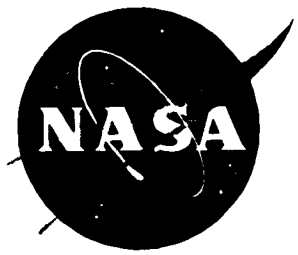

NASA Contractor Report 4661
Part 2

Space Environmental Effects on Spacecraft: LEO Materials Selection Guide

Edward M. Silverman

Contract NAS1-19291
Prepared for Langley Research Center

August 1995

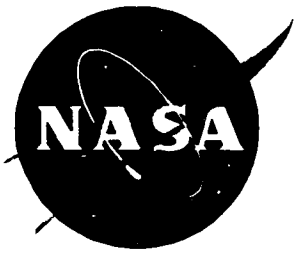

NASA Contractor Report 4661
Part 2

Space Environmental Effects on Spacecraft: LEO Materials Selection Guide

Edward M. Silverman
TRW Space & Electronics Group • Redondo Beach, California

National Aeronautics and Space Administration
Langley Research Center • Hampton, Virginia 23681-0001

Prepared for Langley Research Center
under Contract NAS1-19291

August 1995

Printed copies available from the following:

NASA Center for AeroSpace Information
800 Elkridge Landing Road
Linthicum Heights, MD 21090-2934
(301) 621-0390

National Technical Information Service (NTIS)
5285 Port Royal Road
Springfield, VA 22161-2171
(703) 487-4650

FOREWORD

This report describes the work accomplished under the "Mission Systems Operations Analysis of NASA Space Station Freedom Advanced Concepts (MSOA) contract NAS1-19291, Task 12 (April 1993 through March 1995). Sponsorship for this program was provided by National Aeronautics and Space Administration, Langley Research Center, Hampton, Virginia.

Ms. Joan G. Funk and Dr. Stephen S. Tompkins were the NASA Task Technical Monitors. The following aerospace personnel provided critical support throughout the program:

Brian Blakkolb	TRW Space & Electronics Group
Dennis Rhoads	TRW Space & Electronics Group
Dr. Robert Stillwell	TRW Space & Electronics Group
Dr. Gary Pippin	Boeing Defense & Space Group
Harry Dursch	Boeing Defense & Space Group
Dr. Hank Babel	McDonnell Douglas
Dr. Alan Tribble	Rockwell International

ABBREVIATIONS, ACRONYMS, AND SYMBOLS

Å	Angstrom
Al	Aluminum
AL	Anomalously Large
AO	Atomic Oxygen
A*p*	Geomagnetic Activity Index (daily)
a*p*	Geomagnetic Activity Iindex (3-hourly)
AR	Anti-reflectance
ASTM	American Society for Testing Materials
AXAF	Advanced X-Ray Astrophysics Facility
BOL	Beginning of Life
BRDF	Bi-directional Reflection Distribution Function
C	Centigrade
CAA	Chromic Acid Anodize
CERES	Cloud and the Earth's Radiant Energy System
CLEO	Circular Low Earth Orbit
CN	Cumulative Number
cm	Centimeter
CTE	Coefficient of Thermal Expansion
CVCM	Collectible Volatile Condensable Material
DHW	Double Halfwave
DoD	Department of Defense
DSP	Defense Support Program
DSCS	Defense Satellite Communications System
EDAC	Error detection and correction
EECC	Environmental Exposure Control Canister
EIS	Experiment Initiate System
EMI	Electromagnetic Interference
EPDM	Ethylene Propylene Diene Monomer
ESCA	Electron Spectroscopy for Chemical Analysis
ESD	Electro Static Discharge
ESH	Equivalent Sun Hours
EO	Electro-optical
EOS	Earth Orbiting Satellite
EOL	End-of-Life
EPDS	Experiment Power & Data System
ESA	European Space Agency
EURECA	European Retrievable Carrier
EUV	Extreme ultraviolet

eV	Electron Volt
$F_{10.7}$	10.7 Centimeter Solar Radio Noise Flux
°F	Fahrenheit
FEP	Fluorinated Ethylene Propylene
FEWS	Follow-on Early Warning Satellite
FRECOPA	FREnch COoperative Passive Payload
FTIR	Fourier Transform Infrared
g	gram
GCR	Galactic Cosmic Ray
GEO	Geosynchronous Orbit
GeV	Ggaelectron Volt
Ghz	Gigahertz
GPS	Global Positioning System
GSFC	Goddard Space Flight Center
HEO	Highly Elliptical Orbit
HSLA	High Strength Low Alloy
HVI	Hypervelocity Impact
Hz	Hertz
IBEX	Ion Beam Textured and Coated Surfaces Experiment
IDE	Interplanetary Dust Experiment
IR	Infrared
Isc	Short-Circuit Current
ITO	Indium-Tin Oxide
I-V	Current-Voltage
JPL	Jet Propulsion Laboratory
JSC	Johnson Space Center
K	Kelvin
KeV	Kiloelectron volt
kg	Kilogram
kHz	KiloHertz
km	Kilometer
KSC	Kennedy Space Center
LaRC	Langley Research Center
LMSC	Lockheed Missiles & Space Company
LDEF	Long Duration Exposure Facility
LEO	low Earth orbit
LeRC	Lewis Research Center

LSI	Large-scale integration
m	Meter
MEO	Medium Earth Orbit
MeV	Megaelectron Volt
Mhz	Megahertz
MIL-STD	Military Standard
MLI	Multilayer Insulation
MDSSC	McDonnell Douglas Space Systems Company
mm	Millimeter
M/OD	Micrometeoroids/Orbital Debris
MSFC	Marshall Space Flight Center
MTM	Magnetic Tape Module
mV	Millivolt
MW	Megawatt
NASA	National Aeronautics and Space Administration
nm	Nanometer
OCLI	Optical Coating Laboratory, Inc
OSO-H	Orbiting Solar Observatory
OSR	Optical Solar Reflector
PL	Phillips Laboratory
Pmp	Maximum Power Point
PTFE	Polytetrafluoroethylene
QCM	Quartz Crystal Microbalances
RCC	Removable Cassette Container
R_e	Earth radii
rf	Radio Frequency
RMS	Remote Manipulator System
SAEF-2	Spacecraft Assembly and Encapsulation Facility - 2
SAMPLE	Solar Array Materials Passive LDEF Exposure
sec	Second
SEM	Scanning Electron Microscopy
SEU	Single Event Upset
SEL	Single Event Latchup
SIG	Special Investigation Group
SMM	Solar Maximum Mission
SPENV	Space Environment
SAA	Sulfuric Acid Anodize
SSF	Space Station Freedom

SSM	Second Surface Mirror
SSN	Sunspot Number
TCSE	Thermal Control Surfaces Experiment
TML	Total Mass Loss
TOMS	Total Ozone Mapping System
TRMM	Tropical Rainfall Measuring Mission
UHCRE	High Resolution Study of Ultra-Heavy Cosmic Ray Nuclei
ULE	Ultra Low Expansion
UV	Ultraviolet
UTIAS	University of Toronto Institute for Aerospace Studies
UTRC	United Technologies Research Center
VDA	Vapor Deposited Aluminum
VLSID	Very Large-Scale Integrated Device
Voc	Open Circuit Voltage
ZOT	Zinc Orthotitanate
α	absorptivity
ε	emissivity
μ	micron, micrometer
λ	wavelengths

TABLE OF CONTENTS
PART 1*

*Published under separate cover.

PART 2

10. THERMAL CONTROL SYSTEM

10.1 INTRODUCTION

10.1.1 Thermal Environment

Throughout the various phases of every spacecraft mission there are significant variations in the internal heat dissipated by components and in the external heating fluxes. Spacecraft components must also be maintained within specified operational temperature limits for high reliability, although wider limits can be tolerated for spacecraft survival. Factors that must be considered by the spacecraft thermal control system designer include allowable operating temperatures, mission modes, energy absorbed by the spacecraft, internal heat generation, and external heat radiation.

10.1.1.1 Allowable Operating Temperatures

The allowable operating temperatures are key factors in the design of a spacecraft or a major subsystem. Typical subsystem design temperature levels for a spacecraft are as follows:

- 0 to 60°C (32 to 140°F) for all systems in general;
- -18 to 50°C (0 to 120°F) for electronic equipment
- 0 to 20°C (32 to 68°F) for storage batteries;
- 4 to 50°C (40 to 122°F) for propulsion system;
- 21°C ± 1°C (70°F ± 2°F) for precision optical systems; and
- -184 to 121°C (-300 to +250°F) for solar array.

A relatively cool, narrow operating temperature range extends the useful lifetime of batteries. Propulsion systems, on the other hand, may need a warm environment to avoid freezing of propellants, i.e., hydrazine. A very tightly controlled temperature of 21°C (70°F) for precision optical systems avoids optical performance degradation due to thermal deformation of optical elements. And very low temperatures for some solid state detectors assure minimum internal thermal noise and thus maximum signal-to-noise ratios.

10.1.1.2 Typical Mission Modes

A spacecraft is exposed to a wide range of thermal conditions from prelaunch through transfer orbit to operational orbit. Three possible mission modes are:

- Near-Earth Orbit, in which Earth emission and albedo (solar radiation reflected from Earth) significantly affect the thermal design;
- Synchronous orbit, approximately 22,400 miles from Earth, where emission and albedo are not particularly significant except at cryogenic temperatures; and
- Interplanetary flights in which the spacecraft moves toward or away from the sun.

10.1.1.3 External Energy Characteristics and Absorptance

The energy absorbed by a spacecraft depends on the thermal characteristics and area of its outer surface, its orientation to the source of thermal radiation, and the characteristics of that source. Geometric considerations determine in part how much energy is absorbed on the outer surface due to area size and spacecraft orientation. However, radiation source characteristics and thermal surface properties are interrelated and require some amplification.

Important external radiation sources include the sun, albedo (planetary reflection), and Earth emission. The intensity of solar radiation - parallel sun rays are assumed at these distances - varies with the distance from the sun according to the inverse square law. The intensity also varies spectrally, i.e., according to the wavelength spectrum, with the following approximate energy distribution:

- Ultraviolet (wavelength less than 0.38 μm): 7%
- Visible (wavelength between 0.38 and 0.76 μm): 45.5%
- Infrared (wavelength greater than 0.76 μm): 47.5%

The Earth's albedo is almost diffuse, which means that from any fixed point on Earth, the intensity of reflected radiation is almost uniformly distributed out from that point and is not dependent upon the angle of incident radiation. The Earth's albedo is not a fixed value but varies considerably with local conditions such as cloud cover. The spectral distribution is approximately the same as the source (the sun). While not precise statements, for thermal design purposes it is

adequate to consider the albedo as diffuse and its spectrum that of the sun. The Earth's emission, on the other hand, is based on an apparent "black body" temperature of the Earth and its atmosphere. (A "black body" emits the maximum amount of radiant energy at a given temperature and wavelength.) A temperature of 450°R is commonly assumed, with the emission considered to be diffuse.

The spectral distribution of the energy source is particularly important in spacecraft thermal design since spacecraft coatings and surfaces are spectrally responsive to the radiation source. A black coating absorbs almost all of the impinging solar energy and has a flat spectral response, i.e., the same response to all wavelengths. A second surface mirror (e.g., glass or quartz, aluminized or silvered on the back side, attached with adhesives to the spacecraft exterior), on the other hand, reflects most of the solar radiation and shows a marked change over the spectrum, except for a flat response in the solar band (see Figure 10-1).[1] Other coatings, in general, have surface characteristics that vary between those of black bodies and second surface mirrors

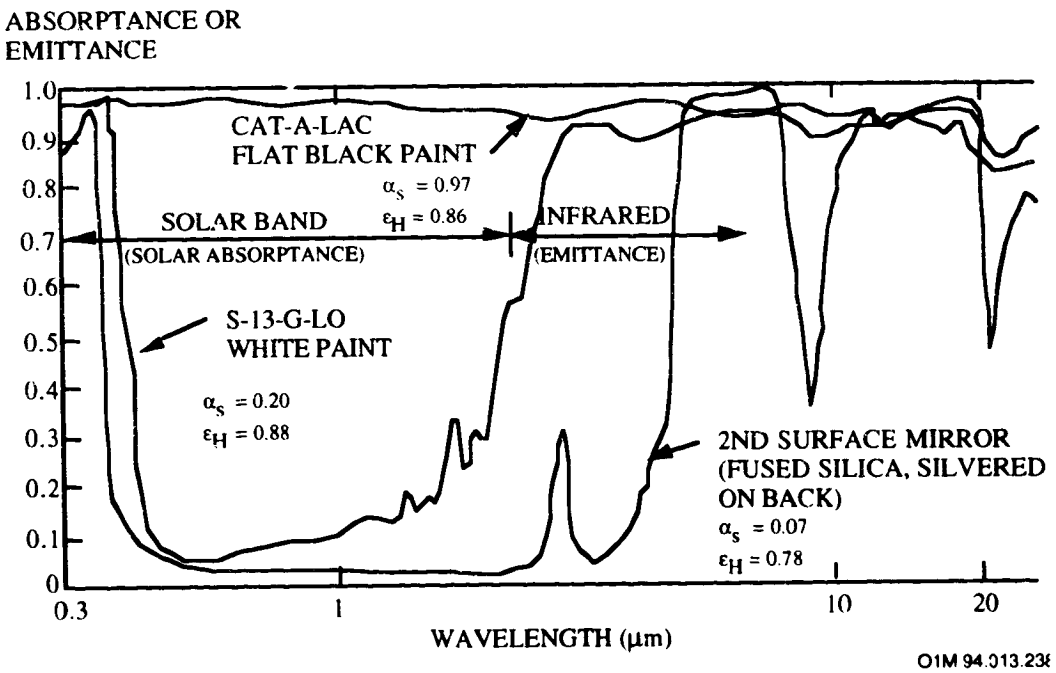

Figure 10-1. Spectral Absorptance/Emittance of Several Materials and Coatings

The solar absorptance of spacecraft materials will, in general, increase over the lifetime of a mission - the longer the mission, the larger the increase. The magnitude of this increase cannot be precisely determined, but must nevertheless be considered in all spacecraft thermal design. Absorptance changes can be induced by the ultraviolet spectrum of solar radiation, by energetic

particles, by contamination from materials outgassing during the various mission phases, and by other factors such as high temperatures and the vacuum of space.

10.1.1.4 Internal Heat Generation

The heat generated by spacecraft components often presents difficult thermal design problems becaus of local high heat densities, high dissipation, and wide changes over time. Sources of this heat include electronic components, batteries, solar cells, and radioisotope thermoelectric generators. These components, including both payload and support equipment, are located inside the spacecraft, on the external surface, or deployed away from the spacecraft body by means of supports. Heat generated by internal equipment is conducted and/or radiated to radiator surfaces that reject it to space. Radiator surfaces are finished with selected coatings to minimize the external flux absorbed and maximize radiation to deep space. Any external surfaces not used as radiators are usually covered with multilayer insulation blankets. Major design considerations include locating heat sources so as to temper the wide variations of heat in local regions, and minimizing the temperature drop from the heat-generating component to the "radiator" (the major panels or surfaces that radiate the heat to space).

10.1.2 Thermal Management Systems

The primary function of the thermal control system is to maintain nominal temperatures for all components on board the spacecraft in all external environments and under all operational modes. The thermal control design may include a combination of suitable external coatings and/or surfaces and insulation, the particular internal placement of components, and the use of other thermal control hardware such as heat pipes, louvers, and heaters. Radiators are used to maintain the heat balance within the space vehicle. The excess heat is radiated into deep space to maintain relatively constant temperatures. Temperature levels are controlled by using selective absorbers to limit absorbed solar or albedo energy, balanced with solar array electrically generated heat dissipated from electronic boxes, and through energy previously stored in batteries and distributed via heaters.

The spacecraft engineer has two methods to control temperature. These are the passive and active methods. The overall thermal design is generally a combination of the two methods.

10.1.2.1 Passive Thermal Control

The passive method controls temperature by the use of conductive and radiative heat paths. This is done by selecting the proper geometrical surface configuration and optical properties of the materials. Thermal coatings, thermal insulation, heat sinks, doublers, second surface mirrors, and tapes are used to maintain the temperature in the passive thermal control method.

Thermal Coating Materials. The external spacecraft surfaces are radiatively coupled to space, as the space is considered to be at absolute zero. Because these surfaces are also exposed to external sources of energy, like the Sun, their radiative properties must be selected to balance the internal dissipation, external energy sources, and the heat rejection to space, while maintaining the desired operating temperature. The two properties of primary importance for external surfaces are the emittance and solar absorptance. Generally, emittance is a function of temperature. For many materials, however, an emittance at 300° C can be used over the expected temperature range of a spacecraft with acceptable accuracy. Spacecraft radiators are covered with thermal control coatings to minimize the heat flux absorbed and to maximize heat radiation to space. These coatings have a low solar absorptance and a high infrared emittance. Table 10-1 lists the thermal optical properties of some common thermal control coatings and components.

Table 10-1. Thermal Optical Properties of Coatings and Components

Material	Absorptivity	Emissivity
Aluminum (polished)	0.10	0.05
Aluminum silicone paint	0.25	0.28
Aluminized Kapton	0.35	0.60
Silvered Teflon	0.14	0.76
Silicon Oxide on polished metal	0.10	0.90
Titanium	0.80	0.18
White Paint (epoxy base)	0.22	0.81
Black Paint	0.84	0.80
Gold	0.40	0.06
Ablative material	0.90	0.90
Second Surface Mirrors, 0.15--mm silvered fused silica	0.07	0.78
Solar cells	0.70	0.82

A coating consists of a layer (or layers) of any substance(s) upon a substrate. Optical coatings have been used to control the temperature of satellites since the first successful orbital flight in 1958. Since then coating materials have been developed to the point where reasonably stable coatings are available that give a wide range of values of hemispherical emittance, ε, between .1 and .9, and selected values of the solar absorptance, α, between .1 and .9.

Three types of coatings can be identified:

1. Pigmented coatings that are mixtures of a pigment and a vehicle.
2. Contact coatings, formed by layers of a substance coated on a substrate without chemical reaction occurring between the coating material and the substrate.
3. Conversion coatings that are layers of compounds formed by the chemical reaction of the substrate with another material.

Radiators. Spacecraft thermal radiators require a low solar absorptance to minimize absorbed solar and albedo heating, and a high infrared emittance to minimize radiator size for a fixed heat rejection rate and radiator temperature. Second surface mirrors consist of a metal (usually silver or aluminum) deposited on one side of a quartz sheet, installed with the glass or quartz surface facing outward. The glass of the second surface mirror is transparent over most of

the solar wavelengths so that most of the solar energy reaches the mirror surface i.e., the back side metal, and is reflected back out into space. Equipment heat is conducted into the second surface mirrors and to the glass or quartz front surface from which it radiates to space. Glass is an excellent emitter over the infrared spectrum. Figure 10-2 shows a schematic of a typical second surface mirror application. Silvered Teflon functions in an identical manner.

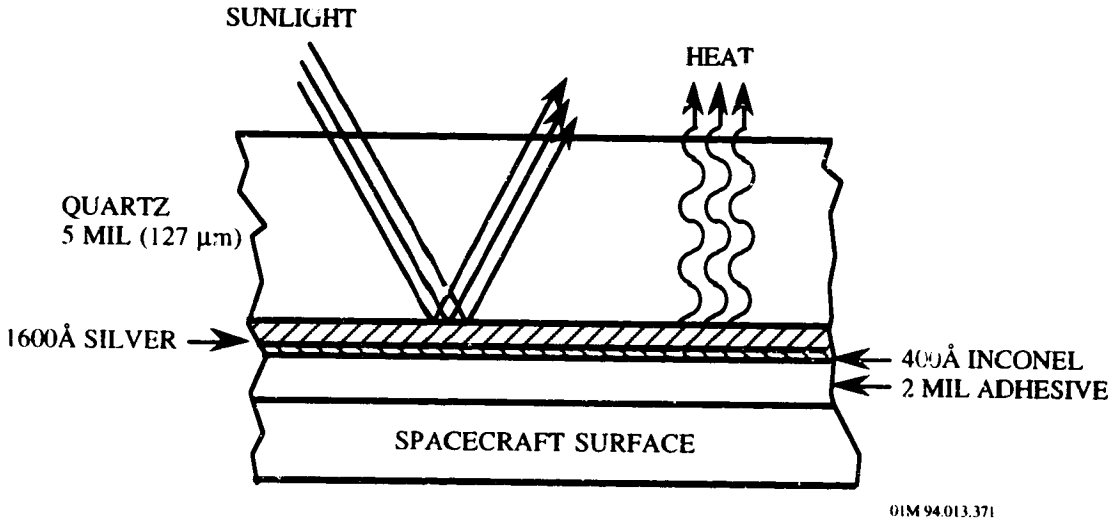

Figure 10-2. Cross- Sectional View of Second Surface Thermal Control Mirrors

Thermal Insulation. Thermal insulation reduces the rate of heat flow per unit area between two boundary surfaces. Multilayer insulations are used to reduce the temperature fluctuations in components caused by time varying external radiative heat fluxes, and to minimize the temperature gradients in components caused by nonuniform external heating. These blankets are also used to isolate internal components when necessary, and may also be used to obtain more controlled values of performance. Hence, multilayer insulation reduces environmental heating effects, cold case heater power requirements and the temperature gradients across structures.

Multilayer insulation blankets consist of several alternating layers of vacuum deposited aluminized 25 µm Kapton and double aluminized crinkled innerlayers of Mylar or Kapton to achieve a low emittance. These radiation shields are crinkled so that the conductance from shield-to-shield is reduced by having only point contacts over a small fraction of the area, and allow trapped gases to be replaced by high vacuum which is an excellent insulator in space. Instead of crinkling, Dacron net separators or embossed plastic film are used to separate the radiation shields and minimize the shield-to-shield conductance. All blankets are electrically grounded and provide for venting during launch. Figure 10-3 shows a schematic of a typical blanket consisting of

several alternating layers of aluminized Kapton and crinkled inner layers, and optional Dacron net separators.

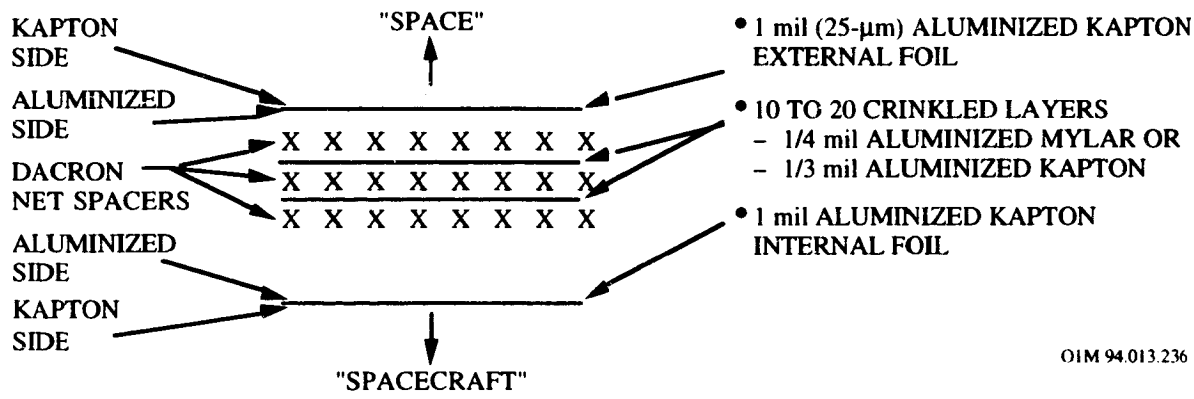

Figure 10-3. Typical Multilayer Blanket Composition

For effective performance, the residual gas pressure within multilayer insulations must be less than 10^{-4} torr. To accomplish this and to protect the insulation from damage, adequate venting is provided during ascent. Multilayer insulators are usually vented through the edges of blankets or by perforations in the shields. Installation of multilayer insulation often involves cutting, taping, and tailoring to fit the contours.

10.1.2.2 Active Thermal Control

Passive temperature control does have its limitations: added mass and surface area; poor response to large variations in equipment power dissipation; and degradations in the optical properties. To overcome these limitations, active thermal control methods are used to complement the passive techniques. In this method, the temperature of the equipment is continuously monitored, and thermal control hardware is turned on or off when preset temperature limits are reached. In this way, the equipment temperature is controlled and maintained within the desired range. Thus, the thermal control hardware reacts to changing heating rates by adjusting the thermal properties in accordance with preset temperature limits. Heaters and thermostats, louvers, heat pipes, and spaceborne cooling systems are employed in the active thermal control method. For example, for spacecraft with high-power-dissipation equipment, such as high-power TWTA (traveling wave tube amplifier), it may be more efficient in terms of added mass to use heat pipes to increase thermal conductivity in place of heat sinks. A brief review of active control elements can be found in books by P.R.K. Chetty and B.N. Agrawal.[2,3]

10.1.3 Design Implications to Future Spacecraft

The basic requirement for a coating to be used in spacecraft is long-term space stability for periods of months and even of years. End of life (EOL) properties must be considered in designing a thermal control system because most coatings are known to degrade with time. The degradation varies as a function of time as well as the orbit. The degradation is caused by the combined effects of high vacuum, charged particles, ultraviolet radiation from the sun, and contamination. Contamination sources are: improper handling of thermal coatings; outgassing from the shroud during ascent; thruster firings; and condensation of outgassed constituents of the spacecraft materials, e.g., volatile materials and other thermal coatings. Person-tended vehicles may have additional contamination from extra-vehicle activities and vented waste products.

The solar absorptance (α_S) of spacecraft materials will, in general, increase over the lifetime of a mission - the longer the mission, the larger the increase. Absorptance changes can be induced by the ultraviolet spectrum of solar radiation. In contrast, emittance (ε) remains roughly constant. Usually, paints are much more susceptible to this damage than mirrors or metallized polymeric films. Contamination can produce immediate, significant increases in solar absorptance. Atomic oxygen at low altitudes tends to erode many unprotected materials, such as Kapton, silver, and carbon. The magnitude of this change cannot be precisely determined, but must nevertheless be considered in all spacecraft thermal design.

Spacecraft designers frequently need coatings with α_S and ε values tailored for a particular application. These requirements range from low α_S/high ε for many thermal radiator applications to many other combinations of low-to-high α_S and low-to-high ε. Figure 10-4[4] shows the range of coatings and films that can be prepared in the laboratory. Hence, different materials and surface coatings can be used to provide almost any desired combination of absorptance and emittance characteristics. Black paints, for example, have high solar absorptance, while white paints have low absorptance; both, however, exhibit high emittance. By mixing black and white paints in various proportions, various shades of gray can be created to provide coatings with high emittance and a range of solar absorptance. The same results may be achieved by a geometric black-and-white checkerboard pattern. White paints and second-surface mirrors attached to the surface with adhesives provide the high emittance and low solar absorptance required for many spacecraft surfaces, especially those used to radiate internally generated heat into space. Although second-surface mirrors are costlier than paints, they are used more often because they are less subject to degradation in space over long-life missions.

Figure 10-5 shows that even though the selection is more limited there is still a wide range of coatings suitable for short term applications (< 5 years). For long term applications (> 5 years), this range of suitable materials is severely limited (see Figure 10-6). The "LDEF test" validated only a few of these coatings for long term applications. These include Z-93 and YB-71 white ceramic coatings, silver Teflon (when properly applied), thin chromic acid anodized aluminum and possibly D-111 black ceramic coating.

Because of the different combinations of space environment constituents, the range of coatings that are usable in geosynchronous orbit (GEO) are somewhat different than for LEO applications but are also very limited (see Figure 10-7).

With the limited range of proven coatings, designers of space hardware for long term missions must accommodate the optical properties (α_s, ε) of these coatings. The behavior of coatings in the space environment is still not well understood and conservative end-of-life estimates for coatings must be used. Until this materials/environment interaction is better understood and improved coatings are developed, the stability of coatings in the space environment will continue to be a limiting factor in the technology for long term missions.

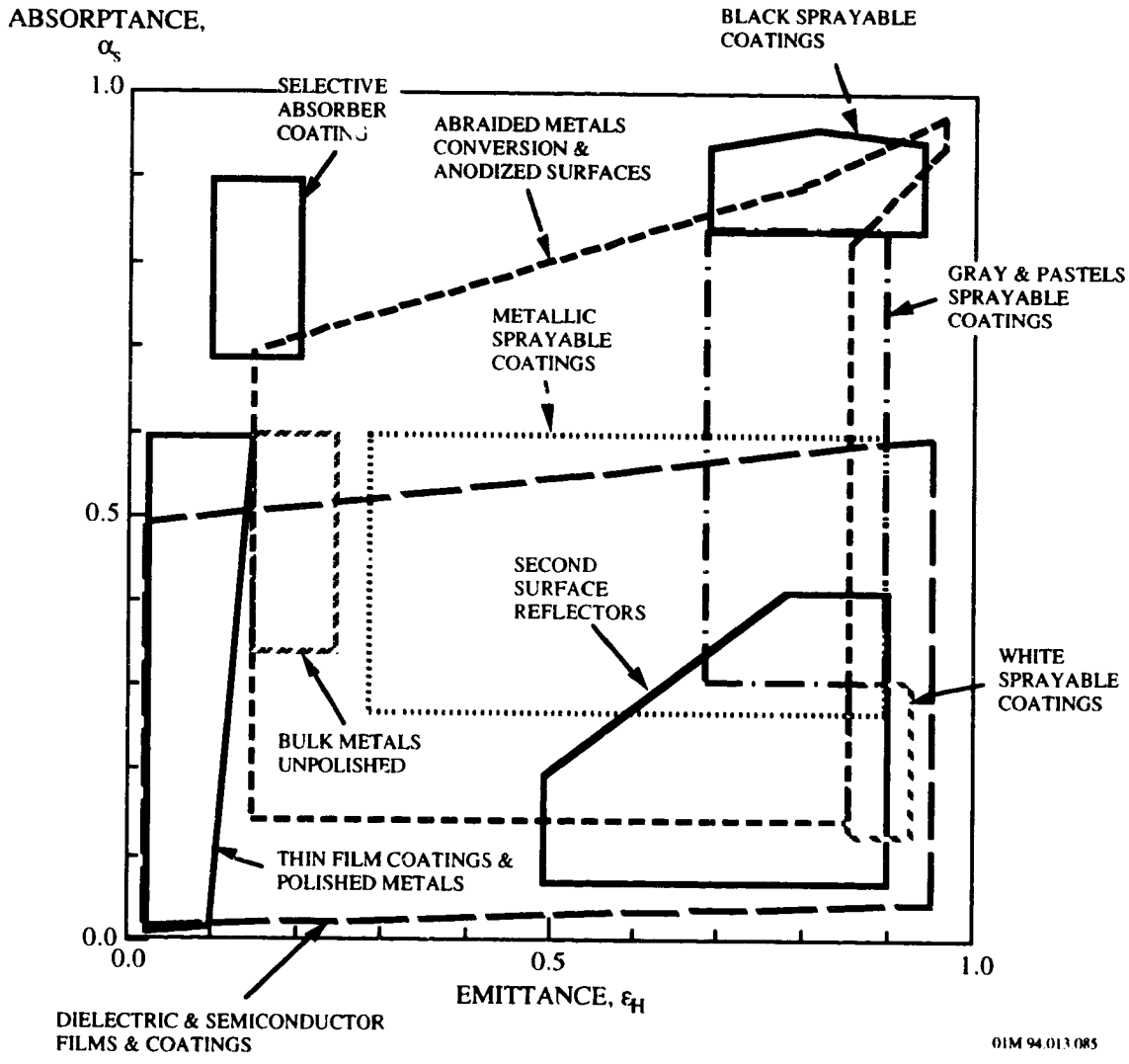

Figure 10-4. Available Coatings and Surfaces

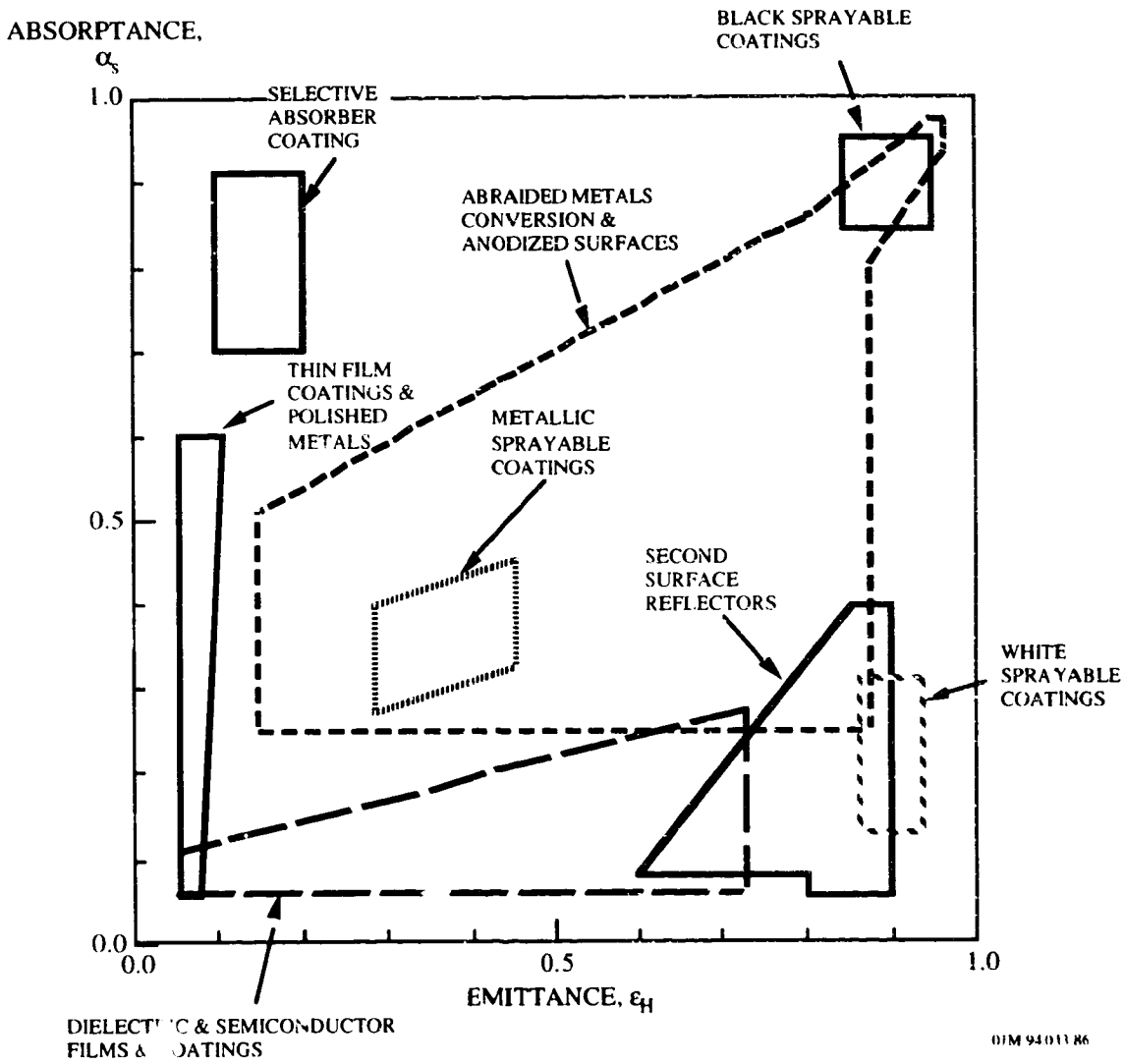

Figure 10-5. Usable Coatings and Surfaces - LEO Short Term

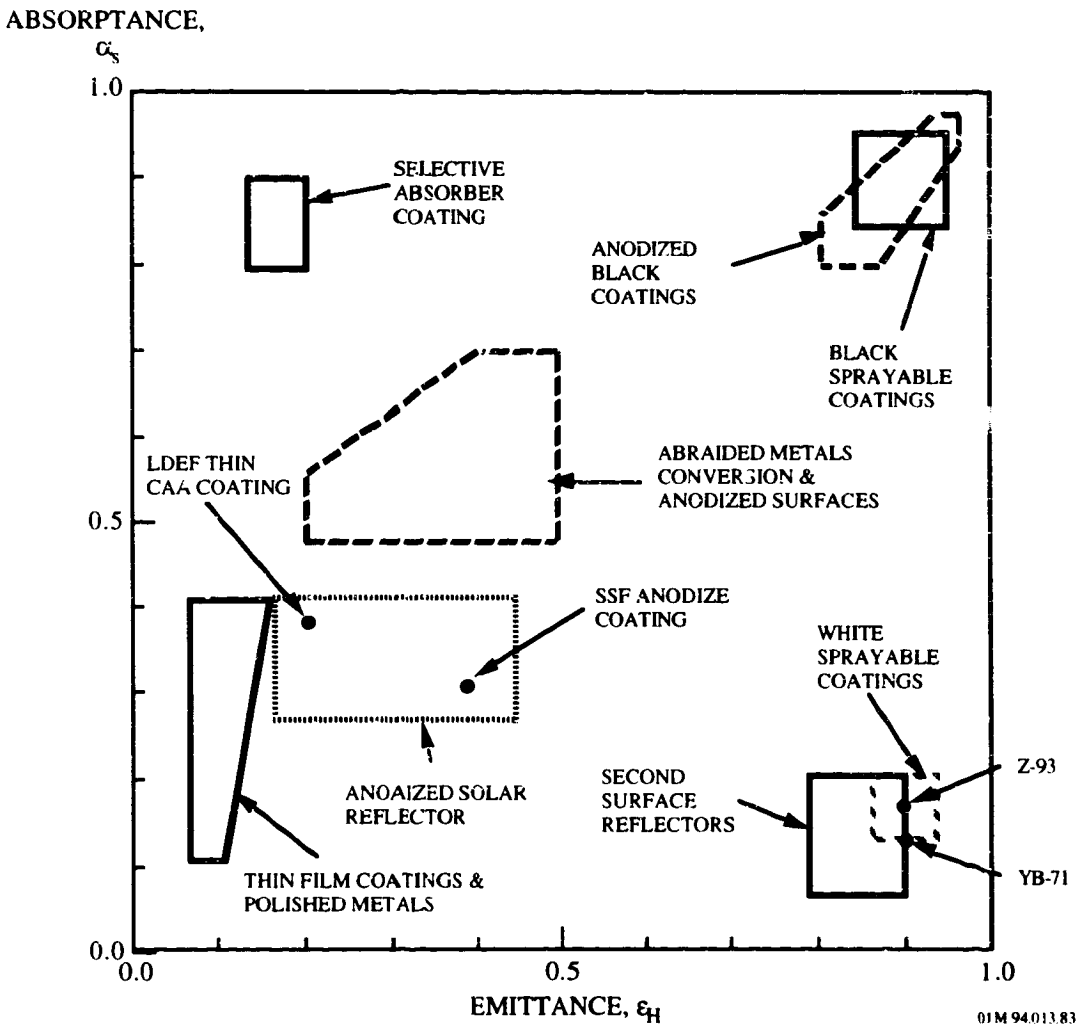

Figure 10-6. Usable Coatings and Surfaces - LEO > 5 years

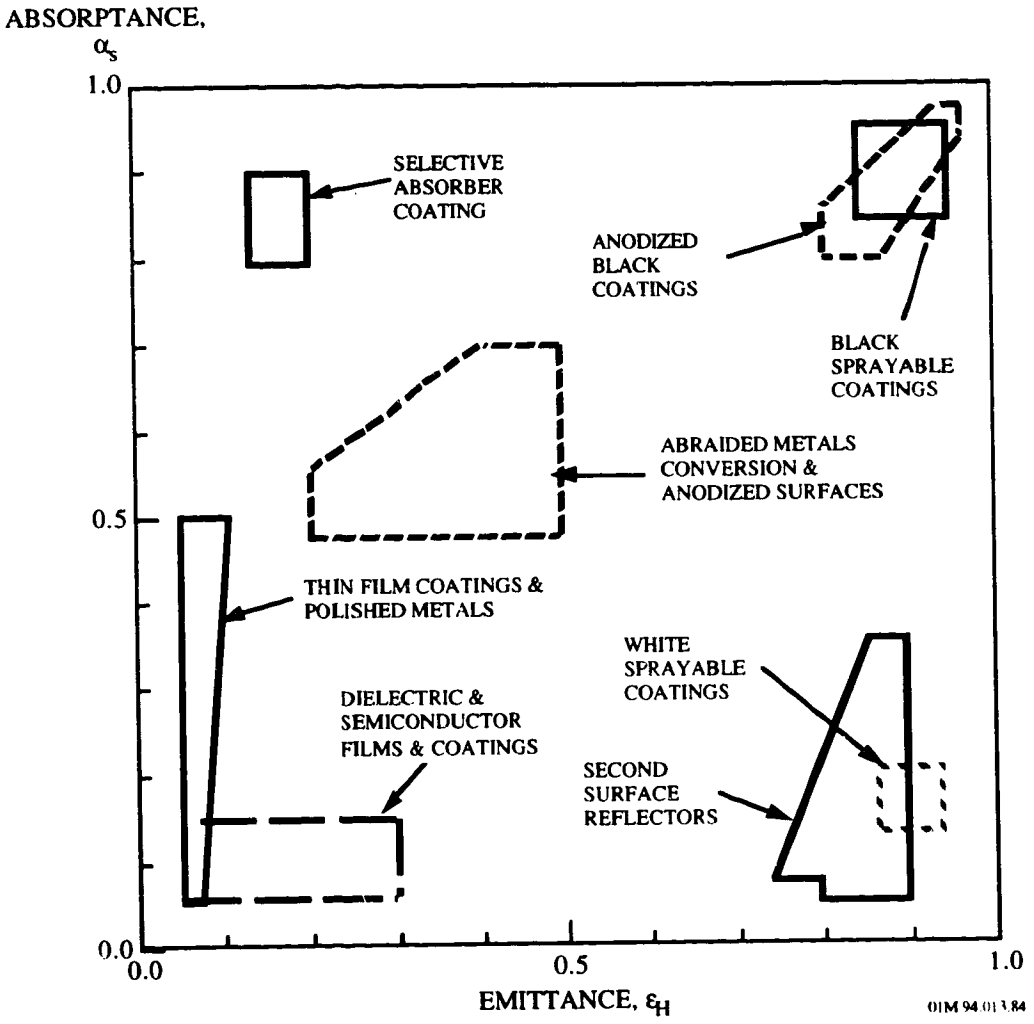

Figure 10-7. Usable Coatings and Surfaces - GEO 1-7 Years

10.2 SUMMARY OF FLIGHT EXPERIMENT RESULTS

With the exception of the limited experimentation conducted aboard Skylab, the LDEF (69 months) and the COMES experiments (13 months, 2 days) on the MIR satellite have provided the only retrievable space exposure opportunity to test the long term performance of thermal control coatings. Many of the 57 LDEF experiments exposed thermal control coatings to the LDEF environment either as test specimens or as operational coatings. In addition, several coatings were used as thermal control surfaces on LDEF itself. The available thermal control coatings data from the LDEF experiments and from the LDEF system have been reviewed. Tables 10-2 and 10-3 list the experiments, their location on LDEF, and the coatings that are considered in this design guide document.

Table 10-4 provides a summary of the space environment effects on LDEF thermal control materials. More detailed sample evaluation and data analysis are provided in the subsequent sections categorized by thermal control materials. This analysis has provided a wealth of information that is now being made available to aid in the design of future spacecraft. As an example of this, International Space Station Alpha plans to employ the thermal control coating Z-93 extensively on large and complex structures. This is due in large part to the confidence generated by the stability Z-93 demonstrated on the LDEF mission.

However, when the available data on these materials are evaluated along with the preparation, exposure, and measurement conditions, there are several factors that complicate this analysis. In many cases there were no ground and/or flight control samples to establish a measurement baseline and to determine the effects of aging alone on these materials. Where there were control samples, many were either not stored under controlled conditions or were lost over the unanticipated five year delay in the recovery of LDEF. This long and uncertain mission duration also resulted in lost or incomplete pre-flight data and documentation. In addition, some test samples were prepared using different techniques, procedures, material batches, and sample thicknesses. Finally, except for the 15 month in-flight data generated by the TCSE LDEF Experiment S0069, all the thermal control coating data from LDEF consisted of measurements conducted in air at nominal values of room temperature and humidity. It is important to note that the measurements of solar absorptance and thermal emittance made after LDEF flight exposure were taken on samples which had more or less recovered from the UV and radiation damage experienced in flight. If this degradation were observed in the vacuum of space during flight, these values of solar absorptance and thermal emittance may have been different.

Table 10-2. Selected LDEF Experiments with Thermal Control Coatings

Exp #	Ref	LDEF Row	AO Atoms/cm^2	UV esh	Title	PI	Organization
S0069	4,5,67	9 (8°)[a]	8.99x10^{21}	11,200	Thermal Control Surfaces Experiment (TCSE)	Wilkes, Zwiener	AZ Technology NASA/MSFC
A0171	8	8 (38°)	7.15x10^{21}	9,400	Solar Array Materials Passive LDEF Exposure (SAMPLE)	Whitaker	NASA/MSFC
A0114	9	3 9	1.3x10^{17} 8.99x10^{21}	11,100 11,200	Interaction of Atomic Oxygen with Solid Surfaces at Orbital Altitudes	Gregory, Peters	Univ. of Al-HSV NASA/MSFC
M0003-5	10	3 9	1.3x10^{17} 8.99x10^{21}	11,100 11,200	Thermal Control Materials	Hurley	UDRI
M0003-18	11,12	3(TE)[b] 4,8 9(LE)[b]	8.72x10^{4} to 8.99x10^{21}	10,500 to 11,200	DOD Materials Experiment Sub-Experiment 18	Jaggers, Meshishnek	Aerospace Corp.
A0138-6	13	3 (TE)	1.3x10^{17}	11,100	FRECOPA	Guillaumon, Paillous	CERT
M0003-8 M0003-10	14,15 16	1-12 Space & Earth Ends	2.7x10^{3} to 9.0x10^{21}	4,500 to 14,500	LDEF Materials SIG Analysis	Golden, Pippin, Bourassa	The Boeing Co.
S1003	17	6	4.94x10^{19}	6,400	Ion Beam Textured and Coated Surfaces Experiment	Mirtich, Rutledge	NASA/LaRC
S1001 A0076	10, 18	3(TE) 9(LE)	1.3x10^{17} 8.99x10^{21}	11,100 11,200	Low Temperature Heat Pipe Experiment and Cascade Variable Conductance Heat Pipe Experiment	Kauder	NASA/GSFC
S0010	19	9 (8°)	8.99x10^{21}	11,200	Exposure of Spacecraft Coatings	Slemp Young	NASA/LeRC
A0034	20,21	3 (TE) 9 (LE)	1.3x10^{17} 8.99x10^{21}	11,100 11,200	AO Stimulated Outgassing	Linton	NASA/MSFC
A0178	10,2223 ,24,25, 26	1,2,4-8 10,11	1.4x10^{17} to 8.4x10^{21}	6,400 to 10,700	High Resolution Study of Ultra-Heavy Cosmic-Ray Nuclei	See References	ESTEC, Boeing, Aerospace, JPL, NASA
P0004-1	10,20	2 (Tray F)	1.54x10^{17}	9,600	Space Exposed Expt Developed for Students	See References	Boeing, Aerospace

(a) Angle of ram
(b) LE = Leading Edge; TE=Trailing Edge

Table 10-3. Thermal Control Coatings on LDEF Experiments

Thermal Coating	S0069 TCSE	A0114 (UAH)	A0171 Sample	S1003 (IBEX)	S1001 A0076	M0003-5 (Dayton)	M0003	A0138-6 FRECOPA	A0178	P0004-1	MSIG
Z-93	X	X				X	X(6)				
S13G/LO	X	X	X	X	X	X	X	X(6)			X
A276	X	X	X			X	X	X			X
YB-71	X					X	X				
D111	X					X	X				
Z302	X	X	X			X		X			
Z306	X	X	X			X		X(7)			X
Chromic Acid Anodize	X					X					X
RTV 670/ A276	X										
OI650/ A276	X										
Al/ Kapton									X		
Ag/ Teflon					X		X		X	X	

Notes for Table 10-3:

[1]401-C10 (Nextel) Black, Z853 Yellow, Tiodize K17 Black, Tiodize K17 White

[2]401-C10 (Nextel) Black, Black Chrome

[3]SiOx over Kapton; 200, 500, 700, 1000Å

[4]Acrylic/Urethane over Kapton; Silicone over Kapton, RTV 615 white paint

[5]NS43G; White Silicone Eu 203 MeSi, a Al 203 MeSi, PV100, TiO2 MeSi, DC 92-007

[6]White paints similar to S13G and Z-93: PY100, 536, PSB, SG11, FD, PSG 120 FD, and conductive white paints PCB-2, PCB-T, PCB 119

[7]Black Paints similar to Z306: PU1, Cuvertin 306, VHT SP 102, HT 650, Electrodag 501, L300, PNC, PUC

Table 10-4. Summary of Performance of LDEF Thermal Control Materials

Observations	Principal Exposures	Engineering Significance
White Paints		
A276 (leading edge) binder erosion, retention of optical properties	2-9 x 10^{21} atoms/cm^2 6000-11,000 esh UV	Maintained thermal control capability. EOL absorptivity retained Mechanical integrity lost.
A276 (trailing edge) Specimens darkened, Reflown samples partially recovered absorptivity	2.3x10^{21} atoms/cm^2 1450-11,000 esh UV	EOL absorptivity dominated by thin outer layer of binder.
Z93 remained white	AO, UV	Maintained thermal control capability.
YB-71 remained white	AO, UV	Maintained thermal control capability.
PCB-Z remained white	AO, UV	Maintained thermal control capability.
S13G/LO binder darkened	AO, UV	Absorptance increase limits performance lifetime.
Black Paints		
D-111	AO, UV	Maintained thermal control capability.
Z306 (leading edge) Binder erosion, absorptance and emittance changes within measurement accuracy	AO, UV, Thermal cycling	Maintains thermal and optical properties. Mechanical integrity lost.
Z302 (leading edge) Loss of binder and pigment essentially to substrate, absorptivity intact, emittance reduced	AO, UV, Thermal cycling	Specular property lost. Emittance reduction limits use as thermal control in AO environment.[a]
Silvered Teflon (Ag/FEP)		
Thickness changes in FEP layer of silvered Teflon	AO	Optical property changes - slight decrease in emissivity no change in absorptivity -reflectance more diffuse
Bonded Ag/FEP to rigid substrate	UV and/or AO	Increases in solar absorptivity from UV darkening of adhesive that diffused through cracked Ag (due to improper application procedures which pre-cracked the Ag layer)
Embrittled FEP outer surface	UV	Reduced mechanical properties
FEP tape ripped along interface between Al and blankets	Thermal cycling with mechanical motion	Failure in FEP tape
Anodizations		
Black chromium plated aluminum exhibited large variations in optical properties for complex exposure histories on various panels)	AO, UV	Performance predictions not easily made, use with caution
Chromic Acid Anodized Aluminum showed only slight increases in absorptance on trailing edge	AO, UV	Good potential for space applications

(a) Suspect the Z306 was applied thicker than the Z302, which may account for differences in erosion end results.

10.3 WHITE PAINTS

10.3.1 Natural Space Environmental Effects on White Paints

The optical properties of white paints are summarized in Table 10-5. Some of these are conventional white-pigment-in-a-clear-binder paints, but white ceramics (which could be used by themselves for thermal control surfaces) are also included. The values of solar absorption (α) and thermal emissivity (ε) are included.

Based on the results from the Space Shuttle flights and the LDEF mission, the expected natural space environmental effects on these white paints are listed in Table 10-6.[27] While the geomagnetic field and the Earth's ionosphere are not expected to affect these paints, all the other environments may affect α. It is the organic binders that are especially vulnerable to crosslinking and the production of color centers produced by solar UV and the particulate radiation in the Van Allen belts. The organics also outgas (in space vacuum) and suffer erosion (in atomic oxygen). The oxides are not expected to be affected by vacuum and atomic oxygen, but will be vulnerable (as are the other paints) to impact damage.

Table 10-5. Optical Properties of White Paints Exposed to the LEO Environment

Paint	Pigment	Binder	α	ε
A276 White	TiO_2	Polyurethane	0.29	0.90
Z-93 White	ZnO	K_2SiO_3	0.15	0.92
YB-71 White	Zn_2TiO_4	K_2SiO_3	0.15	0.90
S-13G/LO White	ZnO	Methylsilicone	0.37	0.90
Chemglaze Z302 Black	Carbon	Polyurethane	0.97	0.91
D-111 Black	Carbon	Silicate	0.98	0.93
Clear Anodize	Al_2O_3	-	0.2-0.3	0.7-0.9
	BeO	-	0.09	0.66
	MgO	-	~0.095	~0.9
Inorganic Materials	TiO_2	-	~0.2	~0.9
	ZnS	-	~0.09	~0.5
	ZnO	-	0.2	~0.4
	ZnO_2	-	0.29	0.78

Table 10-6. Natural Environmental Effects on White Paints

Environment / Material	Sunlight	Vacuum	Van Allen Belts	Micrometeoroid Objects	Hot Plasma	Gases
S-13G/LO	May increase α	Outgas	May increase α	May increase α	May increase α	May increase α
Z-93	May increase α	Outgas	May increase α	May increase α	May increase α	May increase α
Chemglaze Z302	May increase α	Outgas	May increase α	May increase α	May increase α	May increase α
A276	May increase α	Outgas	May increase α	May increase α	May increase α	May increase α
YB-71	May increase α	Outgas	May increase α	May increase α	May increase α	May increase α
Clear anodize (Al_2O_3)				May increase α		
BeO	-	-	-	May increase α	May increase α	May increase α
MgO	-	-	-	May increase α	May increase α	May increase α
Inorganic TiO_2	-	-	-	May increase α	May increase α	May increase α
ZnS	May increase α	-	-	May increase α	May increase α	May increase α
ZnO	-	-	-	May increase α	May increase α	-
ZrO_2						
Primary Concern:	Solar UV at all altitudes Atomic oxygen in LEO Van Allen belts in MEO Hot plasma in GEO			May increase α		

10.3.1.1 Thermal-Optical Properties

10.3.1.1.1 Effects of Mission Duration

The optical properties variations of several white paints on the LDEF satellite are summarized in Table 10-7 (ref. 4). These white paints, part of the Thermal Control Surfaces Experiment (TCSE) S0069 experiment, are good reflectors of solar energy while also being good emitters of thermal energy to the cold sink of space, i.e., they have a low solar absorptance (α_S) and a high room temperature emittance (ε_N). The TCSE experiment combined in-space measurements with extensive post-flight analyses of thermal control surfaces to determine the effects of exposure to the low Earth orbit space environment.

Table 10-7. Optical Property Variations of White Paint Coatings on LDEF TCSE Experiment

Material	Solar Absorptance (α_s)[a,b,c]				Emittance (ε_N)[d]		
	Pre-flt	In-flt (15 Mo)	Post-flt	$\Delta\alpha_S$	Pre-flt	Post-flt	$\Delta\varepsilon_N$
A276	.25	.30	.24	-.01	.90	.93	.03
A276 w/RTV670	.27	.53	.62	.35	.91	.88	-.03
A276 w/Ox650	.25	.54	.59	.34	.91	.89	-.01
Z-93	.14	.13	.15	.01	.90	.92	.01
S13G/LO	.18	.22	.37	.19	.90	.89	-.01
YB-71	.13	.12	.15	.02	.85	.89	-.01
YB-71 over Z-93	.10	.11	.11	.01	.66	.87	.02

(a) Mission Duration: The TCSE operated for 582 days before battery depletion. The battery power was finally expended while the sample carousel was being rotated. This left the carousel in a partially closed position. This carousel position caused 35 of the samples to be exposed for the complete LDEF mission (69.2 months), and 14 exposed for only 582 days (19.5 months) and therefore protected from the space environment for the subsequent four years.

(b) Space Environmental Exposure: The LDEF was deployed with the TCSE located on the leading edge (row 9) and at the Earth end of this row (position A9). In this configuration, the TCSE was facing the ram direction. The LDEF was rotated about the long axis where row 9 was offset from the ram direction by about 8°. The exposure environment for the TCSE were:

Atomic oxygen fluence	8.99×10^{21} atoms/cm^2
Solar UV exposure	11,200 esh
Thermal cycles	~34,000 cycles; -29°C (-20°F) to 71°C (160°F), ± 10°C (20°F)
Radiation (at surface)	3.0×10^5 rads

(c) The primary TCSE in-space measurement was total hemispherical reflectance as a function of wavelength (100 wavelength steps from 250 to 2500 nm) using a scanning integrating sphere reflectometer. The measurements were repeated at preprogrammed intervals over the mission duration. The secondary measurement used calorimetric methods to calculate solar absorptance and thermal emittance from temperature-versus-time measurements.

(d) Laboratory measurements of spectral reflectance were obtained using Beckman DK-2A spectrophotometer equipment with a Gier-Dunkle 203 mm integrating sphere.

Solar absorptance, α_S, and normal emittance, ε_N, of several white paints on an aluminum substrate on LDEF Experiment S0010, Exposure of Spacecraft Coatings (ref. 19), are summarized in Table 10-8. Also shown are the 5-year 9-month exposure conditions for this experiment, which was located in Tray B on Row 9, the leading edge of LDEF. The experimental canister was opened for 10 months, early in the LDEF mission. This allowed flight data to be obtained for 10-month and 5-year 9-month exposures on the selected coating specimens.

Table 10-8. Optical Property Variations of White Coatings on LDEF Experiment S0010

Coating	Preflight		10 Months Exposure		5.8 Years Exposure	
	α_S	ε_N	α_S	ε_N	α_S	ε_N
S13G/LO White Paint	.158	0.90	.182	0.89		
Zinc oxide-silicone	.163	0.90			.206	.89
A276 White Paint	.229	0.89	.237	0.90	-	-
Chemglaze	.243	0.91	-	-	.259	0.88
YB-71 White Paint	.121	0.91	.123	0.91	-	-
Zinc orthotitinate-silicate	.128	0.90	-	-	.125	0.90

(a) Exposure Conditions For Tray B on Row 9:

Atomic oxygen	8.99×10^{21} atoms/cm^2
UV radiation	100-400 nm; 11,000 hrs
Particulate radiation	e- and p+: 2.5×10^5 rad surface fluence Cosmic: 10 rads
Vacuum	1.33×10^{-4} - 1.33×10^{-5} N/m^2 (10^{-6} - 10^{-7} torr)
Thermal cycles	~34,000 cycles: -29 to 71 °C, ±11°C (-20 to 160 °F, ±20°F)

The results show that the YB-71 (zinc orthotitinate/potassium silicate) paint has stable optical properties when exposed to the LEO environment. Similar results were reported by B. Stein,[28] who reported stable optical properties for both the YB-71 and Z-93 white paints. The solar absorptance for A276 increased to 0.259 from 0.243 after 5.8 years of space exposure. In contrast, S13G/LO (treated zinc oxide/silicone) exhibited a 25 % increase in solar absorptance in this study and in the study by Hurley,[10] although subjected to atomic oxygen in space and oxygen from air upon return to Earth. This is surprising since exposure to air (oxygen) after UV exposure is known to "bleach" the reflectance degradation caused by the UV.

X-ray Photoelectron Spectroscopy (XPS) and Energy Dispersive X-ray (EDS) studies of these coatings indicate that a silicone molecular contamination film was deposited on the specimens during LDEF. Such contamination films were also identified in other experiments on LDEF.[29,30,31,32] Since these silicones are typically converted to a silicate when exposed to atomic oxygen,[33] they are not easily removed from the surface of coatings. This contamination may influence the mass loss and optical property data generated by this experiment.

10.3.1.1.2 Effects of Varying Oxygen Exposures

Several thermal control paints were flown on LDEF (LDEF Experiment M0003 Sub-Experiment 18),[11] including the white paints Chemglaze A276, S13G/LO, and YB-71. Both S13G/LO and YB-71 were located on trays D9 (LE) and D3 (TE). The leading edge tray was exposed to 11,200 equivalent sun hours of UV radiation and an atomic oxygen fluence of 8.99×10^{21} atoms/cm^2 while the trailing edge tray was exposed to 11,100 equivalent sun hours of UV radiation and an atomic oxygen fluence of 1.32×10^{17} atoms/cm^2. In addition, the A276 and S13G/LO white paints were used on LDEF as a thermal control coating on the Experiment Power and Data System (EPDS) sunshields (painted with Chemglaze A276) and the signal conditioning unit (SCU) covers (painted with S13G/LO). These covers were used to protect data system instrumentation for other experiments. These covers were located on the leading edge (row 8) and trailing edge (row 4) of the spacecraft; row 8 is located 30° from the perpendicular of the atomic oxygen vector, and row 4 is located 30° from the perpendicular of the wake region. Consequently, these trays were exposed to different levels of UV radiation and atomic oxygen; samples from row 8 (referred to as leading edge samples) were exposed to 9,400 equivalent sun hours of UV radiation and an atomic oxygen fluence of 7.15×10^{21} atoms/cm^2, while samples from row 4 (referred to as trailing edge samples) was exposed to 10,500 equivalent sun hours of UV radiation and an atomic oxygen fluence of 2.31×10^{5} atoms/cm^2.

A summary of the solar absorptances for the thermal control paints are listed in Table 10-9. The effects of low Earth orbit, which includes those induced by UV radiation and atomic oxygen, varied significantly with each paint and its location on LDEF.

A276 White Paint. Samples of Chemglaze A276 located on the trailing edge of LDEF darkened significantly due to UV-induced degradation of the paint's polyurethane binder, while leading edge samples remained white but exhibited severe atomic oxygen erosion of the binder. Although the thermal control properties of the surface are not deleteriously affected, the surface has lost its physical integrity and is easily damaged upon contact.

S13G/LO White Paint. Although the response of S13G/LO to low Earth orbit is much more complicated, it also exhibited greater darkening on trailing edge samples as compared to leading edge samples. The solar absorptance of the trailing edge has increased threefold from an initial value of 0.15. The leading edge has also degraded, but its solar absorptance has only increased to 0.23. Almost all of the degradation occurs in the visible and ultraviolet wavelengths, with very little degradation occurring above 1200 nm. The absorption peaks above 1200 nm have

been identified as methyl silicone (binder) absorption peaks and are present in leading edge, trailing edge, and control samples. The increase in solar absorptance of S13G/LO is due to UV-induced damage of the methyl silicone binder on both the leading and trailing edge samples. However, based on reflectance data, there is no evidence of damage to the encapsulated zinc oxide pigment. This damage is not bleachable and does not recover upon exposure to air, even after one year. Both the leading and trailing edge surfaces show oxidation of the methyl silicone binder to silica, which is accompanied by a loss of methyl groups and a formation of a cracking network on the surface. The extent of this cracking network depends largely on the atomic oxygen fluence that the surface received. However, unlike A276 there was no preferential removal of the binder by atomic oxygen from the leading edge surface.

YB-71 White Paint. YB-71 exhibited an apparent increase in its solar absorptance to 0.183 for both the leading and trailing edge samples from 0.130 on a laboratory controlled sample. No measurements were made on th flight samples prior to launch. The LDEF investigators concluded that this white paint remained relatively stable and showed minimal degradation since the similar values measured on the leading and trailing edge locations indicated no significant effects of contamination or atomic oxygen.

Table 10-9. Effects of Varying UV/Atomic Oxygen Fluences on the Solar Absorptances of White Paints on LDEF Experiment M0003-18

Type	Location	α_s	UV (sun-hrs)	Atomic Oxygen (atoms/cm^2)
S13G/LO	Control	0.147	-	-
	D9(LE)	0.232	11,200	8.99×10^{21}
	D9(LE)	0.228	11,200	8.99×10^{21}
	D3(TE)	0.458	11,100	1.32×10^{17}
	D3(TE)	0.473	11,100	1.32×10^{17}
	D8(LE-SCU)	0.257	9,400	7.15×10^{17}
	D4(TE-SCU)	0.496	10,500	2.31×10^{5}
A276	Control	0.282	-	-
	D8(LE-SS)	0.228	9,400	7.15×10^{17}
	D4(TE-SS)	0.552	10,500	2.31×10^{5}
YB-71	Control	0.130	-	-
	D9(LE)	0.182	11,200	8.99×10^{21}
	D3(TE)	0.182	11,100	1.32×10^{17}

TE=trailing edge; LE=leading edge; SS=sun shield cover; SCU=signal conditioning unit cover

10.3.1.1.3 AO and UV Synergistic Effects

The prediction of material degradation due to the space environment is essential for the design of spacecraft thermal systems. The space environment has several components, such as the vacuum, atomic oxygen (in low Earth orbit), solar ultra-violet irradiation, the particles fluxes (electrons and protons), micrometeoroids and debris, to which must be added the effects of thermal cycling and contamination (both by chemical compounds with a low molecular weight and by dust). However, it is difficult to reproduce in a laboratory the synergistic effects of these different components and to recreate the real, complete space environment of a given mission (in particular with respect to far ultra-violet radiation). Hence, experimenting in-orbit is of very great interest for the study of material degradation due to the synergistic effects of the space environment. In addition, it enables the validation of ground based simulations effects. Several experiments on the LDEF and MIR spacecraft observed the results of the synergistic effects of the space environment on the optical properties of white paint coatings.

LDEF Experiment A0034

Multiple specimens of five different types of white thermal control coatings, four white zinc oxide or orthotitanate pigment with silicone or silicate binder based paint and one titanium dioxide/polyurethane based paint, were exposed on LDEF Experiment A0034.[20,21] A summary of the five thermal coatings and their characteristic formulation is provided in Table 10-10.

Table 10-10. White Thermal Control Coatings on LDEF Experiment A0034

S13G	zinc oxide in RTV602 silicone binder
S13G/LO	zinc oxide in RTV602 silicone binder, improved formulation for low outgassing
Z-93	zinc oxide in potassium silicate binder
YB-71	zinc orthotitanate
A276	titanium dioxide pigment in polyurethane binder

This experiment consisted of both a leading edge and trailing edge module, which housed 25 specimens of thermal control coatings in a sandwiched array of apertured compartments. The module mounted on the leading edge of the LDEF provided direct exposure to the combined space environment, including atomic oxygen, while the other module, mounted on the trailing edge, was intended to provide comparable environmental exposure in the relative absence of atomic oxygen. Additional levels of control for analysis were included by sealing the apertures of selected specimen compartments in each module with quartz windows and metal covers. The

windows were intended to exclude atomic oxygen while transmitting damaging solar ultraviolet radiation. The metal covers provided controlled exposure to space vacuum in the absence of atomic species and all but the most energetic of space radiation.

The thermal control coatings retrieved from the leading edge and trailing edge of A0034 were exposed to the maximum and the minimum levels of atomic oxygen, respectively, with other environmental exposure relatively equal. Based on the restricted field-of-view (approximately 25 degrees) and estimates of coating UV sensitivity, the estimated level of solar UV irradiation to specimens of A0034 was 1500 equivalent sun hours. Table 10-11 summarized the space exposure conditions for LDEF Experiment A0034.

Table 10-11. Space Exposure Condition of LDEF Experiment A0034

LDEF Position		Space Exposure Condition		
		Atomic Oxygen atoms/cm^2	Ultraviolet esh	Vacuum
Leading Edge	Open	8.99×10^{21}	1500	Yes
	Quartz Window	-	1500	Yes
	Metal Cover	-	-	Yes
Trailing Edge	Open	1.32×10^{17}	1500	Yes
	Quartz Window	-	1500	Yes
	Metal Cover	-	-	Yes

Tables 10-12 and 10-13 present the variations of the solar absorptance and emissivity of the various white paint samples after their flight on LDEF. The effects of extended space exposure on thermal control coatings of LDEF experiment A0034 are dependent on several factors, including the type or composition of the coating and the combination of incident environmental factors. For a few specimens, variant response to the same environmental exposure indicates influences of specific coating formulation or preparation. LDEF leading edge exposure, characterized by the degree of atomic oxygen exposure, apparently reversed the damage induced by incident solar radiation. The principal exception is one of the S13G specimens, which are known to rapidly recover from UV damage when exposed to oxygen, exposed under an open aperture on the leading edge.

The visual appearance and optical properties of the polyurethane coating exposed under open apertures on the leading edge were little changed despite the erosion of binder material by atomic oxygen. Significant degradation of the A276 specimen exposed under a quartz window

appears to be duplicated in an area of the open aperture specimen that was shadowed from direct atomic oxygen impingement.

The most significant degradation to the zinc oxide or zinc orthotitanate coatings was found in specimens of S13G and S13G/LO exposed to the aperture-limited level of solar radiation and the minimal atomic oxygen fluence on the trailing edge. Specimens of Z-93 coatings were least affected of all by exposure on the leading or trailing edge modules. Specimens of YB-71 coatings were affected only slightly more than Z-93 coatings. Preliminary results of BRDF and surface profiling measurements indicated that the AO exposure on these coatings did not significantly alter the diffuse properties.

Observations of fluorescence changes induced in the exposed coatings provided additional evidence of environmental interaction. Suppression and color shifting of visibly color specific fluorescence are strikingly evident in the three zinc oxide based coatings (S13G, S13G/LO, and Z-93). The intrinsic yellow glow of these type coatings is visibly extinguished in the specimens exposed through open apertures on the leading edge of the LDEF. Those on the trailing edge are affected to a lesser degree. The fluorescence of these trailing edge specimens, under black light illumination, is shifted to longer wavelengths (orange appearance). In contrast, the intrinsic yellow fluorescence Z-93 coatings is visibly extinguished for specimens exposed through open apertures on both the Leading and trailing edges. The visible fluorescence of these zinc oxide based coatings is little changed by exposure under the quartz windows of either experiment module; the differences are detectable only in the visual intensity or hue of the yellow glow. These effects can be gauged from the relative black-light illuminated tones. The YB-71 coating specimens provide no evidence of natural or induced fluorescence.

Table 10-12. Synergistic Environment Effects on the Solar Absorptance of White Paints

Exposure: Coating	Total Space Exposure (Open) Average	Control Vacuum Only (Metal Cover) Average	UV Only (Window) Average
	LDEF	**Leading Edge**	
S13G	0.17[a]	0.17	0.18
S13G/LO	0.19	0.18	0.19
Z-93	0.17	0.16	0.17
YB-71	0.17	0.16	0.19
A276	0.20	0.21	0.35
	LDEF	**Trailing Edge**	
S13G	0.26	0.18	0.20
S13G/LO	0.28	0.17	0.21
Z-93	0.17	0.16	0.16
YB-71	0.19	0.16	0.19

(a) Solar absorptance determined by measuring the spectral diffuse reflectance in the 200-2200 nanometers range using a Varian/Cary 2300 spectrometer

Table 10-13. Synergistic Environment Effects on the Emittance of White Paints

Exposure: Coating	Total Space Exposure (Open) Average	Control Vacuum Only (Metal Cover) Average	UV Only (Window) Average
	LDEF	**Leading Edge**	
S13G	0.88[a]	0.90	0.90
S13G/LO	0.87	0.89	0.89
Z-93	0.92	0.91	0.93
YB-71	0.89	0.89	
A276	0.92	0.87	0.87
	LDEF	**Trailing Edge**	
S13G	0.89	0.90	0.90
S13G/LO	0.91	0.89	0.89
Z-93	0.90	0.91	0.91
YB-71	0.89	0.89	0.89
C9 "Leading Edge" 8.1°: AO Fluence = 8.99×10^{21} atoms/cm^2; UV = 11,200 esh. C3 "Trailing Edge" 171.9° AO Fluence = 1.32×10^{17} atoms/cm^2; UV = 11,100 esh..			

(a) Thermal emittance measured with a Gier-Dunkle DB-100 reflectometer

FRECOPA/LDEF and COMES/MIR Experiments

The COMES experiment consisted of four panels which were deployed by an cosmonaut in space outside of MIR with the possibility of exposing samples on both sides, conventionally identified as "V" and "R". Experiment AO 138-6 was part of the FRECOPA experiment located on the trailing edge (row 3) of LDEF. The experiment was designed to allow exposure of a part of the samples to the whole spacecraft environment, including launch and re-enty, by being laid directly on the FRECOPA tray surface, while the other samples were protected from the external environment of LDEF for all mission phases except free flight, by the means of a vacuum-tight FRECOPA canister in which they were stored.

Space Environment Conditions on the LDEF and MIR Space Experiments: Due to its position on the trailing edge of LDEF, the AO 138-6 experiment did not receive any oxygen atoms during the mission, with the exception of a short period during the retrieval when it received an estimated fluence of 1.32×10^{17} atoms cm^{-2}. The solar illumination was 11,100 esh for the samples located on the tray and only 1448 esh for the samples inside the canister. The particle irradiation dose (mainly due to the electron flux) was weak: 3×10^{5} rads. The number of temperature cycles was ~34,000 with temperatures within the ranges shown in Table 10-14. The COMES/MIR space environment conditions for the "V" and "R" faces are also listed.

Table 10-14. Space Environment Conditions for LDEF FRECOPA and MIR COMES

	FRECOPA-LDEF		COMES-MIR	
ENVIRONMENT	CANISTER	TRAY	FACE V	FACE R
Oxygen atoms cm^{-2}	0	1.3×10^{17}	1.2×10^{18} to 7.5×10^{19} (1)	3.5×10^{20} to 5.8×10^{20} (1)
Solar UV (esh)	1448	11,100	2850(2)	1900(2)
Temp. Cold (°C)	-20 to -26	-43 to -52	-60 to -70	-60 to -70
Temp. Hot (°C)	+67 to +85	+45 to +63	+10 to +30	+50 to +60

(1) Estimated from AO reactivity erosion of Kapton (3.0×10^{-24} $cm^3 atom^{-1}$)and Terphane (3.0×10^{-24} $cm^3 atom^{-1}$) samples

(2) Estimated from data of experiment calorimeter

Experimental Description. The solar reflection measurements were made with a Beckman DK2A spectrophotometer with an integrating sphere, and the infrared emissivity measurements were made with the Gier & Dunkle DB 100 device. It is important to underline that the measurements were all taken in air on samples which had thus experienced more or less intense recovery of the radiation damage.

Table 10-15 presents the variations of the emissivity of various common white paint samples after their flight on FRECOPA/LDEF and COMES/MIR.[34]

Table 10-15. Emissivity Variations of White Paints After Their Flight on FRECOPA/LDEF and COMES/MIR

Material	$\varepsilon_{initial}$	AO 138-6 LDEF		COMES	
		Canister $\Delta\varepsilon$	Tray $\Delta\varepsilon$	Face V $\Delta\varepsilon$	Face R $\Delta\varepsilon$
A276	0.877	-0.005		+0.005	+0.036
S36	0.856	0.001	-0.001		
PV100	0.865	-0.001			
PSB	0.895	-0.001	-0.003	-0.003	
SG11FD	0.854			-0.005	-0.005
PSG 120 FD	0.876	-0.002		0.000	+0.002
PCB-Z - conductive	0.872	0.000		+0.006	+0.003
PCB-T - conductive	0.815	0.000			
PCB 119 - conductive	0.861			+0.008	+0.006

Table 10-16 presents the variations of the solar reflectance of various white paint samples after their flight on FRECOPA/LDEF and COMES/MIR (ref. 34).

Table 10-16. Solar Reflectance Variations of White Paints After Their Flight on FRECOPA/LDEF and COMES/MIR

Material	$Rs_{initial}$	AO 138-6 LDEF		COMES	
		Canister ΔRs	Tray ΔRs	Face V ΔRs	Face R ΔRs
A276	0.75	-0.24		-0.01	+0.05
S36	0.81	-0.04	-0.08		
PV100	0.78	-0.08			
PSB	0.83	-0.05	-0.01	-0.01	
SG11FD	0.82			-.0.04	-0.01
PSG 120 FD	0.80	-0.07		-0.04	-0.02
PCB-Z - conductive	0.78	-0.04		-0.01	-0.02
PCB-T - conductive	0.72	-0.10			
PCB 119 - conductive	0.79			-0.01	0.01

From these two tables, one observes that the white paints were less deteriorated following the COMES experiment than after the FRECOPA experiment. This was especially true for the A276 paint. It seems clear that the atomic oxygen cures the effects of the UV radiation. On the R side, which received the most oxygen atoms, the solar reflectance of the A276 paint even seems to have increased following the flight.

Table 10-17 shows the deterioration in the solar reflectance for different samples exposed to different environments on the V side of the COMES experiment. See Table 10-14 for the space environment exposure conditions.

Table 10-17. Synergistic Space Environment Effects on the Solar Reflectance Degradation ΔR_S of White Paints on the V Side of COMES

Material	Chemical Nature	UV + AO + vacuum ΔR_S(a)	UV (λ>190 nm) ΔR_S(b)	UV (λ>360 nm) ΔR_S(c)	Vacuum ΔR_S(c)
PCBZ - Conductive	Zinc Orthostannate/ silicone	-0.01	-0.01	-0.01	+0.01
PSG 120 FD(Astral) SG 120 FD (MAP)	ZnO/silicone	-0.04	-0.03	0.00	0.00
A 276	Polyurethane	-0.01	-0.14	0.00	+0.01
PCB 119 - Conductive	Zinc Orthotitanate (doped)/Silicone	-0.01	0.00	+0.01	+0.01
SG 11 FD	Zinc Orthotitanate/ Silicone	-0.04	-0.01	0.00	0.00
PSB	Zinc Orthotitanate/ silicate	0.00	0.00	+0.01	0.00

(a) an exposure to all of the parameters: ultraviolet solar radiation (including far UV), atomic oxygen, vacuum and the temperature, ΔR_S=final R_S-initial R_S

(b) an exposure to ultra-violet radiation with a wavelength greater than 190 nm, to the vacuum and to the temperature

(c) an exposure to radiations with a wavelength greater than 360 nm, to the vacuum and to the temperature

(d) an exposure to the vacuum and to the temperature.

The deterioration generally found on the white paints is relatively low whether submitted to the complete environment or under UV. The A276 paint is an exception; it suffered very strong deterioration under UV with a wavelength greater than 190 nm but on the other hand its solar reflectance is stable under UV + atomic oxygen. In the case of this paint, it has been confirmed that the atomic oxygen decreases the extent of damage which would be experienced under UV radiation acting alone, as had been clearly shown by many observations on LDEF. On

the R side of COMES which received the most oxygen atoms, the solar reflectances of the A276 paint and the PCB 119 even seem to have increased following the flight. But the PSG 120 FD and SG 11 FD paints on the other hand, appear to deteriorate more under UV + atomic oxygen than under ultraviolet radiation alone.

MIR/Recoverable Cassette Container-1 (RCC) Experiment

The Russian RCC-1 Thermal Control Coatings experiment contained nine white thermal control paints, of which only two were chemically similar to the U.S. white paints, Z-93 and YB-71. Tables 10-18 and 10-19 summarize the effects of the space environment on the thermal optical properties of the RCC-1 thermal control coating materials.[35] These materials were exposed to an AO fluence of ~10 x 10^{21} atoms-cm^{-2} and ~600 UV esh.

Table 10-18. Space Exposure Effects on the Solar Absorptance of White Paints on the Mir/RCC-1 Experiment

Reference	Chemical Nature	Solar Absorptance		
		Pre-Flight	Post-Flight	$\Delta\alpha$
AK-512-w	TiO_2 + ZnO/acrylic resin	0.30	0.30	0.00
KO-5191	ZnO/silicone resin	0.18	0.20	0.02
KO-5258	ZnO + TiO/silicone resin	0.27	0.31	0.04
TP-co-2	ZnO/potassium metasilicate	0.18	0.18	0.00
TP-co-10M	ZnO/asbestos	0.20	0.20	0.00
TP-co-11	ZnO/orthotitanate-potassium metasilicate	0.14	0.14	0.00
TP-co-12	ZnO/potassium metasilicate	0.19	0.19	0.00
TP-co-90	Zr titanate/potassium metasilicate	0.15	0.15	0.00
40-1-12-88	ZrO_2/silicone resin	0.21	0.28	0.07

Table 10-19. Space Exposure Effects on the Emittance of White Paints on the Mir/RCC-1 Experiment

Reference	Chemical Nature	Emittance		
		Pre-Flight	Post-Flight	$\Delta\alpha$
AK-512-w	TiO_2 + ZnO/acrylic resin	0.88	0.88	0.00
KO-5191	ZnO/silicone resin	0.89	0.89	0.00
KO-5258	ZnO + TiO/silicone resin	0.90	0.89	-0.01
TP-co-2	ZnO/potassium metasilicate	0.97	0.94	-0.03
TP-co-10M	ZnO/asbestos	0.84	0.84	0.00
TP-co-11	ZnO/orthotitanate-potassium metasilicate	0.93	0.91	-0.02
TP-co-12	ZnO/potassium metasilicate	0.96	0.94	-0.02
TP-co-90	Zr titanate/potassium metasilicate	0.95	0.94	-0.01
40-1-12-88	ZrO_2/silicone resin	0.92	0.91	-0.01

A number of these materials did not experience any significant changes in solar absorptance or emittance. The TP-co-2, TP-co-11, and TP-co-12 coatings were the most stable. This result agrees with the LDEF findings (Z-93, YB-71) in that zinc oxide and zinc oxide orthotitanate in metasilicate binders are the most stable upon exposure to the space environment. The solar absorptance and emittance values for these materials are very similar, indicating consistency of results. Furthermore, the diffuse reflectance spectra for TP-co-2 and TP-co-12 are in general agreement with the U.S. equivalent Z-93, and the reflectance spectrum for TP-co-11 is similar to YB-71.

In contrast, the 40-1-12-88 exhibited the highest increase in solar absorptance, 0.07, due to the degrading effect of the solar UV. White paint 40-1-12-88 was found to be the least stable material. This material is based on ZrO_2 and is known to be very sensitive to UV radiation. Because this material exhibited no mass change (see below) it can be concluded that it is relatively immune to AO attack, thereby preventing any cleaning erosion effect. Conversely, the coatings TP-co-10M and TP-co-90 showed a mass decrease, but no change in optical properties. This is consistent with the optical stability of these materials was maintained by AO erosion on the exterior surface. No significant changes in emittance were observed for any of the materials.

10.3.1.2 Mass Loss

The mass loss variations of several white paints on an aluminum substrate on the LDEF satellite are summarized in Table 10-20. These white paints were part of the LDEF experiment S0010, Exposure of Spacecraft Coatings (ref. 19).

Table 10-20. Mass Loss of White Paint Coatings in LDEF Experiment S0010

Test Material Description	Mass Loss[a] mg/cm^2
YB-71 on Aluminum	.15
S-13GLO on Aluminum	.19
A276 on Aluminum	.23

[a]Atomic Oxygen Fluence = 2.6×10^{20} atoms/cm^2

Mass loss was observed on the majority of the Russian RCC-1 Thermal Control Coatings experiment white paints due to erosion by AO, as shown in Table 10-21.[35] KO-5191 and TP-co-11 demonstrated no mass changes, while the porous ceramic coating TP-co-12 demonstrated a significant increase of 1.1 mg. It is believed that this increase is due to contamination from the Mir Orbital Station condensing on the materials surface when cooled by the Earth's shadow. For coatings which exhibited a mass increase, the contamination deposition effect obviously prevailed over the AO erosion effect.

Table 10-21. Environment Effects on the Mass Loss of White Paints on the Mir/RCC-1 Experiment

Reference	Chemical Nature	Mass (g)		
		Pre-Flight	Post-Flight	Δm (mg)
AK-512-w	TiO_2 + ZnO/acrylic resin	4.3844	4.3837	-0.7
KO-5191	ZnO/silicone resin	4.5258	4.5258	0.0
KO-5258	ZnO + TiO/silicone resin	4.6203	4.6206	0.3
TP-co-2	ZnO/potassium metasilicate	4.6200	4.6197	-0.3
TP-co-10M	ZnO/asbestos	4.6992	4.6973	1.9
TP-co-11	ZnO/orthotitanate-potassium metasilicate	4.5807	4.5807	0.0
TP-co-12	ZnO/potassium metasilicate	4.5260	4.5271	1.1
TP-co-90	Zr titanate/potassium metasilicate	4.6095	4.6068	-2.7
40-1-12-86	ZrO_2/silicone resin	4.6222	4.6223	0.1

10.3.1.3 Summary of Flight Experiments Findings

The following are the major conclusive findings from flight and ground-based simulation experiments for white paints

- Z-93, YB-71, PCB-Z white paints are stable.

  Z-93P white paint has been requalified. In contrast, YB-71P has not been successfully requalified. Hence, future use of this white paint is not recommended.

- A276 white paint is affected by AO and UV.

  Chemglaze A276 is not recommended as a white thermal control paint for spacecraft that require any significant mission lifetimes due to its susceptibility to UV degradation and atomic oxygen erosion. Ultraviolet radiation causes a significant increase in the material's solar absorption, while atomic oxygen erosion of the binder results in a fragmented surface and could cause particulate contamination to other areas of the spacecraft. Its low cost and ease of application, however, make it much more desirable for boosters and upper stage rockets that do not require long mission lifetimes.

- S-13G/LO white paint on LDEF gave variable results.

  A 100% increase in absorptivity should be accounted for in the spacecraft thermal design of S13G/LO paint. S13GP/LO-1 has been successfully requalified.

- Potassium silicate binders are stable; organic binders are not stable.

10.3.2 A276 White Paint

Chemglaze A276 polyurethane white paint, used on many short term space missions including Spacelab, is formulated for space applications requiring high reflectivity and low outgassing, and provides excellent gloss and color retention.

It has a low solar absorptance (α_S) of 0.23 ±0.01 and a high room temperature normal emittance (ε_N) of 0.90 ±.05. Outgassing measurements according to ASTM E595-77 are %TML = 0.99 and %CVCM=0.08.[36]

A276 is known to degrade moderately under long term UV exposure and to be susceptible to AO erosion.

10.3.2.1 Composition

Binder: Polyurethane

Pigment: Titanium dioxide

10.3.2.2 Source

Manufacturer: Lord Chemical Products
2000 West Grandview Blvd
Erie, PA
Telephone. 814 868-3611

Cost: $61.50/gallon (1994 price)

10.3.2.3 Effects of the Space Environment

10.3.2.3.1 Thermal-Optical Properties

Absorptance and Emittance Properties. *The average α values for A276 white thermal control paint ranged from 0.22 $\pm$0.02 for the white appearance to 0.45 $\pm$0.05 for the dark brown finish, apparently due to contamination and UV degradation during flight. Actual measurements ranging from 0.20 to 0.55. The white control sample had an α of 0.29. The ε values for the A276 showed no change from the control sample value of 0.88 even though there was severe color change.* This can be attributed to the fact that the emissivity of painted coatings are more a function of coating thickness and chemical matrix than other factors such as color. Table 10-22 summarizes the α and ε measurements for A276 white paint after 5 years and 9 months exposure on several LDEF experiments and on thermal control test disks located on selective tray clamps placed around the LDEF periphery.[37]

Table 10-22. LDEF Post Flight Absorptance and Emittance Results for A276 White Paint.

Location on LDEF	AO atoms/cm^2	Description	Sample #	α_s (1)	ε_N (2)	α/ε
E-12, H-6,F-6	4.94×10^{19} to 1.33×10^{21}	White to light tan color	6	.22±.02	.91±.01	.24
E-12, H-6,F-6	4.94×10^{19} to 1.33×10^{21}	Medium tan in color	2	.36±.03	.88	.41
E-12, H-6,F-6	4.94×10^{19} to 1.33×10^{21}	Medium tan to dark brown	4	.45±.05	.88±01	.51
Tray clamp E-3#8	1.32×10^{17}	Brown in color	1	.53	.38	.60
Tray clamp E-6#8	4.94×10^{19}	Tan non-uniform color	1	.42	.87	.48
Tray clamp E-9#6	8.99×10^{21}	White in color	1	.32	.90	.36
Tray clamp E-12#6	1.33×10^{21}	Dull cream beige color	1	.36	.87	.41
Tray clamp		Control Sample - white	4	.29±.01	.88	.33

(1) Solar Reflectance: Devices & Services Solar Reflectomerter SSR-ER, Ver. 5.0
(2) Infrared Reflectance: Gier Dunkle Infrared Reflectometer DB-100, Normal Emittance

The key result is that the environmental effects depend a great deal on the location of the white paint on the spacecraft. For example, the specimens located on the leading edge (ram direction) of LDEF showed that the organic binder of the A276 paint had been broken down by the attack from AO which left only a white chalky pigment. In contrast, the specimens located on the trailing edge (shielded from AO) had developed a hardened dark brown finish while other specimens showed only patches of brown depending upon their orientation with respect to the AO flux. This is demonstrated by comparing the experiment tray coated with A276 paint located on row 6 with the tray located on the opposite row 12. Both trays received the same intensity of UV flux during the mission, but because the LDEF was yawed 8°, the row 12 tray was exposed to a ~2700% larger increase in AO flux than the row 6 tray. The result was that row 6 tray remained brown in color while the row 12 tray was bleached white with brown spots. The dark brown areas were due to the UV polymerization of the A276 organic binder with an average α almost twice as high as the white control sample α of 0.29.

Atomic oxygen exposure counteracts the effects of the UV radiation by removing the material affected by UV. This is substantiated by the less deterioration exhibited by the A276 coating following the 1.1 year COMES/MIR flight experiment in comparison to the 9-month exposure in a FRECOPA canister during the LDEF missions as shown in Table 10-23 (ref. 34). The COMES experiment consisted of four panels which were deployed by a cosmonaut in space outside of MIR with the possibility of exposing samples on both sides, conventionally identified as "V" and "R". Experiment AO 138-6, part of the FRECOPA experiment located on the trailing edge of LDEF, was designed to allow exposure of a part of the samples to the whole spacecraft environment by being laid directly on the FRECOPA tray surface, while the remainder of the samples were protected from the external environment of LDEF for all mission phases, except free flight, by the means of a vacuum-tight FRECOPA canister in which they were stored. On the R side which received the most oxygen atoms, the solar reflectance of the A276 paint increased (α_s decreased) following the flight.

The A276 white paint on the side V of the COMES experiment suffered very strong deterioration under UV with a wavelength greater than 190 nm but was stable under combined UV and atomic oxygen exposures. Table 10-24 shows the deterioration in the solar reflectance property for different A276 white paint samples exposed to the different environments. In the case of this paint, it has been confirmed that the atomic oxygen has a repairing effect on damage due to UV radiation, as has been clearly shown by the several observations on LDEF.

Table 10-23. Solar Reflectance and Emissivity Variations of A276 White Paint After its Flight on FRECOPA/LDEF and COMES/MIR

Thermal Property		AO 138-6 LDEF		AO 138-6 LDEF		COMES		COMES	
$Rs_{initial}$	$\varepsilon_{initial}$	Canister ΔRs	Tray ΔRs	Canister $\Delta\varepsilon$	Tray $\Delta\varepsilon$	Face V ΔRs	Face R ΔRs	Face V $\Delta\varepsilon$	Face R $\Delta\varepsilon$
0.75	0.877	-0.24		-0.005		-0.01	+0.03	+0.003	+0.036

Environmental Variations of LDEF and MIR Space Experiments: Due to its position on the trailing edge of LDEF, the AO 138-6 experiment did not receive any oxygen atoms during the mission, with the exception of a short period during the capture when it received a fluence evaluated at 1.32×10^{17} atoms cm^{-2}. The solar illumination was 11,100 equivalent sun hours (esh) for the samples located on the tray and only 1448 esh for the samples inside the canister. The particular irradiation dose (mainly due to the electron flux) was weak: 3×10^5 rads. The number of temperature cycles was ~34,000 with temperatures within the ranges shown in the table below.

Experimental Description. The solar reflection measurements were made with a Beckman DK2A spectrophotometer with an integrating sphere, and the infrared emissivity measurements were made with the Gier & Dunkle DB 100 device. It is important to underline that the measurements were all taken in air on samples which had thus experienced more or less intense recovery of the radiation damage.

ENVIRONMENT	FRECOPA-LDEF		COMES-MIR	
	CANISTER	TRAY	FACE V	FACE R
Oxygen atoms cm^{-2}	0	1.3×10^{17}	1.2×10^{18} to 7.5×10^{19} (1)	3.5×10^{20} to 5.8×10^{20} (1)
Solar UV (esh)	1448	11,100	2850(2)	1900(2)
Temp. Cold case (°C)	-20 to -26	-43 to -52	-60 to -70	-60 to -70
Temp. Hot case (°C)	+67 to +85	+45 to +63	+10 to +30	+50 to +60

(1) Estimated from AO reactivity erosion of Kapton (3.0×10^{-24} $cm^3 atom^{-1}$) and Terphane (3.0×10^{-24} $cm^3 atom^{-1}$) samples

(2) Estimated from data of experiment calorimeter

Table 10-24. Synergistic Space Environment Effects on the Solar Reflectance Degradation ΔR_S of A276 Coating on the V Side of COMES.

Type	Chemical Nature	UV + AO + vacuum ΔR_S(a)	UV (λ>190 nm) ΔR_S(b)	UV (λ>360 nm) ΔR_S(c)	Vacuum ΔR_S(d)
White Paint	Polyurethane	-0.01	-0.14	0.00	+0.01

(a) an exposure to all of the parameters: ultraviolet solar radiation (including far UV), atomic oxygen, vacuum and the temperature; ΔR_S=final R_S-initial R_S

(b) an exposure to ultraviolet radiation with a wavelength greater than 190 nm, to the vacuum and to the temperature

(c) an exposure to radiations with a wavelength greater than 360 nm, to the vacuum and to the temperature

(d) an exposure to the vacuum and to the temperature.

10.3.2.3.2 IR Reflectance Measurements

Figure 10-8 shows the pre-flight, in-space, and post-flight measurement of the IR reflectance curves for the A276 thermal control paint located on LDEF leading edge (row 9),[4,15] which was exposed to an atomic fluence of 8.99×10^{21} atoms/cm^2. The unprotected A276 showed degradation early in the 5.8 year exposure of the LDEF mission as the solar absorptance increased to 0.305 from 0.253 after 15 months. . These TCSE in-space measurements showed there was not a sufficient amount of AO present early in the mission to inhibit UV degradation (see Table 10-7).

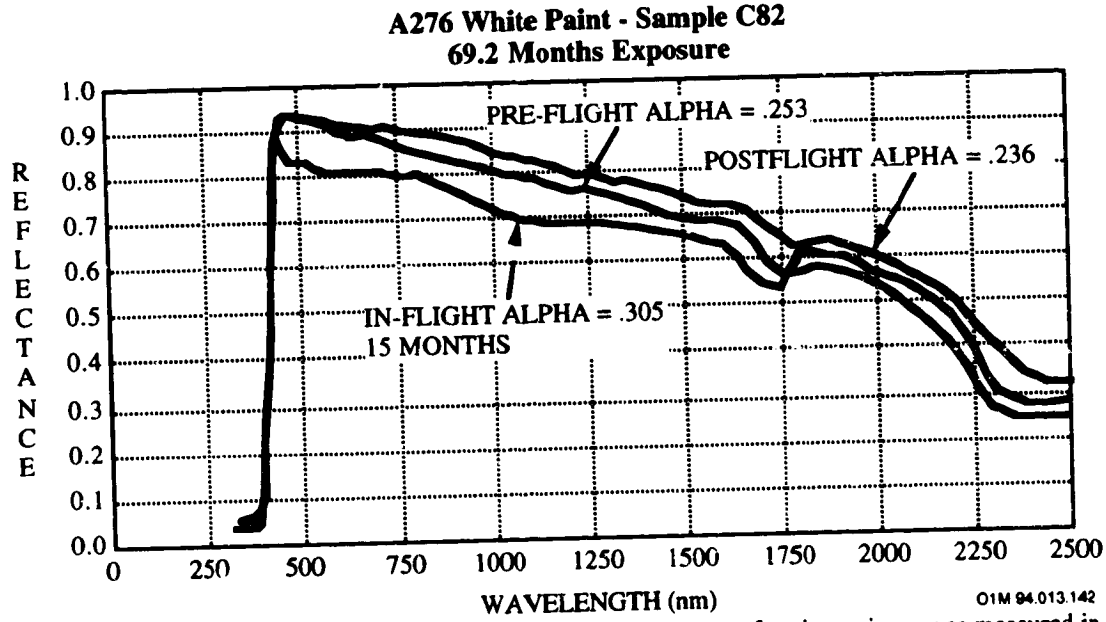

To derive the solar absorptance values, the spectral diffuse reflectance of each specimen was measured in the range 200 - 2200 nanometers using a Varian/Cary 2300 spectrometer with integrating sphere attachment and calibrated standards.

Figure 10-8. IR Reflectance of Exposed A276 White Paint on the LDEF TCSE Experiment

Diffuse and specular IR reflectance measurements were made on several white paint specimens. The spectral diffuse reflectance, as a measure of solar absorptance, increased ($\Delta\alpha$=+0.15) for the A276 specimen exposed under a UV grade quartz window (see Table 10-12).[21]

10.3.2.3.3 Atomic Oxygen Effects.

Space Shuttle Flight Experiments. Experiments from Shuttle Missions STS-5 and STS-8 demonstrated the effects of atomic oxygen exposure on material degradation.[38,39,40,41] Whitaker reported the effects of atomic oxygen on several paints from the STS-5 mission, including Chemglaze A276.[42] Based on SEM results, she noted that the Chemglaze A276 developed a porous surface, probably due to the atomic oxygen reacting with the polyurethane binder. However, the total atomic oxygen fluence incident on the samples was only 9.9×10^{19} atoms/cm^2, which is significantly less than the fluence received on the leading edge of LDEF. Additionally, the limited duration of the STS-5 Space Shuttle flight did not permit the evaluation of long-term UV radiation effects.

LDEF Experiment. The effects of the LEO space exposure on the thermo-optical design values of A276 white thermal control coating were determined by the Boeing Defense & space Group on LDEF subexperiment M0003-8.[15,43] Atomic oxygen fluences greater than 10^{21} atoms/cm^2 was observed to maintain the optical performance of the A276 coating by eroding the solar ultraviolet radiation-induced dark surface layer, i.e., "cleaning" the white paint surface. Organic paint binders, such as the polyurethane used in the A276 paint, are affected by solar ultraviolet radiation, which darkens their surface (i.e., raising α_s). It is postulated that the A276 ram-facing surfaces darkened during the earlier part of the mission when atomic oxygen flux was relatively low, then were "cleaned up" during the last few weeks of the mission, when atomic oxygen flux was substantially higher.

Figure 10-9 shows the changes in α_s for A276 paint disks[a] as a function of location on LDEF. Multiple specimens measured along a particular row indicated limited variability in absorptance. The white paint surfaces facing the front of LDEF (rows 7 to 12 where the AO fluence ranged from 3.99×10^{21} to 8.99×10^{21} atoms/cm^2) retained the α_s of the control specimen (i.e., control specimen α_s was comparable to that from specimens on rows 9 and 10), while those

---

[a] Sample Description: White-on-black disks of polyurethane thermal control paint was applied to over two hundred of the LDEF experiment tray clamps. The thermal control disks are four cm diameter disks of Chemglaze Z306 black polyurethane thermal control paint applied to the approximately center of 38% of the anodized 6061-T6 aluminum tray clamps. A three cm diameter aluminum foil disk, which had been coated with Chemglaze A276 white polyurethane thermal control pant, was adhesively bonded in the center of each black disk. Chemglaze 9924 primer was used prior to the application of Z306 on the tray clamps, and prior to the application of A276 to the adhesive backed aluminum foil. Approximately one hundred A276 white paint thermal control coating disks were measured for absorptance and emittance. The measurements were made without removing the disks from the clamps.

on the trailing edge of LDEF (rows 1 to 6 where AO fluence ranged from 2.31×10^5 to 4.94×10^{19} atoms/cm^2) showed a doubling of α_s, compared to that of the control specimen.

Absorptance as a function of AO fluence is presented in Figure 10-10. The fluence levels are based on predictions from the LDEF AO fluence model developed by Boeing.[44,45] Absorptance data from Earth and space end disks are not included in Figure 10-10, due to a scatter in those data which will be discussed in Section 10.3.2.3.4, Figure 10-13. From Figure 10-10, a fluence level of 10^{21} oxygen atoms per cm^2 was necessary to cause sufficient resin erosion in the A276 white thermal control paint to maintain coating optical performance, removing the darkened resin which degraded the coating's absorptance.

Emissivity, ε, was not affected during the flight as shown in Figure 10-11. Statistical analysis indicates a marginally significant increase in emittance for leading edge specimens (0.88 ± 0.02) as compared to trailing edge specimens (0.86 ± 0.02).[15] Control specimen emittance was comparable to measurements made for specimens on trailing edge surfaces, rows 1 through 6.

The absorptance and emittance measurements versus angle of AO incidence are shown in Figure 10-12. The incidence angles are based on an assumed 8° offset in yaw angle for the LDEF satellite. Figure 10-12 shows that the erosion effect of atomic oxygen maintains low absorptance levels for the A276 paint for incidence angles up to 80°, with an apparent atomic oxygen effect discernible to an incidence angle of 100°. Statistical analysis conducted on the emittance measurements shown in Figure 10-12 indicated a marginal but significant increase in emittance for leading edge white paint specimens (incidence angle less than 70°, $\varepsilon = 0.89 \pm 0.01$) as compared to the control ($\varepsilon = 0.87$) and to trailing edge specimens (incidence angle greater than 100°, $\varepsilon = 0.86 \pm 0.01$). The increase in emittance is consistent with the roughening of leading edge surfaces observed by microscopy, caused by atomic oxygen erosion of the paint resin.

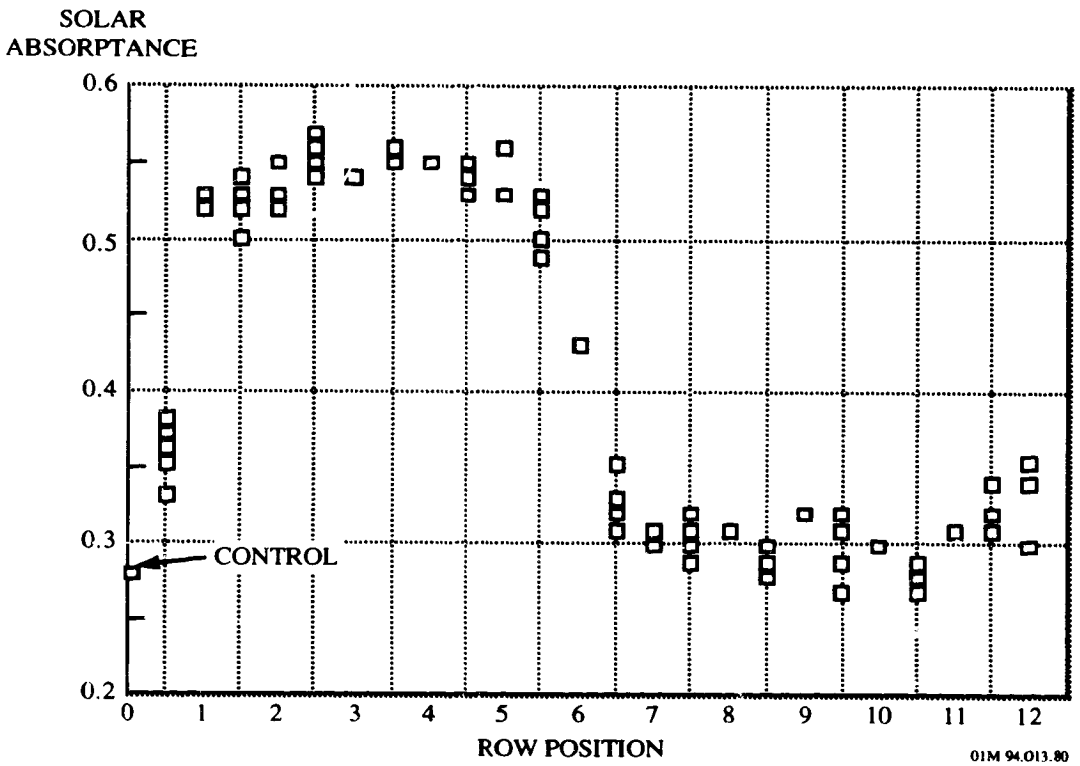

Figure 10-9. Solar Absorptance For A276 White Paint Disks Versus LDEF Row Position

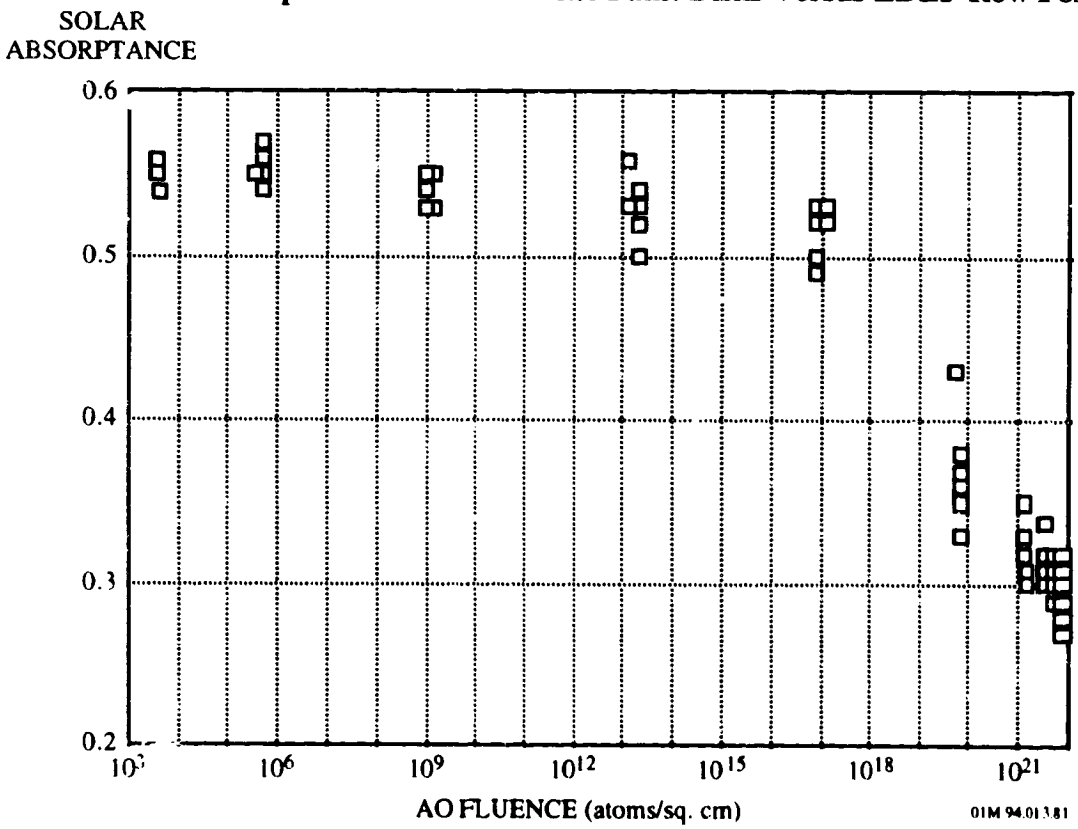

Figure 10-10. Solar Absorptance For A276 White Paint Disks Versus Atomic Oxygen Fluence

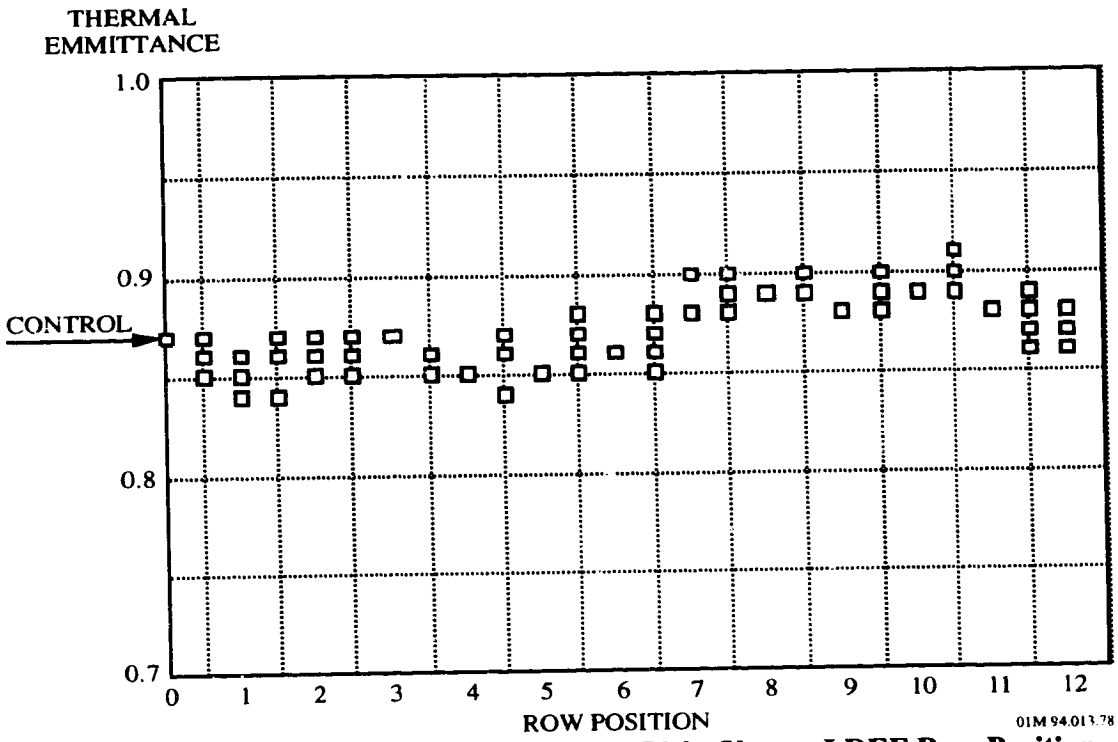

Figure 10-11. Emittance For A276 White Paint Disks Versus LDEF Row Position

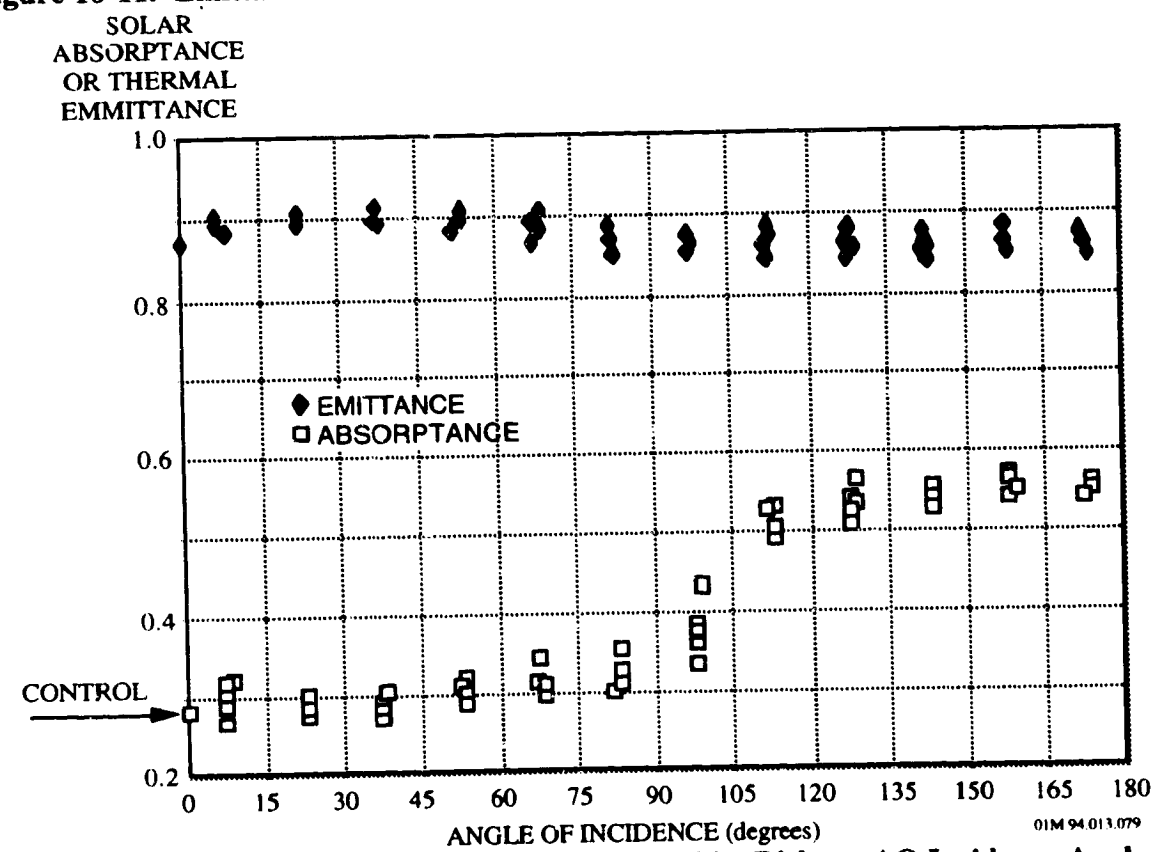

Figure 10-12. Absorptance and Emittance for A276 White Disks vs AO Incidence Angle

10.3.2.3.4 Ultraviolet Radiation Effects

Figure 10-13 shows the solar absorptance measur ements for all of the A276 white thermal control disks on LDEF subexperiment M0003-8 (ref. 44), including Earth and space end disks, as a function of predicted solar fluence in equivalent sun hours.[44] Also included in Figure 10-13 are data from LDEF Thermal Control Surfaces Experiment (TCSE-S0069) for comparison.[46] This experiment was located on the leading edge (row 9) of LDEF and at the Earth end of this row (position A9). In this configuration, the TCSE was facing the ram direction, which received an AO fluence of 8.99 x 10^{21} atoms/cm^2 and a solar UV exposure of 11,200 esh.

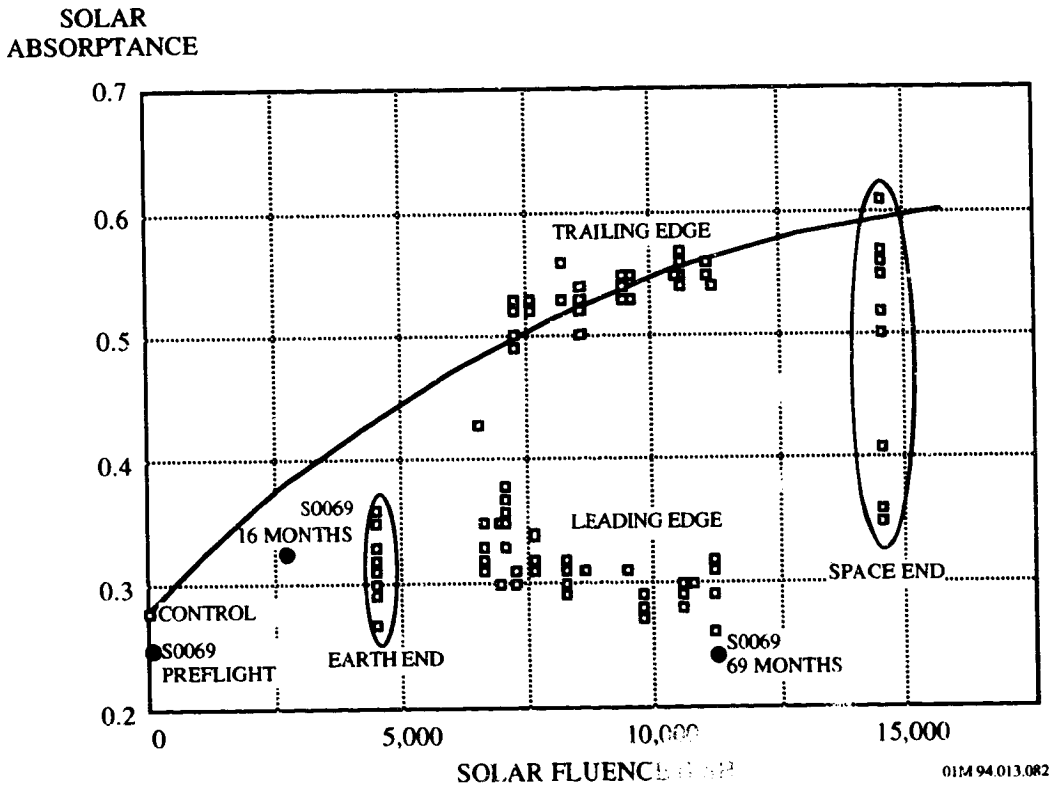

Note: The scatter in data obtained for the Earth and space ends disks of LDEF is shown in Figure 10-13. Both Earth and space end disks were predicted to receive approximately the same fluences of atomic oxygen, assuming no vehicle pitch offset or over-riding effects of local environments. However, it is apparent that there were some local differences in atomic oxygen fluence which resulted in the observed scatter. The trend of increased absorptance with increasing UV exposure is still intact with the Earth and space end disk data. But the ends of LDEF were in the transition region with regards to atomic oxygen fluence, where slight differences in surface orientation and position could markedly affect atomic oxygen fluence. When compared to absorptance data from the disks on LDEF side trays, data from the space end disks indicate incidence angles ranging from 85 to 105 degrees.

Figure 10-13. Solar Absorptance For A276 White Paint Disks vs. Ultraviolet Radiation Exposure

Figure 10-13 suggests a gradual absorptance increase for A276 with increasing UV exposure in the absence of AO. This trend is confirmed by experiment S0069 data, which showed an increase in the absorptance of A276 occurring in the early, low AO flux portion of the LDEF mission. The data in Figure 10-13 suggest that all of the A276 paint disks were darkened according to this trend in the initial years when LDEF was still in a relatively high orbit. With orbital altitude decay, the AO flux began to increase rapidly. The AO fluence model predicted that ~54% of the AO fluence on LDEF occurred in the last six months of the mission. It is postulated that during this latter phase the AO erosion removed UV damaged paint resin and restored A276 absorptance to nominal values on leading edge specimens. It does not appear that the trailing edge specimens have yet reached an end-of-life condition versus UV exposure, although the apparent rate of absorptance degradation with UV exposure has decreased significantly for the highest level UV exposed specimens. It does, however, appear that the leading edge specimens have reached an end-of-life condition versus AO exposure.

Results from LDEF Experiment M0003 Sub-Experiment 18 (ref. 11), confirmed the UV interactions with A276 white paint. In this experiment A276 was used as a thermal control coating on the Experiment Power and Data System (EPDS) sunshield covers. These covers were used to protect data system instrumentation for other experiments. These covers were located near the leading edge (row 8) and trailing edge (row 4) of the spacecraft; row 8 is located 30° from the perpendicular of the atomic oxygen vector, and row 4 is located 30° from the perpendicular of the wake region. Consequently, these trays were exposed to different levels of UV radiation and atomic oxygen; samples from row 8 (referred to as leading edge samples) were exposed to 9,400 equivalent sun hours of UV radiation and an atomic oxygen fluence of 7.15×10^{21} atoms/cm^2, while samples from row 4 (referred to as trailing edge samples) was exposed to 10,500 equivalent sun hours of UV radiation and an atomic oxygen fluence of 2.31×10^{5} atoms/cm^2.

A summary of the solar absorptances, listed in Table 10-25, indicated that the leading edge A276 samples darkened significantly due to UV-induced degradation of the paint's polyurethane binder, while leading edge samples remained white but exhibited severe AO erosion of the binder. Although the thermal control properties of the surface are not deleteriously affected, the surface has lost its physical integrity and is easily damaged upon contact.

Table 10-25. Effects of Varying UV/Atomic Oxygen Fluences on the Solar Absorptances of A276 on LDEF Experiment M0003-18

Location	UV (esh)	Atomic Oxygen (atoms/cm^2)	α_s
Control	-	-	0.282
D8(LE-SS)	9,400	7.15×10^{21}	0.228
D4(TE-SS)	10,500	2.31×10^{5}	0.552

Note: TE = trailing edge; LE = leading edge; SS = sun shield cover

The effects of UV radiation on the optical properties of titanium dioxide have been investigated previously.[47] The reflectance spectra of titanium dioxide degrades significantly more in the visible than the IR region, but almost completely recovers to the pre-irradiation values after exposure to an oxidizing atmosphere. This suggests that most of the UV induced damage to the Chemglaze A276 pigment could recover upon return of the LDEF spacecraft to Earth or on interaction with atomic oxygen.

10.3.2.3.5 Chemglaze A276 White Paint with Coatings

Comparison of the thermo-optical properties of A276 samples flown on LDEF with and without silicone overcoatings provides an excellent example of the synergistic effects of solar UV and AO. Two materials used as protective coatings over A276 included RTV670[b] and OI650.[c] Post-flight measurements of solar absorptance for the protected and unprotected A276 samples showed that although both coatings protected A276 from AO erosion, the A276 white paint and silicone overcoat degraded from solar UV exposure. Figures 10-14 to 10-17 show the changes in the solar absorptance and reflectance for the uncoated and coated A276 white paint samples on the LDEF TCSE-S0069 experiment.

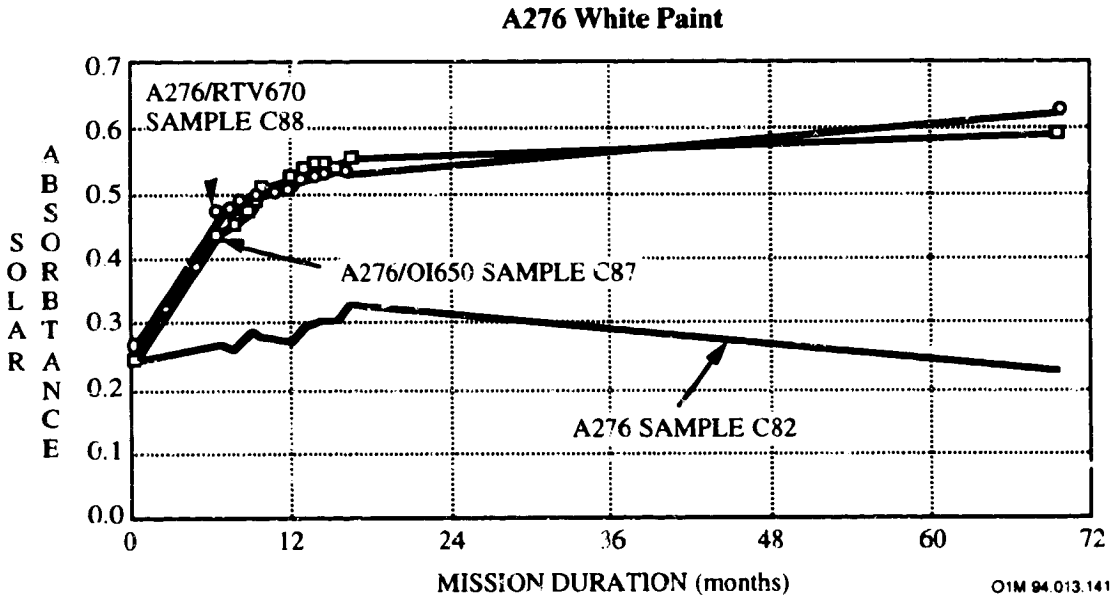

Figure 10-14. Solar Absorptance for Uncoated and Coated A276 White Paint

The AO erosion of the unprotected A276 on the LDEF leading edge removed the UV damaged material, leaving a fresh undamaged surface and minimum solar absorptance changes. Apparently, the oxidation and subsequent loss of the polyurethane binder prevented significant build-up of damaged material. The TCSE in-space measurements from the unprotected A276 showed there was sufficient AO present during the almost six year mission to inhibit UV degradation (ref. 4).

---

b Manufactured by General Electric. No longer being produced.

c Manufactured by Owens Illinois, Television Products Division.

In contrast, when protected from AO, the UV damaged surface material and contaminants resulted in large increases in α_S. A276 has been known to degrade readily under solar UV exposure, much like the A0114 trailing edge sample and the clear overcoated TCSE samples. Apparently, the overcoat prevented material loss, but allowed solar UV damage of the A276 coating and possibly damage and darkening of the silicone protective layer. Figure 10-15 shows the A276/RTV670 degradation model. Preflight, in-space, and post-flight measurements of reflectance for the A276 white paint protected with both coatings are presented in Figures 10-16 and 10-17.

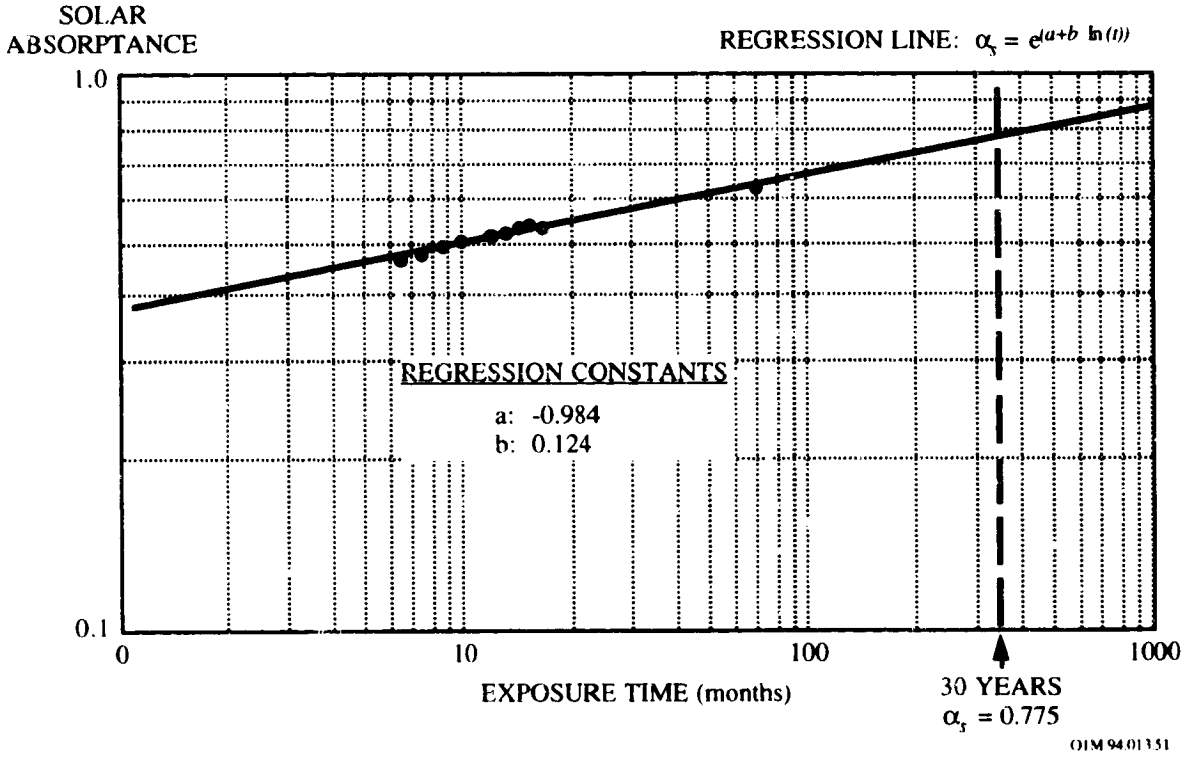

Figure 10-15. A276/RTV670 Degradation Model

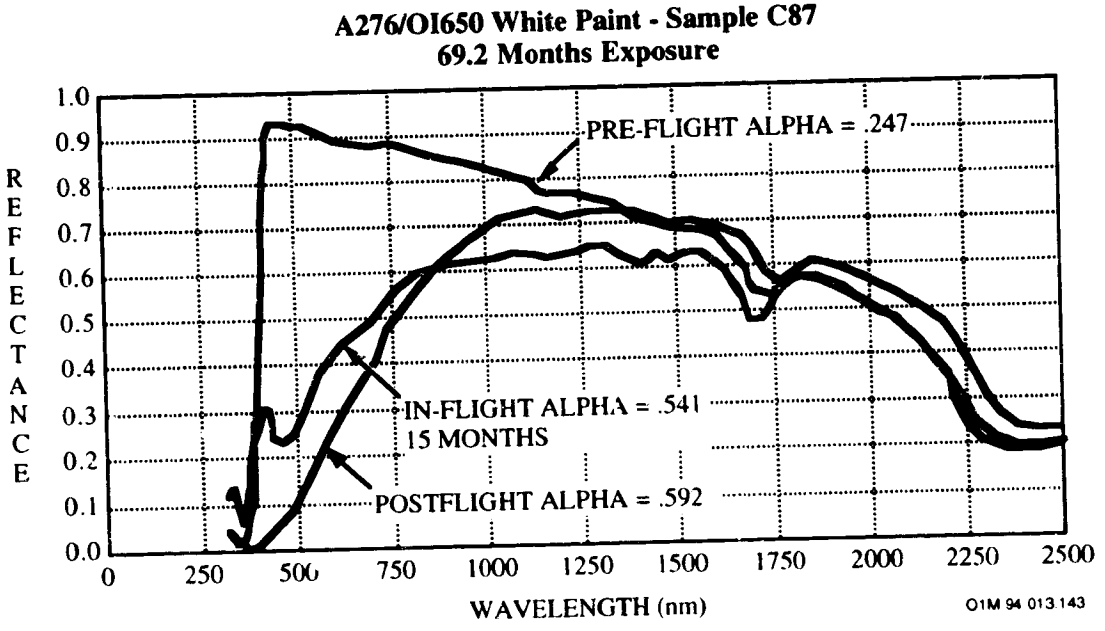

Figure 10-16. Solar Reflectance for Coated A276/OI650 White Paint

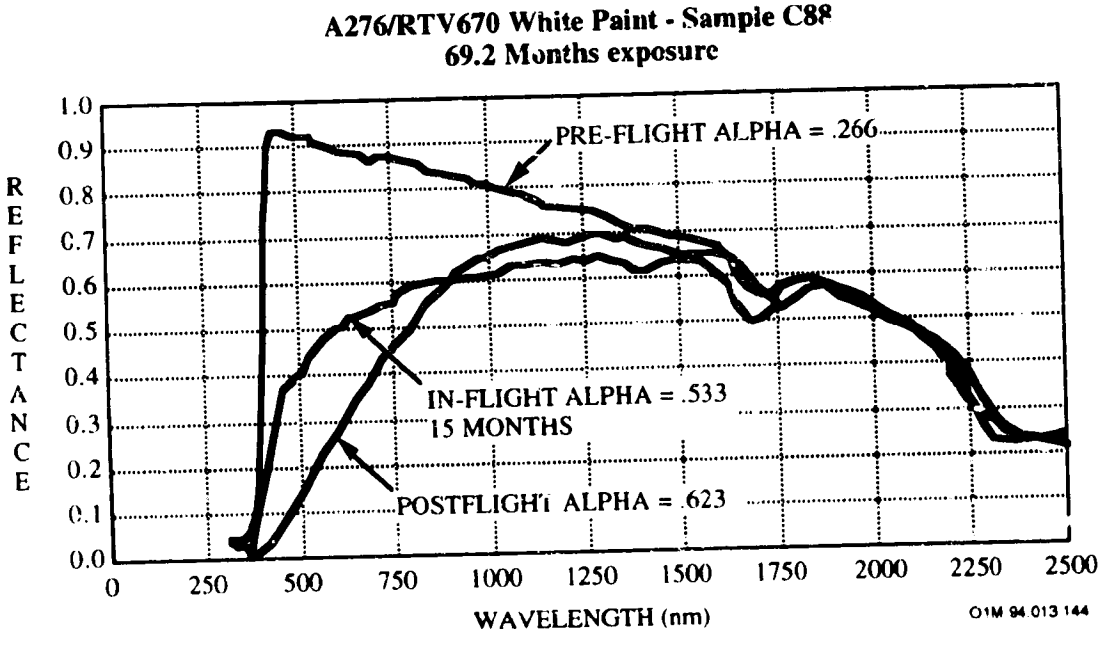

Figure 10-17. Solar Reflectance for Coated A276/RTV670 White Paint

10.3.2.3.6 Designs Considerations for the Space Environment

The A276 thermal control paint suffered from long exposure to the low Earth orbit space environment. The LDEF study revealed that the A276 white paint displayed varying degrees of thermo-optical property degradation depending upon the location on LDEF relative to the AO flux and the amount of UV exposure received, as well as whether A276 had a silicone coating, hence, providing an excellent example of the synergistic effects of solar UV and AO impingement. Thermo-optical properties as a function of LDEF location and the effects of silicone coatings are shown Figures 10-18 and 10-19.

The paint pigment binder was susceptible to both UV polymerization and AO erosion. The AO erosion removed the binder from the A276. AO erosion effects, apparent on the paint surfaces up to an incident angle of 100 degrees, prevented significant build-up of UV-damaged material. On LDEF, the majority of the AO exposure occurred in the latter few months of the mission. This AO exposure apparently eroded away the small amount of degraded surfaces (approximately over 20% during the first 15 months) seen on the ram-exposed S0069 samples during the first part of the mission (see Figure 10-18). In contrast, when protected from AO the intact surface and contaminants resulted in large increases in α_s (see Figure 10-19). Darkening of the trailing edge white paint surfaces appears to be largely due to the solar UV induced degradation of the paint resin, with some additional effect from degraded surface contaminants.

The following are recommendations for use of the A276 white paint coating:

- A 100% increase in absorptivity would be needed to account for in the spacecraft thermal design if these paints are used.
- The use of the A276 white paint on spacecraft requiring precise thermal control on extended low Earth orbit missions could produce unwanted thermal excursions as these coatings degrade over time.
- Chemglaze A276 is not recommended as a white paint for spacecraft that require any significant mission lifetimes due to its susceptibility to UV degradation and AO erosion. UV radiation causes a significant increase in the material's solar absorption, while AO erosion of the binder results in a fragmented surface, which could cause particulate contamination to other areas of the spacecraft. Its low cost and ease of application, however, make it much more desirable for boosters and upper stage rockets that do not require long mission lifetimes.

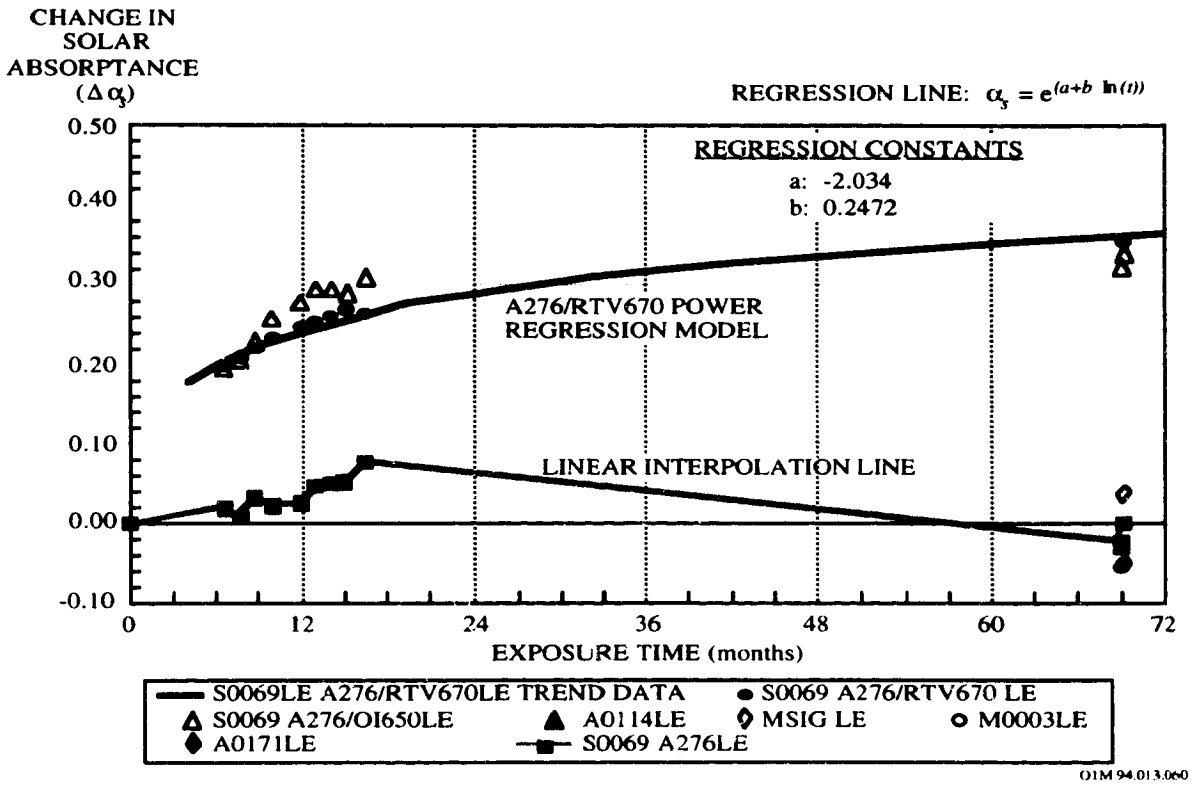

Figure 10-18. Performance of A276 and A276 with overcoats on LDEF-Leading Edge

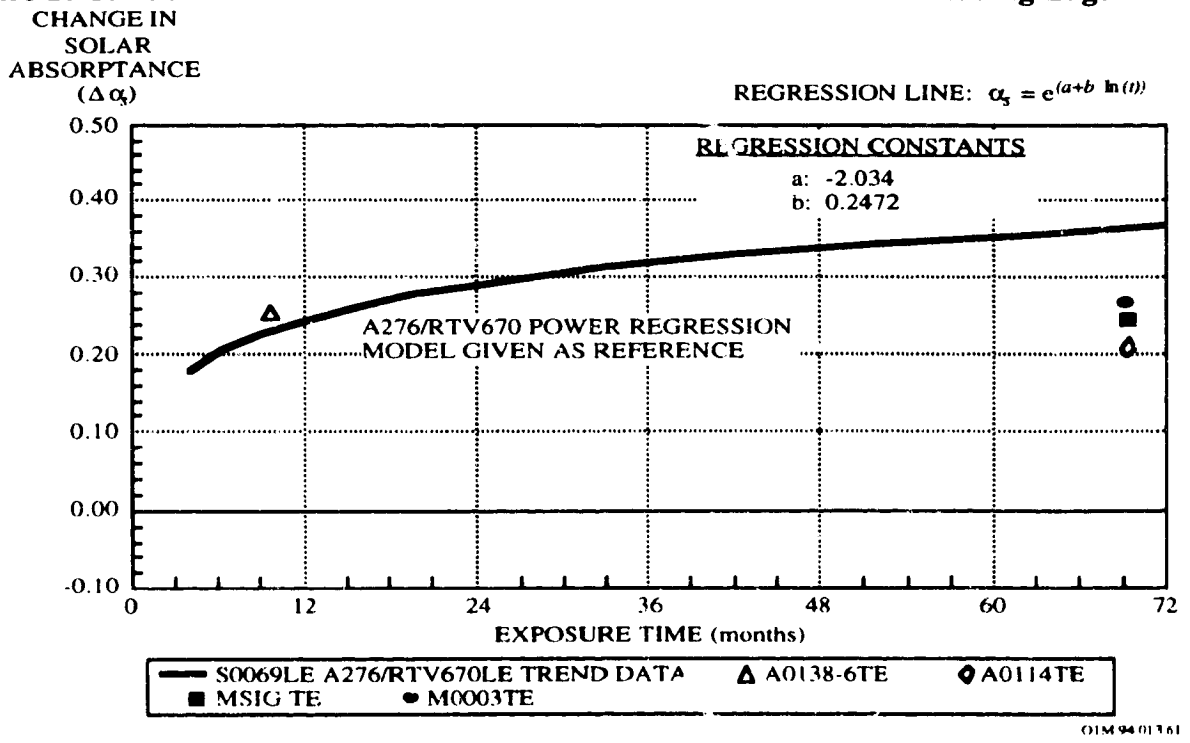

Figure 10-19. Performance of A276 on LDEF Trailing Edge: $\Delta\alpha_s$ vs. Exposure Time

10.3.3 Z-93 White Paint

The ceramic non-specular white thermal control coating Z-93 (manufactured by the IIT Research Institute) has a low solar absorptance (α_S) of 0.15 ±0.01 and a high room temperature normal emittance (ε_T) of 0.90 ±.05 for a typical 0.005 ±0.001 inch coating thickness.

The Z-93 white paint has demonstrated excellent stability in the LEO environment. The results from the 69 month LDEF mission, and in particular the Thermal Control Surfaces Experiment (TCSE-S0069),[48] have demonstrated this stability through the in-flight optical data that were not subjected to the uncertainties of data generated from pre- and post-flight sample measurements alone.

In addition to its stability in LEO, this coating can be deposited onto large, complex structures with relative ease and with low weight and cost per square area. As a result of these characteristics, Z-93 has been baselined for use on the radiators and some of the antennas which will compose the critical and intricate structure of Space Station Freedom.

10.3.3.1 Composition

Binder:	PS7 Potassium silicate[d]
Pigment:	Zinc oxide (New Jersey Zinc Co., SP 500)

10.3.3.2 Source

Manufacturer:	IIT Research Institute 10 West 35 Street Chicago Illinois 60616 Telephone: 312 567-4432
Cost:	$125/pint

d This coating (Z-93P) is being requalified with PQ Corporation's Kasil 2130 potassium silicate binder.

10.3.3.3 Ground-Based Simulation Testing

Comparative simulated space radiation testing was conducted on the original Z-93 and the reformulated Z-93P white paint. The solar absorptance results, summarized in Table 10-26, indicated that the reformulated paint, Z-93P performed comparably to the original version.[49]

Table 10-26. Comparative Solar Absorptance Values for Original and Reformulated Z-93

Simulated Space Environment	K2130 Binder		PS7 Binder	
	Pre-Exposure	Post-Exposure	Pre-Exposure	Post-Exposure
Atomic Oxygen:[1] $2..1x10^{22}$ atoms/cm^2	.165	.164	.159	.156
Atomic Oxygen:[2] $1x10^{21}$ atoms/cm^2 VUV: 9400 esh (130 nm)	.143	.155	.145	.149

1. Exposed in the Atomic Oxygen Drift Tube System (ACDTS)
   - <0.1 eV thermal energy AO neutral atoms
   - $5x10^{16}$ atoms/cm^2/sec AO Neutral Flux
2. Princeton Plasma Physics laboratory (PPPL) System
   - 10^{16} atoms/cm^2/sec AO flux
   - Plasma generated by 2.45 GHz, 1kW R-F Field
   - VUV radiation generated by plasma

10.3.3.3 Effects of the Space Environment

The optical properties variations of the Z-93 white paint on the LDEF satellite are summarized in Table 10-27 (ref. 4). This white paint, part of the Thermal Control Surfaces Experiment (TCSE) S0069 experiment, was selected because it is a good reflector of solar energy while also being good emitters of thermal energy to the cold sink of space.

Table 10-27. Optical Property Variation of Z-93 White Paint on the LDEF TCSE Experiment

Material	Solar Absorptance (α_s)[a,b,c]				Emittance (ε_N)[d]		
	Pre-flt	In-flt (15 Mo)	Post-flt	$\Delta\alpha_s$	Pre-flt	Post-flt	$\Delta\varepsilon_N$
Z-93	.14	.13	.15	.01	.90	.92	.02

(a) Mission Duration: The TCSE operated for 582 days before battery depletion. The battery power was finally expended while the sample carousel was being rotated. This left the carousel in a partially closed position. This carousel position caused 35 of the samples to be exposed for the complete LDEF mission (69.2 months), and 14 exposed for only 582 days (19.5 months) and therefore protected from the space environment for the subsequent four years.

(b) Space Environmental Exposure: The LDEF was deployed with the TCSE located on the leading edge (row 9) and at the Earth end of this row (position A9). In this configuration, the TCSE was facing the ram direction. The LDEF was rotated about the long axis where row 9 was offset from the ram direction by about 8°. The exposure environment for the TCSE were:

Atomic oxygen fluence	8.99×10^{21} atoms/cm^2
Solar UV exposure	11,200 esh
Thermal cycles	~34,000 cycles: -29 to 71 °C, ± 11°C (-20 to 160 °F, ±20°F)
Radiation (at surface)	3.0×10^5 rads

(c) The primary TCSE in-space measurement was total hemispherical reflectance as a function of wavelength (100 wavelength steps from 250 to 2500 nm) using a scanning integrating sphere reflectometer. The measurements were repeated at preprogrammed intervals over the mission duration. The secondary measurement used calorimetric methods to calculate solar absorptance and thermal emittance from temperature-versus-time measurements.

(d) Laboratory measurements of spectral reflectance were obtained using Beckman DK-2A spectrophotometer equipment with a Gier-Dunkle 203 mm integrating sphere.

10.3.3.4 Design Considerations for the Space Environment

10.3.3.4.1 Thermo-Optical Properties

The unique in-space optical measurements performed on the LDEF Thermal Control Surfaces Experiment (TCSE-S0069) provide a time history of changes in α_S. In Figures 10-20 and 10-21, Z-93 solar absorptance data is plotted against exposure time from several experiments on the LDEF's leading and trailing edges, respectively. A small improvement in solar absorptance occurred early in the mission which is typical of potassium silicate coatings like Z-93. Only a small degradation was seen for the remainder of the mission. The data from the Z-93 samples indicated that it was very stable over the LDEF mission, and data from three experiments corroborated these findings for both leading and trailing edge samples. The solar absorptance of Z-93 was also not effected by the AO environment as shown by the AO114 trailing edge sample (see Figure 10-21).

These in-space measurements also allowed investigators to develop a trend analysis and a prediction model for the material and to better understand the damage mechanisms affecting its optical stability (see Figures 10-22 and 10-23). The trend analysis studies also provide some insight into the small changes that were measured.

There appears to be at least two mechanisms affecting the Z-93 solar absorptance for the LDEF mission. The first is a decrease in α_S typical of silicate coatings in thermal vacuum. This decrease is normally associated with loss of interstitial water from the ceramic matrix. Ground laboratory simulation tests have shown this process takes a much shorter time than the TCSE flight data suggest. This slower loss of water may be due to the cold temperature of the TCSE Z-93 sample mounted on a thermally isolated calorimeter. The temperature of the Z-93 sample ranged from approximately -55°C to +6°C but remained well below 0°C most of the time. The short term decrease in α_S is dominant for the first year of exposure after which a long term increase in α_S becomes dominant (ref. 4).

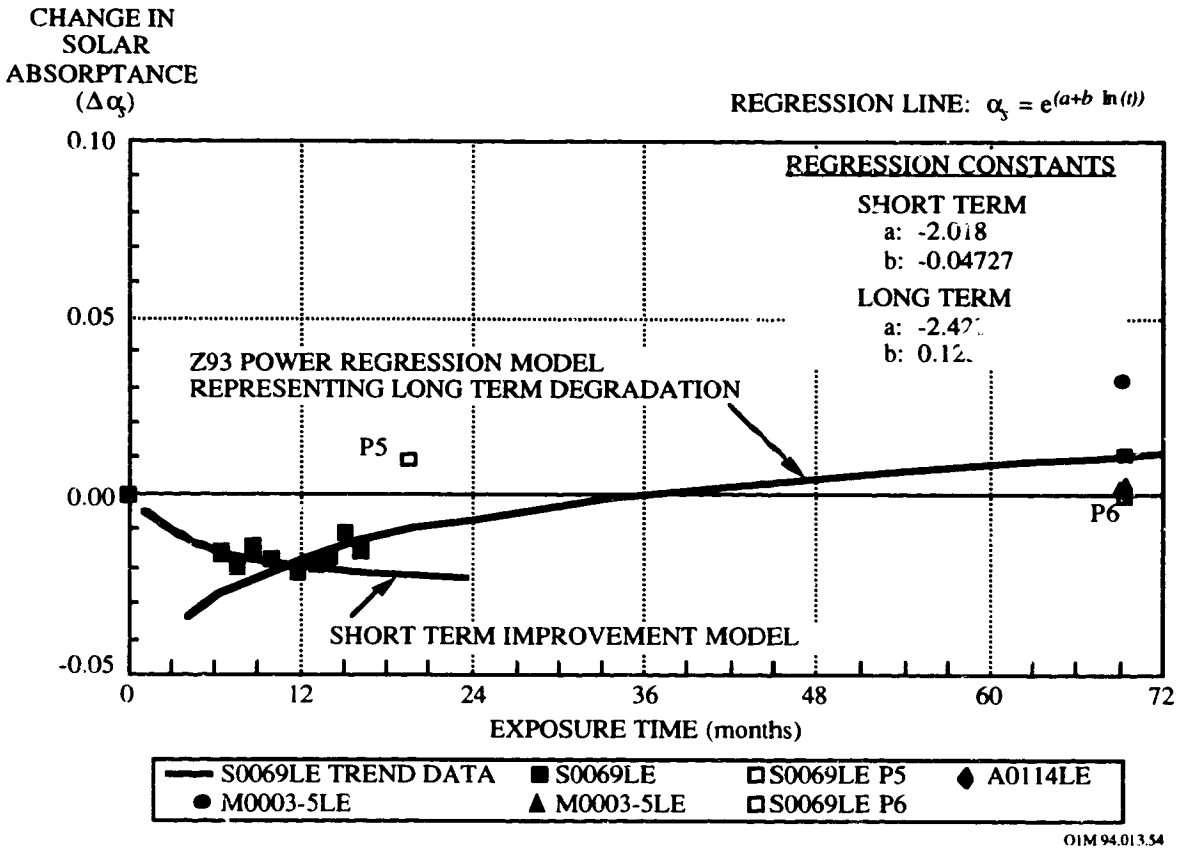

Figure 10-20. Performance of Z-93 on LDEF - Leading Edge $\Delta\alpha_s$ vs. Exposure Time

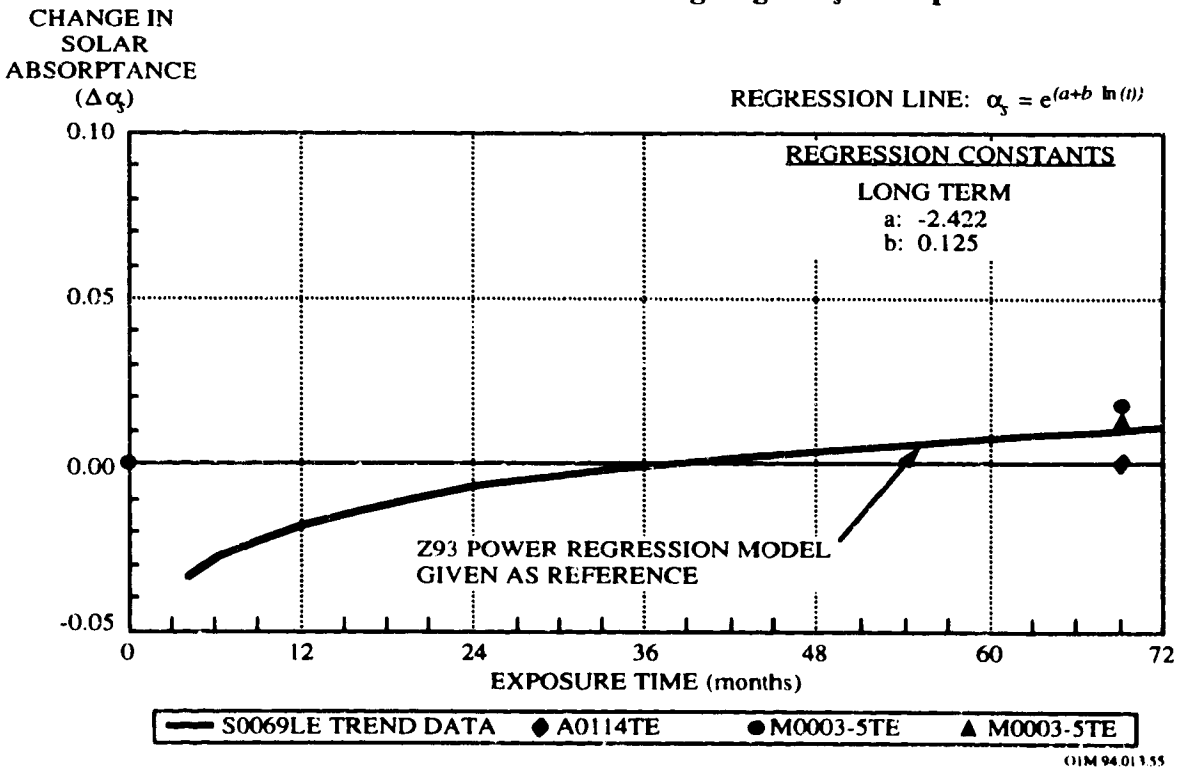

Figure 10-21. Performance of Z-93 on LDEF - Trailing Edge $\Delta\alpha_s$ vs. Exposure Time

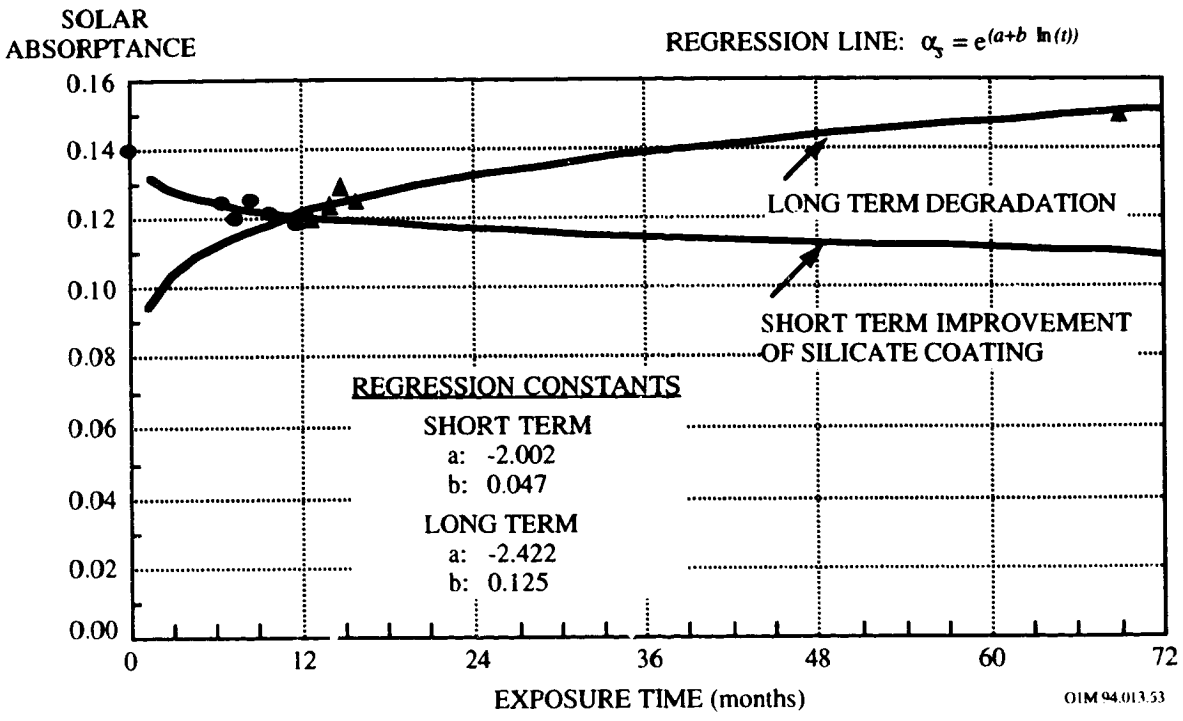

Figure 10-22. Power Regression Analysis of Z-93

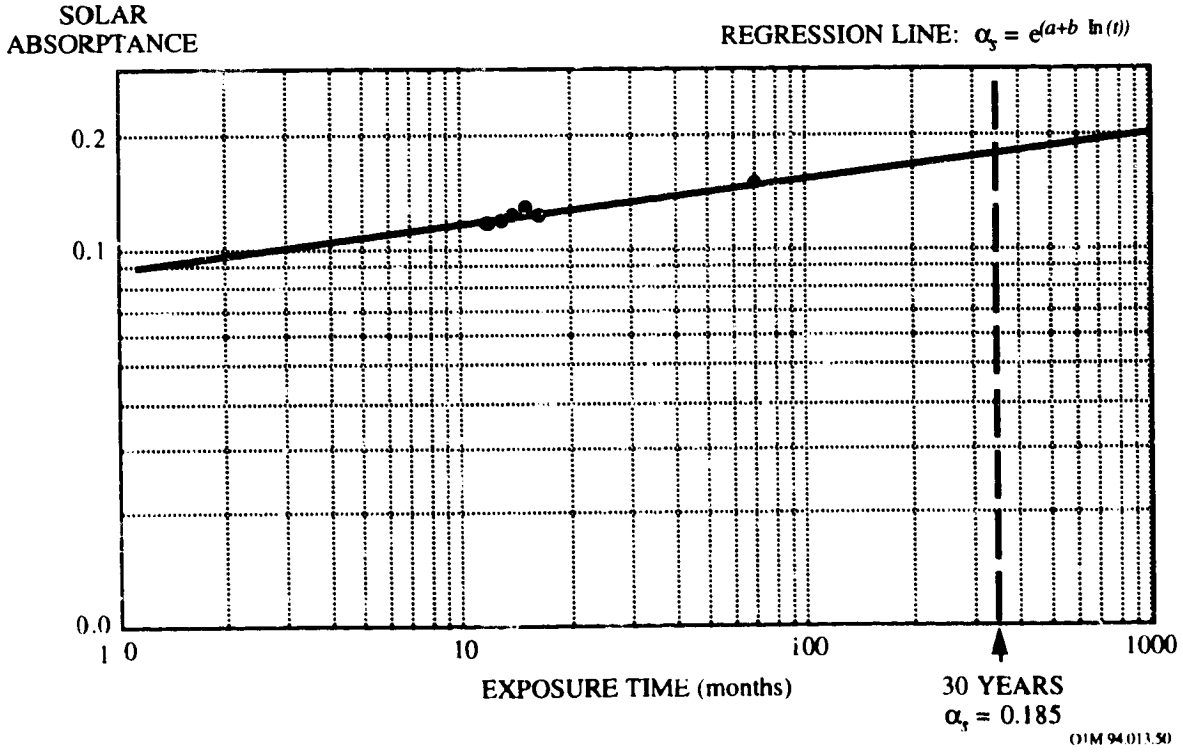

Figure 10-23. Z-93 Degradation Model

10.3.4.4.2 Micrometeoroid/Debris Impacts

The effects of multiple impact craters on the thermal radiative properties of Z-93 as a function of time were calculated using an equation based on the fraction of damaged surface area.[50]

$$A_s\,(\text{Beta}) = A_o - \left[D_{a.e} * F_a * T_{yr}\right]$$

where:	A_s (Beta, time)	=	effective or average value of solar absorptance or emittance at each Beta angle
	Beta	=	degrees from velocity vector or ram direction
	A_o	=	solar absorptance or emittance of original coating
	$D_{a.e}$	=	difference between coating and substrate absorptance or emittance
	F_a	=	fraction of damaged surface area per year
	T_{yr}	=	number of years exposed

Figures 10-24 and 10-25 show the results of impacts on Z-93 white coating for three different Beta angles of 0, 90, and 180 degrees, for up to 30 years in orbit. Both solar absorptance and thermal emittance decrease slightly with time. The larger spall/crater diameter ratio for Z-93 and other ceramic binder paints does not significantly affect the solar absorptance or thermal emittance values. When the coating and substrate thermal radiative properties are significantly different, then the effect of impacts is greater. This effect is shown in Figure 10-24 and 10-25, by comparing the larger change in emittance than in absorptance. Bare aluminum substrate has a very low emittance ~4%, compared to the Z-93 value of ~92%. In comparison aluminum absorptance is ~4% (low value) and Z-93 ~14%. Actually, the exposed aluminum absorptance in the spalled area is probably closer to the Z-93, which means the changes shown on Figure 10-24 are even less.

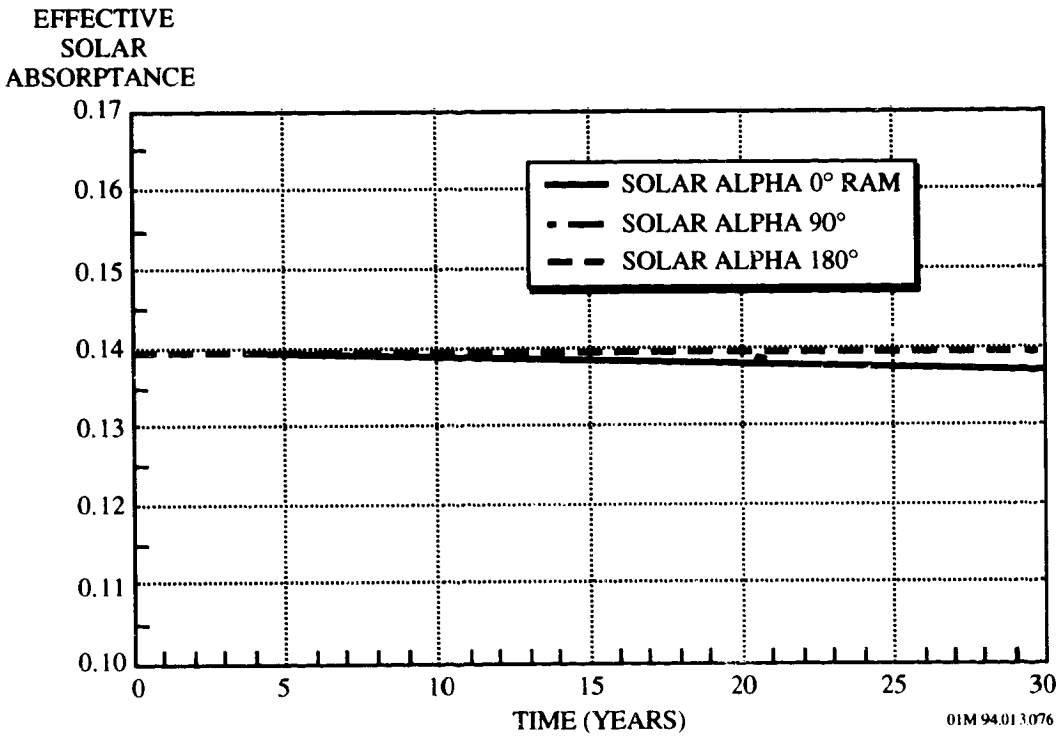

Figure 10-24. Z-93 M/OD Effect on Solar Absorptance vs Time

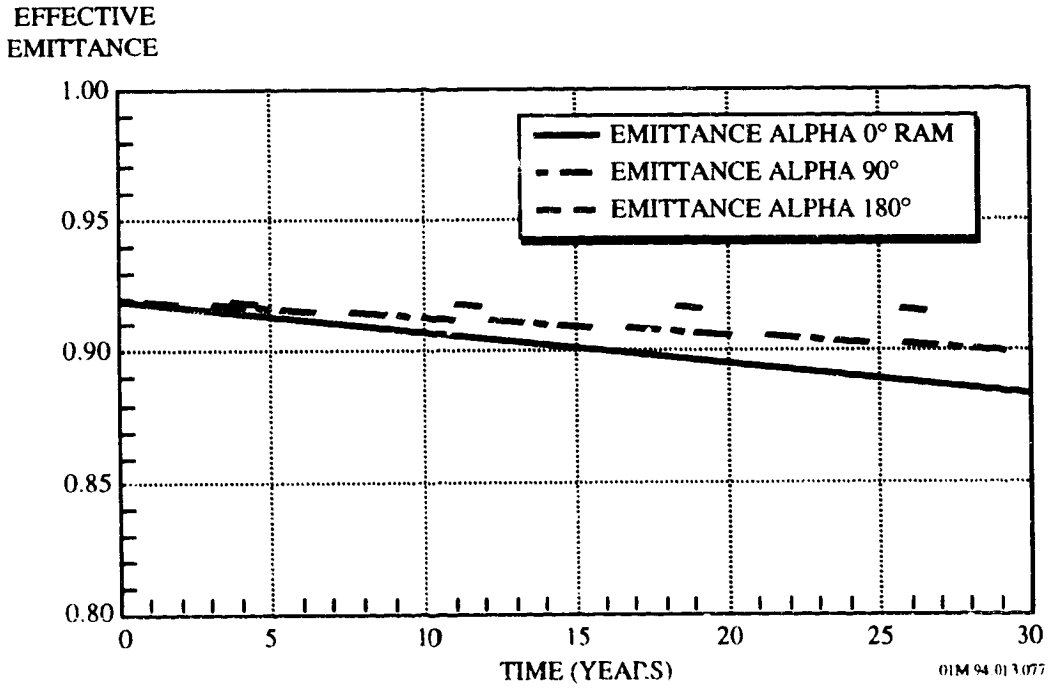

Figure 10-25. Z-93 M/OD Effect on Emittance vs Time

10.3.4 YB-71 White Paint

YB-71 white paint is a ceramic non-specular zinc orthotitanate (ZOT) white coating. It has a low solar absorptance (α_S) of 0.12 ± 01 and a high room temperature emittance (ε_T) of 0.90 ±.05.

10.3.4.1 Composition

Pigment:	Zn_2TiO_4 (IIT Research Institute)
Binder:	PS7 Potassium silicate[e] (GTE Sylvania Inc.)

10.3.4.2 Source

Manufacturer:	IIT Research Institute 10 West 35 Street Chicago Illinois 60616 Telephone: 312 567-4432
Cost:	$950/pint

e This coating (YB-71P) is being requalified with PQ Corporation's Kasil 2130 potassium silicate binder.

10.3.4.3 Ground-Based Simulated Space Testing

Comparative simulated space radiation testing was conducted on the original YB-71 and the reformulated YB-71P white paint. The solar absorptance results, summarized in Table 10-28, indicated that the reformulated paint, Z-93P did not performed comparably to the original version.[51]

Table 10-28. Comparative Solar Absorptances for Original and Reformulated YB-71

Simulated Space Environment	K2130 Binder		PS7 Binder	
	Pre-Exposure	Post-Exposure	Pre-Exposure	Post Exposure
Atomic Oxygen:[1] 1.0×10^{23} atoms/cm^2 VUV: 22,000 ESH	.125	.125	.133	.126
Atomic Oxygen:[2] 1×10^{21} atoms/cm^2 VUV: 9400 esh (130 nm)	.127	.193	.133	.152

1. Exposed in the Atomic Oxygen Drift Tube System (AODTS)
   - <0.1 eV thermal energy AO neutral atoms
   - 5×10^{16} atoms/cm^2/sec AO Neutral Flux
2. Princeton Plasma Physics laboratory (PPPL) System
   - 10^{16} atoms/cm^2/sec AO flux
   - Plasma generated by 2.45 GHz, 1kW R-F Field
   - VUV radiation generated by plasma

10.3.4.3 Effects of the Space Environment

This white paint were part of the LDEF Thermal Control Surfaces Experiment (TCSE) S0069 experiment, and was selected because it is a good reflector of solar energy while also being a good emitter of thermal energy to the cold sink of space. The optical properties variations of the YB-71 white paint on the LDEF satellite are summarized in Table 10-29 (ref. 4). The YB-71 coatings on the TCSE behaved similarly to the Z-93 samples. A small increase in the infrared reflectance early in the mission caused a decrease in α_S. This was offset by a slow long-term degradation resulting in a small overall increase in α_S. The samples with YB-71 applied over a primer coat of Z-93 had a somewhat lower absorptance that the other YB-71 samples. Current YB-71 samples are consistently below 0.10 solar absorptance (ref. 4).

Table 10-29. Optical Property Variations of YB-71 White Paint on the LDEF TCSE Experiment

Material	Solar Absorptance $(\alpha_s)^{a,b,c}$				Emittance $(\varepsilon_N)^d$		
	Pre-flt	In-flt (15 Mo)	Post-flt	$\Delta\alpha_S$	Pre-flt	Post-flt	$\Delta\varepsilon_N$
YB-71	.13	.12	.15	.02	.90	.89	-.01
YB-71 over Z-93	.10	.11	.11	.01	.85	.87	.02

(a) Mission Duration: The TCSE operated for 582 days before battery depletion. The battery power was finally expended while the sample carousel was being rotated. This left the carousel in a partially closed position. This carousel position caused 35 of the samples to be exposed for the complete LDEF mission (69.2 months), and 14 exposed for only 582 days (19.5 months) and therefore protected from the space environment for the subsequent four years.

(b) Space Environmental Exposure: The LDEF was deployed with the TCSE located on the leading edge (row 9) and at the Earth end of this row (position A9). In this configuration, the TCSE was facing the ram direction. The LDEF was rotated about the long axis where row 9 was offset from the ram direction by about 8^{o}. The exposure environment for the TCSE were:

Atomic oxygen fluence	8.99×10^{21} atoms/cm^2
Solar UV exposure	11,200 esh
Thermal cycles	~34,000 cycles: -29 to 71 °C, ±11°C (-20 to 160 °F, ±20°F)
Radiation (at surface)	3.0×10^5 rads

(c) The primary TCSE in-space measurement was total hemispherical reflectance as a function of wavelength (100 wavelength steps from 250 to 2500 nm) using a scanning integrating sphere reflectometer. The measurements were repeated at preprogrammed intervals over the mission duration. The secondary measurement used calorimetric methods to calculate solar absorptance and thermal emittance from temperature-versus-time measurements

(d) Laboratory measurements of spectral reflectance were obtained using Beckman DK-2A spectrophotometer equipment with a Gier-Dunkle 203 mm integrating sphere.

10.3.4.4 Designs Considerations for the Space Environment

Figures 10-26 and 10-27 show the change in α_s of several YB-71 samples located on the leading and trailing edges of LDEF, respectively. The YB-71 samples were flown on both the TCSE-S0069 and M0003-5 LDEF experiments. A regression analysis performed on the TCSE leading edge solar absorptance values calculated from the spectral reflectance data yielded a power regression line (see Figure 10-26). (Although log/log plots of experimental data can be misleading, trend analysis are useful to examine the possibility of trends and the potential of an empirical performance prediction model.) The YB-71 coatings on the TCSE behaved similarly to the Z-93 thermal control coating. A small increase in the infrared reflectance early in the mission caused a decrease in solar absorptance (see Figure 10-26). This was offset by a slow long term degradation resulting in a small overall increase in solar absorptance.

The M0003-5 YB-71 showed a slightly higher $\Delta\alpha_s$ than those samples on TCSE. There was no significant difference in the performance of leading and trailing edge samples on M0003-5. In addition, the TCSE samples were consistently more stable than the M0003 samples. The YB-71 samples were prepared for LDEF before the development of YB-71 was finalized. These differences could be due to batch variations of this new coating.

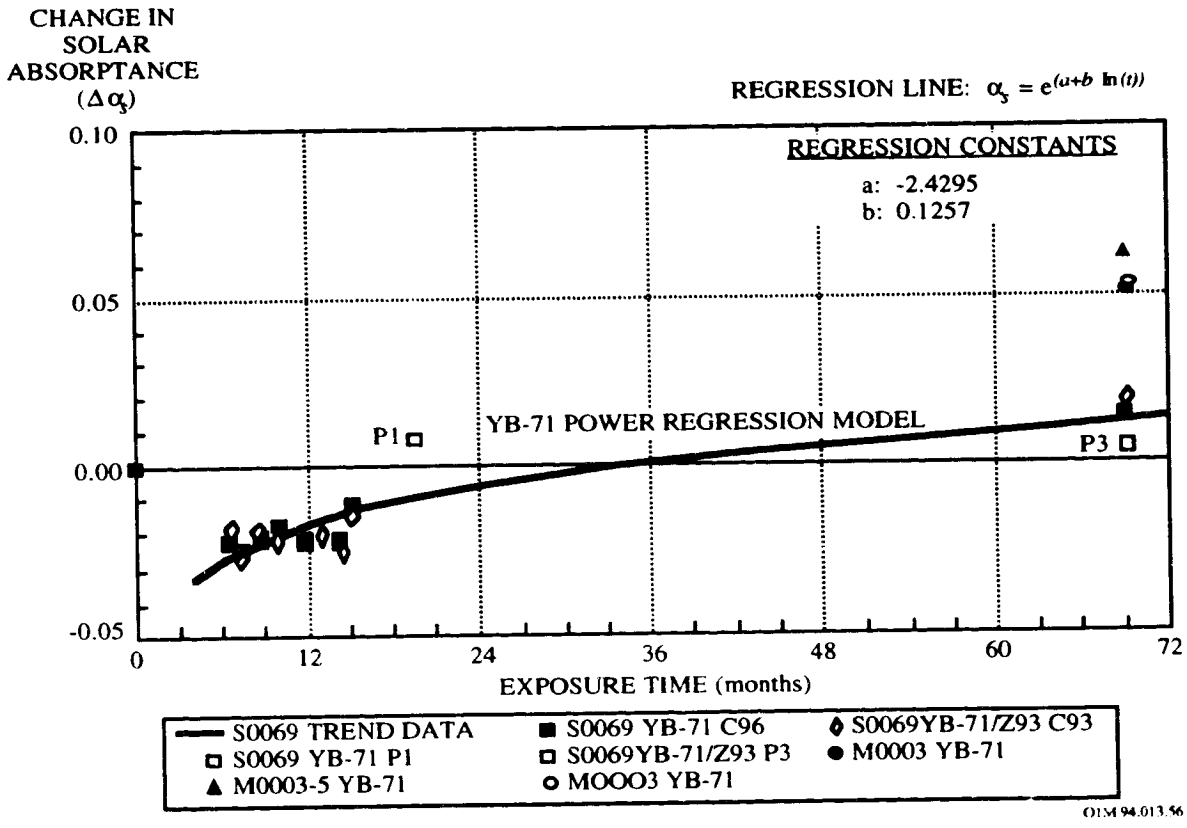

Figure 10-26. Solar Absorptance of YB-71 and YB-71/Z-93 on LDEF Leading Edge

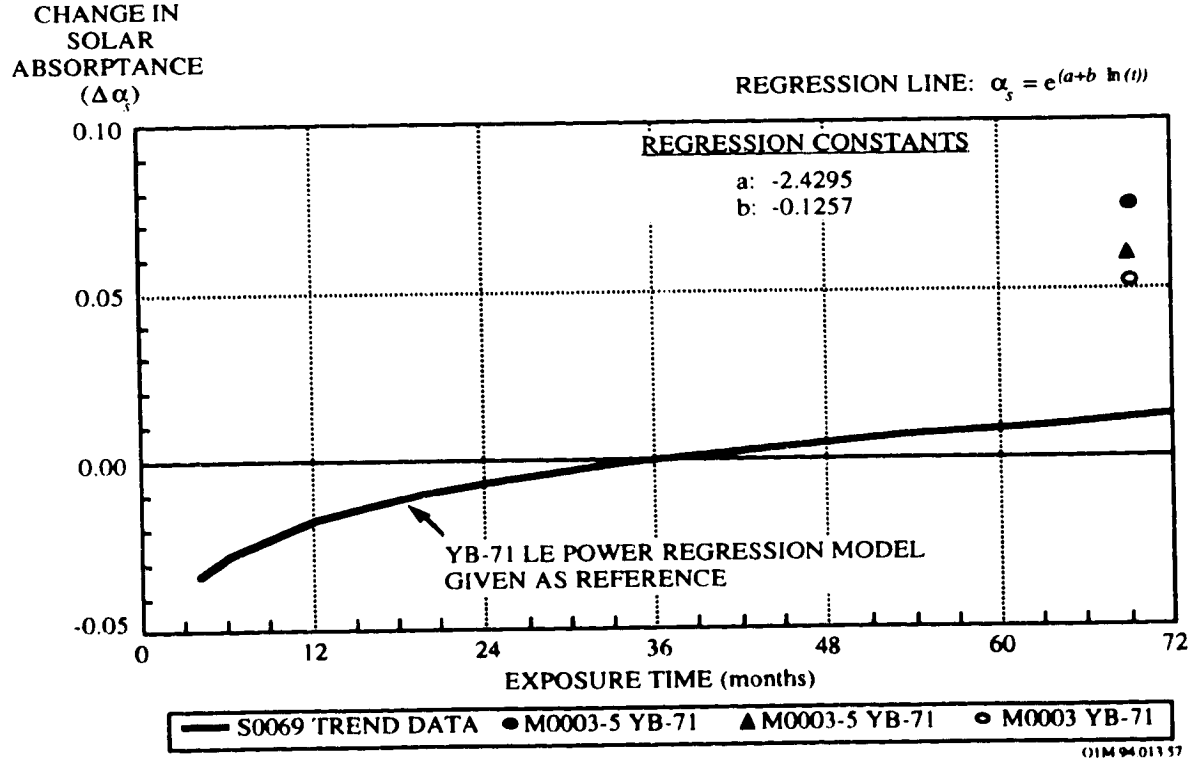

Figure 10-27. Solar Absorptance of YB-71 and YB-71/Z-93 on LDEF Trailing Edge

10.3.5 S13G/LO White Paint

S13G/LO white paint is a non-conductive zinc-oxide methylsilicone non-specular white coating.[f] It has a low solar absorptance (α_S) of 0.18 ±0.1 and a high room temperature emittance (ε_T) of 0.90 ±0.05 for a typical 0.008 ±0.001 inch coating thickness.

10.3.5.1 Composition

Binder:	Stripped methylsilicone (General Electric RTV 602).
Pigment:	Zinc oxide SP500 (New Jersey Zinc Co.), PS7-treated
Solvent:	Toluene, USP (US Pharm.)

S13G/LO is a white thermal control paint that incorporates a zinc oxide pigment in a methyl silicone binder. The ZnO pigment is reactively encapsulated in slurry with the PS7 potassium silicate to enhance its stability against UV radiation. Outgassing characteristics are enhanced by devolatiliztion of the binder at 423 K and a vacuum of the order of 7×10^{-4} Pa for 24 hr.

Zinc oxide was originally thought to be one of the most stable white pigments to UV irradiation in vacuum.[52] However, in 1965 serious doubts arose due to discrepancies between ground-based and in-flight experiments.[53,54] As a result, it was determined that the original zinc oxide-based silicone coatings (S-13) were not as stable as first predicted. This instability has been attributed to the formation of an easily bleachable (by oxygen) infrared absorption band (~700 - 2800 nm).[55] This damage was not observed by post-exposure reflectance measurements performed in air, since exposure to the atmosphere resulted in a rapid and complete recovery of the UV-induced damage.[56]

Since the ultraviolet-induced infrared absorption band develops rapidly in zinc oxide and is easily reversed upon exposure to oxygen, it has been suggested that the infrared phenomenon is not related to bulk phenomena but is associated with the photodesorption of oxygen. Gilligan[53]

---

[f] The S13G/LO white paint evaluated in the LDEF experiments is no longer in production. Due to the withdrawal of the RTV-602 binder and the PS-7 encapsulant for the zinc oxide pigment, the coatings is being reformulated and requalified. A new methylsilicone binder 884 from Wacker is being evaluated with PQ Corporation's Kasil 2130 potassium silicate being used as the pigment encapsulant. Data presented in this section are for the discontinued version of S13G/LO. The new version designation will be S13GP/LO-1.

explained the infrared optical behavior of ZnO on the basis of a free-carrier absorption mechanism. Absorbed photons create electron-hole pairs in a "depletion zone" with the holes discharging adsorbed oxygen from the surface of the pigment particles. The zinc oxide pigments therefore becomes electron rich with the electrons accumulating in the infrared-active conduction band, resulting in an increase in the infrared absorption.

The methyl silicone binder itself does not offer an effective barrier to photodesorption reaction on the surface of zinc oxide since it does not "wet" the pigment particles. Consequently, a method was developed to reactively encapsulate the zinc oxide pigment particles with potassium silicate to provide stability to the surface. Studies have shown that the reactively-encapsulated zinc oxide pigment greatly reduces UV-induced infrared degradation.[57]

There is additional UV-induced degradation observed in the S13G/LO paint system due to degradation of the silicone binder. When exposed to ultraviolet radiation, the methyl silicone binder exhibits induced ultraviolet-visible absorption. Only a portion of this damage observed in S13G/LO recovered upon exposure to oxygen,[55,58] indicating that the degradation is not limited to bleachable surface defects but may be the result of bulk polymer degradation.[55] Gaseous products have been observed to evolve during exposure of a methyl silicone/TiO_2 paint system to UV radiation in vacuum and are primarily hydrocarbon molecules. These hydrocarbon molecules are a result of bulk degradation of the methyl silicone binder.[59]

10.3.5.2 Source

Manufacturer:	IIT Research Institute 10 West 35 Street Chicago Illinois 60616 Telephone: 312 567-4432
Cost:	$480/pint

10.3.3.3 Ground-Based Simulation Testing

Comparative simulated atomic oxygen space environmental testing was conducted on the S13G/LO (no longer in production) and the reformulated S13GP/LO-1 white paint (a new methylsilicone binder 884 from Wacker is being evaluated with PQ Corporation's Kasil 2130 potassium silicate being used as the encapsulant for the zinc oxide pigment) The solar absorptance results, summarized in Table 10-30, indicated that the reformulated paint, S13GP/LO-1, performed comparably to the original version.[60]

Table 10-30. Comparative Solar Absorptance Values for Original and Reformulated Z-93

Simulated Space Environment	K2130 Binder		PS7 Binder	
	Pre-Exposure	Post-Exposure	Pre-Exposure	Post-Exposure
Atomic Oxygen:[a] 1.0×10^{21} atoms/cm^2 VUV: 22,000 esh	.204	.204	.209	.214
Atomic Oxygen:[b] 1×10^{21} atoms/cm^2 VUV: 9400 esh (130 nm)	.203	.209	.210	.215

(a) Exposed in the Atomic Oxygen Drift Tube System (AODTS)
- <0.1 eV thermal energy AO neutral atoms
- 5×10^{16} atoms/cm^2/sec AO Neutral Flux

(b) Princeton Plasma Physics laboratory (PPPL) System
- 10^{16} atoms/cm^2/sec AO flux
- Plasma generated by 2.45 GHz, 1kW R-F Field
- VUV radiation generated by plasma

10.3.5.3 Effects of the Space Environment

Previous atomic oxygen experiments on Shuttle Missions STS-5 and STS-8 did not reveal any noticeable degradation to S13G/LO.[61] Solar absorptivity and scanning electron microscope (SEM) photographs did not indicate any atomic oxgyen erosion of the surface of S13G/LO.

The S13G/LO samples on the LDEF Thermal Control Surfaces Experiment (TCSE) S0069 experiment degraded significantly on the LDEF mission. The TCSE experiment combined in-space measurements with extensive post-flight analyses of thermal control surfaces to determine the effects of exposure to the low Earth orbit space environment. This white paint was original selected because it is a good reflector of solar energy while also being good emitters of thermal energy to the cold sink of space. The optical properties variations are summarized in Table 10-31 (ref. 4).

Table 10-31. Optical Property Degradation of S13G/LO White Paint on the LDEF TCSE Experiment

Material	Solar Absorptance $(\alpha_s)^{a,b,c}$				Emittance $(\varepsilon_N)^d$		
	Pre-flt	In-flt (15 Mo)	Post-flt	$\Delta\alpha_S$	Pre-flt	Post-flt	$\Delta\varepsilon_N$
S13G/LO	.18	.22	.37	.19	.90	.89	-.01

(a) Mission Duration: The TCSE operated for 582 days before battery depletion. The battery power was finally expended while the sample carousel was being rotated. This left the carousel in a partially closed position. This carousel position caused 35 of the samples to be exposed for the complete LDEF mission (69.2 months), and 14 exposed for only 582 days (19.5 months) and therefore protected from the space environment for the subsequent four years.

(b) Space Environmental Exposure: The LDEF was deployed with the TCSE located on the leading edge (row 9) and at the Earth end of this row (position A9). In this configuration, the TCSE was facing the ram direction. The LDEF was rotated about the long axis where row 9 was offset from the ram direction by about 8°. The exposure environment for the TCSE were:

Atomic oxygen fluence	8.99×10^{21} atoms/cm^2
Solar UV exposure	11,200 esh
Thermal cycles	~34,000 cycles: -29 to 71 °C, ±11°C (-20 to 160 °F, ±20°F)
Radiation (at surface)	3.0×10^5 rads

(c) The primary TCSE in-space measurement was total hemispherical reflectance as a function of wavelength (100 wavelength steps from 250 to 2500 nm) using a scanning integrating sphere reflectometer. The measurements were repeated at preprogrammed intervals over the mission duration. The secondary measurement used calorimetric methods to calculate solar absorptance and thermal emittance from temperature-versus-time measurements.

(d) Laboratory measurements of spectral reflectance were obtained using Beckman DK-2A spectrophotometer equipment with a Gier-Dunkle 203 mm integrating sphere.

Figure 10-28 shows the degradation in the reflectance spectra for the S13G/LO samples on the TCSE and AO114 LDEF experiments in Figures10-28 and 10-29, respectively.[62]

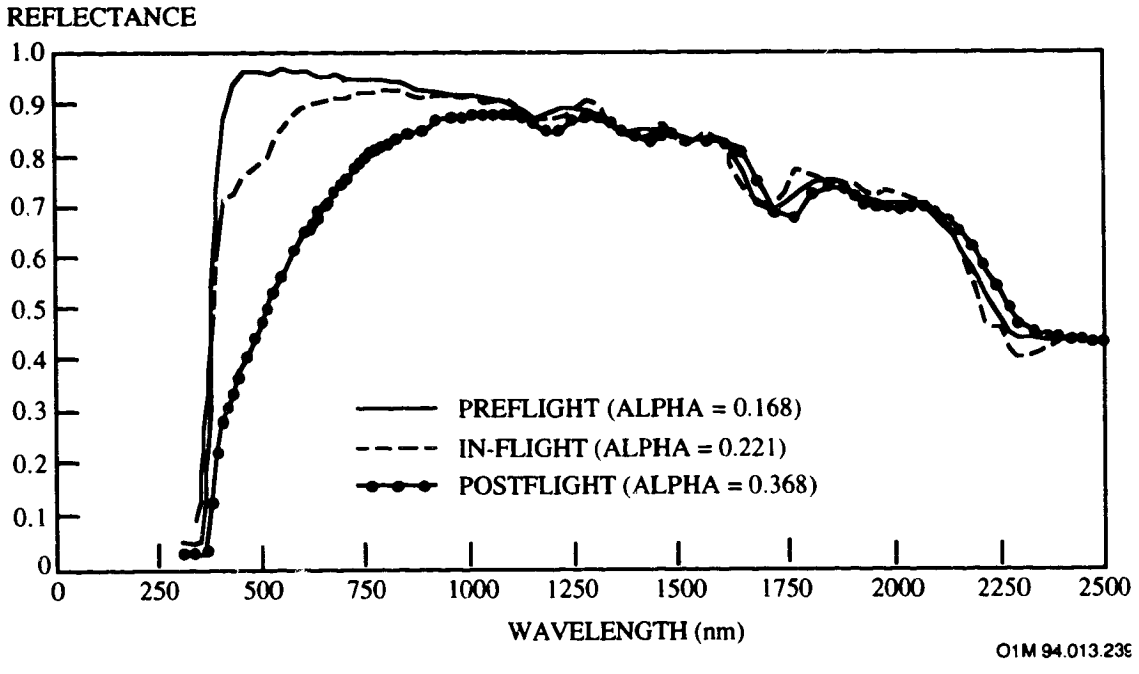

Figure 10-28. Reflectance Spectra for S13G/LO White Paint on LDEF TCSE Experiment

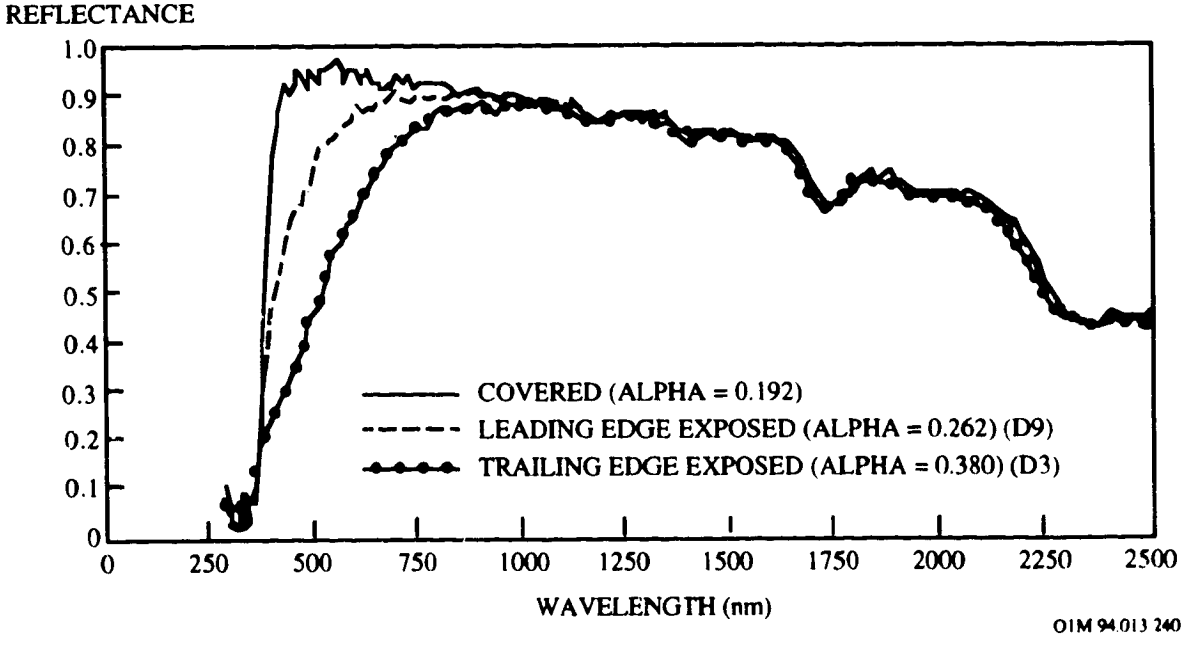

Figure 10-29. Reflectance Spectra for S. /LO White Paint on LDEF A0114 Experiment

S13G/LO was flown on LDEF Experiment M0003 Sub-Experiment 18 (ref. 11) on trays D9 (LE) and D3 (TE). The leading edge tray was exposed to 11,200 equivalent sun hours of UV radiation and an atomic oxygen fluence of 8.99×10^{21} atoms/cm,^{2} whereas the trailing edge tray was exposed to 11,100 equivalent sun hours of UV radiation and an atomic oxygen fluence of 1.32×10^{17} atoms/cm.^{2} In addition, the S13G/LO white paint was used on LDEF as a thermal control coating on the signal conditioning unit (SCU) covers. These covers were used to protect data system instrumentation for other experiments. These covers were located on the leading edge (row 8) and trailing edge (row 4) of the spacecraft; row 8 is located 30° from the perpendicular of the atomic oxygen vector, and row 4 is located 30° from the perpendicular of the wake region. Hence, these trays were exposed to different levels of UV radiation and atomic oxygen; samples from row 8 (referred to as leading edge samples) were exposed to 9,400 equivalent sun hours of UV radiation and an atomic oxygen fluence of 7.15×10^{21} atoms/cm,^{2} while samples from row 4 (referred to as trailing edge samples) was exposed to 10,500 equivalent sun hours of UV radiation and an atomic oxygen fluence of 2.31×10^5 atoms/cm.^{2}

A summary of the solar absorptance variations is listed in Table 10-32. S13G/LO exhibited greater darkening on trailing edge samples compared to leading edge samples. The solar absorptance of the trailing edge increased threefold from an initial value of 0.15. The leading edge also degraded, but its solar absorptance only increased to 0.23. Almost all of the degradation occurred in the visible and ultraviolet wavelengths, with very little degradation occurring above 1200 nm. The absorption peaks above 1200 nm are methyl silicone (binder) absorption peaks and are present in leading edge, trailing edge, and control samples.

Table 10-32. Effects of Varying UV/Atomic Oxygen Fluences on the Solar Absorptances of S13G/LO on LDEF Experiment M0003-18

Location	UV (esh)	Atomic Oxygen (atoms/cm^2)	α_s
Control	-	-	0.147
D9(LE)	11,200	8.99×10^{21}	0.232
D9(LE)	11,200	8.99×10^{21}	0.228
D3(TE)	11,100	1.32×10^{17}	0.458
D3(TE)	11,100	1.32×10^{17}	0.473
D8(LE-SCU)	9,400	7.15×10^{21}	0.257
D4(TE-SCU)	10,500	2.31×10^5	0.496

Note: TE = trailing edge; LE = leading edge; SCU = signal conditioning unit cover

The increase in solar absorptance of S13G/LO on both the leading and trailing edge samples is attributed to UV-induced damage of the methyl silicone binder since reflectance data revealed no evidence of damage to the reactively-encapsulated zinc oxide pigment. This damage is not bleachable and does not recover upon exposure to air, even after one year. Both the leading and trailing edge surfaces showed oxidation of the methyl silicone binder to silicate (SiO_x), which is accompanied by a loss of methyl groups and a formation of a cracking network on the surface. The extent of this cracking network depends largely on the atomic oxygen fluence that the surface received.

S13G/LO white paint was also used as a thermal control coating on a few experiment surfaces and cover shields on LDEF.[63] Summarized in Table 10-33 are the exposed surface coating optical properties and α/ε averages for the S13G/LO white paint. The absorptivity for the white surface S13G/LO was 0.20 ±0.02 , which increased to 0.35 ±0.05 for the yellow surfaces. The actual measurements ranged from 0.17 for the white surfaces to a 0.43 for the darkest yellow surfaces. The typical unexposed paint α/ε specification for S13G/LO is 0.18/0.90. The emissivity for the S13G/LO, like that of the A276, did not vary with color change and the average for all readings was 0.89 ±0.01. Reflectance spectra of S13G/LO test samples from trays D9 (LE) and D3 (TE) are shown in Figure 10-29

Table 10-33. LDEF Post-Flight Absorptance and Emittance Results for Exposed S13G/LO

Location on LDEF	Space Environment	Description	No. of Samples	α_S (1)	ε_N (2)	α/ε
C-3 Trailing Edge	1.32×10^{17} atoms/cm^2 11,100 esh	Dark Yellow to Brown	2	.39	.89	.44
D-3 Trailing Edge	1.32×10^{17} atoms/cm^2 11,100 esh	Yellow-Tan in color	4	.35±.05	.89±.01	.39
G-6 Earth End	3.33×10^{20} atoms/cm^2 4,500 esh	White to Tan in Color	8	.21±.02	.90	.23
C-9 Leading Edge	8.9^{c} 10^{21} atoms/cm^2 ,200 esh	White w/Brown spots	5	.20±.02	.87±.01	.23
D-9 Leading Edge	8.99×10^{21} atoms/cm^2 11,200 esh	White-Beige in Color	3	.27±.05	.89±.01	.30

(1) Solar Reflectance: Devices & Services Solar Reflectomerter SSR-ER, Ver. 5.0
(2) Infrared Reflectance: Gier Dunkle Infrared Reflectometer DB-100, Normal Emittance

The significant change in the solar absorptance of this white paint agrees with the early flight data obtained on S-13 G coating. Figure 10-30 shows the change in solar absorptance of S-13 G coating versus flight time in esh as measured from several flight experiments.[64] The degradation of the S-13G coating that was observed on OSO III[g] is similar to the LDEF data. The duration of the data acquisition for OSO III was less than one month. Data for Mariner V and the Lunar Orbiters exhibit increased damage due to the particulate environment in deep space.

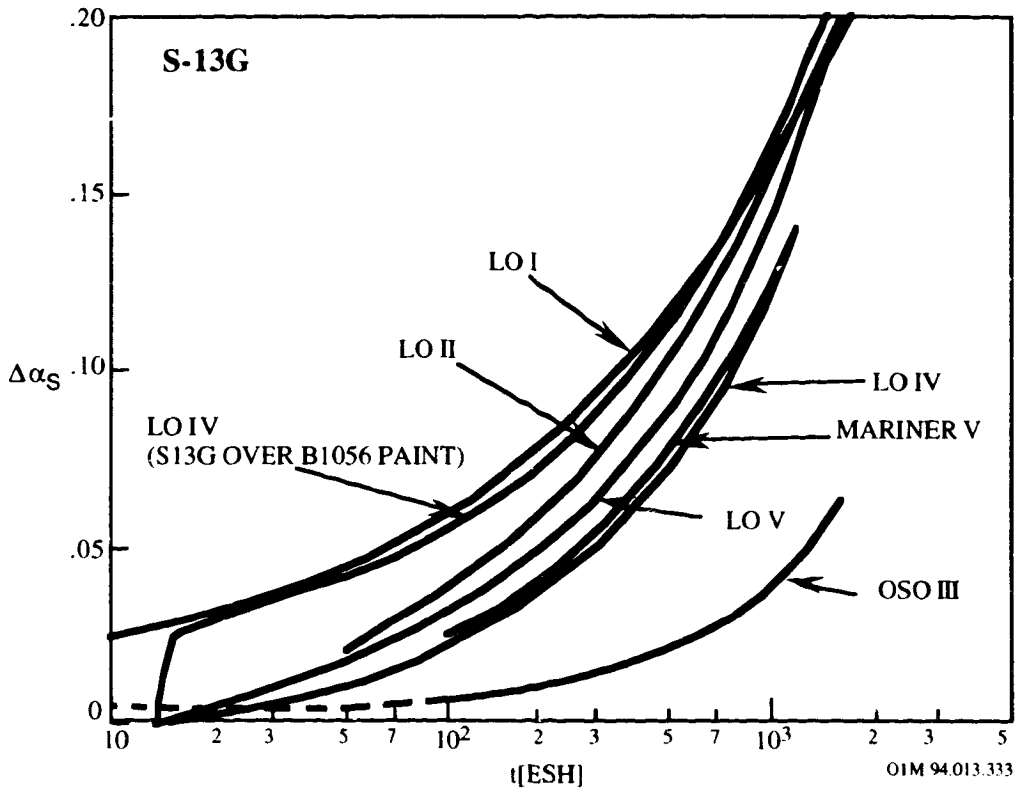

Figure 10-30. Comparative Solar Absorptance Changes of S-13 G Coating vs Flight Time for Early Space Missions

---

[g] OSO III was launched on March 8, 1967 in a near circular orbit (of about 550 km) with a 33° angle of inclination relative to the Equator.

10.3.5.4 Design Considerations for the Space Environment

10.3.5.4.1 Thermal-Optical Properties

There is a wide variation in the results from the different LDEF experiments for S13G/LO. These differences are unexplained at this time. Figures 10-31 and 10-32 show the change in α_S of several S13G/LO samples located on the leading and trailing edges of LDEF. There does not appear to be any clear correlation between ram and wake locations with respect to degradation in α_S. A regression analysis performed on the α_S values calculated from the spectral reflectance data taken in space and in post-flight measurements yielded a power regression line. This power regression model,[65] shown in Figure 10-33, falls in the middle of the spread of data reported for the various experiments (see Figures 10-31 and 10-32). The regression model predicts a 30 year end-of-life value of 0.61 for S13G/LO. Although log/log plots of experimental data can be misleading, trend analysis are useful to examine the possibility of trends and the potential of an empirical performance prediction model.

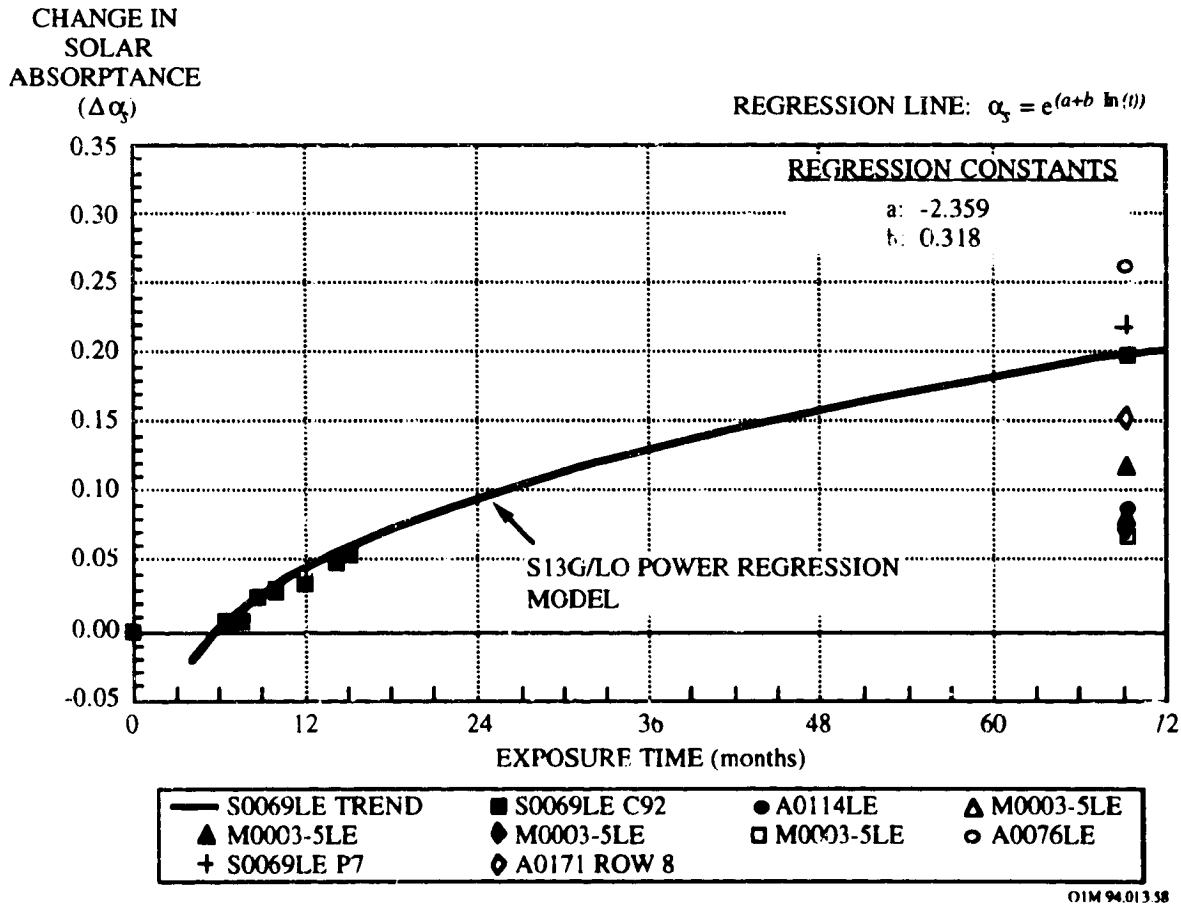

Figure 10-31. Performance of S13G/LO on LDEF - Leading Edge $\Delta\alpha_s$ vs. Exposure Time

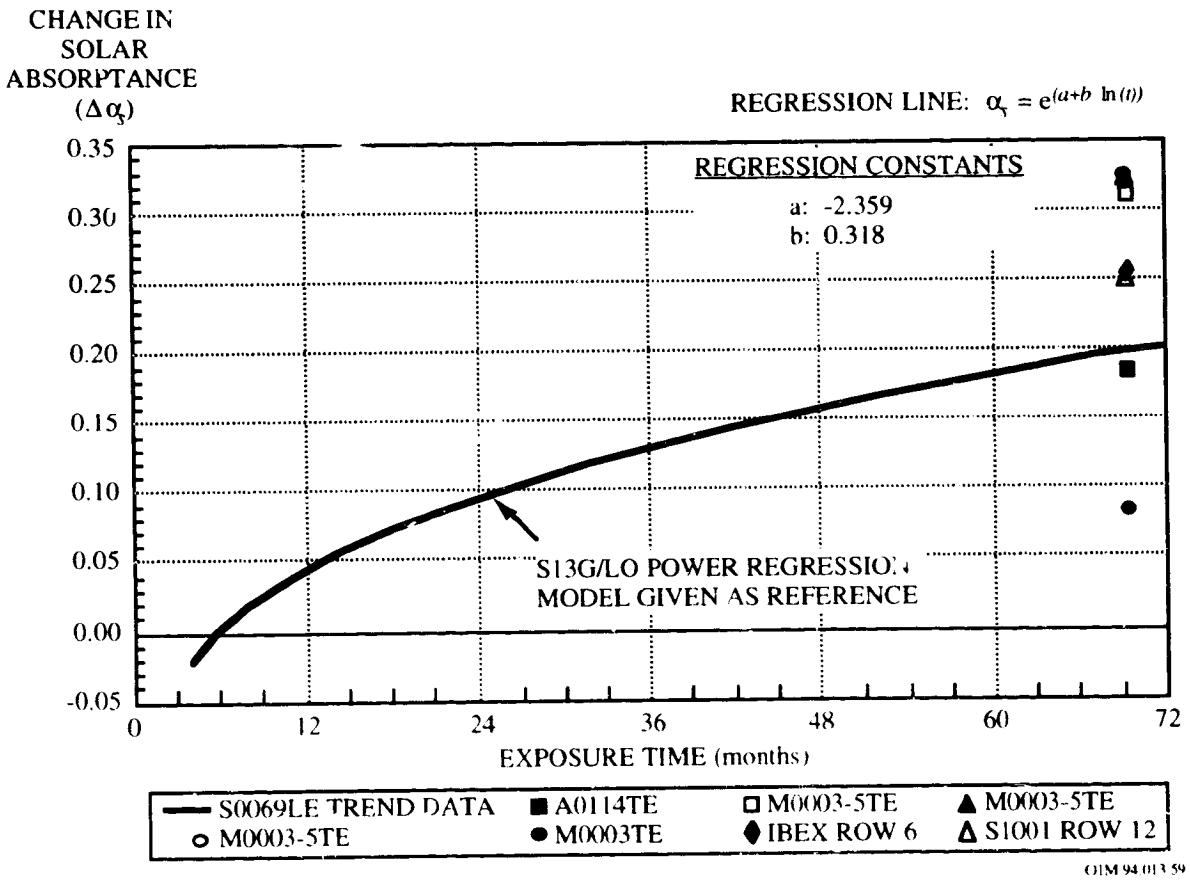

Figure 10-32. Performance of S13G/LO on LDEF - Trailing Edge $\Delta\alpha_s$ vs. Exposure Time

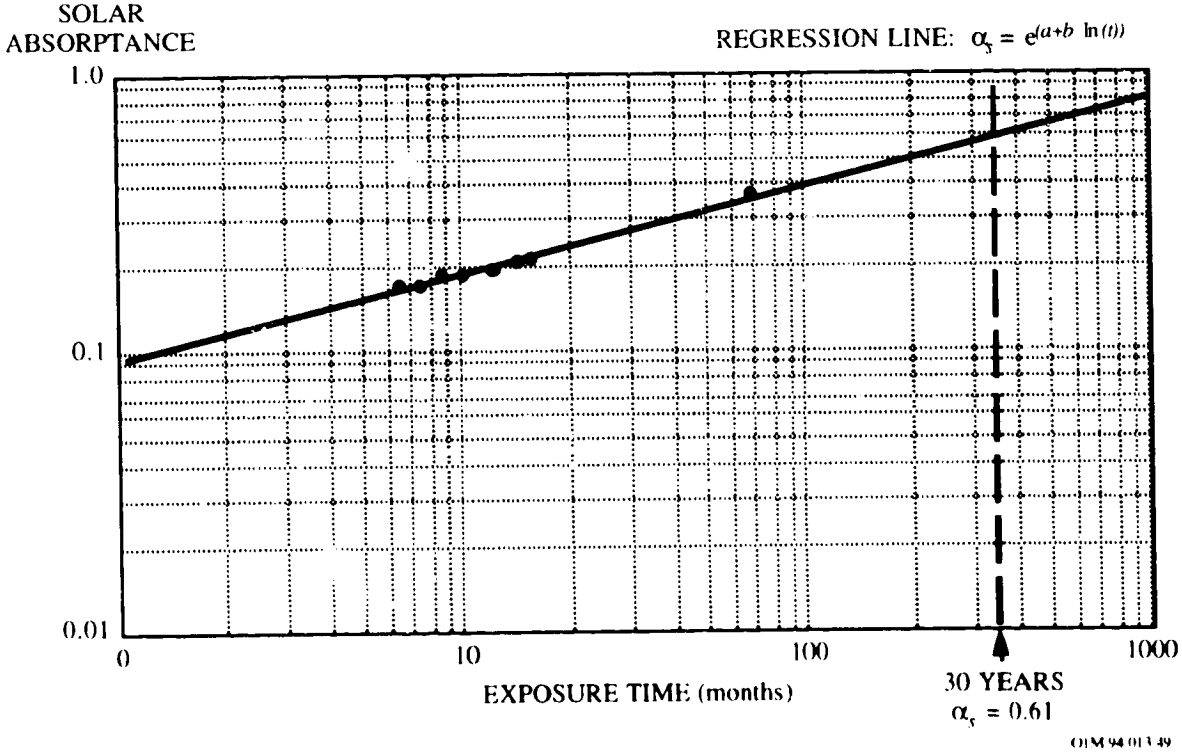

Figure 10-33. Degradation Rate Study of S13G/LO

The LDEF experiments revealed that the paint S13G/LO, as well as A276 and Z306, suffered from long term exposure to the low Earth orbit space environment. The paint pigment binders were susceptible to both UV polymerization and AO erosion. LDEF also revealed that the A276 and S13G/LO white paints displayed varying degrees of thermo-optical property degradation depending upon the location on LDEF relative to the AO flux and the amount of UV exposure received.

Although laboratory testing of the reformulated S13GP/LO-1 white paint indicate similar solar absorptance performance to the discontinued S13G/LO white paint (see Table 10-30), additional flight test data are needed to predict its long-term degradation for extended low Earth orbit missions. In the interim, it is recommended that a 100% increase in absorptivity should be accounted for in the spacecraft thermal design if the S13GP/LO-1 paint is used.

10.3.5.4.2 Micrometeoroid/Debris Impacts

The effects of multiple impact craters to the thermal radiative properties of S13G/LO as a function of time were calculated using an equation based on the fraction of damaged surface area (ref. 52).

$$A_s\,(\text{Beta}) = A_o - \left[D_{a.e} * F_a * T_{yr}\right]$$

where:	A_s (Beta, time)	=	effective or average value of solar absorptance or emittance at each Beta angle
	Beta	=	degrees from velocity vector or ram direction
	A_o	=	solar absorptance or emittance of original coating
	$D_{a.e}$	=	difference between coating and substrate absorptance or emittance
	F_a	=	fraction of damaged surface area per year
	T_{yr}	=	number of years exposed

The effects on S13G/LO are minimal (see Figures 10-34 and 10-35) since the spall to crater ratio is low. For this coating, the atomic oxygen, ultraviolet radiation, and contamination will have a greater long-term effect than meteoroid/debris impacts (ref. 4).

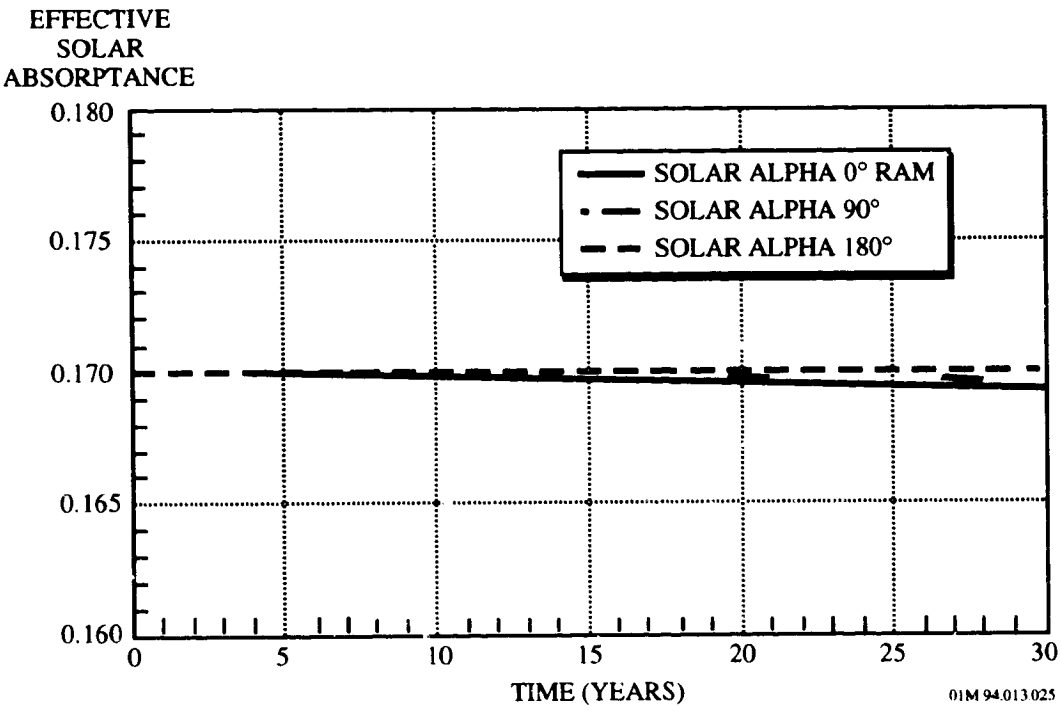

Figure 10-34. S13G/LO M/OD Effect on Solar Absorptance vs Time

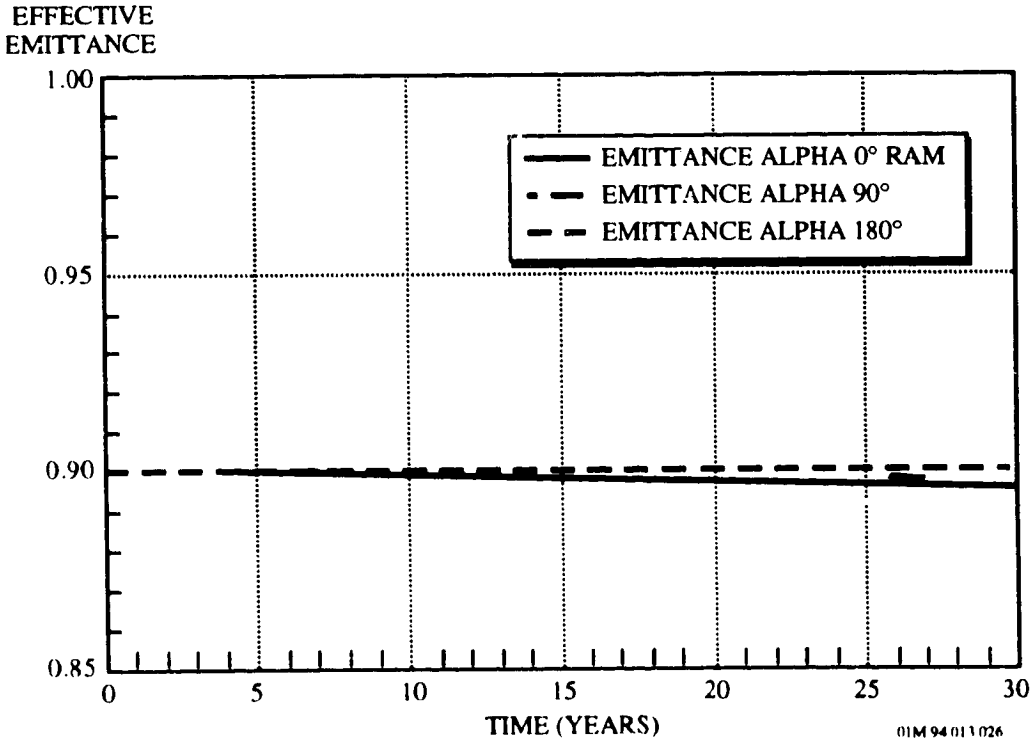

Figure 10-35. S13G/LO M/OD Effect on Emittance vs Time

10.3.6 White Tedlar Film

10.3.6.1 Composition

Polyvinylflouride film

Thermal properties: $\alpha_s = 0.250$, $\varepsilon_N = 0.890$

10.3.6.2 Source

Manufacturer: DuPont

10.3.6.3 Effects of the Space Environment

White Tedlar is another material that was expected to degrade over the 5.8 year LDEF mission due to solar UV exposure. Instead, the optical properties of this material improved slightly (ref. 4). Figure 10-36 shows the solar absorptance data (ref. 64). White Tedlar was located on the leading edge, row 9, of the LDEF S0069 TCSE Experiment, which received an atomic oxygen fluence of 8.99×10^{21} atoms/cm^2. The surface remained diffuse and white, similar to pre-flight observations.

As with A276, Tedlar has been shown to be susceptible to AO erosion. The erosion effect of AO is the apparent reason for the lack of surface degradation of these flight samples. The TCSE in-flight data showed that only a small degradation in solar absorptance was seen early in the LDEF mission. The solar absorptance increase to 0.26 from 0.25. This indicated that, as with the A276 samples, there was sufficient AO early in the mission to erode away damaged material or otherwise inhibit significant degradation. The subsequent high AO fluence eroded away all the damaged surface materials, and even provided a slight improvement in solar absorptance. The post-flight solar absorptance after 69 months was 0.22 compared to the pre-flight solar absorptance measurement of 0.25.

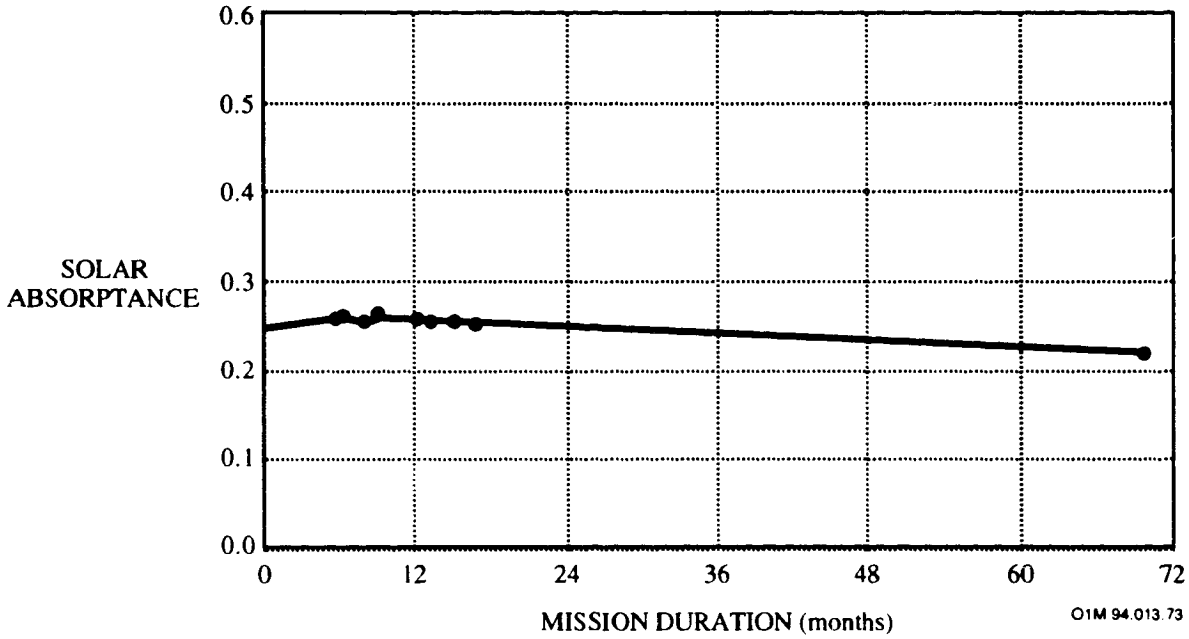

Figure 10-36. Solar Absorptance Variations With Space Exposure for White Tedlar

10.3.7 PCBT White Paint

PCBT is a flexible tin orthotitanate/silicone conductive non-specular white coating. The white paint is typically used as a coating for Kapton and Mylar substrates.

Thermal properties: $\alpha_s = 0.26 \pm 0.02$; $\varepsilon_H = 0.78 \pm 0.04$

After UV irradiation of 750 esh at 25°C; $\Delta\alpha_s = 0.08$

10.3.7.1 Composition

Binder:	Elastomer Silicone (Dow Corning R4-3117)
Pigment:	Tin orthotitanate

10.3.7.2 Source

Manufacturer:	MAP Company Z.I. Chemin de la Rijole 09100 Pamiers, France Tel. 33 61 60 27 00; Fax. 33 61 60 23 30
Cost:	6,000 French francs/K (1994 prices)

10.3.7.3 Effects of the Space Environment

10.3.7.3.1 Thermal-Optical Properties

The PCBT coating showed promise during a 9-month LDEF FRECOPA experiment and during the 1.1 year COMES/MIR flight experiment, as shown in Table 10-34 (ref. 34). Experiment AO 138-6 was part of the FRECOPA experiment located on the trailing edge of LDEF. The solar reflection measurements were made with a Beckmann DK2A spectrophotometer with an integrating sphere, and the infrared emissivity measurements were made with the Gier & Dunkle DB 100 device. It is important to underline that the measurements were all taken in air on samples which had thus experienced more or less intense recovery of the radiation damage.

Table 10-34. Solar Reflectance and Emissivity Variations For PCBT White Paint on LDEF

Type	$Rs_{initial}$	$\varepsilon_{initial}$	AO 138-6 LDEF		AO 138-6 LDEF	
			Canister ΔRs	Tray ΔRs	Canister $\Delta\varepsilon$	Tray $\Delta\varepsilon$
White paint conductive	0.72	0.815	-0.10		0.000	

Environmental Variations of LDEF AO 138-6 FRECOPA Space Experiment: Due to its position on the trailing edge of LDEF, the AO 138-6 experiment did not receive any oxygen atoms during the mission, with the exception of a short period during the capture when it received a fluence evaluated at 1.32×10^{17} atoms cm^{-2}. The solar illumination was 11,100 equivalent sun hours (esh) for the samples located on the tray and only 1448 esh for the samples inside the canister. The particle irradiation dose (mainly due to the electron flux) was weak: 3×10^{5} rads. The number of temperature cycles was ~34,000 with temperatures within the ranges shown in the table below.

ENVIRONMENT	CANISTER	TRAY
Oxygen atoms cm^{-2}	0	1.32×10^{17}
Solar UV (esh)	1448	11,110
Temp. Cold case (°C)	-20 to -26	-43 to -52
Temp. Hot case (°C)	+67 to +85	+45 to +63

10.3.8 PCBZ White Paint

PCBZ white paint is a rigid zinc orthostannate/silicone conductive non-specular white thermal control paint. It is typically used as a coating for rigid aluminum alloy surfaces.

Thermal properties: $\alpha_s = 0.26$; $\varepsilon_H = 0.83$

After UV irradiation of 1045 esh at 25°C: $\Delta\alpha_s = 0.03$

10.3.8.1 Composition

Binder:	Methyl phenyl silicone (Rhone Poulenc Rhodorsil 10 336)
Pigment:	Zinc orthostannate Zn_2SnO_4

10.3.8.2 Source

Manufacturer:	MAP Company Z.I. Chemin de la Rijole 09100 Pamiers, France Tel. 33 61 60 27 00; Fax. 33 61 60 23 30
Cost:	7,400 French francs/K (1994 prices)

10.3.8.3 Space Environmental Effects

10.3.8.3.1 Thermal-Optical Properties

The PCBZ coating showed promise during a 9-month LDEF FRECOPA experiment and during the 1.1 year COMES/MIR flight experiment, as shown in Table 10-35 (ref. 34). The COMES experiment consisted of four panels which were deployed by an cosmonaut in space outside of MIR with the possibility of exposing samples on both sides, conventionally identified as "V" and "R". Experiment AO 138-6 was part of the FRECOPA experiment located on the trailing edge of LDEF. The experiment was designed to allow exposure of a part of the samples to the whole spacecraft environment by being laid directly on the FRECOPA tray surface, while the other part of samples was protected from the external environment of LDEF for all mission phases, except free flight, by the means of a vacuum-tight FRECOPA canister in which they were stored. Comparison of the LDEF and MIR flight data indicated less degradation for PCBZ following the FRECOPA experiment than after the COMES experiment

Table 10-35. Solar Reflectance and Emissivity Variations of PCBZ White Paint on FRECOPA/LDEF and COMES/MIR

			AO 138-6 LDEF		AO 138-6 LDEF		COMES		COMES	
Type	$Rs_{initial}$	$\varepsilon_{initial}$	Canister ΔRs	Tray ΔRs	Canister $\Delta\varepsilon$	Tray $\Delta\varepsilon$	Face V ΔRs	Face R ΔRs	Face V $\Delta\varepsilon$	Face R $\Delta\varepsilon$
White paint conductive	0.78	0.872	-0.03		0.000		-0.01	-0.02	+0.006	+0.003

Environmental Variations of LDEF and MIR Space Experiments : Due to its position on the trailing edge of LDEF, the AO 138-6 experiment did not receive any oxygen atoms during the mission, with the exception of a short period during the capture when it received a fluence evaluated at 1.32×10^{17} atoms cm^{-2}. The solar illumination was 11,100 equivalent sun hours (esh) for the samples located on the tray and only 1448 esh for the samples inside the canister. The particle irradiation dose (mainly due to the electron flux) was weak: 3×10^{5} rads. The number of temperature cycles was ~ 34,000 with temperatures within the ranges shown in the table below.

	FRECOPA-LDEF		COMES-MIR	
ENVIRONMENT	CANISTER	TRAY	FACE V	FACE R
Oxygen atoms cm^{-2}	0	1.3×10^{17}	1.2×10^{18} to 7.5×10^{19} (1)	3.5×10^{20} to 5.8×10^{20} (1)
Solar UV (esh)	1448	11,110	2850(2)	1900(2)
Temp. Cold case (°C)	-20 to -26	-43 to -52	-60 to -70	-60 to -70
Temp. Hot case (°C)	+67 to +85	+45 to +63	+10 to +30	+50 to +60

(1) Estimated from AO reactivity erosion of Kapton (3.0×10^{-24} $cm^3 atom^{-1}$) and Terphane (3.0×10^{-24} $cm^3 atom^{-1}$) samples

(2) Estimated from data of experiment calorimeter

Experimental Description. The solar reflection measurements were made with a Beckman DK2A spectrophotometer with an integrating sphere, and the infrared emissivity measurements were made with the Gier & Dunkle DB 100 device. It is important to underline that the measurements were all taken in air on samples which had thus experienced more or less intense recovery of the radiation damage.

Table 10-36 shows for the deterioration in the solar reflectance of PCBZ exposed to different environments on the V side of the COMES experiment. The deterioration generally found on this white paint is relatively low whether submitted to the complete environment or under UV.

Table 10-36. Synergistic Space Environment Effects on the Solar Reflectance Degradation ΔR_S of PCBZ on the V Side of COMES

Type	Chemical Nature	UV + AO + vacuum ΔR_S(a)	UV (λ>190 nm) ΔR_S(b)	UV (λ>360 nm) ΔR_S(c)	Vacuum ΔR_S(d)
Conductive White Paint	Zinc Orthostannate/ silicone	-0.01	-0.01	-0.01	+0.01

(a) an exposure to all of the parameters: ultraviolet solar radiation (including far UV), atomic oxygen, vacuum and the temperature; ΔR_S=final R_S-initial R_S

(b) an exposure to ultra-violet radiation with a wavelength greater than 190 nm, to the vacuum and to the temperature

(c) an exposure to radiations with a wavelength greater than 360 nm, to the vacuum and to the temperature

(d) an exposure to the vacuum and to the temperature.

Space Environment on the V side of the COMES experiment:

Atomic Oxygen, atoms cm^{-2}	$1.2x10^{18}$ to $7.5x10^{19}$ (1)
Solar UV (esh)	2850(2)
Temp. Cold case (°C)	-60 to -70
Temp. Hot case (°C)	+10 to +30

(1) Estimated from AO reactivity erosion of Kapton (3.0×10^{-24} $cm^3 atom^{-1}$)and Terphane (PET) (3.0×10^{-24} $cm^3 atom^{-1}$) samples

(2) Estimated from data of experiment calorimeter

10.3.9 PCB 119

PCB 119 is a conductive non-specular white coating.

Thermal properties: $\alpha_s = 0.15$; $\varepsilon_N = 0.83$

10.3.9.1 Composition

Binder:	Silicone (Rhone Poulenc Rhodorsil 10336)
Pigment:	Zinc orthotitanate (doped)

10.3.9.2 Source

Manufacturer:	MAP Company Z.I. Chemin de la Rijole 09100 Pamiers, France Tel. 33 61 60 27 00; Fax. 33 61 60 23 30
Cost:	7,400 French francs/K (1994 prices)

10.3.9.3 Space Environmental Effects

10.3.9.3.1 Thermal-Optical Properties

The PCB 119 showed promise during the 1.1 year COMES/MIR flight experiment as shown in Table 10-37 (ref. 34). The COMES experiment consisted of four panels which were deployed by a cosmonaut in space outside of MIR with the possibility of exposing samples on both sides, conventionally identified as "V" and "R". The solar reflection measurements were made with a Beckmann DK2A spectrophotometer with an integrating sphere, and the measurements of infra-red emissivity with the Gier & Dunkle DB 100 device. It is important to underline that the measurements were all taken in air on samples which had thus experienced more or less intense recovery of the radiation damage.

Table 10-37. Solar Reflectance and Emissivity Variations of PCB 119 on the COMES/MIR

Type	Rs initial	ε initial	Face V ΔRs	Face R ΔRs	Face V $\Delta\varepsilon$	Face R $\Delta\varepsilon$
White paint conductive	0.79	0.861	-0.01	0.01	+0.008	+0.006

Environmental Variations of MIR Space Experiments:

ENVIRONMENT	FACE V	FACE R
Oxygen atoms cm^{-2}	$1.2x10^{18}$ to $7.5x10^{19}$ (1)	$3.5x10^{20}$ to $5.8x10^{20}$ (2)
Solar UV (esh)	2850(2)	1900(2)
Temp. Cold case (°C)	-60 to -70	-60 to -70
Temp. Hot case (°C)	+10 to +30	+50 to +60

(1) Estimated from data of experiment calorimeter

(2) Estimated from AO reactivity erosion of Kapton (3.0×10^{-24} $cm^3 atom^{-1}$)and Terphane (PET) (3.0×10^{-24} $cm^3 atom^{-1}$) samples

Table 10-38 shows the deterioration in the solar reflectance for the PCB 119 white paint exposed to different environments for the COMES experiment. The deterioration generally found on this white paint is relatively low whether submitted to the complete environment or under UV. It should be remembered that the degradations considered here are those recorded after the samples have been returned to the air; those which might have been observed in orbit would have been different. On the R side of COMES which received the most oxygen atoms, the solar reflectance of the PCB 119 even seem to have increased following the flight.

Table 10-38. Synergistic Space Environment Effects on the Solar Reflectance Degradation ΔR_S of PCB 119 on the V Side of COMES

Type	Chemical Nature	UV + AO + vacuum ΔR_S(a)	UV (λ>190 nm) ΔR_S(b)	UV (λ>360 nm) ΔR_S(c)	Vacuum ΔR_S(c)
Conductive White Paint	Zinc Orthotitanate (doped)/Silicone	-0.01	0.00	+0.01	+0.01

(a) an exposure to all of the parameters: ultraviolet solar radiation (including far UV), atomic oxygen, vacuum and the temperature; ΔR_S=final R_S-initial R_S

(b) an exposure to ultra-violet radiation with a wavelength greater than 190 nm, to the vacuum and to the temperature

(c) an exposure to radiations with a wavelength greater than 360 nm, to the vacuum and to the temperature

(d) an exposure to the vacuum and to the temperature.

Space Environment on the V side of the COMES experiment:

Atomic Oxygen, atoms cm^{-2}	$1.2x10^{18}$ to $7.5x10^{19}$ (1)
Solar UV (esh)	2850(2)
Temp. Cold case (°C)	-60 to -70
Temp. Hot case (°C)	+10 to +30

(1) Estimated from AO reactivity erosion of Kapton (3.0×10^{-24} $cm^3 atom^{-1}$)and Terphane (PET) (3.0×10^{-24} $cm^3 atom^{-1}$) samples

(2) Estimated from data of experiment calorimeter

10.3.10 PSB

PSB is a non-conductive white silicate thermal control paint.

Thermal properties: $\alpha_s = 0.14 \pm 0.02$; $\varepsilon_H = 0.90 \pm 0.04$

After UV irradiation of 1080 esh at 25°C: $\Delta\alpha_s = 0.02$

10.3.10.1 Composition

Binder:	Potassium silicate
Pigment:	Zinc orthotitonate

10.3.10.2 Source

Manufacturer:	MAP Company Z.I. Chemin de la Rijole 09100 Pamiers, France Tel. 33 61 60 27 00; Fax. 33 61 60 23 30
Cost:	7,200 French francs/K (1994 prices)

10.3.10.3 Space Environmental Effects

10.3.10.3.1 Thermal-Optical Properties

The PSB coating showed promise during a 9-month LDEF FRECOPA experiment and during the 1.1 year COMES/MIR flight experiment, as shown in Table 10-39 (ref. 34). The COMES experiment consisted of four panels which were deployed by a cosmonaut in space outside of MIR with the possibility of exposing samples on both sides, conventionally identified as "V" and "R". Experiment AO 138-6 was part of the FRECOPA experiment located on the trailing edge of LDEF. The experiment was designed to allow exposure of a part of the samples to the whole spacecraft environment by being laid directly on the FRECOPA tray surface, while the other part of samples was protected from the external environment of LDEF for all mission phases, except free flight, by the means of a vacuum-tight FRECOPA canister in which they were stored.

Table 10-39. Solar Reflectance and Emissivity Variations of PSB White Paint on FRECOPA/LDEF and COMES/MIR

			AO138-6 LDEF		AO138-6 LDEF		COMES		COMES	
Type	$Rs_{initial}$	$\varepsilon_{initial}$	Canister ΔRs	Tray ΔRs	Canister $\Delta\varepsilon$	Tray $\Delta\varepsilon$	Face V ΔRs	Face R ΔRs	Face V $\Delta\varepsilon$	Face R $\Delta\varepsilon$
White paint	0.83	0.895	-0.05	-0.01	-0.001	-0.003	-0.01		-0.003	

Environmental Variations of LDEF and MIR Space Experiments: Due to its position on the trailing edge of LDEF, the AO 138-6 experiment did not receive any oxygen atoms during the mission, with the exception of a short period during the capture when it received a fluence evaluated at 1.32×10^{17} atoms cm^{-2}. The solar illumination was 11,100 equivalent sun hours (esh) for the samples located on the tray and only 1448 esh for the samples inside the canister. The particle irradiation dose (mainly due to the electron flux) was weak: 3×10^5 rads. The number of temperature cycles was ~34,000 with temperatures within the ranges shown in the table below.

Experimental Description. The solar reflection measurements were made with a Beckman DK2A spectrophotometer with an integrating sphere, and the infrared emissivity measurements were made with the Gier & Dunkle DB 100 device. It is important to underline that the measurements were all taken in air on samples which had thus experienced more or less intense recovery of the radiation damage.

	FRECOPA-LDEF		COMES-MIR	
ENVIRONMENT	CANISTER	TRAY	FACE V	FACE R
Oxygen atoms cm^{-2}	0	1.3×10^{17}	1.2×10^{18} to 7.5×10^{19} (1)	3.5×10^{20} to 5.8×10^{20} (1)
Solar UV (esh)	1448	11,100	2850(2)	1900(2)
Temp. Cold case (°C)	-20 to -26	-43 to -52	-60 to -70	-60 to -70
Temp. Hot case (°C)	+67 to +85	+45 to +63	+10 to +30	+50 to +60

(1) Estimated from AO reactivity erosion of Kapton (3.0×10^{-24} $cm^3 atom^{-1}$) and Teflon (3.0×10^{-24} $cm^3 atom^{-1}$) samples

(2) Estimated from data of experiment calorimeter

From Table 10-39, one observes that the PSB white paint was less deteriorated following LEO exposure during the COMES experiment than during the FRECOPA canister experiment. Apparently, the higher atomic oxygen fluence level on the V-side of the COMES experiment removed the material affected by the UV radiation.

Table 10-40 shows for the COMES experiment the deteriorations in the solar reflectance for the PSB coating exposed to different environments. The deterioration generally found on this white paint is relatively low whether submitted to the complete environment or under UV. However, the solar reflectance degradations reported are those recorded after the samples have been returned to the air; the solar reflectance values which might have been observed in orbit could have been different.

Table 10-40. Synergistic Space Environment Effects on the Solar Reflectance Degradation ΔR_S of PSB Coating on the V Side of COMES

Type	Chemical Nature	UV + AO + vacuum ΔR_S(a)	UV (λ>190 nm) ΔR_S(b)	UV (λ>360 nm) ΔR_S(c)	Vacuum ΔR_S(d)
White Paint	Zinc Orthotitanate/ silicate	0.00	0.00	+0.01	0.00

(a) an exposure to all of the parameters: ultraviolet solar radiation (including far UV), atomic oxygen, vacuum and the temperature; ΔR_S=final R_S-initial R_S

(b) an exposure to ultra-violet radiation with a wavelength greater than 190 nm, to the vacuum and to the temperature

(c) an exposure to radiations with a wavelength greater than 360 nm, to the vacuum and to the temperature

(d) an exposure to the vacuum and to the temperature.

Space Environment on the V side of the COMES experiment:

Atomic Oxygen, atoms cm^{-2}	$1.2x10^{18}$ to $7.5x10^{19}$ (1)
Solar UV (esh)	2850(2)
Temp. Cold case (°C)	-60 to -70
Temp. Hot case (°C)	+10 to +30

(1) Estimated from AO reactivity erosion of Kapton (3.0×10^{-24} $cm^3 atom^{-1}$) and Terphane (PET) (3.0×10^{-24} $cm^3 atom^{-1}$) samples

(2) Estimated from data of experiment calorimeter

10.3.11 SG 11 FD

SG 11 FD is a non-conductive silicone white paint.

Thermal properties: $\alpha_s = 0.13 \pm 0.02$; $\varepsilon_H = 0.80 \pm 0.04$

After UV irradiation of 1000 esh at 25°C: $\Delta\alpha_s = 0.02$

10.3.11.1 Composition

Binder:	Silicone (Rhone Poulenc RTV 121)
Pigment:	Zinc orthotitanate

10.3.11.2 Source

Manufacturer:	MAP Company Z.I. Chemin de la Rijole 09100 Pamiers, France Tel. 33 61 60 27 00; Fax. 33 61 60 23 30
Cost:	7,400 French francs/K (1994 prices)

10.3.11.3 Space Environmental Effects

10.3.11.3.1 Thermal-Optical Properties

The SG 11 FD coating showed promise during the 1.1 year COMES/MIR flight experiment, as shown in Table 10-41 (ref. 34). The COMES experiment consisted of four panels which were deployed by a cosmonaut in space outside of MIR with the possibility of exposing samples on both sides, conventionally identified as "V" and "R". The solar reflection measurements were made with a Beckmann DK2A spectrophotometer with an integrating sphere, and the infrared emissivity measurements were made with the Gier & Dunkle DB 100 device. It is important to underline that the measurements were all taken in air on samples which nad thus experienced more or less intense recovery of the radiation damage.

Table 10-41. Solar Reflectance and Emissivity Variations of SG 11 FD on COMES/MIR

Type	Rs initial	$\varepsilon_{initial}$	Face V ΔRs	Face R ΔRs	Face V $\Delta\varepsilon$	Face R $\Delta\varepsilon$
White paint	0.82	0.854	-0.04	-0.01	-0.005	-0.005

Environmental Variations of MIR Space Experiments:

ENVIRONMENT	COMES/MIR	
	FACE V	FACE R
Oxygen atoms cm^{-2}	$1.2x10^{18}$ to $7.5x10^{19}$ (1)	$3.5x10^{20}$ to $5.8x10^{20}$ (1)
Solar UV (esh)	2850(2)	1900(2)
Temp. Cold case (°C)	-60 to -70	-60 to -70
Temp. Hot case (°C)	+10 to +30	+50 to +60

(1) Estimated from AO reactivity erosion of Kapton (3.0×10^{-24} cm^3atom^{-1})and Terphane (PET) (3.0×10^{-24} cm^3atom^{-1}) samples

(2) Estimated from data of experiment calorimeter

Table 10-42 shows for the COMES experiment the deterioration in the solar reflectance for the SG 11 FD white paint exposed to different environments. The deterioration generally found on this white paint appear to deteriorate more under UV + atomic oxygen than under ultra-violet radiation alone. However, the solar reflectance degradations reported are those recorded after the samples have been returned to the air; the solar reflectance values which might have been observed in orbit could have been different.

Table 10-42. Synergistic Space Environment Effects on the Solar Reflectance Degradation ΔR_S of SG 11 FD on the V Side of COMES

Type	Chemical Nature	UV + AO + vacuum ΔR_S(a)	UV (λ>190 nm) ΔR_S(b)	UV (λ>360 nm) ΔR_S(c)	Vacuum ΔR_S(c)
White Paint	Zinc Orthotitanate /Silicone	-0.04	-0.01	0.01	0.00

(a) an exposure to all of the parameters: ultraviolet solar radiation (including far UV), atomic oxygen, vacuum and the temperature; ΔR_S=final R_S-initial R_S

(b) an exposure to ultra-violet radiation with a wavelength greater than 190 nm, to the vacuum and to the temperature

(c) an exposure to radiations with a wavelength greater than 360 nm, to the vacuum and to the temperature

(d) an exposure to the vacuum and to the temperature.

Space Environment on the V side of the COMES experiment:

Atomic Oxygen, atoms cm^{-2}	$1.2x10^{18}$ to $7.5x10^{19}$ (1)
Solar UV (esh)	2850(2)
Temp. Cold case (°C)	-60 to -70
Temp. Hot case (°C)	+10 to +30

(1) Estimated from AO reactivity erosion of Kapton (3.0×10^{-24} cm^3atom^{-1})and Terphane (PET) (3.0×10^{-24} cm^3atom^{-1}) samples

(2) Estimated from data of experiment calorimeter

10.3.12 PSG 120 FD

PSG 120 FD is a non-conductive zinc oxide methylsilicone white thermal control paint

10.3.12.1 Composition

Binder:	Silicone elastomer (Rhone Poulenc RTV 121)
Pigment:	Zinc oxide SP 500 (New Jersey Zinc Co.,)

10.3.12.2 Source

Manufacturer:	ASTRAL Peintures et Vernis, 164 rue Ambroise Croizat, 93024 Saint-Denis. Cedex 1, France

10.3.12.3 Space Environmental Effects

10.3.12.3.1 Thermal-Optical Properties

The PSG 120 FD coating showed promise during a 9-month LDEF FRECOPA experiment and during the 1.1 year COMES/MIR flight experiment, as shown in Table 10-43 (ref. 34). The COMES experiment consisted of four panels which were deployed by a cosmonaut in space outside of MIR with the possibility of exposing samples on both sides, conventionally identified as "V" and "R". Experiment AO 138-6 was part of the FRECOPA experiment located on the trailing edge of LDEF. The experiment was designed to allow exposure of a part of the samples to the whole spacecraft environment by being laid directly on the FRECOPA tray surface, while the other part of samples was protected from the external environment of LDEF for all mission phases, except free flight, by the means of a vacuum-tight FRECOPA canister in which they were stored.

Table 10-43. Solar Reflectance and Emissivity Variations of PSG 120 FD White Paint on FRECOPA/LDEF and COMES/MIR

			AO 138-6 LDEF		COMES			
Type	$Rs_{initial}$	$\varepsilon_{initial}$	Canister ΔRs	Canister Δε	Face V ΔRs	Face R ΔRs	Face V Δε	Face R Δε
White paint	0.80	0.876	-0.07	-0.002	-0.04	-0.02	0.000	-0.002

Environmental Variations of LDEF and MIR Space Experiments: Due to its position on the trailing edge of LDEF, the AO 138-6 experiment did not receive any oxygen atoms during the mission, with the exception of a short period during the capture when it received a fluence evaluated at 1.32×10^{17} atoms cm^{-2}. The solar illumination was 11,100 equivalent sun hours (esh) for the samples located on the tray and only 1448 esh for the samples inside the canister. The particle irradiation dose (mainly due to the electron flux) was weak: 3×10^{5} rads. The number of temperature cycles was ~34,000 with temperatures within the ranges shown in the table below.

	FRECOPA-LDEF		COMES-MIR	
ENVIRONMENT	CANISTER	TRAY	FACE V	FACE R
Oxygen atoms cm^{-2}	0	1.3×10^{17}	1.2×10^{18} to 7.5×10^{19} (1)	3.5×10^{20} to 5.8×10^{20} (1)
Solar UV (esh)	1448	11,100	2850(2)	1900(2)
Temp. Cold case (°C)	-20 to -26	-43 to -52	-60 to -70	-60 to -70
Temp. Hot case (°C)	+67 to +85	+45 to +63	+10 to +30	+50 to +60

(1) Estimated from AO reactivity erosion of Kapton (3.0×10^{-24} $cm^3 atom^{-1}$) and Terphane (3.0×10^{-24} $cm^3 atom^{-1}$) samples

(2) Estimated from data of experiment calorimeter

Experimental Description. The solar reflection measurements were made with a Beckman DK2A spectrophotometer with an integrating sphere, and the infrared emissivity measurements were made with the Gier & Dunkle DB 100 device. It is important to underline that the measurements were all taken in air on samples which had thus experienced more or less intense recovery of the radiation damage.

From Table 10-43, one observes that the PSG 120 FD white paint was less deteriorated following LEO exposure during the COMES experiment than during the FRECOPA canister experiment. Apparently, the higher atomic oxygen fluence level on the V-side of the COMES experiment removed the material affected by the UV radiation.

Table 10-44 shows for the COMES experiment the deteriorations in the solar reflectance for the PSG 120 FD white paint exposed to different environments. The deterioration generally found on this white paint appear to deteriorate more under UV + atomic oxygen than under ultra-violet radiation alone. However, the solar reflectance degradations reported are those recorded after the samples have been returned to the air; the solar reflectance values which might have been observed in orbit could have been different.

Table 10-44. Synergistic Space Environment Effects on the Solar Reflectance Degradation ΔR_S of PSG 120 FD on the V Side of COMES

Type	Chemical Nature	UV + AO + vacuum ΔR_S(a)	UV (λ>190 nm) ΔR_S(b)	UV (λ>360 nm) ΔR_S(c)	Vacuum ΔR_S(c)
White Paint	ZnO/silicone	-0.04	-0.03	0.00	0.00

(a) an exposure to all of the parameters: ultraviolet solar radiation (including far UV), atomic oxygen, vacuum and the temperature; ΔR_S=final R_S-initial R_S

(b) an exposure to ultra-violet radiation with a wavelength greater than 190 nm, to the vacuum and to the temperature

(c) an exposure to radiations with a wavelength greater than 360 nm, to the vacuum and to the temperature

(d) an exposure to the vacuum and to the temperature.

Space Environment on the V side of the COMES experiment:

Atomic Oxygen, atoms cm^{-2}	$1.2x10^{18}$ to $7.5x10^{19}$ (1)
Solar UV (esh)	2850(2)
Temp. Cold case (°C)	-60 to -70
Temp. Hot case (°C)	+10 to +30

(1) Estimated from AO reactivity erosion of Kapton (3.0×10^{-24} $cm^3 atom^{-1}$) and Terphane (PET) (3.0×10^{-24} $cm^3 atom^{-1}$) samples

(2) Estimated from data of experiment calorimeter

10.4 BLACK PAINTS

10.4.1 Natural Space Environmental Effects on Black Paints

10.4.1.1 Thermal-Optical Properties

Black paints use carbon as a pigment, which gives them near-unity values of α and ε. The optical properties of black paints are summarized in Table 10-45.[66]

Table 10-45. Optical Properties of Typical Black Paints

Material	Pigment	Binder	α	ε
Chemglaze Z302	Carbon	Polyurethane	0.97	0.91
D-111	Carbon	Silicate	0.98	0.93
Thermatrol	Carbon		0.94	0.92
3M Velvet	Carbon	Polyester	0.95	0.92
Kemacryl	Carbon		0.92	0.92
CAT-A-LAC	Carbon	Epoxy	0.95	0.92
Anodize	Organic Dye	$Al_2O_3+H_2O$	0.8-0.9	0.7-0.9

Table 10-46 is a listing of the expected effects of the natural space environments on these black paints (ref. 68). The net effects of solar UV, Van Allen belts, impact damage, hot plasma, and atomic oxygen will be to reduce α (make the paints less absorptive of sunlight). Only the geomagnetic field and the Earth's ionosphere are not expected to affect these black paints. The organic binders limit the radiation and the proton resistance of these paints.

Table 10-46. Expected Natural Environmental Effects on Black Paints

Material	Sunlight	Vacuum	Van Allen Belts	Objects	Hot Plasma	Gases
Chemglaze	decrease α	Outgas	decrease α	decrease α	decrease α	Erosion, Glow decrease α
Thermatrol	decrease α	Outgas	decrease α	decrease α	decrease α	Erosion, glow decrease α
3M Velvet	decrease α	Outgas	decrease α	decrease α	decrease α	Erosion, glow decrease α
Kemacryl	decrease α	Outgas	decrease α	decrease α	decrease α	Erosion, glow decrease α
Cat-A-Lac-	decrease α	Outgas	decrease α	decrease α	decrease α	Erosion, glow decrease α
Anodize	-	-	-	decrease α	-	

Primary Concern is decrease in α for the following environments:
- Solar UV at all altitudes
- Atomic oxygen in LEO
- Van Allen Belts in MEO
- Hot plasma in GEO

10.4.1.1.1 Effects of Mission Duration

The space environment effects on the optical properties of several black paints on the LDEF satellite are summarized in Table 10-47. These black paints were part of the Thermal Control Surfaces Experiment (TCSE) S0069 experiment. The TCSE experiment combined in-space measurements with extensive post-flight analyses of thermal control surfaces to determine the effects of exposure to the low Earth orbit space environment. The primary TCSE in-space measurement was hemispherical reflectance as a function of wavelength (100 wavelength steps from 250 to 2500 nm) using a scanning integrating sphere reflectometer. The measurements were repeated at preprogrammed intervals over the mission duration. The secondary measurement used calorimetric methods to calculate solar absorptance and thermal emittance from temperature-versus-time measurements.

Table 10-47. Optical Property Variations of Black Paints on LDEF TCSE Experiment

Material	Solar Absorptance (α_s)[a,b,c]				Emittance (ε_N)[d]		
	Pre-flt	In-flt (15 Months)	Post-flt	$\Delta\alpha_S$	Pre-flt	Post-flt	$\Delta\varepsilon_N$
D111 Black	.98	.99	.99	.01	.93	.90	-.03
Z302 Black	.97	.98	.98	.01	.91	.92	.01
Z302 w/OI650	.98	.99	.99	.01	.90	.90	0
Z302 w/RTV670	.98	.99	.99	.01	.91	.90	-.01

(a) Mission Duration: The TCSE operated for 582 days before battery depletion. The battery power was finally expended while the sample carousel was being rotated. This left the carousel in a partially closed position. This carousel position caused 35 of the samples to be exposed for the complete LDEF mission (69.2 months), and 14 exposed for only 582 days (19.5 months) and therefore protected from the space environment for the subsequent four years.

(b) Space Environmental Exposure: The LDEF was deployed with the TCSE located on the leading edge (row 9) and at the Earth end of this row (position A9). In this configuration, the TCSE was facing the ram direction. The LDEF was rotated about the long axis where row 9 was offset from the ram direction by about 8°. The exposure environment for the TCSE were:

Atomic oxygen fluence	8.99×10^{21} atoms/cm^2
Solar UV exposure	11,200 esh
Thermal cycles	~34,000 cycles: -29 to 71 °C, ±11°C (-20 to 160 °F, ±20°F)
Radiation (at surface)	3.0×10^5 rads

(c) The primary TCSE in-space measurement was total hemispherical reflectance as a function of wavelength (100 wavelength steps from 250 to 2500 nm) using a scanning integrating sphere reflectometer. The measurements were repeated at preprogrammed intervals over the mission duration. The secondary measurement used calorimetric methods to calculate solar absorptance and thermal emittance from temperature-versus-time measurements.

(d) Laboratory measurements of spectral reflectance were obtained using Beckman DK-2A spectrophotometer equipment with a Gier-Dunkle 203 mm integrating sphere.

10.4.1.1.2 AO and UV Synergistic Effects

FRECOPA/LDEF and COMES/MIR

Table 10-48 presents the effects of different space environments on the solar reflectance and the emissivity for various black paints on FRECOPA/LDEF and COMES/MIR (ref. 34).

Table 10-48. Solar Reflectance and Emissivity Variations of Black Paints on FRECOPA/LDEF and COMES/MIR

Material	Rs initial	$\varepsilon_{initial}$	AO 138-6 LDEF		COMES/MIR			
			Canister ΔRs	Canister Δε	Face V ΔRs	Face R ΔRs	Face V Δε	Face R Δε
PU1	0.03	0.885	+0.04	-0.002	+0.06	+0.06	+0.032	+0.032
Z306	0.04	0.906	+0.035		+0.06		+0.026	
Cuvertin 306	0.03	0.910			+0.03		+0.025	
VHT SP102	0.05	0.860	+0.013	+0.001				
HT650	0.03	0.873	0.01	— 0.001				
Electrodag 501	0.04	0.791			+0.02		+0.014	
L300	0.05	0.843	+0.035	-0.013				
PNC	0.08	0.796	+0.02	-0.040				
PUC	0.07	0.757			+0.03	+0.01	+0.127	+0.119

Environmental Variations of LDEF and MIR Space Experiments: Due to its position on the trailing edge of LDEF, the AO 138-6 experiment did not receive any oxygen atoms during the mission, with the exception of a short period during the capture when it received a fluence evaluated at 1.32×10^{17} atoms cm^{-2}. The solar illumination was 11,100 equivalent sun hours (esh) for the samples located on the tray and only 1448 esh for the samples inside the canister. The particle irradiation dose (mainly due to the electron flux) was weak: 3×10^{5} rads. The number of temperature cycles was ~34,000 with temperatures within the ranges shown in the table below.

ENVIRONMENT	FRECOPA-LDEF		COMES-MIR	
	CANISTER	TRAY	FACE V	FACE R
Oxygen atoms cm^{-2}	0	1.3×10^{17}	1.2×10^{18} to 7.5×10^{19} (1)	3.5×10^{20} to 5.8×10^{20} (1)
Solar UV (esh)	1448	11,100	2850(2)	1900(2)
Temp. Cold case (°C)	-20 to -26	-43 to -52	-60 to -70	-60 to -70
Temp. Hot case (°C)	+67 to +85	+45 to +63	+10 to +30	+50 to +60

(1) Estimated from AO reactivity erosion of Kapton (3.0×10^{-24} $cm^3 atom^{-1}$) and Terphane (3.0×10^{-24} $cm^3 atom^{-1}$) samples

(2) Estimated from data of experiment calorimeter

Experimental Description. The solar reflection measurements were made with a Beckman DK2A spectrophotometer with an integrating sphere, and the infrared emissivity measurements were made with the Gier & Dunkle DB 100 device. It is important to underline that the measurements were all taken in air on samples which had thus experienced more or less intense recovery of the radiation damage.

MIR/Recoverable Cassette Container-1 (RCC) Experiment

The Russian RCC-1 Thermal Control Coatings experiment contained two black paints, both of which were separately uncovered and protected by quartz glass to the space environment. Tables 10-49 and 10-50 summarize the effects of the space environment on the thermal optical properties of the RCC-1 thermal control coating materials.[67] These materials were exposed to an AO fluence of ~10 x 10^{21} cm^{-2} and ~600 UV esh.

Table 10-49. Space Exposure Effects on the Solar Absorptance of Black Paints on the Mir/RCC-1 Experiment

Reference	Chemical Nature	Condition	Absorptance		
			Pre-Flight	Post-Flight	$\Delta\alpha$
AK-243	Black pigment/acrylic resin	Uncovered	0.98	0.92	-0.06
		Protected by quartz glass	0.98	0.97	-0.01
FP-5246	Black pigment/fluoroplastic solution	Uncovered	0.98	0.96	-0.02
		Protected by quartz glass	0.98	0.98	0.00

Table 10-50. Space Exposure Effects on the Emittance of Black Paints on the Mir/RCC-1 Experiment

Reference	Chemical Nature	Condition	Emittance		
			Pre-Flight	Post-Flight	$\Delta\varepsilon$
AK-243	Black pigment/acrylic resin	Uncovered	0.95	0.94	-0.01
		Protected by quartz glass	0.95	0.95	0.00
FP-5246	Black pigment/fluoroplastic solution	Uncovered	0.92	0.91	-0.01
		Protected by quartz glass	0.92	0.91	-0.01

Both black paints were degraded by space environment exposure. These coatings revealed a significant decrease in solar absorptance. The AK-243 and FP-5246 coatings that were protected by quartz glass did not experience noticeable changes in their characteristics.

10.4.1.2 Mass Loss

Mass loss was observed on the black paints flown on the Russian RCC-1 Thermal Control Coatings experiment, as shown in Table 10-51 (ref. 69). The greatest mass loss was observed on the black paint FP-5246 and is related to the carbon content in the coating pigment binder which is susceptible to AO

Table 10-51. Space Exposure Effects on the Mass Loss of Black Paints on the Mir/RCC-1 Experiment

Reference	Chemical Nature	Condition	Mass (g)		
			Pre-Flight	Post-Flight	Δm mg
AK-243	Black pigment/acrylic resin	Uncovered	4.3839	4.3784	-5.5
		Protected by quartz glass	4.3619	4.3608	-1.1
FP-5246	Black pigment/fluoroplastic solution	Uncovered	4.3783	4.3717	-6.6
		Protected by quartz glass	4.4102	4.4099	-0.3

10.4.1.2 Summary of Flight Experiment Findings

The following are the conclusive findings from flight experiments for black paints:

- D-111 black paint is stable
- Potassium silicate binders are stable (e.g., D-111)
- Organic binders are not stable (e.g., Z302, Z306)

10.4.2 Chemglaze Z302 and Z306 Black Paints

Z302 and Z306 are polyurethane based gloss and flat black paints, respectively.

Both Z302 and Z306 black paints are primarily used for substrates in space applications requiring low outgassing characteristics while providing high thermal absorptivity properties. Both Z302 and Z306 have a high solar absorptance (α_S) of 0.95 ±0.01 and a high room temperature normal emittance (ε_N) of 0.90 ±05. Outgassing measurements according to ASTM E595-77 are %TML = 1.39 and %CVCM=0.01% for Z302, and TML = 1.0, and %CVCM=0.02 for Z306.[68] Z302 has a gloss rating of 93 at an incident angle of 60°, whereas Z306 has a maximum gloss rating of 15 at an incident angle of 85°.

Both Z302 and Z306 are known to degrade moderately under long term UV exposure and to be susceptible to AO that results in erosion of the polyurethane binder and the carbon pigment.

10.4.2.1 Composition

Binder:	Polyurethane
Pigment:	Carbon

10.4.2.2 Source

Manufacturer:	Lord Chemical Products 2000 West Grandview Blvd Erie, PA Telephone. 814 868-3611
Cost:	Z302: $50.40/gallon (1994 prices) Z306: $42.00/gallon (1994 prices)

10.4.2.3 Effects of the Space Environment

10.4.2.3.1 Thermal-Optical Properties

Z302 gloss black paint, flown on the TCSE/LDEF S0069 experiment, was observed to be susceptible to AO interactions that resulted in significant erosion of the polyurethane binder and carbon pigment when not protected from AO effectively. Two of the S0069 Z302 coatings were exposed to the environment for the total 5.8 years of the LDEF mission. These unprotected Z302 sample surfaces eroded down to the primer coat. Two other samples were exposed for only 19.5 months and, while they did erode, still had good solar absorptance properties (ref. 4) as summarized in Table 10-52.[65]

Table 10-52. Optical Properties of Black Paint Z302 on LDEF TCSE Experiment

Material	Solar Absorptance (α_s)[a,b,c]				Emittance (ε_N)[d]		
	Pre-flt	In-flt 15 Months	Post-flt 19.5 Months	$\Delta\alpha_s$	Pre-flt	Post-flt	$\Delta\varepsilon_N$
Z302 Black	.97	.98	.98	.01	.91	.92	.01

(a) Mission Duration: The TCSE operated for 582 days before battery depletion. The battery power was finally expended while the sample carousel was being rotated. This left the carousel in a partially closed position. This carousel position caused 35 of the samples to be exposed for the complete LDEF mission (69.2 months), and 14 exposed for only 582 days (19.5 months) and therefore protected from the space environment for the subsequent four years.

(b) Space Environmental Exposure: The LDEF was deployed with the TCSE located on the leading edge (row 9) and at the Earth end of this row (position A9). In this configuration, the TCSE was facing the ram direction. The LDEF was rotated about the long axis where row 9 was offset from the ram direction by about 8°. The exposure environment for the TCSE were:

Atomic oxygen fluence	8.99×10^{21} atoms/cm^2
Solar UV exposure	11,200 esh
Thermal cycles	~34,000 cycles: -29 to 71 °C, ±11°C (-20 to 160 °F, ±20°F)
Radiation (at surface)	3.0×10^5 rads

(c) The primary TCSE in-space measurement was total hemispherical reflectance as a function of wavelength (100 wavelength steps from 250 to 2500 nm) using a scanning integrating sphere reflectometer. The measurements were repeated at preprogrammed intervals over the mission duration. The secondary measurement used calorimetric methods to calculate solar absorptance and thermal emittance from temperature-versus-time measurements.

(d) Laboratory measurements of spectral reflectance were obtained using Beckman DK-2A spectrophotometer equipment with a Gier-Dunkle 203 mm integrating sphere.

Unprotected samples of Z302 located on the trailing edge of the LDEF AO114 experiment showed considerable change (decrease) in α_s, presumable due to a loss of material even with the reduced AO exposure. The AO114 Z302 sample was completely eroded from the unprotected and uncovered portion of the AO114 sample.

In contrast, Z306 was observed to be optically stable for an A0114 (leading edge) and an A0171 (row 8) sample after 69 months exposure to the LEO environment (see Figure 10-37). However, an A0114 sample and an A0138-6 (FRECOPA) sample, both wake positioned, exhibited solar absorptance changes of about -0.04, as shown in Figure 10-37.

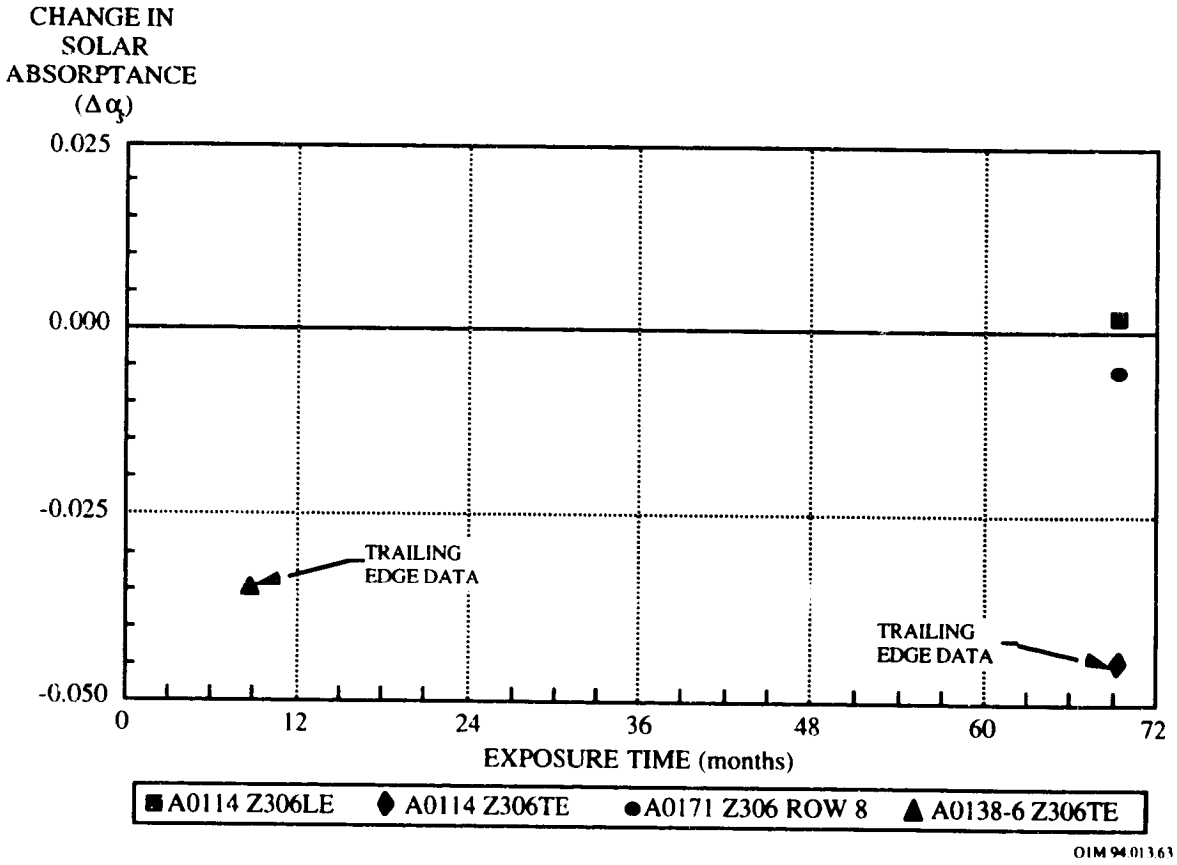

Figure 10-37. Performance of Z306 Black Paint on LDEF - Leading and Trailing Edge $\Delta\alpha_s$ vs. Exposure Time

The Z306 coating on a Kapton substrate experienced more degradation after the 1.1 year COMES/MIR flight experiment (complementary bleaching due to the higher atomic oxygen fluence levels) in comparison to the 9-month exposure in a FRECOPA canister during the LDEF mission, as shown in Table 10-53 (ref. 34). The COMES experiment exposed samples on both sides of four panels, conventionally identified as "V" and "R." Experiment AO 138-6, part of the FRECOPA experiment located on the trailing edge of LDEF, was designed to allow exposure of some of the samples to the whole spacecraft environment by being laid directly on the FRECOPA tray surface, while the remaining samples were protected from the external environment of LDEF for all mission phases, except free flight, by the means of a vacuum-tight FRECOPA canister in which they were stored.

Table 10-53. Solar Reflectance and Emissivity Variations of Z306 Black on FRECOPA/LDEF and COMES/MIR

Type	$Rs_{initial}$	$\varepsilon_{initial}$	AO 138-6 LDEF		COMES	
			Canister ΔRs	Canister $\Delta\varepsilon$	Face V ΔRs	Face V $\Delta\varepsilon$
Black paint	0.04	0.906	+0.035	-0.008	+0.06	+0.026

Environmental Variations of LDEF and MIR Space Experiments: Due to its position on the trailing edge of LDEF, the AO 138-6 experiment did not receive any oxygen atoms during the mission, with the exception of a short period during the capture when it received a fluence evaluated at 1.32×10^{17} atoms cm^{-2}. The solar illumination was 11,100 equivalent sun hours (esh) for the samples located on the tray and only 1448 esh for the samples inside the canister. The particle irradiation dose (mainly due to the electron flux) was weak: 3×10^{5} rads. The number of temperature cycles was ~34,000 with temperatures within the ranges shown in the table below.

ENVIRONMENT	FRECOPA-LDEF		COMES-MIR	
	CANISTER	TRAY	FACE V	FACE R
Oxygen atoms cm^{-2}	0	1.3×10^{17}	1.2×10^{18} to 7.5×10^{19} (1)	3.5×10^{20} to 5.8×10^{20} (1)
Solar UV (esh)	1448	11,100	2850 (2)	1900 (2)
Temp. Cold case (°C)	-20 to -26	-43 to -52	-60 to -70	-60 to -70
Temp. Hot case (°C)	+67 to +85	+45 to +63	+10 to +30	+50 to +60

(1) Estimated from AO reactivity erosion of Kapton (3.0×10^{-24} $cm^3 atom^{-1}$) and Terphane (3.0×10^{-24} $cm^3 atom^{-1}$) samples

(2) Estimated from data of experiment calorimeter

Experimental Description. The solar reflection measurements were made with a Beckman DK2A spectrophotometer with an integrating sphere, and the infrared emissivity measurements were made with the Gier & Dunkle DB 100 device. It is important to underline that the measurements were all taken in air on samples which had thus experienced more or less intense recovery of the radiation damage.

The optical properties of the Z306 black paint on an aluminum substrate on the LDEF satellite are summarized in Table 10-54. This black paint was part of the LDEF experiment S0010, "Exposure of Spacecraft Coatings."[19]

Table 10-54. Optical Property Changes of Z306 Black Paint Exposed on LDEF S0010

Coating	Preflight		10 Months Exposure		5.8 Years Exposure	
	α_S	ε_N	α_S	ε_N	α_S	ε_N
Z306 Black Paint	.926	0.91	.911	0.91	-	-
Chemglaze	.922	0.92	-	-	.902	0.910

Space Environment Exposure Conditions For Tray B on Row 9 of LDEF S0010

Atomic oxygen	8.99×10^{21} atoms/cm^2
UV radiation	100-400 nm; 11,200 hrs
Particulate radiation	e- and p+: 2.5×10^5 rad surface fluence Cosmic: 10 rads
Vacuum	1.33×10^{-4} - 1.33×10^{-5} N/m^2 (10^{-6} - 10^{-7} torr)
Thermal cycles	~34,000 cycles:-29 to 71 °C, ±11°C (-20 to 160 °F, ±20°F)

Chemglaze Z306 black paint was used as the primary thermal control coating on all LDEF interior structural members and experiment tray bottoms. The Z306 measurements taken from the LDEF interior gave an average α/ε of 0.96/0.92 with a small variation of $\pm$0.01 for both α and ε. The Z306 showed good durability on the interior surfaces of the LDEF, but these surfaces were not subjected to direct AO and UV exposure (see Table 10-55).[69]

Table 10-55. Absorptance and Emittance Post Flight Results for LDEF Chemglaze Z306 Black Paint.

Location on LDEF	Atomic Oxygen atoms/cm^2	Description	No. of Samples	α_S (1)	ε_N (2)	α/ε
E-9 Leading Edge	8.99×10^{21}	Black w/primer visible	3	.91 ±.06	.93 ±.01	.98
LDEF Interior	None	Black	5	.96 ±.01	.92 ±.01	1.04

(1) Solar Reflectance: Devices & Services Solar Reflectomerter SSR-ER, Ver. 5.0
(2) Infrared Reflectance: Gier Dunkle Infrared Reflectometer DB-100, Normal Emittance

The Z306 thermal control coating was exposed on the leading edge module of LDEF Experiment A0034.[20,70] Cumulative exposure to solar radiation was restricted by geometry of the coating compartments and apertures from the unobstructed mission integrated level. Based on the restricted field-of-view (approximately 25 degrees) and estimates of coating UV sensitivity the estimated level of solar UV irradiation to specimens of A0034 was 1500 equivalent sun hours. Table 10-56 summarizes the space environmental conditions for this experiment. Each module of this experiment housed 25 specimens of thermal control coatings in a sandwiched array of aperture compartments. The module mounted on the leading edge of the LDEF provided direct exposure to the combined space environment, including atomic oxygen. Additional levels of control for analysis were included by sealing the apertures of selected specimen compartments in each module with quartz windows and metal covers. The windows were intended to exclude atomic oxygen while transmitting damaging solar ultraviolet radiation. The metal covers provided controlled exposure to space vacuum in the absence of atomic species and all but the most energetic of space radiation.

Table 10-56. Space Exposure Conditions of LDEF Experiment A0034

LDEF Position		Atomic Oxygen atoms/cm^2	Ultraviolet esh	Vacuum
Leading Edge	Open	9.0×10^{21}	1500	Yes
	Quartz Window	-	1500	Yes
	Metal Cover	-	-	Yes

The LEO environment effects on the solar absorptance and on the infrared emittance of the Z306 black paint are summarized in Table 10-57. The visual appearance and optical properties of the polyurethane coatings exposed under open apertures on the leading edge were little changed despite the erosion of binder material by atomic oxygen. Observations of fluorescence changes induced in the exposed coatings provide additional evidence of environmental interaction. An olive-green fluorescent emission was observed in specimens of Z306 black absorber coatings exposed under open or quartz windowed apertures, in contrast to the unexposed control material which was not visibly fluorescent. The intensity of the stimulated glow was comparatively weak for the specimen exposed under the window, and the coloration was only observed when the specimen was viewed at a small angle.

Table 10-57. LDEF Leading dge Space Exposure Effects on the Solar Absorptance and nittance of Z306 Black Paint

Property	Total Space Exposure[c] (Open)	Control Vacuum Only (Metal Cover)	UV Only (Window)
Infrared Emittance ε_{IR}[a]	0.80	0.84	0.83
Solar Absorptance α_s[b]	0.96	0.95	0.95

(a) Thermal emittance measured with a Gier-Dunkle DB-100 reflectometer
(b) Solar absorptance determined by measuring the spectral diffuse reflectance in the 200-2200 nanometers range using a Varian/Cary 2300 spectrometer
(c) average values on LDEF Leading Edge

10.4.2.3.2 Mass Loss

Mass loss of the Z306 black paint on an aluminum substrate on the LDEF satellite is summarized in Table 10-58. This black paint was part of the LDEF experiment S0010, "Exposure of Spacecraft Coatings."[19]

Table 10-58. Mass Loss of Black Paint Z306 in LDEF Experiment S0010

Materials	Mass Loss[a] mg/cm^2
Z306 on Aluminum	.26
(a) Atomic Oxygen Fluence = 2.6 x 10^{20} atoms/cm^2	

10.4.2.3.3 Coated Z302 Black Paint

In anticipation of erosion effects, protective OI650 and RTV670 coatings were applied over some of the Z302 samples to evaluate their effectiveness. Two of the TCSE Z302 coatings were exposed to the environment for the total 5.8 year LDEF mission. The samples with overcoats of either RTV670 or OI650 showed little change in solar absorptance as shown in Table 10-59. However, the surface of the silicone overcoatings have undergone some significant morphological changes. These changes are demonstrated primarily through the formation of fissures in the silicone likely resulting from the shrinkage of the overcoat material as it lost mass from AO, radiation and general LEO space environmental exposure.

Table 10-59. Optical Property Variations of Coated Z302 Black Paint on LDEF TCSE Experiment

Material	Solar Absorptance (α_s)[a,b,c]				Emittance (ε_N)[d]		
	Pre-flt	In-flt (15 Months)	Post-flt	$\Delta\alpha_S$	Pre-flt	Post-flt	$\Delta\varepsilon_N$
Z302 Black	.97	.98	.98[a]	.01	.91	.92[a]	.01
Z302 w/OI650	.98	.99	.99	.01	.90	.90	0
Z302 w/RTV670	.98	.99	.99	.01	.91	.90	-.01

(a) Mission Duration: The TCSE operated for 582 days before battery depletion. The battery power was finally expended while the sample carousel was being rotated. This left the carousel in a partially closed position. This carousel position caused 35 of the samples to be exposed for the complete LDEF mission (69.2 months), and 14 exposed for only 582 days (19.5 months) and therefore protected from the space environment for the subsequent four years.

(b) Space Environmental Exposure: The LDEF was deployed with the TCSE located on the leading edge (row 9) and at the Earth end of this row (position A9). In this configuration, the TCSE was facing the ram d tion. The LDEF was rotated about the long axis where row 9 was offset from the ram direction by about 8°. The exposure environment for the TCSE were.

Atomic oxygen fluence	8.99×10^{21} atoms/cm^2
Solar UV exposure	11,200 esh
Thermal cycles	~34,000 cycles: -29 to 71 °C, ±11°C (-20 to 160 °F. ±20°F)
Radiation (at surface)	3.0×10^5 rads

(c) The primary TCSE in-space measurement was total hemispherical reflectance as a function of wavelength (100 wavelength steps from 250 to 2500 nm) using a scanning integrating sphere reflectometer. The measurements were repeated at preprogrammed intervals over the mission duration. The secondary measurement used calorimetric methods to calculate solar absorptance and thermal emittance from temperature-versus-time measurements.

(d) Laboratory measurements of spectral reflectance were obtained using Beckman DK-2A spectrophotometer equipment with a Gier-Dunkle 203 mm integrating sphere.

Performance comparison of Z302 and Z302 with overcoats is shown in Figure 10-38.

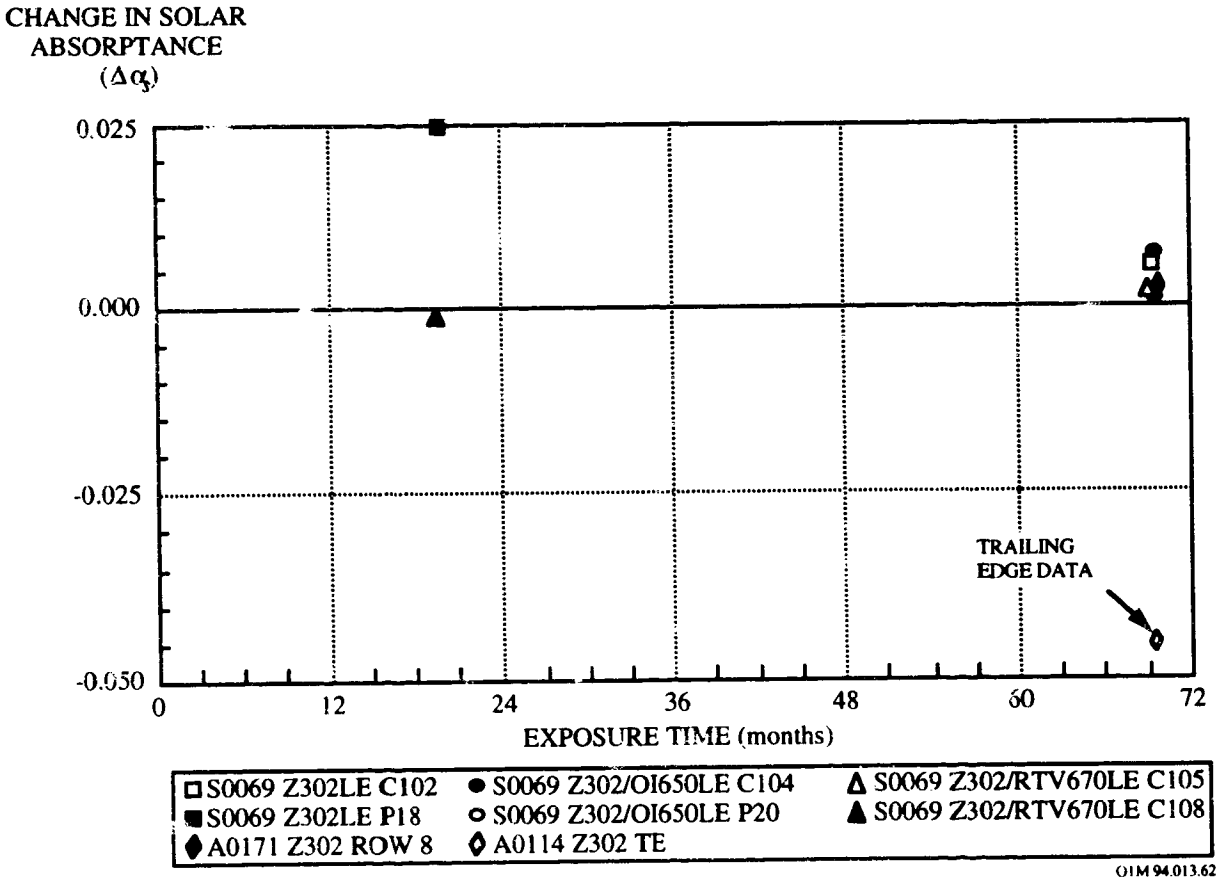

Figure 10-38. Performance of Z302 and Z302 with Overcoats on LDEF - Leading and Trailing Edge $\Delta\alpha_s$ vs. Exposure Time

Z302 with overcoated paints were evaluated on the STS-41G Space Shuttle flight and the results are summarized in Table 10-60.[71]

Table 10-60. Optical Property Variations of Coated Z302 Black Paint on STS-41G

Evaluations	Z302 Glossy Black with OI651 Overcoat	Z302 Glossy Black with RTV-602 Overcoat	Z302 Glossy Black with MN41-1104-0 Overcoat
Exposed flight specimens optical property, absorptivity (α)	.972	.969	.970
Nominal control values of absorptivity (α)	.972	.973	.972
Mass loss of flight specimen due to atomic oxygen exposure	none	negligible	negligible
Comments on Exposure effects	Maintains specular character of Z302	Loss of Z302 specular character	Loss of Z302 specular character

10.4.2.3.4 Design Considerations for the Space Environment

The study revealed that the paint Z306 suffered from long term exposure to the low Earth orbit space environment. The paint polyurethane binders is susceptible to both UV polymerization and AO erosion.

10.4.3 D-111 Black Paint

D-111 black paint, a non-specular black coating, is recommended for applications with small surface areas. It is not recommended for applications with large surface areas.

Thermal properties: $\alpha_s = 0.98 \pm 0.02$; $\varepsilon_N = 0.93 \pm 0.04$

10.4.3.1 Composition

Binder:	Silicate
Pigment:	Carbon

10.4.3.2 Source

Manufacturer:	IIT Research Institute 10 West 35 Street Chicago Illinois 60616 Telephone: 312 567-4432
Cost:	$125/pint

10.4.3.3 Effects of the Space Environment

D111 black coating samples flown on LDEF demonstrated to be relatively stable in both optical properties and appearance in the LEO environment in both the ram and wake orientations. A summary of the performance of the D-111 black paint on both the leading and trailing edge of LDEF is presented in Figure 10-39.

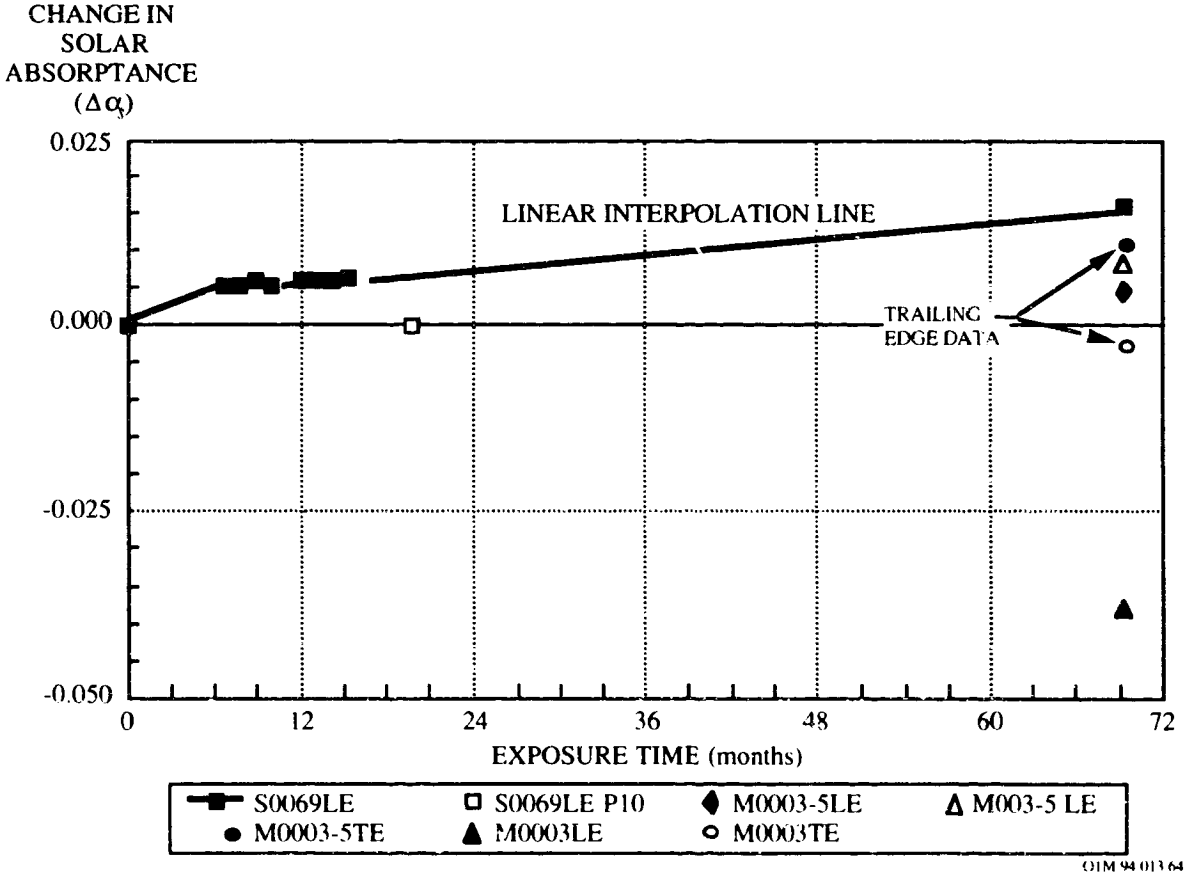

Figure 10-39. Performance of D-111 Black Paint on LDEF - Leading and Trailing Edge: $\Delta\alpha_s$ vs. Exposure Time

This black paint specimens were part of the LDEF Thermal Control Surfaces Experiment (TCSE) S0069 experiment, which combined in-space measurements with extensive post-flight analyses of thermal control surfaces to determine the effects of exposure to the low Earth orbit space environment. The optical properties are summarized in Table 10-61. The D-111 coating was observed to be very stable with exposures to atomic oxygen fluence. This was not expected since the pigment is a carbonous material and one may have expected some AO reaction with the pigment. However it may be assumed that the glass binder effectively protected the pigment from AO interaction.

Table 10-61. Optical Property Variations of Black Paint D-111 on LDEF TCSE Experiment

Material	Solar Absorptance (α_s)[a,b,c]				Emittance (ε_N)[d]		
	Pre-flt	In-flt (15 Months)	Post-flt	$\Delta\alpha_S$	Pre-flt	Post-flt	$\Delta\varepsilon_N$
D111 Black	.98	.99	.99	.01	.93	.90	-.03

(a) Mission Duration: The TCSE operated for 582 days before battery depletion. The battery power was finally expended while the sample carousel was being rotated. This left the carousel in a partially closed position. This carousel position caused 35 of the samples to be exposed for the complete LDEF mission (69.2 months), and 14 exposed for only 582 days (19.5 months) and therefore protected from the space environment for the subsequent four years.

(b) Space Environmental Exposure: The LDEF was deployed with the TCSE located on the leading edge (row 9) and at the Earth end of this row (position A9). In this configuration, the TCSE was facing the ram direction. The LDEF was rotated about the long axis where row 9 was offset from the ram direction by about 8°. The exposure environment for the TCSE were:

Atomic oxygen fluence	8.99×10^{21} atoms/cm^2
Solar UV exposure	11,200 esh
Thermal cycles	~34,000 cycles: -29 to 71 °C, ±11°C (-20 to 160 °F, ±20°F)
Radiation (at surface)	3.0×10^5 rads

(c) The primary TCSE in-space measurement was total hemispherical reflectance as a function of wavelength (100 wavelength steps from 250 to 2500 nm) using a scanning integrating sphere reflectometer. The measurements were repeated at preprogrammed intervals over the mission duration. The secondary measurement used calorimetric methods to calculate solar absorptance and thermal emittance from temperature-versus-time measurements.

(d) Laboratory measurements of spectral reflectance were obtained using Beckman DK-2A spectrophotometer equipment with a Gier-Dunkle 203 mm integrating sphere.

The effects of the low Earth orbit UV radiation and atomic oxygen space environment on the solar absorptance of the black paint D-111 are summarized in Table 10-62. This black paint was located on both the leading and trailing edge of LDEF Experiment M0003 Sub-Experiment 18 (ref. 11). The D-111 coating was stable for both of these positions with the exception of one of the M0003 trailing edge sample. As with the YB-71 black paint, the D-111 remained relatively stable and showed minimal degradation with the different locations on LDEF. This behavior is in contrast to trailing edge samples of A276 which darkened significantly due to UV-induced degradation of the paint's binder, while leading edge samples remained white but exhibited severe atomic oxygen erosion of the binder. Although the response of S13G/LO to low Earth orbit is much more complicated, it also exhibited greater darkening on trailing edge samples as compared to leading edge samples.

Table 10-62. Effects of UV/Atomic Oxygen on the Solar Absorptance of D111 Black Paint

LDEF Location	Space Environment		α_s
	UV (esh)	Atomic Oxygen (atoms/cm^2)	
Control			0.971
D9(LE)	11,200	8.72×10^{21}	0.933
D3(TE)	11,100	1.32×10^{17}	0.968

Note: TE = trailing edge; LE = leading edge

10.4.3.4 Designs Considerations for the Space Environment

D-111 is a diffuse black paint that performed very well with little change in either optical properties or appearance as a result of the LDEF mission.

10.4.4 MH21S/LO and MH21I Black Paints

These paints are ceramic flat, non-specular black coatings. These non-urethane coatings are being considered for space applications where a low- or high-temperature condition exists, and where applications can tolerate a surface coated with a silicone having a unique combination of desirable features. At present, the urethanes are the predominantly used flat-black coating materials because of their ease of application, their durability, their ease of maintenance, and their acceptable optical properties. However, urethane based black coatings have been shown to be susceptible to the atomic oxygen space environment. In addition, these paints replace the D-111 black paint that contains a carbon pigment, which may be susceptible to atomic oxygen erosion effects.

10.4.4.1 Composition

MH21S/LO

Binder:	Silicone
Pigment:	Glass ceramic

MH21I

Binder:	Silicate (Kasil 2130)
Pigment:	Glass ceramic

10.4.4.2 Source

Manufacturer:	IIT Research Institute 10 West 35 Street Chicago Illinois 60616 Telephone: 312 567-4432
Cost:	$950/pint

10.4.4.3 Thermal-Optical Properties.

Figure 10-40 shows the measured reflectance for MH21S/LO at angles varying from 20 to 80 degrees.[72] Optical measurements were performed with a Perkin-Elmer Lambda-9 spectrophotometer, having an accuracy of ±0.02, in accordance with ASTM-E-903. The solar absorptance/reflectance was measured as a function of wavelength and angle of incidence (20, 40, 60, and 80 degrees). The absorptance values at the varying angles were calculated from these measurements, and are also shown in Figure 10-40.

MH21S/LO black paint has a total hemispherical emittance of $\varepsilon_H = 0.86$. This result, shown in Figure 10-41, was obtained using the vacuum calorimetric method as described in NASA Reference Document TND-1716 over a temperature range of -100 to +100°C.

The total normal emittance value, $\varepsilon_N = 0.90$, was measured using a Gier-Dunkel DB-100 infrared reflectometer according to ASTM-408. The emittance represents an integrated value for the 5- to 25-μm wavelengths with a ±0.02 accuracy.

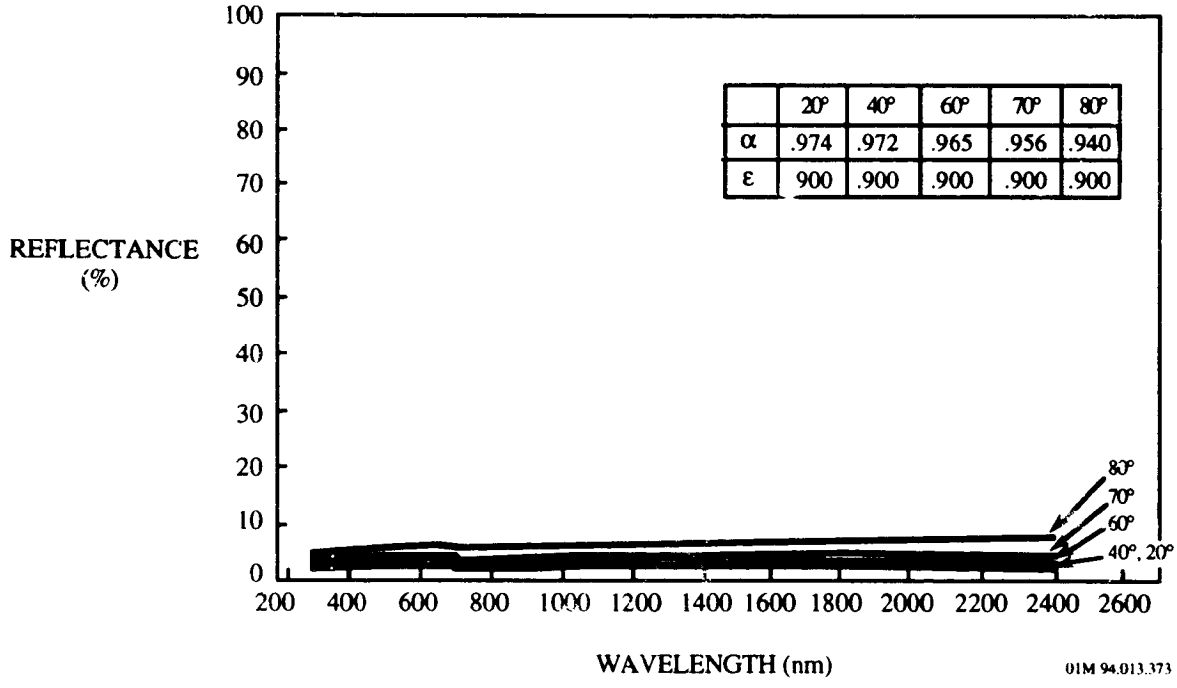

Figure 10-40. Reflectance Measurements of MH21S/LO Silicone Paint from 20 to 80 Degrees as a Function of Wavelength and Angle of Incidence.

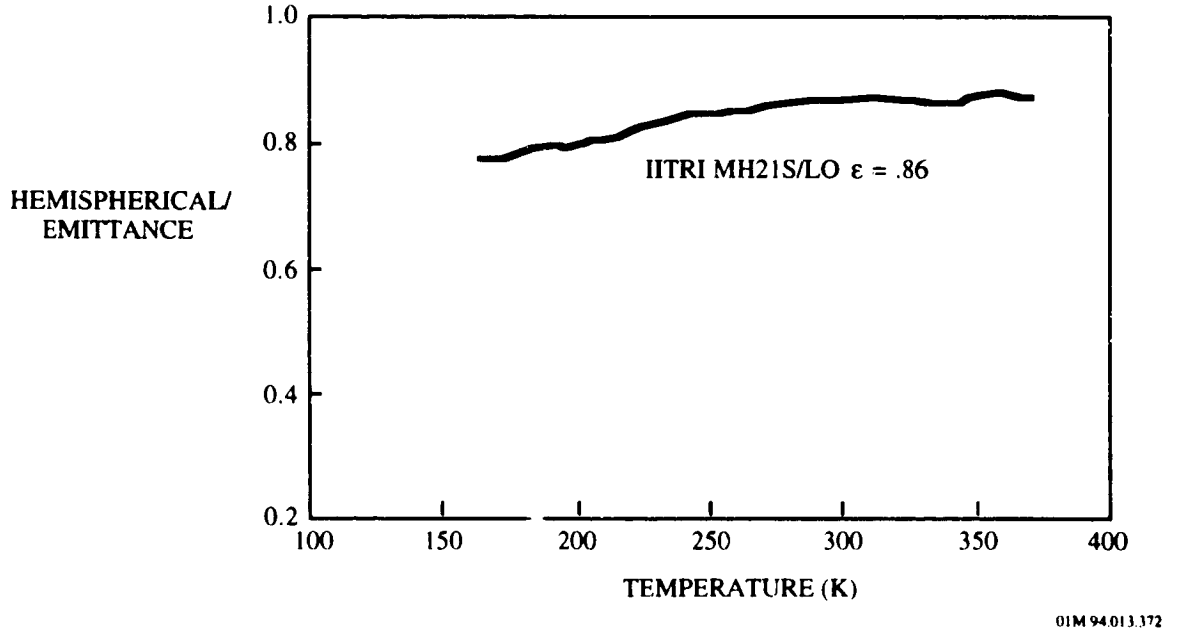

Figure 10-41. Total Hemispherical Emittance vs. Temperature for MH21S/LO Silicone Black Paint

10.4.4.4 Effects of the Simulated Space Environment

10.4.4.4.1 Ultraviolet

A 1,000-hour equivalent sun hours (esh) ultraviolet degradation test was performed on the MH21S/LO black paint at a pressure of 10^{-6} torr with reflectance measurements being made in situ. A Spectrolab X-25 solar simulator using a Xenon lamp with an air-mass-zero filter was used to provide the one-Sun exposure. Reflectance measurements were made in air prior to UV exposure and under vacuum. The measurements in vacuum were made after 100, 200, 500, and 1,000 hours. No change on the reflectance values was observed from the pre-test values. [73]

10.4.4.4.2 Atomic Oxygen Exposure

An atomic oxygen test was performed on the MH21S/LO silicone black paint by exposing it to an anisotropic oxygen plasma to estimate its stability relative to Kapton under the same environmental conditions. The result shown that this black paint is 19 times less affected by the oxygen plasma under the same environmental conditions than Kapton.

10.4.4.4.3 Particle Irradiation

The MH21S/LO silicone black paint was simultaneously exposed to low-energy, 3.5-KeV protons at a fluence level of 3.02×10^{15} p/cm^2, obtained with a flux of 2×10^9 p/cm^2/sec in conjunction with 428 esh of UV exposure. No change or degradation in reflectance was observed.

The MH21S/LO silicone black paint was exposed sequentially to one MeV electron and then to one MeV proton. The fluences were 7.5×10^{13} e/cm^2, obtained with a flux of 4.6×10^{10} e/cm^2/sec, and 1.5×10^{13} p/cm^2, obtained with a flux of 9.29×10^{10} p/cm^2/sec. Reflectances were obtained before and after each exposure. No change or degradation in reflectance was observed.

10.4.4.4.4 Electrostatic Charge

An electrostatic charge test was carried out on the MH21S/LO silicone black paint on a coated 6- by 6-in. aluminum plate. The painted plate, while in vacuum, was irradiated with 10-KeV electrons at a current density of a 10-nA/cm^2 beam from an electron flood gun. The

resulting charge buildup was then measured with a contactless electrostatic probe. The MH21S/LO silicone paint charged to a high 7600 volts. This test measurement gives a relative indication of the sample's propensity for a charge buildup in a space environment.

10.4.4.4.5 Outgassing Test

The outgassing test was performed in accordance with ASTM E-595. The MH21S/LO silicone black paint was spray coated onto primed, thin aluminum foils, then allowed to cure at ambient temperature for a minimum of 7 days. After the high-vacuum exposure at 125°C for 24 hours, the IITRI MH21S/LO silicone black paint exhibited a final TML of 0.19% and a CVCM of 0.01%. These results are based on an average of two test samples. This silicone paint meets the outgassing criteria for space applications with ample margin.

10.4.4.4.6 Surface Contamination Test

The MH21S/LO black paint was tested for surface contamination by using the adhesive tape-lift method to determine the amount and particle size removed from the surface. This paint exhibited clean surfaces with a 300-500 cleanliness class level. The different class levels are described in MIL STD-1246B and the measuring and counting are described in ASTM F24.

10.4.4.4.7 Thermal Cycling

The MH21S/LO silicone black paint was sprayed onto three different substrates: 0.062-in. aluminum 6062; 0.005-in. Kapton H film; and 0.062-in. G-10 epoxy fiberglass. This paint was easily applied to all three primed substrates with a smooth, uniform thicknesses without paint buildup or flow from the surfaces during the application process. An adhesion test was conducted on the substrates after thermal vacuum cycling from -100°C to +150°C for the Kapton and G-10 epoxy fiberglass samples, and from -100°C to +225°C for the aluminum sample. This cycling test was done at a controlled rate of 2°C per minute in a 10^{-6} torr vacuum. None of the test samples showed any crazing or loss of adhesion after 100 cycles in any of the three adhesion tests.

10.4.5 PU1 Black Paint

PU1 is a non-conductive black polyurethane coating.

Thermal properties: $\alpha_s = 0.96 \pm 0.02$; $\varepsilon_H = 0.89 \pm 0.04$

10.4.5.1 Composition

Binder:	Polyurethane
Pigment:	Carbon

10.4.5.2 Source

Manufacturer:	MAP Company Z.I. Chemin de la Rijole 09100 Pamiers, France Tel. 33 61 60 27 00; Fax. 33 61 60 23 30
Cost:	1,520 French francs/K (1994 prices)

10.4.5.3 Effects of the Space Environment

10.4.5.3.1 Thermal-Optical Properties

The PU1 coating showed promise during a 9-month LDEF FRECOPA experiment and during the 1.1 year COMES/MIR flight experiment, as shown in Table 10-63 (ref. 34). The COMES experiment consisted of four panels which were deployed by a cosmonaut in space outside of MIR with the possibility of exposing samples on both sides, conventionally identified as "V" and "R". Experiment AO 138-6 was part of the FRECOPA experiment located on the trailing edge of LDEF. The experiment was designed to allow exposure of a part of the samples to the whole spacecraft environment by being laid directly on the FRECOPA tray surface, while the other part of samples was protected from the external environment of LDEF for all mission phases, except free flight, by the means of a vacuum-tight FRECOPA canister in which they were stored. From Table 10-63, one observes that the black paint deteriorated more for COMES than for FRECOPA (complementary bleaching due to the atomic oxygen).

Table 10-63. Solar Reflectance and Emissivity Variations of PU1 Black Paint on FRECOPA/LDEF and COMES/MIR

Type	Rs initial	$\varepsilon_{initial}$	AO 138-6 LDEF		COMES			
			Canister ΔRs	Canister $\Delta\varepsilon$	Face V ΔRs	Face R ΔRs	Face V $\Delta\varepsilon$	Face R $\Delta\varepsilon$
Black paint	0.03	0.885	+0.04	-0.002	+0.06	+0.06	+0.032	+0.032

Environmental Variations of LDEF and MIR Space Experiments: Due to its position on the trailing edge of LDEF, the AO 138-6 experiment did not receive any oxygen atoms during the mission, with the exception of a short period during the capture when it received a fluence evaluated at 1.32×10^{17} atoms cm^{-2}. The solar illumination was 11,100 equivalent sun hours (esh) for the samples located on the tray and only 1448 esh for the samples inside the canister. The particle irradiation dose (mainly due to the electron flux) was weak: 3×10^5 rads. The number of temperature cycles was ~34,000 with temperatures within the ranges shown in the table below.

ENVIRONMENT	FRECOPA-LDEF		COMES-MIR	
	CANISTER	TRAY	FACE V	FACE R
Oxygen atoms cm^{-2}	0	1.3×10^{17}	1.2×10^{18} to 7.5×10^{19} (1)	3.5×10^{20} to 5.8×10^{20} (1)
Solar UV (esh)	1448	11,100	2850(2)	1900(2)
Temp. Cold case (°C)	-20 to -26	-43 to -52	-60 to -70	-60 to -70
Temp. Hot case (°C)	+67 to +85	+45 to +63	+10 to +30	+50 to +50

(1) Estimated from AO reactivity erosion of Kapton (3.0×10^{-24} $cm^3 atom^{-1}$) and Terphane (3.0×10^{-24} $cm^3 atom^{-1}$) samples

(2) Estimated from data of experiment calorimeter

Experimental Description. The solar reflection measurements were made with a Beckman DK2A spectrophotometer with an integrating sphere, and the infrared emissivity measurements were made with the Gier & Dunkle DB 100 device. It is important to underline that the measurements were all taken in air on samples which had thus experienced more or less intense recovery of the radiation damage.

10.4.6 Cuvertin 306 Black Paint

Cuvertin 306 is a non-conductive black coating.

Thermal properties: $\alpha_s = 0.97 \pm 0.02$; $\varepsilon_H = 0.88 \pm 0.04$

10.4.6.1 Composition

Binder:	Polyurethane
Pigment:	Carbon

10.4.6.2 Source

Manufacturer:	Henckel
	Allemagne, France

10.4.6.3 Effects of the Space Environment

10.4.6.3.1 Thermal-Optical Properties

The Cuvertin 306 coating showed promise during a 9-month LDEF FRECOPA experiment and during the 1.1 year COMES/MIR flight experiment, as shown in Table 10-64 (ref. 34). The COMES experiment consisted of four panels which were deployed by a cosmonaut in space outside of MIR with the possibility of exposing samples on both sides, conventionally identified as "V" and "R". The solar reflectance measurements were made with a Beckman DK2A spectrophotometer with an integrating sphere, and the infrared emissivity measurements were made with the Gier & Dunkle DB 100 device. It is important to underline that the measurements were all taken in air on samples which had thus experienced more or less intense recovery of the radiation damage.

Table 10-64. Solar Reflectance and Emissivity Variations of Cuvertin 306 Black Paint on COMES/MIR

Type	$Rs_{initial}$	$\varepsilon_{initial}$	Face V ΔRs	Face R ΔRs	Face V $\Delta\varepsilon$	Face R $\Delta\varepsilon$
Black paint	0.03	0.910	+0.03		+0.025	

Environmental Variations of MIR Space Experiments:

ENVIRONMENT	COMES/MIR	
	FACE V	FACE R
Oxygen atoms cm^{-2}	$1.2x10^{18}$ to $7.5x10^{19}$ (1)	$3.5x10^{20}$ to $5.8x10^{20}$ (1)
Solar UV (esh)	2850(2)	1900(2)
Temp. Cold case (°C)	-60 to -70	-60 to -70
Temp. Hot case (°C)	+10 to +30	+50 to +60

(1) Estimated from AO reactivity erosion of Kapton (3.0×10^{-24} $cm^3 atom^{-1}$) and Terphane (PET) (3.0×10^{-24} $cm^3 atom^{-1}$) samples

(2) Estimated from data of experiment calorimeter

10.4.7 Electrodag 501 Black Paint

Electrodag 501 is a ceramic non-conductive non-specular black coating.

Thermal properties: $\alpha_s = 0.96 \pm 0.02$; $\varepsilon_N = 0.80 \pm 0.03$

10.4.7.1 Composition

Binder:	Fluorocarbon
Pigment:	Carbon

10.4.7.2 Source

Manufacturer:	Acheson Port Huron, Michigan

10.4.7.3 Effects of the Space Environment

10.4.7.3.1 Thermal-Optical Properties

The Electrodag 501 coating showed promise during a 9-month LDEF FRECOPA experiment and during the 1.1 year COMES/MIR flight experiment, as shown in Table 10-65 (ref. 34). The COMES experiment consisted of four panels which were deployed by a cosmonaut in space outside of MIR with the possibility of exposing samples on both sides, conventionally identified as "V" and "R". The solar reflection measurements were made with a Beckman DK2A spectrophotometer with an integrating sphere, and the infrared emissivity measurements were made with the Gier & Dunkle DB 100 device. It is important to underline that the measurements were all taken in air on samples which had thus experienced more or less intense recovery of the radiation damage.

Table 10-65. Solar Reflectance and Emissivity of Electrodag 501 Black Paint On COMES/MIR

Type	$Rs_{initial}$	$\varepsilon_{initial}$	Face V ΔRs	Face R ΔRs	Face V $\Delta\varepsilon$	Face R $\Delta\varepsilon$
Black paint	0.04	0.791	+0.02		+0.014	

Environmental Variations of MIR Space Experiments:

ENVIRONMENT	COMES/MIR	
	FACE V	FACE R
Oxygen atoms cm^{-2}	$1.2x10^{18}$ to $7.5x10^{19}$ (1)	$3.5x10^{20}$ to $5.8x10^{20}$ (1)
Solar UV (esh)	2850(2)	1900(2)
Temp. Cold case (°C)	-60 to -70	-60 to -70
Temp. Hot case (°C)	+10 to +30	+50 to +60

(1) Estimated from AO reactivity erosion of Kapton (3.0×10^{-24} $cm^3 atom^{-1}$) and Terphane (PET) (3.0×10^{-24} $cm^3 atom^{-1}$) samples

(2) Estimated from data of experiment calorimeter

10.4.8 PUC Black Paint

PUC is a conductive black polyurethane coating.

Thermal properties: $\alpha_s = 0.94 \pm 0.02$; $\varepsilon_H = 0.80 \pm 0.04$

10.4.8.1 Composition

Binder:	Polyurethane
Pigment:	Carbon and graphite

10.4.8.2 Source

Manufacturer:	MAP Company Z.I. Chemin de la Rijole 09100 Pamiers, France Tel. 33 61 60 27 00; Fax. 33 61 60 23 30
Cost:	1,600 French francs/K (1994 prices)

10.4.8.3 Effects of the Space Environment

10.4.8.3.1 Thermal-Optical Properties

The PUC coating showed promise during a 9-month LDEF FRECOPA experiment and during the 1.1 year COMES/MIR flight experiment, as shown in Table 10-66 (ref. 34). The COMES experiment consisted of four panels which were deployed by a cosmonaut in space outside of MIR with the possibility of exposing samples on both sides, conventionally identified as "V" and "R". The solar reflection measurements were made with a Beckman DK2A spectrophotometer with an integrating sphere, and the infrared emissivity measurements were made with the Gier & Dunkle DB 100 device. It is important to underline that the measurements were all taken in air on samples which had thus experienced more or less intense recovery of the radiation damage.

Table 10-66. Solar Reflectance and Emissivity Variations of PUC Black Paint on COMES/MIR

Type	$Rs_{initial}$	$\varepsilon_{initial}$	Face V ΔRs	Face R ΔRs	Face V $\Delta\varepsilon$	Face R $\Delta\varepsilon$
Black paint	0.07	0.757	+0.03	+0.01	+0.127	+0.119

Environmental Variations of MIR Space Experiments

ENVIRONMENT	COMES/MIR	
	FACE V	FACE R
Oxygen atoms cm^{-2}	$1.2x10^{18}$ to $7.5x10^{19}$ (1)	$3.5x10^{20}$ to $5.8x10^{20}$ (1)
Solar UV (esh)	2850(2)	1900(2)
Temp. Cold case (°C)	-60 to -70	-60 to -70
Temp. Hot case (°C)	+10 to +30	+50 to +60

(1) Estimated from AO reactivity erosion of Kapton (3.0×10^{-24} $cm^3 atom^{-1}$) and Terphane (PET) (3.0×10^{-24} $cm^3 atom^{-1}$) samples

(2) Estimated from data of experiment calorimeter

10.5 THERMAL CONTROL BLANKETS

10.5.1 Silver/FEP Teflon

10.5.1.1 Composition

Flexible second surface mirror radiators based on metallic-coated Teflon (FEP) tapes are frequently employed in spacecraft thermal control management applications. Fluorocarbon polymers, i.e., fluorinated ethylene propylene (FEP), have long been considered physically and chemically stable materials suitable for spacecraft applications. By choosing the proper Teflon thickness and the appropriate metal it is possible to specify a thermal control surface within a wide range of α/ε values. Silver Teflon (FEP) tape is a thermal control coating whose high emittance is controlled by the thickness of the Teflon film, and its low solar absorptance (high reflectance) is controlled by a metallic silver second surface. The incident light (solar flux) transmits through the smooth clear Teflon and specularly reflects off the silver layer. Figure 10-42 is a schematic of the silver Teflon thermal control blankets from the LDEF satellite (ref. 24).

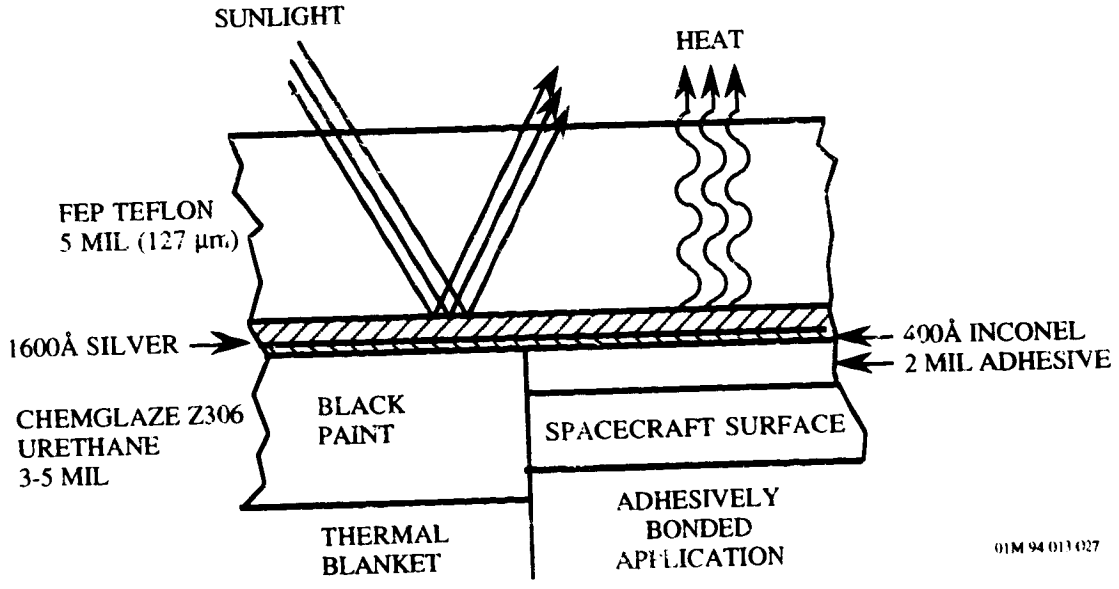

Figure 10-42. Cross-Sectional View of LDEF Silver Teflon Thermal Control Blankets

Figure 10-43 explains the radiation characteristics of the second surface mirror silver Teflon coating.[74] The reflectance of the coating and the transparency of the polymeric film must occur from 0.2 to 3.0 micrometers, the region of maximum solar energy. But the coating is radiating heat away from a spacecraft which has a maximum temperature of about 100°C. Therefore, this energy is found in the infrared from 10 to 50 micrometers. The characteristic absorption bands of polymers provide this infrared emittance.

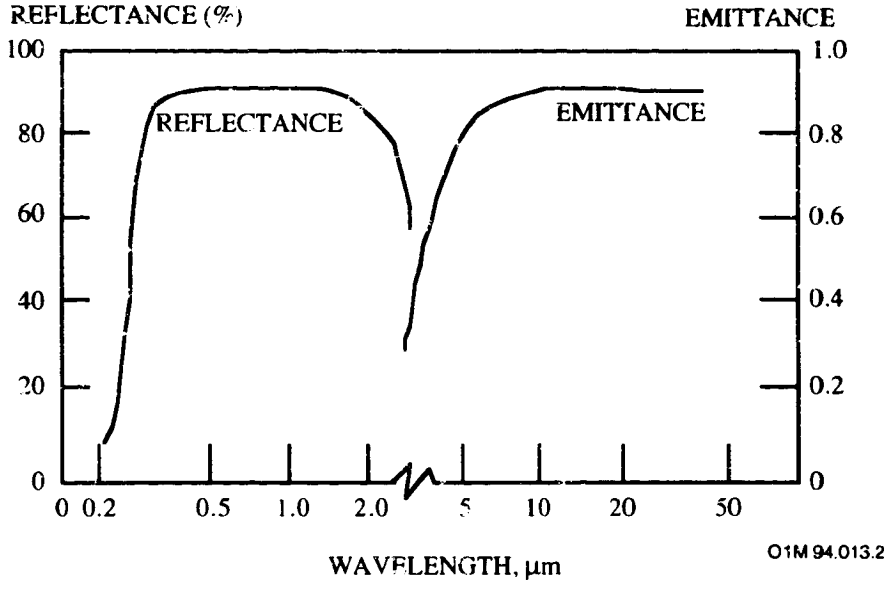

Figure 10-43. Radiation Characteristics of SSM Coating

10.5.1.2 Source

FEP resin is sold in the U.S. under the Teflon trademark by Du Pont Co.

Silver Teflon film is produced by Sheldahl, Northfield, MN (Tel: 507/663-8000).

Table 10-67 shows typical thermo-optical properties of silver Teflon blankets.[75]

Table 10-67. Typical Thermo-Optical Properties of Unexposed Silver/Teflon

Sample Description	α_s (1)	ε_H (2)	α_s / ε_H	Weight gms/in^2
0.5 mil Type A Teflon x vacuum deposited silver x vacuum deposited Inconel	≤0.09	≥0.40	0.17	0.018
1.0 mil Type A Teflon x vacuum deposited silver x vacuum deposited Inconel	≤0.09	≥0.48	0.14	0.035
2.0 mil Type A Teflon x vacuum deposited silver x vacuum deposited Inconel	≤0.09	≥0.60	0.11	0.070
5.0 mil Type A Teflon x vacuum deposited silver x vacuum deposited Inconel	≤0.09	≥0.75	0.09	0.176
7.5 mil Type A Teflon x vacuum deposited silver x vacuum deposited Inconel	≤0.09	≥0.80	0.12	0.264
10.0 mil Type A Teflon x vacuum deposited silver x vacuum deposited Inconel	≤0.09	≥0.85	0.11	0.352
Transparent Conductive Coating x 5.0 mil Type A Teflon x vacuum deposited silver x vacuum deposited Inconel	≤0.14	≥0.75	0.15	0.175

(1) Solar absorptance testing was done with a dual beam, ratio recording Beckman DK-2A UV-VIS-NIR spectrophotometer. Solar absorptance was computed based on 25 equal energy intervals centered on wavelengths from 314 nanometers to 2191 nanometers. These wavelengths are computed from tables of spectra in NASA SP-8005 and ASTM E490-73a.

(2) An approximation to total hemispherical emittance was obtained from a Lion Research Corporation emissometer. This instrument responds to the IR energy emitted from a sample through a potassium bromide window into the detector. The wavelength range is 3-30 microns. This method equates to ASTM E408, Method B.

10.5.1.3 Effects of the Space Environment

Silver Teflon thermal control blankets have been used on many satellites. Extensive data on the performance of this material exist from post-flight analysis of specimens from LDEF, the Solar Max Recovery Mission, and several Space Shuttle experiments.

10.5.1.3.1 LDEF Flight Experiments

The LDEF mission is the source of the most recent data on long-life radiator coatings, particularly for silver Teflon. The available data on silver Teflon from the LDEF experiments are summarized in Table 10-68.

Table 10-68. LDEF Experiments on Silver/Teflon

Organization	Expt No	Title	PI	Ref
Boeing	A0178 P0004-1	Ultra-Heavy Cosmic- Ray Nuclei Experiment Space Exposed Expt Developed for Students	Pippin Crutcher Rousslang	22
Aerospace	A0178 P0004-1 M0003 A0076	Ultra-Heavy Cosmic Ray Nuclei Experiment Space Exposed Expt Developed for Students Aerospace Corp Cascade Variable-Conductance Heat Pipe Expt	Hemminger Stuckey Uht	76
NASA/JPL	A0178 P0004-1	Ultra-Heavy Cosmic- Ray Nuclei Experiment Space Exposed Expt Developed for Students	Brinza Stiegman Staszak Laue Liang	77
ESTEC	A0178	High Resolution Study of Ultra-Heavy Cosmic-Ray Nuclei Experiment	Levadou Froggatt	78
NASA Langley	S0010	Exposure of Spacecraft Coatings	Young Slemp	79
CNES, CERT-DERTS	AO 138-6	FRECOPA	Guillaumon, Paillous	13
NASA Lewis	A0178	High Resolution Study of Ultra-Heavy Cosmic-Ray Nuclei Experiment	Banks Devers Gebauer Hill	80
Thermal Control Properties Group	A0178 P0004-1	Ultra-Heavy Cosmic- Ray Nuclei Experiment Space Exposed Expt Developed for Students	Stein	81
Wright-Patterson	A0178 P0004-1	Ultra-Heavy Cosmic- Ray Nuclei Experiment Space Exposed Expt Developed for Students	Jones	82
NASA Marshall	S0069	Thermal Control Surfaces Experiment (TCSE)	Zwiener	83
AZ Tech/ NASA Marshall	S0069	Thermal Control Surfaces Experiment (TCSE)	Wilkes Brown Hummer Zwiener	4
D R I	M0003-5	Thermal Control Materials Experiment	Hurley	10
NASA Lewis/ OSU/CSU	S1003	Ion Beam Textured and Coated Surfaces Experiment (IBEX)	Mirtich Rutledge Stevens Olle Merrow	84

10.5.1.3.2 Absorptance and Emittance

Solar absorptance and emissivity properties for 127 μm (5 mil) silver Teflon thermal blankets exposed 5 years and 9 months to the LEO environment on the LDEF Thermal Control Surfaces Experiment (TCSE) (ref. 4) did not degrade significantly after exposures to an AO fluence of 8.99×10^{21} atoms/cm^2 and 11,200 esh (see Table 10-69). This experiment was located on row 9 and orientated approximately 8° to the AO ram vector.

Table 10-69. Optical Properties of Silver Teflon on the LDEF TCSE Experiment

	Solar Absorptance (α_s)[a,b,c]				Emittance (ε_N)[d]		
Material	Pre-flt	In-flt (15 Months)	Post-flt	$\Delta\alpha_s$	Pre-flt	Post-flt	$\Delta\varepsilon_N$
Silver Teflon 127 μm (5 mil)	.06	.06	.08	.02	.81	.78	-.03
Silver Teflon 127 μm textured	.07	.08	.10	.03	.82	.79	-.03
Silver Teflon 51 μm (2 mil)	.07	.08	.16	.09	.66	.46	.20

(a) Mission Duration: The TCSE operated for 582 days before battery depletion. The battery power was finally expended while the sample carousel was being rotated. This left the carousel in a partially closed position. This carousel position caused 35 of the samples to be exposed for the complete LDEF mission (69.2 months), and 14 exposed for only 582 days (19.5 months) and therefore protected from the space environment for the subsequent four years.

(b) Space Environmental Exposure: The LDEF was deployed with the TCSE located on the leading edge (row 9) and at the Earth end of this row (position A9). In this configuration, the TCSE was facing the ram direction. The LDEF was rotated about the long axis where row 9 was offset from the ram direction by about 8°. The exposure environment for the TCSE were:

Atomic oxygen fluence	8.99×10^{21} atoms/cm^2
Solar UV exposure	11,200 esh
Thermal cycles	~34,000 cycles: -29 to 71 °C, ±11°C (-20 to 160 °F, ±20°F)
Radiation (at surface)	3.0×10^5 rads

(c) The primary TCSE in-space measurement was total hemispherical reflectance as a function of wavelength (100 wavelength steps from 250 to 2500 nm) using a scanning integrating sphere reflectometer. The measurements were repeated at preprogrammed intervals over the mission duration. The secondary measurement used calorimetric methods to calculate solar absorptance and thermal emittance from temperature-versus-time measurements.

(d) Laboratory measurements of spectral reflectance were obtained using Beckman DK-2A spectrophotometer equipment with a Gier-Dunkle 203 mm integrating sphere.

Typical pre-flight absorptance values for the 127 μm (5 mil) silver Teflon blankets used on LDEF ranged from 0.06 to 0.10. The end-of-life (EOL) solar absorptivity was 0.10, which is less than 0.03 degradation from the pre-flight values. The change in absorptivity is most likely due to UV radiation and a roughening of the surface due to AO. The surface of the silver Teflon radiator underwent significant appearance changes where the surface color was changed to a

diffuse, whitish appearance with brown discoloration. This change was caused by the eroding effect of atomic oxygen and resulted in a rough, light scattering surface. Similar results were observed on LDEF Experiment S0010.[h]

Figure 10-44 shows a long term solar absorptance degradation model for a 127 μm (5 mil) silver Teflon (ref. 4). Spectral analysis and post flight surface analysis have demonstrated the complex nature of the behavior of materials in the space environment, with trends often appearing near the noise level. The models are thus offered for use with caution. In particular, they are viewed as representing the most likely case, not the worst case.

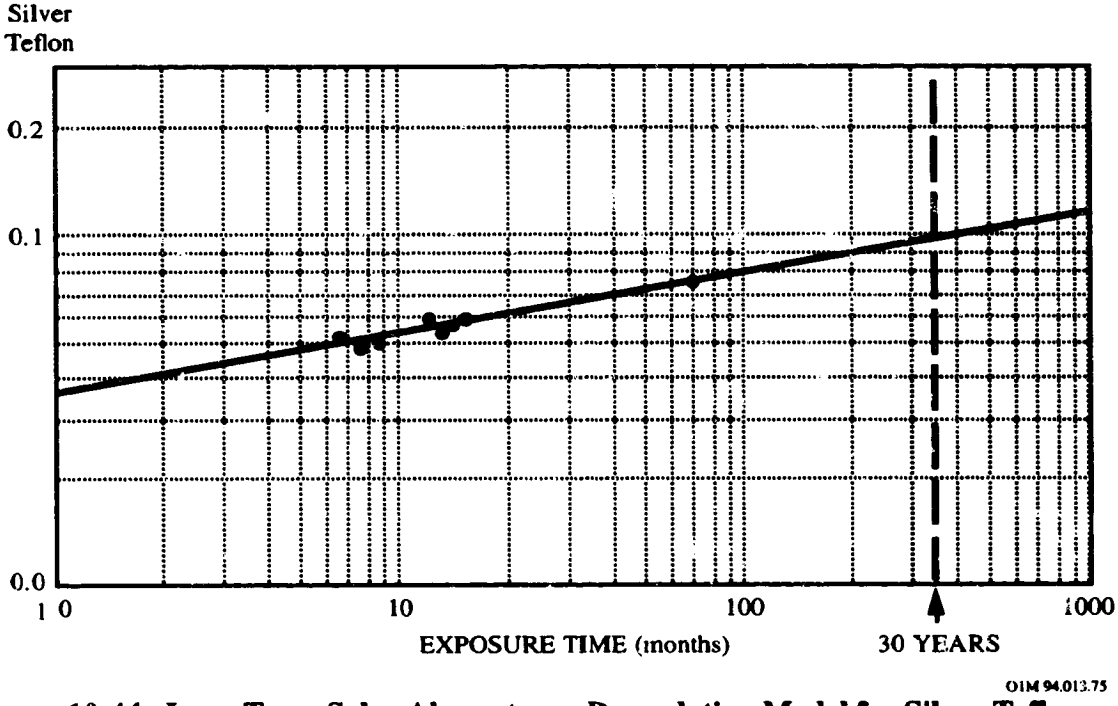

Figure 10-44. Long Term Solar Absorptance Degradation Model for Silver Teflon

---

[h] **LDEF Experiment S0010 Exposure of Spacecraft Coatings.** The effects of the LEO environment during the LDEF mission on the optical properties of silver Teflon flown on LDEF Experiment S0010, Exposure of Spacecraft Coatings, are summarized in the table below. (Ref.: S.W. Slemp and P.R. Young, "LDEF Thermal Control Coatings Post-Flight Analysis," Second Post-Retrieval Symposium, NASA CP 3194, June 1992, pp. 1093-1097). This experiment was located in Tray B on Row 9, the leading edge of LDEF. The experimental canister was opened for 10 months, early in the LDEF mission which allowed flight data to be obtained for 10-month and 5-year 9-month exposures. The silver Teflon retained its initial solar absorptance after 5.8 years of exposure, although the surface roughness increased and the Teflon thickness decreased by 28 μm (1.1 mil).

Coating	Preflight		10 Months Exposure		5.8 Years Exposure	
	α_s	ε_N	α_s	ε_N	α_s	ε_N
Silvered FEP Teflon	.069	0.80	.068	0.80		
127 μm (5 mil)	.070	0.80			.073	0.78

A very slight increase in solar absorptance, α_S, with increasing equivalent sun hours of ultraviolet exposure was observed for the Ag/FEP thermal blankets taken from the LDEF experiment A0178 "A High Resolution Study of Ultra-Heavy Cosmic Ray Nuclei." Table 10-70 summarizes the thermo-optical values measured by Boeing along with the atomic oxygen fluences and equivalent sun hours at the end of the mission for all rows, including the fluence received during the retrieval excursion (ref. 22).

Table 10-70. Absorptance and Emittance of Silver Teflon as a Function of LDEF Location

Blanket No. [b]	Angle off ram	UV esh	AO atom/cm^3	Absorptance [a]		Emittance [a]	
				Exposed	Unexposed	Exposed	Unexposed
D1	111.9°	7400	2.92×10^{17}	0.062	0.063	0.804	0.804
A2	141.9°	9600	1.54×10^{17}	0.073, 0.15 [c]		0.805	
E2	141.9°	9600	1.54×10^{17}	0.067		0.800	
F2	141.9°	9600	1.54×10^{17}	0.062		0.803	
A4	158.1°	10500	2.31×10^{5}	0.087		0.803	
F4	158.1°	10500	2.31×10^{5}	0.064		0.791	
B5	128.1°	8200	9.60×10^{12}	0.062		0.804	
C5	128.1°	8200	9.60×10^{12}	0.065		0.807	
D5	128.1°	8200	9.60×10^{12}	0.062	0.064	0.804	0.799
C6	98.1°	6400	4.94×10^{19}	0.061		0.799	
B7	68.1°	7100	3.39×10^{21}	0.059		0.789	
D7	68.1°	7100	3.39×10^{21}	0.060		0.793	
C8	38.1°	9400	7.15×10^{21}	0.062, 0.24 [c]		0.777	
A10	21.9°	10700	8.43×10^{21}	0.070	0.061	0.776	0.803
E10	21.9°	10700	8.43×10^{21}	0.072		0.779	
C11	51.9°	8500	5.61×10^{21}	0.066		0.786	
D11	51.9°	8500	5.61×10^{21}	0.064		0.799	

(a) The absorptance and emittance values are measured through the Teflon surface. Each value is the average of three measurements.

(b) These blankets were fabricated as follows (from top layer to bottom layer): FEP (4-6 mils); Silver (1600 Å); Inconel (400 Å); and Chemglaze black paint (2-3 mils).

(c) Contaminated specimens.

Measurements of solar absorptance versus equivalent sun hours of ultraviolet exposure made at both ESTEC and Boeing indicated a very slight increase in absorptance with increased solar exposure (see Figure 10-45).[85] It should be pointed out, however, that the absolute error associated with such measurements is at least ±0.02 absorptance units. The differences between the absolute values obtained by the two laboratories are within this error and are most likely due to differences in calibration of the instruments used.

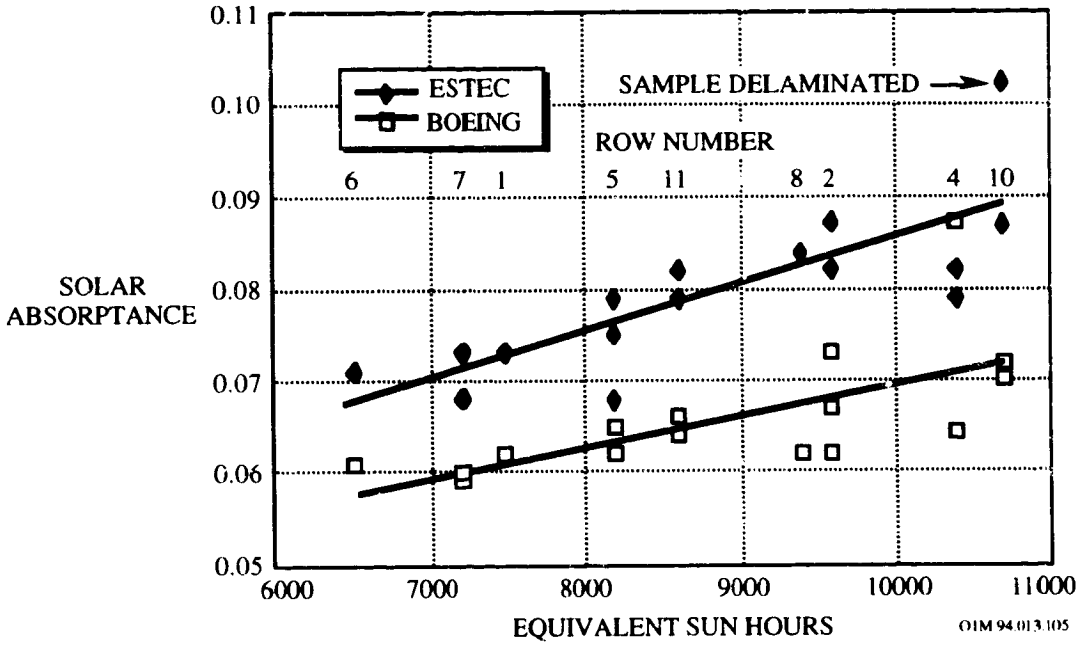

Figure 10-45. Effects of Equivalent Sun Hours on the Solar Absorptance of Silver Teflon

Comparison of the solar absorptance changes for the silver Teflon blankets flown on LDEF with those flown on the STS-8 and the Solar Maximum Mission (SMM) is shown in Figure 10-46. The silver Teflon, used on the SMM spacecraft on a thermal radiator and as trim on louver assemblies,[86] was 127 μm (5 mils) thick with a 150 Å thick layer of silver and a 100 Å thick layer of Inconel. The Teflon side were exposed to the orbit environment with some material exposed on the silver/Inconel side, due to its unique application as trim on the louver system.

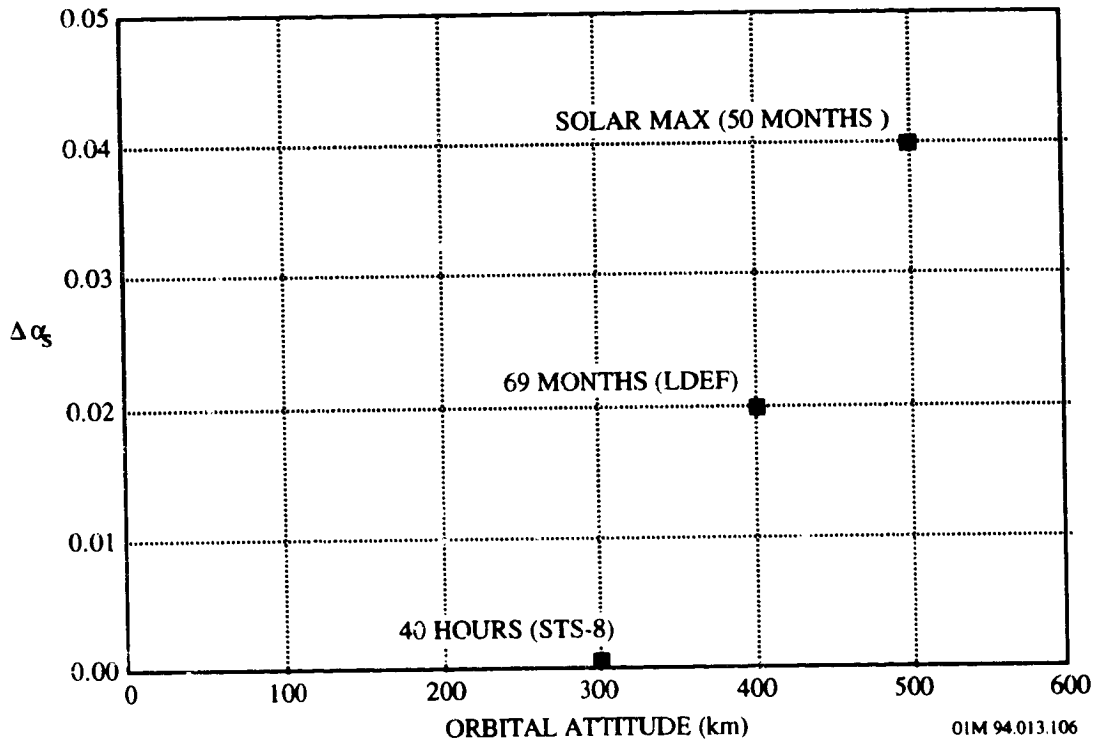

Figure 10-46. Comparison of Solar Absorptance Changes of Silver Teflon on Different Flight Experiments

The solar absorptance of the Teflon film samples with non-eroded silver/Inconel surfaces on the Solar Max increased by a maximum of 0.04. The solar absorptance of the Teflon film prior to on-orbit exposure is typically 0.05 to 0.07. The Teflon samples with the greatest absorptance change were those exposed to the orbit environment on both sides of the film, and those contaminated by spacecraft outgassing. In these samples, the solar absorptance increased by as much as 0.22 to 0.29. This large change in absorptance indicates a potentially large change in the performance of the Teflon film.

Observations of the Teflon exposed surfaces on the Solar Max showed evidence of a reaction to the long duration exposure of the low-Earth orbit environment. Reactions ranged from cracks in the Inconel layer to a total depletion of silver and Inconel. The cracks in the Inconel surface may be due to temperature cycling under varying orbit conditions. Other evidence has indicated that the reaction of Inconel with atomic oxygen causes removal of the Inconel layer. Silver oxide deposits have been found on sample surfaces. The silver oxide may have come to the Inconel surface through the apparent cracks after the exposed silver reacted with atomic oxygen. Exposure tests indicate that the silver/Inconel depletion may be caused by exposure to atomic oxygen alone, or to a combination of atomic oxygen and UV. This suggests a mechanism for the loss of Inconel and silver. First, the atomic oxygen and temperature cycling causes the loss of Inconel and the formation of cracks. Silver oxide (and perhaps silver peroxide) forms and then flakes off in response to temperature cycling. This cycle continues until Teflon is exposed, and the Teflon reacts to atomic oxygen and UV resulting in the formation of the cone structures.[i]

[i] It is important to note that this type of degradation can only occur when the Inconel side is exposed to the atomic oxygen, which is not the intended or normal use of silver/FEP since the a/e of Inconel is about 2.0. In addition, the Inconel is only 200 to 400 Å thick and contain many tiny "pin-holes". Each one of these holes is a potential reaction site for AO oxidation of the silver. This reaction spreads causing release of the silver from the FEP and subsequent release of more Inconel. When sunlight gets to both sides of the silver/FEP as in the Solar Max situation, this all occurs at a very high temperature with the back side having an a/e of 2 and the front side degrading with AO exposure.

The normal emittance measurements of the exposed LDEF 127 μm (5 mil) silver Teflon thermal blankets showed a small but reproducible decrease. As shown in Table 10-70 for the 127 μm thick thermal blanket, an emissivity decrease of only 0.03 from 0.81 to 0.78 occurred for high fluence atomic oxygen exposure (8.99×10^{21} atoms/cm^2), reflecting the slightly decreased thickness of leading edge specimens.

The bonded silver Teflon radiator sample on the LDEF TCSE mission lost 0.025 mm (1 mil) of material from the original thickness of 127 μm. (Silver Teflon is much less susceptible to atomic oxygen erosion than Kapton.) However, a 0.025 mm loss of Teflon from the two mil sample caused a significant loss of emittance (see Table 10-69). Figure 10-47 shows emissivity as a function of thickness.

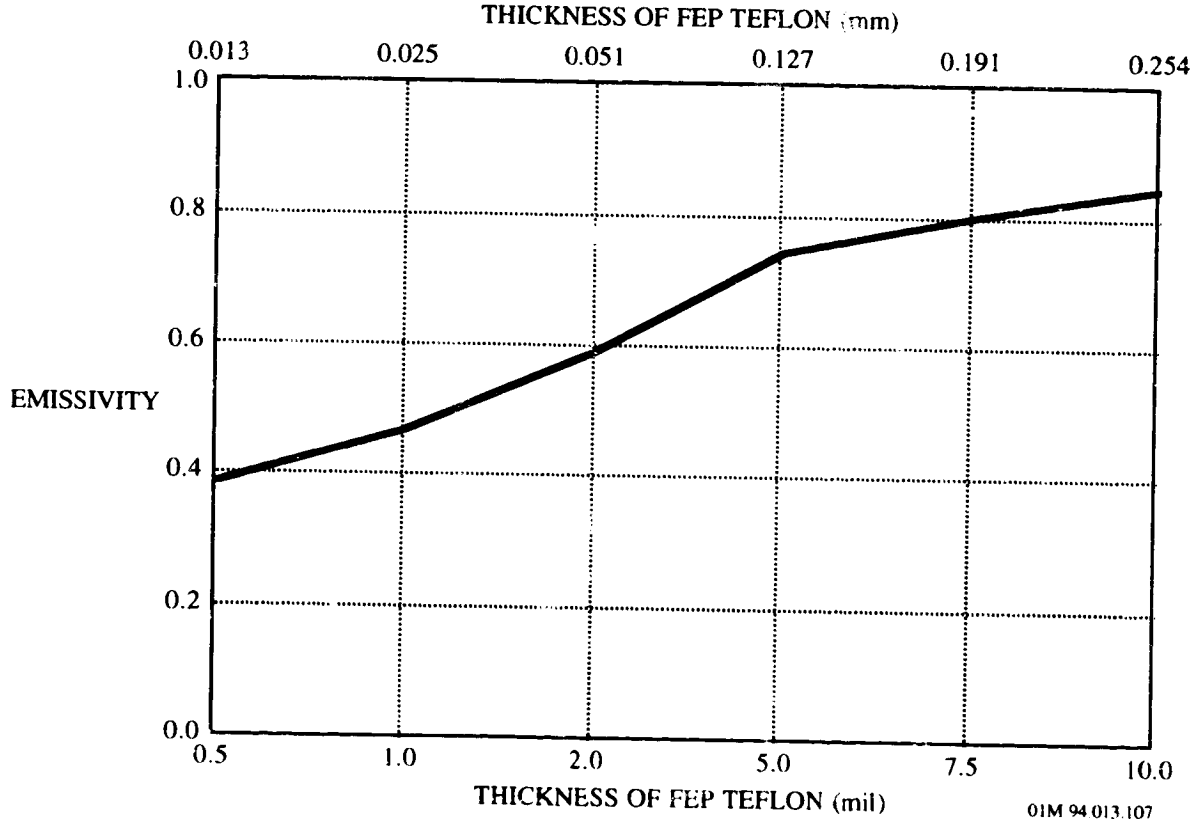

Figure 10-47. Emissivity as a Function of Coating Thickness for Silver Teflon

Small decreases in normal emissivity were also observed on the LDEF FRECOPA[j] and UHCRE experiments.[85] The measurements by ESTEC and Boeing on the UHCRE thermal blankets of rows 1-11 revealed a small decrease as indicated in Figure 10-48. The effect of atomic oxygen on the leading rows (rows 7,8,10,11) to the ram velocity can clearly be seen. The spread in the data is due mainly to initial thickness differences rather than uncertainty in the measurements (the reproducibility of the equipment used, Gier-Dunkle DB 100, is ±0.003).

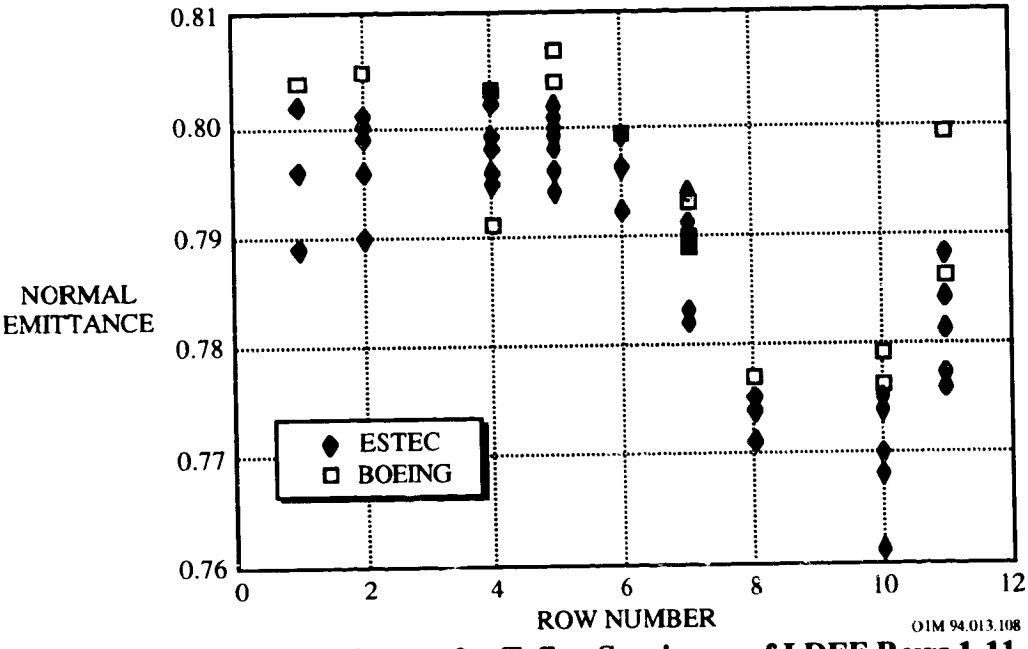

Figure 10-48. Normal Emittance for Teflon Specimens of LDEF Rows 1-11

---

[j] **LDEF Experiment AO 138-6 FRECOPA.** The minimum effect of the LEO environment on the emissivity of silvered Teflon film samples after their flight on FRECOPA (Experiment AO 138-6) (Reference: Guillaumon, J.C., et al., "Spacecraft Thermal Control Coatings", First Post-Retrieval Symposium, NASA CP 3194, pp. 945-960) is shown in the table below. This experiment, located on LDEF trailing edge, exposed a part of the samples to the whole spacecraft environment by being laid directly on the FRECOPA tray surface, while the other samples were protected from the external environment for all mission phases, except free flight, by the means of a vacuum-tight FRECOPA canister in which they were stored.

Material	Mfg.	$\varepsilon_{initial}$	Canister $\Delta\varepsilon$	Tray $\Delta\varepsilon$
Silvered FEP (127 microns)	Sheldahl	0.795		0
Silvered FEP (127 microns) + adhesive	Sheldahl	0.795	0	
Silvered FEP (127 microns)	Sheldahl	0.795	0.001	

Environmental Variations of LDEF Space Experiments: Because of its position on side 3 of the LDEF, the AO 138-6 experiment did not receive any oxygen atoms during the mission, with the exception of a short period during the capture when it received a fluence evaluated at 1.32×10^{17} atoms/cm^2. The solar illumination was 11100 equivalent sun hours (esh) for the samples located on the tray and only 1448 esh for the samples inside the canister. The particular irradiation dose (mainly due to the electron flux) was weak: 3×10^5 rads. The number of temperature cycles was 34000 within the ranges shown.

	CANISTER	TRAY
Oxygen atoms/cm^2	0	1.3×10^{17}
Solar UV (esh)	1448	11,110
Temp. Cold case (°C)	-20 to -26	-43 to -52
Temp.Hot case (°C)	+67 to +85	+45 to +63

The post-flight visual appearance of the low-fluence LDEF surfaces (rows 1-6) was transparent and specular, similar to that of unexposed (control) specimens; the appearance of the high-fluence LDEF surfaces (rows 7-11) was quite different, milky and diffuse due to AO erosion, leading to supposition that the thermal control properties of this widely used second-surface mirror blanket material had been significantly degraded. However a plot of α_s/ε ratios for Ag/FEP samples from a number of LDEF locations disproved this supposition as shown in Figure 10-49,[87] which shows only a slight increase in the absorptance to emittance ratio with increasing solar exposure. Samples from rows 7 through 11 received much higher AO fluences than those from rows 1 through 6 (see Table 10-70), but all samples retained the α_s/ε ratio of control specimens except for one sample from row 8, which had a heavy contamination stain on it. (There is a slight influence of UV irradiation on the solar absorptance which appears to be independent of atomic oxygen erosion.) The visual appearance change of the uncontaminated Ag/FEP was entirely due to a change in reflectance type from specular to diffuse, but not in magnitude of total reflectance (see Section 10.5.1.3.4 below).

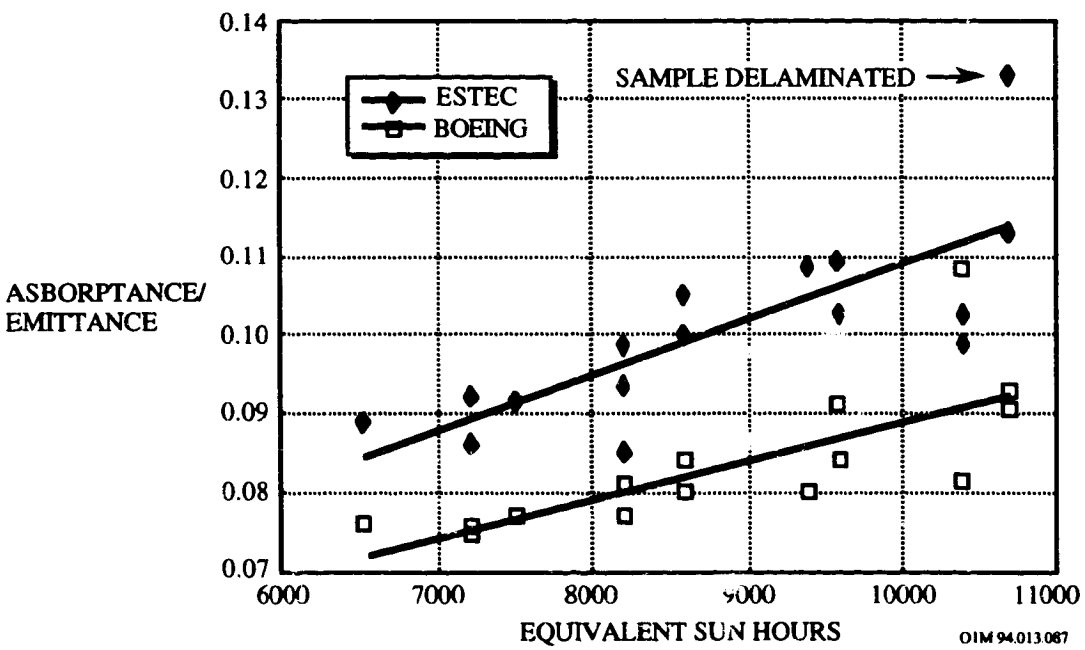

Note: Measurements were made on areas of the blankets free from any noticeable impacts and represent the least damaged areas of the blanket. The fraction of areas punctured and delaminated by impact must be considered when determining the overall thermal efficiency (see Section 10.5.1.3.7).

Figure 10-49. Effects of Equivalent Sun Hours on Absorptance/Emittance Ratios for Silver/Teflon Blankets of LDEF Rows 1-11

10.5.1.3.3 Reflectance

The minimum effects of the LEO environment on the solar reflectance of silver Teflon samples after their flight on AO 138-6 FRECOPA/LDEF and on the 1.1 year COMES/MIR flight experiment (ref. 34) are shown in Table 10-71. Compared to the COMES experiment, the FRECOPA experiment did not receive a high flux of atomic oxygen because of its position on the trailing edge of LDEF.

Table 10-71. Solar Reflectance Variations of Silver Teflon Second Surface Mirrors on the FRECOPA and COMES Experiments

Material	Mfg.	Rs initial	AO 138-6 LDEF		COMES	
			Canister ΔRs	Tray ΔRs	Face V ΔRs	Face R ΔRs
Silver FEP (127 μm)	Sheldahl	0.93		-0.01	-0.03	
Silver FEP (127μm)+adhesive	Sheldahl	0.92	-0.01			
Silver FEP (127 μm)	Sheldahl	0.93	-0.02			

Environmental Variations of LDEF and MIR Space Experiments: Due to its position on the trailing edge of LDEF, the AO 138-6 experiment did not receive any oxygen atoms during the mission, with the exception of a short period during the capture when it received a fluence evaluated at 1.32×10^{17} atoms cm^{-2}. The solar illumination was 11,100 equivalent sun hours (esh) for the samples located on the tray and only 1448 esh for the samples inside the canister. The particle irradiation dose (mainly due to the electron flux) was weak: 3×10^5 rads. The number of temperature cycles was ~34,000 with temperatures within the ranges shown in the table below.

ENVIRONMENT	FRECOPA-LDEF		COMES-MIR	
	CANISTER	TRAY	FACE V	FACE R
Oxygen atoms cm^{-2}	0	1.3×10^{17}	1.2×10^{18} to 7.5×10^{19} (1)	3.5×10^{20} to 5.8×10^{20} (1)
Solar UV (esh)	1448	11,100	2850(2)	1900(2)
Temp. Cold case (°C)	-20 to -26	-43 to -52	-60 to -70	-60 to -70
Temp. Hot case (°C)	+67 to +85	+45 to +63	+10 to +30	+50 to +60

(1) Estimated from AO reactivity erosion of Kapton (3.0×10^{-24} $cm^3 atom^{-1}$) and Terphane (3.0×10^{-24} $cm^3 atom^{-1}$) samples

(2) Estimated from data of experiment calorimeter

Experimental Description. The solar reflection measurements were made with a Beckman DK2A spectrophotometer with an integrating sphere, and the infrared emissivity measurements were made with the Gier & Dunkle DB 100 device. It is important to underline that the measurements were all taken in air on samples which had thus experienced more or less intense recovery of the radiation damage.

Comparison of the reflectance spectra between a control and a LDEF-exposed adhesively bonded silver Teflon samples showed a significantly increased diffuse component, especially in the visible region (400 to 600 nm) for the space exposed specimen. Figure 10-50 compares the reflectance spectra of the control sample and an LDEF exposed silver Teflon specimen.[88] The total reflectance (diffuse plus specular), however, of the two specimens was virtually the same.

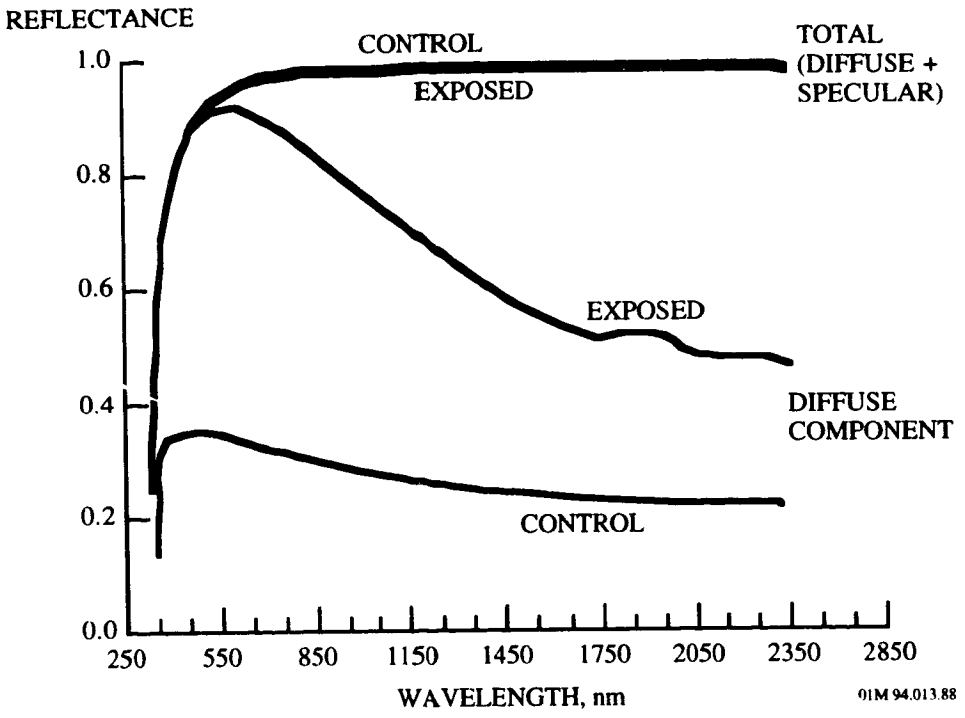

Figure 10-50. Reflectance Spectrum of a Control and a LDEF-Exposed Silver Teflon

Depending on the atomic oxygen fluence, the silver Teflon second surface mirror coating changed from specular reflector of radiation to a diffuse reflector due to surface roughening as revealed by scanning electron microscopy. The diffuse reflectance is extremely low for trailing edge specimens and increases as a function of increased atomic oxygen exposure, until the diffuse component is the major portion of the total reflectance in the visible region of the spectrum. Samples located on rows with high atomic oxygen fluence had a significant increase in diffuse reflectance, compared to those which were unexposed, or exposed to minimal atomic oxygen fluence. The increase in diffuse reflectance caused by the microscopic surface texture produced a milky-appearing diffuse-reflecting surface, as opposed to the original smooth, specular, reflecting surface. Hence, high fluence exposed samples are dominated by diffuse reflectance, whereas low fluence exposed samples are dominated by specular reflectance. For example, compare Figure 10-51 of a Ag/FEP exposed to a low atomic oxygen fluence (1.09×10^{13} atoms/cm^2) to Figure 10-52 of a Ag/FEP sample exposed to a high atomic oxygen fluence (7.78×10^{21} atoms/cm^2).[8] There was little change in total reflectance between high and low fluence atomic oxygen exposure of the silver Teflon samples. Diffuse reflectance measured in the region of the spectrum between 4000 and 5000 nm showed only a slight increase for oxygen exposed specimens relative to solar exposed specimens.

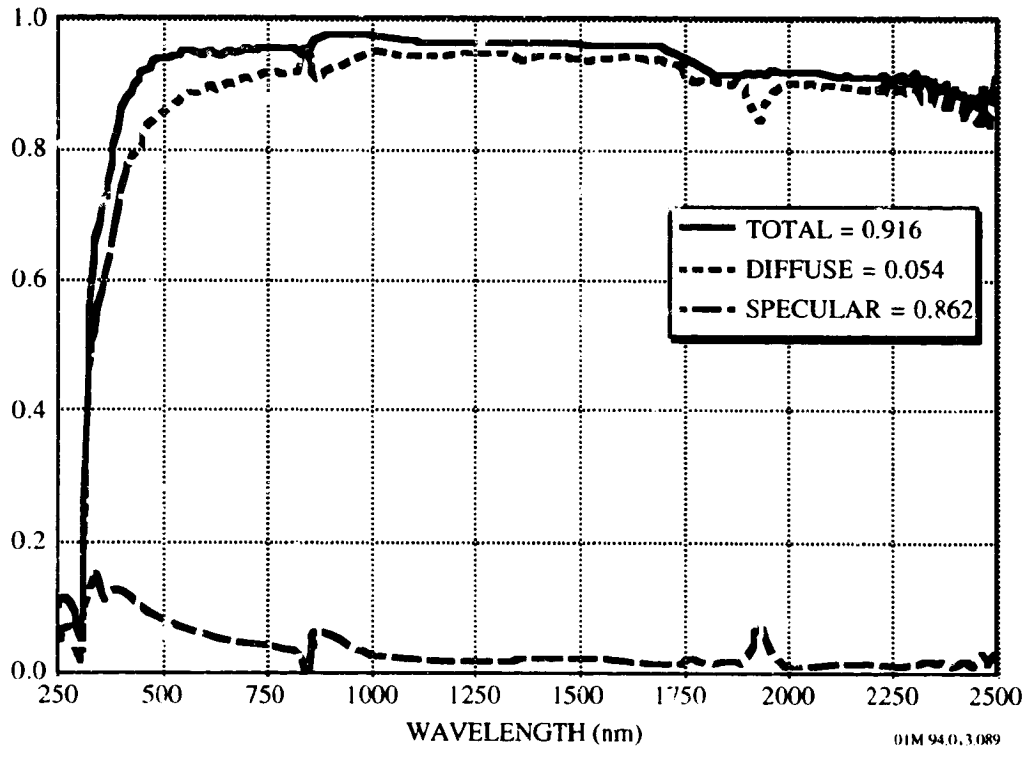

Figure 10-51. Solar Reflectance of Ag/FEP sample exposed to a low AO fluence

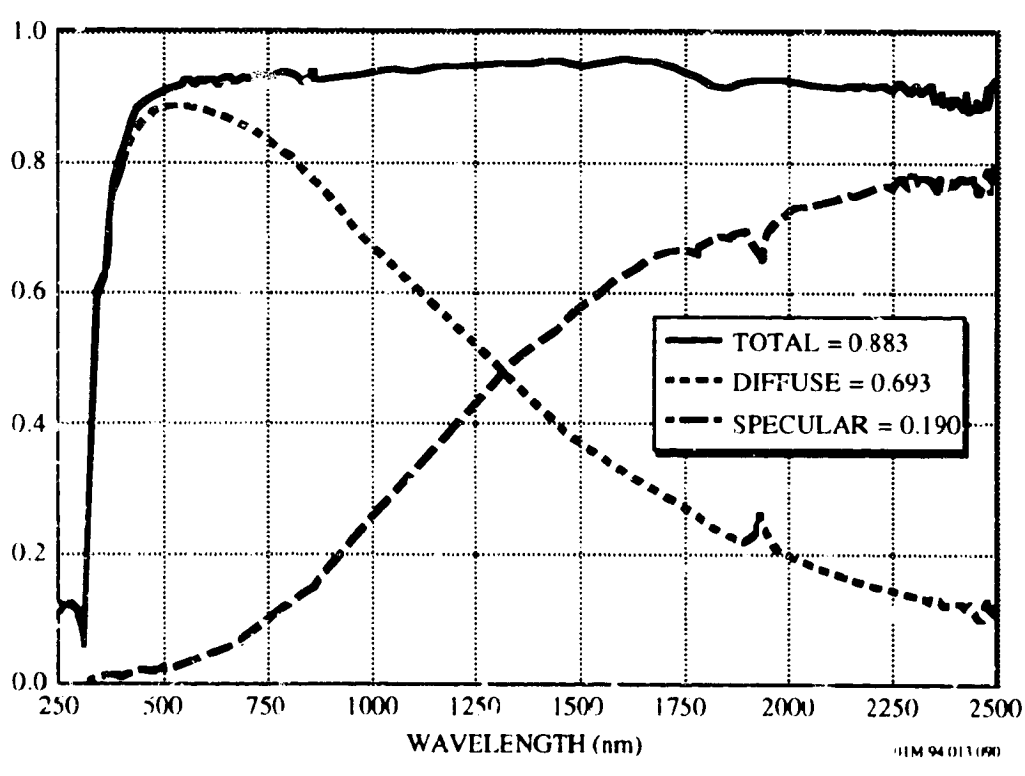

Figure 10-52. Solar Reflectance of Ag/FEP sample exposed to a high AO fluence

Bi-directional reflectance distribution function (BRDF) measurements show a large increase in diffuse reflectance for specimens exposed to AO as shown in Figure 10-53 (ref. 22). BRDF measurements of samples from C11 and A10 are asymmetric due to orientation of the sample with respect to the incident laser beam and the directionality of the roughened surface of these specimens. The surface texturing of blankets exposed to atomic oxygen causes the diffuse appearance of those blankets.

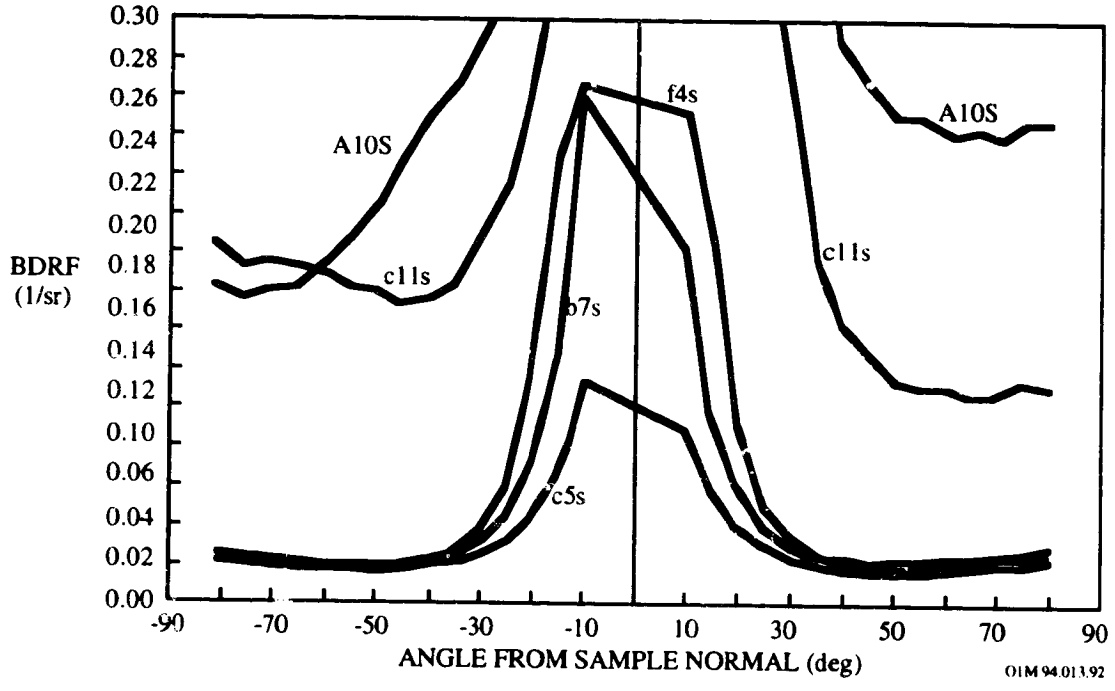

Figure 10-53. BRDF Measurements of Ag/FEP Specimens from Rows 4,5,7,10, and 11

10.5.1.3.4 Atomic Oxygen Erosion Yield and Surface Recession

The predicted average atomic oxygen erosion yield or atomic oxygen reaction efficiency for the Ag/Teflon samples exposed on LDEF is 3.65 $\pm$0.05x10^{-25} cm^3/atom for normal incidence atomic oxygen at ram.[87] Figure 10-54 shows the erosion yield (AO reaction efficiency) for the designated rows versus the cosine of the atomic oxygen atoms incident angle. The angles off ram for each row were: 68° for row 7; 51° for row 11; 38° for row 8; and 21° for row 10. The erosion yield for individual specimen measurements shows a wide range of values within each row, which is attributed to the uncertainty of the initial specimen thickness.[k] The atomic oxygen fluences, which are dependent on atmospheric model density values, have its own uncertainty. The AO erosion yield or reaction efficiency (R_e) is derived by dividing the atomic oxygen recession measurements (Δx) by the atomic oxygen fluence (F_t), i.e., $R_e = \Delta x/F_t$. The best power fit through the mean values for each row gives a power 0.32 of the cos of angle from ram and a value of 3.65 $\pm$0.05x10^{-25} cm^3/atom. This value is about 10 times higher than the recession expected for the LDEF flight based on previous measurements. The power curve 0.5 of the cos of angle from ram, previously reported by B. Banks of NASA LeRC, is also plotted for comparison.[90]

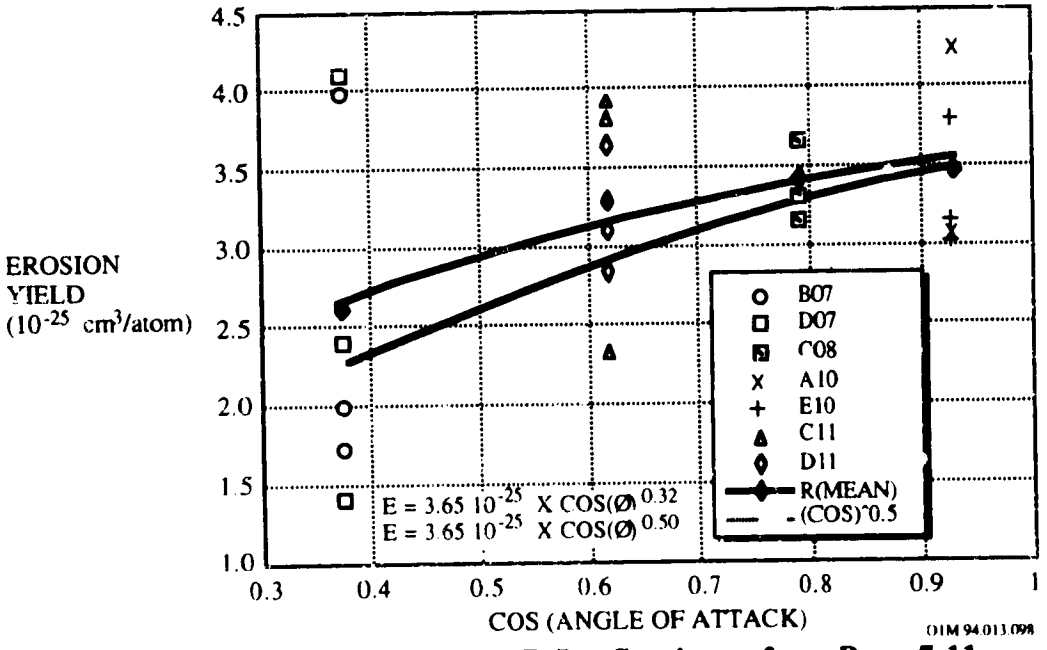

Figure 10-54. Erosion Yield for Teflon Specimens from Rows 7-11.

---

[k] Blanket thicknesses were determined using cross sectional photomicrographs of specimens exposed and unexposed areas from blankets located toward the trailing edge and unexposed areas from blankets located toward the ram direction. The average thickness determined was 5.2 mil

This atomic oxygen erosion yield value is about 10 times higher than the recession value expected for the LDEF flight based on previous low fluence flight data measurements on Space Shuttle flights where exposure levels were near 1.00×10^{20} atoms/cm^2 and < 40 esh solar exposure.[91] The atomic oxygen erosion yield of FEP Teflon has generally been reported to be less than 1×10^{-25} cm^3/atom with the most accepted value being 3.7×10^{-26} cm^3/atom.[90] Thus, with polyimide Kapton H having an erosion yield of 3×10^{-24} cm^3/atom, FEP Teflon was assumed to have an erosion yield of only 1.2% that of Kapton H. Instead, the atomic oxygen erosion yield of FEP Teflon is approximately 12.1% that of Kapton H (see Table 10-72). Hence, this erosion yield or atomic oxygen reaction efficiency determined from the LDEF mission is considerably higher than previous data generated for Ag/FEP material samples exposed for several days at high AO flux in the Space Shuttle Orbiter payload bays during the Space Shuttle missions STS-5 and STS-8.

Table 10-72. Comparative AO Reaction Efficiencies (cm^3/atom) of Teflon and Kapton

Materials	Flight Experiments		
	LDEF	STS-8	Solar Max
Kapton H	3×10^{-24}	3×10^{-24}	3×10^{-24}
FEP Teflon	0.365×10^{-24}	$<0.05 \times 10^{-24}$	–
Silver Teflon	0.365×10^{-24}	-	1×10^{-4}

This lower than expected erosion rate can be attributed to either (1) comparative low fluence exposures of 3.5 x 10^{20} atoms/cm^2 on STS-8, (2) high fluence sweeping atomic oxygen exposure of material which had uncertain surface chemistry due to pre-flight cleaning procedures (Solar Max retrieval), or (3) synergistic effects of UV and atomic oxygen exposures. The STS-8 exposure conditions had a low ratio of solar UV, i.e., < 40 esh, compared to the accelerated atomic fluence of 3.5 x 1020 atoms/cm2, which is equivalent to about one year of AO in nominal LEO orbit. In contrast, LDEF at a 250 nautical mile orbit had exposure conditions of 2.6 x 10^{20} atoms/cm^2 atomic oxygen and 2,300 esh in the first 10 months (Row 9). This information also implies an induction period prior to the onset of significant mass loss due to AO erosion for Ag/FEP thermal blankets in LEO.[92]

The decrease in the thickness of the Teflon film from the leading edge exposed specimens (row 7,8,10,11) on LDEF, on which the erosion yields are based, are plotted as a function of atomic oxygen fluences in Figure 10-55.[93] The thickness of the leading edge exposed specimens measured was determined from the mass measurements and the assumption of 2.15 g/cm^3 FEP density. The data points at the left edge of the graph show the variation in the range of thickness for unexposed specimens from the trailing edge for comparison. This figure shows the correlation between mesurements at ESTEC and Boeing. The fits to the data give recession yields of 3.41 and 3.34 x 10^{-25} cm^3/atom, respectively.

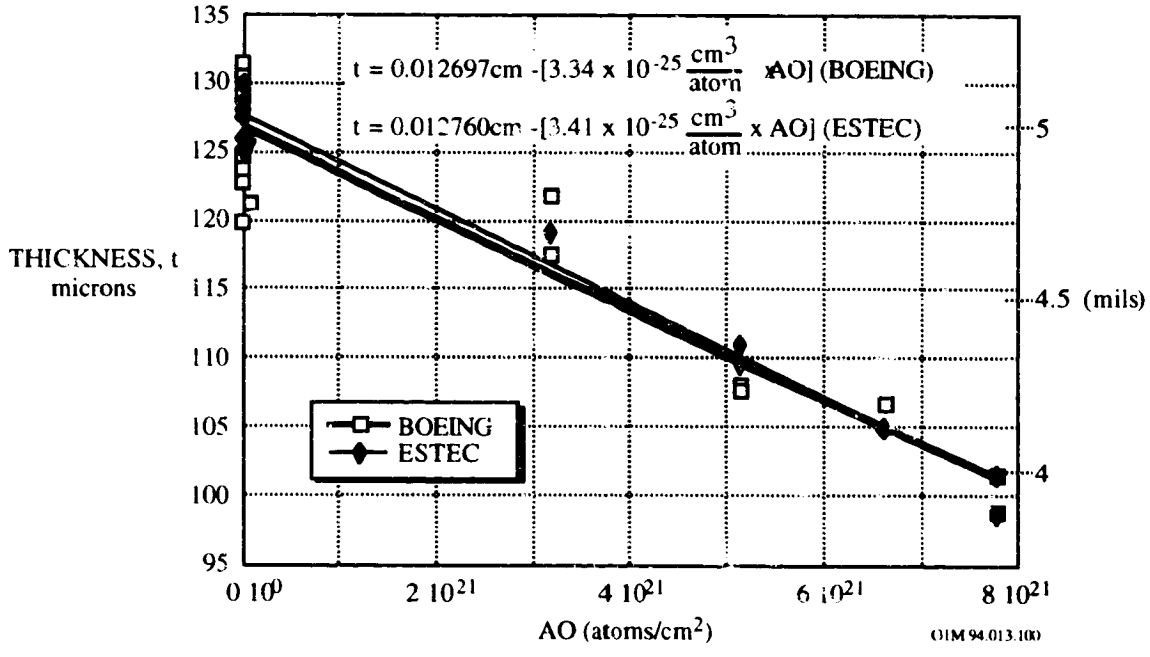

Figure 10-55. Thickness of Teflon from Leading Edge Exposed Specimens

The recession for specimens from rows 7, 8 10, 11 plotted against the angle from ram is shown in Figure 10-56. The angles off ram for each row were: 68° for row 7; 51° for row 11; 38° for row 8; and 21° for row 10. The calculated curve is based on an erosion yield of 3.65 $\pm$0.05x10^{-25} cm^3/atom and the power 1.5 of cos of angle from ram (ref. 99).

The recession of the Teflon layer as a function of cos of angle from ram is plotted in Figure 10-57 (ref. 99). An extrapolation of the plotted power regression curve predicts about 31 microns (1.22 mils) surface recession in the ram direction i.e., cosine

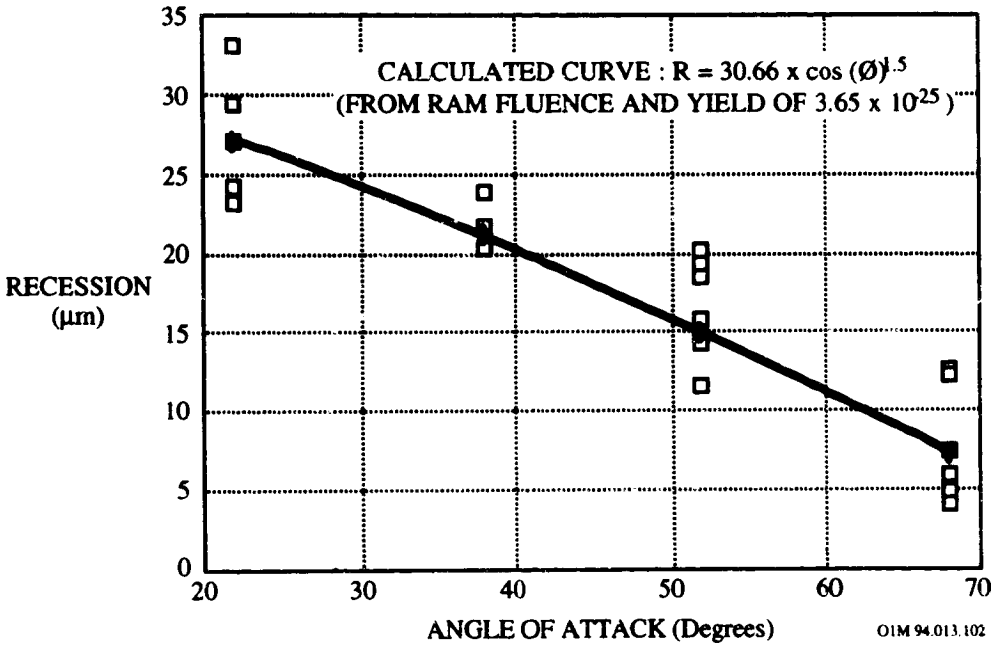

Figure 10-56. Teflon Surface Recession vs Atomic Oxygen Angle of Attack

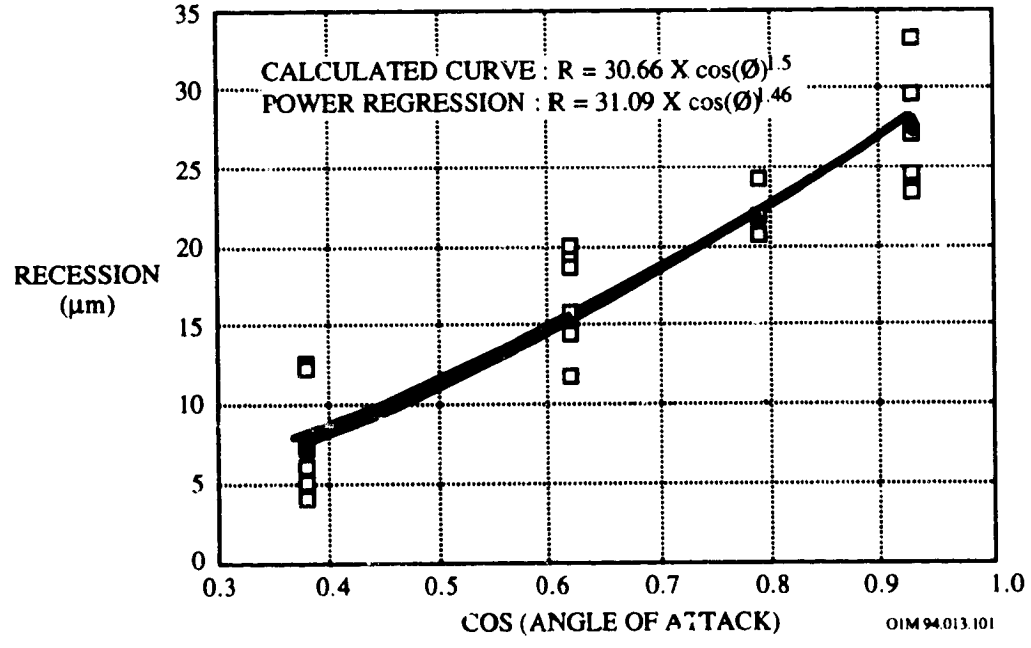

Figure 10-57. Teflon Surface Recession vs. Cosine of AO Attack

The angle of impact of the atomic oxygen affects the rate of surface erosion with an angular sensitivity proportional to the cosine of the angle with respect to the surface normal to the 1.5 power as opposed to the cosine to the 1 power, as would normally be expected. This may be an indicative that highly inclined surfaces may have a higher probability of specular scattering. The Teflon recession rate due to AO exposure was found to have the same general dependence upon angle of arrival of atomic oxygen as Kapton and Mylar, all of which have the $(\cos \phi)^{1/2}$ angular dependence, where ϕ is the angle between the surface normal and atomic oxygen arrival direction.[94] The angular dependence of the erosion yield for FEP Teflon samples flown on the LDEF High resolution Study of Ultra-Heavy Cosmic Ray Nuclei Experiment (A0178) is shown in Figure 10-58.[95] The erosion yield thus follows a $(\cos \phi)^{1/2}$ because the fluence drops off approximately as the cos ϕ (except near 90° where significant differences occur). Thus, it appears that FEP Teflon, similar to Kapton and Mylar, experiences mass loss per unit area dependence upon $(\cos \phi)^{1/2}$. As can be seen from the figure, the predicted FEP Teflon erosion yield for normal atomic oxygen incidence is 3.64×10^{-25} cm^3/atom with an uncertainty of approximately $\pm 0.5 \times 10^{-25}$ cm^3/atom.

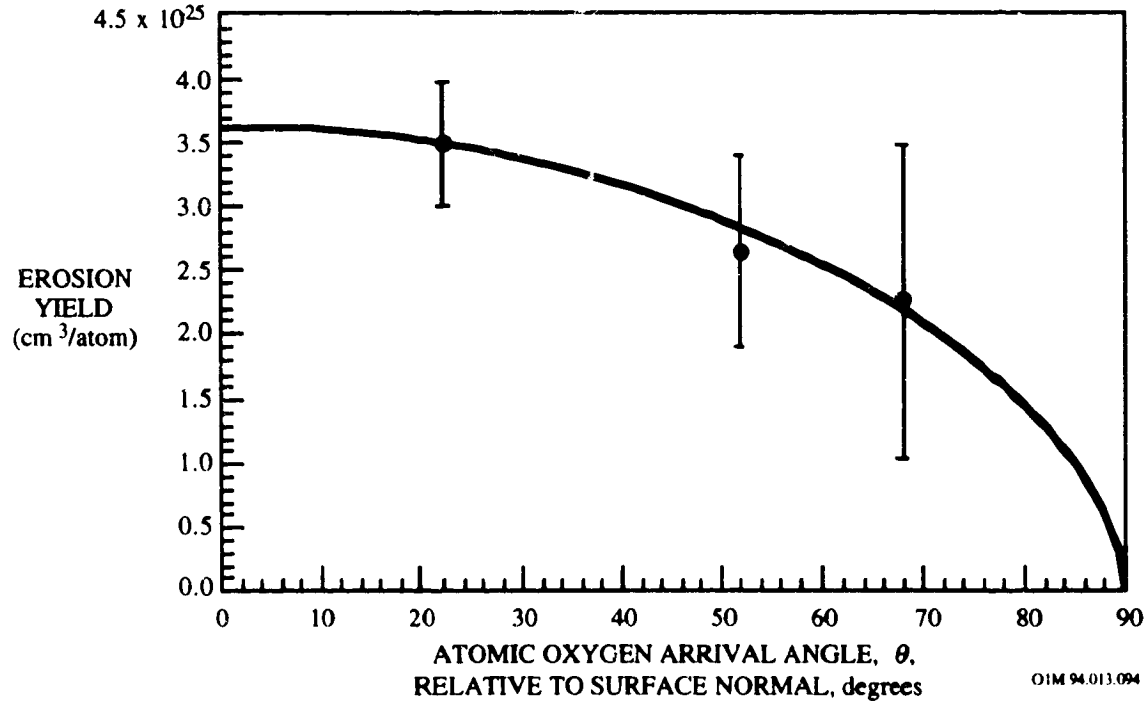

Figure 10-58. Atomic Oxygen Erosion Yield Angular Dependence for FEP Teflon.

10.5.1.3.5 AO and UV Synergism Effects on Surface Recession

The depth of the erosion of the Teflon surface of the Ag/FEP blanket caused by atomic oxygen was approximately ~31 μm (1.2 mil). Based on short-term LEO exposure data in LEO[94], the predicted erosion depth was on the order of ~4 μm (0.15 mil), approximately eight times lower than that measured after the flight. Hence, atomic oxygen erosion of FEP Teflon was higher than that predicted on the basis of short-time LEO exposures. This may be an example of AO/UV synergism wherein a threshold of UV exposure is reached after which the erosion is accelerated, as postulated by Koontz et al.[92]

Ground-based laboratory atomic oxygen exposure of FEP Teflon has generally produced erosion yields which have greatly exceeded those observed in low fluence flight tests. This may have been due in part of synergistic effects associated with significant vacuum UV exposure of the FEP Teflon in ground-based laboratory facilities. Vacuum UV is believed to accelerate the oxidation rate of FEP Teflon in low energy ground-based laboratory facilities.[92] Flight data from a Lockheed experiment, reported in 1985, for atomic oxygen exposures up to 1.85×10^{22} atoms/cm^2 and approximately 300 esh solar UV show an induction period of over a month prior to onset of recession. These results show clearly that UV plays a significant role in altering the FEP surface and allowing increased recession rates over long exposure periods.

Predictions of material lifetime for recession of ram facing surfaces based on LDEF specimens only allows estimates of a lower bound of FEP thickness necessary for long term use (ref. 22). If the recession rate of FEP under combined exposure is controlled by the UV exposure rate, then less than 5 mil thickness loss could be expected over a thirty year period for a ram facing surface. This is based on the observed recession over the 5 year and 10 month exposure and the fact that the solar UV exposure rate should be essentially constant over the 30 year period. If the recession rate is controlled by the atomic oxygen exposure rate, then ~16 mil thickness loss could be expected over thirty years. This prediction is based on Space Station Freedom receiving an estimated ram fluence of 1.5×10^{23} oxygen atoms/cm^2. To maintain constant absorptance and emittance values over this time period would require at least seven mils of FEP. These estimates assume constant rates of degradation. The rate may accelerate given an induction period prior to the onset of the mass loss.

The results demonstrate that UV alone does not cause recession of FEP. It has not yet been determined experimentally that oxygen alone is sufficient or if UV is necessary for erosion to occur. However, it is probable that UV is required, at least initially, to produce sites in the

polymer susceptible to oxidation. Deposited molecular contamination films alter the recession rate by "consuming" oxygen or UV. There is more material with which to react, and formation of oxide films may block attack on the substrate. These effects probably slow the observed recession rate relative to clean material.

In conclusion, the FEP blanket material was effective in protecting the silver second surface mirror for the entire mission. End of life optical properties were unchanged from preflight values and the blankets maintained their mechanical integrity. Expected surface texturing was observed for areas exposed to atomic oxygen. The average recession rate was greater than values reported for experiments flown on Space Shuttle flight.

10.5.1.3.6 Mechanical Properties

The effects of the LDEF environment on the mechanical properties of FEP film taken from the silver Teflon thermal blankets are shown in Figures 10-57 to 10-59, which shows data from films exposed to the space environment and from control specimens flown on LDEF which were protected from the environment.[96]

Individual tensile strength measurements, plotted as a function of atomic oxygen (AO) fluence in Figure 10-59, show essentially two populations: one group of blankets exposed to a high AO fluence showing only small decreases in tensile strength and in percent elongation compared with unexposed specimens from the same blankets; and one group of blankets exposed to low AO fluence showing a 30% decreased in tensile strength and a 25% decrease in percent elongation relative to unexposed specimens.

Blankets exposed simultaneously to solar radiation and atomic oxygen lost mass and became thinner. Although the Teflon surface was eroded by the atomic oxygen exposure on rows 7 to 11 (and thus, the load carrying capability of the film was reduced), the tensile strength was not affected, as shown in Figure 10-60. However, on LDEF rows 1 to 6, where AO fluence was low, exposure to solar ultraviolet and vacuum ultraviolet embrittled FEP, decreasing the percent elongation to failure and the ultimate tensile strength, as shown in Figure 10-61. The implication is that for one group of blankets (i.e., high AO fluence), erosion of the UV-affected surface layer by AO resulted in no degradation of the film strength (based on the remaining cross-sectional area, after erosion), while for the other group (i.e., low AO fluence), the changes in the chemical structure and embrittlement due to the effects of long-term solar ultraviolet radiation has occurred in the bulk of the FEP.

Solar UV radiation of sufficiently short wavelengths has enough energy to break bonds in the FEP backbone and induce crosslinking in the polymer, making it more brittle. Under simultaneous exposure, UV induced bond breaking provides reaction sites for the atomic oxygen to attack the polymer backbone, producing volatile products which then leave, exposing new reaction sites. Similar processes occur with hydrocarbon materials outgassed onto the FEP surface. Brinza et al[77] also presents data on this phenomenon. Polyethylene films on LDEF exhibited similar effects.

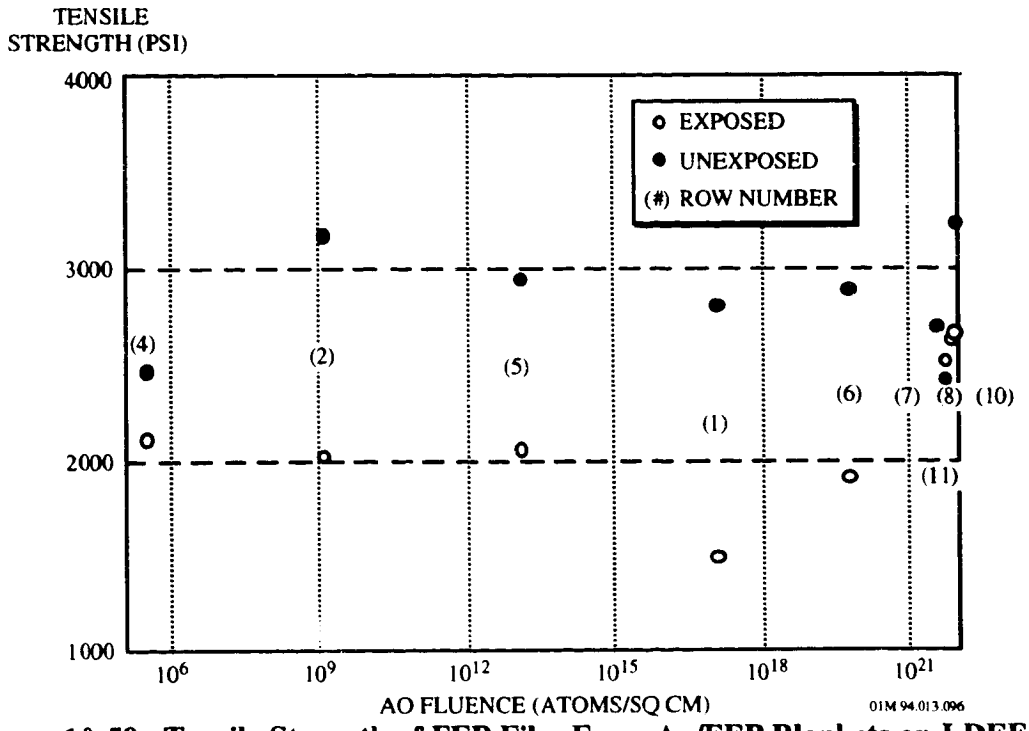

Figure 10-59. Tensile Strength of FEP Film From Ag/FEP Blankets on LDEF as a Function of Atomic Oxygen Fluence

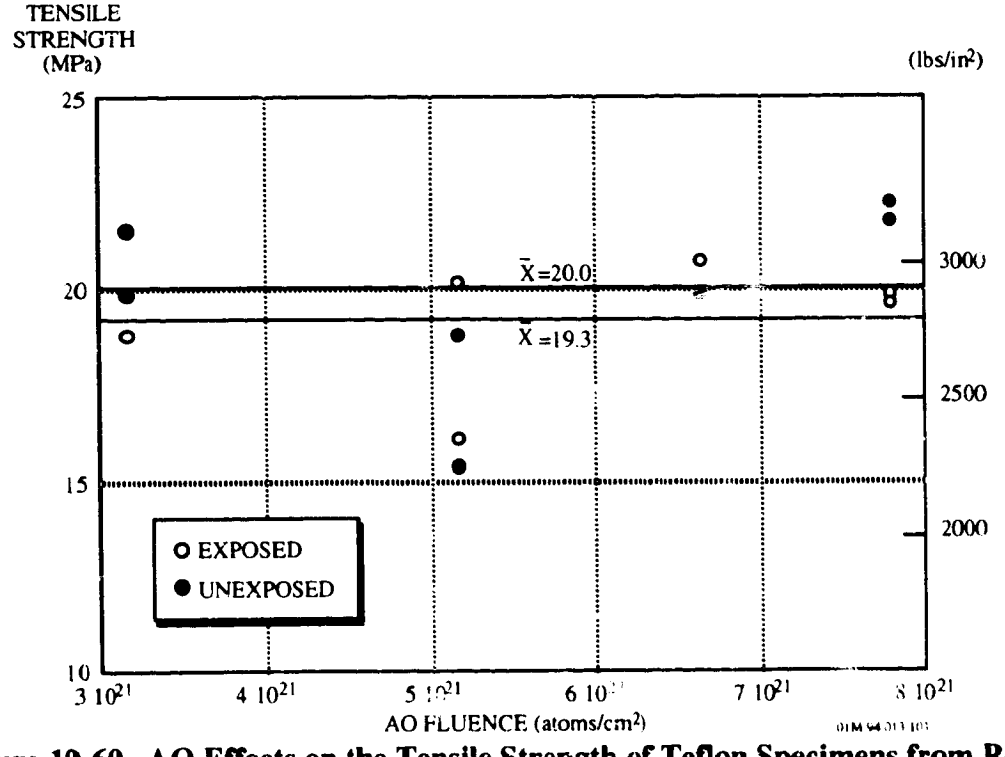

Figure 10-60. AO Effects on the Tensile Strength of Teflon Specimens from Row 7-11.

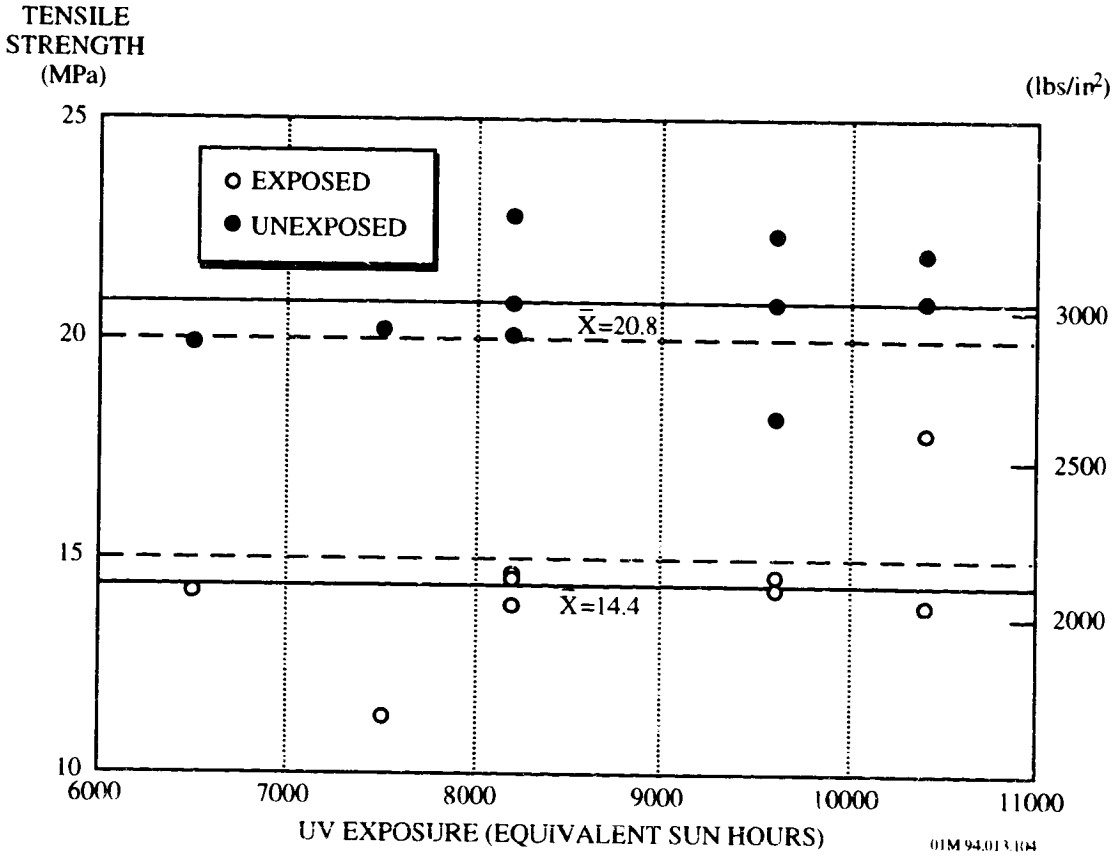

Figure 10-61. UV Effects on the Tensile Strength of Teflon Specimens from Rows 1-6.

10.5.1.3.7 Micrometeoroid and Debris Impacts

Silver Teflon thermal blankets, which covered large areas of LDEF, provided a large data base for determining spall or effective damage area by micrometeoroid/debris impacts. The LDEF A0178 thermal blankets provided a large, uniform meteoroid detection surface randomly spaced around the spacecraft; only Rows 3, 9, 12 did not house an A0178 experiment tray. These blankets were silver Teflon (Sheldahl G411500) with a back surface coating of Chemglaze Z306 black paint. The approximate thickness of the blanket was 200 microns. Table 10-73 describes the number of impacts the M&D SIG identified on each experiment tray surface (excluding the experiment tray bolts, clamps, shims, and flanges).

Table 10-73. M/D Impacts on the Experimental Tray Surfaces of LDEF

Row	Tray	<0.3 mm	>0.3 mm
1	D1	130	11
2	A2	103	7
	E2	87	17
4	A4	49	8
	F4	28	8
5	B5	58	9
	C5	20	8
	D5	228	10
6	C6	-	40
7	B7	376	60
	D7	-	58
8	C8	-	40
10	A10	497	87
	E10	276	121
11	C11	344	48
	D11	320	59

Damage Assessment. The penetrations though the thermal blankets typically possessed a central circular to elliptical-shaped hole surrounded by a raised lip of melted Teflon material. Each of these penetrations was surrounded by an associated delamination zone, a discoloration due to AO exposure of the silver layer, and delamination of the black thermal control paint on the back surface. Commonly the Teflon layer would be separated or delaminated from the underlying layers of the blanket for up to 10 or more penetration hole diameters around the penetration hole. Many penetrations possessed several sharp distinct, colored rings, while others exhibited a more continuous halo phenomenon where the change from one color or ring to another was more

diffuse or gradational. However, all rings/halos were not circular in appearance. These blankets were attached to the trays by velcro, which worked very well. The attachment lasted throughout the entire mission and, in fact, could still be used for attachment off the blankets into their respective carrying cases. When impacts occurred into the velcro which supported the thermal blanket materials, large delamination areas were very common around the penetration.

Figure 10-62 is a schematic of the damage morphology and diameter measurements for impacts into thermal control blankets and laminated materials.[97] This represents the typical damage for silver Teflon blankets (Sheldahl G411500) with a back surface coating of Chemglaze Z306 black paint (e.g., LDEF A0178 thermal control blanket). Impacts on the blankets lead to many penetration through the Teflon, allowing access of AO to the silver layer. Photographs of the impacted A0178 silver Teflon blankets can be found in the LDEF M&D SIG Final Report. The numerous black dots observed on the blankets represent a penetration through the Teflon, allowing access of AO to the silver layer. Instead of being reflective (as on pre-flight) the entire blanket is very milky in color. This is caused by the high amount of light scattering from the newly textured surface of the Teflon. The Teflon surface was textured by AO erosion. The ring structure growing around the smaller penetration due to AO degradation (i.e., discoloration) of the silver, forming a silver oxide area.

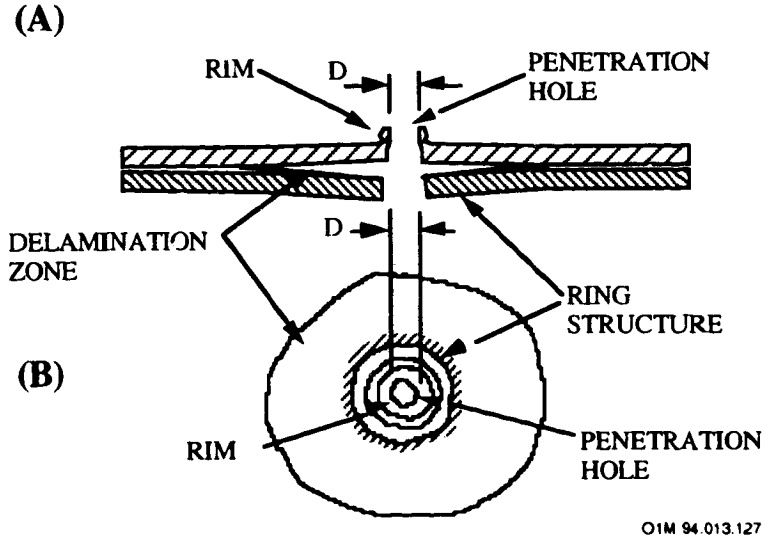

(A) Cross-sectional view depicting the delamination of the Teflon layer from the underlying silver/Inconel/paint surface
(B) Top view showing the extent of the delamination zone and the presence of the "rings" generally found in association with these features.

Figure 10-62. Schematic Diagram of Damage Morphology and Diameter Measurements for Impacts into Thermal Control Blankets and Laminated Materials

Thermal blankets on the trailing edge were not subjected to AO, but instead to UV light which embrittled the Teflon. Without the mitigating effects of the AO erosion, the Teflon became very brittle. While the penetration has the typical raised melted lips and an underlying (but smaller) delamination from the silver and black paint layers, it does not have AO-created rings in the silver. Instead, there are multiple cracks running out from the central penetration hole. These cracks are located in the Teflon, not in the silver or black-painted back surface.

Thermo-Optical Properties. The effects of multiple impact craters to the thermal radiative properties of silver Teflon as a function of time were calculated using an equation based on the fraction of damaged surface area (ref. 52).

$$A_s\,(Beta) = A_o - \left[D_{a,e} * F_a * T_{yr}\right]$$

where:

A_s (Beta, time) absorptance or	=	effective or average value of solar emittance at each Beta angle
Beta	=	degrees from velocity vector or ram direction
A_o	=	solar absorptance or emittance of original coating
$D_{a,e}$	=	difference between coating and substrate absorptance or emittance
F_a	=	fraction of damaged surface area per year
T_{yr}	=	number of years exposed

Changes to the thermal radiative properties of silver Teflon blankets utilized the damaged area measured by Nerren.[98] The percent of area darkened from impacts was analyzed by Nerren & Sullivan.[83] The photograph image of the silver Teflon blanket flown on LDEF Experiment A0178 on row 10E was scanned to determine the damage area. The Ag/FEP blanket analyzed was positioned +22 degrees from the velocity vector. A total of 322 penetrations were counted and their associated darkened area measured. The darkened area included the impact penetration hole area and the discolored area surrounding the impacts, resulting in a 1.44% damaged surface area. The darkened area had a higher solar absorptance than the original Ag/FEP, which increased the overall effective solar absorptance. The overall effect to thermal radiative properties are plotted in Figures 10-63 and 10-64 utilizing the above equation. However, this equation is only an approximation for determining the effective emittance reduction as the delaminated area was greater than the rings or the damaged area as shown in Figure 10-62. This delaminated area represents a "greenhouse effect" where the effective emittance is greatly reduced as no thermal conductance tapes place between the Ag and the FEP.[99]

C-3

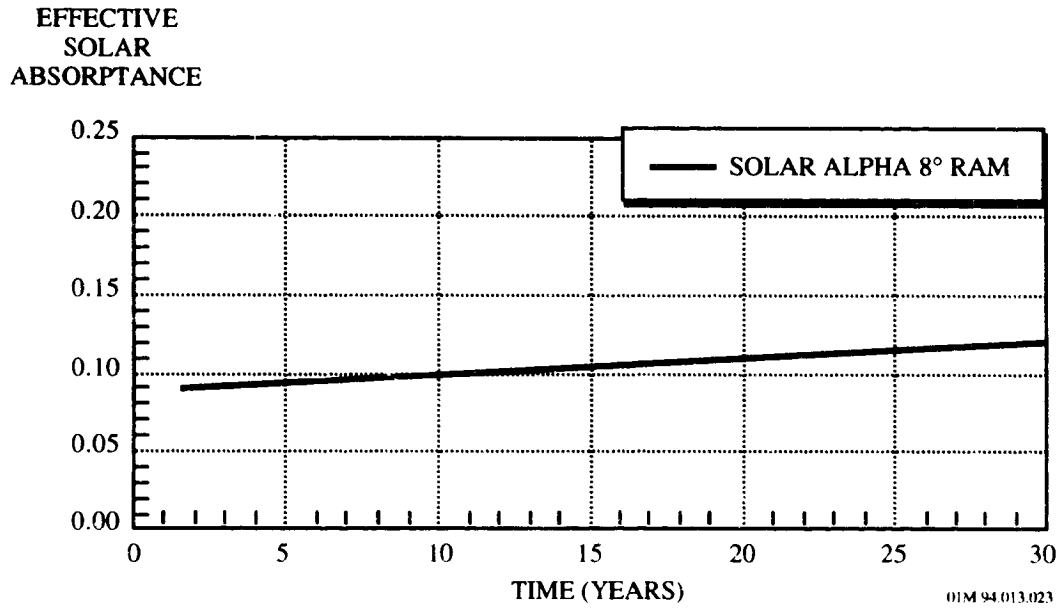

Figure 10-63. Silver/Teflon M/OD Effect on Solar Absorptance vs Time

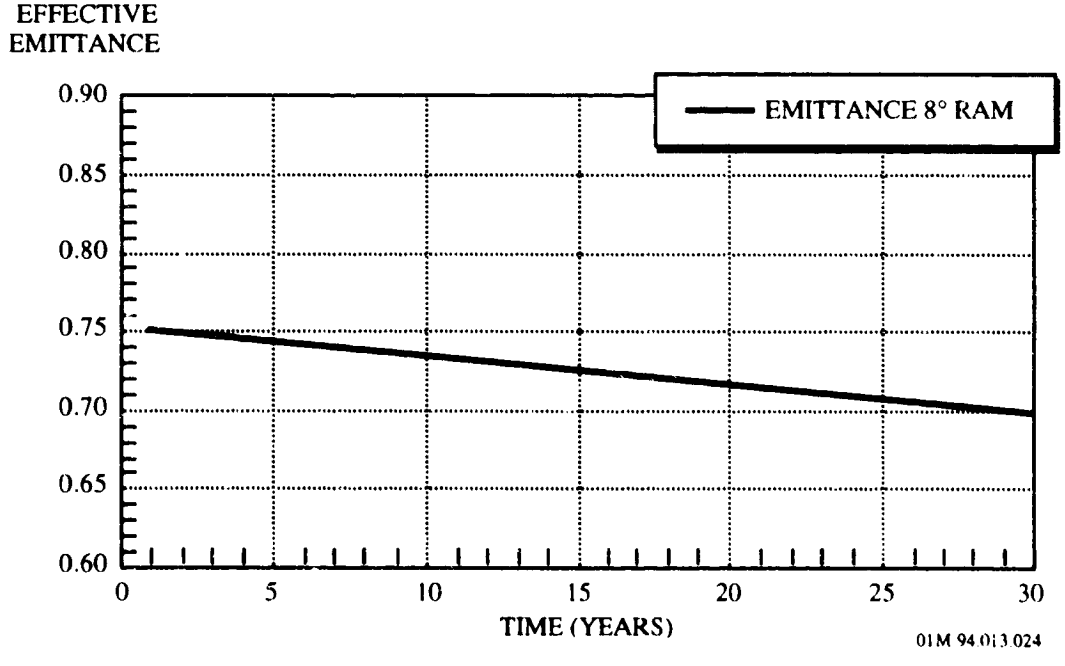

Figure 10-64. Silver/Teflon M/OD Effect on Emittance vs Time

10.5.1.3.8 Microcracking Effects on Solar Absorptance

Microcracking occurred in the silver/Inconel layer of silver Teflon (Ag/FEP) second-surface mirror insulation blankets. Adhesive backed Ag/FEP requires 'gentle' handling when the adhesive release paper is removed. The material should not be excessively stretched or bent during this process. Mishandling can crack the silver layer, allowing adhesive bleed through and subsequent darkening upon exposure to solar UV radiation. Experience from Solar Max and LDEF shows delaminated areas cause increases in absorptance to 0.1. Such microcracking has been shown to be preventable by modifying the adhesive-backed Ag/FEP application procedures. This microcracking resulted in bleed-through of adhesive to the base of the FEP during the LDEF flight; when the adhesive in the microcracked areas was affected by solar ultraviolet radiation, it darkened and the solar absorptance of the Ag/FEP substantially increased.[83]

10.5.1.3.9 Contamination-Induced Solar Absorptance Degradation of Silver Teflon.

The absorptance of Ag/Teflon may be substantially changed by surface accumulation of a molecular contaminant film (generally hydrocarbons and silicones). The contaminant is an absorbing layer, hence the α of contaminated Ag/Teflon rises as the contaminant thickness increases, eventually approaching an asymptotic value equal to the α of the contaminant.[1]

Changes in solar absorptance attributable to contamination have been observed on many satellites. On the NOAA-7 spacecraft,[100] which was launched in 1981 and orbited at an altitude of 833 km, the deposition of contaminants onto Temperature-controlled Quartz Crystal Microbalances (TQCM's) were measured for 2 years. It was found that α leveled off after about 1000 Å were deposited on the TQCM's. By then, α had increased by a factor of 2.5 and 3.3 for several TQCMs. If this contamination changed a silver Teflon surface by the same factor, then the initial α would be 0.1 and the final α approximately 0.3. The rate of change with contaminant thickness (assuming linearity) would be 0.2 per 1000 Å, or 0.02 per 100 Å.

Most of the Ag/Teflon samples on the Solar Maximum Mission satellite[101] had a very small change in α (delta $\alpha \leq 0.04$), but samples which were visibly contaminated went from an initial α of 0.06 to a final α of 0.28. This was after 4 years of flight at an altitude of ~500 km. Unfortunately, the contaminant layer thickness was not measured.

A silicon-containing molecular contamination was observed on selected silver Teflon second surface mirror specimens on the LDEF UHCRE Experiment, as shown in Figure 10-65. The amber-colored silicon-containing contamination may have resulted from the outgassing of the adhesive which secured the velcro hook and loop tape onto the thermal blankets which, in turn, secured the thermal blanket on the experiment tray. These pads, some as large as 1 inch by 4 inches, were bonded with DC6-1104 RTV silicon adhesive. A visual inspection of two velcro strips on a section of blanket showed that the adhesive had been liberally applied. Approximately 50 pads were attached to the blanket material. A matching set of pads were bonded to the tray itself. Thus a significant amount of silicon adhesive was used in this particular application, since at least 16 blankets were held in place using this technique. The silicon from this source, perhaps

---

[1] Note that although the absolute value of α depends on the initial absorptance of the clean Ag/Teflon, the change in α depends only on the contaminant layer thickness and the chemical identity of the contaminant. Therefore contamination data involving substrates other than Ag/Teflon can still be used to predict solar absorptance degradation. [This argument applies only to degradation by contaminant films or UV-polymerized contaminant f ilms. Degradation by atomic oxygen, UV alone, or radiation is highly dependent on the substrate.]

in the form of an organic silicone, probably contributed to the general molecular contamination observed at various locations on LDEF experiments and structure. Infrared analysis performed on wipes of the contamination were taken from several positions on the experiment tray corners.

The IR spectrum indicates a silicone contaminant. It was concluded that these stains are a result of oxidation of outgassed silicones by atomic oxygen.[102] The potential significance of this particular contaminant is the possibility of conversion to an inorganic silicate due to reaction with atomic oxygen. Silica/silicates have been shown to be effective barriers to AO erosion. Thus, surfaces which were covered with this contaminant may have responded differently to the LDEF environment than surfaces which were not contaminated.

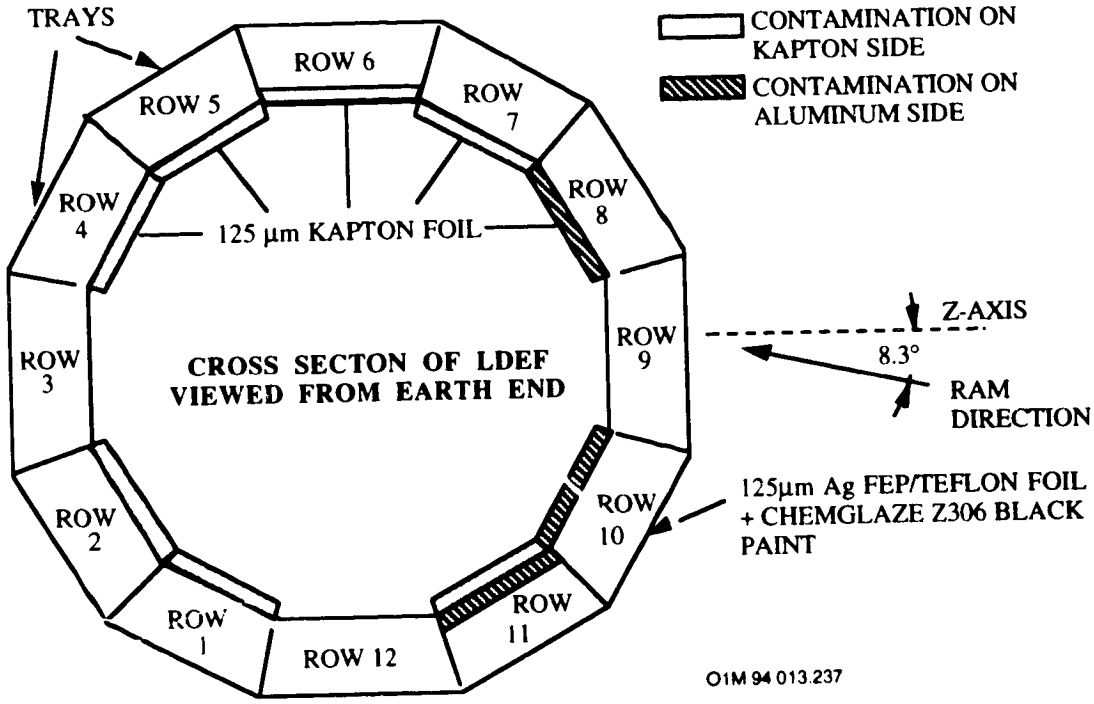

Contamination stains were also mapped on the Kapton foil. Foils in rows 8, 10, and 11 were contaminated on the aluminized side and that foils in rows 1, 2, 4, 5, 6, 7, and 11 were contaminated on the Kapton side. The most heavily contaminated surfaces were the Kapton side of foils 2, 4, 5 and the aluminized foils 8, 10, and 11. As the contamination in the majority of cases is facing the ram direction, and by analysis of the layer, is confirmed to contain silicon and oxygen, one can suppose that outgassed silicone products have been oxidized by atomic oxygen to form a silicon oxide layer on the foils. Silicon oxide being resistant to atomic oxygen erosion would not be removed by the cleaning action of atomic oxygen and thus form a protective layer for the Kapton.

Figure 10-65. Contamination on LDEF Satellite.

The foregoing data indicate that the change in α due to contamination is anywhere from 0.01 to 0.05 per 100Å of deposited contaminant.[m] The large variation is most likely due to the different absorptivities of different species of contaminants as well as the extent of the UV degradation of the contaminants.

Previous and recent contamination analyses for the Earth Orbiting Satellite (EOS) predict worst-case depositions after 5 years of 300 to 500 Å in the vicinity of the instruments. The exact deposition obviously depends on instrument location and the facing direction of contamination-sensitive surfaces.

Combining the observed α degradations with the predicted EOS contamination levels, the minimum, nominal, and maximum changes in α can be calculated:

$$(\text{delta } \alpha)\text{min} = 300\text{Å } (0.01/100\text{Å}) = 0.03$$

$$(\text{delta } \alpha)\text{nom} = 400\text{Å } (0.03/100\text{Å}) = 0.12$$

$$\text{delta } \alpha)\text{max} = 500\text{Å } (0.05/100\text{Å}) = 0.25$$

For Ag/Teflon, with an initial α of 0.10, the end-of-life α values would then be 0.13 minimum, 0.22 nominal, and 0.35 maximum. Since one generally designs to a plausible worst case scenario, assuming an end-of-life α of approximately 0.3 for silver Teflon would not be unreasonable.

---

[m]There are very few spacecraft on which both α changes and contaminant layer thickness were measured. Furthermore, the change in α depends on the chemical species of contaminant, and there are no flights for which α, contaminant thickness, and contaminant species are all measured. Even if there were, the actual deposition on any spacecraft surface is a complicated combination of all the condensable species outgassed by the spacecraft. The best that can be done is to give the range of observed delta α vs. thickness values for past spacecraft and assume that future spacecraft are going to outgas similar species and therefore exhibit similar solar absorptance degradation.

10.5.1.4 Design Considerations for the Space Environment

The following design and performance lessons are obtained from a number of flight experiments.

- Between 80 and 90 percent of the silver Teflon surfaces maintained its thermal control properties throughout the mission. The thermal performance showed minimal degradation from the solar UV exposures of up to 11,000 esh.
- At low LEO altitudes atomic oxygen erosion may result in degraded properties, depending on total fluence levels.
- The average recession rate of 3.64×10^{-25} cm^3/atom for the 69-month LDEF mission was an order of magnitude greater than values reported for experiments flown on the shorter mission duration Space Shuttle flights.
- The recession rate of silver Teflon increases under combined UV and AO exposure.
- Atomic oxygen induced roughening on the ram-facing surfaces (e.g., LDEF leading edge specimens), leading to increased diffuse reflectance. Hence, precautions must be taken if this material is to be used near critical optical surfaces.
- Certain areas of a trailing edge specimen on LDEF (blanket A4) showed surface texturing and shadowing indicating exposure to atomic oxygen. The evidence indicates that atomic oxygen scattered from a scuff plate and was able to reach the surface of the A4 blanket. Indirect scattering must be considered when critical surfaces are designed and located on a spacecraft in LEO.
- Hypervelocity impacts did not compromise the thermal-optical properties of the silver Teflon blankets and the mechanical integrity remained intact.
- The adhesion of silver to the Teflon was much better for trailing edge specimens than for leading edge specimens, which were separated with ease.
- Heavy contamination cause increases in solar absorptance to around 0.25. For silver Teflon, with an initial α of 0.10, the end-of-life a values would then be 0.13 minimum, 0.22 nominal, and 0.35 maximum. Since one generally designs to a plausible worst case scenario, assuming an end-of-life α of approximately 0.3 for silver Teflon would not be unreasonable.

10.5.1.5 Performance Life Estimates

Materials performance lifetime limits can be determined by several factors: increases in the α/ε ratio, causing increases in temperature above the allowed performance values; mechanical failure of the material; tearing due to thermal-cycling-induced stresses; embrittlement by solar UV radiation, causing subsequent cracking; impact damage, creating punctures and associated damage and/or darkening of a portion of the blanket; and redeposition of outgassed contaminant materials that darken and change the absorptance characteristics of the materials. An estimate of the expected environmental degradation for a specified mission can be made from the mission profile, which establishes the orbit and required lifetime.

The designer must establish end-of-life requirements for the optical properties of silver Teflon. In GEO, the SCATHA degradation curves could be used to estimate the performance life with exposure to the trapped radiation charged particle belt.[103] In 5 years, both 5-mil and 2-mil silver Teflon had degraded to α_s values of greater than 0.24 due to electron and proton radiation.

In LEO orbits, the atomic oxygen flux is strongly dependent upon altitude and solar activity. The atomic oxygen and solar UV fluences are determined based on the mission profile, and the total recession over the life of the mission is predicted. The minimum required thickness of the silver Teflon material at end-of-life is based on the well established values for emittance of Teflon as a function of thickness.

The actual recession rate used will depend on the expected duration of the mission. For short periods of time in LEO, recession rates of $<0.05 \times 10^{-25}$ cm^3/atom will be sufficient to establish thickness loss. For missions of greater length, the LDEF value 3.64×10^{-25} cm^3/atom is clearly more appropriate. In practice, the known reaction efficiency and expected oxygen fluence are used to predict the expected life of a film with a given initial thickness.

Lifetime predictions should also include consideration of the fraction of the blanket surface that will likely be darkened or destroyed by impacts and potential absorptance increases due to contaminant films over a fraction of the surface. These considerations were minor for LDEF. Impacts darkened 2 percent or less of the surface area of each LDEF blanket and delaminated <5 percent of the blanket area. Contaminant films caused absorptance values as high as about 0.25, but only for relatively small surface areas. The minimum area required for a given radiator would need to be scaled up by only 5 percent to 10 percent to compensate for these effects.

10.5.2 Aluminized FEP Teflon

10.5.2.1 Composition

Aluminum/Teflon (FEP) tape is a thermal control coating whose high emittance is controlled by the thickness of the Teflon film, and its low solar absorptance (high reflectance) is controlled by a metallic silver second surface. The incident light (solar flux) transmits through the smooth clear Teflon and specularly reflects off the aluminum layer. Table 10-74 shows typical thermo-optical properties of aluminum/Teflon thermal control blankets.[104]

Table 10-74. Typical Thermo-Optical Properties of Unexposed Aluminum/Teflon

Sample Description	α_s (1)	ε_H (2)	α_s / ε_H	Weight gms/in^2
0.5 mil Teflon x vacuum deposited aluminum	≤0.14	≥0.40	0.29	0.018
1.0 mil Teflon x vacuum deposited aluminum	≤0.14	≥0.48	0.24	0.035
2.0 mil Teflon x vacuum deposited aluminum	≤0.14	≥0.60	0.19	0.070
5.0 mil Teflon x vacuum deposited aluminum	≤0.14	≥0.75	0.15	0.176
7.5 mil Teflon x vacuum deposited aluminum	≤0.15	≥0.80	0.18	0.264
10.0 mil Teflon x vacuum deposited aluminum	≤0.15	≥0.85	0.17	0.352

(1) Solar absorptance testing was done with a dual beam, ratio recording Beckman DK-2A UV-VIS-NIR spectrophotometer. Solar absorptance was computed based on 25 equal energy intervals centered on wavelengths from 314 nanometers to 2191 nanometers. These wavelengths are computed from tables of spectra in NASA SP-8005 and ASTM E490-73a.
(2) An approximation to total hemispherical emittance was obtained from a Lion Research Corporation emissometer. This instrument responds to the IR energy emitted from a sample through a potassium bromide window into the detector. The wavelength range is 3-30 microns. This method equates to ASTM E408, Method B.

10.5.2.2 Source

FEP resin is sold in the U.S. under the Teflon trademark by Du Pont Co.

Aluminum Teflon film is produced by Sheldahl, Northfield, MN (Tel: 507/663-8000).

10.5.2.3 Effects of the Space Environment

No flight experiment data available.

10.5.3 Aluminized Kapton Multilayer Insulation

10.5.3.1 Multilayer Insulation Composition

A multilayer insulation (MLI) blanket consists of second surface mirrors (SSM) and single surface reflector mirrors. A typical blanket construction, consists of the following layers (see Figure 10-66):

- 1/2 to 5 mil Kapton (Kapton side facing the space environment) x vacuum deposited aluminum outer layer
- 10 crinkled layers of 0.3 mil Kapton x vacuum deposited aluminum
- 1/2 to 5 mil Kapton (Kapton side facing spacecraft structure) x vacuum deposited aluminum inside layer
- 1-inch and 2-inch wide perforated 3.0 mil Teflon x vacuum deposited aluminum x 966 acrylic pressure sensitive adhesive tape (used for fastening MLI)

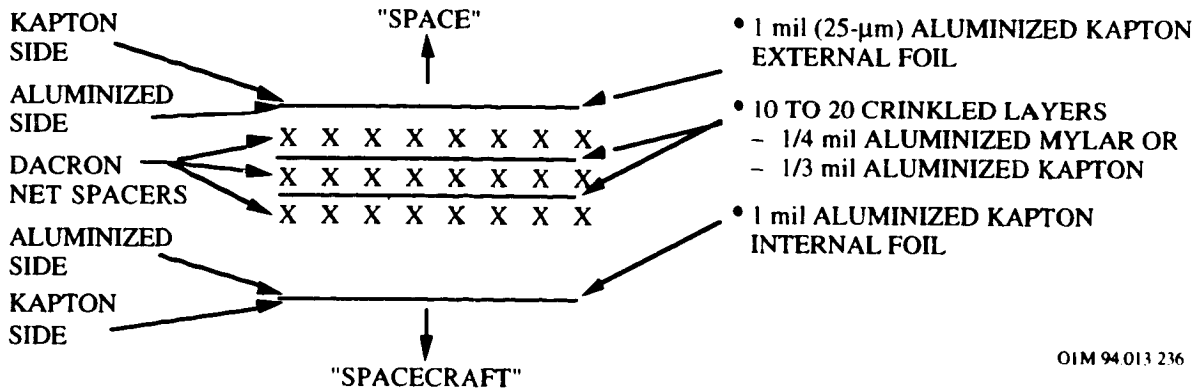

Figure 10-66. Typical Multilayer Blanket Composition

10.5.3.2 Pre-Flight Thermal-Optical Properties

Aluminized Kapton SSM. Table 10-75 shows typical thermo-optical properties of aluminized Kapton second surface mirrors (ref. 116). As with Teflon, the Kapton thickness provides the emittance property desired, and hence, emittance increases with increasing Kapton thickness. Aluminum is most often used as the mirror metal. Kapton has a characteristic transparent orange color whose density increases with increasing thickness. This results in increasing absorptance with increasing film thickness. Hence, the α/ε ratio remains ~2.0 for any material construction.

Table 10-75. Typical Thermo-Optical Properties of Aluminized Kapton SSM

Kapton Thickness		Typical $\alpha^{(a)}$	Typical ε
Inches	Microns		
0.0005	12	.56	.33
0.001	25	.70	.35
0.002	50	.79	.38
0.003	75	.85	.41
0.005	125	.93	.45

(a) The absorptance and emittance values are measured through the Kapton surface.

The single aluminized Kapton is being recommended as a light block in the Space Station MLI blankets. With a much higher infrared emittance facing away from the blanket than toward the blanket, it prevents an increase in temperature in the reflector layers by preventing solar radiation from striking the reflector layers and by radiating infrared radiation away from the blanket. This improves the thermal efficiency of the blanket.

Kapton Aluminum Reflectors. First-surface mirrors are made using Kapton or Mylar substrates (see Section 10.5.7). These mirrors are commonly used in multilayer insulation blankets for the multiple layers of infrared heat shield. Aluminum is most often used for the mirror followed by gold and on rare occasions, silver. All provide very low emittances. The maximum infrared hemispherical emittance of the aluminized inner cover of the MLI design is expected to be 0.04, so that the majority of the radiation will be radiated to space rather than to the interior of the blanket. Large areas of material are needed in fabricating MLI blankets and for this reason aluminized Kapton is often used to keep costs down. However, sometimes high temperature resistance and/or requirements for nonburning materials dictate the use of Kapton

base film. Table 10-76 shows typical thermo-optical properties of Kapton aluminum thermal control materials (ref. 116).

Table 10-76. Typical Thermo-Optical Properties of Kapton Aluminum

Material Description	α_s (1)	ε_H (2)	α_s/ε_H	Temp. Range Continuous °C (°F)	Approx. Weight gms/in^2
Vacuum deposited aluminum x 0.5 mil Kapton	≤0.14 (3)	≥0.05 (3)	4.0	-251 to 288 (-420 to 550)	0.012
Vacuum deposited aluminum x 1.0 mil Kapton	≤0.14	≥0.05	4.0	-251 to 288 (-420 to 550)	0.023
Vacuum deposited aluminum x 0.5 mil Kapton x vacuum deposited aluminum	≤0.14	≥0.05	4.0	-251 to 288 (-420 to 550)	0.012
Vacuum deposited aluminum x 0.5 mil Kapton x vacuum deposited aluminum	≤0.14	≥0.05	4.0	-251 to 288 (-420 to 550)	0.023

(1) Solar absorptance testing was done with a dual beam, ratio recording Beckman DK-2A UV-VIS-NIR spectrophotometer. Solar absorptance was computed based on 25 equal energy intervals centered on wavelengths from 314 nanometers to 2191 nanometers. These wavelengths are computed from tables of spectra in NASA SP-8005 and ASTM E490-73a.

(2) An approximation to total hemispherical emittance was obtained from a Lion Research Corporation emissometer. This instrument responds to the IR energy emitted from a sample through a potassium bromide window into the detector. The wavelength range is 3-30 microns. This method equates to ASTM E408, Method B.

(3) The absorptance and emittance values are measured through the aluminum surface.

10.5.3.3 Source

Manufacturer: Sheldahl
Northfield, MN 55057
Tel: (507) 663-2180

10.5.3.4 Space Environment Effects - MLI

10.5.3.4.1 Atomic Oxygen Effects

The LDEF Cascade 1 Variable Conductance Heat Pipe Experiment No. A0076 revealed the effects of atomic oxygen on the performance of Al/Kapton multilayer blankets. The experiment, located in Tray F 9 of LDEF where it received an atomic oxygen (AO) fluence of 8.99×10^{21} atoms/cm^2 almost normal to its surface and 11,200 equivalent sun hours, was covered on all sides by MLI.[105]

The majority of the tray was covered by aluminized Kapton polyimide multilayer insulation blankets, which also covered the inner sides and bottom of the tray. The outermost layer of the MLI was 0.076 mm (0.003 inch) unperforated Kapton light block, aluminized only on the inner side, and all other layers were 0.0076 mm (0.0003 inch), double aluminized, perforated Kapton. There was a total of 15 layers of 0.0003 inch Kapton under the 0.003 inch layer. All were separated by polyester scrim cloth to minimize heat leaks between layers. The MLI blankets were attached to the sides of the experiment tray using Velcro tape.

The exposed MLI showed substantial changes caused by atomic oxygen erosion and debris particle impact. The appearance of the experiment changed from the bronze color of the outer Kapton layer to the shiny metallic finish of the exposed aluminum. Most of the exposed outermost Kapton layer of the (0.76 mm) 0.003 inch MLI and the polyester scrim cloth under it were lost, and there was evidence of contaminant deposition which discolored the edges of the MLI blanket. Some of the aluminizing shielded sections of the scrim cloth during the remainder of the exposure and accounted for the survival of some areas of the scrim cloth. The aluminizing on the underlying double aluminized Kapton layers remained firmly attached and protected the Kapton from the space environment.

10.5.3.3.2 AO Undercutting of LDEF Aluminized-Kapton Multilayer Insulation

An aluminized-Kapton multilayer insulation sample which was located on the leading edge of LDEF (F9), was used to study LEO directed atomic oxygen undercutting.[106] Cracks in the aluminzation of a Kapton MLI sample allowed characterization of LEO direct ram AO undercutting. AO undercut profile shapes and sizes were found to vary with crack width which is

proportional to the number of oxygen atoms entering the crack. Undercut widths exceeded crack widths by a factor of 2.5 to 12.5 for horizontal cracks, and 3.1 to 16.6 for vertical cracks.

10.5.3.3.3 Mass Loss Degradation

There were two different forms of MLI insulation blankets returned to Earth from the Solar Maximum Mission.[107] In both forms, the top layer was made of Kapton with an aluminum layer vapor deposited on the inside surface. The bottom layer, the layer facing the spacecraft systems, is also made of aluminized Kapton, with the aluminum facing the inner layers of the MLI. In both forms, every layer was separated and supported by a Dacron mesh.

The MLI blankets that covered the Modular Attitude Control System (MACS) module were composed entirely of aluminized Kapton. The top and bottom layers were made of 2 mil Kapton. There were six to ten inner layers of 1/4 mil Kapton, aluminized on both sides. The MLI taken from the Main Electronics Box was made of aluminized Kapton and aluminized Mylar. The top layer was 3 mil Kapton and the bottom layer was 1 mil Kapton. There were fifteen inner layers of 1/4 mil Mylar, aluminized on both sides.

The MLI materials were analyzed using optical microscopes and Scanning Electron Microscopes (SEM). In addition, infrared spectroscopy was used to detect potential changes in the Kapton polymer structure, and a solar reflectometer measured solar absorptance.

The most apparent change in the MLI was the dull appearance of the top Kapton layers as compared to the shiny surface of new Kapton samples. Findings on STS-8 as well as SMM indicated that changes in the Kapton were most likely due to the presence of atomic oxygen. Infrared spectroscopy indicated that while there was obvious degradation in the Kapton, the actual polymer structure has not changed. Measurements of thickness of the top Kapton layer from the front of the MACS indicated that the Kapton suffered mass losses ranging from 0.54 percent to 31.4 percent.

The significance of the Kapton degradation to spacecraft designers lies in potential changes in the MLI performance. Measurements have been made of solar absorptance of the Kapton material. The solar absorptance of the Kapton material is typically 0.37 to 0.41 prior to on-orbit exposure. The post-flight measurements indicated that the solar absorptance of the SMM Kapton samples had increased by 0.03 to 0.04. This increase is probably due to the optical scattering effect of the degraded Kapton surface. This small increase should have little effect on

the performance of the MLI insulation blankets. However, greater degradation of the top Kapton layer that may significantly affect the performance of the MLI, cannot be ruled out in future missions.

10.5.3.3.4 Micrometeoroid Effects

LDEF Cascaded Variable Conductance Heat Pipe Experiment No. A0076. The 14 m^2 sample of the ram-facing LDEF MLI blanket provided an opportunity to study the effects of high velocity impacts (HVI). The 1.3 mm thick single aluminized Kapton outer layer had been eroded away by AO, releasing vapor-deposited aluminum on the back surface The first layer of Dacron (DuPont trademark) isolator cloth was then exposed and also eroded away. The underlying double aluminized reflector layers and the remaining Dacron layers were intact except for eight small rips in the first reflector layer, caused by HVI. Reflector layers are commonly perforated with 3%-10% open area to aid venting during ascent into space. The additional open area due to HVI damage was negligible in terms of the blanket performance. Meteoroid and debris hits caused small penetrations and rips in the MLI layers, and in some cases left cloudy areas where the vapor plume caused by a hit condensed on the next layers. There were no visible changes in the MLI blanket which was underneath the experiment. It was shielded from solar radiation, atomic oxygen, and debris by the exposed MLI layer and by the parts of the experiment.[108]

Solar Maximum Mission. Analyses were conducted on some of the particles that impacted the various MLI blankets and the louvers from the MACS on the SMM. These analyses determined the sources of the various particles and the effect of impacts on the MLI materials and on the aluminum louvers. A survey of approximately one-half square meter of MLI revealed over 1500 impact sites. Of these, 432 impacts resulted in craters in the Kapton greater than 40 microns in diameter. In the 75-micron thick Kapton (Main Electronics Box), craters greater than 100 microns in diameter were perforated through the Kapton layer. In the 50 micron Kapton (MACS), craters larger than 70 microns in diameter penetrated through the Kapton. When the survey totaled approximately 0.7 square meters of Kapton surface, about 160 impact craters penetrating the Kapton layer were found.

A number of particles completely penetrated all of the MLI layers. One particle penetrated the MLI near a star tracker, making an impression in the star tracker's aluminum shield. Approximately half of the particles that impacted the MACS louvers penetrated the first of the two aluminum sheets, as evidenced by impressions in the second sheet.

Chemical analyses of a number of the impacts has shown that sources of the particles fall into one of four groups. The first group of particles is meteoric material, evidenced by the elements silicon, magnesium, iron, calcium, aluminum with minor amounts of iron-nickel sulfide. The second group of particles is paint particles. This is characterized by titanium and zinc, and the chemistry includes potassium, silicon, aluminum and chlorine. The third group of particles is aluminum droplets, probably from the MLI. The fourth group of particles is waste particles as evidenced by one impact that penetrated three layers of MLI. The chemistry includes sodium, potassium chloride, phosphorus and minor amounts of sulfur. Investigators believed that this particle may have come from the Orbiter's waste management system.

Two of the large impacts have been investigated in more detail. In both cases, the impact particle apparently disintegrated upon impact with the outer Kapton layer of the MLI. The disrupted material was sprayed inward in a cone shaped pattern, lodging on the second layer of the MLI.

In the case of the first impact particle, a small portion of disrupted material penetrated the second layer of the MLI. This impact particle caused a hole 280 microns in diameter with a raised rim. The second MLI layer has a ring of tiny holes and craters surrounding a roughed up area of about 5 millimeters in diameter. Particles from the back of the first layer and from the front of the second layer have been analyzed showing that about 75% are fragments or melted droplets of Kapton. Of the non-Kapton particles, most are composed of magnesium, silicon and iron. Next in number were aluminum particles. Investigators believed that the aluminum was derived from the MLI. Other particles were composed of iron, sulfur, and nickel.

The second reported impact particle caused a crater 355 microns in diameter with a raised rim in the Kapton layer. The second layer has a wedge shaped pattern of concentric, elongated holes. Particles of the second impact were composed primarily of iron, sulfur, and nickel.

An examination of the aluminized Mylar films and the Dacron mesh from the inner layers of the MLI which was used to cover the MEB reveled no erosion in these materials. The only apparent damage to these materials was caused by the impact particles.

10.5.3.5 Space Environmental Effects - SSM

10.5.3.5.1 Solar Reflectance

LEO exposure does not appear to significantly affect the solar reflectance of aluminized Kapton samples after their flight on FRECOPA/LDEF and on the 1.1 year COMES/MIR flight experiment (ref. 34). As shown in Table 10-77, the aluminized Kapton displayed analogous behavior in both experiments.

Table 10-77. Solar Reflectance Degradation ΔRs of Aluminized Kapton Second Surface Mirrors Measured After the FRECOPA and COMES Flight Experiments

Material	Mfg	$Rs_{initial}$	AO 138-6 LDEF		COMES	
			Canister ΔRs	Tray ΔRs	Face V ΔRs	Face R ΔRs
Aluminized Kapton (25 microns)	Rexor	0.65		-0.03	-0.02	-0.10
Aluminized Kapton (12 microns)	CAMVAC	0.67		-0.04		
Aluminized Kapton (25 microns)	CAMVAC	0.66	-0.02			
Aluminized Kapton (25 microns)	Rexor	0.64	-0.02			
Aluminized Kapton (25 microns)	Sheldahl	0.64	-0.030			

Environmental Variations of LDEF and MIR Space Experiments: Due to its position on the trailing edge of LDEF, the AO 138-6 experiment did not receive any oxygen atoms during the mission, with the exception of a short period during the capture when it received a fluence evaluated at 1.32×10^{17} atoms cm^{-2}. The solar illumination was 11,100 equivalent sun hours (esh) for the samples located on the tray and only 1448 esh for the samples inside the canister. The particle irradiation dose (mainly due to the electron flux) was weak: 3×10^{5} rads. The number of temperature cycles was ~34,000 with temperatures within the ranges shown in the table below.

ENVIRONMENT	FRECOPA-LDEF		COMES-MIR	
	CANISTER	TRAY	FACE V	FACE R
Oxygen atoms cm^{-2}	0	1.3×10^{17}	1.2×10^{18} to 7.5×10^{19} (1)	3.5×10^{20} to 5.8×10^{20} (1)
Solar UV (esh)	1448	11,100	2850(2)	1900(2)
Temp. Cold case (°C)	-20 to -26	-43 to -52	-60 to -70	-60 to -70
Temp. Hot case (°C)	+67 to +85	+45 to +63	+10 to +30	+50 to +60

(1) Estimated from AO reactivity erosion of Kapton (3.0×10^{-24} $cm^3 atom^{-1}$) and Terphane (3.0×10^{-24} $cm^3 atom^{-1}$) samples

(2) Estimated from data of experiment calorimeter

Experimental Description. The solar reflection measurements were made with a Beckman DK2A spectrophotometer with an integrating sphere, and the infrared emissivity measurements were made with the Gier & Dunkle DB 100 device. It is important to underline that the measurements were all taken in air on samples which had thus experienced more or less intense recovery of the radiation damage.

10.5.3.5.2 Emissivity

LEO exposure does not appear to significantly affect the emissivity of aluminized Kapton samples after their flight on FRECOPA/LDEF (ref. 13), as shown in Table 10-78.

Table 10-78. Emissivity Variations of Aluminized Kapton Second Surface Mirrors (SSM) Measured After the FRECOPA Flight Experiment

Material	Mfg.	$\varepsilon_{initial}$	AO 138-6 LDEF	
			Canister $\Delta\varepsilon$	Tray $\Delta\varepsilon$
Aluminized Kapton (25 microns)	Rexor	0.667		-0.003
Aluminized Kapton (12 microns)	CAMVAC	0.556		-0.014
Aluminized Kapton (25 microns)	CAMVAC	0.551	-0.001	
Aluminized Kapton (25 microns)	Rexor	0.667	-0.005	
Aluminized Kapton (25 microns)	Sheldahl	0.650	-0.002	

Experimental Description: Experiment AO 138-6 was part of the FRECOPA experiment located on the trailing edge of LDEF. The experiment was designed to allow exposure of a part of the samples to the whole spacecraft environment by being laid directly on the FRECOPA tray surface, while the remaining samples were protected from the external environment of LDEF for all mission phases, except free flight, by the means of a vacuum-tight FRECOPA canister in which they were stored.

Environmental Variations of LDEF Space Experiments: Due to its position on the trailing edge of LDEF, the AO 138-6 experiment did not receive any oxygen atoms during the mission, with the exception of a short period during the capture when it received a fluence evaluated at 1.32×10^{17} atoms cm^{-2}. The solar illumination was 11,100 equivalent sun hours (esh) for the samples located on the tray and only 1448 esh for the samples inside the canister. The particle irradiation dose (mainly due to the electron flux) was weak: 3×10^5 rads. The number of temperature cycles was ~34,000 with temperatures within the ranges shown in the table below.

	FRECOPA-LDEF	
	CANISTER	TRAY
Oxygen atoms cm^{-2}	0	1.3×10^{17}
Solar UV (esh)	1448	11,110
Temp. Cold case (°C)	-20 to -26	-43 to -52
Temp.Hot case (°C)	+67 to +85	+45 to +63

10.5.3.6 Space Environmental Effects - Reflectors

10.5.3.6.1 Thermal-Optical Properties

LEO exposure does not appear to significantly affect the solar reflectance and the emissivity of double aluminized Kapton sample after its flight on FRECOPA/LDEF (ref. 13), as shown in Table 10-79. Experiment AO 138-6 was part of the FRECOPA experiment located on the trailing edge of LDEF. The experiment was designed to allow exposure of a part of the samples to the whole spacecraft environment by being laid directly on the FRECOPA tray surface.

Table 10-79. Optical Property Variations of VDA Kapton

Material	Mfg.	$Rs_{initial}$	$\varepsilon_{initial}$	AO 138-6 LDEF	
				Tray ΔRs	Tray $\Delta\varepsilon$
Kapton H (25 microns)/ Aluminum both sides	Rexor	0.91	0.027	-0.010	-0.002

Experimental Description: Experiment AO 138-6 was part of the FRECOPA experiment located on the trailing edge of LDEF. The experiment was designed to allow exposure of a part of the samples to the whole spacecraft environment by being laid directly on the FRECOPA tray surface, while the remaining samples were protected from the external environment of LDEF for all mission phases, except free flight, by the means of a vacuum-tight FRECOPA canister in which they were stored.

Environmental Variations of LDEF Space Experiments Due to its position on the trailing edge of LDEF, the AO 138-6 experiment did not receive any oxygen atoms during the mission, with the exception of a short period during the capture when it received a fluence evaluated at 1.32×10^{17} atoms cm^{-2}. The solar illumination was 11,100 equivalent sun hours (esh) for the samples located on the tray and only 1448 esh for the samples inside the canister. The particle irradiation dose (mainly due to the electron flux) was weak: 3×10^{5} rads. The number of temperature cycles was ~34,000 with temperatures within the ranges shown in the table below.

	FRECOPA-LDEF	
	CANISTER	TRAY
Oxygen atoms cm^{-2}	0	1.3×10^{17}
Solar UV (esh)	1448	11,110
Temp. Cold case (°C)	-20 to -26	-43 to -52
Temp.Hot case (°C)	+67 to +85	+45 to +63

10.5.4 Gold-Coated Kapton

10.5.4.1 Composition

A polyimide with vacuum deposited gold. Typical properties are provided in Tables 10-80 and 10-81 (ref. 116).

Table 10-80. Typical Thermo-Optical Properties of Gold-Coated Kapton

Material Description	$\alpha_s^{(1)}$	$\varepsilon_H^{(2)}$	α_s/ε_H	Temp. Range Continuous °C (°F)	Approx. Weight gms/in^2
Vacuum deposited gold[3] x 0.3 mil Kapton	~0.3	≤0.03	15.0	-251 to 288 (-420 to 550)	0.007
Vacuum deposited gold x 0.5 mil Kapton	~0.3	≤0.03	15.0	-251 to 288 (-420 to 550)	0.012
Vacuum deposited gold x 1.0 mil Kapton	~0.3	≤0.03	15.0	-251 to 288 (-420 to 550)	0.023
Vacuum deposited gold x 2.0 mil Kapton	~0.3	≤0.03	15.0	-251 to 288 (-420 to 550)	0.046
Vacuum deposited gold x 3.0 mil Kapton	~0.3	≤0.03	15.0	-251 to 288 (-420 to 550)	0.070
Vacuum deposited gold x 5.0 mil Kapton	~0.3	≤0.03	15.0	-251 to 288 (-420 to 550)	0.117

(1) Solar absorptance testing was done with a dual beam, ratio recording Beckman DK-2A UV-VIS-NIR spectrophotometer. Solar absorptance was computed based on 25 equal energy intervals centered on wavelengths from 314 nanometers to 2191 nanometers. These wavelengths are computed from tables of spectra in NASA SP-8005 and ASTM E490-73a.

(2) An approximation to total hemispherical emittance was obtained from a Lion Research Corporation emissometer. This instrument responds to the IR energy emitted from a sample through a potassium bromide window into the detector. The wavelength range is 3-30 microns. This method equates to ASTM E408, Method B.

(3) 750 Å

(4) The absorptance and emittance values are measured through the Kapton surface.

Table 10-81. Typical Thermo-Optical Properties of Gold-Coated Kapton

Material Description	$\alpha_s^{(1)}$	$\varepsilon_H^{(2)}$	α_s/ε_H	Temp. Range Continuous °C (°F)	Approx. Weight gms/in^2
Vacuum deposited gold[4] x 0.3 mil Kapton	~0.31[4]	.50[4]	0.62	-251 to 288 (-420 to 550)	0.007
Vacuum deposited gold x 0.5 mil Kapton	~0.31	.55	0.56	-251 to 288 (-420 to 550)	0.012
Vacuum deposited gold x 1.0 mil Kapton	~0.33	.65	0.51	-251 to 288 (-420 to 550)	0.023
Vacuum deposited gold x 2.0 mil Kapton	~0.34	.75	0.45	-251 to 288 (-420 to 550)	0.046
Vacuum deposited gold x 3.0 mil Kapton	~0.37	.81	0.46	-251 to 288 (-420 to 550)	0.070
Vacuum deposited gold x 5.0 mil Kapton	~0.41	.86	0.48	-251 to 288 (-420 to 550)	0.117

(1) Solar absorptance testing was done with a dual beam, ratio recording Beckman DK-2A UV-VIS-NIR spectrophotometer. Solar absorptance was computed based on 25 equal energy intervals centered on wavelengths from 314 nanometers to 2191 nanometers. These wavelengths are computed from tables of spectra in NASA SP-8005 and ASTM E490-73a.

(2) An approximation to total hemispherical emittance was obtained from a Lion Research Corporation emissometer. This instrument responds to the IR energy emitted from a sample through a potassium bromide window into the detector. The wavelength range is 3-30 microns. This method equates to ASTM E408, Method B.

(3) 750 Å

(4) The absorptance and emittance values are measured through the Kapton surface.

10.5.4.2 Source

Manufacturer: Sheldahl
Northfield, MN 55057
Tel: (507) 663-2180

10.5.4.3 Effects of the Space Environment

Not available.

10.5.5 Germanium-Coated Kapton

10.5.5.1 Applications

Germanium/Kapton is used in blanket and closeout applications, and as an interstitial layer between the photovoltaic cells and the face sheet on solar array panels. A coating of germanium is applied to Kapton blanket material to achieve required thermo-optical properties as well as to protect the polymer from the space environment, in particular erosion caused by atomic oxygen. The coating has good abrasion resistance and is readily cleaned by wiping with standard solvents.

10.5.5.2 Method of Application

The germanium is applied to the Kapton by sputter deposition in a batch process to produce coated material which may then be cut to size. The coating may also be applied to pre-cut pieces of blanket if necessary. The coated blanket is installed in the usual manner with the germanium side typically facing outward. Coating thickness may be varied to tailor thermal properties of the blanket, but nominal germanium thickness is 1500 Å.

10.5.5.3 Effects of the Space Environment

Germanium coated Kapton is a possible material for advanced photovoltaic solar arrays. There are limited short-term environmental exposure data available for germanium/Kapton. Specimens were integrated into the heated trays and passive tray of the JPL EOIM-3 experiments.[n] Thermal property data for germanium/Kapton are summarized in Table 10-82 below. The material evaluated was 1500 Å germanium on 2 mil Kapton.

---

[n]Flight exposure of germanium/Kapton took place on the Evaluation of Oxygen Interactions with Materials, Mission 3 (EOIM-3) flight experiment sponsored by NASA/BMDO Space Environmental Effects program. Results documented in TRW Advanced Interceptor Technologies Program report No. 57888.93.440-003; total atomic oxygen fluence of 2×10^{21} atoms/cm^2 over 42 hours.

Table 10-82. Space Exposure Data for Germanium/Kapton

Specimen Condition	IR Reflectance ρ_R	Solar Absorptance α_s	Emittance ε_h	α/ε_h
Preflight	0.384	0.483	0.617	0.78
Control	0.384	0.482	0.616	0.78
Flight	0.386	0.485	0.614	0.79

Estimated Germanium Oxide layer thicknesses were determined by ESCA as shown in Table 10-83.[109] Possible formation of volatile GeO (direct reaction and/or disproportionation).

Table 10-83. GeO_x thicknesses for Coated Kapton Specimens

Specimen Location	GeO_x Thickness (Å)
Passive (10^o - 40^oC)	60
60^oC Strip	40
200^oC Strip	20

10.5.5.4 Design Consideration

Germanium/Kapton is stable in the LEO space environment, exhibiting no quantitatively significant degradation in thermal properties from short term space exposure. However, pin-holes in the coating characteristic of the coating process may allow atomic oxygen to erode the Kapton, thus undermining the structural integrity of the blanket. This phenomenon should not significantly affect the thermal performance of the blanket until undercutting has progressed to the point where fragments of the material come free from the body of the blanket. The dislocated fragments may also present a contamination hazard to other systems on a spacecraft. There are no definitive measures of the rate at which this phenomenon occurs, but a conservative estimate would take the erosion rate of uncoated Kapton at the orbit of interest and multiply by a factor of one-half. There are no long-term data on the space-stability of germanium/Kapton, but the germanium coating is expected to be stable in the space environment.

10.5.6 Black Kapton

Black Kapton is used to provide a solar shield for high gain antennas. It provides RF and IR transparency with low light transmission and low light reflectivity. Typical properties are provided in Table 10-84 (ref. 116).

Table 10-84. Typical Thermo-Optical Properties of Black Kapton

Material Description	α [a]	ε	Typical α/ε	Temp. Range Continuous °C (°F)	Approx. Weight gms/in^2
Carbon filled 1.0 mil Kapton (100CB) x vacuum deposited aluminum				-251 to 288 (-420 to 550)	0.023
First Side	≥0.85	≥0.81	~1.0		
Second Side	≤0.18	≤0.05	~3.0		
Electrically Conductive Carbon Kapton	0.93	0.84	~1.1	-251 to 121 (-420 to 250)	0.021

(a) The absorptance and emittance values are measured through the carbon surface.

10.5.6.1 Composition

Polyimide with black carbon

10.5.6.2 Source

DuPont

10.5.6.3 Effects of the Space Environment

Black Kapton was flown on the STS-5 mission to measure reaction of surfaces with atomic oxygen in the low Earth orbital environment. Samples on STS-5 were exposed to an atomic oxygen sweeping impingement across the surfaces with a total exposure fluence of $9.9x19^{19}$ atoms/cm^2 for 43.5 hrs. Average film thickness loss is summarized in Table 10-85.

Table 10-85. STS-5 Black Kapton Film Thickness Loss

Thickness μm [a]	Thickness Loss μm	Fluence 10^{20} atoms/cm^2	Reaction Efficiency 10^{-24} cm^3/atom [b]
25.4	1.35	0.99	1.4

(a) Film thickness of 25.4 μm correspond to 1.0 mil
(b) Most probable error is +30 to 40%

10.5.7 Aluminized Mylar

Two of the most common materials used in the aerospace industry for reflector layers in MLI are aluminized Mylar and aluminized Kapton.

10.5.7.1 Composition

First-surface mirrors are made using Mylar or Kapton substrates (see Section 10.5.3). These mirrors are commonly used in multilayer insulation blankets for the multiple layers of infrared heat shield. Aluminum is most often used for the mirror followed by gold and on rare occasions, silver. All provide very low emittances. Large areas of material are needed in fabricating MLI blankets and for this reason aluminized Mylar is often used to keep costs down. However, sometimes high temperature resistance and/or requirements for nonburning materials dictate the use of a Kapton base film. Table 10-86 shows typical thermo-optical properties of Kapton aluminum thermal control materials (ref. 116).

Table 10-86. Typical Thermo-Optical Properties of Mylar Aluminum

Material Description	α_s (1)	ε_H (2)	α_s / ε_H	Temp. Range Continuous °C (°F)	Approx. Weight gms/in^2
Vacuum deposited aluminum x 0.5 mil Mylar	≤0.14 (3)	≤0.05 (3)	4.0	-251 to 288 (-420 to 550)	0.011
Vacuum deposited aluminum x 1.0 mil Mylar	≤0.14	≤0.05	4.0	-251 to 288 (-420 to 550)	0.021
Vacuum deposited aluminum x 0.5 mil Mylar x vacuum deposited aluminum	≤0.14	≤0.05	4.0	-251 to 288 (-420 to 550)	0.011

(1) Solar absorptance testing was done with a dual beam, ratio recording Beckman DK-2A UV-VIS-NIR spectrophotometer. Solar absorptance was computed based on 25 equal energy intervals centered on wavelengths from 314 nanometers to 2191 nanometers. These wavelengths are computed from tables of spectra in NASA SP-8005 and ASTM E490-73a.

(2) An approximation to total hemispherical emittance was obtained from a Lion Research Corporation emissometer. This instrument responds to the IR energy emitted from a sample through a potassium bromide window into the detector. The wavelength range is 3-30 microns. This method equates to ASTM E408, Method B.

(3) The absorptance and emittance values are measured through the aluminum surface.

The following data of Table 10-87 are typical optical properties of single-sided aluminized Mylar tested on the Mylar side. The aluminum thickness is 1,000 Å.

Table 10-87. Optical Properties of Aluminized Mylar

Mylar Thickness	α_s (1)	ε_H (2)
0.25 mil	0.16	0.33
0.5 mil	0.16	0.46
1.0 mil	0.19	0.57
2.0 mil	0.23	0.72
3.0 mil	0.25	0.77
5.0 mil	0.27	0.81

(1) Solar absorptance testing was done with a dual beam, ratio recording Beckman DK-2A UV-VIS-NIR spectrophotometer. Solar absorptance was computed based on 25 equal energy intervals centered on wavelengths from 314 nanometers to 2191 nanometers. These wavelengths are computed from tables of spectra in NASA SP-8005 and ASTM E490-73a.
(2) An approximation to total hemispherical emittance was obtained from a Lion Research Corporation emissometer. This instrument responds to the IR energy emitted from a sample through a potassium bromide window into the detector. The wavelength range is 3-30 microns. This method equates to ASTM E408, Method B.

10.5.7.2 Source

Manufacturer: Sheldahl
Northfield, MN 55057
Tel: (507) 663-2180

10.5.7.3 Effects of the Space Environment

LDEF FRECOPA Experiment. A Teflon glass fabric and a Mylar sheet aluminized on its internal face were the materials for the heat shield for the LDEF FRECOPA Experiment. The aluminized Mylar face was painted black. Visual inspection of the aluminized Mylar heat shield showed a change in its initial silver white color to a golden yellow.[110] When the plate was returned, it was torn on one side and there were numerous cracks near the attachment points. Due to the extreme embattlement of Mylar, mechanical tests were not conduct. Thickness measurements showed a slight increase in thickness of up to 8%. This variation depends on the degree of exposure.

The study of thermo-mechanical properties using differential scanning calorimetry showed a reduction in the melting temperature of the material of about 4%, and using thermomechanical analysis an increase in the CTE of about 25%. The structure of Mylar therefore appeared to be considerably modified by exposure to the environment, particularly to thermal conditions, UV and thermal cycling. Thermo-Optical properties were also modified, with a slight variation in IR emissivity (0.57 to 0.60) and an increase in solar absorption (0.15 to 0.23 and up to 0.37 in the most exposed areas).

The presence of contaminants on the surface is minimal, with evidence of fluorine and nitrogen in particular. These could be produced by decomposition of the Teflon glass fabric, particularly the fluorine which is one of its components.

The MLIs also showed the same aging characteristics. The first layer of Mylar became yellow and brittle. Tensile tests were conducted on the following layers, and these results showed a slight increase in ultimate strength.

Mylar is therefore very sensitive to the environment. It undergoes physical and chemical changes which are considerably prejudicial to its use if not properly protected.

10.5.8 Protected Coated Thermal Control Blankets

Multilayer insulation (MLI) blankets are efficient, lightweight insulation systems for use in a vacuum. In order to achieve long life for blankets directly exposed to the LEO environment the outer layers of the MLI blankets will have a coating. For example, a transparent conductive coating, such as indium tin oxide (ITO), is typically applied to the front surface of second-surface mirrors to provide a means of draining static electricity induced by Van Allen radiation belts. Without this conductive coating, it is possible to build up charges of 20 000 to 30,000 volts on the surface of a second-surface mirror. AO-resistant MLI outer layers must be developed.

In addition, MLI directly exposed to the LEO environment must also be designed for resistance to UV radiation and high velocity impacts, as well as AO. However, the outer layers of these blankets frequently use materials such as Teflon as well as Kapton and Mylar (DuPont trademarks), which are eroded by AO. Although MLI blankets have not been designed and qualified with AO-resistant outer layers, coating materials have been developed and examined to determine its feasibility as an AO-resistant outer layer for MLI blankets. For example, polycrystalline ceramic films, such as SiO_x (where $1.9 < X < 2.0$), SiO_2, fluoropolymer-filled SiO_2, and Al_2O_3 (see Section 8) have been demonstrated in both ground and space tests (i.e., LDEF) to be effective in protecting polyimide Kapton from oxidation by LEO atomic oxygen.[111,112] These films are often used as an environmental protective coating due to its resistant to atomic oxygen exposure, and provides improved radiative properties during space environment exposure. Other materials under consideration as an AO-resistant outer layer include an aluminum foil laminated to the substrate (e.g., Mylar) or some other flexible, metalized material.[o]

[o]Specifically, the candidate material is a thin Mylar film sandwiched between two aluminum foil layers to form a foil laminate. Such a laminate would be very resistant to AO. Preliminary thermal vacuum tests indicate that there are design problems associated with using a thermally conductive material as an outer layer on an insulation blanket. Heat conduction at blanket overlaps and at areas where the MLI is compressed (for example, at seams and penetrations) may dominate the insulative properties.

10.5.8.1 SiO_X-Coated Silver Teflon

10.5.8.1.1 Composition

5.0 mil Type A Teflon x vacuum deposited silver x vacuum deposited Inconel x 966 acrylic pressure sensitive adhesive tape with SiO_x coated on Teflon side.

10.5.8.1.2 Manufacturing Process

The Sheldahl proprietary ion-beam assist process applies a SiO_x coating to the Teflon side of the vacuum deposited aluminum Teflon sample in thin layers by allowing multiple passes of the depositing cathode. The total SiO_x coating thickness resulting from the multiple pass application process is 1000 Å. Handling of SiO_x coated samples results in minimum generation of particulate flakes due to the thinness of the SiO_x layers. In addition, the SiO_x adheres well to the substrate as demonstrated by a MIL-STD adhesion test where the adhesive is pulled off the tape and sticks to the SiO_x coating. The SiO_x coating produced by the ion-beam assist process also contains less pinhole type defects than one step processes due to the multiple passes of the depositing cathode.

The cost of the SiO_x coated materials is approximately two to three times the cost of uncoated materials. This additional cost includes the extra processing required as well as testing of optical properties, thermal shock, adhesion, blocking, flexibility, outgassing, thermal cycling, solvent wipe, and humidity resistance.

10.5.8.1.3 Effects of the Space Environment

Not Available

10.5.8.2 ITO-Coated Silver Teflon

10.5.8.2.1 Composition

A transparent conductive coating, such as indium tin oxide (ITO) is typically applied to the front surface of second-surface mirrors to provide a means of draining static electricity induced by Van Allen radiation belts. Without this conductive coating, it is possible to build up charges of 20,000 to 30,000 volts on the surface of a second-surface mirror. The ITO coating has a surface resistivity of approximately 10,000 ohms per square. The coating increases the solar absorptance three percent and the emittance is unaffected. Table 10-88 shows typical thermo-optical properties of transparent conductive coating/Teflon/silver thermal control materials (ref. 116).

Table 10-88. Typical Thermo-Optical Properties of ITO-Coated Teflon/Silver

Material Description	α_s (1)	ε_H (2)	α_s / ε_H	Temp. Range Continuous °C (°F)	Approx. Weight gms/in^2
ITO x 2.0 mil Teflon x vacuum deposited silver x vacuum deposited Inconel	≤0.14 (3)	≥0.60 (3)	0.19	-73 to 66 (-100 to 150)	0.070
ITO x 5.0 mil Teflon x vacuum deposited silver x vacuum deposited Inconel	≤0.14	≥0.75	0.15	-73 to 66 (-100 to 150)	0.175

(1) Solar absorptance testing was done with a dual beam, ratio recording Beckman DK-2A UV-VIS-NIR spectrophotometer. Solar absorptance was computed based on 25 equal energy intervals centered on wavelengths from 314 nanometers to 2191 nanometers. These wavelengths are computed from tables of spectra in NASA SP-8005 and ASTM E490-73a.
(2) An approximation to total hemispherical emittance was obtained from a Lion Research Corporation emissometer. This instrument responds to the IR energy emitted from a sample through a potassium bromide window into the detector. The wavelength range is 3-30 microns. This method equates to ASTM E408, Method B.
(3) The absorptance and emittance values are measured through the Teflon surface.

10.5.8.2.2 Source

Manufacturer: Sheldahl
Northfield, MN 55057
Tel: (507) 663-2180

10.5.8.2.3 Effects of the Space Environment

Table 10-89 presents the variations of the solar reflectance of ITO-coated silver Teflon samples after their flight on FRECOPA/LDEF and on the 1.1 year COMES/MIR flight experiment (ref. 34). The COMES experiment consisted of four panels which were deployed by an astronaut in space outside of MIR with the possibility of exposing samples on both sides, conventionally identified as "V" and "R". Experiment AO 138-6, part of the FRECOPA experiment, was located on the trailing edge of LDEF. The experiment was designed to allow exposure of a part of the samples to the whole spacecraft environment by being laid directly on the FRECOPA tray surface, while the other part of samples was protected from the external environment of LDEF for all mission phases, except free flight, by the means of a vacuum-tight FRECOPA canister in which they were stored. Compared to the COMES/MIR experiment, the AO 138-6 FRECOPA experiment did not receive a high flux of atomic oxygen because of its position on LDEF.

Table 10-89. Solar Reflectance Degradation ΔRs of ITO Silver Teflon Second Surface Mirrors Measured After the FRECOPA and COMES Flight Experiments

Material	Mfg.	$Rs_{initial}$	AO 138-6 LDEF		COMES	
			Canister ΔRs	Tray ΔRs	Face V ΔRs	Face R ΔRs
Silver FEP + ITO	GE	0.89		0	-0.07	
Silver FEP + ITO	GE	0.91		-0.04		
Silver FEP (125 microns) + ITO	Sheldahl	0.91		-0.03		
Silver FEP (125 microns) + ITO	Sheldahl	0.90	0			
Silver FEP (125 microns) + ITO	GE	0.90	0			

Environmental Variations of LDEF and MIR Space Experiments: Due to its position on the trailing edge of LDEF, the AO 138-6 experiment did not receive any oxygen atoms during the mission, with the exception of a short period during the capture when it received a fluence evaluated at 1.32×10^{17} atoms cm^{-2}. The solar illumination was 11,100 equivalent sun hours (esh) for the samples located on the tray and only 1448 esh for the samples inside the canister. The particle irradiation dose (mainly due to the electron flux) was weak: $\sim 10^5$ rads. The number of temperature cycles was ~34,000 with temperatures within the ranges shown in the table below.

ENVIRONMENT	FRECOPA-LDEF		COMES-MIR	
	CANISTER	TRAY	FACE V	FACE R
Oxygen atoms cm^{-2}	0	1.3×10^{17}	1.2×10^{18} to 7.5×10^{19} (1)	3.5×10^{20} to 5.8×10^{20} (1)
Solar UV (esh)	1448	11,100	2850(2)	1900(2)
Temp. Cold case (°C)	-20 to -26	-43 to -52	-60 to -70	-60 to -70
Temp. Hot case (°C)	+67 to +85	+45 to +63	+10 to +30	+50 to +60

(1) Estimated from AO reactivity erosion of Kapton (3.0×10^{-24} $cm^3 atom^{-1}$) and Terphane (3.0×10^{-24} $cm^3 atom^{-1}$) samples

(2) Estimated from data of experiment calorimeter

Experimental Description. The solar reflection measurements were made with a Beckman DK2A spectrophotometer with an integrating sphere, and the infrared emissivity measurements were made with the Gier & Dunkle DB 100 device. It is important to underline that the measurements were all taken in air on samples which had thus experienced more or less intense recovery of the radiation damage.

The silver FEP with ITO deteriorated more for COMES than for FRECOPA.

Table 10-90 presents the variations of the emissivity of ITO-coated silver Teflon samples after their flight on FRECOPA/LDEF (ref. 13). Experiment AO 138-6 was part of the FRECOPA experiment located on the trailing edge of LDEF. The experiment was designed to allow exposure of a part of the samples to the whole spacecraft environment by being laid directly on the FRECOPA tray surface, while the other part of samples was protected from the external environment of LDEF for all mission phases, except free flight, by the means of a vacuum-tight FRECOPA canister in which they were stored.

Table 10-90. Emissivity Variations of ITO Silver Teflon Conductive Second Surface Mirrors (SSM) Measured After the FRECOPA Flight Experiment

Material	Mfg.	$\varepsilon_{initial}$	AO 138-6 LDEF	
			Canister $\Delta\varepsilon$	Tray $\Delta\varepsilon$
Silver FEP + ITO	GE	0.804		0.011
Silver FEP + ITO	GE	0.81		0.009
Silver FEP (125 microns) + ITO	Sheldahl	0.803		0.007
Silver FEP (125 microns) + ITO	Sheldahl	0.804	0.002	
Silver FEP (125 microns) + ITO	GE	0.810	0.006	

Experimental Description: Experiment AO 138-6 was part of the FRECOPA experiment located on the trailing edge of LDEF. The experiment was designed to allow exposure of a part of the samples to the whole spacecraft environment by being laid directly on the FRECOPA tray surface, while the remaining samples were protected from the external environment of LDEF for all mission phases, except free flight, by the means of a vacuum-tight FRECOPA canister in which they were stored.

Environmental Variations of LDEF Space Experiments: Due to its position on the trailing edge of LDEF, the AO 138-6 experiment did not receive any oxygen atoms during the mission, with the exception of a short period during the capture when it received a fluence evaluated at 1.32×10^{17} atoms cm^{-2}. The solar illumination was 11,100 equivalent sun hours (esh) for the samples located on the tray and only 1448 esh for the samples inside the canister. The particle irradiation dose (mainly due to the electron flux) was weak: 3×10^{5} rads. The number of temperature cycles was ~34,000 with temperatures within the ranges shown in the table below.

	FRECOPA-LDEF	
	CANISTER	TRAY
Oxygen atoms cm^{-2}	0	1.3×10^{17}
Solar UV (esh)	1448	11,110
Temp. Cold case (°C)	-20 to -26	-43 to -52
Temp.Hot case (°C)	+67 to +85	+45 to +63

10.5.8.3 In_2O_3-Coated Silver Teflon

10.5.8.3.1 Composition

An overcoat of In_2O_3 is ion beam sputter deposited on Teflon/Ag to provide surface conductivity for thermal and spacecraft charge control.

10.5.8.3.2 Source

10.5.8.3.3 Space Environmental Effects

Silver Teflon with an ion beam sputter deposited thin conductive coating of In_2O_3 on the Teflon side provided a pre-flight sheet resistance of approximately 900 ohms/square. This sample was flown in low-Earth orbit on the Long Duration Exposure Facility (LDEF) for 5.8 years with the In_2O_3 side exposed to space. Because of its location on LDEF (98° from the ram direction), the material was primarily exposed to vacuum ultraviolet (6500 esh), radiation, thermal cycling (33,700 thermal cycles), the vacuum of space, the micrometeoroid and debris environment, and grazing incidence atomic oxygen.

Measurements of solar absorptance and thermal emitttance (pre- and post-flight) showed no changes. However, photomicrographs showed cracking and a decrease in electrical conductivity to 2000 ohms/square.[113] (See also J.Guillaumon and Alain Paillous, "Spacecraft Thermal Control Coatings", First Post-Retrieval Flight Symp., NASA CP 3134, pp.945-960.) In_2O_3 coating on Kapton and Teflon appeared to provide protection from atomic oxygen erosion (ref. 10).

10.5.8.5 ITO-Coated Aluminized Teflon

10.5.8.5.1 Composition

A transparent conductive coating, such as indium tin oxide (ITO) is typically applied to the front surface of second-surface mirrors to provide a means of draining static electricity induced by Van Allen radiation belts. Without this conductive coating, it is possible to build up charges of 20,000 to 30,000 volts on the surface of a second-surface mirror. The ITO coating has a surface resistivity of approximately 10,000 ohms per square. The coating increases the solar absorptance three percent and the emittance is unaffected. Table 10-91 shows typical thermo-optical properties of transparent conductive coating/Teflon/aluminum thermal control materials (ref. 116).

Table 10-91. Typical Thermo-Optical Properties of ITO-Coated Teflon/Aluminum

Material Description	$\alpha^{(a)}$	ε	Typical α/ε	Temp. Range Continuous °C (°F)	Approx. Weight gms/in^2
ITO x 2.0 mil Teflon x vacuum deposited aluminum	≤0.19	≥0.60	0.27	-73 to 66 (-100 to 150)	0.070
ITO x 5.0 mil Teflon x vacuum deposited aluminum	≤0.19	≥0.75	0.22	-73 to 66 (-100 to 150)	0.175

(a) The absorptance and emittance values are measured through the Teflon surface.

10.5.8.5.2 Source

10.5.8.5.3 Effects of the Space Environment

No Data Available.

10.5.8.6 SiO_X-Coated Aluminized Kapton

10.5.8.6.1 Composition

Silicon oxide sputter deposited coatings have been successfully applied over Kapton and are effective in protecting this substrate from erosion by atomic oxygen. Results from LDEF have demonstrated this fact.

10.5.8.6.2 Manufacturing Process

The SiO_x coating, produced by Sheldahl is a 1300 Å thick sputter deposited overcoating. The cost of the SiO_x coated materials is approximately two to three times the cost of uncoated materials. This additional cost includes the extra processing required as well as testing of optical properties, thermal shock, adhesion, blocking, flexibility, outgassing, thermal cycling, solvent wipe, and humidity resistance.

10.5.8.6.3 Effects of the Space Environment

Specimens of 1/3, 1/2, 1 and 5 mil vacuum deposited aluminum (VDA) Kapton coated with thin film oxide were flown at three locations aboard LDEF to evaluate their resistance to atomic oxygen erosion. Post flight emittance and solar absorptance measurements compared with pre flight values are summarized in Table 10-92.[114]

Table 10-92. Comparison of Pre-Flight and Post Flight Solar Absorptance and Emittance for Selected Thermal Control Coatings

Coating	Substrate	Location on LDEF	α	ε_N
200A SnO_2/In_2O_3	Kapton 1/2 mil	F9 F12 H1	0.35 0.31 0.35	0.59 0.60 0.64
200A SiO_x	Kapton 1/2 mil	Control F12 H1	0.34 0.36 0.36	0.56 0.57 0.58
500A SiO_x	Kapton 1/2 mil	Control F12 H1	0.33 0.34 0.37	0.57 0.57 0.60
700A SiO_x	Kapton 1/2 mil	Control F12 H1	0.32 0.32 0.36	0.57 0.56 0.60
1000A SiO_x	Kapton 1/2 mil	Control F12 H1	0.33 0.34 0.40	0.58 0.57 0.61
No Coating	Kapton 1 mil	Control F12 H1	0.35 0.35 0.35	0.65 0.57 0.59
Acrylic/Urethane	Kapton 1/2 mil	Control F12	0.36 0.40	0.87 0.85
DC Q9-6312 clear silicone	Kapton 1/2 mil	Control F12 H1	- 0.41 0.37	- 0 83 0.79
S13GLO	Kapton 5 mil	Control F9 F12 H1	0.16 0.42 0.41 0.47	0.90 0.88 0.89 0.89
RTV 615 white paint	Kapton 1/3 mil	Control F9 F12 H1	0.23 0.47 0.33 0.40	0.87 0.85 0.86 0.86

Space Environmental Exposure Conditions:

F9: Samples flown in the ram direction on top of the MLI blanket of the Cascade Variable Conductance Heat Pipe Experiment. These samples saw UV (11,100 esh) and AO (8.32×10^{21} atoms/cm^2)

F12: Samples flown on top of the MLI blanket of the Low Temperature Heat Pipe Experiment perpendicular to the ram direction. These samples saw UV (6,900 esh) and much less AO (1.2×10^{21} atoms/cm^2)

H1: Samples flown on the perimeter of the Low Temperature Heat Pipe Experiment power tray on the space end of the satellite. These samples saw UV (14,500 esh) and AO (3.64×10^{20} atoms/cm^2)

Degradation of the thermal control coatings was observed on each of the experiment trays, either due to surface contamination or due to an inherent property of the coatings. Initial analysis indicate that much of the observed degradation was caused by outgassing of methyl silicon species from coatings, adhesives or rubber products aboard the spacecraft. These outgassing products were then turned brown by the action of UV and atomic oxygen near the end of the flight. The Kapton samples overcoated with silicon oxide suffered the least degradation and erosion. Small change in solar absorptance was observed but was probably due to the general contamination experienced by all parts of the spacecraft. The Kapton samples overcoated with indium oxide and indium tin oxide however did not fair as well as the silicon oxide coated samples. The worst degradation was observed in the unprotected Kapton. In some instances 5 mil Kapton had patches which were completely eroded away. Urethane and silicone overcoating of some of the Kapton did little to prevent their eventual erosion by atomic oxygen. Although the black paint samples (Z306 and RTV615 with carbon black) showed little change in absorptance or emittance they did show some signs of contamination and tended to curl as did the white paints. This curling was probably caused by shrinkage of the paints.

10.5.8.7 ITO-Coated Aluminized Kapton

10.5.8.7.1 Composition

A transparent conductive coating, such as indium tin oxide (ITO) is typically applied to the front surface of second-surface mirrors to provide a means of draining static electricity induced by Van Allen radiation belts. Without this conductive coating, it is possible to build up charges of 20,000 to 30,000 volts on the surface of a second-surface mirror. The ITO coating has a surface resistivity of approximately 10,000 ohms per square. The coating increases the solar absorptance three percent and the emittancce is unaffected. Table 10-93 shows typical thermo-optical properties of transparent conductive coating/Kapton/aluminum thermal control materials (ref. 116).

Table 10-93. Typical Thermo-Optical Properties of ITO-Coated Kapton/Aluminum

Material Description	α_s (1)	ε_H (2)	α_s / ε_H	Temp. Range Continuous °C (°F)	Approx. Weight gms/in^2
ITO x 1.0 mil Kapton x vacuum deposited aluminum	≤0.44 (3)	≥0.62 (3)	~0.50	-184 to 260 (-300 to 500)	0.023
ITO x 2.0 mil Kapton x vacuum deposited aluminum	≤0.49	≥0.71	~0.50	-184 to 260 (-300 to 500)	0.046

(1) Solar absorptance testing was done with a dual beam, ratio recording Beckman DK-2A UV-VIS-NIR spectrophotometer. Solar absorptance was computed based on 25 equal energy intervals centered on wavelengths from 314 nanometers to 2191 nanometers. These wavelengths are computed from tables of spectra in NASA SP-8005 and ASTM E490-73a.

(2) An approximation to total hemispherical emittance was obtained from a Lion Research Corporation emissometer. This instrument responds to the IR energy emitted from a sample through a potassium bromide window into the detector. The wavelength range is 3-30 microns. This method equates to ASTM E408, Method B.

(3) The absorptance and emittance values are measured through the Kapton surface.

10.5.8.7.2 Source

Manufacturer: Sheldahl
Northfield, MN 55057
Tel: (507) 663-2180

10.5.8.7.3 Effects of the Space Environment

Table 10-94 presents the variations of the solar reflectance of aluminized Kapton samples after their flight on FRECOPA/LDEF and on the 1.1 year COMES/MIR flight experiment (ref. 34). The COMES experiment consisted of four panels which were deployed by an astronaut in space outside of MIR with the possibility of exposing samples on both sides, conventionally identified as "V" and "R". Experiment AO 138-6, part of the FRECOPA experiment, was located on the trailing edge of LDEF. The experiment was designed to allow exposure of a part of the samples to the whole spacecraft environment by being laid directly on the FRECOPA tray surface, while the other part of samples was protected from the external environment of LDEF for all mission phases, except free flight, by the means of a vacuum-tight FRECOPA canister in which they were stored. Compared to the COMES/MIR experiment, the AO 138-6 FRECOPA experiment did not receive a high flux of atomic oxygen because of its position on LDEF.

The aluminized Kapton with ITO displayed analogous behavior in both experiments.

Table 10-94. Solar Reflectance Degradation ΔRs of ITO Aluminized Kapton Second Surface Mirrors Measured After the FRECOPA and COMES Flight Experiments

Material	Mfg	$Rs_{initial}$	$\varepsilon_{initial}$	AO 138-6 LDEF		COMES	
				Canister ΔRs	Tray ΔRs	Face V ΔRs	Face R ΔRs
Aluminized Kapton + ITO	GE	0.61	.762		-0.02	-0.02	-0.02
Aluminized Kapton + ITO	GE	0.60	.762	-0.02			

Environmental Variations of LDEF and MIR Space Experiments: Due to its position on the trailing edge of LDEF, the AO 138-6 experiment did not receive any oxygen atoms during the mission, with the exception of a short period during the capture when it received a fluence evaluated at 1.32×10^{17} atoms cm^{-2}. The solar illumination was 11,100 equivalent sun hours (esh) for the samples located on the tray and only 1448 esh for the samples inside the canister. The particle irradiation dose (mainly due to the electron flux) was weak: 3×10^5 rads. The number of temperature cycles was ~34,000 with temperatures within the ranges shown in the table below.

ENVIRONMENT	FRECOPA-LDEF		COMES-MIR	
	CANISTER	TRAY	FACE V	FACE R
Oxygen atoms cm^{-2}	0	1.3×10^{17}	1.2×10^{18} to 7.5×10^{19} (1)	3.5×10^{20} to 5.8×10^{20} (1)
Solar UV (esh)	1448	11,100	2850(2)	1900(2)
Temp. Cold case (°C)	-20 to -26	-43 to -52	-60 to -70	-60 to -70
Temp. Hot case (°C)	+67 to +85	+45 to +63	+10 to +30	+50 to +60

(1) Estimated from AO reactivity erosion of Kapton (3.0×10^{-24} $cm^3 atom^{-1}$) and Terphane (3.0×10^{-24} $cm^3 atom^{-1}$) samples

(2) Estimated from data of experiment calorimeter

Experimental Description. The solar reflection measurements were made with a Beckman DK2A spectrophotometer with an integrating sphere, and the infrared emissivity measurements were made with the Gier & Dunkle DB 100 device. It is important to underline that the measurements were all taken in air on samples which had thus experienced more or less intense recovery of the radiation damage.

Table 10-95 presents the variations of the emissivity of aluminized Kapton samples after their flight on FRECOPA/LDEF (ref. 13). Experiment AO 138-6 was part of the FRECOPA experiment located on the trailing edge of LDEF. The experiment was designed to allow exposure of a part of the samples to the whole spacecraft environment by being laid directly on the FRECOPA tray surface, while the other part of samples was protected from the external environment of LDEF for all mission phases, except free flight, by the means of a vacuum-tight FRECOPA canister in which they were stored.

Table 10-95. Emissivity Variations of ITO Aluminized Kapton Second Surface Mirrors (SSM) Measured After the FRECOPA Flight Experiment

Material	Mfg	$\varepsilon_{initial}$	Canister $\Delta\varepsilon$	Tray $\Delta\varepsilon$
Aluminized Kapton + ITO	GE	.762		-0.013
Aluminized Kapton + ITO	GE	.762	-0.041	

Experimental Description: Experiment AO 138-6 was part of the FRECOPA experiment located on the trailing edge of LDEF. The experiment was designed to allow exposure of a part of the samples to the whole spacecraft environment by being laid directly on the FRECOPA tray surface, while the remaining samples were protected from the external environment of LDEF for all mission phases, except free flight, by the means of a vacuum-tight FRECOPA canister in which they were stored.

Environmental Variations of LDEF Space Experiments: Because of its position on side 3 of the LDEF, the AO 138-6 experiment did not receive any oxygen atoms during the mission, with the exception of a short period during the capture when it received a fluence evaluated at 1.32×10^{17} atoms cm^{-2}. The solar illumination was 11,100 equivalent sun hours (esh) for the samples located on the tray and only 1448 esh for the samples inside the canister. The particle irradiation dose (mainly due to the electron flux) was weak: 3×10^{5} rads. The number of temperature cycles was ~34,000 with temperatures within the ranges shown in the table below.

	FRECOPA-LDEF	
	CANISTER	TRAY
Oxygen atoms cm^{-2}	0	1.3×10^{17}
Solar UV (esh)	1448	11,110
Temp. Cold case (°C)	-20 to -26	-43 to -52
Temp.Hot case (°C)	+67 to +85	+45 to +63

10.5.8.8 In_2O_3-Coated Aluminized Kapton

10.5.8.8.1 Composition

10.5.8.8.2 Source

10.5.8.8.3 Space Environmental Effects

In_2O_3 coating on Kapton appeared to provide protection from atomic oxygen erosion (ref. 4).

10.5.9 Beta Cloth

The function of the PTFE impregnated Beta cloth cover is to improve the handling characteristics of MLI blankets.

10.5.9.1 Composition and Optical Properties

Solar absorptance and thermal emittance measurements on Beta cloth material are shown in Table 10-96. The data were obtained on as-supplied materials, unexposed to either atomic oxygen or ultraviolet radiation. The use of a strong outer-ply material for multilayer insulation reduces manufacturing costs. Light-weight continuous film materials are easily damaged and are difficult to handle. The glass fabric used in the beta cloth should be of a fine, tight weave to resist erosion by atomic oxygen.

Table 10-96. Optical Properties Measurements for Beta Cloth

Material	Surface Tested	Solar Absorptance	Thermal Emittance
Chemgals-250, PTFE impregnated, aluminized on one side	Unaluminized Side	0.33	0.90
Chemglas-250, PTFE impregnated, aluminized on one side. Same as Above	Aluminized Side	0.33	0.15
Sheldahl prepared sample thermal control blanket. Surface ply was Beta cloth, PTFE impregnated without metalization of either surface.	Beta cloth surface ply over metalized light block and reflector plies.	0.22	0.90

10.5.9.2 Source

DuPont, General Electric

10.5.9.3 Effects of the Space Environment

PTFE Teflon impregnated Beta cloth was used on LDEF near the leading edge and portions of this material was directly exposed to atomic oxygen throughout the flight. Teflon exposed to direct impingement on the surface of the beta cloth was completely removed. However, the erosion did not extend through the woven fabric. Table 10-97 and Table 10-98 present the variations of the solar reflectance and emissivity of various Teflon-impregnated glass fabric (beta cloth) after their flight on the 9-month FRECOPA/LDEF experiment and the 1.1-year

COMES/MIR flight experiment (ref. 34). The COMES experiment consisted of four panels which were deployed by a cosmonaut in space outside of MIR with the possibility of exposing samples on both sides, conventionally identified as "V" and "R". Experiment AO 138-6 was part of the FRECOPA experiment located on the trailing edge of LDEF. The experiment was designed to allow exposure of a part of the samples to the whole spacecraft environment by being laid directly on the FRECOPA tray surface, while the other part of samples was protected from the external environment of LDEF for all mission phases, except free flight, by the means of a vacuum-tight FRECOPA canister in which they were stored.

Table 10-97. Solar Reflectance Variations of Beta Cloth Measured After the FRECOPA and COMES Flights Experiments

Material	Mfg	$Rs_{initial}$	AO 138-6 LDEF		COMES	
			Canister ΔRs	Tray ΔRs	Face V ΔRs	Face R ΔRs
Teflon-impregnated glass fabric (beta cloth)	DuPont	0.700		-0.140		-0.07
Teflon-impregnated glass fabric (beta cloth)	DuPont	0.680	-0.100		0	
Astroquartz/FEP/aluminum (silica fabric)	GE	0.830		-0.050		

Environmental Variations of LDEF and MIR Space Experiments: Due to its position on the trailing edge of LDEF, the AO 138-6 experiment did not receive any oxygen atoms during the mission, with the exception of a short period dur the capture when it received a fluence evaluated at 1.32×10^{17} atoms cm^{-2}. The solar illumination was 11,100 equivalent sun hours (esh) for the samples located on the tray and only 1448 esh for the samples inside the canister. The particle irradiation dose (mainly due to the electron flux) was weak: 3×10^{5} rads. The number of temperature cycles was ~34,000 with temperatures within the ranges shown in the table below.

ENVIRONMENT	FRECOPA-LDEF		COMES-MIR	
	CANISTER	TRAY	FACE V	FACE R
Oxygen atoms cm^{-2}	0	1.3×10^{17}	1.2×10^{18} to 7.5×10^{19} (1)	3.5×10^{20} to 5.8×10^{20} (1)
Solar UV (esh)	1448	11,100	2850(2)	1900(2)
Temp. Cold case (°C)	-20 to -26	-43 to -52	-60 to -70	-60 to -70
Temp. Hot case (°C)	+67 to +85	+45 to +63	+10 to +30	+50 to +60

(1) Estimated from AO reactivity erosion of Kapton (3.0×10^{-24} $cm^3 atom^{-1}$) and Terphane (3.0×10^{-24} $cm^3 atom^{-1}$) samples

(2) Estimated from data of experiment calorimeter

Experimental Description. The solar reflection measurements were made with a Beckman DK2A spectrophotometer with an integrating sphere, and the infrared emissivity measurements were made with the Gier & Dunkle DB 100 device. It is important to underline that the measurements were all taken in air on samples which had thus experienced more or less intense recovery of the radiation damage.

From Table 10-97, one observes that the reflectance of the beta cloth deteriorated significantly in both experiments. Significant emissivity changes were observed for the astroquartz/FEP/aluminum (silica fabric) as shown in Table 10-98.

Table 10-98. Emissivity Variations of Beta Cloth Measured After the LDEF FRECOPA Experiment

Material	Mfg	$e_{initial}$	AO 138-6 LDEr	
			Canister Δe	Tray Δe
Teflon-impregnated glass fabric (beta cloth)	DuPont	0.895		0.001
Teflon-impregnated glass fabric (beta cloth)	DuPont	0.895	0	
Astroquartz/FEP/aluminum (silica fabric)	GE	0.845		-0.760

Experimental Description: Experiment AO 138-6 was part of the FRECOPA experiment located on the trailing edge of LDEF. The experiment was designed to allow exposure of a part of the samples to the whole spacecraft environment by being laid directly on the FRECOPA tray surface, while the remaining samples were protected from the external environment of LDEF for all mission phases, except free flight, by the means of a vacuum-tight FRECOPA canister in which they were stored.

Environmental Variations of LDEF Space Experiments: Due to its position on the trailing edge of LDEF, the AO 138-6 experiment did not receive any oxygen atoms during the mission, with the exception of a short period during the capture when it received a fluence evaluated at 1.32×10^{17} atoms cm^{-2}. The solar illumination was 11,100 equivalent sun hours (esh) for the samples located on the tray and only 1448 esh for the samples inside the canister. The particle irradiation dose (mainly due to the electron flux) was weak: 3×10^5 rads. The number of temperature cycles was ~34,000 with temperatures within the ranges shown in the table below.

	FRECOPA-LDEF	
	CANISTER	TRAY
Oxygen atoms cm^{-2}	0	1.3×10^{17}
Solar UV (esh)	1448	11,110
Temp. Cold case (°C)	-20 to -26	-43 to -52
Temp.Hot case (°C)	+67 to +85	+45 to +63

LDEF Experiment S1001. Beta cloth impregnated with PTFE was used on LDEF Experiment S1005, which was a heat pipe experiment sponsored by NASA-Marshall.[114] The atomic oxygen fluence to this experiment was 8.43×10^{21} atoms/cm^2 during the LDEF mission. Examination of the Beta cloth following flight by NASA-Marshall personnel revealed that the PTFE was eroded from the exposed surfaces of the fabric to a depth of approximately 0.001 inch. It is expected that exposed glass fibers would shield and protect the PTFE from further erosion, if the blanket were exposed to more atomic oxygen. The inside surface of the Beta cloth showed no signs of degradation. The use of the Beta cloth on LDEF was not intended as an experiment. The manufacturer and designation of the material are not known at this time.

10.6 ALUMINUM SURFACE COATINGS

10.6.1 Anodized Aluminum

10.6.1.1 Thermal-Optical Properties

Aluminum anodizing using chromic or sulfuric acid can produce a/e ratios of between 0.2 and 2.0. Anodizing is recommended for all exposed aluminum hardware except for some radiators that have extremely low a/e requirements.[P] Anodized coatings with a/e ratios near 1:1 are used to minimize the use of heaters where equipment must be maintained at relatively high temperatures. Anodized aluminum provides a corrosion-resistant coating on the ground, is resistant to AO in space, and reduces spectral reflection. In addition, there are standard procedures for adding inorganic dyes to sulfuric acid anodized aluminum to produce additional optical property options. Table 10-99 lists the optical properties of a number of chromic acid and sulfuric acid anodized aluminum alloys.[115]

Table 10-99. Optical Properties of Several Anodized Aluminum Alloys

Alloy	Anodizing Process			
	Chromic		Sulfuric	
	α	ε	α	ε
2219-T37 sheet	0.42	0.71	0.35	0.82
5052-H34 sheet	0.55	0.60	0.32	0.82
5657-H25 sheet	0.45	0.55	0.16	0.80
6061-T6 sheet	0.43	0.50	0.40	0.84

Anodic coatings have intrinsic benefits other than potentially low degradation in optical properties. The absorptance-to-emittance ratio of anodic coatings can be tailored such that the maximum surface temperatures do not exceed the temperature limit of 235°C for the astronauts' gloves. Anodic coatings are rugged for handling, and integral with their substrate so that debonding of the coating from the substrate does not occur.

[P] Radiators require a low absorptance in order to reflect the incident solar energy, and a high emittance to radiate as much heat as possible. Developing a chromic acid anodic coating with a sufficiently high emittance ($e > 0.9$) to make it a candidate for a radiator coating would be difficult, if not possible. Because conventional chromic acid anodizing is a self-limiting thickness process, and because emittance is dependent on thickness, it is very difficult to achieve the high emittance required for radiators with chromic acid anodizing. However, chromic acid anodic coatings are candidates for other applications not requiring high emittances.

10.6.1.2 Manufacturing Process

MIL-STD-8625, Anodic Coatings for Aluminum and Aluminum Alloys, Type I, specify the anodize process for aluminum alloys. Studies conducted at NASA Langley[116] showed that a broad range of properties could be obtained by varying the chromic acid anodize processing parameters. Figures 10-67 and 10-68 graphically show the effect of anodizing time on the optical properties of 6061-T6 sheet. Initially, the optical properties change rapidly with anodizing time but stabilize at longer anodizing times. The values listed in Table 10-99 are in the region in which the optical properties have stabilized. With shorter processing times, a broader range of optical properties can be obtained. However, the process must be tightly controlled and achieving a uniform coating with the desired optical properties is more difficult, particularly with chromic acid anodizing. Standard deviation of between (0.01 and (0.02 has been achieved for both absorptance and emittance of chromic acid anodic coatings using tighter controls on processing conditions. The emittance of chromic acid anodic coatings varies more with anodize time than that of sulfuric acid anodic coatings.

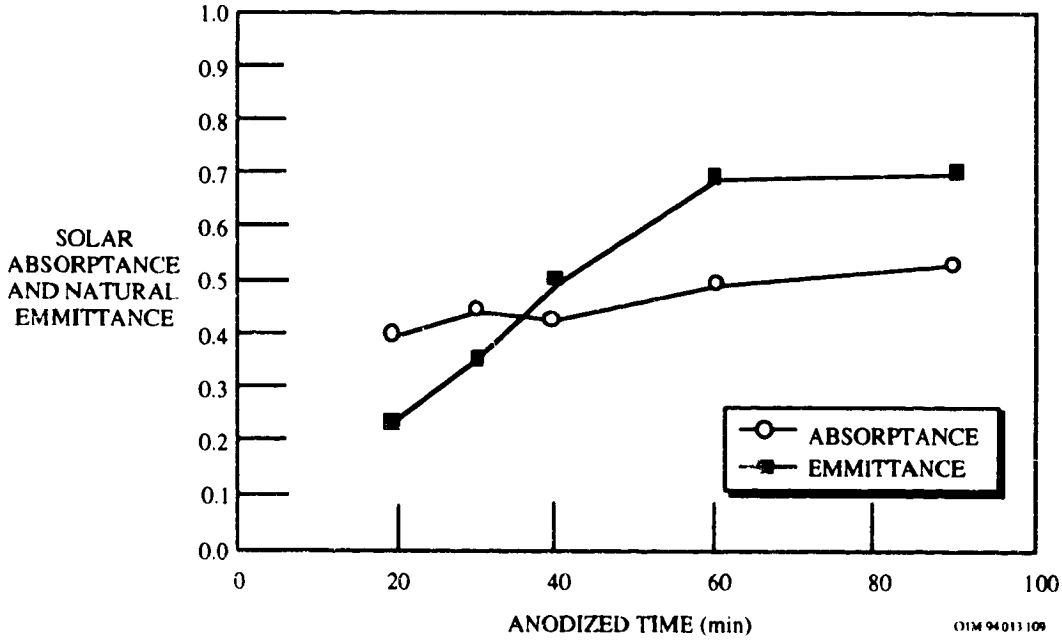

Figure 10-67. Optical Properties of Chromic Acid Anodized 6061-T6 as a Function of Anodizing Time.

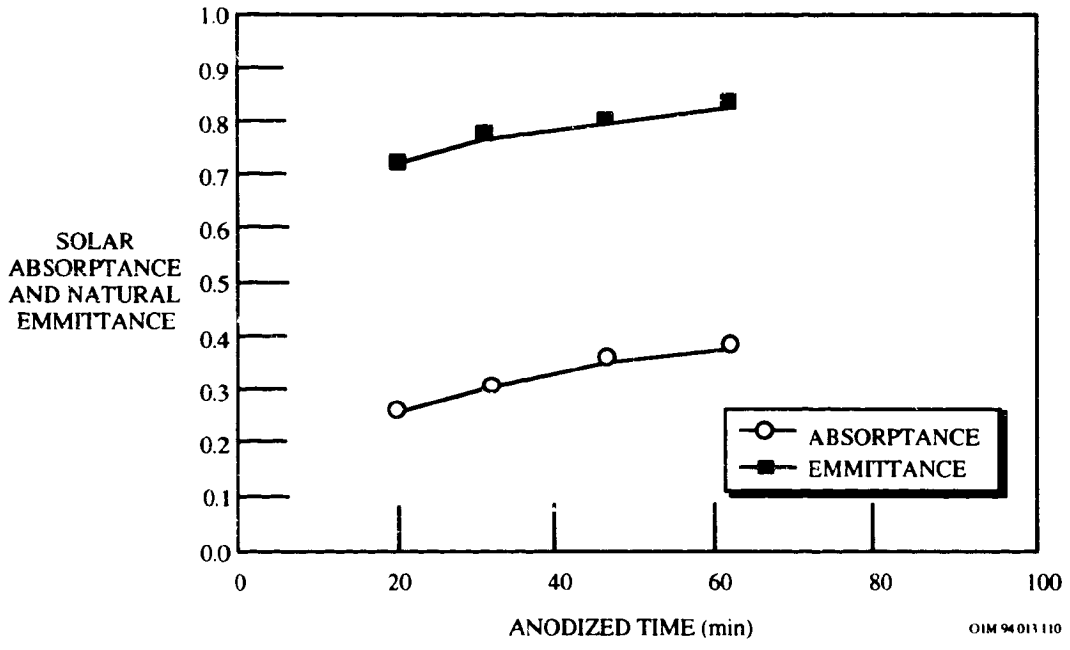

Figure 10-68. Optical Properties of Sulfuric Acid Anodized 6061-T6 as a Function of Anodizing Time

10.6.1.2 Effects of the Space Environment

Although anodic coatings offer many attractive features, there are a number of unfavorable characteristics that must be accommodated during the design phase. Because UV radiation normally causes the absorptivity of anodic coatings to increase with exposure while the emissivity remains constant, the a/e ratio increases. The coating should be designed to accommodate this increase without exceeding the allowable touch temperature limits. Thermal analysis indicates that increases in absorptance of greater than 0.2 would result in significant weight penalties for most hardware. Therefore, a maximum allowable absorptance increase of 0.2 from all sources is recommended, with a maximum UV degradation of 0.1. The rest of the absorptance degradation is expected to be primarily from contamination. In addition, the maximum allowable emittance decrease from all sources should be 0.05.

Anodic coatings can also begin to craze if thermally cycled, particularly when cycled to high temperatures. In one study,[117] this crazing increased the absorptivity of several nominally 0.025 mm thick anodized coatings by about 0.02 to 0.03, and decreased the emissivity by 0.04 to 0.07. Other investigators using other alloys have reported no change in optical properties with thermal cycling.

10.6.1.2.1 Solar Absorptance and Thermal Emittance

Chromic acid anodize was used as part of the passive thermal management system for LDEF. The anodize process used for LDEF structures was actually a modification of the standard chromic acid anodize process, as specified by MIL-STD-8625, Anodic Coatings for Aluminum and Aluminum Alloys, Type I. The modified process used for LDEF was developed by Gilliland at the NASA Langley Research Center (LaRC), and permits tailoring of solar absorptance and thermal emittance through the selection and control of anodizing voltage and time. LDEF structural components were constructed of 6061-T6 aluminum alloy and were anodized using the modified chromic acid process to achieve an average absorptance of 0.31 $\pm$0.01 and an emittance of 0.15 $\pm$0.01.[118]

Absorptivity and emissivity measurements were taken at 397 locations (exposed and unexposed) on the LDEF structure (intercostals, longerons, and center ring), 55 exposed locations on the space end thermal control panels, 60 exposed locations on the black chrome Earth end panels, and 221 exposed and unexposed locations on the tray lip flanges. Unexposed surface measurements were taken on areas of the facility which were shadowed by tray flanges and mounting clamps and therefore were not directly exposed to the AO and UV flux. The exposed anodized aluminum thermal control coatings measured survey represented 539 ft^2 (33%) out of the total exposed LDEF surface area. To determine the effects of the low Earth orbit environment on the anodized coatings, measurements were taken on both exposed and unexposed surfaces and compared to QA measurements taken at the time of hardware fabrication in 1978. The results are summarized in Tables 10-100 through 10-102.[119]

Table 10-100. Solar Absorptance Results for Chromic Acid Anodized Aluminum on LDEF

Item	1978 QA α	Unexposed α	Exposed α
Structure	.31 ±.02	.33 ±.04	.36 ±05
3" Tray Flange	.33 ±.02	.33 ±.03	.36 ±04
6" & 12" Tray Flanges	.33 ±.01	.35 ±.03	.37 ±.03
Space Therm Panels	.34 ±.02	—	.37 ±03
Earth Therm Panels	0.9	—	.92 ±.03

Table 10-101. Thermal Emittance Results for Chromic Acid Anodized Aluminum on LDEF

Item	1978 QA ε	Unexposed ε	Exposed ε
Structure	.15 ±.03	.18 ±.04	.15 ±.03
3" Tray Flange	.25 ±.01	.24 ±.04	.23 ±.04
6" & 12" Tray Flanges	.17 ±.02	.18 ±.02	.18 ±.03
Space Therm Panels	.15 ±.01	—	.15 ±.02
Earth Therm Panels	0.09	—	.08 ±.01

Table 10-102. Solar Absorptance/Thermal Emittance Results for Chromic Acid Anodized Aluminum on LDEF

Item	1978 QA α/ε	Unexposed α/ε	Exposed α/ε
Structure	2.07	1.83	2.37
3" Tray Flanges	1.32	1.38	1.56
6" & 12" Tray Flanges	1.94	1.94	2.06
Space Therm Panels	2.27	-	2.47
Earth Therm Panels	10.0	-	11.5

Solar Absorptance. The average absorptivity of 246 exposed structural surface measurements taken around the LDEF periphery was 0.36 ±0.05 which was an increase of 0.05 over the QA log average of 0.31 (0.02 (see Table 10-100). The observed average 0.05 degradation (16%) is consistent with a LaRC solar stability test done at the time when the variable anodizing process was being developed. This test showed the solar degradation to be no more than 15% for over 2000 hours of a one sun exposure in a vacuum test chamber. The average absorptivity for the 125 unexposed structural surfaces was 0.33 (0.04, a 6.5% increase over the original 0.31 value. This small change in absorptivity most likely can be attributed to the different measuring instruments employed or the presence of contamination on the unexposed surfaces.

Absorptance degradation on LDEF did not appear to be a function of the total UV exposure, but was related more to orientation relative to the velocity direction. Average row absorptivities versus LDEF row location for the QA log, unexposed, and exposed structural surface measurements showed that almost no change in absorptivity on the leading edge (row 9), to approximately a 24% increase in absorptivity on the trailing edge (row 3). As shown in Figure 10-69, surfaces in the wake direction saw more absorptance degradation than surfaces in the ram

direction.[120] The absorptance degradation of less than 0.015 in the ram direction is small, although it received 11,000 esh UV exposure.

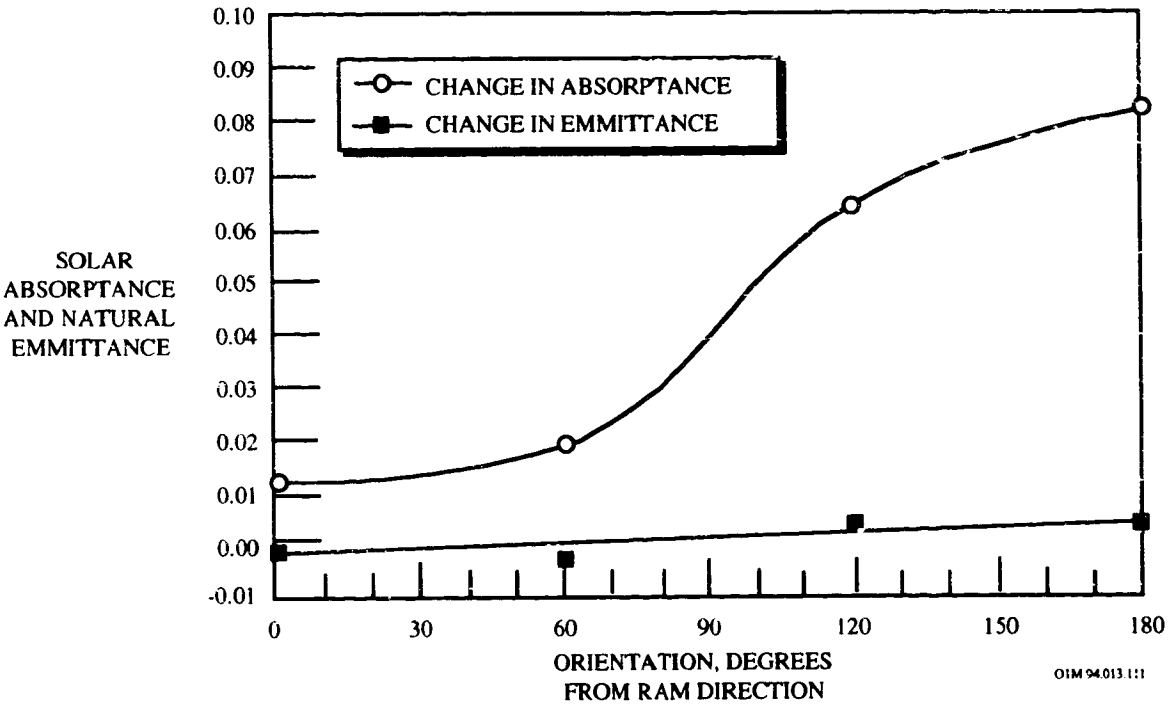

Figure 10-69. Change in Absorptance and Emittance of Chromic Acid Anodized 6061-T6 as a Function of Orientation to Ram Direction-LDEF Data.

In a study by Boeing,[121] a correlation was observed in absorptance measurement changes with decreasing AO fluence, but not with solar radiation fluence. This small amount of degradation is consistent with ground test results, which showed degradation of between 0.01 to 0.045 after 1000 esh near-UV testing.[122] In the wake direction, the 0.08 degradation in absorptance appears to be primarily due to contaminant deposition and UV degradation of the contaminant layer. In a study at NASA Langley,[123] the chromic acid anodized 1145 aluminum 3 mil foil used to coat composite tubes was found to be very stable to simulated solar UV radiation. A solar absorptance increase of only 0.02 was observed after 4,000 esh (2,000 hours x 2 solar constants), as shown in Figure 10-70.

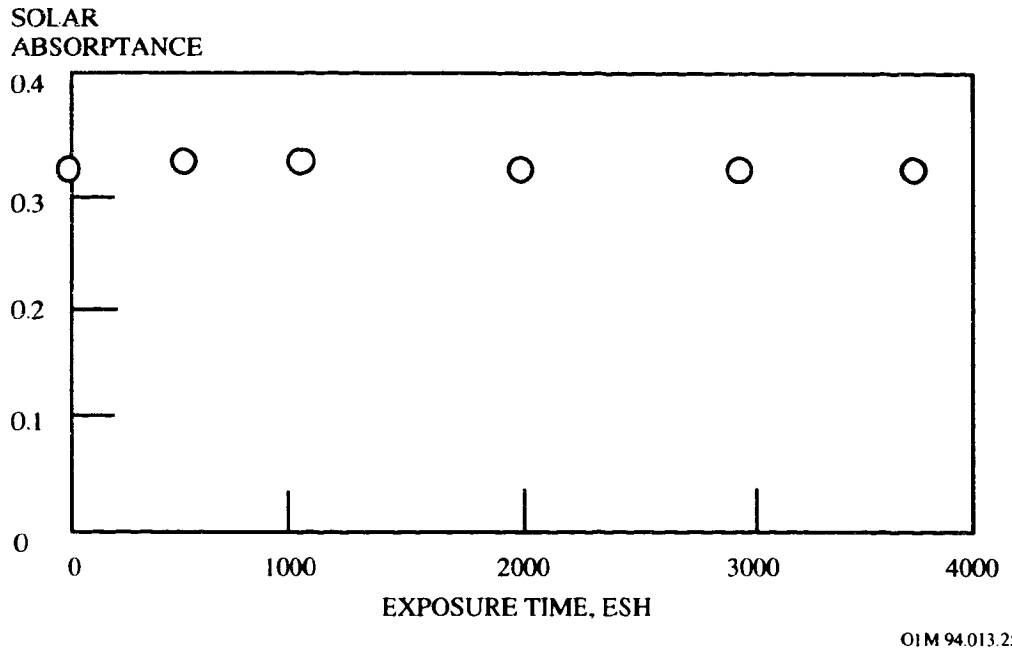

Figure 10-70. Effects of UV on Solar Absorptance of Chromic-Acid Anodized Aluminum

Thermal Emittance. The average normal emissivity for exposed surfaces was 0.15 ±0.03 which was the same as the QA log average. One consistent trend observed while surveying the structure was the 20.0% increase in unexposed surface average emissivity (0.18 ±0.04) over the QA average emissivity values (see Table 10-101).

Absorptance/Emittance Ratio. A plot of the average row a/e ratio versus row location on the spacecraft shows that the leading edge rows are much closer to the QA log ratios than the trailing edge rows which were shielded from the AO flux. The results indicate that the overall exposed and unexposed average a/e values remained within the design range of 1.67 to 2.43 throughout the six year LDEF mission, even though locally the a/e varied depending upon which row location was being examined on the LDEF (see Table 10-102).

Space and Earth Facing Panels. The LDEF employed thin aluminum panels at each end of the facility to control heat flow in and out of the ends of the spacecraft. The space facing panels used a clear chromic anodized finish with a design a/e from 1.78 to 2.57. The average absorptivity increased 8.8% from 0.34 in 1978 to 0.37 by the end of the LDEF mission (see Table 10-100), and the average emissivity for the panels showed no change except for tolerances from beginning to end of mission (0.15 ±0.01 versus 0.15 ±0.02; see Table 10-101). The Earth facing panels were black chrome anodized for an a/e range from 7.75 to 10.88. On these 12 panels, the surface properties remained very stable over the LDEF mission with the average absorptivity

increasing only 0.02 from the QA of 0.90 to 0.92 for the end of mission (see Table 10-100). The emissivity also showed very little change from the QA measured value of 0.09 to the end of mission value of 0.08 (see Table 10-101). Unexposed measurements were not available for either the space or the Earth end panels. Overall changes in the a/e values for the anodized surfaces were small relative to the accuracies of the measurements taken, but the consistency in observed trends indicates that the results presented are valid.

The thermo-optical property measurements, shown in Table 10-103, indicate that the chromic acid anodize specimens were not significantly affected by either short-term (10 months, 2300 esh UV and $<2.6 \times 10^{20}$ AO atoms/cm^2) or long term (5.8 years, 11200 esh UV and 9×10^{21} AO atoms/cm^2) exposure.[124]

Table 10-103. Solar Absorptance and Thermal Emittance Measurements for 6061 Aluminum Chromic Acid Anodize Test Specimens on LDEF Experiment S0010

	Preflight		10 Month Exposure		5.8 Year Exposure	
Coating	α	ε	α	ε	α	ε
Thin CAA	0.295	0.16	0.299	0.17	—	—
	0.288	0.18	—	—	0.296	0.19
Med. CAA	0.292	0.43	0.287	0.43	—	—
	0.306	0.45	—	—	0.311	0.46
Thick CAA	0.33	0.71	0.337	0.71	—	—
	0.341	0.75	—	-	0.354	0.75

10.6.1.2.2 Specular Reflectance

The chromic acid anodizing process provides less than 5 percent specular reflectance at 0.5 micrometers, the peak solar wavelength. In contrast, the sulfuric acid process has nearly 40 percent specular reflectance as shown in Figure 10-71.[123] For satellites with optical experiments it is highly desirable to have a low solar absorptance coating on the composite structural members which would not be a specular reflector. Hence, minimizing the amount of sunlight reflected from these members.

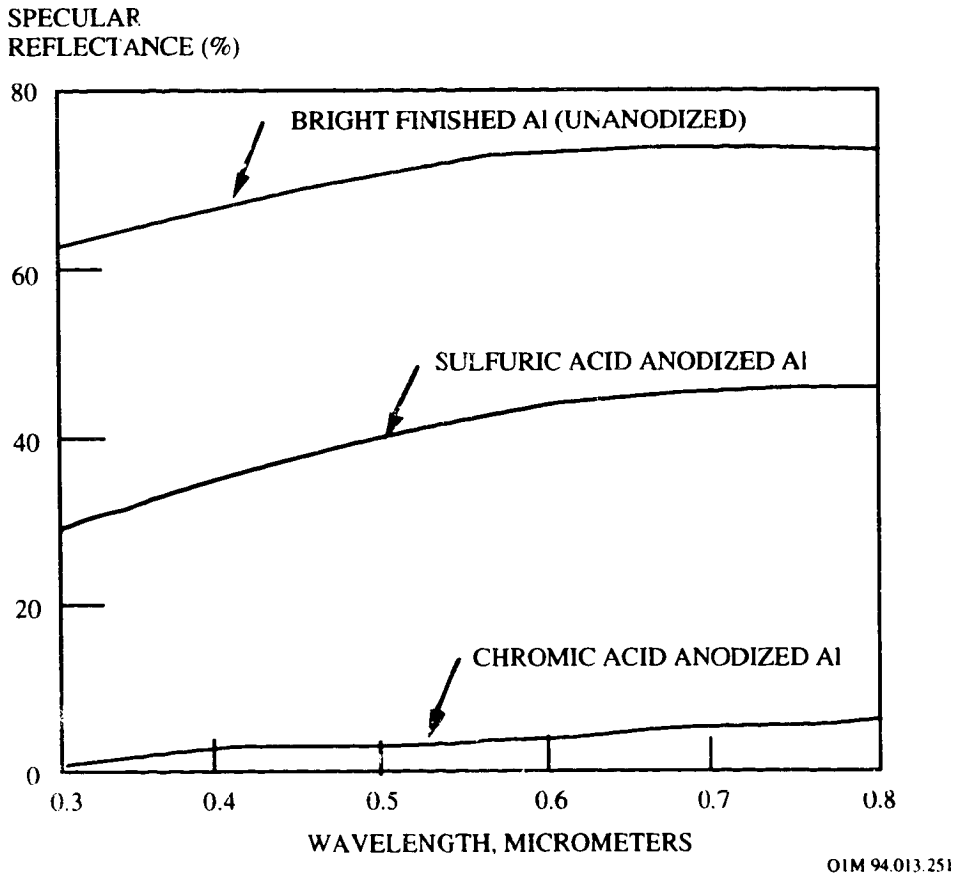

Figure 10-71. Specular Reflectance of Chemically Treated Aluminum

10.6.1.2.3 Effect of Contamination of Thermo-Optical Properties

Contamination is expected to increase the absorptance of a surface by an amount dependent on the thickness of the contaminant layer, and the optical properties (transmission, absorption and refractive indices) of the layer and the substrate. The LDEF Materials Special Investigation Group has indicated that the contaminant film on the LDEF satellite varied between

0.1 mm to 100 mm and averaged approximately 3 mm (30,000 Å).[125] This contaminant film consisted primarily of silicones from sources such as the Z-306 paint used on the interior of the structure, and hydrocarbons. Silicone sources were found to be widespread on LDEF despite low pre-flight reporting. Although outgassing requirements were imposed on LDEF, further experience has shown that more rigorous controls are needed to minimize contamination.

For the chromic acid anodized coatings, it has been suggested that ram-direction AO reacted with the silicone contaminant layer, resulting in a clear contaminant layer which did not significantly affect absorptance.[126] A contaminant layer of up to 30,000 Å had a negligible effect on emittance on the chromic acid anodic coatings with low initial emittances.

10.6.1.2.4 Effect of Hypervelocity Impact on Thermo-Optical Properties

Hypervelocity impact from micrometeoroids and orbital debris can remove areas of the oxide layer, exposing bare aluminum with different optical properties than the initial oxide. In addition, the ratio of the coating spall diameter to the crater diameter can influence the overall optical effects of multiple impact craters on coatings. Dependent upon the bond strength and type of coating, different amounts of coating can be removed during impact. The shock waves from the initial impact can cause coatings to spall. Impacts on conversion coatings such as chromic acid anodize (CAA) did not product any apparent spall, resulting in changes much less than 0.1% in even 100 years for effective absorptance and emittance (ref. 52). Of course, this assumes the orbital debris environment does not change significantly from what LDEF experienced.

10.6.1.2.5 Summary

From the results of the LDEF external a/e surface survey, it can be concluded that the clear chromic acid anodizing process as developed by Duckett and Gilliand has proven to be a stable spacecraft thermal control coating. Measurements have confirmed that the exposed surface (intercostals and longerons) average absorptivity degraded no more than 16% over the life of the LDEF mission. Furthermore the exposed surface average emissivity also showed very little degradation from new values.

10.6.2 MgF_2/Aluminum Coating

10.6.2.1 Manufacturing Process

MTO

10.6.2.2 Effects of the Space Environment

Table 10-104 presents the variations of the solar reflectance and the emissivity of various white paint samples after their flight on FRECOPA/LDEF (ref. 13). Experiment AO 138-6 was part of the FRECOPA experiment located on the trailing edge of LDEF. The experiment was designed to allow exposure of a part of the samples to the whole spacecraft environment by being laid directly on the FRECOPA tray surface, while the other part of samples was protected from the external environment of LDEF for all mission phases, except free flight, by the means of a vacuum-tight FRECOPA canister in which they were stored.

Table 10-104. Optical Property Variations of MgF_2/Aluminum Surface Coatings

Material	Mfg.	$Rs_{initial}$	$\varepsilon_{initial}$	AO 138-6 LDEF		AO 138-6 LDEF	
				Canister ΔRs	Tray ΔRs	Canister Δe	Tray Δe
MgF_2/Aluminum Coating	MTO	0.890	0.025	-0.03		-0.001	

Environmental Variations of LDEF and MIR Space Experiments: Due to its position on the trailing edge of LDEF, the AO 138-6 experiment did not receive any oxygen atoms during the mission, with the exception of a short period during the capture when it received a fluence evaluated at 1.32×10^{17} atoms cm^{-2}. The solar illumination was 11,100 equivalent sun hours (esh) for the samples located on the tray and only 1448 esh for the samples inside the canister. The particle irradiation dose (mainly due to the electron flux) was weak: 3×10^5 rads. The number of temperature cycles was ~34,000 with temperatures within the ranges shown in the table below.

ENVIRONMENT	FRECOPA-LDEF		COMES-MIR	
	CANISTER	TRAY	FACE V	FACE R
Oxygen atoms cm^{-2}	0	1.3×10^{17}	1.2×10^{18} to 7.5×10^{19} (1)	3.5×10^{20} to 5.8×10^{20} (1)
Solar UV (esh)	1448	11,100	2850(2)	1900(2)
Temp. Cold case (°C)	-20 to -26	-43 to -52	-60 to -70	-60 to -70
Temp. Hot case (°C)	+67 to +85	+45 to +63	+10 to +30	+50 to +60

(1) Estimated from AO reactivity erosion of Kapton (3.0×10^{-24} $cm^3 atom^{-1}$) and Terphane (3.0×10^{-24} $cm^3 atom^{-1}$) samples
(2) Estimated from data of experiment calorimeter

Experimental Description. The solar reflection measurements were made with a Beckman DK2A spectrophotometer with an integrating sphere, and the infrared emissivity measurements were made with the Gier & Dunkle DB 100 device. It is important to underline that the measurements were all taken in air on samples which had thus experienced more or less intense recovery of the radiation damage.

10.6.3 Vacuum Deposited Aluminum

Vacuum deposited aluminum coatings are intended for use as either passive thermal control surfaces in the space environment for improving the electrical grounding of parts, and/or for use on non-metallic surfaces for radar reflectance in a space environment. Typical thermo-optical properties include a solar absorptance of 0.13 maximum, and a room temperature normal emittance of 0.04 maximum.

10.6.3.1 Manufacturing Process

Vacuum deposited aluminum may be deposited, to form an opaque film, on any metal or non-metallic substrate able to withstand 163(C (325(F). This coating ha · mirror-like appearance and requires special handling and packaging to prevent damage or contamination to the coating. Blind holes, slits, etc., which might entrap liquids during cleaning, must be avoided in the design of the parts to be coated. The trapped liquid outgasses and causes film degradation during the vacuum metallization process. If such designs are necessary, a vacuum bake operation must be specified to follow any vapor and/or liquid cleaning operations.

10.6.3.2 Effects of the Space Environment

Table 10-105 presents the variations of the solar reflectance and the emissivity of various vacuum deposited aluminum samples after their flight on FRECOPA/LDEF (ref. 13). Experiment AO 138-6 was part of the FRECOPA experiment located on the trailing edge of LDEF. The experiment was designed to allow exposure of a part of the samples to the whole spacecraft environment by being laid directly on the FRECOPA tray surface, while the other part of samples was protected from the external environment of LDEF for all mission phases, except free flight, by the means of a vacuum-tight FRECOPA canister in which they were stored.

Table 10-105. Optical Property Variations of VDA Surface Coating

Material	$Rs_{initial}$	$\varepsilon_{initial}$	AO 138-6 LDEF		AO 138-6 LDEF	
			Canister ΔRs	Tray ΔRs	Canister Δε	Tray Δε
Vacuum deposited aluminum	0.90	0.023	-0.010		-0.002	
Vacuum deposited aluminum	0.91	0.023		0		0.002
Vacuum deposited aluminum	0.90	0.023		0		0.001

Experimental Description: Experiment AO 138-6 was part of the FRECOPA experiment located on the trailing edge of LDEF. The experiment was designed to allow exposure of a part of the samples to the whole spacecraft environment by being laid directly on the FRECOPA tray surface, while the remaining samples were protected from the external environment of LDEF for all mission phases, except free flight, by the means of a vacuum-tight FRECOPA canister in which they were stored.

Environmental Variations of LDEF Space Experiments Due to its position on the trailing edge of LDEF, the AO 138-6 experiment did not receive any oxygen atoms during the mission, with the exception of a short period during the capture when it received a fluence evaluated at 1.32×10^{17} atoms cm^{-2}. The solar illumination was 11,100 equivalent sun hours (esh) for the samples located on the tray and only 1448 esh for the samples inside the canister. The particle irradiation dose (mainly due to the electron flux) was weak: 3×10^{5} rads. The number of temperature cycles was ~34,000 with temperatures within the ranges shown in the table below.

	FRECOPA-LDEF	
	CANISTER	TRAY
Oxygen atoms cm^{-2}	0	1.3×10^{17}
Solar UV (esh)	1448	11,110
Temp. Cold case (°C)	-20 to -26	-43 to -52
Temp.Hot case (°C)	+67 to +85	+45 to +63

10.6.4 PSG 173 Aluminum/Silicone Paint

PSG 173 aluminum paint provides low absorptance, low emittance, and low outgassing under vacuum conditions to limit temperature gradients and excursions. This paint can be applied directly onto aluminum alloys.

10.6.4.1 Composition

Binder:	purified silicone
Pigment:	aluminum
Solvent:	aromatics

10.6.4.2 Source

Manufacturer: ASTRAL
Peintures et Vernis, 164 rue Ambroise Croizat, 93024
Saint-Denis. Cedex 1, France

10.6.4.3 Effects of the Space Environment

10.6.4.3.1 Thermal-Optical Properties

The PSG 173 coating showed promise during a 9-month LDEF FRECOPA experiment and during the 1.1 year COMES/MIR flight experiment, as shown in Table 10-106 (ref. 34). The COMES experiment consisted of four panels which were deployed by a cosmonaut in space outside of MIR with the possibility of exposing samples on both sides, conventionally identified as "V" and "R". Experiment AO 138-6 was part of the FRECOPA experiment located on the trailing edge of LDEF. The experiment was designed to allow exposure of a part of the samples to the whole spacecraft environment by being laid directly on the FRECOPA tray surface, while the other part of samples was protected from the external environment of LDEF for all mission phases, except free flight, by the means of a vacuum-tight FRECOPA canister in which they were stored.

Table 10-106. Solar Reflectance and Emissivity Variations of PSG 173 Aluminum Paint After the FRECOPA/LDEF and COMES/MIR Flight Experiments

Type	$R_{s\ initial}$	$\varepsilon_{initial}$	AO 138-6 LDEF		COMES	
			Canister ΔR_s	Canister $\Delta\varepsilon$	Face V ΔR_s	Face V $\Delta\varepsilon$
aluminum paint	0.69	0.317	-0.08	-0.006	-0.06	-0.009

Environmental Variations of LDEF and MIR Space Experiments: Due to its position on the trailing edge of LDEF, the AO 138-6 experiment did not receive any oxygen atoms during the mission, with the exception of a short period during the capture when it received a fluence evaluated at 1.32×10^{17} atoms cm^{-2}. The solar illumination was 11,100 equivalent sun hours (esh) for the samples located on the tray and only 1448 esh for the samples inside the canister. The particle irradiation dose (mainly due to the electron flux) was weak: 3×10^5 rads. The number of temperature cycles was ~34 000 with temperatures within the ranges shown in the table below.

ENVIRONMENT	FRECOPA-LDEF		COMES-MIR	
	CANISTER	TRAY	FACE V	FACE R
Oxygen atoms cm^{-2}	0	1.3×10^{17}	1.2×10^{18} to 7.5×10^{19} (1)	3.5×10^{20} to 5.8×10^{20} (1)
Solar UV (esh)	1448	11,100	2850(2)	1900(2)
Temp. Cold case (°C)	-20 to -26	-43 to -52	-60 to -70	-60 to -70
Temp. Hot case (°C)	+67 to +85	+45 to +63	+10 to +30	+50 to +60

(1) Estimated from AO reactivity erosion of Kapton (3.0×10^{-24} $cm^3 atom^{-1}$) and Terphane (3.0×10^{-24} $cm^3 atom^{-1}$) samples

(2) Estimated from data of experiment calorimeter

Experimental Description. The solar reflection measurements were made with a Beckman DK2A spectrophotometer with an integrating sphere, and the infrared emissivity measurements were made with the Gier & Dunkle DB 100 device. It is important to underline that the measurements were all taken in air on samples which had thus experienced more or less intense recovery of the radiation damage.

From Table 10-106 one observes that the PSG 173 FD aluminum paint reflectance deteriorated significantly in both the canister on LDEF and on the V-face of the COMES experiment. Emissivity change was not significant.

10.6.5 Polyurethane Leafing Aluminum Thermal Control Coating

10.6.5.1 Composition

Leafing aluminum thermal control coating consists of a Chemglaze Z001 clear glossy, moisture curing, polyurethane binder and an aluminum pigment filler. Leafing is defined as the propensity of metallic flakes to align themselves in parallel surfaces thus, providing both a barrier to atomic oxygen and ultraviolet light penetration.

10.6.5.2 Source

Chemglaze Z001 flexible polyurethane glossy clear paint is available from R.D. Abbott Company inc., Long Beach, CA. The aluminum pigment powder is available from Alcan-Toyo America, 1717 North Naper Blvd., Naperville, IL.

10.6.5.3 Properties

Leafing pigments with suitable binders can be used to control emissivity. It is a thermal control coating which is used when a ratio of solar absorptance to normal emittance of near 1 is desired.

Solar absorptance values are dependent upon the coating thickness as well as the substrate material. Table 10-107 illustrates the coating's thermal properties at different thickness and on different substrates.

Table 10-107. Thermal Properties of Leafing Aluminum Paint

Substrate Material	Coating Thickness Inch	α_s	ε_N	α/ε
Carbon Composite	0.00025 - 0.0005	0.31	0.28	1.1
Carbon Composite	0.002	0.23 - 0.24	0.21 - 0.22	1.0 - 1.1
Aluminum	0.002	0.23 - 0.24	0.21 - 0.22	1.9 - 1.1

10.6.5.4 Effects of the Space Environment

Since the Z001 coating is a TDI (toluene diisocyanate) polyurethane, some loss of gloss and yellowing tendencies should be expected. After 10 years in a space environment, the solar absorptance is expected to reach 0.36 and no significant change in hemispherical emittance is expected. Accelerated UV exposure tests (multiple - 3 suns) performed show that the solar absorptance increases from 0.23 to 0.26 after 1244 hours of UV. exposure.

No atomic oxygen stability data are available at this time for the Chemglaze Z001 coating material. The erosion yield should be similar to the Chemglaze Z302 specular black coating and is expected to have poor atomic oxygen stability.

Chemglaze Z001 has a maximum short term service (1 hour) temperature of 177^{o}C (350^{o}F) and can withstand regular service between -184 to 121(C (-300 to 250^{o}F). Extended exposure to higher temperature (177(C and above) can cause the solar absorptance to reach the 0.36 end of life value at an accelerated rate.

10.7 YELLOW PAINT

A971 yellow polyurethane paint.

10.7.1 Composition

Binder: Polyurethane

Pigment:

10.7.2 Source

Manufacturer: Lord Chemical Products
2000 West Grandview Blvd
Erie, PA
Telephone. 814 868-3611

Cost: $92/gallon (1994 prices)

10.7.3 Effects of the Space Environment

10.7.3.1 Thermal-Optical Properties

The A971 yellow polyurethane coating specimens were parts from the trunnion scuff plate assemblies, located between trays C3 and D3 and between trays C9 and D9 on the LDEF center ring frame, located on the trailing and leading edges, respectively. The trunnion scuff plates are part of the interface between LDEF and the Space Shuttle payload bay. The trailing edge specimen was exposed to 1.3×10^{17} oxygen atoms/cm^2 and 11,100 esh of UV radiation. The leading edge specimen was exposed to 9.0×10^{21} oxygen atoms/cm^2 and 11,200 esh of UV radiation.

Optical properties were analyzed for the A971 yellow coating on the LDEF scuff plates, and the results are shown in Table 10-108 (ref. 44). Solar absorptance for the trailing edge specimen was 0.12 higher than what was measured on a vendor supplied sample. It is significant that the absorptance of the trailing edge A971 coating was comparable to that measured for A276 white polyurethane paint exposed to the same environmental conditions (see Section 10.3.2). The absorptance of the leading edge A971 specimen was slightly degraded compared to the control.

Apparently not quite all of the UV damaged polyurethane resin had been removed by atomic oxygen erosion from the scuff plate surface .

The thermal emittance for the trailing edge specimen was 0.87, essentially what was expected for a gloss polyurethane paint without atomic oxygen exposure and consistent with observations for comparably exposed A276 white polyurethane paint. However, comparison to the control was poor, indicating a difference in coating thicknesses for the two specimens. The leading edge thermal emittance was slightly higher than that measured for the trailing edge specimen, again comparable to what was observed for the A276 white paint disks based on increased surface roughness due to AO erosion.

Table 10-108. Optical Properties For A971 Yellow Polyurethane Coating

Specimen	Space Environment		Solar Absorptance	Thermal Emittance
	AO atoms/cm^2	UV esh		
Vendor Control			0.46	0.83
Leading Edge Scuff Plate Segment	9.0×10^{21}	11,200	0.50	0.89
Trailing Edge Scuff Plate Segment	1.3×10^{17}	11,100	0.58	0.87

10.8 OPTICAL SOLAR REFLECTORS

10.8.1 OSR OCLI

10.8.1.1 Composition

Metallic silver, vacuum deposited on one surface of fused silica. The silver is overcoated with dielectric or conductive materials to protect it form degradation. A typical description, shown in Figure 10-72, is as follows:

- Coating: Silver 10^{-7} m thick
- Overcoating: Inconel $5x10^{-8}$ m thick (both depositions made in the same chamber without breaking vacuum
- Fused Silica: Corning Glass Works No. 7940, .008" ($2x10^{-4}$ m) thick.

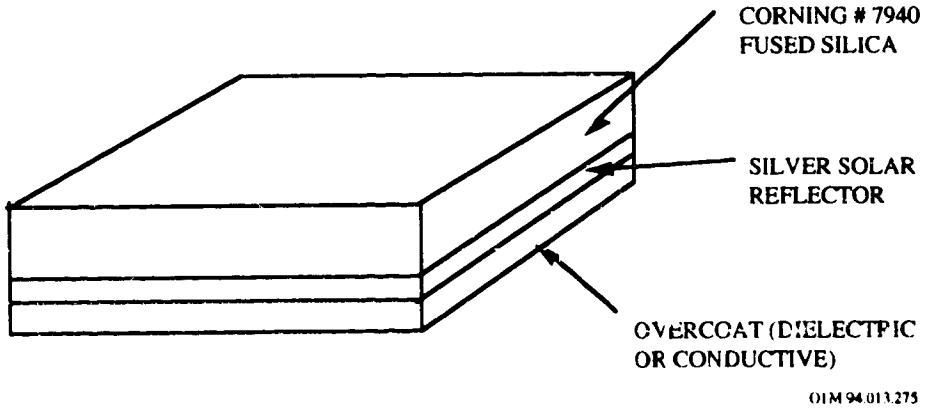

Figure 10-72. Silver Vacuum Deposited on Fused Silica

This coating system is also called Rigid Optical Solar Reflector (Rigid OSR), or second surface thermal control mirror (SSM).

10.8.1.2 Manufacturing Process

The OSR fused silica mirrors are supplied by Optical Coating Laboratory, Inc., Santa Rosa, California. The OSR fused silica mirrors can be fabricated in a variety of shapes and sizes. The most common configuration presently in use is that of 2.54×10^{-2} m squares. Squares of 3.81×10^{-2} m have been also manufactured. Larger sizes can be produced while maintaining the fused silica thickness , however, the breakage factor during fabrication and handling leads to increased costs. The OSR fused silica mirrors can be bonded to the substrate with an adhesive or a double-backed tape. Silicone cements provide the most desirable characteristics.

10.8.1.3 Effects of the Space Environment

10.8.1.3.1 Thermal-Optical Properties

The OSR OCLI coating showed promise during a 9-month LDEF FRECOPA experiment and during the 1.1 year COMES/MIR flight experiment, as shown in Table 10-109 (ref. 34). The COMES experiment consisted of four panels which were deployed by a cosmonaut in space outside of MIR with the possibility of exposing samples on both sides, conventionally identified as "V" and "R". Experiment AO 138-6 was part of the FRECOPA experiment located on the trailing edge of LDEF. The experiment was designed to allow exposure of a part of the samples to the whole spacecraft environment by being laid directly on the FRECOPA tray surface, while the other part of samples was protected from the external environment of LDEF for all mission phases, except free flight, by the means of a vacuum-tight FRECOPA canister in which they were stored.

Table 10-109 presents the variations of the solar reflectance and the emissivity of OSR OCLI samples after their flight on FRECOPA/LDEF and COMES/MIR. No significant change in emissivity and solar reflectance was observed for the OSR OCLI samples that were flown in the LDEF canister and on the COMES experiment. Hence, the OSR OCLI material was very stable for both experiments.

Table 10-109. Solar Reflectance Emissivity Variations for Silver Silica Optical Surface Reflectors (OSR)

Pre-Flight Properties		AO 138-6 LDEF		COMES	
$Rs_{initial}$	$\varepsilon_{initial}$	Canister $\Delta\varepsilon$	Canister ΔRs	Face V ΔRs	Face R ΔRs
0.94	0.798	0.000	-0.01	-0.01	0.000
0.94	0.798	0.000	-0.01		
0.94	0.798	0.000	-0.01		
0.94	0.798	0.000	-0.01		

Environmental Variations of LDEF and MIR Space Experiments : Due to its position on the trailing edge of LDEF, the AO 138-6 experiment did not receive any oxygen atoms during the mission, with the exception of a short period during the capture when it received a fluence evaluated at 1.32×10^{17} atoms cm^{-2}. The solar illumination was 11,100 equivalent sun hours (esh) for the samples located on the tray and only 1448 esh for the samples inside the canister. The particle irradiation dose (mainly due to the electron flux) was weak: 3×10^5 rads. The number of temperature cycles was ~34,000 with temperatures within the ranges shown in the table below.

ENVIRONMENT	FRECOPA-LDEF		COMES-MIR	
	CANISTER	TRAY	FACE V	FACE R
Oxygen atoms cm^{-2}	0	1.3×10^{17}	1.2×10^{18} to 7.5×10^{19} (1)	3.5×10^{20} to 5.8×10^{20} (1)
Solar UV (esh)	1448	11,100	2850 (2)	1900 (2)
Temp. Cold case (°C)	-20 to -26	-43 to -52	-60 to -70	-60 to -70
Temp. Hot case (°C)	+67 to +85	+45 to +63	+10 to +30	+50 to +60

(1) Estimated from AO reactivity erosion of Kapton (3.0×10^{-24} $cm^3 atom^{-1}$) and Terphane (3.0×10^{-24} $cm^3 atom^{-1}$)

(2) Estimated from data of experiment calorimeter

Experimental Description. The solar reflection measurements were made with a Beckman DK2A spectrophotometer with an integrating sphere, and the infrared emissivity measurements were made with a Gier & Dunkle DB 100 device. It is important to underline that the measurements were all taken in air on samples which had thus experienced more or less intense recovery of the radiation damage

10.8.1.3.2 Contamination

Several Department of Defense satellites have seen significant solar absorptance degradation of fused silica/silver second surface mirrors.[127] The degradation has been attributed to contamination, with the rate of change in a being 0.01 per 100 Å (this is the average rate; the maximum is 0.025 per 100 Å).

In addition, contamination-induced degradation of OSR's has been observed on several European communications satellites and was measured on one of them, ECS-1.[128] This satellite was launched into geosynchronous orbit in June 1983. Two sets of calorimeters and TQCM's were mounted on the satellite's radiators. The calorimeters measured an increase in a of 0.020 per year while the TQCM's simultaneously accumulated 37.5 Å of contaminant per year. The rate of change in a was therefore approximately 0.05 per 1000 Å. The entire change was attributed to contamination because OSR's have not been observed to degrade significantly due to other environmental effects such as radiation and UV.

RELATIONSHIPS OF SPACE ENVIRONMENT - MATERIAL INTERACTIONS

Contamination

Thermal Control Surfaces

Solar Absorptance Increase (Da_S) of 0.03 per 100 Å of molecular film 10-164

[1] TRW Internal Document

[2] P.R.K. Chetty, Satellite Technology and Its Applications, TAB Professional and Reference Books, 1991.

[3] B.N. Agrawal, Design of Geosynchronous Spacecraft, Prentice-Hall, Inc., 1986.

[4] D.R. Wilkes et al., "Initial Materials Evaluation of the Thermal Control Surfaces Experiment (S0069)," LDEF First Post-Retrieval Symposium, NASA CP-3134, 1991, pp. 899-917.

[5] D.R. Wilkes et al., "Thermal Control Surfaces on the MSFC LDEF Experiments," LDEF Materials Workshop 1991, NASA CP 3162, 1992, pp. 187-209.

[6] J. Zwiener et al., "Unusual Materials Effects Observed on the Thermal Control Surface Experiment (S0069)," LDEF First Post-Retrieval Symposium, NASA CP 3134, 1991, pp. 919-934.

[7] D.R. Wilkes et al., "The Continuing Materials Analysis of the Thermal Control Surfaces Experiment," LDEF Second Post-Retrieval Symposium, NASA CP 3194, 1993, pp. 1061-1073.

[8] A.F. Whitaker et al., "Atomic Oxygen Effects on LDEF Experiment AO171," LDEF Second Post-Retrieval Symposium, NASA CP 3194, 1993, pp. 1125-1135.

[9] J.M. Zwiener, R.J. Mell, P.N. Peters, J.C. Gregory, D.R. Wilkes, and E.R. Miller, "Fluorescence Measurements of the Thermal Control Experiments Coatings on LDEF S0069 and A0114," LDEF Second Post-Retrieval Symposium, NASA CP 3194, 1993, pp. 1111-1123.

[10] C.J. Hurley, "Long Duration Exposure Facility Experiment M0003-5 Thermal Control Materials," LDEF First Post-Retrieval Symposium, NASA CP 3134, 1991, pp. 961-974.

[11] C. Jaggers et al., "Thermal Control Paints on LDEF: Results of M0003 Sub-Experiment 18," LDEF Second Post-Retrieval Symposium, NASA CP 3194, 1993, pp.1075-1092.

[12] C.S. Hemminger, W.K. Stuckey, and J C. Uht, "Space Environmental Effects on Silvered Teflon Thermal Control Surfaces," LDEF First Post-Retrieval Symposium, NASA CP 3134, 1991, pp.831-874.

[13] J.C. Guillaumon et al., "Spacecraft Thermal Control Coatings," LDEF First Post-Retrieval Symposium, NASA CP 3194, 1991, pp. 945-960.

[14] H.G. Pippin and E.R. Crutcher, "Contamination on LDEF: Sources, Distribution, and History," LDEF Second Post-Retrieval Symposium, NASA CP 3194, 1993, pp. 1023-1040.

15 J.L. Golden, "Results of Examination of the A276 White and Z306 Black Thermal Control Paint Disks Flown on LDEF," LDEF First Post-Retrieval Symposium, NASA CP 3134, 1991, pp.975-988.

16 H.G. Pippin et al., "Survey of Results from the Boeing Modules on the M0003 Experiment on LDEF," LDEF First Post-Retrieval Symposium, NASA CP 3134, 1991, pp. 1109-1114.

17 M. Mirtich et al., "Ion Beam Textured and Coated Surfaces Experiment (IBEX)," LDEF First Post-Retrieval Symposium, NASA CP 3134, 1991, pp. 989-1004.

18 L. Kauder, "Preliminary Results for the LDEF/HEPP Thermal Control Samples," LDEF First Post-Retrieval Symposium, NASA CP 3134, 1991, pp. 797-800.

19 W.S. Slemp and P.R. Young, "LDEF Thermal Control Coatings Post-Flight Analysis," LDEF Second Post-Retrieval Symposium, NASA CP 3134, 1993, pp. 1093-1097.

20 R.A. Linton, "Effects of Space Exposure on Thermal Control Coatings," AIAA 92-0795, January 6-9, 1992, Reno, NV.

21 R.C. Linton et al., "LDEF Experiment A0034: Atomic Oxygen Stimulated Outgassing," LDEF First Post-Retrieval Symposium, NASA CP 3134, 1991, pp.763-779.

22 K. Rousslang, E. Crutcher, and G. Pippin, "Results of Examination of Silvered Teflon from LDEF," LDEF First Post-Retrieval Symposium, NASA CP 3134, 1991, pp. 847-859.

23 D.E. Brinza, A.E. Stiegman, P.R. Staszak, E.G. Laue, and R.H. Liang, "Vacuum Ultraviolet (VUV) Radiation-Induced Degradation of Fluorinated Ethylene Propylene (FEP) Teflon Aboard the LDEF," LDEF First Post-Retrieval Symposium, NASA CP 3134, 1991, pp. 817-829.

24 F. Levadou, M. Froggatt, M. Rott, and E. Schneider, "Preliminary Investigation into UHCRE Thermal Control Materials," LDEF First Post-Retrieval Symposium, NASA CP 3134, 1991, pp.875-898.

25 P.R. Young and W.S. Slemp, "An Analysis of LDEF-Exposed Silvered FEP Teflon Thermal Blanket Material," NASA TM 104096, December 1991.

26 B.A. Banks, J.A. Dever, L. Gebauer, and C.M. Hill, "Atomic Oxygen Interactions with FEP Teflon and Silicones on LDEF," LDEF First Post-Retrieval Symposium, NASA CP 3134 1991, pp.801-815.

27 J.W. Haffner et al., "Natural Environmental Effects on SDIO Spacecraft Surface Materials," Air Force Geophysics Laboratory, Report No. AFGL-TR-89-0084, May 1989.

28 B.A. Stein, "LDEF Materials: An Overview of the Interim Findings," LDEF Materials Workshop '91, NASA CP 3162, 1992, pp. 1-56.

[29] E.R. Crutcher and K.J. Warner, "Molecular Films Associated with LDEF," LDEF First Post-Retrieval Symposium, NASA CP 3134, 1991, pp. 155-177.

[30] G.A. Harvey "Organic Contamination of LDEF," LDEF First Post-Retrieval Symposium, NASA CP 3134, 1991, pp.179-196.

[31] R. Crutcher, "Materials SIG Quantification and Characterization of Surface Contaminants," LDEF Materials Workshop 1991, NASA CP 3162, 1992, pp. 95-140.

[32] C.S. Hemminger, "Surface Contamination on LDEF Exposed Materials," LDEF Materials Workshop 1991, NASA CP 3162, 1992, pp. 159-174.

[33] G.A. Harvey, "Sources and Transport of Silicone NVR," LDEF Materials Workshop 1991, NASA CP 3162, 1992, pp.175-185.

[34] J.C. Guillaumon and A. Paillous, "Spacecraft Materials: Comparison between Flight Results Obtained on LDEF and MIR," LDEF Materials Results for Spacecraft Applications, NASA CP-3257, 1994, pp. 485-498.

[35] A.C. Tribble, R. Lukins, and E. Watts, "Low Earth Orbit Thermal Control Coatings Exposure Flight Tests: A Comparison of U.S. and Russian Results," NASA Contract NAS1-19243, Task 16, Rockwell International Space Systems Division, August 1994.

[36] Lord Corporation Brochure.

[37] T.R. Sampair and W. M. Berrios, "Effects of Low Earth Orbit Environment on the Long Duration Exposure Facility Thermal Control Coatings," LDEF First Post-Retrieval Symp., NASA CP-3134, 1991, pp. 935-944.

[38] L.J. Leger, I.K. Spiker, J.F. Kuminecz, and J.T. Visentine, "STS Flight 5 LEO Effects Experiments - Background Description and Thin Film Results," AIAA-83-2631-CP, October 1983.

[39] L.J. Leger, J.F. Visentine, and J.F. Kuminecz, "Low Earth Orbit Atomic Oxygen Effects on Surfaces," AIAA-84-0548, January 1984.

[40] J.T. Visentine, L.J. Leger, J.F. Kumineca, and I.K. Spiker, "STS-8 Atomic Ocygen Effects Experiments, Paper presented at AIAA 23rd Aerospace Sciences Meeting, Reno, NV, January 1985.

[41] B.D. Green, G.E. Caledonia, and T.D. Wilderson, "The Shuttle Environment: Gases, Particulates and Glow," J. Spacecraft and Rockets, Vol. 22, no. 5, 1985, pp. 500-511.

[42] A.F. Whitaker, "LEO Atomic Oxygen Effects on Spacecraft Materials - STS-5 Results," NASA-TM-86463, August 1984.

[43] J.L. Golden, "Results of the Examination of LDEF Polyurethane Thermal Control Coatings," NASA Contractor Report 4617, Boeing Defense & Space Group, July 1994.

[44] R.J. Bourassa, "Atomic Oxygen and Ultraviolet Radiation Mission Total Exposures for LDEF Experiments," LDEF First Post-Retrieval Symposium, NASA CP-3134, 1992, pp. 643-661.

[45] R.J. Bourassa and H.G. Pippin, "Model of Spacecraft Atomic Oxygen and Solar Exposure Microenvironments," LDEF Materials Results for Spacecraft Applications Conference, NASA CP 3257, 1994, pp. 105-114.

[46] M.J. Brown et al., "Measurement and Analysis of LDEF/TCSE Flight Samples", AZ Technology Report No. 90-2-107-1, February 1991.

[47] T.E. Firle and T.M. Flanagan, "Mechanisms of Degradation of Polymeric Thermal Control Coatings: Part II. Effects of Radiation on Selected Pigments," AFML-TR-68-334, Part II, March 1970.

[48] D.R. Wilkes et al., "Initial Materials Evaluation of the Thermal Control Surfaces Experiment (S0069)," LDEF First Post-Retrieval Symposium, NASA CP-3134, 1991, pp. 899-917.

[49] Air Force/Industry Debriefing on White Thermal Control Coating Requalification, October 25-26, 1994, Los Angeles, CA.

[50] J.M. Zwiener and M.M. Finckenor, "Micrometeoroid/Space Debris Effects on Materials," LDEF Materials Results for Spacecraft Applications Conference, NASA CP-3257, 1994, pp. 259-280.

[51] Air Force/Industry Debriefing on White Thermal Control Coating Requalification, October 25-26, 1994, Los Angeles, CA.

[52] G.A. Zerlaut, Y. Harada, and E.H. Tompkins, "Ultraviolet Irradiation of White Spacecraft Coatings in Vacuum," Symposium of Thermal Radiation of Solids, NASA-SP-55, Washington, D.C., 1965.

[53] B.D. Pearson, Jr., "Preliminary Results from the Ames Emissivity Experiment on OSO-II" Progress in Astronautics and Aeronautics, Vol. 18, Academic Press, New York, 1966, pp. 459-472.

[54] C.F. Schafer and T.C. Bannister, "Peagasus Thermal Control Coatings Experiment," AIAA-66-419, June 1966.

[55] J.E. Gilligan, "The Induced Optical Properties of Zinc Ocide," AIAA-67-214, January 1967.

[56] H.F. MacMillan, A.F. Sklensky, and L.A. McKellar, "Apparatus for Spectral Bidirectional Reflectance Measurements During Ultraviolet Irradiation in Vacuum," Thermophysics and Temperature Control of Spacecraft and Entry Behicles," Academic Press, New York, 1966, pp. 129-149.

[57] R.J. Mell and Y. Harada, "Space Stable Thermal Control Coatings," AFWAL-TR-87-4010, May 1987.

[58] J.E. Gilligan and G.A. Zerlaut, "The Space Environment Stability Problem in White Pigment Coatings," Institute of Environmental Science, Technical Meeting, Proceedings, Vol. 17, 1971, pp. 447-457.

[59] J.S. Choate, S.W. Johnson, and V.L. Mongold, "Analysis of Products Evolved From Selected Thermal Control Coating Materials During Ultrviolet Radiation in Vacuum" AIAA-69-640, June 1969.

[60] Air Force/Industry Debriefing on White Thermal Control Coating Requalification, October 25-26, 1994, Los Angeles, CA.

[61] A.F. Whitaker, "LEO Atomic Oxygen Effects on Spacecraft Materials - STS-5 Results," NASA-TM-86463, August 1984.

[62] D.R. Wilkes et al., "Thermal Control Surfaces on the MSFC LDEF Experiments," LDEF Materials Workshop '91, NASA CP 3162, 1992, pp. 187-209.

[63] T.R. Sampair and W. M. Berrios, "Effects of Low Earth Orbit Environment on the Long Duration Exposure Facility Thermal Control Coatings," LDEF First Post-Retrieval Symposium, NASA CP-3134, 1991, pp. 935-944.

[64] Y. S. Touloukian, D.P. DeWitt, and R.S. Hernicz, "Thermal Radiative Properties of Coatings," Thermophysical Properties of Matter, Vol. 9, IFI/Plenum, New York, 1972.

[65] D.R. Wilkes et al, "The Performance of Thermal Contgrol Coatings opn LDEF and Implications to Future Spacecraft," LDEF Materials Results for Spacecraft Applications, NASA CP-3237, 1994, pp. 3-20.

[66] J.W. Haffner et al., "Natural Environmental Effects on SDIO Spacecraft Surface Materials," Air Force Geophysics Laboratory, Report No. AFGL-TR-89-0084, May 1989.

[67] A.C. Tribble, R. Lukins, and E. Watts, "Low Earth Orbit Thermal Control Coatings Exposure Flight Tests: A Comparison of U.S. and Russian Results," NASA Contract NAS1-19243, Task 16, Rockwell International Space Systems Division, August 1994.

[68] Lord Corporation Brochure.

[69] R.S. Sampair W. M. Berrios, "Effects of Low Earth Orbit Environment on the Long Duration Exposure Facility Thermal Control Coatings," LDEF First Post-Retrieval Conference, NASA CP-3134, 1991, pp. 935-944.

[70] R.C. Linton, R.R. Kamenetzky, J.M. Reynolds, and C.L. Burris, "LDEF Experiment A0034: Atomic Oxygen Stimulated Outgassing," First Post-Retrieval Symposium, NASA CP 3134, 1991, pp.763-779.

[71] J.T. Visentine and A.F. Whitaker, "Material Selection Guidelines to Limit Atomic Oxygen Effects on Spacecraft Surfaces,", NASA TM-100351, February 1989.

72 C.H. Clatterbuck and J.J. Scialdone, "An Evaluation of Two Flat-Black Silicone Paints for Space Application," NASA TM 100768, December 1990.

73 NASA TM-100768, December 1990.

74 W.S. Slemp, "Ultraviolet Radiation Effects," NASA/SDIO Space Environmental Effects Workshop, NASA CP 3035, 1988.

75 Sheldahl Catalogue, "Thermal Control Material & Metalized Films,", Northfield, MN.

76 C.S. Hemminger, WK Stuckey, and J.C. Uht, "Space Environmental Effects on Silver Teflon Thermal Control Surfaces," LDEF First Post-Retrieval Symposium, NASA CP 3134, 1991, pp.831-845.

77 D.E. Brinza, A.E. Stiegman, P.R. Staszak, E.G. Laue, and R.H. Liang, "Vacuum Ultraviolet (VUV) Radiation-Induced Degradation of Fluorinated Ethylene Propylene (FEP) Teflon Aboard the LDEF," LDEF First Post-Retrieval Symposium, NASA CP 3134, 1991, pp. 817-829.

78 F. Levadou, M. Froggatt, M. Rott, and E. hneider, "Preliminary Investigation into UHCRE Thermal Control Materials," LDE First Post-Retrieval Symposium, NASA CP 3134, 1991, pp.875-898.

79 P.R. Young and W.S. Slemp, "An Analysis of LDEF-Exposed Silver FEP Teflon Thermal Blanket Material," NASA Technical Memorandum 104096, December 1991.

80 B.A. Banks, J.A. Dever, L. Gebauer, and C.M. Hill, "Atomic Oxygen Interactions with FEP Teflon and Silicones on LDEF," LDEF First Post-Retrieval Symposium, NASA CP 3134, 1991, pp.801-815.

81 B. Stein and A. Whitaker, "TCPG Interlaboratory Evaluation of Silver Teflon Thermal Blanket Materials Exposed on LDEF," Memorandums to participating laboratories.

82 M. Jones, "Data transmittal worksheet for the LDEF Ad Hoc TCP Round Robin Testing.

83 M. Zweiner, "Unusual Material Effects Observed on the Thermal Control Surfaces Experiment (S0069)," LDEF First Post-Retrieval Symposium, NASA CP 3134, 1991, pp. 919-933.

84 M.J. Mirtich et al., "Ion Beam Textured and Coated Surfaces Experiment (IBEX)," LDEF First Post-Retrieval Symposium, NASA CP 3134, 1991, pp.989-1004.

85 F. Levadou and G. Pippin, "Effects of the LDEF Environment on the Ag/FEP Thermal Blankets," LDEF Materials Workshop '91, NAsA CP 3162, 1992, pp. 311-344.

86 Satellite Servicing Project Goddard Space Flight Center, "Proceedings of the SMRM Degradation Study Workshop," NASA-TM-89274, pp. 1-32.

87 F. Levadou, M. Froggatt, M. Rott, and E. Schneider, "Preliminary Investigation into UHCRE Thermal Control Materials", LDEF First Post-Retrieval Symposium, CP-3134, 1991, pp.875-898.

88 P.R. Young and W.S. Slemp, "An Analysis of LDEF-Exposed Silvered FEP Teflon Thermal Blanket Material," NASA Technical Memorandum 104096, December 1991.

89 B.A. Banks, J.A. Dever, L. Gebauer, and C.M. Hill, "Atomic Oxygen Interactions with FEP Teflon and Silicones on LDEF," LDEF First Post-Retrieval Symposium, NASA CP-3134, 1991, pp. 801-816.

90 B.A. Banks, S.K. Rutledge, P.E. Paulsen, and T.J. Stueber, "Simulation of the Low-Earth-Orbital Atomic Oxygen Interaction with Materials by Means of an Oxygen Ion Beam," NASA TM 101971, 1989.

91 J.T. Visentine, L.J. Leger, J.F. Kumineca, and I.K. Spiker, "STS-8 Atomic Oxygen Effects Experiment," AIAA Paper 85-0415, 1985.

92 S. Koontz, L. Leger, and K. Albyn, "Vacuum Ultraviolet Radiation/Atomic Oxygen Synergism in Materials Reactivity," Journal of Spacecraft and Rockets, May-June 1990.

93 F. Levadou and G. Pippin, "Effects of the LDEF Environment on the Ag/FEP Thermal Blankets," LDEF Materials Workshop '91, NAsA CP 3162, 1992, pp. 311-344.

94 J.T. Visentine, L.J. Leger, J.F. Kumineca, and I.K. Spiker, "STS-8 Atomic Oxygen Effects Experiment," AIAA Paper 85-0415, 1985.

95 B.A. Banks, L. Gebauer, and C.M. Hill, "Atomic Oxygen Interactions with FEP Teflon and Silicones on LDEF," LDEF First Post-Retrieval Symposium, NASA CP-3134, 1991, pp. 801-815.

96 K. Rousslang, E.R. Crutcher, and G. Pippin, "Results of Examination of Silvered Teflon from the Long Duration Exposure Facility," LDEF First Post-Retrieval Symposium, NASA CP 3134, 1991, pp. 847-860.

97 M. Allbrooks and D. Atkinson, "The Magnitude of Impact Damage on LDEF Materials," NASA Contractor Report NCR 188258, July 11, 1992.

98 B. Nerren and R. Sullivan-Holt, Unpublished data, George C. Marshall Space Flight Center, Huntsvillle, Ala., April 1990.

99 Wayne Slemp, private communications

100 Goddard Space Flight Center internal memo entitled "Summary of Results to Date of QCM Data from the NOAA-7 Spacecraft" from 732/Thermal Engineering Branch to 480/Tiros Instrument Manager, January 1984.

[101] Proceedings of the Solar Maximum Repair Mission Degradation Study Workshop, Goddard Space Flight Center, May 1985. Document #408-SMRM-79-0001. See especially the paper by G.D. Rhoads of Lockheed entitled "Solar Maximum Thermal Surface Assessment."

[102] F. Levadou, M. Froggatt, M. Rott, and E. Schneider, "Preliminary Investigation into UHCRE Thermal Control Materials," LDEF First Post-Retrieval Symposium, NASA CP-3134, 1991, pp. 975-998.

[103] D.F. Hall and A.A. Fote, "Thermal Control Coatings Performance at Near Geosynchronous Altitude," AIAA J. Thermophysics and Heat Transfer, Vol. 6, No. 4, October-December 1992, pp. 665-671.

[104] Sheldahl Data, "Thermal Control Material & Metalized Films."

[105] M.G. Grote, "Results from the LDEF/A0076 Cascaded Variable Conductance Heatpipe Experiment," LDEF First Post-Retrieval Symposium, NASA CP 3134, 1991, pp.1455-1466.

[106] K.deGroh and B.A. Banks, "AO Undercutting of LDEF Aluminized-Kapton Multilayer Insulation," LDEF Second Post-Retrieval Symposium, NASA CP 3162, 1993, pp.781-795.

[107] Satellite Servicing Project Goddard Space Flight Center, "Proceedings of the SMRM Degradation Study Workshop," NASA-TM-89274, pp. 1-32.

[108] C.A. Smith, M.M. Hasegawa, and C.A. Jones, "Space Station WP-2 Application of LDEF MLI Results," LDEF Materials Results for Spacecraft Applications, NASA CP 3257, 1994, pp. 47-60.

[109] D.E. Brinza, "Early Results from the JPL Experiments on the Evaluation of Oxygen Interactions with Materials (EOIM-3) Experiment Aboard STS-46," Presented at the EOIM-3 BMDO Flight Experiment Workshop, June 22, 1993.

[110] C.Durin and I. Alet, "Results of the Post Flight Analyses on System Materials for the LDEF FRECOPA Experiment," Materials in a Space Environment, CNES, Toulouse, September 1991, pp.47-74.

[111] B.A. Banks, M.J. Mirtich, S.K. Rutledge, D.M. Swec, and H.K. Nahra, "Ion Beam Sputter-Deposited Thin Film Coatings for the Protection of Spacecraft Polymers in Low Earth Orbit," NASA TM-87051, paper presented at the 23rd Aerospace Sciences Meeting, Reno, Nevada, January, 1985.

[112] S.K. Rutledge and R.M. Olle, "Durability Evaluation of Photovoltaic Blanket Materials Exposed on LDEF Tray S1003," LDEF First Post-Retrieval Symposium, NASA CP-3134, 1991, pp.1379-1394.

113 M.J. Mirtich and S.K. Rutledge, "Ion Beam Textured and Coated Surfaces Experiment (IBEX)," LDEF First Post-Retrieval Symposium, NASA CP 3134, 1991, pp.989-1011.

114 L. Kauder, "Preliminary Results for LDEF/HEPP Thermal Control Samples," LDEF First-Post Retrieval Symposium, NASA CP-3134, 1991, pp. 797-800.

115 H.W. Babel, K.E. Simpson, and C.A. Jones, "Material Considerations for Space Station Freedom", 41st Congress of the International Astronautical Federation, Report No. IAF-90-278, October, 1990.

116 R.J. Duckett and C.S. Gilliland, "Variable Anodic Thermal Control Coatings on Aluminum," AIAA Paper No. AIAA-83, June 1983, AIAA 18th Thermophysics Conference, Montreal, Canada.

117 D. Duffy, "Final Report on Development of Durable/Long-Life Radiator Coatings," Acurex Technical Report FR-88-100/ESD for NASA Lyndon B. Johnson Space Center, Acurex Corp. Environmental Systems Division, Mountain View, CA, April 1988.

118 J. Golden, "Anodized Aluminum on LDEF," LDEF Materials Results for Spacecraft Applications, NASA CP-3257, 1994, pp.61-72.

119 T.R. Sampair and W.M. Berrios, "Effects of Low Earth Orbit Environment on the Long Duration Exposure Facility Thermal Control Coatings," LDEF First Post-Retrieval Symposium, NASA CP-3134, 1991, pp. 935-944.

120 K.E. David and H.W. Babel, "Optical Property Degradation of Anodic Coatings in the Space Station Low Earth Orbit," Presented to AIAA Materials Specialist Conference, Dallas, TX, April 1992.

121 W.L. Plagemann, "Space Environmental Effects on the Integrity of Chromic Acid Anodized Coatings," LDEF First Post-Retrieval Symposium, NASA CP 3134, 1991, pp. 1023-1040.

122 R.J. Duckett and C.S. Gilliland, "Variable Anodic Thermal Control Coatings on Aluminum," AIAA Paper No. AIAA-83, June 1983, AIAA 18th Thermophysics Conference, Montreal, Canada.

123 W.S. Slemp, "Ultraviolet Radiation Effects," NASA/SDIO Space Environmental Effects Workshop, NASA CP 3035, 1988.

124 J. Golden, "Anodized Aluminum on LDEF," LDEF Materials Results for Spacecraft Applications, NASA CP-3257, 1994, pp.61-72.

125 Preliminary Report on LDEF-Related Contaminants, LDEF Materials Special Investigation Group, prepared by Boeing Aerospace, August 1990.

126 E.R. Crutcher and K.J. Warner "Molecular Films Associated with LDEF," First Post-Retrieval Symposium, NASA CP-3134, 1991, pp. 155-178.

127 T.B.Stewart, G.S. Arnold, D.F. Hall, D.C. Marvin, W.C. Hwang, R.D. Chandler, and H.D. Marten, "Photochemical Spacecraft Self-Contamination: Laboratory Results and Systems Impact," AIAA-88-2728, June 1988.

128 F. Levadou, K. Derbyshire, and A. Paillous, "Enhancement of Solar Absorptance Degradation due to Contamination of Solar Radiator Panels in Geosynchronous Orbit," in Proceedings of the 15th International Symposium on Space Technology and Science, Tokyo, May 1986.

11. POWER SYSTEMS

The different elements of the power system include energy sources, energy converters, energy storage, power conditioning, and control systems. The amount of electrical power required on board a spacecraft is dictated by the mission goals, i.e., the operational requirements of the payloads, the antenna characteristics, the data rate, and the spacecraft orbit. For communication satellites the power requirements range from 500 W to 2000 W depending upon the channel capacity. Further, the power requirements are to be met uninterrupted for durations typically in excess of five to seven years. In contrast, unmanned scientific probes with mission life varying from a few months to three to four years and manned space stations (e.g., Skylab, Space Stations) require 2 to 100 kW of power depending upon the load and the specific nature of the mission.

The generation of electrical power on board a spacecraft generally involves four basic elements:

- A primary source of energy such as direct solar radiation or nuclear power generators, chemical batteries.
- A device for converting the primary energy into electrical energy.
- A device for storing the electrical energy to meet peak and/or eclipse demands.
- A system for conditioning, charging, discharging, regulating and distributing the generated electrical energy at the specified voltage levels.

Foremost among the sources of primary power for use in spacecraft is the solar radiation that impinges in the vicinity of Earth at a level of 135.3 mW/cm^2. Nearly all the spacecraft use solar radiation as the primary source of power. However, use of solar radiation would need a supplementary source that can store the electrical energy. Chemical sources such as rechargeable storage batteries serve such a purpose. These batteries employing electrochemical processes have typical efficiency of 75%. As an alternate to solar energy, radioactive isotope generators have also been used especially for outer planetary missions because of the distance effects resulting in a low level of solar radiation. For example, the solar radiation reduces to about 58 mW/cm^2 in the Mars orbit and to about 5 mW/cm^2 in Jupiter orbit. So it becomes necessary to use other primary sources of energy for spacecraft on missions to Jupiter and beyond.

The basic configuration of a spacecraft power system based on a solar energy source consists of (a) solar cell array, (b) rechargeable secondary storage batteries for energy storage and (c) the power conditioning and control system (PCCS) which transfers power from the solar cell array directly and/or indirectly through the battery to the different loads.

11.1 SOLAR CELLS AND ARRAYS

11.1.1 Introduction

The solar cell basically works on the principle of photovoltaic effect and converts incident radiation into electrical energy usually represented by the so-called Johnson curve. Solar cells are made using different materials. Since 1955, all significant practical applications of solar cells utilize silicon devices, since none of the other materials provide higher efficiencies than silicon for production-type cells, e.g., 15%.[a] Recently GaAs solar cells are being made and used with efficiencies greater than 18 percent. They have lower power performance degradation with temperature and degrade less under charged particle irradiation than conventional silicon solar cells. Although GaAs cells presently cost more per watt as delivered from the manufacturer, their characteristics make GaAs arrays more competitive with silicon arrays when cost per watt-hour for long life missions are taken into consideration.

The spectral response curve of a typical silicon solar cell in relation to the solar radiation is shown in Figure 11-1.[1] The cell response extends over the wavelength 0.35 μm to 1.10 μm. For a maximum output, it is desirable to have the peak spectral response of the cell at the maximum energetic response of the solar spectrum, i.e., in the neighborhood of 0.5 μm. In fact, for technological reasons, the maximum of this response is located around 0.8 μm.

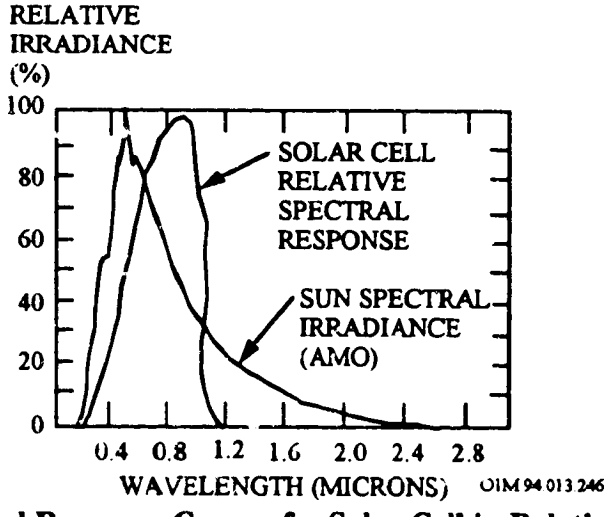

Figure 11-1. Spectral Response Curve of a Solar Cell in Relation to the Solar Radiation.

[a] The silicon solar cells were developed first at the Bell Laboratory in 1953. They were used for the first time in space application in 1958 on board the VANGUARD-1 Spacecraft for the generation of electrical power. Since then, there have been continuous improvements in the performance characteristics of solar cells. And to date, these cells continue to be the primary means of generating electrical power in Earth orbiting spacecraft.

The solar cells on board the spacecraft undergo a large number of thermal cycles (from > +60°C to <-170°C in the case of GEO orbits). Figure 11-2 shows how the current-voltage (I-V) characteristic of a typical cell varies due to different temperatures (ref. 1).

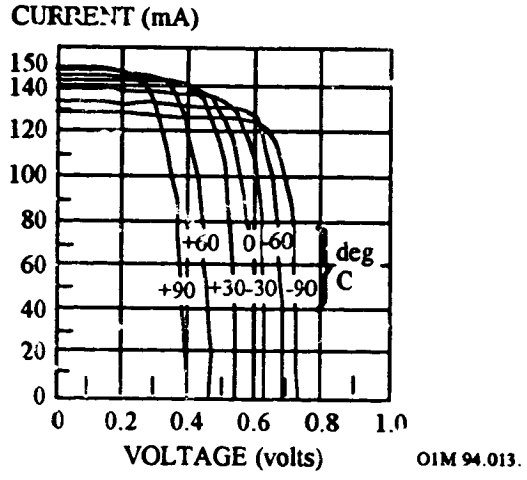

Figure 11-2. I-V Characteristic of a Typical Solar Cell for Various Temperatures.

11.1.2 Solar Cells

11.1.2.1 Charged Particle Radiation Degradation Effects

The efficiency of the solar cell decreases as a function of time in space due to its susceptibility to the particle radiation. A large flux of protons and electrons arise in the spacecraft environment because of the Van Allen Radiation Belts (trapped radiation) and solar flares. Most of the solar cell degradation effects occur because of the solar flare protons and trapped electrons. The energy of these particles varies from a few KeV to several MeV in the case of electrons and is in the range of several hundred MeV for protons.

The bombardment of these high energy particles produces crystalline defects in the solar cells, which then become recombination centers. Low energy particles create damage close to the junction and therefore, raise the dark current and lower the open circuit voltage. High energy particles penetrate far into the base and lower the lifetime of electron hole pairs, thereby decreasing the short circuit current. This results in a reduced cell power output. Figure 11-3 shows the effects of successive doses of 1 MeV electrons in the I-V characteristics of solar cells (ref. 1).

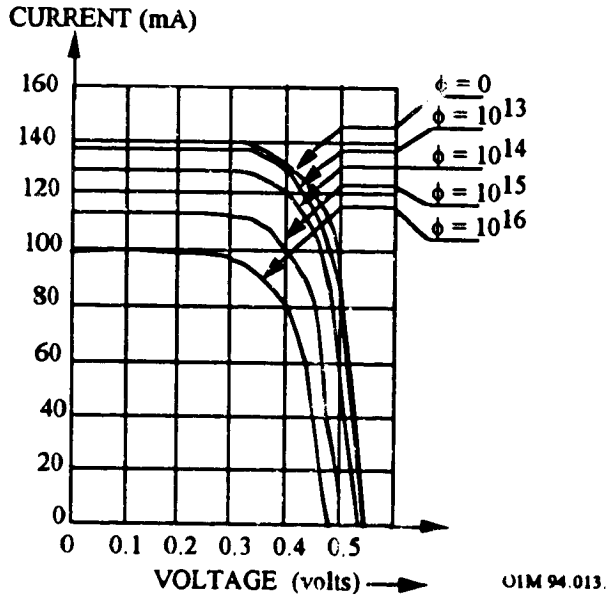

Figure 11-3. I-V Characteristic of a Typical Solar Cell Subjected to Successive Doses of 1 MeV Electrons.

The radiation effects can be minimized by protecting the cells using cover glasses, which are usually made of quartz or sapphire or cerium doped silica. In general, a 150 to 300 microns thick cover slip is attached to the solar cell with UV resistant adhesive for the purpose

of thermal control and protection from radiation and mircrometeorites. The amount of radiation degradation to the cells depends on the radiation level, which is a function of the orbital altitude, and on the thickness of the cover glass employed as shown in Figure 11-4 (ref. 1). The cover slip incorporates an antireflection coating (e.g., silicon monoxide) on the front surface optimized at 0.6 microns and a multilayer UV rejection filter at the back surface. The cover glass will have 98% transmittance over the spectral range of 0.35 microns to 1.10 microns. Temperature of the cells has to be kept low to obtain higher output power and hence the ratio of solar absorptivity to the black body emissivity (α/ε) of the cells should be made a minimum. The cover glasses, which act as a filter to cut down the total energy absorbed by the cell, achieve this to a good extent. A solar cell complete with its cover glass exhibits an α/ε of around 0.94.

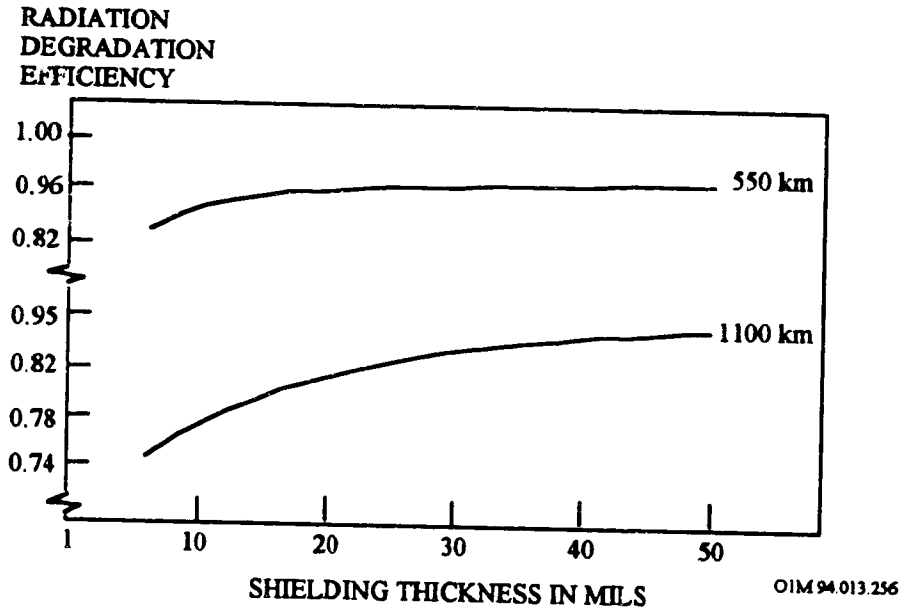

Figure 11-4. Radiation Degradation Efficiency versus Shielding Thickness and Orbital Altitude

11.1.2.2 Micrometeoroid and Debris Impact Effects

Photovoltaic cells (solar cells) were flown in a variety of locations on the Long Duration Exposure Facility (LDEF). The Solar-Array-Materials Passive LDEF Experiment (SAMPLE-A0171)[2] was located 38 degrees off the LDEF leading edge and the Advanced Photovoltaic Experiment (APEX-S0014)[3] was located on the leading edge. A total of over 350 cells representative of the late 1970's and early 1980's technology were flown. Eleven of these cells were gallium-arsenide and the remaining cells were silicon.

LDEF APEX Experiment. The APEX-S0014 experiment consisted of 144 Si type solar cells and 11 LPE GaAs solar cells solicited from different industrial and governmental groups.[b] The cells were mounted on 127 aluminum plates of different sizes and configurations. Most of the solar cells were protected with the conventional (glass) coverslides. The APEX cells provided by the NASA Marshall Space Flight Center (MSFC) contained both conventional and polymer coverslides.

APEX sustained a large number of impact from micrometeoroids and debris due to its position on the leading edge. A survey of APEX conducted in SAEF-2 at the Kennedy Space Center at the time of deintegration yielded a count of 632 impacts, 569 of which were 0.5 mm in diameter or smaller.[4] The remainder were greater in diameter than 0.5 mm, with the largest crater 1.8 mm in diameter. Several of the cells were cratered from micrometeoroid and/or debris impacts, with the range of damage spanning from microscopic craters in the coverglass surface to penetration of the coverglass and cell and cratering of the underlying aluminum mounting plate.[5] Hence, damage[c] to the cells included cratered and cracked coverglasses, craters extending into the cell itself, and in one case, a small portion of a silicon cell and coverglass was removed as the particle continued into the aluminum substrate.[6]

Although electrical continuity was maintained in the few cells in which the cratering extended into the solar cell itself, or caused a crack in the coverglass cell, results of the impacts and subsequent cratering did caused extensive electrical degradation of the cells. Figure 11-5 (ref. 5) shows the illuminated current-voltage performance of cell M-3 taken in a laboratory simulator. This cell is a 5.9 cm. x 5.9 cm. silicon cell with a wrap-around front

---

[b] AF Wright Aeronautical Laboratory, Applied Solar Energy Corporation, COMSAT Laboratories, European Space Agency, Jet Propulsion Laboratory, NASA Lewis Research Center, NASA Marshall Space Flight Center, Solarex Corporation, Spectrolab, Inc..

[c] Damage caused by impacts is typically described in terms of crater or perforation diameters, with only an occasional reference to spallation areas.

contact on the four corners. The development of this cell was undertaken to provide power for the Shuttle on extended missions and is similar to the wrap-through technology selected for Space Station Freedom. This cell sustained a small crater in the coverglass which did not penetrate to the silicon cell itself. From Figure 11-5 it can be seem that little change in performance resulted.

The silicon solar cell designated NA-9 had the largest diameter (1.8 millimeter) crater on APEX. The crater extends into the silicon cell through the coverglass, although neither the cell nor cover are cracked. Figure 11-5 is the pre- and post-flight simulator data. The approximately 100 mV drop in open-circuit voltage is due to shunting of the cell pn junction at the sight of the crater. The 5% drop in current is due to area loss associated with the crater and a contaminating layer evident on the cell.

The current-voltage characteristic of another large area, wrap-around silicon cell (M-9) is also shown in Figure 11-5. In this case, however, the micrometeoroid/debris damage extended into the cell itself, cracking both the coverglass and the silicon cell. The crack in the solar cell extend about 90% of the way across the cell while the coverglass crack extends from side to side, although on a different path than the cell crack. The wrap-around feature of cell front contact provides sufficient redundancy to maintain electrical continuity. The loss in fill factor evident in Figure 11-5 is due to this cell crack, but the short-circuit current and open-circuit voltage are unchanged.

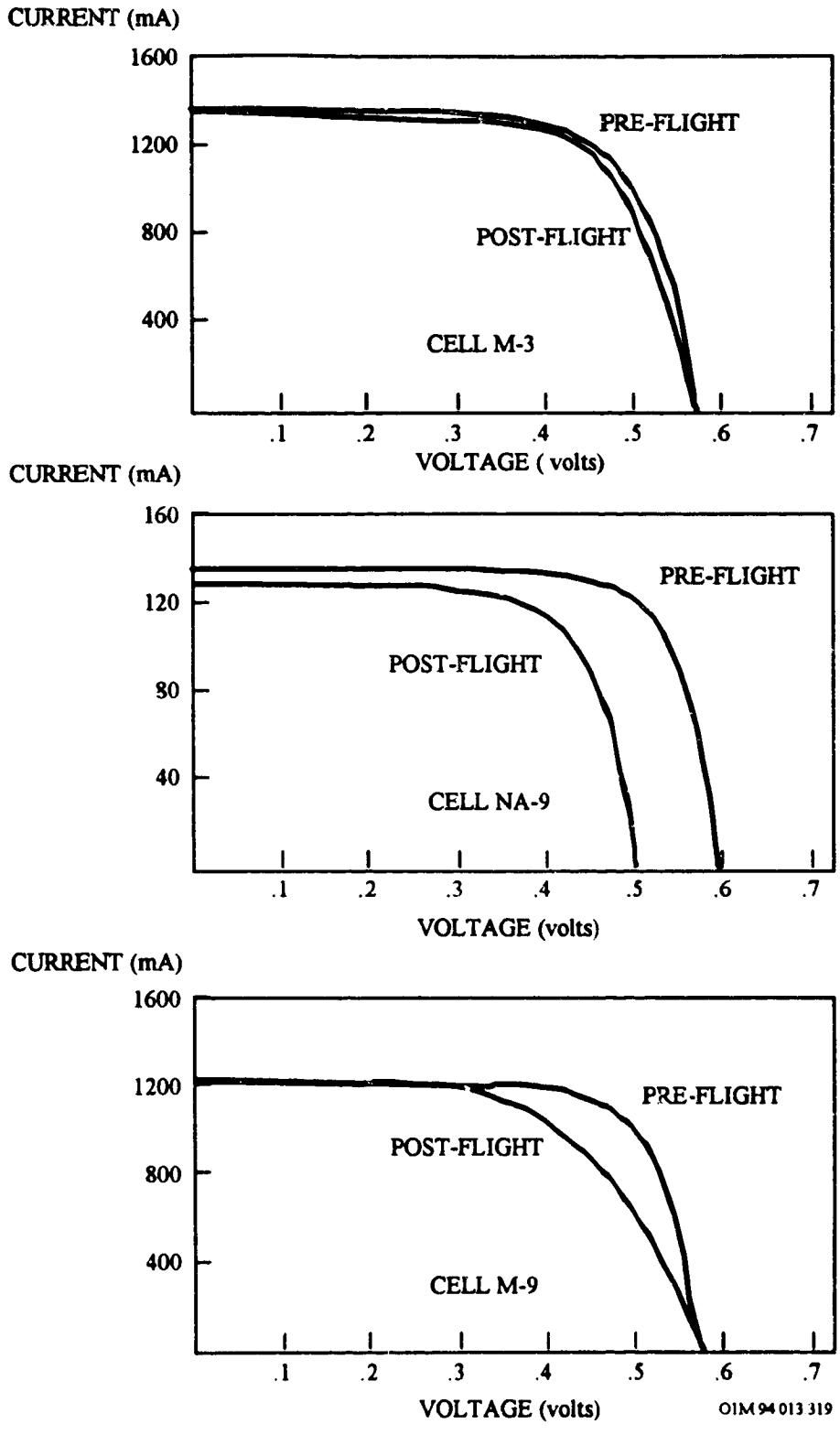

Figure 11-5. Illuminated Current-Voltage Performance of Cells M-3, NA-9, and M-9

LDEF SAMPLE Experiment. Micrometeoroids and debris impacts were also observed on the solar cells flown on the JPL and MSFC portions of the LDEF SAMPLE experiment,[d] which was located 38° off the ram position. A relatively high fluence of ~0.130 impacts/cm^2 of size $\geq$ 0.05 mm diameter was observed by the JPL investigators over the mission duration (ref. 2). These were typically of small size and of high energy, as evidenced by penetrations of materials such as Invar tabs and thin silicon solar cells. Most impacts appear to be normal to the plate (circular crater). Evidence from a number of LDEF experiments suggests that the majority of the impacts observed on this experiment were of space debris, rather than micrometeorite origin.[7] The MSFC investigators observed micrometeorite/debris craters on the solar cells with a flux calculated at 0.148 impacts/cm^2.

In contrast to the results on some of the solar cells located on the APEX experiment, no micrometeorite damage was found to cause significant electrical degradation to the solar cells flown on the JPL and MSFC SAMPLE experiments. Electrical properties of the solar cells were minimally affected by impacts, as reported by Stella (ref. 2) and Young (ref. 3). An impact to a silicon cell on the JPL portion of the SAMPLE experiment left a well-defined crater with any ejected material blown completely away. The silicon cell was completely penetrated (~0.1 mm central hole), with the formation of a near hexagonal-shaped through hole. Hence, cracking of the cover glass and even penetrations to the solar cell only had a local effect.

Instead, the degradation in cell performance for all samples was due to a loss of cell current due to a darkening of the adhesive and/or coverglass due to exposure to UV, charged particles, and AO fluence. Changes in the electrical performance (i.e., Isc, short circuit current) for each cover/encapsulant type category are discussed in Section 11.1.3.

---

[d] The JPL portion of SAMPLE consisted of an 28 cm x 41.4 cm (11-in. x 16.3-in.) aluminum plate with 30 different combinations of thin silicon solar cell/cover samples, as summarized in the table below. The cells were Solarex Corporation fabricated 50 μm thick 2 x 2 cm^2 silicon devices with silver-plated Invar tabs welded to the N and P contacts.. Each cell and tab assembly was bonded to a slightly oversize sheet of 25 μm thick Kapton insulation bonded to the aluminum plate. The bonding materials were standard space-type silicone RTVs.

Experimental List of the Materials Aboard JPL Portion of SAMPLE

Number of Cells	Coverglass Materials	Coverglass Thickness	Adhesive/Encapsulant
6	microsheet	100 micron	5 silicone adhesives, including DC 93-500
10	FEP Teflon	50 micron	5 different silicone adhesives
10	None		6 different hard/soft silicone encapsulants
2	None		GE X-76 polyimide encapsulant
2	None		Bergstron and Assoc./GE BE225HUP silicone-polyimide

The MSFC protion of SAMPLE consisted of 4 multi-cell modules and 5 single cells. Conventional (glass) coverslides were flown as part of the solar cell assemblies on the MSFC SAMPLE experiments.

11.1.3 Solar Cell Coverslides

The purpose of a coverglass is to prevent energetic protons from damaging the semiconductor material and degrading its electronic transport properties, which, in turn, reduces cell conversion efficiency. The choice of coverglass material and its thickness are determined by the energy and flux of the protons, which varies with orbital inclination and altitude. Proton damage is evidence by the drop in Isc (short-circuit current) as well as the substantial loss of Voc (open-circuit voltage) .

Post-flight evaluation of the solar array experiments revealed that some components/materials are very resistant to the environment to which they were exposed while others need protection, modification, or replacement. The LDEF flight provided a means to directly evaluate the behavior of the cover materials in the space environment, including their ability to protect the cells. The post flight experiment review consisted of visual examination, cell electrical performance measurements and data analysis. The effects of the LDEF mission environment (micrometeorite/debris impacts, atomic oxygen, UV and particulate radiation) on the samples are reviewed below.

11.1.3.1 Atomic Oxygen

Coverglass slides were flown in a variety of locations on the Long Duration Exposure Facility (LDEF). The Solar-Array-Materials Passive LDEF Experiment (SAMPLE-A0171) (ref. 2) was located 38 degrees off the LDEF leading edge and the Advanced Photovoltaic Experiment (APEX-S0014) (refs. 5 and 6) was located on the leading edge. The longer than planned (5.8 years versus 1 year) LDEF flight provided an increased amount of atomic oxygen fluence in the ram direction and 38 degrees off the ram direction; 8.99×10^{21} atoms/cm^2 and 7.15×10^{21} atoms/cm^2, respectively.

In general, this increased atomic oxygen fluence combined with UV and charged particles exposure account for the degradation in cell performance for all solar cell samples that were not covered or covered with the non-conventional coverslides (e.g., polymer). Apparently, the loss of open-circuit voltage and short-circuit current is instead attributed to a darkening of the adhesive and/or coverglass. As expected, very little degradation in cell conversion efficiency was demonstrated by post-flight performance measurements for the solar cells covered with the conventional (glass) coverslides.

LDEF APEX Experiment. A representative sampling of the post-flight illuminated current-voltage (I-V) characteristic of some of the cells flown on APEX, described in Table 11-1, are shown in Figures 11-6 to 11-15 (ref. 6). Also included for comparison in the figures are the pre-flight values of short-circuit current (ISC), open circuit voltage (Voc) and fill factor (F.F.).[e]

Table 11-1. Solar Cells on APEX Experiment

Silicon Cells			
Cell Number	**Description**	**Coverglass**	**Remarks**
IV#7 B-1L	Spectrolab, Solar Maximum Mission	12 mil Crng. 7940	Little pre- to post-flight change
ISC#95 M-5	ASEC, Large Area, Wrap Around Contact SSF predecessor	6 mil Fused Silica	Little pre- to post-flight change
ISC#112 B-2R	COMSAT Very High Blue Sensitivity V-grooved cover	30 mil 7070	Little pre- to post-flight change
ISC#114 B-4R	COMSAT Non-Reflecting Textured surface High current	12 mil Fused Silica	Little pre- to post-flight change
ISC#63 NA-10	Solarex, Back Surface Field/Reflector	No cover	ΔVoc = 65 mV ΔIsc = 13.4 mA
ISC#83 B-21R	LeRC A/C Standard	No cover	ΔVoc = 46 mV ΔIsc = 4.7 mA
Gallium Arsenide Cells			
Cell Number	**Description**	**Coverglass**	**Remarks**
ISC#111 A-2	JPL, AMOS Only heterostructure cell on APEX	Unknown material	Increase in current from pre- to post-flight
ISC#71 NB-15L	Hughes, Dj = 0.5 μm	12 mil Fused Silica	ΔVoc = 10 mV ΔIsc = 17.5 mA
ISC#76 NB-29R	Hughes, Dj = 0.5 μm	No Cover	ΔVoc = 65 mV ΔIsc = 21.7 mA
ISC#77 NB-29L	Hughes, Dj = 0.35 μm	No Cover	ΔVoc = 85 mV ΔIsc = 23.7 mA

[e] The fill factor is a measure of how close to ideal (100 percent) the cell is performing. It is the ratio of the product of max-power-current and max-power-voltage divided by the product of short-circuit-current and open-circuit-voltage (ImpxVmp)/(IscxVoc).

All of the silicon cells are n-p type, the standard configuration for silicon space cells due to its superior radiation tolerance. Cell IV#7 (Mount B-1L) was manufactured by Spectrolab for the Solar Maximum Mission satellite. The base resistivity of the cell was 10 Ω-cm with an anti-reflection coating of Ta_2O_5. As can be seen in Figure 11-6, little change in cell performance due to time on-orbit has occurred. The small differences in Isc and Voc are within experimental accuracy.

The cell of Figure 11-7, ISC#95, is a large area (5.9 x 5.9 cm) cell in which the front contact wraps around the edge of the cell enabling all leads to be attached from the rear. This cell is the predecessor to the Space Station Freedom cell. Seven such cells were flown. Little change in Isc or Voc was noticed, however the drop in fill factor of about 2 percentage points was typical of this set of cells. A set of four cells with the same design but with conventional top/bottom contacts also showed little change in Isc or Voc. The drop in fill factor was larger, ranging from 6 to 18 percentage points.

Cell ISC#112 (see Figure 11-8) has a base resistivity of 1 Ω-cm and an anti-reflection coating of Ta_2O_5. Its 30 mil coverglass is the thickest on LDEF APEX experiment, and the only grooved design. The grooves are situated above the cell collection fingers and serve to reflect light to those areas where it can be collected. No decrease in performance was seen.

The cell of Figure 11-9, ISC#114, and a companion cell, IV#11, employed a texturized surface to optimize photon absorption and thus increase short-circuit current. The cells have a base resistivity of 10 Ω-cm and also use a Ta_2O_5 anti-reflection coating. The post-flight currents of the cells, in excess of 189 ma, are the largest current densities of the APEX cell complement.

The last two silicon cells of Table 11-1 were two of fifteen silicon cells which did not have coverglasses. Proton damage is evidenced by the drop in Isc as well as the substantial loss of Voc. Similar drops in performance were seen in the entire set of unglassed cells. Cell ISC#83 has a base resistivity of 10 Ω-cm and is consequently more radiation tolerant than the 1 Ω-cm material of cell ISC#63. This is confirmed by the data of Figures 11-10 and 11-11.

A summary of the gallium arsenide solar cells contained in the APEX sample set is provided in Table 11-1. Ten of the eleven were fabricated by Hughes Research Laboratory using the liquid phase epitaxy techniques. Post-flight simulator calibration for the gallium arsenide cells was accomplished using a gallium arsenide aircraft standard of the same design and vintage of these Hughes cells. The remaining cell, ISC#111 (Figure 11-12), is a metal-

oxide-semiconductor structure made at JPL and primarily of interest as a terrestrial cell. The cell is covered with a coverglass of unknown material. At this time the source of the increase in current from pre-flight to post-flight is not known. A change in the junction structure (formed by the metal and oxide layers) is unlikely as the open-circuit voltage is unchanged. The contaminating film covering the cell may have served to improve the anti-reflection properties of the front surface of the coverglass.

The remaining three cells of Table 11-1 (Figure 11-13 through 11-15) are similar in design with the exception of the junction depth (Dj). Each cell, ISC#71, ISC76, ISC77, represents a set of three flown on APEX. The effect of the fused silica coverglass on ISC#71 is most apparent in the open-circuit voltage, with that of the uncovered cells sustaining significant losses. As in the case of the silicon cells, this is due to the energetic protons found in LEO. The decrease in Voc and Isc of cell ISC#77 is greater than that of ISC#76 due to the shallower depth of its junction (0.35 μm versus 0.50 μm).

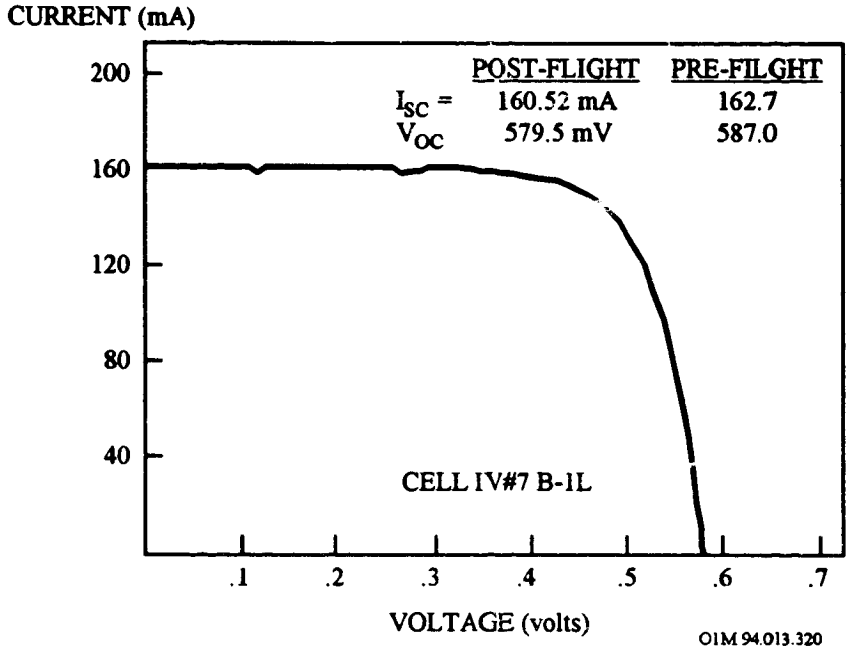

Figure 11-6. Illuminated Performance of Silicon Cell IV#7, B-1L

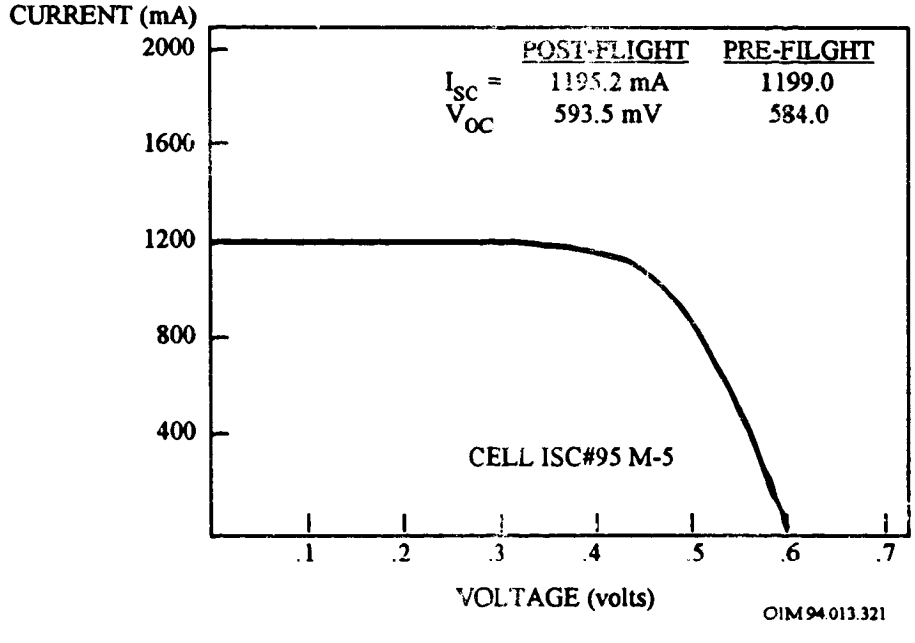

Figure 11-7. Illuminated Performance of Silicon Cell ISC#95, M-5

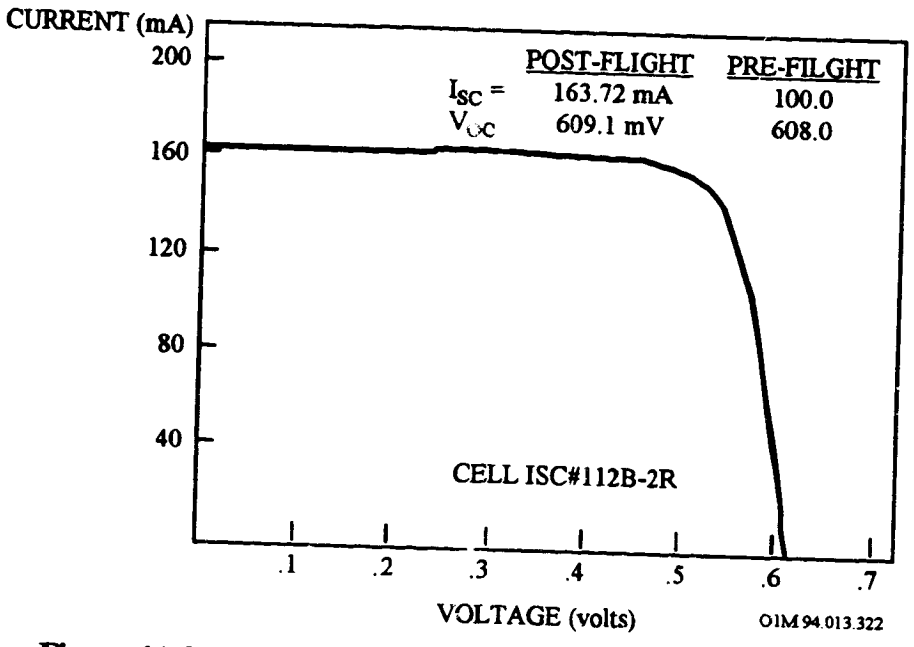

Figure 11-8. Illuminated Performance of Silicon Cell ISC#112, B-2R

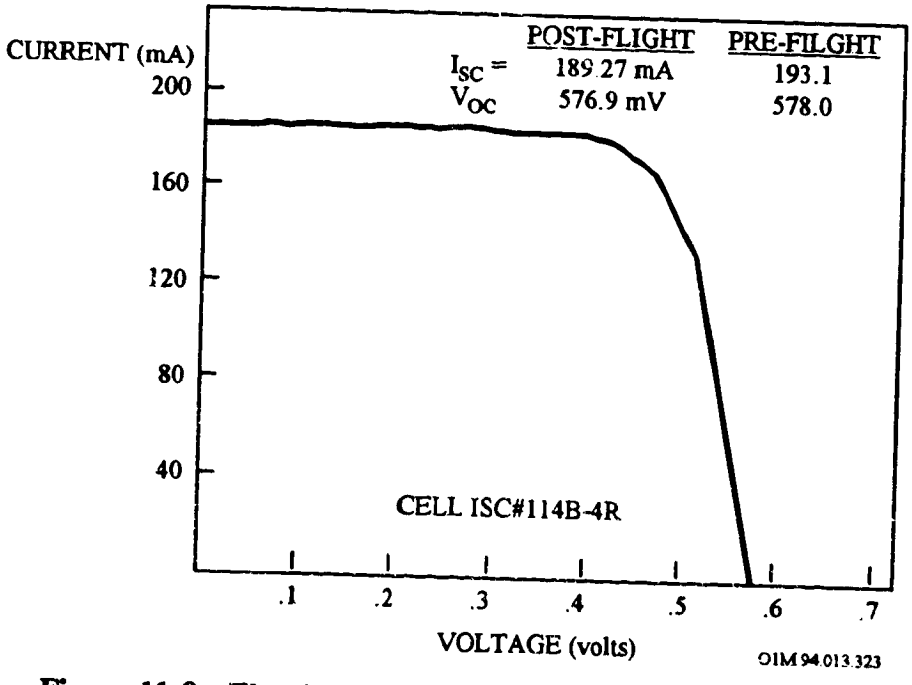

Figure 11-9. Illuminated Performance of Silicon Cell ISC#114, B-4R

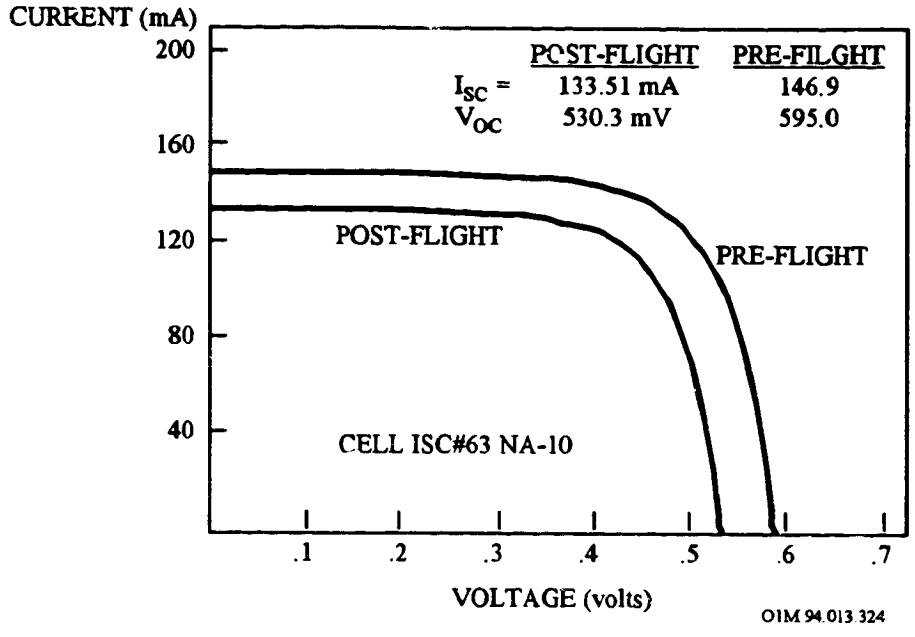

Figure 11-10. Illuminated Performance of Silicon Cell ISC#63, NA-10

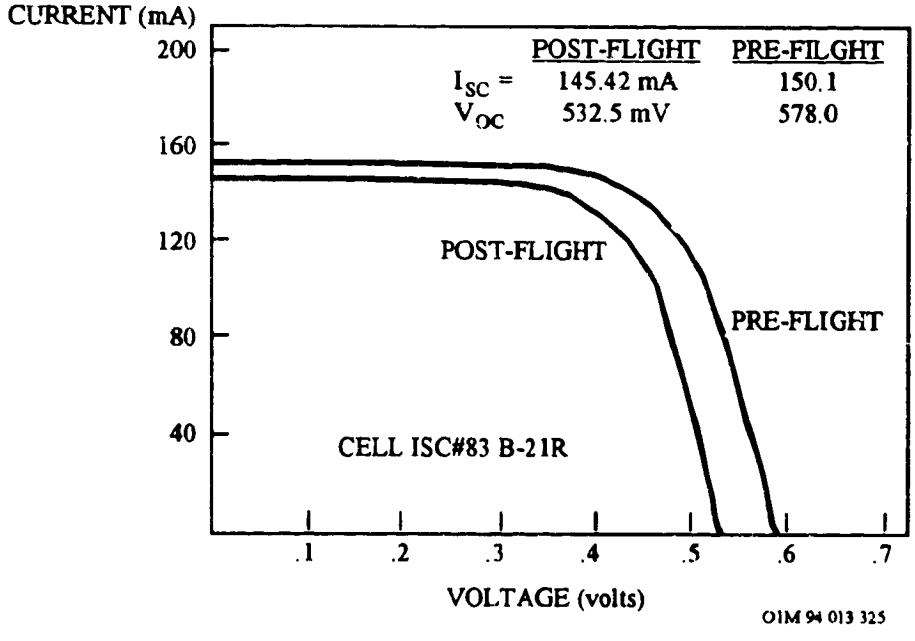

Figure 11-11. Illuminated Performance of Silicon Cell ISC#83, B-21R

c 4

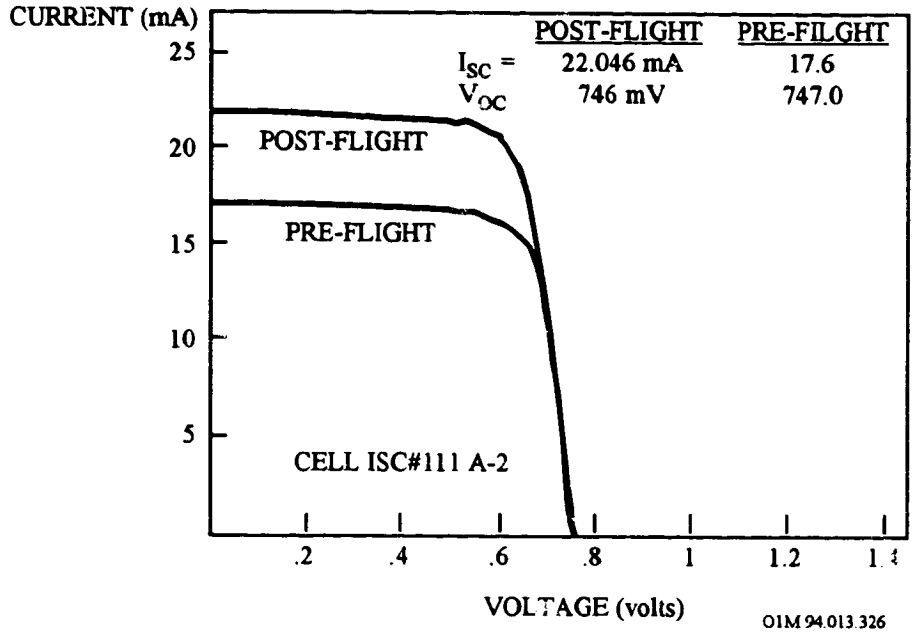

Figure 11-12. Illuminated Performa ce of Gallium Arsenide Cell ISC#111, A-2

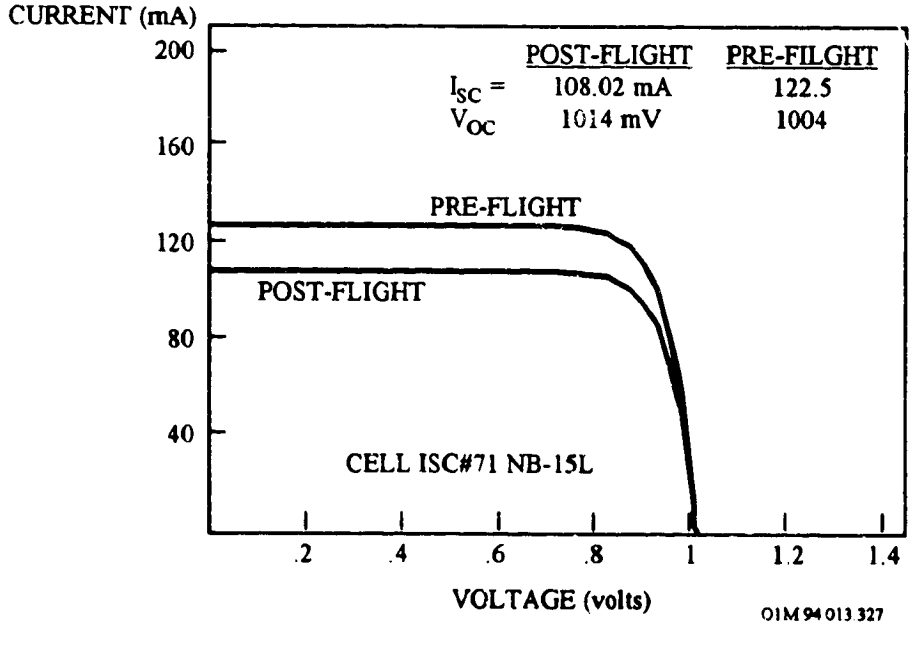

Figure 11-13. Illuminated Performance of Gallium Arsenide Cell ISC#71, NB-15L

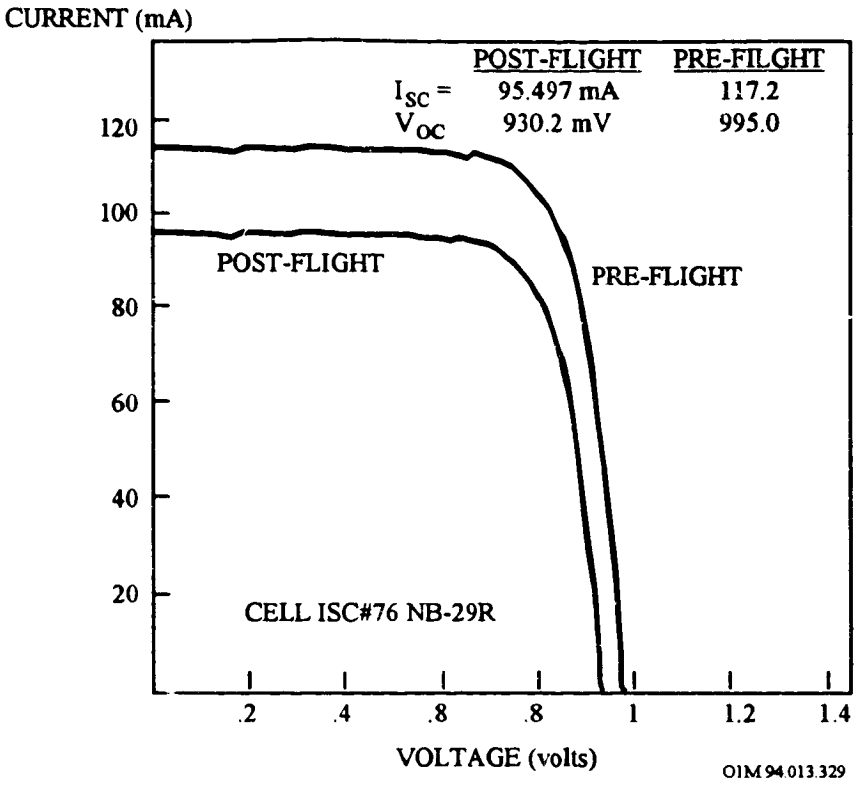

Figure 11-14. Illuminated Performance of Gallium Arsenide Cell ISC#76, NB-29R

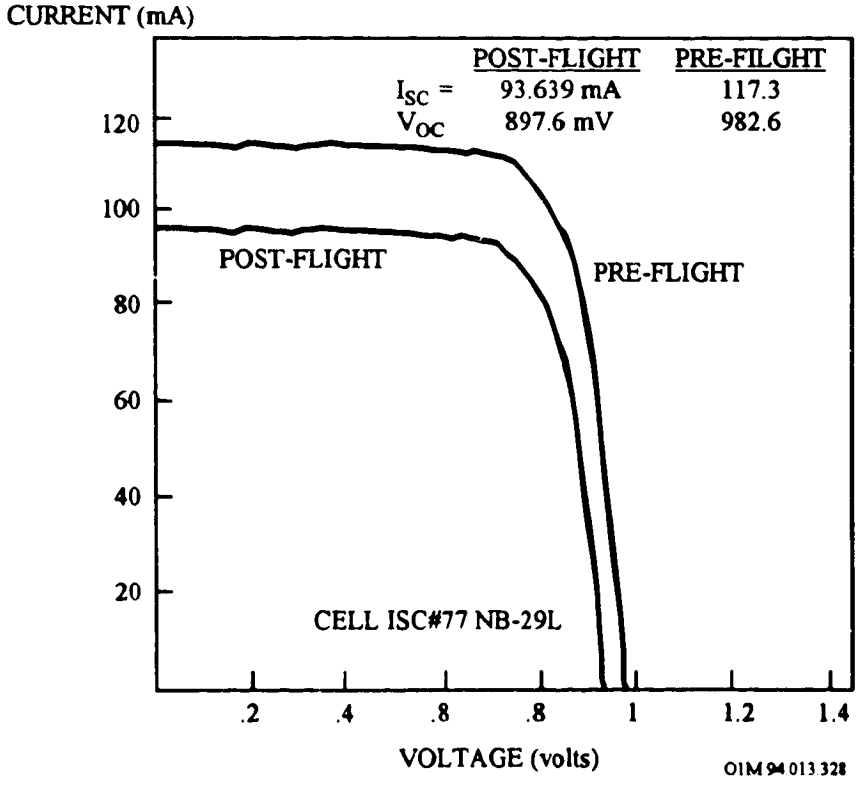

Figure 11-15. Illuminated Performance of Gallium Arsenide Cell ISC#77, NB-29L

The cell assemblies on the MSFC APEX experiment, described in Table 11-2, showed considerable electrical performance degradation for the organic covers. Figure 11-16 compares the pre-flight and post-flight performance (ref. 3).

Table 11-2. Coverslide Characteristics of MSFC APEX Experiments

Coverslide Characteristics	Cell Identification
OCLI, 6 mil, FS, ARC & UVF	B38, B41
Pilkington, 5.5 mil, Ceria Stabilized Microsheet, ARC	B36, B37
Dow Corning 93-500	B32, B33
FEP Teflon	B34, B35
Legend: FS = fused silica, ARC = anti-reflective coating, UVF = ultra violet filter	

Cell assemblies with polymer covers (B32 to B35) degraded more than assemblies with conventional covers. Cells B32 and B33, which used Dow Corning 93-500 adhesive as protective covers, underwent mostly current degradation. Adhesive darkening is the most probable major contributor. Cells B34 and B35, which had LMSC FEP Spraylon protective layers, degraded in VOC and fill-factor; an indication of decreased shunt resistance.

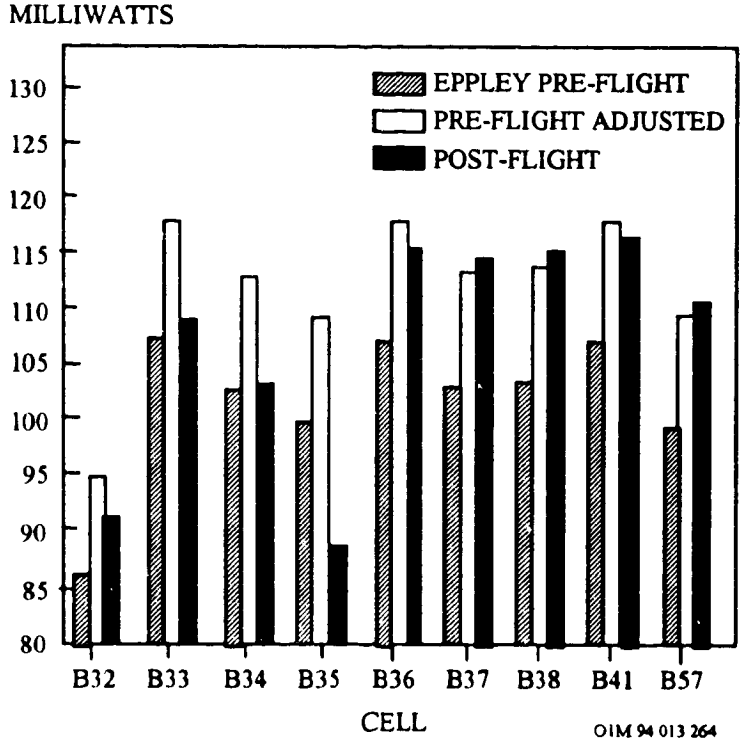

Figure 11-16. Pre- vs Post-flight Maximum Power Point Performance of APEX MSFC Solar Cell Assemblies.

LDEF SAMPLE Experiment. The JPL portion of the LDEF SAMPLE experiment consisted of 30 individual thin silicon solar cell with a variety of protective covers, including conventional cerium doped microsheet platelets and potential candidate materials, such as FEP Teflon film, silicone RTVs, glass resins, polyimides, and a silicone-polyimide copolymer encapsulant. Six cells had 100 μm thick microsheet covers, using five different cell/cover silicone adhesives, including the widely used DC 93-500. Ten cells had 50 μm thick FEP Teflon covers, bonded with five different silicone adhesives. Ten cells were covered with six different silicone encapsulants. Of the ten, six employed soft coatings, such as DC 93-500, and the other four had hard coat silicone encapsulants. Two cells were covered with GE X-76 polyimide, and the remaining two cells with Bergstron and Associates/BE-225HUP silicone-polyimide copolymer. The encapsulant thickness ranged from a low of approximately 12 μm to a high of 75 μm.

Table 11-3 lists the changes in Isc (short circuit current) by each cover/encapsulant type category. The smallest percentage loss measured was for the cerium doped microsheet samples and the BE-225HUP copolymer samples. The latter, however, had very low initial output current and the post-flight samples had cell areas clearly free of encapsulant. The next lowest losses were measured on the polyimide encapsulant, soft silicone encapsulants and the hard coat silicone encapsulants. For the X-76 polyimide, the cell was extensively denuded of encapsulant, so the current shown is in some part that of a bare cell. The hard coat silicones also exhibited some coating loss and crazing. The largest current loss was exhibited by the Teflon covered samples, although the variation was extremely high, ranging from a loss of 10 percent to a loss of 43 percent.

Table 11-3. Solar Cell Assembly Electrical Performance

Cover/Encapsulant	Isc (mA)		Δ (%)	Comments
	Pre-flight	Post-flight		
Microsheet (Ceria)	136.5	132.4	-3	
FEP Teflon	136.8	106	-22	Darkened top surface loss varies from -10% to -43%
Silicone (soft)	132	115	-13	Crazing, some loss near cell edges
Silicone (hard)	135	112	-17	Crazing, flaking, close to complete removal
BE-225 HUP Polyimide-silicone Copolymer	125	121	-3	Partially removed - voids
GE X-76 Polyimide	129.5	119	-8	Encapsulant significantly removed

Hence, all of the non-microsheet cover systems exhibited visible erosion or reaction with the space environment. Coating erosion was sufficient to remove most of the polymer material, allowing damage to occur to the cell grid metallization by atomic oxygen. The most durable polymer material was FEP Teflon, which continued to provide protection against atomic oxygen to the cell below. However, the Teflon material was not free of damage and exhibited visible surface darkening and softening, with some material loss.

11.1.3.2 Charged Particle Radiation Degradation Effects

Solar cells with conventional glass coverslides provided considerable protection against the space environment in comparison to solar cells with no coverslide protection. Conventional glass coverslides were flown as part of the solar cell assemblies (Cell 7 to Cell 10) on the MSFC SAMPLE experiments. Cell 6 had no coverslide. Table 11-4 summarizes the coverslide characteristics of this experiment (ref. 3).

Table 11-4. Coverslide Characteristics of MSFC SAMPLE Experiments

Coverslide Characteristics	SAMPLE
None	Cell 6
OCLI, 6 mil, microsheet, ARC (anti-reflective coating)	Cell 7
OCLI, 6 mil, microsheet ARC & UVF (ultra violet filter)	Cell 8 and Module 5
OCLI, 6 mil, frosted fused silica (FS), ARC & UVF	Cell 9
OCLI, 6 mil, FS, ARC & UVF	Cell 10

Post-flight electrical performance of the MSFC SAMPLE cells Cell 6 through 10 (labelled C6 through C10 in Figure 11-17; ref. 3) indicated that the conventional covers provided considerable protection against the space environment in comparison to Cell 6 with no coverslide. The 20.7 percent degradation in PMP (maximum power point power) experienced by Cell 6 (no coverslide) can be attributed largely to charged particle radiation damage which was equivalent to approximately $5x10^{14}$ 1.0 MeV electrons/cm^2.

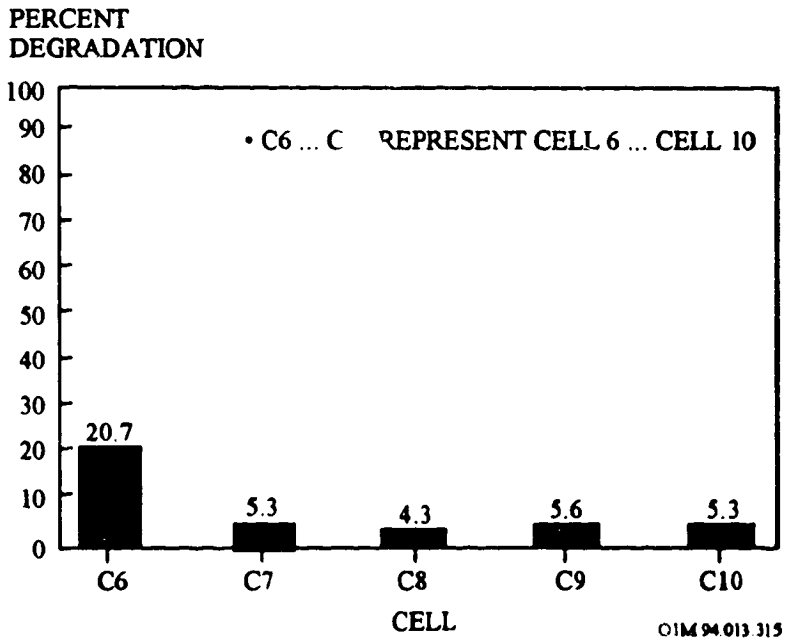

Figure 11-17. MSFC SAMPLE Solar Cell Maximum Power Point Degradation

11.1.3.3 Micrometeoroid and Debris Impact Effects

Electrical properties of the solar cells on the JPL and MFSC portions of the LDEF SAMPLE experiment, located 38 degrees off the ram, were minimally affected by meteoroid/debris impacts to the coverslide as reported by Stella (ref. 2) and Young (ref. 3), respectively. Cracking of the cover glass and even penetrations appeared to only have had a local effect.

On the JPL portion of the LDEF SAMPLE experiment, impact into a 100 micron thick microsheet coverslide left a ~0.1 mm central hole. The microsheet impact was limited in area, and radiating cracks were not visible. It is believed that the impact was spent in the microsheet and that the adhesive was able to absorb any residual gas/debris, without a significant silicon interaction. No degradation was noted in the electrical performance of the covered solar cell. In contrast, an impact particle on solar cell assemblies with polymer cell covers, such as Teflon FEP, penetrated and impacted the silicon cell below. It is clear that the Teflon provided negligible protection against the high energy impacts. However, it was noted that the electrical performance of this cell was not noticeably different from other similarly covered cells, indicating minimal effects from the impact.

On the MSFC portion of the LDEF SAMPLE experiment, the protective glass covers provided sufficient protection to the cell front surface. One of the largest impacts to this experiment caused a crack diagonally across one of the two 0.002-in microsheet coverslides on Module 4. However, electrical performance degradation caused by small craters on the cell coverslide was not discernible in the current/voltage measurement. Instead, the thin Kapton substrate on the solar cell assemblies on Module 5 allowed the larger particles to penetrate the substrate and cause crater damage to the cells back surface and subsequent solar cell electrical performance degradation (see Section 11.1.4.2). Hence, the trend to reduce the weight of solar arrays by reduction of structure should not neglect protection against the micrometeroroid and debris environment.

11.1.4 Solar Array Substrate Materials

Solar array components were flown in a variety of locations on the Long Duration Exposure Facility (LDEF). The Solar-Array-Materials Passive LDEF Experiment (SAMPLE-A0171) (ref. 2) was located 38 degrees off the LDEF leading edge and the Advanced Photovoltaic Experiment (APEX-S0014) was located on the leading edge.

11.1.4.1 Atomic Oxygen Effects

11.1.4.1.1 Polyimide Substrates

The longer than planned (5.8 years versus 1 year) LDEF flight provided an increased amount of atomic oxygen erosion of some of the polyimide substrates which caused significant problems to several of the multi-solar cell modules[f] on the MSFC SAMPLE experiment.[8] Figure 11-18 (ref. 3) shows a cross-sectional sketch of the MSFC SAMPLE solar cell test assemblies. Module 5, the only SAMPLE 12 multicell module not lost to space, experienced degradation in the maximum power point power (PMP) of the individual cells ranging from 4.6 to 80 percent, as shown in Figure 11-19 9 (ref. 3). Current/voltage (I/V) curves, shown in Figure 11-20 indicated a dramatic increase in series resistance of the poorly performing cells (ref. 3). Apparently, the Kapton module substrate had been eroded to the extent that holes/cracks were made that would allow AO flux to impinge upon the silver back-surface metalization and wraparound contacts. It was postulated that interaction of the AO with the wraparounds could cause erosion which would result in increased series resistance.

[f] One module was lost prior to shuttle rendezvous with LDEF, one module was drifting away as LDEF was grappled, and one module (M3) was ~hed by only one corner during the retrieval and was later found on the floor of the cargo bay when LDEF wa. oved from the Shuttle. The fourth module (M4) remained attached to the tray.

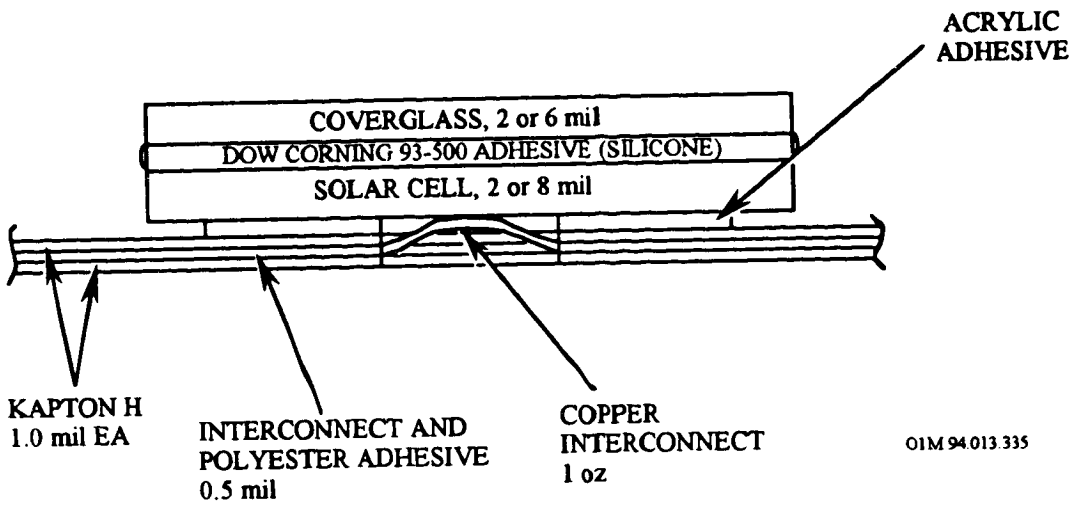

Figure 11-18. Cross-sectional Sketch of MSFC SAMPLE Solar Cell Test Assemblies

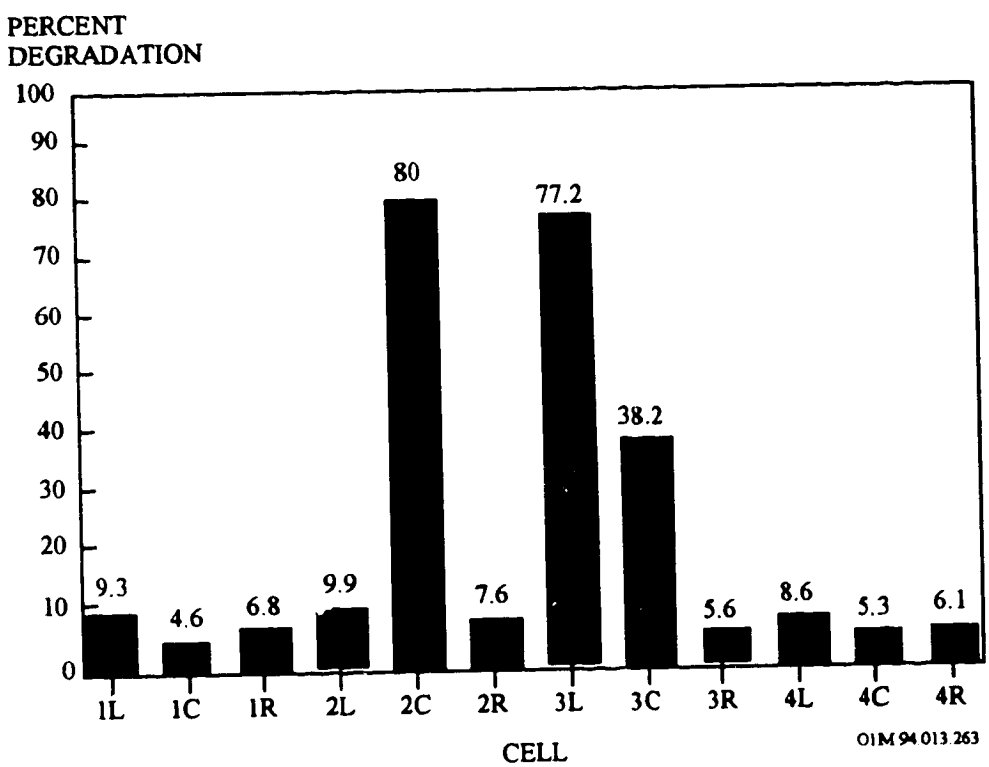

Figure 11-19. MSFC SAMPLE Solar Cell Maximum Power Point Degradation

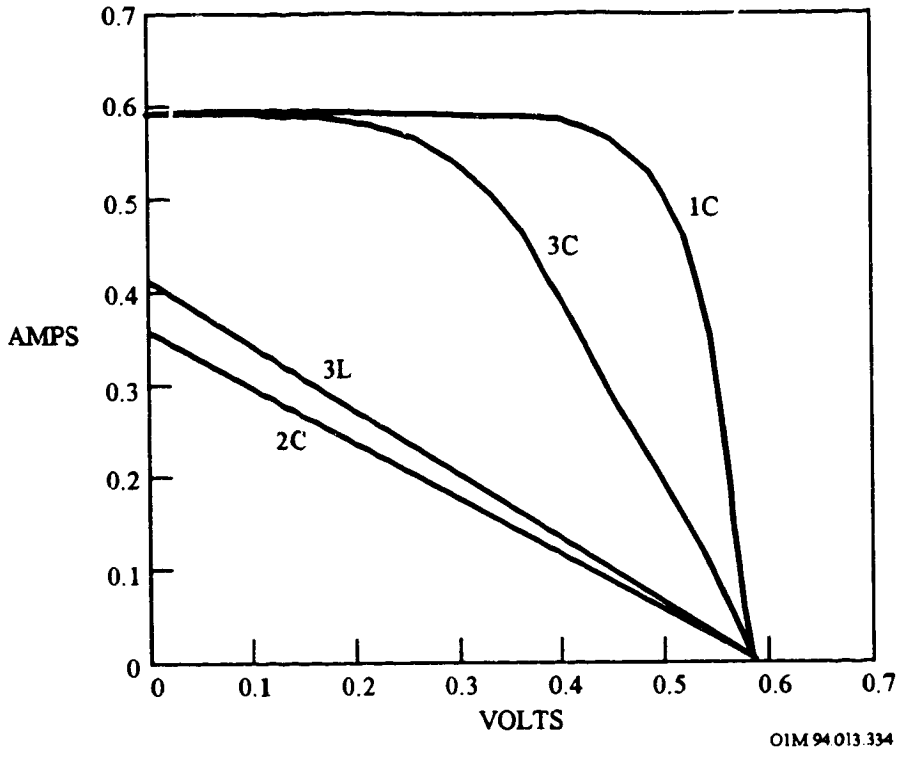

Figure 11-20. Range of SAMPLE Solar Cell Module 5 Individual Cell Electrical Performance

11.1.4.1.2 Silver-Plated Invar Tabs

On the JPL Experiment, all exposed (uncovered by adhesive or encapsulant) silver-plated Invar tab surfaces darkened from the original shiny silver appearance as the result of atomic oxygen interactions. The total fluence of atomic oxygen in the vicinity of this experiment was on the order of $6x10^{21}$ atoms/cm^2. In many cases, the darkened silver tab surfaces showed signs of stress by the formation of platelets. The dark surface material was readily removed by gentle mechanical abrasion revealing a shiny, albeit rough, surface underneath. In some areas, it appeared that the original surface had flaked off during the mission. The resultant surface region was slightly lower than the surrounding regions and the color was less dark; more gray than blue/black suggesting less exposure time to the pertinent environment. Although initially it appeared that the damage to the silver plating did not extend to the Invar, recent efforts to rub off additional blackened regions showed that this was not completely correct. There were a few small areas on the tabs where removal of the darkened surface revealed the Invar surface, suggesting that a minimum thickness of unreacted silver remains on the exposed interconnector. The initial silver thickness was not noted (the problem of atomic oxygen not anticipated at the time of experiment assembly), but typically

ranged from four to six microns. The cover system appearing the least changed was that of the conventional microsheet platelet. These samples generally appeared as if newly assembled.

11.1.4.2 Micrometeoroid and Debris Impact Effects

11.1.4.2.1 Polyimide Substrates

Crater damage to the Kapton substrate can lead to a slight degradation in the cell electrical performance. A comparison of the electrical performance of cells with impact craters (PC1L and PC2R of Module 5) with that of cells without craters (Cell 7 to Cell 10) on the MSFC portion of the LDEF SAMPLE experiment indicated that the crater damage could cause 2- to 4-percent degradation in maximum power point power (PMP). Figure 11-21 compares the solar cell maximum power point degradation (ref. 3). Apparently, the protective glass covers provided sufficient protection to the solar cell front surface, but the thin Kapton substrate on SAMPLE Module 5 allowed the larger particles to penetrate the substrate and cause crater damage to the cells back surfaces. The particles, 100 microns in size, penetrated the Kapton substrate causing craters in the two cells (PC1L and PC2R) that left their signature at the front surface of the cells (cell/coverslide interface). The impacting particle had to first penetrate the Kapton that composed the cell substrate before impacting the cell. However, since these cells have not been evaluated in terms of other performance degradation mechanisms (e.g., polyimide substrates), these values can only be taken qualitatively, i.e., craters up to 100 micron in diameter cause relatively small performance degradation.

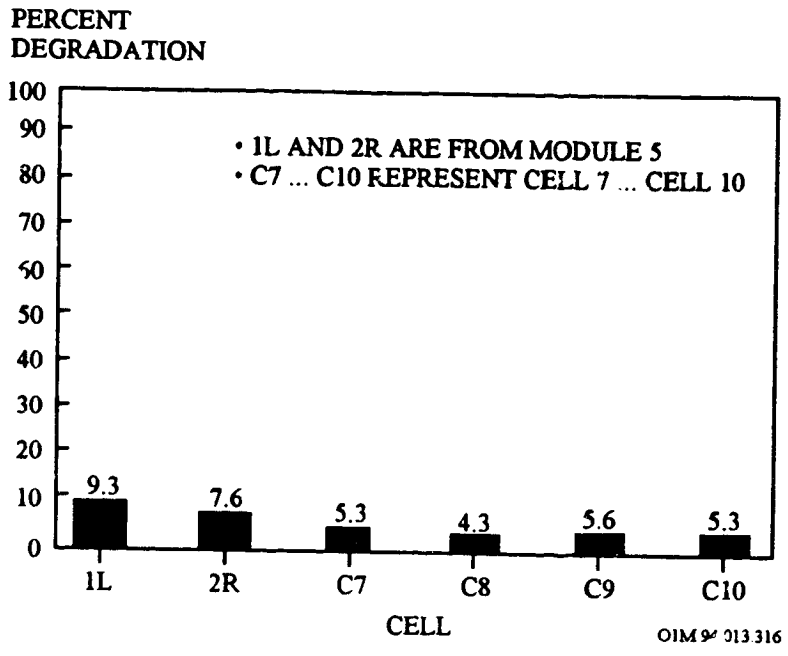

Figure 11-21. MSFC SAMPLE Solar Cell Maximum Power Point Degradation

11.1.4.2.2 Silver-Plated Invar Tabs

Impacts occurred to the silver-plated Invar tabs on the JPL portion of the SAMPLE experiment (ref. 2) where a relatively high fluence of debris/micrometeorite impacts (~0.130 impacts/cm^2) of size $\geq$ 0.05 mm diameter was observed over the mission duration. The results of the impacts were visually surprising, but offer clear indication of the high particle impact velocities and corresponding impact energies. It was observed that the tab had been completely penetrated. The region of Invar immediately surrounding the 0.5 mm diameter penetration hole showed clear indication of melting and resolidifying. In addition, the impact generated gases had peeled the top silver plating away from the Invar and blown those layers out from the impact area. The silver/Invar separation is well-identified by the lack of any atomic oxygen darkened residual silver. Indeed, the inner surface of the peeled back silver plating darkened from atomic oxygen interaction. The remainder of the silver plated Invar tab away from the impact still appears shiny due to a thin layer of silicone adhesive which provided protection during the missions.

11.2 BATTERIES

11.2.1 Introduction

In any spacecraft power system that uses solar radiation, the storage battery is the main source of continuous power, as it is called upon to respond to peak and eclipse demands of power depending upon the spacecraft orbit. The eclipse seasons in a geosynchronous orbit occur twice per year, i.e., in Spring and Autumn. Each season has 45 eclipses. The battery is charged during the sunlit portion of the orbit and discharged during the eclipse. In the case of low-Earth orbit spacecraft, the number of eclipses increases as the altitude decreases. Typically, for a 550 km orbit, there will be about 15 eclipses per day or about 5500 per year. Several times in a year the spacecraft is in continuous sunlight for long periods in the case of high inclination orbits during which the daily average solar array power exceeds the average power demand. Also when the spacecraft comes out of eclipse, the power output of solar array is much higher (as the array is cool and its temperature is very low) than the steady-state power output (when the array attains steady-state temperature). This extra power can be optimally utilized only if the battery is capable of being charged at high rates.

Thus, for spacecraft applications, a storage cell should have high capacity per unit of weight. Chemical effects should not cause deterioration or loss of stored energy. The transformation of electrical into chemical energy as in charging, and of chemical into electrical energy as in discharging, should proceed nearly reversibly. An ideal storage cell should have low impedance, have simplicity and strength of construction, be durable and be producible at low cost.

11.2.2 LDEF Flight Experiments

Three different types of batteries were used on LDEF: $LiSO_2$; lithium carbon monofluoride (LiCF); and NiCd batteries. NASA provided a total of 92 $LiSO_2$ batteries that were used to power all but three of the active experiments. Ten LiCF batteries were used by the two active NASA Marshall Space Flight Center (MSFC) experiments. One NiCd battery, continuously charged by a four-array panel of solar cells, was used to power an active experiment from NASA Goddard Space Flight Center. A detailed review of the investigations into the batteries flown on the LDEF can be found in the the NASA Contractor Report by Harry Dursch.[9]

11.2.2.1 Lithium Sulfur Dioxide ($LiSO_2$) Batteries

The $LiSO_2$ technology is relatively new and has had (prior to LDEF) only a short history of application to space activities. NASA selected the high-energy-density $LiSO_2$ cell as the power supply for the active LDEF experiments. Preflight concerns included the hazards associated with elemental lithium, the electrolyte, the discharge process, and all chemical degradation associated with cell aging and those which may be induced by long-term exposure to the LEO environment. The batteries were in the LEO environment for 69 months, which was a sufficient enough period of time to disclose any design inadequacies. Control batteries remained on Earth in cold storage and undischarged from time of manufacture. The analysis, to date, has shown that all $LiSO_2$ batteries performed satisfactorily for their experiment designed loads (ref. 9).

SAFT America (original manufacturer of the batteries) received ten flight batteries and three control batteries to conduct experimental and destructive physical analysis. The retained capacity testing showed that the capacity loss of the non-flight control batteries over a period of 6 years was around 11% (average of three batteries) versus almost 30% of the initial capacity for an unused flight battery. The difference in capacity loss is tentatively attributed to differences in ambient temperatures. The ground-stored batteries did not see temperatures above 4°C (40°F) and the flight batteries were subjected to temperatures ranging from 4°C to 35°C (41°F to 95°F) over the 69-month mission.[10]

In general, $LiSO_2$ batteries generally exhibited good charge retention, with loss in capacity of less than 3% to 5% per year. LDEF $LiSO_2$ batteries showed charge-retention properties commensurate with that expected, based on the temperatures experienced by these batteries. The favorable performance of LDEF lithium-sulfur-dioxide batteries adds credence

to the selection of lithium-sulfur-dioxide batteries of similar design for the Galileo mission (ref. 9).

11.2.2.2 Lithium Carbon Monofluoride (LiCF) Batteries

Investigation of lithium carbon monofluoride (LiCF) batteries was performed by AZ Technology, NASA MSFC, and Naval Weapons Support Center. Four LiCF batteries were flown on the Thermal Control Surface Experiment (S0069) and six batteries were used on the MSFC heat pipe experiment (S1005). As predicted, all 10 batteries were depleted on return of LDEF. The required experiment life was 12 months, with an expected life of 15 to 18 months. All batteries met or exceeded both of these (ref. 9).

11.2.2.3 Nickel Cadmium Batteries

One nickel cadmium battery, manufactured by General Electric, was flown on the Low Temperature Heat Pipe Experiment Package (Experiment S1001). This battery was continuously charged by a four arrays of solar cells located on the space end of LDEF. Analysis and test of the battery has been conducted by NASA Goddard Space Flight.[11] The battery consisted of 18 cells, which were mounted onto a 0.75-in thick aluminum baseplate. Prior to flight, power analysis for the 12-Ah NiCd battery indicated a need for 2 to 3 amp discharge; however, reduction in the experiment current requirements during flight resulted in a much lower power demand. The resulting overcharge of the battery became a duration test for the NiCd battery. These batteries are not known for their ability to withstand excessive overcharging for long times. The battery survived the entire 6-year usage and was still functioning upon retrieval. A loss of overcharge protection resulted in the development of internal pressures which caused bulging of the NiCd cell cases. However, post-flight testing showed that the battery still had the capability to provide output current in excess of the cell manufacturer's rated capacity of 12.0 ampere-hours (ref. 9).

11.2.3 Lessons Learned

- Lithium-sulfate batteries exhibited excellent long-term charge retention if not drained by their experiment loads. Lithium-carbon monofluoride batteries also met their lifetime objectives, but electrolyte venting might have caused problems if not confined. Electrolyte leakage from E-cells did cause damage to their sockets and adjacent circuit board areas. This phenomenon needs further study to develop improved seals and to prevent damage on missions which may experience delays and extended mission life.

- Rechargeable batteries (e.g., nickel-cadmium) should be provided with protection against overcharging, even if anticipated loads would normally prevent this from occurring. Changes in system loads can occur due to failures or degradation.

REFERENCES

1 P.R.K. Chetty, Satellite Technology and its Applications, McGraw-Hill, Inc. 1991, Chapter 3.

2 P.M. Stella, "LEO Effects on Candidate Solar Cell Cover Materials," LDEF Second-Post Retrieval Symposium, NASA CP 3194, 1993, pp. 1303-1313.

3 L.E. Young, "Impact of LDEF Photovoltaic Experiment Findings Upon Spacecraft Solar Array Design and Development Requirements," LDEF Materials Results for Spacecraft Applications, NASA CP 3257, 1994, pp. 201-215.

4 Meteoroid and Debris Impact Features on the Long Duration Exposure Facility, A Preliminary Report, Meteoroid and Debris Special Investigation Group, Johnson Space Center, August 1990.

5 D.J. Brinker, J.R. Hickey and D.A. Scheiman, "The Effect of the Low Earth Orbit Environment on Space Solar Cells: Results of the Advanced Photovoltaic Experiment (S0014)," LDEF Second-Post Retrieval Symposium, NASA CP 3194, 1993, pp. 1291-1302.

6 D.J. Brinker, J.R. Hickey and D.A. Scheiman, "Advanced Photovoltaic Experiment, S0014: Preliminary Flight Results and Post-Flight Findings," LDEF First Post-Retrieval Symposium, NASA CP-3134, 1991, pp. 1395-1404.

7 D. Ellis, "Micrometeoroid and Debris SIG is Focus for Many Issues," LDEF Spaceflight Environmental Effects Newsletter, Vol. 1, No. 8, January 23, 1991.

8 H.W. Dursch, W.S. Spear, E.A. Miller, G.L. Bohnhoff-Hlavacek, and J. Edelman, NASA Contractor Report 189628, April 1992 p. 145.

9 H.W. Dursch, W.S. Spear, E.A. Miller, G.L. Bohnhoff-Hlavacek, and J. Edelman, "Analysis of Systems Hardware Flown on LDEF - Results of the Systems Special Investigation Group," NASA Contractor Report 189628, April 1992, pp. 116-130.

10 Raman, "Experimentation and Destructive Physical Analysis for the Space Exposed Lithium-Sulfur Dioxide (Li/SO_2) From the Long Duration Exposure Facility (LDEF)," SAFT America, Inc., Attachment 1, 1991.

11 S.L. Tiller and D. Sullivan, "Long Duration Exposure Facility Low-Temperature Het Pipe Experiment Package Power System Results," LDEF First Post-Retrieval Conference, NASA CP-3134, 1992, pp. 1441-1454.

12. OPTICAL COMPONENTS

12.1 INTRODUCTION

There are literally hundreds of optical materials from which a system designer can choose. These are catalogued in references such as the Handbook of Military Infrared Technology and individual glass manufacturer catalogs. A representative set of current, state-of-the art optical materials and designs were tested on LDEF. Detailed results can be found in the Optics Handbook by W. T. Kemp et al.,[1] in the Boeing Mini-Databases,[2] and in the report by M.D. Blue.[3] This experimental data set provides valuable insights into the space response of modern optical materials and designs.

The optics flown on LDEF can be divided according to a number of individual design features: refractive/reflective, substrates/windows, coatings/filters, UV/visible or infrared (IR) transmission, etc. These design features can be categorized into the following three groupings:

- Optical Glasses and Crystals
- Optical Filters and Coatings
- Metal Films/Mirrors

Table 12-1 shows these groupings along with the LDEF material within each group and optical system design parameters (ref. 1).

The LDEF investigations found many common results for optical substrates, filters, and mirrors covering wavelength regions from the ultraviolet to the infrared. In general, most components survived quite well, and space induced degradation was not a major influence on most post-recovery properties. Contamination of the surfaces by a deposited coating of outgassed material was the major influence on optical properties. Off-axis scatter from substrate and filters with a contamination layer was increased by about a factor of ten above the original measurements. Transmission loss from contamination was minor or undetectable in the infrared and visible spectral regions, but catastrophic in the ultraviolet. Soft substrate materials such as halide compounds tended to degrade in space while hard materials such as quartz survived without damage other than the occasional encounter with a micrometeoroid. Multilayer dielectric coatings tended to show effects believed related to aging, compaction, and layer interdiffusion. Changes in optical characteristics, while generally small, were significant in some cases. Performance of most filters and mirrors was degraded.

Table 12- 1. Optical Components Flown on LDEF

Optical Components	LDEF Materials	Design Parameter Responses
Uncoated and Coated Refractive Optics for UV/Visible and IR Systems	Aluminosilicate, borosilicate, lead silicate, potash borosilicate, SiO_2, soda lime silica, soda potash lime, titanium silicate, black glass (low scatter), CaF_2, CdTe, Ge, Si, KRS-5, KRS-6, ZnSe, BaF_2, Al_2O_3, Corning 7940, Suprasil W, Ge (polycrystalline, high purity), and UV-transmissive windows (MgF_2, sapphire [Al_2O_3], CaF_2, LiF, and SiO_2)	• changes in element transmission • scatter increase • reflectivity reduction • image resolution degradation • spectral band shift
Optical Filters and Coatings for UV/Visible and IR Systems	CdSe, Ge, PbTe, PbF_2, SiO, ZnS, Cryolite on SiO_2, SiO on SiO_2, ThF_2 on SiO_2, Antirejection (AR) coating on MgF_2, assorted optical bandpass filters between 0.3 and 1.1 μm (Schott glasses), neutral density filters (Corion), narrow band (Corion), hot mirrors (Corion visible transmitting), Lyman alpha and 1600 Å UV filters, Al_2O_3 on SiO_2, MgF_2 on SiO_2, assorted OCLI filters, and Ge on SiO_2.	• alterations of the wavelength-dependent transmission and reflection properties • contamination of other optical components • loss of mechanical integrity
Mirrors	Ag on SiO_2, Al on SiO_2, Au-plated Al [2024-T351], Au-plated Al [6003], Au on SiO_2, Ir on SiO_2, Nb on SiO_2, Os on SiO_2, Pt on SiO_2, Cu on SiO_2, Ag on C, Ag on SiO_2, Ta on SiO_2, W on SiO_2, Sn on SiO_2, Zn on SiO_2, OSR mirrors [Au, Al, Ag], molybdenum mirror, and diamond turned copper mirror	

12.2 OPTICAL DESIGN CONSIDERATIONS

The effects of the space environment on optical system-related design considerations are summarized in Table 12-2 for the different optical design groupings (ref. 1).

Table 12- 2. Effects of Optical Elements Degradation on System Performance

Optical Elements	Space Environment Effects	Effects on System Performance
Transparent element	darkening, impacts, contamination	• Reduces the throughput of available light for photometric, radiometric, and imaging systems • degrades image resolution • increases scattering which, in turn, increases background noise
Optical coatings	erosion, discoloration, delamination, pitting, contamination	• holes in coating that may alter material wavelength-dependent transmission and reflection properties • Surface contamination on coatings that may decrease throughput of light • Increased scattering which, in turn, increases background noise.
Damaged coatings which encourage other types of damage	contamination, thermal cycling	• Redeposition of contaminants, including damaged coating materials, on other system optics (leading to loss of resolution, reduced throughput, wavelength dependence) • Permanent changes in multilayer-coating thicknesses due to thermal cycling at high temperatures
Diffuse paints or diffuse metal coatings in optical systems	erosion, discoloration	• Baffling efficiency to decrease due to increase in specular reflection or the baffling efficiency to increase due to an increase roughness of baffle surface topography • Redeposition on other materials • Contamination of system optics (leading to loss of resolution, reduced throughput, and/or altered wavelength dependence)
Fiber optics	radiation darkening, impacts, contamination	• Reduced transmission • Complete loss of signal Increased system bit error rate (digital) • Decreased signal-to-noise ratio (analog)

12.3 UNCOATED REFRACTIVE OPTICS FOR UV/VISIBLE AND IR SYSTEMS

A variety of refractive optics materials was flown on LDEF that transmit in both the UV/visible and IR wavelengths. Table 12-3 summarizes the LDEF experiments for the uncoated refractive optics for UV/visible and IR optics (ref. 1). A number of refractive optics for IR systems are equally applicable to UV/visible system (e.g., MgF_2, fused silica)

Table 12- 3. Experiment Summary for UV/Visible and IR Refractive Optics

LDEF Experiment	UV/Visible Optical Materials	IR Optical Materials
AO138-4		ZnSe, ZnSe/ZnS/ThF_4 on ZnSe
AO147	Uncoated fused silica (SiO_2) and fused silica combinations	Uncoated fused silica (SiO_2) and fused silica combinations
AO171	coated fused silica	coated fused silica
AO172	Uncoated fused silica, low iron soda-lime-silica glass, Pyrex 7740 glass, Vycor 7913 glass, BK-7 glass, and Zerodur glass ceramic	Uncoated fused silica, low iron soda-lime-silica glass, Pyrex 7740 glass, Vycor 7913 glass, BK-7 glass, and Zerodur glass ceramic
M0003-2	Uncoated fused silica (T22 Supersil-W1, Amersil) and coated fused silica (MgF_2)	Uncoated fused silica (T22 Supersil-W1, Amersil) and coated fused silica (MgF_2)
M0003-7	Al_2O_3 on SiO_2, Si on SiO_2, NaF_2 on SiO_2	Al_2O_3 on SiO_2, Si on SiO_2, NaF_2 on SiO_2
S0014	Uncoated fused silica	Uncoated fused silica
S0050-1	CaF_2, MgF_2, LiF, Al_2O_3 (synthetic sapphire) and uncoated fused silica	CaF_2, MgF_2, LiF, Al_2O_3 (synthetic sapphire) and uncoated fused silica
S0050-2	Uncoated fused silica, uncoated ULE™, ULE™/Ag coating, and coated fused silica (AR coatings, solar rejection coatings)	Uncoated fused silica, uncoated ULE™, ULE™/Ag coating, and coated fused silica (AR coatings, solar rejection coatings)

12.3.1 Atomic Oxygen Erosion

Fused silica flown on LDEF Experiment S0050-2, Row E5, was found to be resistant to the atomic oxygen environment: 9.60×10^{12} atoms/cm^2. No significant erosion was observed, which is expected for an oxide.

12.3.2 Micrometeoroid Damage

12.3.2.1 Impact

All UV/visible and IR refractive optics samples on the LDEF mission suffered some impact damage due to either micrometeoroids or man-made debris. Table 12-4 summarizes the overall effects of impacts on uncoated refractive optics for both UV/visible and IR systems (ref. 1).

Table 12- 4. Impact Effects for Uncoated Refractive Optics

Material	LDEF Row/ Angle off Ram	Impact Effects
Fused Silica	E5/128° D2/141° D9/8°	• Localized impact damage • Radial cracking does occur but do not propagate a great distance from impact site • Molten glass jetting • Fibers 100 mm long projecting from the fuse zone
SiO_2	D4/158°	• No discernible changes except for debris
Zerodur	D2/141°	• Central pit surrounded by fragmented material with radial cracks • Debris captured in melt zone
Pyrex	D2/141°	• Damage area 5 times central pit radius • Oblique impact produced strongly directional splash • Crater is circular
BK-7	D2/141°	• Temperature and pressure for vaporization exceeded
Soda-Lime-Silica	D2/141°	• Temperature and pressure for vaporization exceeded

In general, impact damage consisted of various nicks and chips, or small quasi-hemispherical craters surrounded by spalls with conchoida surfaces. Spalls extended out by a factor of ~5 times the central crater size. Table 12-5 summarizes the impact site damage size.[4] Radial cracks generally extended two times the spall diameter beyond the spall region. In some cases stringers or fibers of molten material were observed. The major effect of the impact damage is to produce an increase in optical scatter, but apparently, only negligible changes in overall reflectivity or transmission. This is expected because of the overall low value of fractional area affected.

Table 12- 5. Impact Site Damage Size

Sample	Central Melt Pit Diameter (μm)	Crater Diameter (μm)	Spall Surface Diameter (μm)
BK-7	40	100	200
Fused silica	50	120	250
Solda-Lime-Silica	80	175	475
Pyrex	85	200	400
Zerodur (I)	None Measured	100	275
Zerodur (Ii)	75	200	400
Zerodur (III)	50	150	300

The impact damage to the fused silica consisted of various nicks and chips, or small quasi-hemispherical craters surrounded by surface spalls with conshoidal surfaces. The spall produced the equivalent of wide shallow craters around the central craters proper, with the spall extending out by factor of ~5 times the central crater size. In some cases radial cracks extended out beyond the spall region, generally by a factor of about two times the spall diameter, but occasionally by much larger factors. This effect tended to occur only for the larger impact craters. For most cases the impact damage was very localized to the immediate vicinity of the impact sites. In some cases some small residue from the impactor was observed, or "stringers/fibers" of molten fused silica were observed. The number and sizes of the craters were largest on the leading edge, as expected (ref. 4).

Impacts on other optical glasses, including BK-7, Pyrex, ULE, and Zerodur tended to be similar to those in fused silica. This is expected, since the major differences in these glasses (for impact response) are mostly in melting temperatures, compressive yield strengths and/or fracture toughness. Lower melt temperatures, together with the possibility of differential fractionation of the components, associated with BK-7, can be expected to allow bubbles to more readily form, and such were seen surrounding some impact craters. Likewise, lower melt temperatures will promote more "stringer/fiber" production within the craters and a larger "melt zone" around the crater.

In general, fused silica seemed to be more susceptible to impact damage than was SiO_2. However, these samples were placed in different LDEF locations - D9 for fused silica versus D4 for SiO_2, Location D9 is near the leading edge or ram direction; location D4 is near the trailing edge. This seems to imply a directional dependence on the micrometeoroid/debris environment. Other data for uncoated SiO_2 samples flown in other experiments on LDEF near the leading edge were not found. Thus, it is difficult to provide a direct comparison between fused silica and SiO_2 concerning their relative susceptibilities to impact damage.

12.3.2.2 Scatter

Fused silica was found in general not to be resistant to the scatter effects as expected, though no discernible damage was observed except for metallic film fragments on the surface. This high scatter response is consistent with the susceptibility of leading edge samples to impact cratering producing high scatter sites.[5]

12.3.3 Contamination

Satellites in orbit acquire a contamination layer over their surface, and LDEF was no exception. The major cause of contamination on satellites (i.e., LDEF) is from other components, in particular silicon-rich deposits thought to be from outgassing of RTV silicones. The surface of LDEF was covered by a thin brown or yellow-brown stain which was pronounced at openings to the LDEF interior, and much thinner in other regions of the surface. The composition of the layer consisted of silicates and hydrocarbons compounds, among other materials, arising from a variety of sources on the LDEF structure and on the shuttle itself. Specific estimates of the amount of contamination indicate 180 mg/ft^2 at a tray toward the rear of the LDEF satellite and 2 gm/ft^2 for material from an LDEF end-plate scraping.[6] Contamination amounts deposited on components mounted on individual trays varied greatly, ranging from a few monolayers to tenths of microns and higher.

12.3.3.1 Absorption/Transmission/Reflectance

Ultraviolet transmittance of the window materials on LDEF Experiments S0050-2 and S0050-1 was greatly reduced by organic contamination. These window materials consisted of:

- Uncoated fused silica
- Uncoated ULE , ULE /Ag coating
- CaF_2
- MgF_2
- LiF
- Al_2O_3 (synthetic sapphire)

Figure 12-1 (ref. 3) shows the vacuum-ultraviolet transmittance of a MgF_2 window (with front surface contamination only) which was greatly reduced by contamination (other windows were more strongly affected in this spectral region). Because of this organic contamination, there was also a significant decrease in the transmission of LiF, CaF_2, Al_2O_3, and SiO_2. The ratio of the contaminated CaF_2 flight sample to the ground controlled sample showed the transmission monotonically increasing from zero at 200 nm to more than 50 percent at 380 nm. Figure 12-2 shows the ultraviolet transmission for the LiF window, which shows no measurable transmittance in this spectral region (100-200 nm).[7] The higher transmission measure for the MgF_2 window relative to the CaF_2 and LiF windows was probably due to the fact that there was no back film on the MgF_2 window (ref. 7).

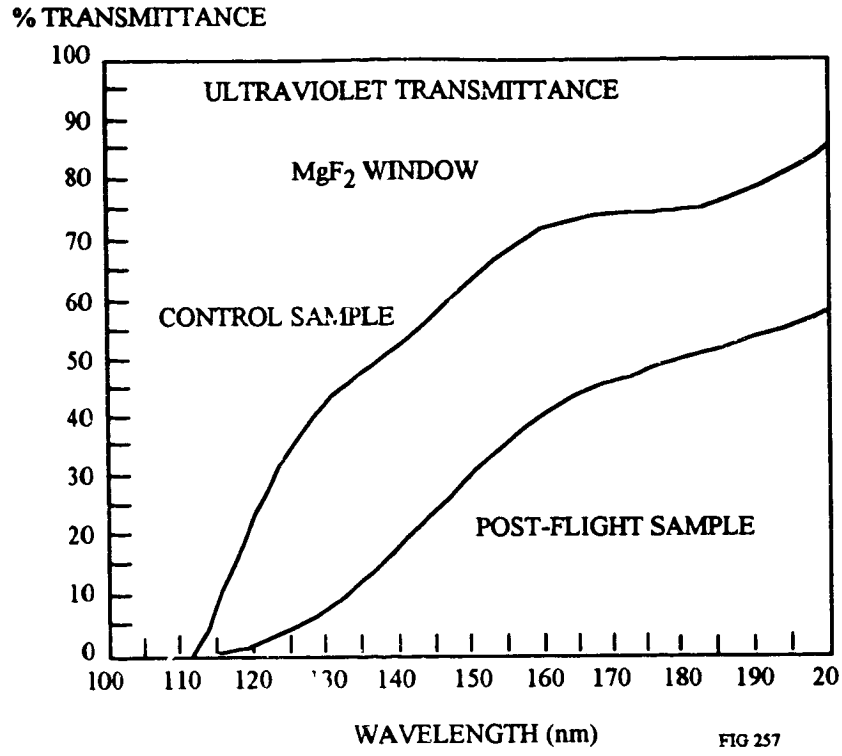

Figure 12-1. VUV Transmittance of a MgF_2 Window as Reduced by Contamination on the Front Surface

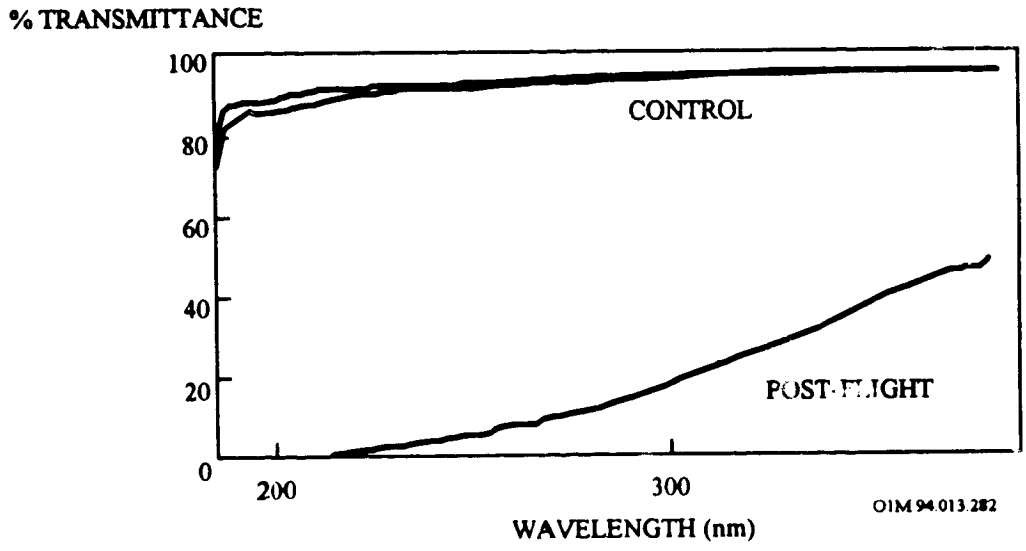

Figure 12-2. Ultraviolet Transmission for LiF Window

There was a significant decrease in transmission of the uncoated ULE glass (up to 45 percent) post-flight over the wavelength range of 350 to 1000 nm. As an example, prior to cleaning, the post-flight transmission of the uncoated ULE sample was reduced from the pre-flight value of 94 percent to 45 percent.[8] Again, this was due to a contaminant film, and the original transmission recovered to nearly the pre-flight values after cleaning. Figure 12-3 shows transmittance for one of the uncoated ULE™ samples where the heaviest deposits were found (ref. 8).

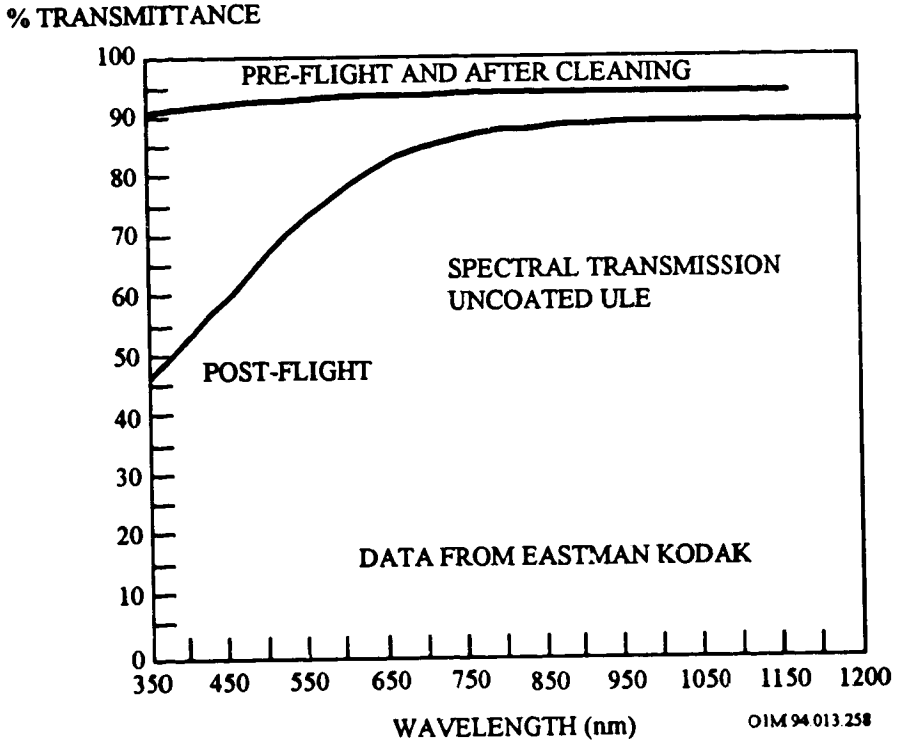

Figure 12-3. UV Transmittance for an Incoated ULE-Glass Sample Showing Transmittance Loss Due to a Contamination Layer

The transmission of uncoated fused silica was observed to decrease by about 30 to 50 percent, mostly in the wavelength range of 200 nm to 700 nm. Figure 12-4 shows the spectral transmission of uncoated fused silica (ref. 7). As an example, prior to cleaning, the post-flight transmission of the uncoated fused silica sample was reduced from the pre-flight value of 94 percent to 68 percent at 350 nm. After cleaning, the transmission generally returned to the pre-flight values within about 1 percent. Hence, the contamination layers on the surface of the components could be removed by cleaning. No data are available on the effects of cleaning on the other samples.

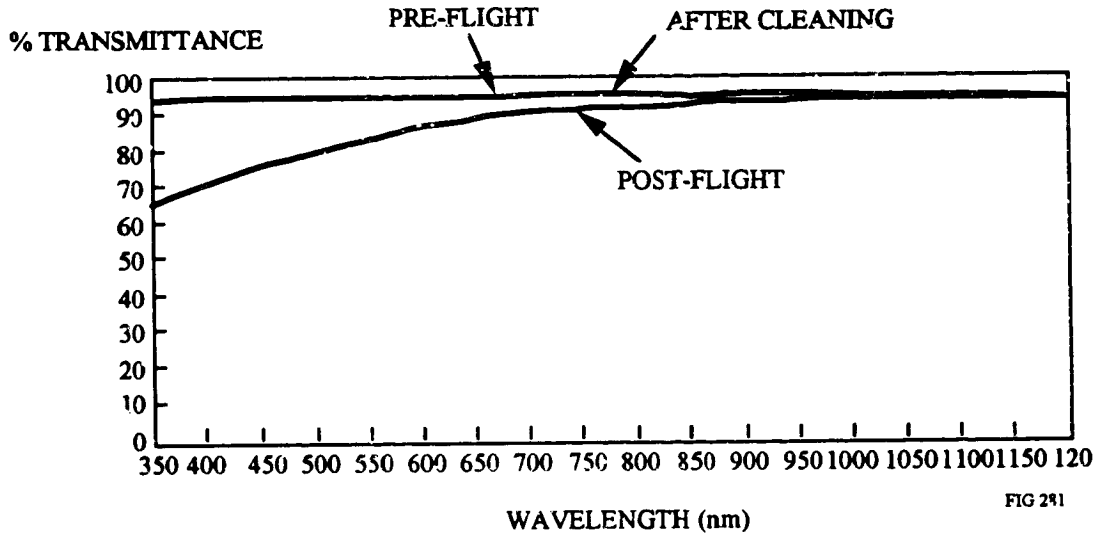

Figure 12-4. Spectral Transmission of Uncoated Fused Silica

Samples flown on experiment AO138-4 (LDEF location B3, leading edge) were tested for spectral performance. Post-flight indicated no significant differences in ZnSe spectral performance.[9]

12.3.3.2 Darkening

Although the ionizing radiation fluence was near $3x10^5$ rads, no radiation darkening was observed in the fused silica, and changes in transmission were associated only with the surface contamination, or (slightly) with impact damage scattering. Also, no darkening was observed for ULE™, even though ULE™ is known to be particularly sensitive to radiation darkening.[10] After cleaning the samples, optical transmittance agreed with prelaunch measurements. Optical transmittance was measured from 350 to 1200 mm. The brown stain reduced transmittance mainly in the short-wave spectral transmittance for one of the uncoated ULE samples where the heaviest deposits were found (see Figure 12-3).

These results are consistent with expectations for the electron, proton, and UV environment in the LDEF orbit where the radiation environments are fairly benign. For higher orbital altitudes, it is anticipated that concerns about radiation darkening should be increased because of the increased severity of the radiation environments.

12.3.3.3 Degradation

A brown discoloration caused by a contaminating film was evident on most of the S0050-1 LDEF samples. The film appeared brittle. No discoloration of bulk optical material was noted. Analysis showed that the brown coating contained carbon as a 30-Å surface layer in addition to a layer of polymer containing Si (in the form of silicones and SiO_2).Table 12-6 summarizes the contamination effects for the uncoated refractive UV/visible and IR optics.

Table 12- 6. Contamination Data Base for Uncoated Refractive UV/Visible and IR Optics

Materials	LDEF Row/ Angle Off Ram	Comments
MgF_2	E5/128°	Organic film appeared brittle. Decrease in transmittance due to contamination
LiF	E5/128°	Organic film present on both surfaces
Al_2O_3	E5/128°	Organic film present or both surfaces
SiO_2	E5/128°	Little contamination. Showed substrate selectivity
CaF_2	E5/128°	Organic film present on both sides.

A Fourier Transform Infrared (FTIR) spectrometer optimized for the 3.4 μm spectral region was used to measure thin organic films on LDEF Experiment S0050-1 samples. Strong

narrow methyl and methylene absorption bands are in this 3.4 μm spectral region. The 3.4 μm contamination measurements on the MgF_2, CaF_2, and LiF windows were typical of many hydrocarbons. This probably is a result of nearby material outgassing. The absence of 3.4 μm absorption on SiO_2 showed substrate selectivity (ref. 8).

12.3.4 Radiation Effects

Table 12-7 lists the radiation resistances of several infrared-transmitting materials, arranged according to their long wavelength cutoffs. The photon resistances are difficult to estimate because most of these materials are transparent to all but short wavelength photons. The wavelength regions shown are those for which the optical transmission through 2 millimeters is at least 10 percent.

The expected natural environmental effects on infrared transmissive materials are listed in Table 12-8. The solar UV could theoretically produce color centers, reducing the infrared transmission of some of these materials. No magnetic field or vacuum effects are expected (with the possible desorption of water under vacuum, since some of these materials are hydroscopic). The Van Allen belts (particularly the low-energy protons) will probably reduce the IR transmissions and solid objects can craze the surfaces or even shatter these materials. No ionospheric effects are expected, but hot plasma can produce electric discharges (since these materials are electrical insulators) degrading their IR transmission. Atomic oxygen may attack (erode) some of these materials and may produce the glow phenomena.

Table 12- 7. Radiation Resistance of Infrared Transparent Materials

Wavelength (μ)	Material	Melt T_M (°K)	$\bar{Z}$	Radiation Resistance (cal/cm^2)	Wave-lengths (μ)	Material	Melt T_M (°K)	$\frac{}{Z}$	Radiation Resistance (cal/cm^2)
0.25-80	CsI	894	54	0.016	7.5-16	InSb	1,001	50	0.020
0.3-55	CsBr	909	45	0.023	0.19-15	NaF	1,253	10	0.63
0.25-45	KI	996	36	0.039	0.25-15	BaF_2	1,553	24.67	0.13
0.42-40	TlBr	733	58	0.011	1.2-15	Si	1,693	14	0.74
0.25-40	KBc	1,003	27	0.069	1.0-15	GaAs	1,553	32	0.076
0.42-35	TiCl	703	49	0.015	1.0-14	INP	1,328	32	0.065
0.21-30	KCl	1,049	18	0.16	0.6-13	AsS_3	573	20.25	0.070
0.4-28	AgCl	728	32	0.036	0.13-12	CaF_2	1,633	12.67	0.51
0.21-26	NaCl	1,074	14	0.27	0.12-9.0	DF	1,143	6	1.59
1.8-23	Ge	1,231	32	0.14	0.25-8.5	MgO	3,073	10	1.54
1.0-20	Se	493	34	0.033	3.5-8.0	Te	725	52	0.020
0.9-16	CdTe	1,314	50	0.026	0.11-7.5	MgF_2	1,669	10	0.83
0.25-16	PbF	1,128	45.5	0.027					

Table 12- 8. Natural Environmental Effects on Infrared Transparent Materials

Material	Sunlight	Van Allen Belts	Objects	Hot Plasma	Gases
CsI	Reduce Transmission	Reduce Transmission	Shatter, Reduce Transmission	May Reduce Transmission	Erosion, Glow Effects
CsBr	Reduce Transmission	Reduce Transmission	Shatter, Reduce Transmission	May Reduce Transmission	Erosion, Glow Effects
KI	Reduce Transmission	Reduce Transmission	Shatter, Reduce Transmission	May Reduce Transmission	Erosion, Glow Effects
KBr	Reduce Transmission	Reduce Transmission	Shatter, Reduce Transmission	May Reduce Transmission	Erosion, Glow Effects
KCl	Reduce Transmission	Reduce Transmission	Shatter, Reduce Transmission	May Reduce Transmission	Erosion, Glow Effects
NaCl	Reduce Transmission	Reduce Transmission	Shatter, Reduce Transmission	May Reduce Transmission	Erosion, Glow Effects
Ge	Reduce Transmission	Reduce Transmission	Shatter, Reduce Transmission	May Reduce Transmission	Erosion, Glow Effects
NaF	Reduce Transmission	Reduce Transmission	Shatter, Reduce Transmission	May Reduce Transmission	Erosion, Glow Effects
Si	Reduce Transmission	Reduce Transmission	Shatter, Reduce Transmission	May Reduce Transmission	Erosion, Glow Effects
CaF_2	Reduce Transmission	Reduce Transmission	Shatter, Reduce Transmission	May Reduce Transmission	Erosion, Glow Effects
MgF_2	Reduce Transmission	Reduce Transmission	Shatter, Reduce Transmission	May Reduce Transmission	Erosion, Glow Effects
Primary Concern: Van Allen Belts in MEO; Debris Objects in LEO; AO in LEO; UV at all Altitudes					

12.4 COATED REFRACTIVE OPTICS FOR UV/VISIBLE AND IR SYSTEMS

A variety of coated refractive optics materials were flown on LDEF that transmit in both the UV/visible and IR wavelengths. Table 12-9 summarizes the LDEF experiments for the coated refractive optics for UV/visible and IR optics. A number of refractive optics for IR systems are equally applicable to UV/visible system (e.g., MgF_2 coated fused silica)

Table 12- 9. Experiment Summary for UV/Visible and IR Refractive Optics

LDEF Experiment	UV/Visible Optical Materials	IR Optical Materials
AO138-4		ZnSe, ZnSe/ZnS/ThF_4 on ZnSe
AO171	Coated fused silica	Coated fused silica
M0003-2	Coated fused silica (MgF_2)	Coated fused silica (MgF_2)
M0003-7	Al_2O_3 on SiO_2 Si on SiO_2 NaF_2 on SiO_2	Al_2O_3 on SiO_2 Si on SiO_2 NaF_2 on SiO_2
S0050-2	ULE™/Ag coating coated fused silica (AR coatings, solar rejection coatings)	ULE™/Ag coating coated fused silica (AR coatings, solar rejection coatings)

12.4.1 Atomic Oxygen Erosion

No data is available. However, solar UV and AO removed the damage layer around the impact layer on the NaF_2 on SiO_2 sample flown on experiment M0003-7 (see Section 12.4.2).

12.4.2 Micrometeoroid and Debris Impact Effects

Table 12-10 summarizes the impact effects on coated UV/Visible Refractive and IR Optics that were flown on the LDEF satellite. The data for these coated optics are also applicable to the data base for the coatings for the UV/visible and IR optics (see Section 12.5). In general, all samples showed some impact effects. Those samples flown on experiment M0003-2 and on the leading edge (at locations D8 and D9) showed several microfractures; the trailing edge samples experienced crazing as the primary effect. The NaF_2 on SiO_2 sample flown on experiment M0003-7 showed delamination, and the damage layer around the impact was subsequent removed by solar UV and AO.

Table 12- 10. Impact Effects for Coated Refractive UV/Visible and IR Optics

Materials\Substrate	LDEF Location Row/Angle off Ram	Comments
MgF_2 on Fused Silica	D9/8°	Damage is localized
NaF_2 on Fused Silica (SiO_2)	D9/8°	Damage layer removed from around impact layer due to UV or AO
ThF_4/Ag/Cr on Mo	D9/8°	Overall damage area is several times crater size. Coating failure is observed
Ag+($Al2O_3$/Si)[3]/ on Polished Silicon	D8/38°	Microfractured, corroded, cratered
Al_2O_3 on SiO_2	D3/171°	Microfractured, flaked
As_2Se_3 on SiO_2	D3/171°	Crazed, discolored
Au/Ni on Al	D4/158°	Unchanged

12.4.3 Contamination

12.4.3.1 Absorption/Transmission/Reflectance

Table 12-11 summarizes the absorption/transmission/reflectance effects for coated refractive UV/visible and IR optics. All of the substrates and coatings experienced a significant performance reduction over the wavelength range of 350 - 1200 nm after flight.

Table 12- 11. Absorption/Transmittance/Reflectance Data Base for Coated Refractive UV/Visible and IR Optics

Materials/ Coatings	LDEF Location Row/Angle off Ram	Comments
Fused Silica/ Ag	E5/113°	Contamination reduced transmission. An increase in scatter was measured.
ULE™/Ag	E5/113°	Contamination reduced transmission. Cleaning returned sample to pre-flight value.
Fused Silica/ Solar rejection	E5/113°	Contamination reduced transmission. Cleaning returned sample to pre-flight value.
Fused silica/ Anti-reflection	E5/113°	Contamination reduced transmission. Normal cleaning methods not effective. Needed exposure to oxygen plasma to improve performance.

Figures 12-5 and 12-6 show the spectral reflection of the coated ULE™ and fused silica samples, respectively (ref. 8). After cleaning with normal solvent drag means (except for the AR-coated samples which could not be cleaned; see Figure 12-7), the samples' optical performance returned to the pre-flight measured values.

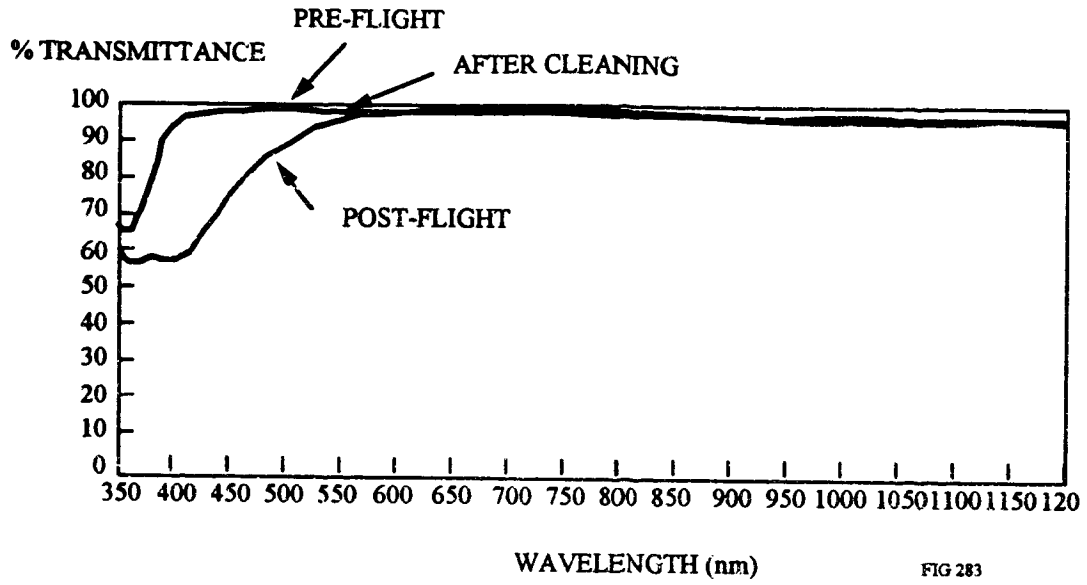

Figure 12-5. Spectral Reflection of Silver Coated ULE™

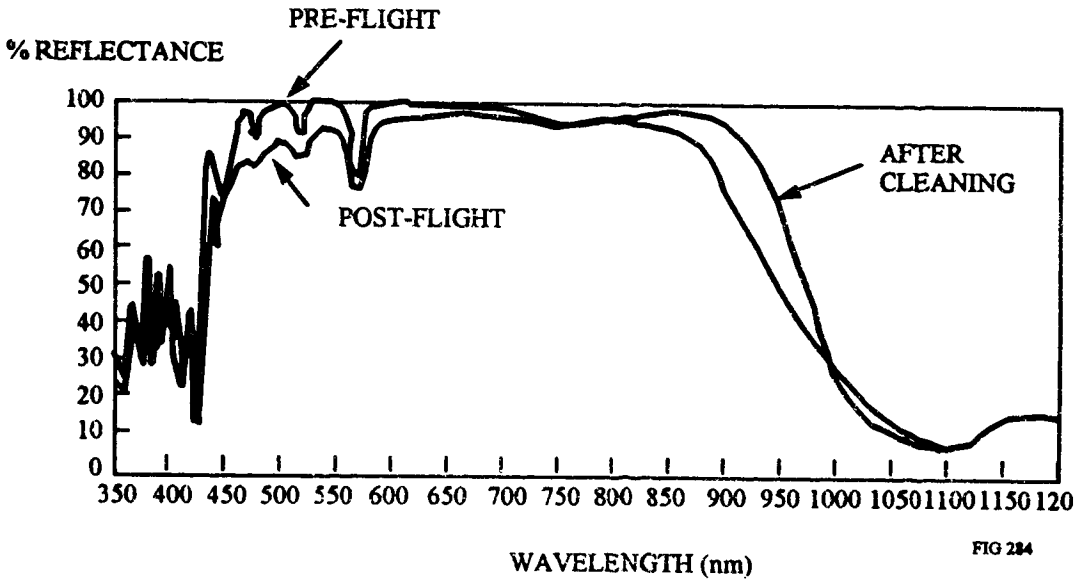

Figure 12-6. Spectral Reflection of Solar Rejection Coated Fused Silica

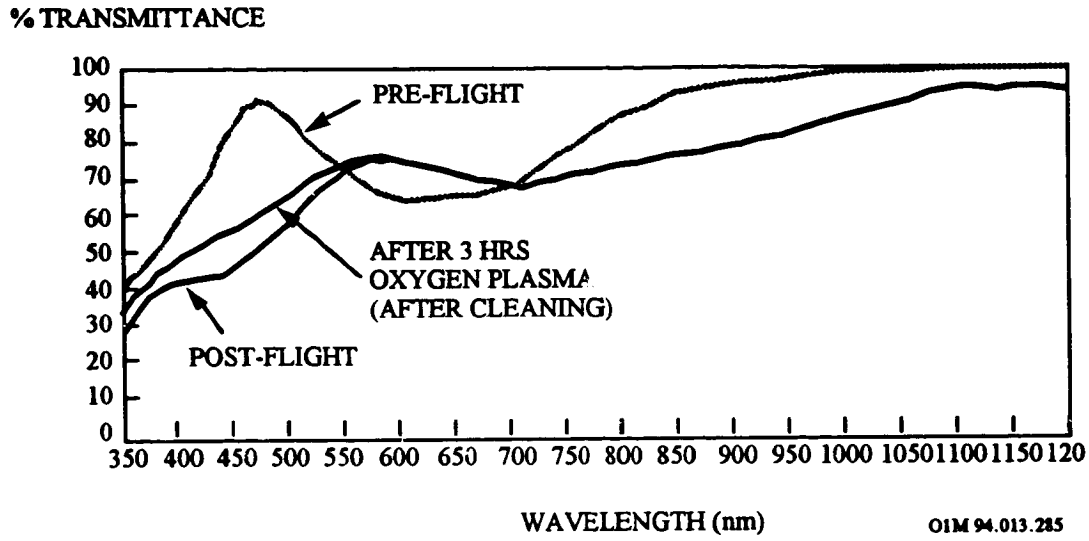

Figure 12-7. Spectral Transmission of Fused Silica Anti-Reflection Coated at 1.06 λ

12.5 COATINGS FOR UV/VISIBLE AND IR SYSTEMS

A number of coatings covered under IR systems are equally applicable to UV/visible systems. Table 12-12 shows a summary of the LDEF experiments containing coatings for UV/visible and IR systems (ref. 1).

Table 12- 12. UV/Visible Optics and IR Optics Coatings Flown on LDEF

LDEF Experiment	UV/Visible Optical Coatings	IR Coatings
A0034	SiO on Pyrex Os/Al on Quartz Ag/Al on Quartz Au/Al on Quartz MgF_2/Al on Quartz	
AO138-4	MgF_2/Al on B1664 glass MgF_2/Al on Kanigened Al MgO/MgF_2 on B1664 glass LaF_3/Chiolite/MgF_2 on B1664 glass ThF_4/Ag on B1664 glass ThF_4/Ag on Kanigened Al LiF/Al on B1664 glass LiF/Al on Kanigened Al Al_2O_3/MgF_2 on Kanigened Al 250 nm dielectric on B1664 glass 1060 nm dielectric/TiO_2/SiO_2 on B1664 glass 10.6 μm mirror/Ge-ZnS-ThF_4 on B1664 glass Al_2O_3/MgF_2/MERK 11611 on B1664 glass	LaF_3/Chiolite/MgF_2 Ge/ZnS/ThF_4 on B1664 glass ThF_4/Ag on B1664 glass Al_2O_3/Ag on Kanigened Al ZnS on Ge
AO138-5	Al on glass Pt on glass	
M0003-2		MgF_2/Fused silica ThF_4/Ag/Cr on Mo MgF_2 ($\lambda = 1.06$ μm)-2-thick on fused silica
M0003-6		Au on Ni/Al
M0003-7		Ag + $(Al_2O_3/Si)^3$ on polished Si Al_2O_3 on SiO_2 As_2Se_3 on SiO_2 ZnS on SiO_2 Al + $(Al_2O_3/ZnS)^4$ on polished Mo Si on SiO_2 PbF_2 on SiO_2 NaF_2 on SiO_2
S0050-2		Ag on ULE™

12.5.1 Atomic Oxygen Erosion

No data available for this effect.

12.5.2 Micrometeoroid and Debris Impact Effects

In general, all samples showed some impact effects. Table 12-13 summarizes the impact effects for IR coatings that are also applicable to UV/Visible coatings (ref. 1).

Table 12- 13. Impact Effects Data Base for Coatings Applicable to IR and UV/Visible Optics

Materials/Substrate	LDEF Row/ Angle off Ram	Comments
MgF_2 on Fused Silica	D9/8°	Damage is localized
ThF_4/Ag/Cr on Mo	D9/8°	Overall damage area is several times crater size. Coating failure is observed.
Ag+$(Al_2O_3/Si)^3$ on Polished Silicon	D8/38°	Microfractured, corroded, cratered
Al_2O_3 on SiO_2	D3/171°	Microfractured, flaked
Ag_2Se_3 on SiO_2	D3/171°	Crazed, discolored
Au/Ni/Al	D4/158°	unchanged
MgF_2(λ=1.06μm)/2 thick on fused silica	D4/158°	Crazed, contaminated
NaF_2 on SiO_2	D9/8°	Damaged layer removed around impact due to UV or AO

Those samples flown on LDEF Experiment M0003-2 and on the leading edge (at locations D8 and D9) showed several microfractures. The trailing edge samples were crazed, but so were the control samples leading the experimenters to the conclusion that crazing is related to coating manufacturing stresses, and not necessarily related to the space environment.

The impact damage to the MgF_2 coating applied to fused silica tended to be less localized than for bare fused silica, with more extensive crazing and a larger tendency to involve long cracks originating at the impact site. Further, local delamination of the coating occurred around the edge of the craters. The clearly-identified craters were much deeper than the coatings, and thus were mostly in the fused silica, and produced the same conshoidal surfaces as for bare silica. Synergistic effects were also observed (e.g., for NaF_2 coatings), such that coating material was sometimes removed around the impact site owing to the further

interactions with either UV and/or AO. The extensive crazing was apparently not only caused by the impacts, however, since even ground controls of MgF_2 displayed similar effects, suggesting that the problem was associated with high in-situ stresses generated at manufacture. Further, there were no indications that the crazing itself significantly interacted with the cratering phenomena, or vice versa. M0003-2 coatings on Mo also showed damage areas many times the crater size leading to coating failure.[11]

From experiment M0003-7, observations show, for $Ag+(Al_2O_3/Si)^3$ on polished Si, three small impact craters, surrounded by localized cracking on the exposed coating surface. The coating was cracked in spirals at the perimeter of the exposure area. The coating appeared to be blistered in the vicinity of the spiral cracks; flaking in the cracked region revealed a corroded and discolored residual surface.[12]

For the Al_2O_3 coating on SiO_2, fine fractures which intersect and terminate in defects in the coating were discernible in the exposed surface areas. There were some small areas where the coating had flaked away revealing the smooth surface of the substrate. A small number of individual blisters or bubbles were discernible in the coating. These features varied in size, were randomly distributed, and were present globally on the surface (ref. 12).

These observations are to be contrasted with the As_2Se_3 coating on SiO_2 sample. After space exposure, the coating appeared nonuniform in color to the eye. At high magnification, it was apparent that the exposed surface was crazed and that the observed variation in color is due to the presence of contiguous green patches in the otherwise pink coating. There were no discernible morphological features associated with the green patches and they did not correspond to the crazed fragments in the coating (ref. 12).

For the M00003-6 experiment, a sample of electroplated Au on Ni/Al, when examined, showed a small quantity of debris on the surface, but no other changes were discernible (ref. 12).

A micrometeoroid impact site was found on one of the samples. The impact crater measured 0.3 mm in diameter by 0.03 mm deep. Multiple fractures occurred in the glass at the impact site (ref. 8).

12.5.3 Contamination

12.5.3.1 Absorption/Transmission/Reflectance

Table 12-14 summarizes the absorption/transmission/reflectance effects for UV/visible and IR coatings (ref. 1).

Table 12- 14. Absorption/Transmission/Reflectance Effects on Coatings for Both UV/Visible and IR Optics

Material	Space Environment	Absorption/Transmission/Reflectance Effects
Al-MgF_2/ B1664 Glass	$1.32x10^{17}$ atoms/cm^2 11,100 esh[1]	Outside/inside samples had significantly-reduced reflectance over all wavelengths
ThF_4-Ag/ B1664 Glass	$1.32x10^{17}$ atoms/cm^2 11,100 esh[1]	Outside/inside samples showed little change in reflectance over all wavelengths
Al_2O_3-Ag/ Kanigen	$1.32x10^{17}$ atoms/cm^2 11,100 esh[1]	Outside/inside samples had significantly-reduced reflectance except at the blue end
Al-MgF_2/ Kanigen	$1.32x10^{17}$ atoms/cm^2 11,100 esh[1]	Inside sample had significant reduction in reflectance at upper end Outside sample had significant reduction across the entire band
MgO-MgF_2/ B1664 Glass	$1.32x10^{17}$ atoms/cm^2 11,100 esh[1]	Inside sample showed slight shift in reflectance Outside sample had little reduction at the blue end but a slight shift to the high end.
Visible 1060 nm mirror/TiO_2-SiO_2 on B1664 Glass	$1.32x10^{17}$ atoms/cm^2 11,100 esh[1]	Remained optically efficient
Al_2O_3/MgF_2/MERK 11611 on B1664 Glass	$1.32x10^{17}$ atoms/cm^2 11,100 esh[1]	slight reduction in transmittance at blue end of spectrum and slight increase in transmittance at high end
Ge-ZnS-ThF_4 on B1664 Glass[2]	$1.32x10^{17}$ atoms/cm^2 11,100 esh[1]	No significant change.

1. Row B3
2. Applies to IR Coating Only

In LDEF experiment AO138-4, the Al/MgF_2 coating on A B1664 glass substrate showed a relative reflectance loss of 16 percent, and a 23 percent reduction on a Kanigened Al substrate. Figures 12-8 and 12-9 (ref. 9) show the reflectance measurements for Al-MgF_2/B1654 glass and Kanigened substrates, respectively. Whether the samples were cleaned prior to post-flight examination is not reported by the experimenter. There was very little degradation in the ThF_4/Ag (Figure 12-10), and in the Al_2O_3/Ag (Figure 12-11) coatings, whether they were on B1664 glass or Kanigened Al substrates (ref. 9).

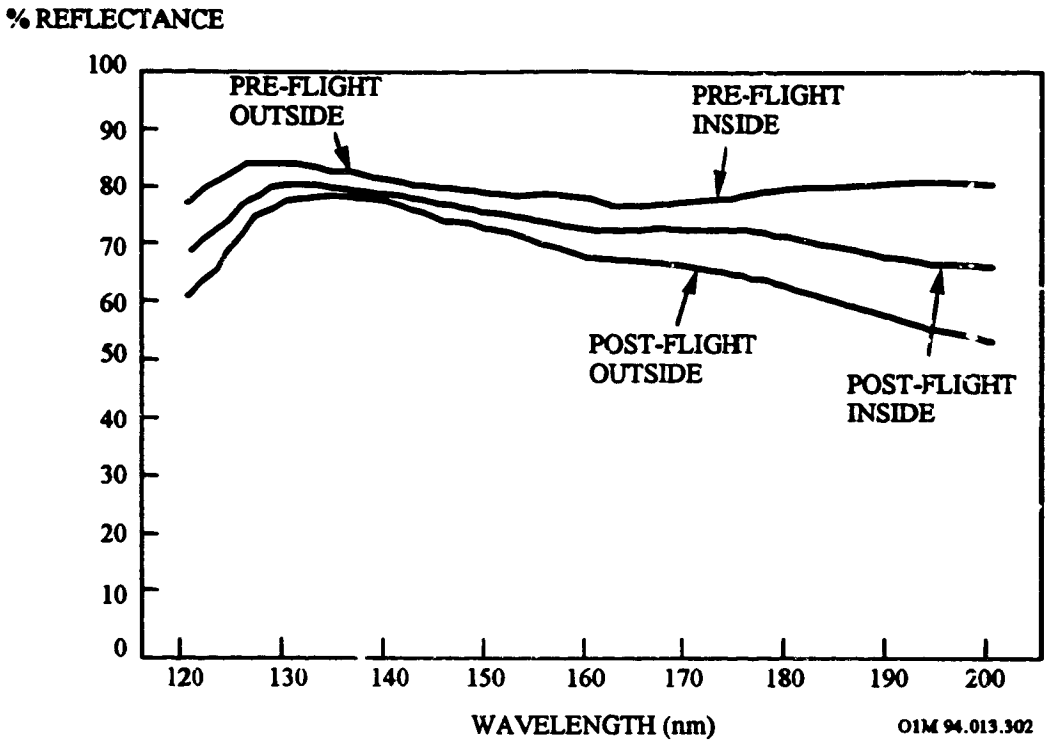

Figure 12-8. Reflectance Measurements for Al-MgF_2/B1664 Glass Mirror

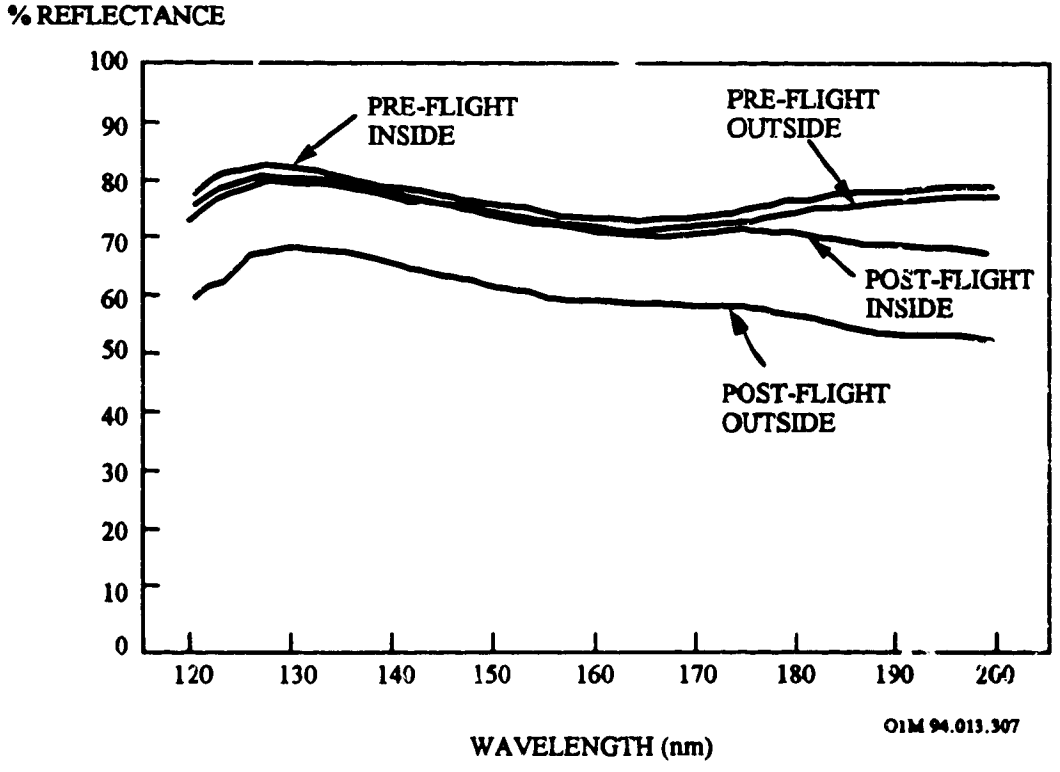

Figure 12-9. Reflectance Measurements for Al-MgF_2/Kanigen Mirror

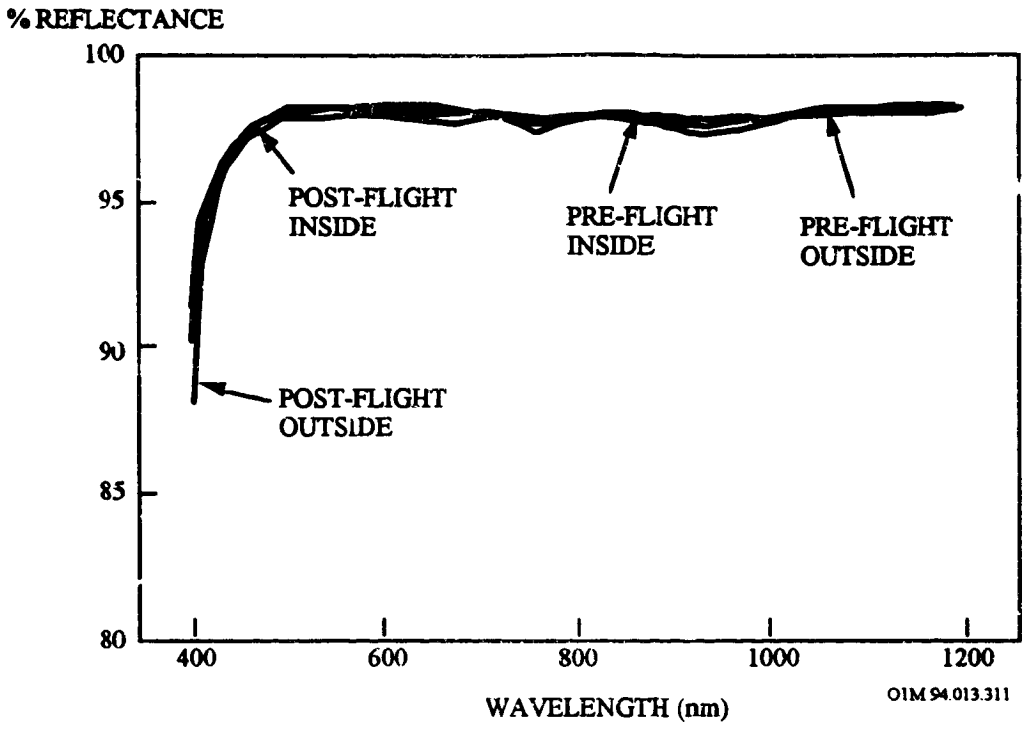

Figure 12-10. Reflectance Measurements for ThF_4-Ag/B1664 Glass Mirror

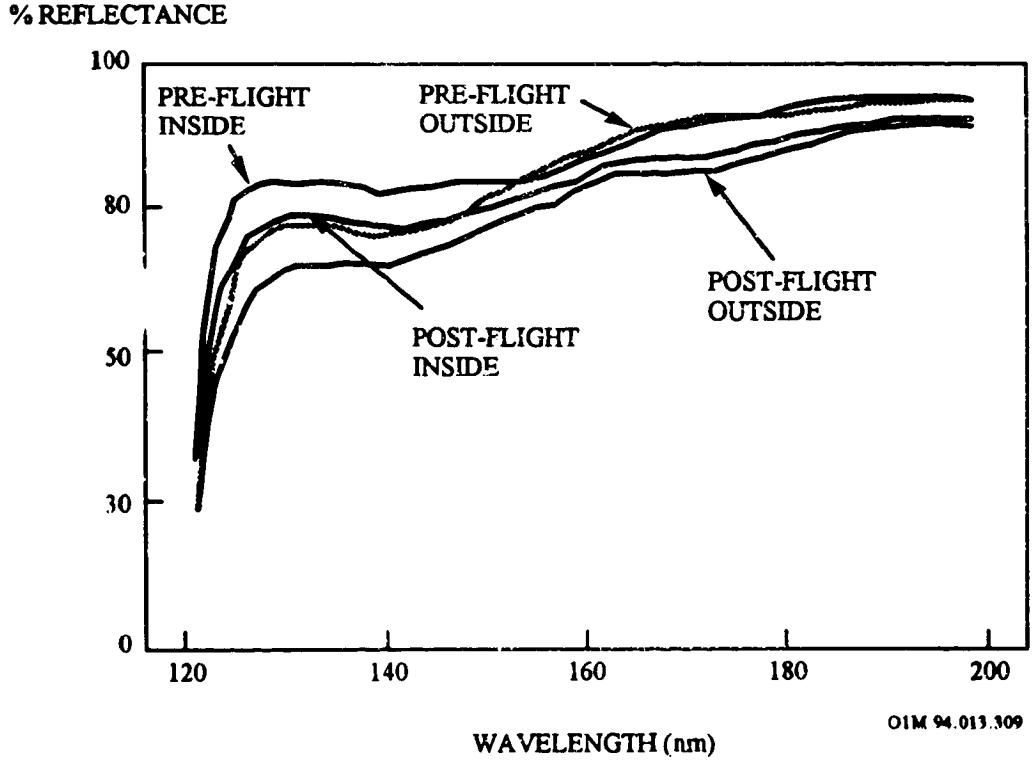

Figure 12-11. Reflectance Measurements for Al_2O_3-Ag/Kanigen Mirror

In LDEF experiment AO138-4, the MgO/MgF_2 coating on B1664 glass showed a significant reduction from 20 to 38 percent in spectral width for each trailing edge flight sample (see Figure 12-12; ref. 9). This is to be compared with the TiO_2/SiO_2 coating on B1664 glass which remained optically-efficient even though the flight sample showed some thin cracking. The Al_2O_3/MgF_2 AR coating showed a very slight (< 1 percent) reduction in average transmittance over a spectral range of 400-100 nm (see Figure 12-13) (ref. 9).

For the case of an antireflection (AR) coating (SiO_2/TiO_2)(λ = 1.06 μm wavelength) the transmission decreased by up to 40 percent at 475 nm and 20 percent at 900 nm, but actually increased by 10 percent at 600 nm. These effects were due to a contamination layer. The contamination was not removable by normal solvent drag means. An attempt to remove the contamination using an oxygen plasma for 3 hours only partially restored the transmission, and the improvement was only about 10 percent and was limited to the wavelength range of 350 to 550 nm (ref. 8).

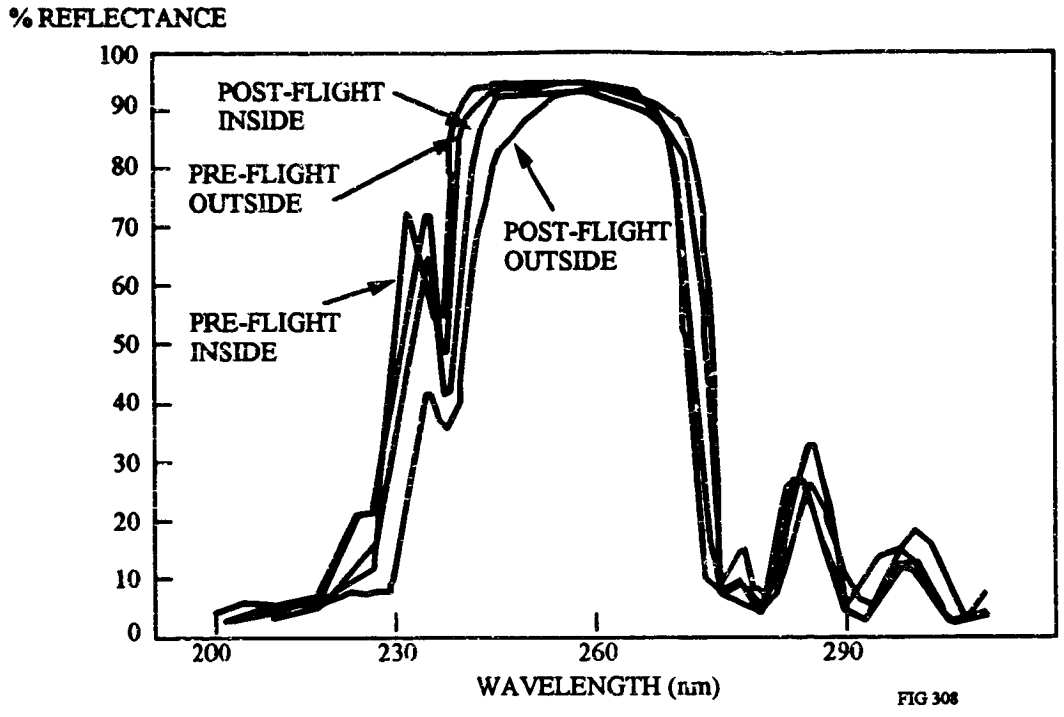

Figure 12-12. Reflectance Measurements for 250 nm Diclectric/Glass Mirror

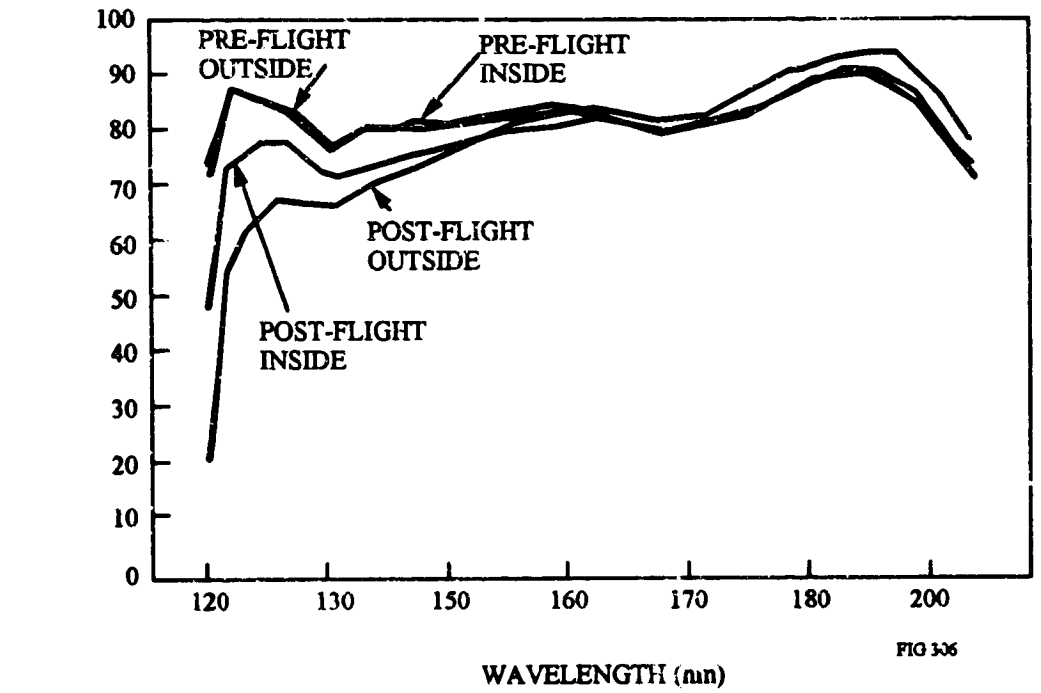

Figure 12-13. Transmission Measurements for AR on B1664 Glass Mirror

12.5.3.2 Degradation

Table 12-15 summarizes the deterioration effects of contamination for UV/visible coatings (ref. 1).

Table 12- 15. Contamination/Deterioration Effects Data Base for UV/Visible Coatings

Materials/Substrate	LDEF Row/ Angle off Ram	Comments
Ge/ZnS/ThF_4 on B1664 Glass	B3/171°	Peeling of coating due to vacuum or thermal cycling
SiO/Al on Pyrex	C3/171° C9/8°	Degradation in UV spectral reflectance due to contamination
Os/Al on Quartz	C3/171° C9/8°	Complete oxidation and evaporative removal of Os film on leading edge
Ag/Al on Quartz	C3/171° C9/8°	Complete oxidation of the silver film in both leading edge and trailing edge samples
Au/Al on Quartz	C3/171° C9/8°	Slight visual difference in leading edge samples. No obvious effect on trailing edge samples
MgF_2/Al on Quartz	C3/171° C9/8°	No visible effect in leading edge or trailing edge samples

The Ge/ZnS/ThF_4 coating on B1664 glass was flown on LDEF experiment AO138-4 and tested at 10.6 μm wavelength. No significant changes in reflectance were measured due to any contamination observed. It is not known whether the sample was cleaned prior to making the reflectance measurements (ref. 9).

The contaminant collector mirrors (SiO/Al/Pyrex, Os/Al/Quartz, Ag/Al/Quartz, Au/Al/Quartz, and MgF_2/Al/Quartz) were flown on experiment AO034. All samples were examined visually and reflectance measurements were made to determine the effect of the observed contaminants. For the SiO sample, contaminant coloration was observed on both leading and trailing edge samples resulting in degraded spectral reflectance. For the Os and Ag samples, oxidation and subsequent surface removal was observed to contaminated the surfaces. The leading and trailing edge samples of the Au and MgF_2 were found to have little or no effect.[13]

Table 12-16 summarizes the deterioration effects of contamination for IR coatings (ref. 1). A number of IR coatings from experiments M0003-2 and -7 were seen to become contaminated and to deteriorate in the space environments.

Table 12- 16. Contamination/Deterioration Effects Data Base for IR Coatings

Materials/Substrate	LDEF Row/ Angle off Ram	Comments
$Ag+(Al_2O_3/ZnS)^4$ on polished Mo	D8/38°	Corroded and hazed
Si/SiO_2	D3/171°	Particle contamination
PbF_2/SiO_2	D3/171°	Dark red contamination
MgF_2(l=1.06μm)/2 thick on Fused Silica	D4/158°	Fibrous matter and film fragments
ZnS/SiO_2	D9/8°	Showed surface cracking and flaking
Al_2O_3/SiO_2	D3/171°	Randomly distributed blisters and flaking
Ag_2Se_3/SiO_2	D3/171°	Slight crack at edge. Contaminated
MgF_2/SiO_2	D4/158°	Entire coating is crazed and blistered around debris spot

The $Ag+(Al_2O_3/ZnS)^4$ coating on Mo appeared hazy and discolored on the exposed surface. Multiple zones of discoloration were apparent. The variation in discoloration was presumed to be the result of varying degrees of dendritic growth. A high density of spots was apparent over the entire coating. Grain boundaries in the substrate were also apparent through the coating (ref. 12).

For the Si/SiO_2 sample, a great deal of debris was on the coating surface, but the surface remained highly specular. The PbF_2/SiO_2 sample had a large number of subsurface polishing scratches. Features, which may be bubbles, pinholes, or growth nodules in the coatings were seen to have formed preferentially along these scratches (ref. 12).

The MgF_2 coating on SiO_2 was seen to be crazed on both the flight and control samples. A great deal of extraneous debris, including fibrous matter and metallic film fragments, was present on the surface. There were three large spots of debris on the spaceward side of the sample where the coating was crazed more extensively. There were also blisters around these debris spots (ref. 12).

The ZnS coating on the SiO_2 substrate was buckled in a regular pattern on two large areas of the surface. The entire coating was blistered. Large blisters, exhibiting many orders of interference rings, were discernible on the surface of the sample at low magnification. In addition, a high density of very small blisters was apparent throughout the coating at magnifications of 200X and greater. The surface was, however, relatively clean of debris (ref. 12).

For the Al_2O_3 coating on SiO_2, fine fractures which intersect and terminate in defects in the coating were discernible in the exposed surface areas. There were some small areas where the coating had flaked away revealing the smooth surface of the substrate. A small number of individual blisters or bubbles were discernible in the coating. These features varied in size, were randomly distributed, and were present globally on the surface (ref. 12).

These observations are to be contrasted with the As_2Se_3 coating on a SiO_2 sample. After space exposure, the coating appeared non-uniform in color to the eye. At high magnification, it was apparent that the exposed surface was crazed and that the observed variation in color is due to the presence of contiguous green patches in the otherwise pink coating. There were no discernible morphological features associated with the green patches and they did not correspond to the crazed fragments in the coating (ref. 12).

12.6 OPTICAL FILTERS FOR UV/VISIBLE SYSTEMS

There were many different filter systems flown on LDEF, including metal-dielectric blockers, metal-dielectric bandpassers, all-dielectric hot mirrors/detector trimmers, and all-dielectric bandpassers. Table 12-17 shows a summary of the experiments containing the UV/visible optical filter systems (ref. 1).

Table 12- 17. Experiment Summary for UV/Visible Optical Filters

Experiment	UV/Visible Optical Filters
AO138-4	Al-MgF_2 on MgF2 Substrate (1216 Å) Al-MgF_2 on MgF_2 Substrate (1270Å) Al-MgF_2 on Quartz Substrate (2430 Å)
A0147	ZnS/Cryolite[i]/Silver on Fused Silica (cemented with Epon 328) ZnS/Cryolite/Silver on Fused Silica (air-spaced, no cement) ThF_4/Cryolite/Al/ZrO_2 on Fused Silica (air-spaced, no cement) ZrO2/Cryolite/Silver on Fused Silica (air-spaced, no cement) ZnS/ThF_4 on Fused Silica (Air-spaced, no cement) ThF_4/Cryolite/Al on Fused Silica (air-spaced, no cement) PbF_2/Cryolite on Fused Silica (air-spaced, no cement) ZnS/Cryolite/silver on Fused Silica (cemented with APCO R313)
S0050-1	Narrow-Band Corion Neutral Density Band Corion Broad-Band Corion

[i] Cryolite is a sodium-aluminum fluoride compound. See "The Infrared Handbook," William L. Wolfe and George J. Zissis, Eds., Environmental Institute of Michigan (1978).

12.6.1 Covered UV/Visible Optical Filters

12.6.1.1 Atomic Oxygen Erosion

No data available.

12.6.1.2 Micrometeoroid and Debris

No data available.

12.6.1.3 Absorption/Transmission/Reflectance

The most common responses for filters was slight to significant reduction in transmittance accompanied by shifts in center wavelength toward the blue. Table 12-18 summarizes the space environment effects for UV/visible optical filters (Ref. 1).

Table 12- 18. Transmittance Data for UV/Visible Optical Filters Exposed Indirectly to Space Environment

Materials	Space Environment	Space Environment Effects
Narrow-Band Corion[(1)]	9.6×10^{12} atoms/cm^2 8,200 esh[1]	Reduced transmission
Neutral Density Band Corion[(1)]	9.6×10^{12} atoms/cm^2 8,200 esh[1]	No change in transmittance
Broad-Band Corion[(1)]	9.6×10^{12} atoms/cm^2 8,200 esh[1]	No change in transmittance
Al-MgF_2 on MgF_2 Substrate (1216 Å)	1.32×10^{17} atoms/cm^2 11,100 esh[2]	Reduced transmittance and shift in center wavelength
Al-MgF_2 on MgF_2 Substrate (1270 Å)	1.32×10^{17} atoms/cm^2 11,100 esh[2]	Reduced transmittance and shift in center wavelength
Al-MgF_2 on Quartz Substrate (2430 Å)	1.32×10^{17} atoms/cm^2 11,100 esh[2]	Reduced transmittance and shit in center wavelength

(1) These filters were provided by Corion Corporation, Holliston, MA. Specific material stack-ups for the filter were not explicitly identified. The narrow-band filters were composed of quarter-wave thick stacks of dielectric materials. The neutral density filters did not use quarter-wave dielectric stacks but were composed of a single layer of Inconel coating which provides approximately uniform attenuation across the visible spectrum. The hot-mirror interference filters were deposited on glass with a ThF_4 layer at the surface. One of the wide-band hot-mirror filters was examined by SEM and was found to be composed of eleven layers of (ThF_4/ZnS) pairs deposited on a glass substrate.

1. Row E5
2. Row B3

The Corion narrow- and broad-band optical filters showed a significant reduction in transmission, as shown in Figure 12-14 and Figure 12-15, respectively. This reduction is believed to be related to the cement degradation used in the filter construction.[14]

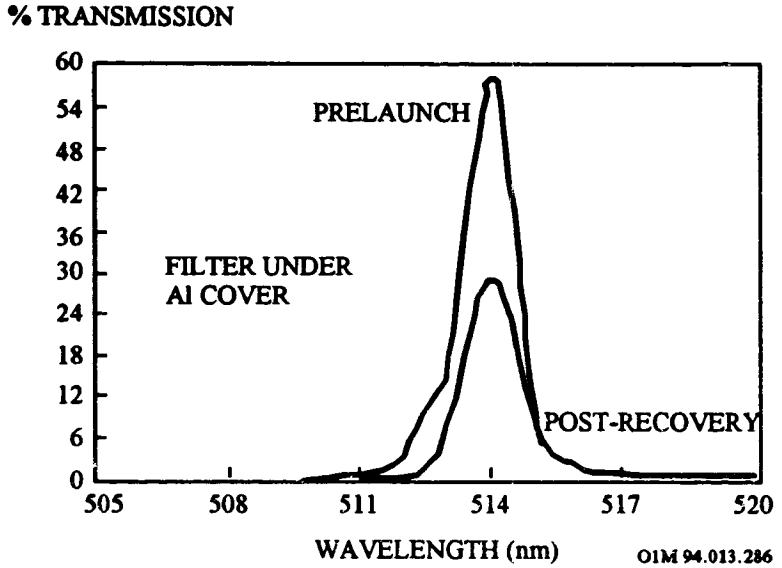

Figure 12-14. Pre-Launch and Post-Recovery Transmission of Corion Narrow-Band Filter #2 (Covered)

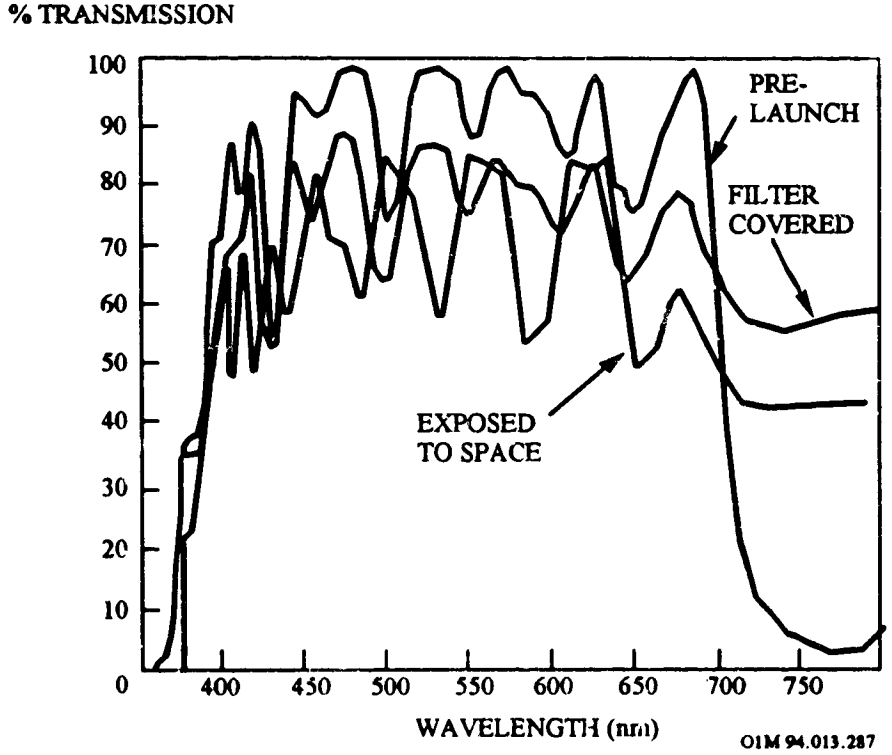

Figure 12-15. Pre-Launch and Post-Recovery Transmission of Corion Broad-band Filter #9 (Covered and Exposed)

The neutral density filters had an Inconel film providing an optical density of about 1.4. For the covered neutral density filter the transmission was unchanged as its transmission curve overlays the pre-launch curve directly, as shown in Figure 12-16. [15] The effects of the space environment for the uncovered neutral density filter is represented by the post-recovery curve as shown in Figure 12-16. The increase in transmission is likely due to erosion of the deposited contaminated layer (see Section 12.6.2).

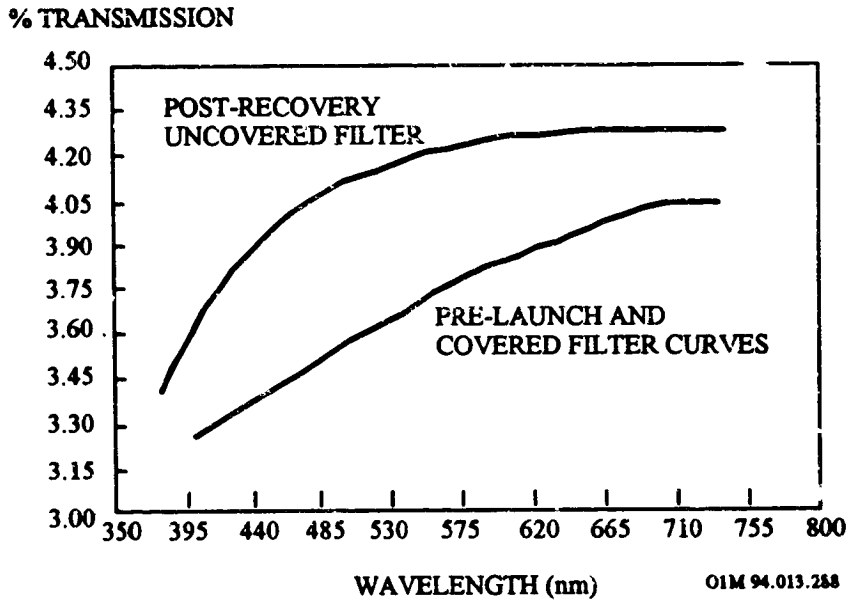

Figure 12-16. Pre-Launch and Post-Recovery Transmission of Corion Neutral Density-Band Filter #6 (Covered and Exposed)

The Al-MgF_2 on MgF_2 Substrate (1216 Å), the Al-MgF_2 on MgF_2 Substrate (1270 Å), and the Al-MgF_2 on Quartz Substrate (2430 Å) filters all showed reduced transmittance and a shift in center wavelength toward the blue (see Figures 12-17 through 12-19) (ref. 11).

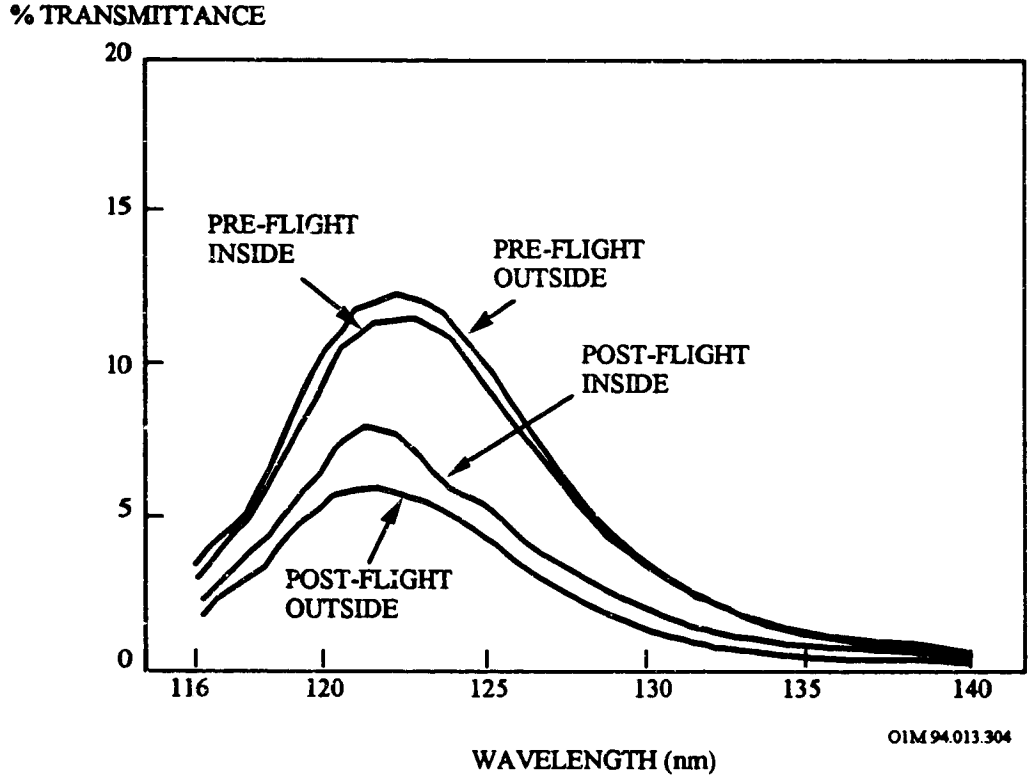

Figure 12-17. Launch and Post-Recovery Transmission of Al/MgF_2 Optical Filter on MgF_2 substrate (1216 Å) (Covered)

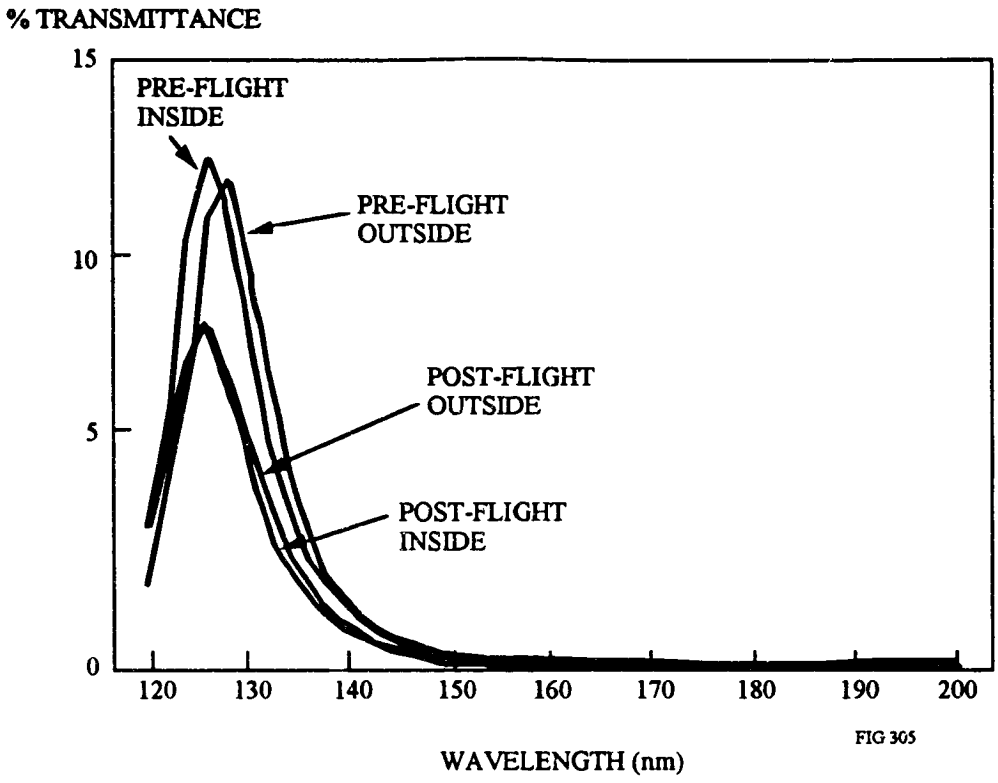

Figure 12-18. Pre-Launch and Post-Recovery Transmission of Al/MgF_2 Optical Filter on MgF_2 Substrate (1270 Å) (Covered)

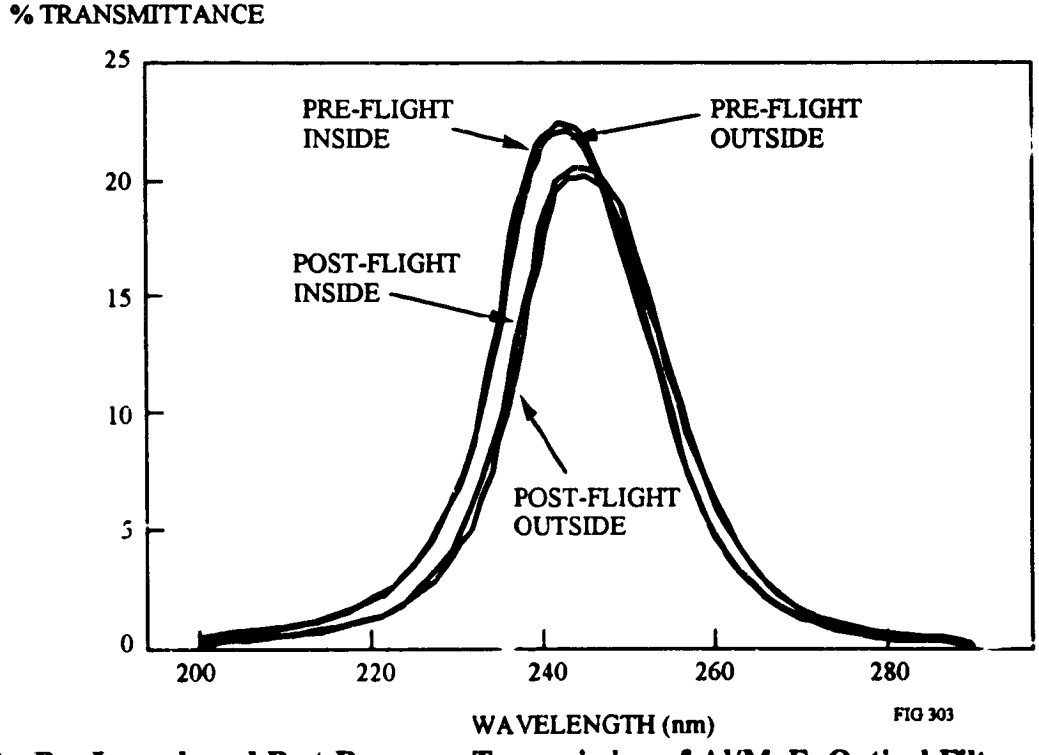

Figure 12-19. Pre-Launch and Post-Recovery Transmission of Al/MgF_2 Optical Filter on SiO_2 Quartz Substrate (2430 Å) (Covered)

12.6.1.4 Darkening

No data available.

12.6.2 Exposed UV/Visible Optical Filters

12.6.2.1 Absorption/Transmission/Reflectance

Table 12-19 summarizes the space environment effects for UV/visible optical filters exposed directly to the space environment (ref. 1).

Table 12- 19. Absorption/Transmittance/Reflectance Data Base for UV/Visible Optical Filters Exposed Directly to Space Environment

Materials	Space Environment	Comments
Narrow-Band Corion	9.6×10^{12} atoms/cm^2 8,200 esh[1]	Reduced transmission, shift in center wavelength, and broadening of bandpass
Neutral Density Band Corion	9.6×10^{12} atoms/cm^2 8,200 esh[1]	Increased transmittance
Broad-band Corion	9.6×10^{12} atoms/cm^2 8,200 esh[1]	Reduced transmittance Deterioration of interference coatings
Al-MgF_2 on MgF_2 Substrate (1216 Å)	1.32×10^{17} atoms/cm^2 11,100 esh[2]	Reduced transmittance and shift in center wavelength
Al-MgF_2 on MgF_2 Substrate (1270 Å)	1.32×10^{17} atoms/cm^2 11,100 esh[2]	Reduced transmittance and shift in center wavelength
Al-MgF_2 on Quartz Substrate (2430 Å)	1.32×10^{17} atoms/cm^2 11,100 esh[2]	Reduced transmittance and shift in center wavelength
ZnS/Cryolite/Silver on Fused Silica (cemented with Epon 828)	7.15×10^{21} atoms/cm^2 9,400 esh[3]	Reduced transmittance
ZnS/Cryolite/Silver on Fused Silica (air-spaced, no cement)	7.15×10^{21} atoms/cm^2 9,400 esh[3]	Slight reduction in transmittance with slight shift of center wavelength
ThF_4/Cryolite on Fused Silica (air-spaced, no cement)	7.15×10^{21} atoms/cm^2 9,400 esh[3]	Increased in transmittance (due to pinholes in some of the metal-dielectric coatings)
ZrO_2/Cryolite/Silver on Fused Silica (air-spaced, no cement)	7.15×10^{21} atoms/cm^2 9,400 esh[3]	Reduced transmittance
ZnS/ThF_4 on Fused Silica (air-spaced, no cement)	7.15×10^{21} atoms/cm^2 9,400 esh[3]	Slight decrease in transmittance near short wave cutoff. Slight increase in transmittance near bluer wavelengths (apparent reduction in extinction coefficient of ZnS)
ThF_4/Cryolite on Fused Silica (air-spaced, no cement)	7.15×10^{21} atoms/cm^2 9,400 esh[3]	Increase in transmission (due to pinholes in some of the metal-dielectric coatings)
PbF_2/Cryolite on Fused Silica (air-spaced, no cement)	7.15×10^{21} atoms/cm^2 9,400 esh[3]	Reduced transmittance (due to increase absorption in the lead compound)
ZnS/Cryolite/Silver on Fused Silica (cemented with APCO R313)	7.15×10^{21} atoms/cm^2 9,400 esh[3]	Slight reduction in transmittance

1. Row E5
2. Row B3
3. Row B8

From LDEF Experiment S0050-1, the Corion narrow- (see Figures 12-20 to 12-23) and broad-band (see Figure 12-15) optical filters showed a small but significant reduction in transmission, which is believed to be related to degradation of the cement used in the filter construction (ref. 15). The broad-band filter 9 showed a slight but measurable shift toward longer wavelengths as a result of space exposure, but with the same bandwidth. For the other narrow-band filters, the shift is toward shorter wavelengths and is more pronounced. The exception is filter number 2, which was under an aluminum cover (see Figure 12-14). For filter number 2 the filter bandwidth was unchanged. For filter number 3, the filter bandwidth increased substantially. For the other two narrow-band filters, the filter bandwidth did not change appreciably with space exposure. Post-recovery measurements of the neutral density filters (Inconel films) showed increased transmission, likely due to erosion of the deposited layer (see Figure 12-16) (ref. 15).

The narrow-band interference filters showed evidence of reduced transmittance, shift of center wavelength, and bandpass broadening. The reduction in narrow-band filter transmittance is the most apparent change in the performance characteristics as a result of the years in space. A reduction in transmittance occurred for all narrow-band filters including the filter under cover. The reduced transmittance has been attributed partly by deterioration of the cement used to attach the two filter halves together and partly by the degradation of the optical design caused by the interdiffusion of the two dielectric materials making up each interface (ref. 3). The effects of interdiffusion of material and compaction/densification of the layers will be dependent upon manufacturing technology and materials, and so will vary among filters from different manufacturers. The shift of center wavelength toward the blue is observed for filters designed for both the ultraviolet and visible spectral regions. A bandpass shift toward the blue may be expected if the temperature cycling causes some realignment and adjustment within the multilayer interference films which tends to decrease the average film layer thickness. Any external effects which disrupt or disturb the interference layer uniformity will tend to broaden the filter bandwidth.[16] Although the magnitude of the shift is only a few nm of wavelength which will be unimportant in many cases, it can be significant where narrow-band energy is to be detected.

The near-infrared suppression (hot mirror) broad-band filters showed a reduction in transmittance and evidence of deterioration of the interference layers as a result of space exposure (see Figure 12-15). These filters combine a low-pass and high-pass filter design to produce the desired spectral characteristic. As Figure 12-15 indicates, the covered filter had somewhat better performance than the filter exposed directly to space. For these filters, the degradation of the interference layers and the reduced interference effectiveness are indicated by the reduced transmittance through the visible region and increased transmittance on the long-wave side.

The radiation exposure of less than 300 krads is below what would be expected to produce observable degradation, and the hot-mirror filter under the aluminum cover would have an exposure of less than one percent of this value. Yet the covered filter suffered a small but significant degradation as shown in Figure 12-15. The atomic oxygen fluence of $4x10^{12}$ atoms/cm^2 provides only one oxygen atom for more than ten surface atoms, insufficient to produce the observed effects. Ultraviolet irradiation would not effect the filter under cover, and normal aging of the hot mirrors should leave them in identical condition. The thousands of temperature cycles would have nearly the same effect for the covered and exposed filters, and do not provide an explanation for the performance differences between the pair.

The neutral density filters are of different construction and reacted differently to the effects of space exposure. The sample exposed to the space environment had slightly increased transmittance. The covered sample was unchanged. The increased transmittance is possibly the result of erosion of the Inconel coating during the 69 months in low Earth orbit as oxide formation should be minimal. The only physical difference noted between this pair of filters was the presence of a contamination layer on the exposed filter which stopped at the rim where the surface was covered by the attachment hardware. The small amount of contamination would reduce transmittance (although the effect is negligible in the visible wavelength region). Erosion would result in increased transmittance.

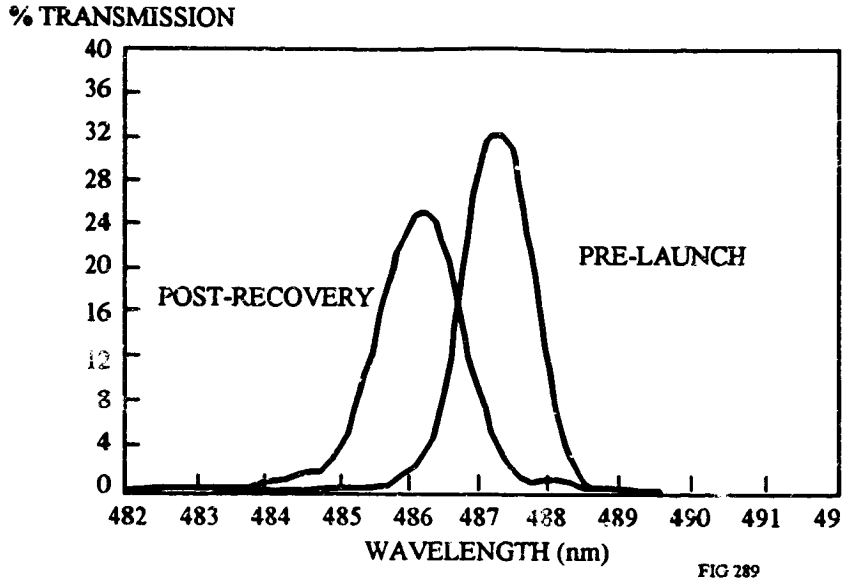

Figure 12-20. Pre-Launch and Post-Recovery Transmission of Corion Narrow-Band Filter #1

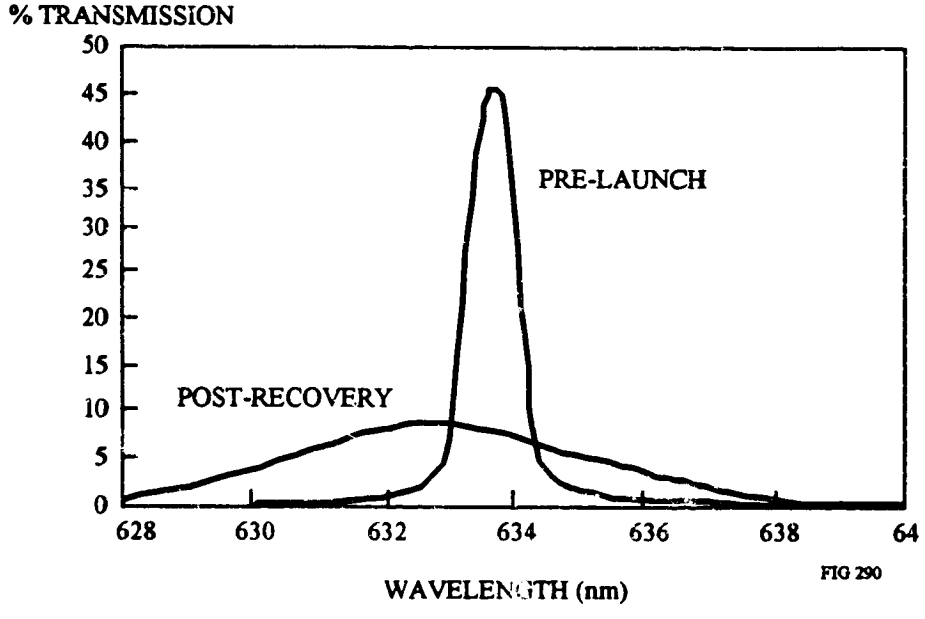

Figure 12-21. Pre-Launch and Post-Recovery Transmission of Corion Narrow-Band Filter #3

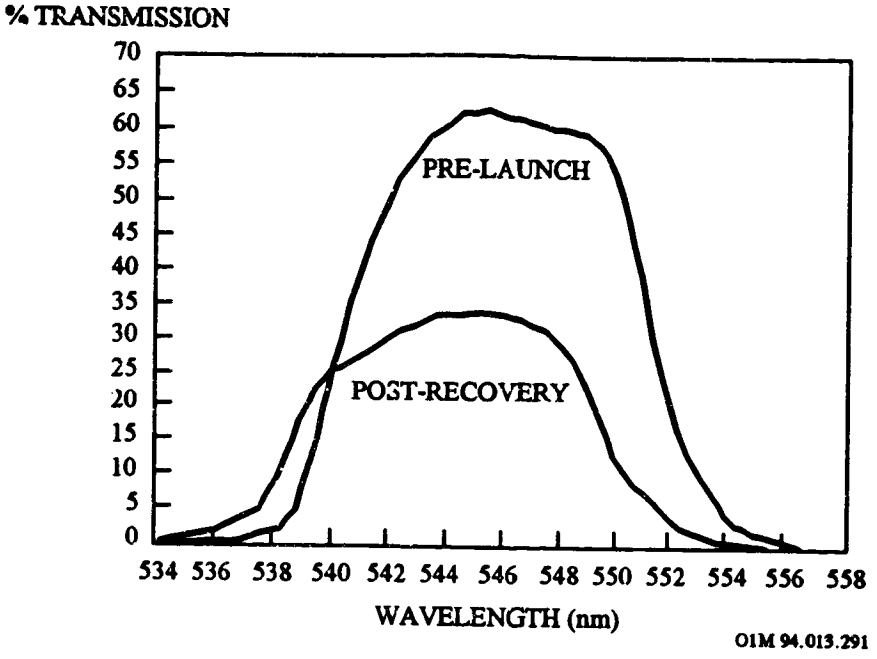

Figure 12-22. Pre-Launch and Post-Recovery Transmission of Corion Narrow-Band Filter #4

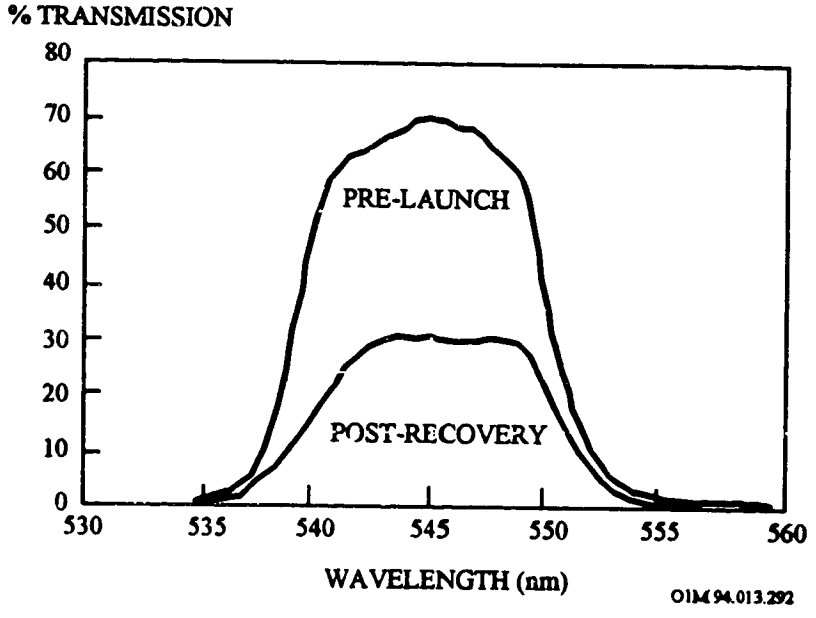

Figure 12-23. Pre-Launch and Post-Recovery Transmission of Corion Narrow-Band Filter #5

The samples from AO138-4 (the 1216 Å, 1270 Å, and 2430 Å filters) all showed reduced transmittance and a shift in center wavelength toward the blue (see Figure 12-24 to 12-26) (ref. 9).

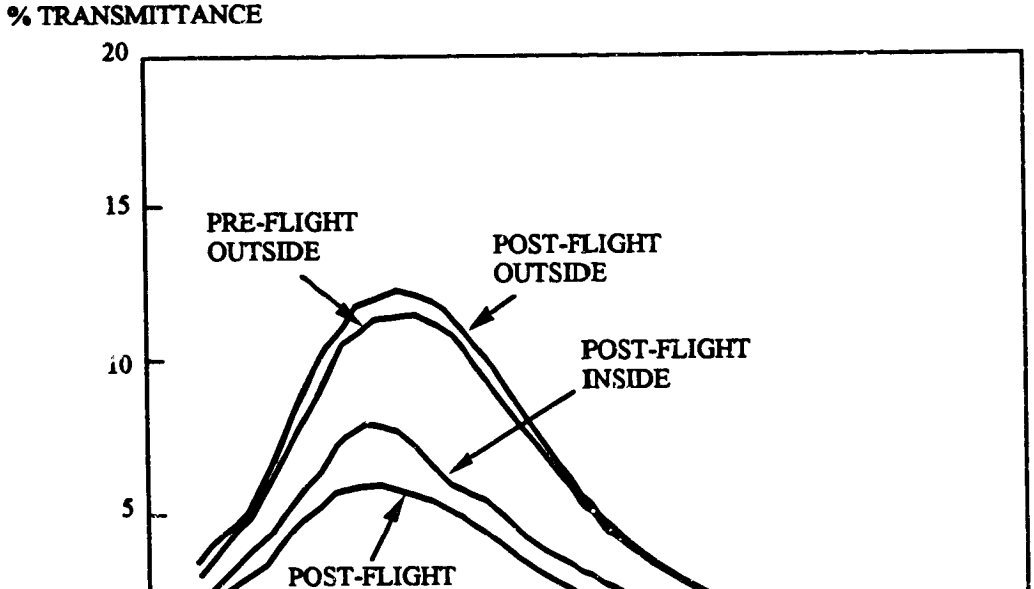

Figure 12-24. Pre-Launch and Post-Recovery Transmission of Exposed Al/MgF_2 Optical Filter on MgF_2 Substrate (1216 Å)

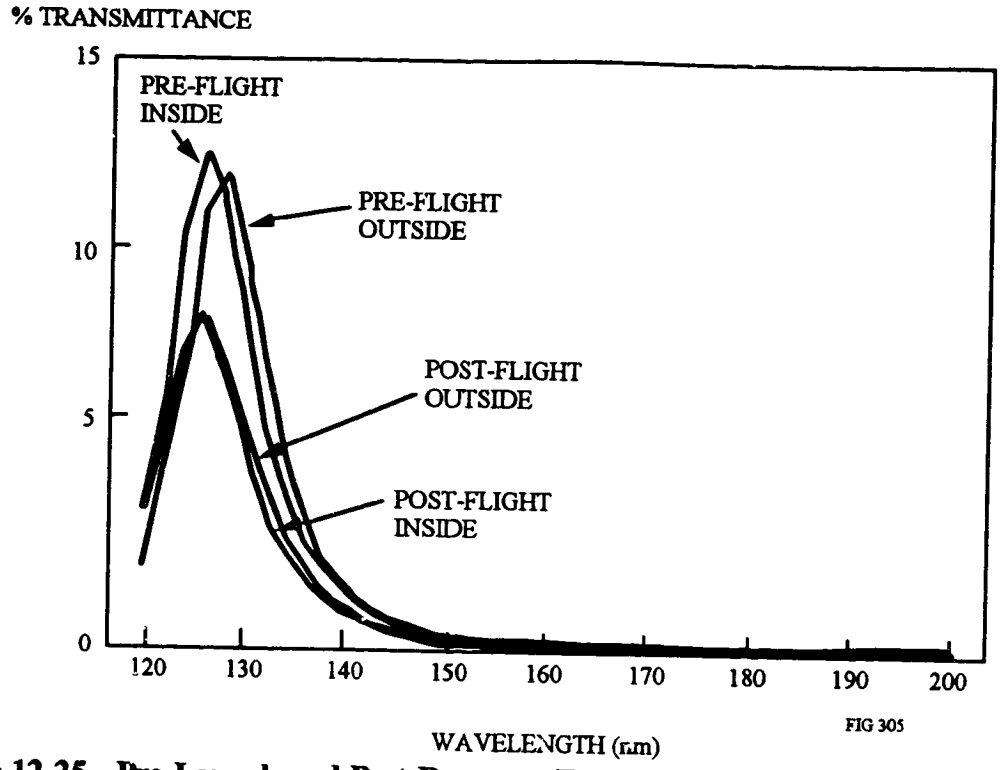

Figure 12-25. Pre-Launch and Post-Recovery Transmission of Exposed Al/MgF_2 Optical Filter on MgF_2 Substrate (1270 Å)

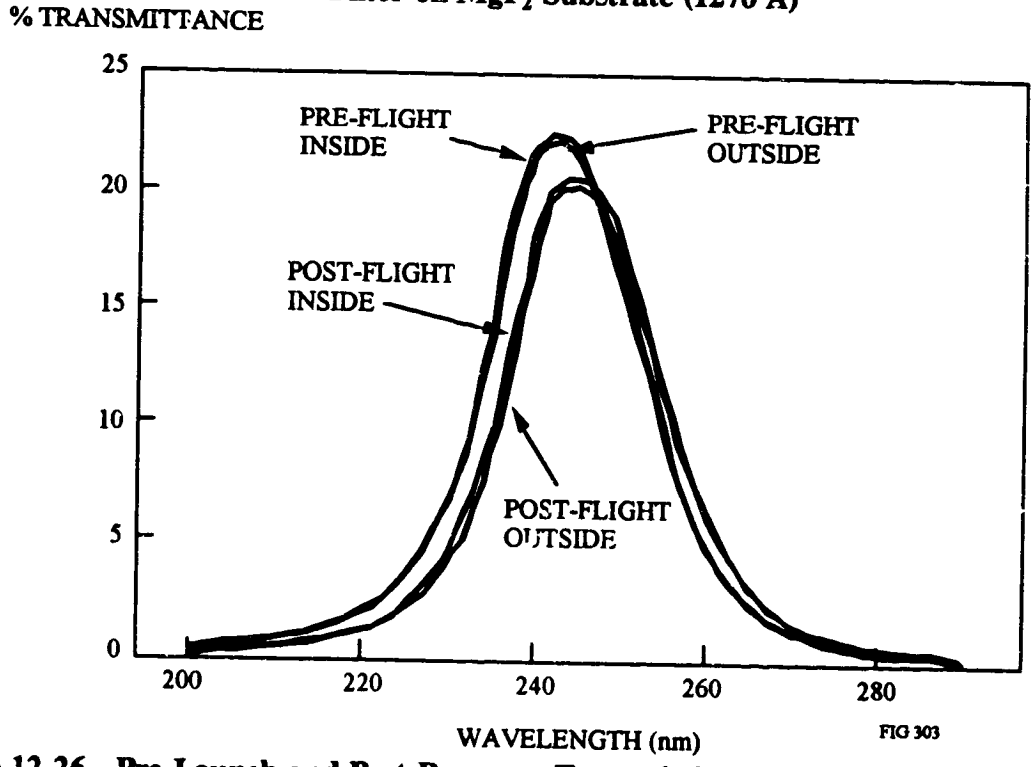

Figure 12-26. Pre-Launch and Post-Recovery Transmission of Exposed Al/MgF_2 Optical Filter on SiO_2 Quartz Substrate (2430 Å)

For the AO147 filters, with the exception of the lead compounds, the filters survived very well, as shown in Figures 12-27 to 12-35.[17] The Epon cement degraded somewhat at 500 nm (other wavelengths were masked by the filter). The failure mode (degradation) of the lead compounds was a wavelength-independent increase in absorption with no change in spectral characteristic. In an instrument, signal would be lost but spectral stability maintained. In the case of filters containing Al layers, the transmission increases were attributed to the pinholes which developed during exposure. This form of failure would reduce signal to noise but would not influence spectral band position or width. The reason for the development of pinholes has not yet been established by the experimenters. One possibility identified is that defects or contamination in the coating caused local heating due to increased absorption which, in turn, caused coating removal.

12.6.2.2 Contamination/Deterioration

A number of filter materials flown on LDEF were retrieved with contamination. A typical example is the set of samples from experiment S0050. On the LDEF tray, the green epoxy-fiberglass mounting strips were changed to a walnut brown where they were exposed to the space environment. Where covered, the original green color was maintained. The tray was covered with a light coating of brown stain which is believed by NASA to be the result of Z-306 thermal-control black paint outgassing in the space environment and becoming fixed in place by the effects of solar UV. The weight density of this material has been estimated to be 0.2 mg/cm^2.[18] For the exposed filter materials, organic deposits were seen on the films. The deposits were greater in the center than along the rim where the samples were covered. Analysis of this contamination is still underway as of this writing.

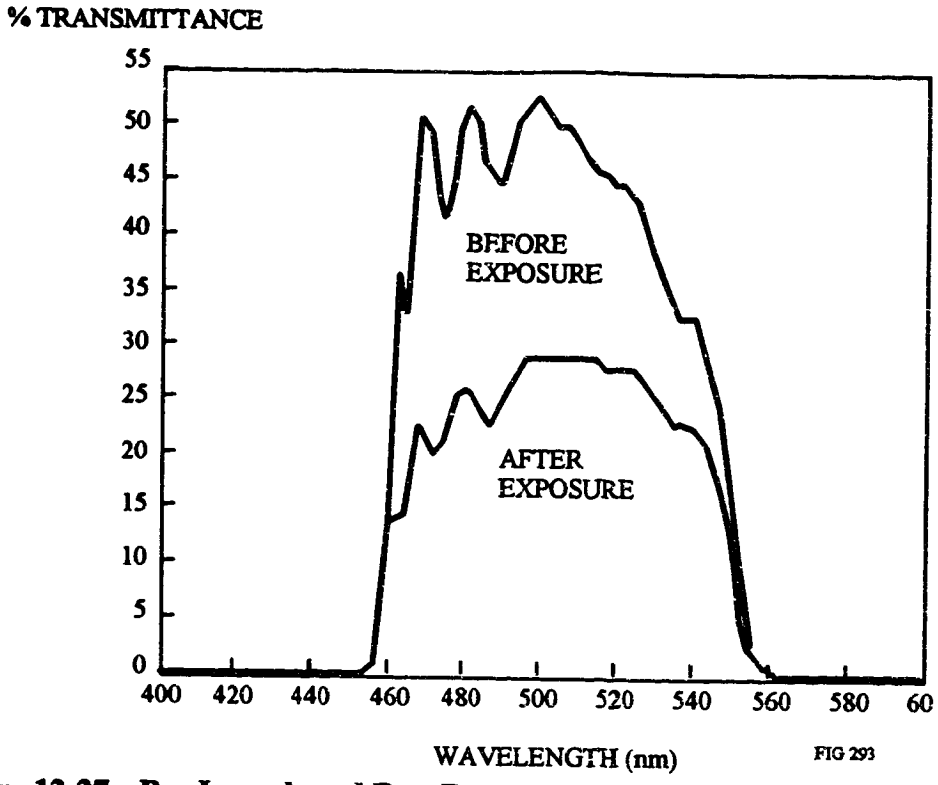

Figure 12-27. Pre-Launch and Post-Recovery Transmission of ZnS/Cryolite/Silver on Fused Silica (cemented with Epon 828)

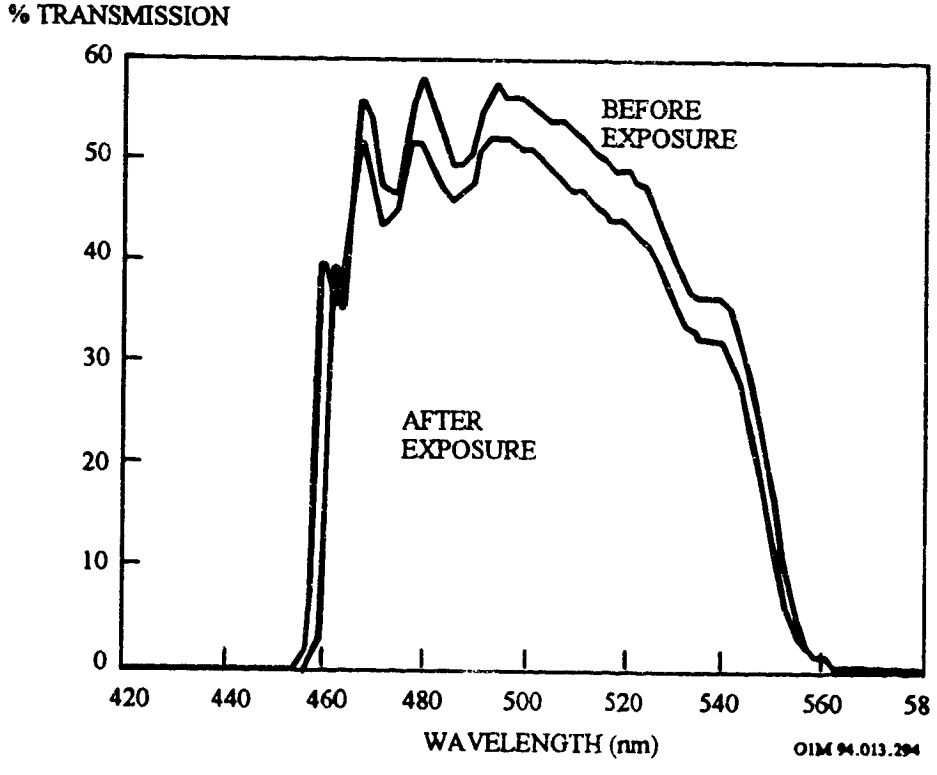

Figure 12-28. Pre-Launch and Post-Recovery Transmission of ZnS/Cryolite/Silver on Fused Silica (air-spaced, no cement)

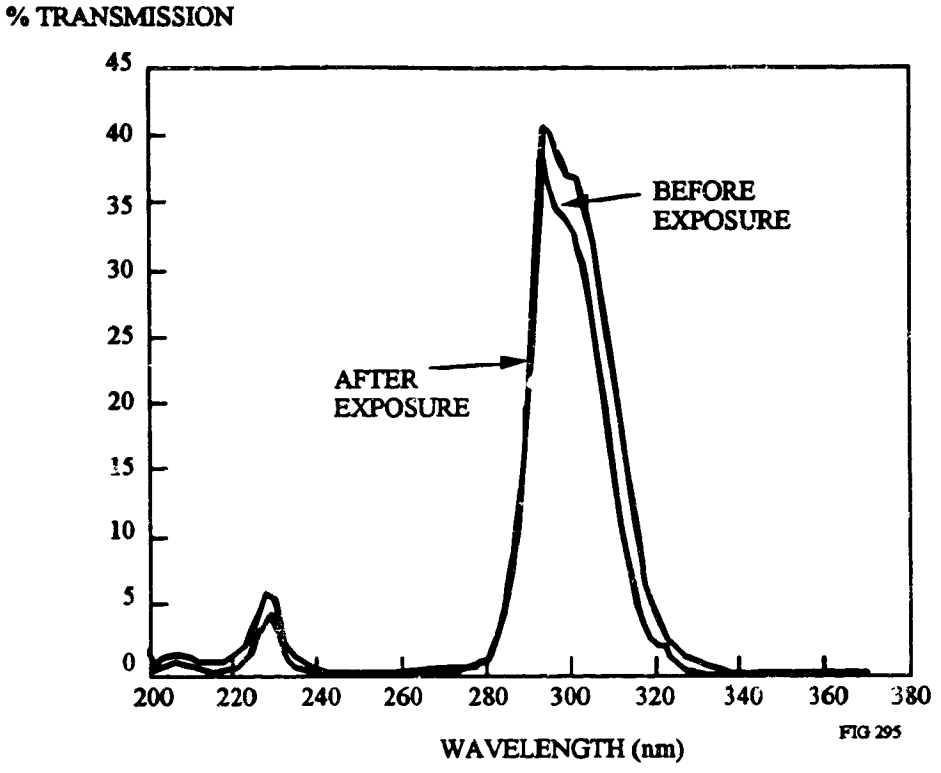

Figure 12-29. Pre-Launch and Post-Recovery Transmission of ThF_4/Cryolite on Fused Silica (air-spaced, no cement)

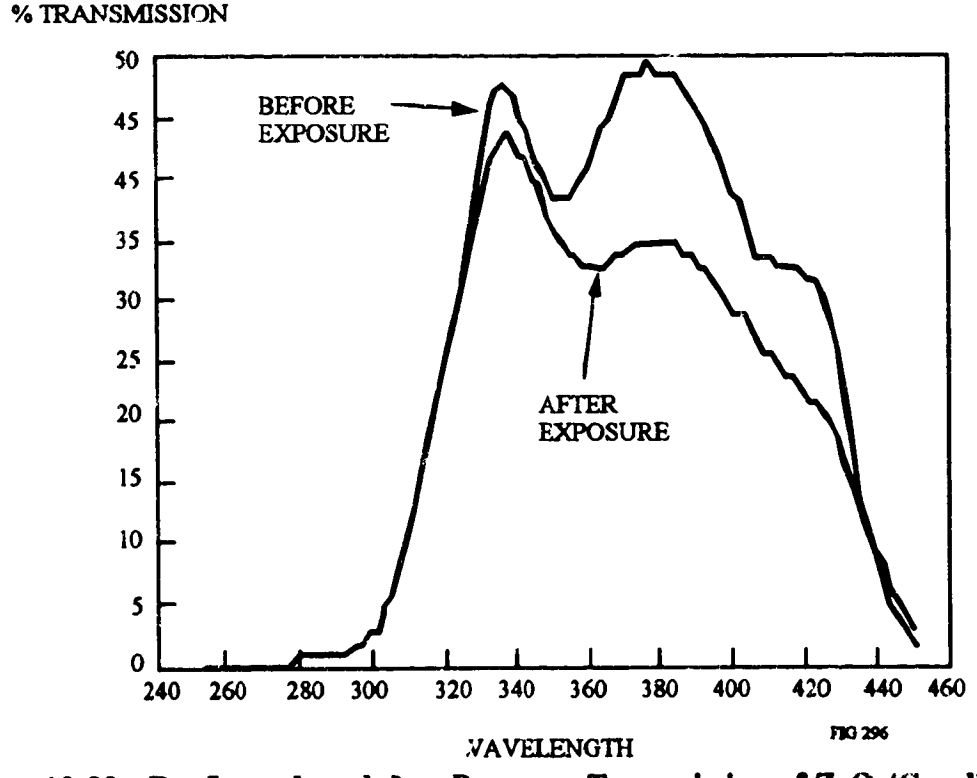

Figure 12-30. Pre-Launch and Post-Recovery Transmission of ZrO_2/Cryolite/Silver on Fused Silica (air-spaced, no cement)

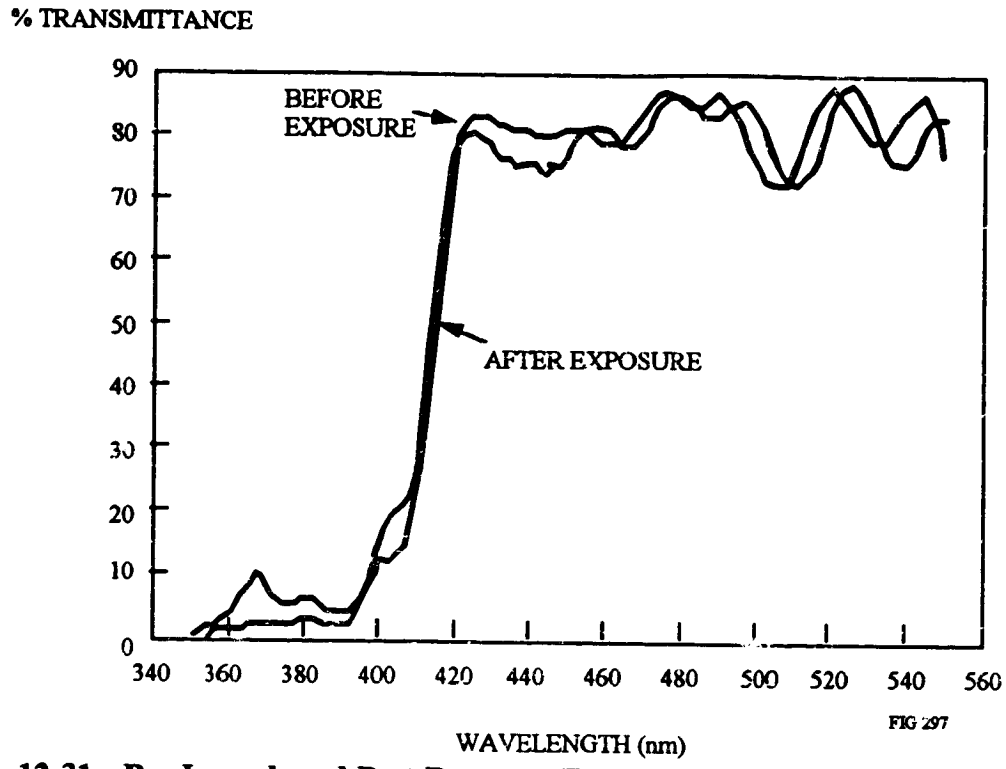

Figure 12-31. Pre-Launch and Post-Recovery Transmission of ZnS/ThF_4 on Fused Silica (air-spaced, no cement)

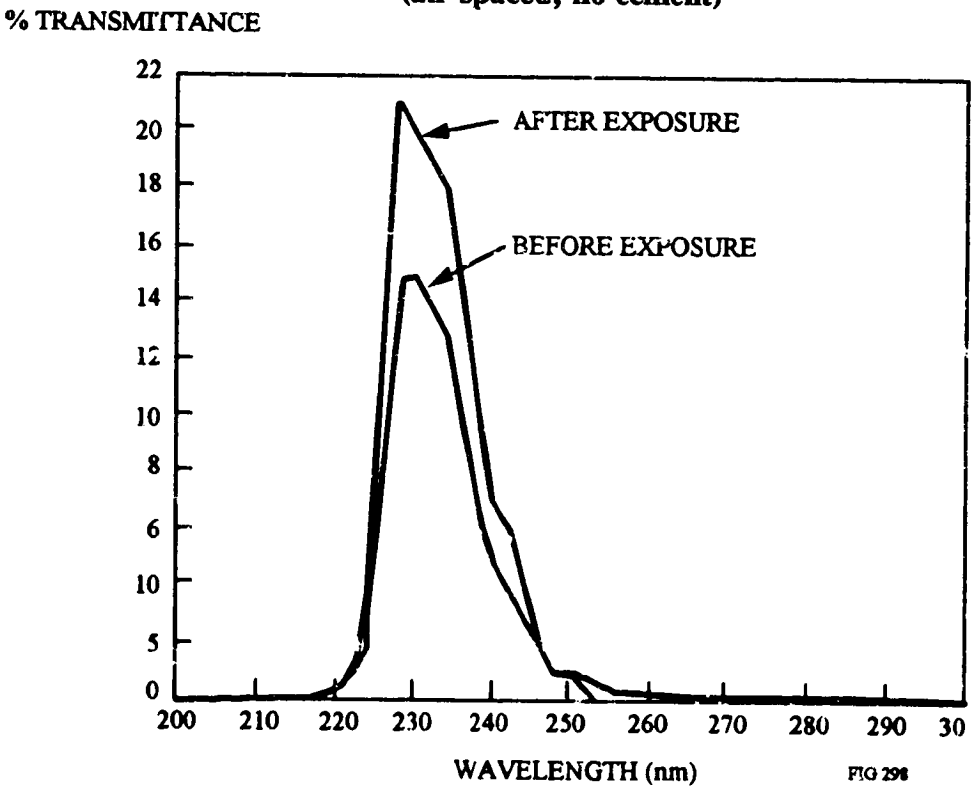

Figure 12-32. Pre-Launch and Post-Recovery Transmission of ThF_4/Cryolite on Fused Silica (air-spaced, no cement)

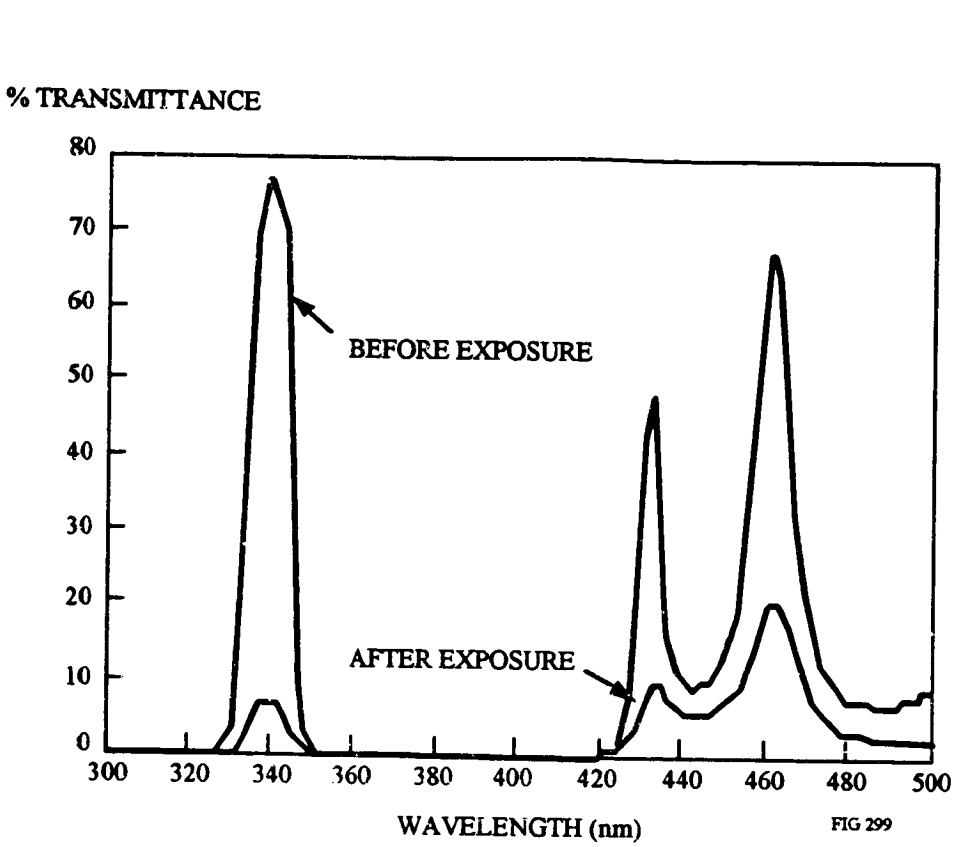

Figure 12-33. Pre-Launch and Post-Recovery Transmission of PbF_2/Cryolite on Fused Silica (air-spaced, no cement)

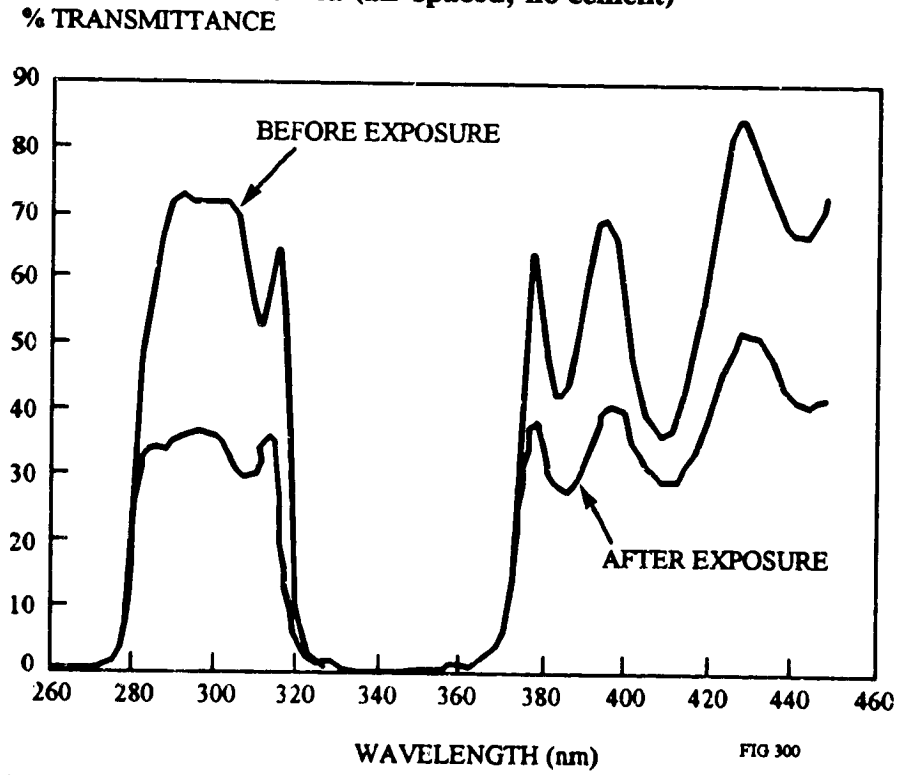

Figure 12-34. Pre-Launch and Post-Recovery Transmission of PbF_2/Cryolite on Fused Silica (air-spaced, no cement)

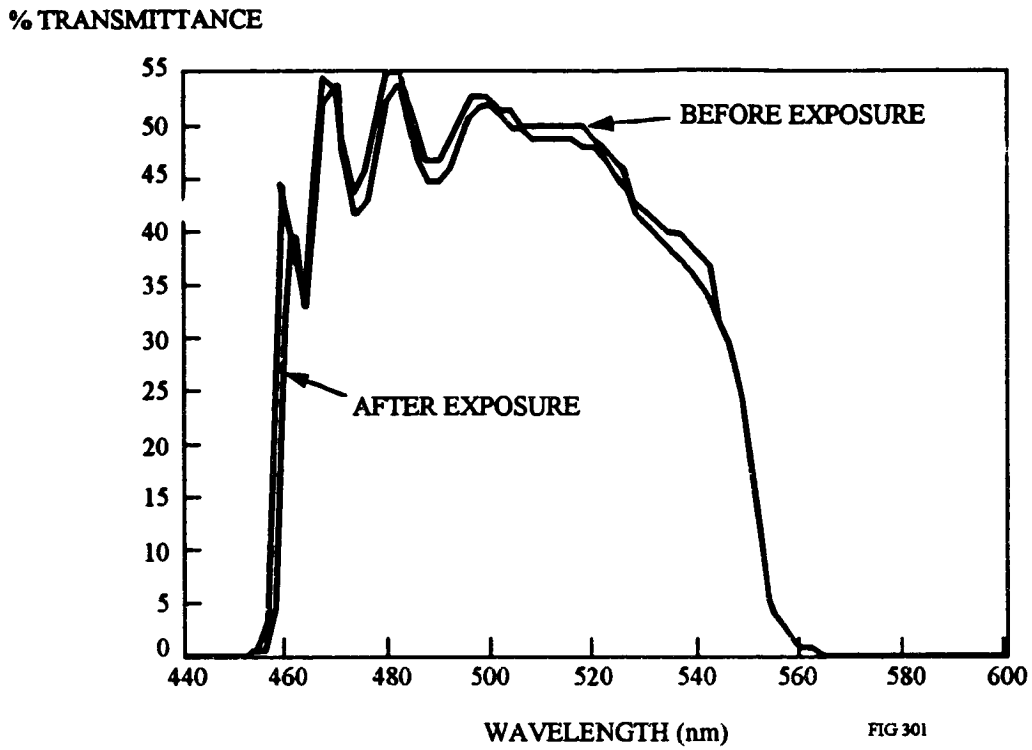

Figure 12-35. Pre-Launch and Post-Recovery Transmission of ZnS/Cryolite/Silver on Fused Silica (cemented with APCO R313)

12.7 OPTICAL FILTERS FOR IR SYSTEMS

Table 12-20 shows a summary of the optical filters for IR systems that were part of the two LDEF experiments (ref. 1).

Table 12- 20. Experiment Summary for IR Optical Filters

Experiment	IR Optical Filters
A0056	CaF_2 Low Index Ratio Quarter-Wave Blocking ZnSe/ZnS/KRS-5 on KRS-6 substrate PbTe/ZnS on Ge Substrate 15 μm 10 percent HBW L-Spacer THW Band-Pass Filter PbTe/ZnS 8-12 μm Tschebyshev Edge Band-Pass Filter (Antireflected on Ge Substrate PbTe/ZnS 14.5 μm 0.7 percent HBW Split-Spacer Fabry-Perot Band-Pass Filter on Ge Substrate
AO138	ZnS/Chiolite on BK7G18 and RG780 Glasses (820 nm Interference Filter)

12.7.1 Atomic Oxygen

No data available.

12.7.2 Impacts

Micrometeoroid/debris impacts on the CaF_2 sample occurred near the edge of the sample holder. The CaF_2 sample was located on Row B8 of LDEF experiment A0056. The impact crater was about 1 mm in diameter with a spallation zone diameter of about 5.5 mm. The substrate cleaved in two directions outward from the crater site to the opposite sides of the sample, and at an angle of about 75°, breaking the sample into three pieces. This verifies the fragile and brittle nature of CaF_2 as a substrate material, while remaining optically-functional.[19]

12.7.3 Scatter

No data available.

12.7.4 Absorption/Transmission/Reflectance

Table 12-21 summarizes the absorption/transmission/reflectance effects of the space environment on IR optical filters (ref. 1). Post-recovery measurements can be placed in two groups. The first group consists of the hard-coated filter materials, primarily Pb-based on Ge substrates. In general, the results of LDEF experiment A0056 indicated that no significant changes were found either in transmission or spectral position of any hard-coated II-VI/PbTe-based multilayers on Ge substrates.[ii] Pre- and post-flight comparisons were well correlated. They showed a small and consistent loss in peak transmission for both (on the order of 5% to 10%), within the accuracy envelope. No cover glasses were used. There was also a displacement of the bandpass to shorter wavelengths (blue) for both the exposed and control samples. However, the shift was small for these filters (on the order of 1 cm^{-1} at 10 μm), and was usually close to the defined measurement accuracy of the spectrometers used for these measurements. These samples are considered stable and show no degradation for the exposure.

In contrast, the softer substrate materials of the second group, KRS-5 (TlBrI)-based multilayers deposited on KRS-5 or KRS-6 (TlClBr) substrates which had much lower transmittance in the infrared region, were adversely affected in their physical and optical properties by the long exposure in space, from a reduced transmission to a complete opacity. Post-flight visual and spectral analysis of the soft materials showed that less degradation had occurred in the Earth-facing tray (G12) than in the leading edge tray (B8).

Finally, the 820 nm interference filter showed a slight reduction in transmission, as shown in Figure 12-36 (ref. 9).

[ii] Hard-coated filter materials comprised spectral filters from atmospheric-sensing, weather forecasting, research and planetary satelites (NIMBUS 4-7, ITOS, TIROS-N, PIONEER, and GAILEO). The filter materials are primarily Pb-based on Ge substrates.

Table 12- 21. Absorption/Transmission/Reflectance Effects Base for IR Optical Filters

Materials	Space Environment	Comments
Low Index Ratio Quarter-Wave Blocking ZnSe/ZnS/KRS-5 on KRS-6 substrate(1)	1.33×10^{21} atoms/cm^2 6,800 esh[1]	Reduced Transmission
PbTe/ZnS on Ge Substrate 15 μm 10 percent HBW L-Spacer THW Band-Pass Filter	1.33×10^{21} atoms/cm^2 6,800 esh[1]	No significant changes in transmission or spectral position
PbTe/ZnS 8-12 μm Tschebyshev Edge Band-Pass Filter (Antireflected on Ge Substrate	7.15×10^{21} atoms/cm^2 9,400 esh[2]	No significant changes in transmission or spectral position
PbTe/ZnS 14.5 μm 0.7 percent HBW Split-Spacer Fabry-Perot Band-Pass Filter on Ge Substrate	7.15×10^{21} atoms/cm^2 9,400 esh[2]	No significant changes in transmission or spectral position
ZnS/Chiolite on BK7G18 and RG780 Glasses (820 nm Interference Filter)	7.15×10^{21} atoms/cm^2 9,400 esh[2]	Slight reduction in transmission

(1) KRS-6 substrate is Thallium-Chlorine-Bromine with a 33-layer ZnS/KRS-5 and ZnSe/KRS-5 coating. KRS-5 is Thallium-Bromine-Iodine.

1. Row G12
2. Row B8

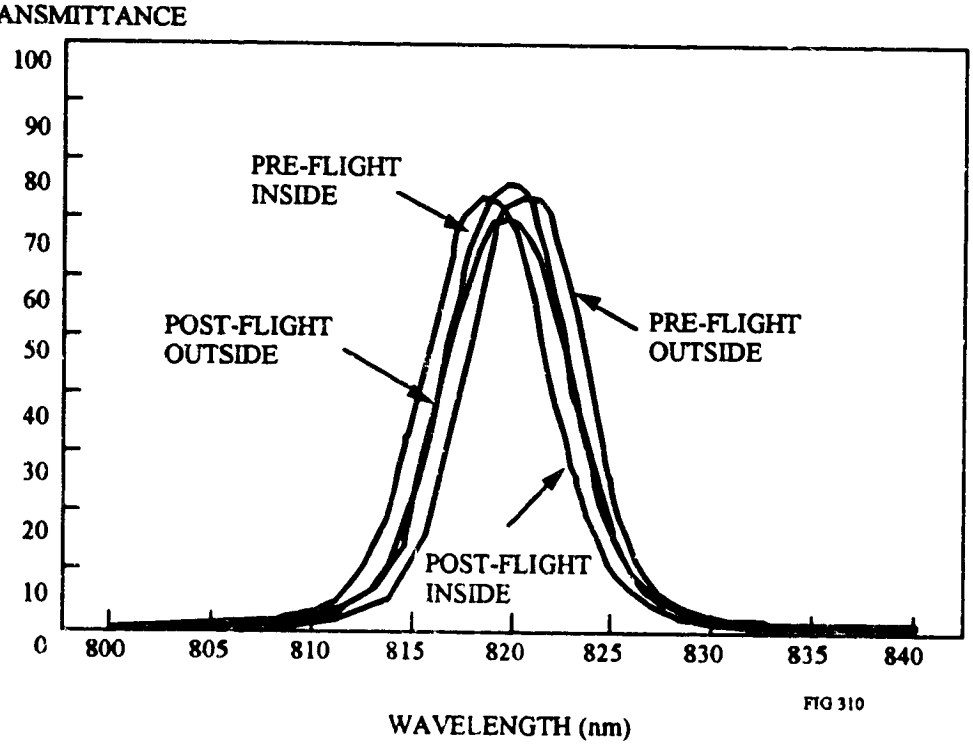

Figure 12-36. Pre-Launch and Post-Recovery Transmission of ZnS/Chiolite on BK7G18 and RG780 Glasses (820 nm Interference Filter)

12.8 MIRRORS

The properties of some metal mirror materials are listed in Table 12-22.[20] Properties include specular reflectivity in three wavelength regions (visible, MWIR, and LWIR), radiation resistance, and photon resistances for two conditions: if they retain their visible wavelength reflectivities, and if they absorb 100 percent of the photon energy. While many materials are good reflectors in all three wavelength bands, beryllium, vanadium, and zirconium make good IR but poor visible light mirrors. Wideband reflection is not always desirable.

Table 12- 22. Properties of Metal Mirror Materials

Material	Specular Reflectivity				Radiation Resistance	Photon Resistance
	Visible 0.4-07μ	MWIR 3-5 μ	LWIR 10-14 μ	(cal/cm^2)	Visible λ Increasing Reflectivity (W/cm^2)	Limit (100% Absorption (W/cm^2)
Be (Z-4)	0.50	0.89	0.92	6.25	66.4	33.2
Mg (Z-12)	0.85			0.30	27.3	4.11
Al (Z-13)	0.91	0.97	0.98	0.26	47.8	4.33
V (Z-23)	0.50	0.91	0.95	0.28	260	131
Co (Z-27)	0.65	0.86	0.97	0.20	157	55
Ni (Z-28)	0.67	0.87	0.94	0.19	152	50.3
Cu (Z-29)	0.70	0.98	0.99	0.10	64	19.2
Zr (Z-40)	0.40	0.85	0.95	0.11	193	116
Rh (Z-45)	0.80	0.93	0.97	0.10	705	141
Ag (Z-47)	0.94	0.98	0.98	0.052	218	131
Au(Z-79)	0.80	0.98	0.99	0.022	90.5	181

Table 12-23 summarizes the mirror materials that were flown on the LDEF (ref. 1).

Table 12- 23. LDEF Experiment Summary for Mirrors

Experiments	Mirror
AO034	SiO/Al on Pyrex Os/Al on Quartz Ag/Al on Quartz Au/Al on Quartz MgF_2/Al on Quartz
AO114	Sputtered Cu on fused silica and OFHC copper
AO138-4	LaF_3/Chiolite/MgF_2 on B1664 Glass Al/MgF_2 on B1664 glass ThF_4/Ag on B1664 Glass Al_2O_3/Ag on Kanigened Al MgO/MgF_2 on B1664 Glass TiO_2/SiO_2 on B1664 Glass Ge/ZnS/ThF_4 on B1664 Glass MgF_2/Al on Kanigened Al
AO138-5	Al on Glass Pt on Glass
M0003-2, -7, and -11	Bare Mo Cu, Diamond-Turned Cu, diamond-Turned Ni-plated Cu, ThF_4/Ag/Cr on Mo $(Si/Al_2O_3)^3$/Ag on Polished Si $(ZnS/Al_2O_3)^4$/Ag on Polished Mo $(ZnS/ThF_4)^5$/Ag on Polished Mo

12.8.1 Atomic Oxygen Erosion

Copper mirrors were flown on the LDEF mission on experiment A0114 on both the leading and trailing edge. The trailing edge showed little effect of AO. The samples on the leading edge received a total fluence of 8.72×10^{21} atoms/cm^2. X-ray diffraction measurements and high resolution profilometry showed that the copper was converted stoichiometrically to Cu_2O.[21]

12.8.2 Impacts

LDEF mirror samples showed localized damage at the sites of impact. Table 12-24 summarizes materials and provides a guide to data contained in this section.

Table 12- 24. Impacts Effects Data Base on Mirrors

Materials	LDEF Row/ Angle of Ram	Comments
Cu	D9/8°	No damage to substrate beyond area of impact
Ni-Cu	D9/8°	Splatter of resolidified matter around craters. Damage is similar to that seen in uncoated Cu.
$(ZnS/Al_2O_3)^4$/Ag on Polished Mo	D8/38°	Impacts revealed multilayer structure. Evidence of melting around impact sites.
$(ZnS/ThF_4)^5$/Ag on Polished Mo	D4/158°	Splatter of resolidified matter around craters.

Cu and Ni-Cu metal mirrors were evaluated for this effect and all of the LDEF samples showed localized damage at the site of impact. No damage to the mirror substrates was observed beyond the area of impact (ref. 11). Impacts on a $(ZnS/Al_2O_3)^4$/Ag/Mo mirror revealed the multilayer structure and also showed signs of melt.[22] On a $(ZnS/ThF_4)^5$Ag/Mo sample, impacts did not reveal the multilayer structure but debris was splattered about the site (ref. 22).

12.8.3 Scatter

The bare Mo mirror sample, which was flown on the leading edge and the trailing edge of LDEF experiment M0003-2 experiment, received exposures of 3 months, 6 months, 9 months, and 69 months. Scatter data were taken at 1.064 μm. All samples were highly scattering. Except for the leading edge, 69-month sample, a trend did not appear between samples exposed on the trailing edge and samples exposed on the leading edge. Even though

all samples were highly scattering, the optic exposed for the full duration of the flight (the 69-month exposure) scatters more than one order of magnitude more light than do samples exposed for 9 months or less.[23]

12.8.4 Absorption/Transmission/Reflectance

A number of absorption/transmission/reflectance effects on UV/visible and IR mirrors were reported on by LDEF experimenters. Table 12-25 summarizes these effects on the mirrors from the LDEF experiments AO138-3, AO138-5 and M0003-7. Table 12-14 discusses the absorption/transmission/reflectance effects for coatings applicable to mirrors.

Table 12- 25. Absorption/Transmission/Reflectance Effects on Mirrors

Materials	Comments
WRe/Si on Glass	Peak reflectivities are within 10 to 15 percent of pre-flight measurements
Al on Glass	Loss of reflectance less than 10% over whole spectral range for samples internal to spacecraft. Loss of reflectance of up to 30% at 220 nm for space-facing samples.
Pt on Glass	Loss of reflectance around 10% at three specific test wavelengths (58.4 nm, 74.4 nm, and 121.6 nm) for samples internal to spacecraft. Loss of reflectance of up to 35% at 121.6 nm for space-facing samples.
$(Si/Al_2O_3)^3$/Ag on polished Si	Minimal reduction in reflectance at the desired wavelength, 2.8 μm, but with an indication of surface oxidation and reduction of reflectance at longer wavelengths (i.e., 3-4 μm).
$(ZnS/Al_2O_3)^4$/Ag on polished Mo	Significant reduction in reflectance with apparent spectral shift of the reflectance maximum. Dendritic growth also apparent.
$(ZnS/ThF_4)^5$/Ag on polished Mo	Significant reduction in reflectance with apparent spectral shift of the reflectance maximum. Dendritic growth also apparent.

The Al and Pt coatings on Glass mirrors facing inward experienced some degradation in reflectance. The Al coating lost less than 10 % reflectivity over the whole spectral range while the Pt coating lost reflectivity of around 10 % for three discrete wavelengths (58.4 nm, 74.4 nm, and 121.6 nm). For the space-facing samples, the Pt mirrors experienced degradations in reflectivity that were more pronounced than for the inward-facing samples. The Al coating lost up to 30 % reflectivity (at 220 nm) while the Pt coating lost up to 35 % reflectivity (at 121.6 nm).[24]

The $(Si/Al_2O_3)^3$/Ag on polished Si mirror showed a minimal reduction in reflectance at the desired wavelength of 2.8 μm, but with an indication of surface oxidation and reduction in reflectance at longer wavelengths (i.e., 3-4 μm). Zinc-sulfide-based coating designs, $(ZnS/Al_2O_3)^4$/Ag on polished Mo and $(ZnS/ThF_4)^5$/Ag on polished Mo, showed significant reductions in reflectance at the desired wavelength with large spectral shifts of the reflectance maxima apparent. Dendritic formations were also seen. A combination of thermal cycling and irradiation effects probably provided energy for the dendrite formation process (ref. 24).

12.8.4 Contamination/Deterioration

Table 12-26 summarizes the contamination/deterioration effects data base for mirrors. Table 12-27 summaries the related materials/effects covered in section 12.5.

Table 12- 26. Contamination/Deterioration Effects Data Base for Mirrors

Materials	LDEF Row	Comments
Ni	D9/8°	Corroded and hazed surrounded by discoloration zone
Diamond-Turned Cu	D4/158°	Hazy, discolored surface with corrosion spots on the surface. Sample showed grain boundaries (ref. 11).

Table 12- 27. Contamination/Deterioration Effects Data Base for IR Coatings Applicable to Mirrors

Materials/ Substrate	LDEF Row/ Angle off Ram	Comments
$(ZnS/Al_2O_3)^4$/Ag Polished Mo	D8 38°	Corroded and hazed
SiO/Al on Pyrex	C3/171° C9/8°	Degradation in UV spectral reflectance due to contamination
Os/Al on Quartz	C3/171° C9/8°	Complete oxidation of the silver film and complete oxidation and evaporative removal of Os film on leading edge
Ag/Al on Quartz	C3/171° C9/8°	Complete oxidation of the silver film in both leading edge and trailing edge samples
Au/Al on Quartz	C3/171° C9/8°	Slight visual difference in leading edge samples. No obvious effect on trailing edge samples
MgF_2/Al on Quartz	C3/171° C9/8°	No visible effect in leading edge or trailing edge samples

12.8.5 Natural Environment Effects

The expected natural space environmental effects on the metal mirror materials are listed in Table 12-28 (ref. 20). Sunlight will only produce heating, while the geomagnetic field will only produce torques on cobalt and nickel. Space vacuum, the ionosphere, and hot plasma are not expected to affect their specular reflectivities, but both the Van Allen belt (low energy protons) and solid objects (micrometeoroids and space debris) will not only affect their reflectivity but will also increase their BRDF (bi-directional reflection distribution function). This BRDF will be due to surface bubbles (produced by low energy protons which become hydrogen gas in metals) and surface pits and craters (produced by object impacts). Atomic oxygen will attack most of these metals, producing a surface oxide layer that will reduce reflectivity (if it adheres to the substrate) and/or increase the BRDF (if it does not adhere or builds up unevenly).

Table 12- 28. Natural Environmental Effects on Metal Mirrors

Material	Sunlight	Van Allen Belts	Objects	Gases
Be	Heating	Reflectance Loss, BRDF Gain	Reflectance Loss, BRDF Gain	Reflectance Loss, Glow
Mg	Heating	Reflectance Loss, BRDF Gain	Reflectance Loss, BRDF Gain	Reflectance Loss, Glow
Al	Heating	Reflectance Loss, BRDF Gain	Reflectance Loss, BRDF Gain	Reflectance Loss, Glow
V	Heating	Reflectance Loss, BRDF Gain	Reflectance Loss, BRDF Gain	Reflectance Loss, Glow
Co	Heating	Reflectance Loss, BRDF Gain	Reflectance Loss, BRDF Gain	Reflectance Loss, Glow
Ni	Heating	Reflectance Loss, BRDF Gain	Reflectance Loss, BRDF Gain	Reflectance Loss, Glow
Cu	Heating	Reflectance Loss, BRDF Gain	Reflectance Loss, BRDF Gain	Reflectance Loss, Glow
Zr	Heating	Reflectance Loss, BRDF Gain	Reflectance Loss, BRDF Gain	Reflectance Loss, Glow
Rh	Heating	Reflectance Loss, BRDF Gain	Reflectance Loss, BRDF Gain	Reflectance Loss, Glow
Ag	Heating	Reflectance Loss, BRDF Gain	Reflectance Loss, BRDF Gain	Reflectance Loss, Glow
Primary Concern: Atomic Oxygen, Space debris effects in LEO, Surface Van Allen Belt Effects in MEO				

12.9 MATERIAL SELECTION GUIDE

The results of the LDEF experiments provide several guidelines and conclusions for the selection and use of optical materials in space. Table 12-29 lists the observed effects of low-Earth orbit space exposure on multilayer filters and mirrors and window substrates (ref. 3).

Table 12- 29. Material Choices for Multi-Layer Filters and Mirrors

- Contamination acquired during six years in storage and six years in space causes an increase in off-axis scattering from optical surfaces of a factor of ten over scattering from the original cleaned surface.
- For irradiation levels under 1/3 Mrad, degradation effects from high-energy radiation are small.
- Radiation-induced absorption and contamination-induced absorption in optical materials is strongest in the UV spectral region, decreasing through the visible region.
- Narrow-band filters exhibit a "blue" shift of 1-9 nm. Effects of compaction/densification and interdiffusion between layers perturb the design of the multilayer filters resulting in loss of performance.
- Stable substrate materials are Si, SiO_2, Al_2O_3, Quartz, ULE Glass
- Suspect materials are fluorides such as MgF_2, CaF_2
- Poor substrate materials are KRS-5, KRS-6

Direct radiation damage effects on all optical components and devices were minimal with few exceptions over the six-year period. Moreover, mounting of components typically gave maximal exposure to these optical components, so that the results of the LDEF experiments represented worst-case conditions. Additional protection from ionizing radiation can easily be provided where desirable. These results from LDEF experiments are in agreement with previous studies indicating that ionizing radiation exposures of less than 1/3 Mrad will not produce significant changes in the properties of substrate materials and optical filters. The effects of the irradiation for both high-energy photon and particulate irradiation on

substrate and window materials make their appearance first as a reduction in ultraviolet transmission for both ionizing and photon irradiations.

Careful and thorough cleaning of all optical components and careful workmanship in fabrication will contribute to the stabilization of properties in space. Contamination deposited on optical components reduces transmittance. The effect was strongest in the ultraviolet region, and became small or undetectable in the visible and infrared regions. Shutters or other means to protect the optical surfaces through the launch and early orbit phases will be necessary to protect critical surfaces from such contamination. Surface protection seems to be essential for optical systems designed to operate in the ultraviolet region.

Multilayer narrow-band filters have the design wavelength shifted toward the blue by an amount that is small (1-4 nm), but significant in many cases. The related increase of bandwidth will depend on the materials used. Material choice is important for filters and mirrors. Soft materials are to be avoided. Zinc sulfide and thorium fluoride compounds showed degradation effects in several components, but not all.

These two compounds are commonly used as interference coatings. Materials such as Si, SiO, and Al_2O_3 showed greater stability under low-Earth orbit conditions. Quartz and ULE glass are stable substrates, as are silicon, germanium. The materials MgF_2 and CaF_2 were suspected as being responsible for poor performance in some experiments.

Soft materials such as KRS-5 and KRS-6, which degraded in orbit in all experiments, are to be avoided. Even when coated, delamination of the coatings deposited on these soft substrates took place in the case of filters. These two materials were unstable under LEO conditions.

Similar considerations apply to dielectric mirrors. Spectral shifts in reflectance may limit the use of such mirrors in space-based laser cavities, but well protected and temperature stabilized components may survive with minimum changes.

Further studies of these complex phenomena are desirable to assure long-term survival and operational stability of optical systems operating in the low-orbit environment.

REFERENCES

1 W.T. Kemp et al., "Long Duration Exposure Facility Space Optics Handbook," Air Force Document PL-TN-93-1067, September 1993.

2 G. Bohnhoff-Hlavacek, "Data Bases for LDEF Results," LDEF First Post-Retrieval Symposium, NASA CP-3134, 1991, pp. 1223-1234.

3 M.D. Blue, "Degradation of Optical Materials in Space," NASA Contract Number NAS1-14654, April 1993.

4 D.E. Wiedlocher and D.L. Kinser, "Cratering in Glasses Impacted by Debris of Micrometeorites," LDEF Second Post-Retrieval Symposium, NASA CP-3194, 1993, pp. 534ff.

5 L.L. DeHainaut, "Degradation of Optical Components in a Space Environment, Experiment M0003, Subexperiment 2," internal report, Phillips Laboratory, Kirtland Air Force Base, NM, July 23, 1993.

6 G.A. Harvey, "Organic Contamination of LDEF," LDEF First Post-Retrieval Symposium, NASA CP 3134, June 1991, pp. 179-196.

7 G.A. Harvey, "Effects of Long-Duration Exposure on Optical System Components," LDEF First Post-Retrieval Symposium, NASA CP 3134, June 1991, p. 1327-1340.

8 K. Havey, A. Mustico, and J. Vallimont, "Effects of Long Term Space Environment Exposure on Optical Substrates and Coatings (S0050-2), Eastman Kodak Co., LDEF Second Post-Retrieval Symposium, NASA CP-3194, 1993, pp. 1389-1397.

9 J. Charlier, "Vacuum Deposited Optical Coatings Experiment," LDEF First Post-Retrieval Symposium, NASA CP-3134, 1991, pp. 1343ff.

10 J. Vallimont and K. Havey, "Effects of Long Term Exposure on Optical Substrates and Coatings (S0050-2)," Eastman Kodak Co., LDEF First Post-Retrieval Symposium, NASA CP-3134, 1991, pp. 1341-1342.

11 L.L. DeHainaut, J.R. Kenemuth, E.C. Tidler, and D.W. Seegmiller, "Degradation of Optical Components in a Space Environment," LDEF Second Post-Retrieval Symposium, NASA CP-3194, 1993, pp. 1361ff.

12 S.R. Gyetvay, J.M. Coggi, and M.J. Meshishnek, Aerospace Corporation LDEF M0003 Sample Observation Data Base, 1993.

13 R.C. Linton, R.R. Kamenetzky, and C.L. Burris, "LDEF Experiment A0034: Atomic Oxygen Stimulated Outgassing," NASA MSFC, LDEF First Post-Retrieval Symposium, NASA CP-3134, 1991, pp. 763ff.

[14] M.D. Blue, LDEF Active Optical System Components Experiment, LDEF First Post-Retrieval Symposium, NASA CP-3134, 1991, pp. 1317ff.

[15] M.D. Blue, "Degradation of Electro-Optical Components Aboard LDEF, LDEF Second Post-Retrieval Symposium, NASA CP-3194, 1993, pp. 1333ff.

[16] Optical Design, U.S. Government Publication MIL-HDBK-141, Military Standardization Series (5 October 1962), Paragraph 20.10.5.1.

[17] T.A. Mooney and A. Smajkiewicz, "Transmittance Measurements of Ultraviolet and Visible Wavelength Filters Flown Aboard LDEF," LDEF First Post-Retrieval Symposium, NASA CP-3134, 1991, pp. 1511ff.

[18] H.W. Dursch, W.S. Spear, E.A. Miller, G.L. Bohnhoff-Hlavacek, and J. Edelman, "Analysis of Systems Hardware Flown on LDEF - Results of the Systems Special Investigation Group, NASA Contractor Report 189628, Boeing, April 1992.

[19] G.J. Hawkins, J.S. Seeley, and R. Hunneman, "Exposure to Space Radiation of High Performance Infrared Multilayer Filters & Materials Technology Experiment (A0056)," LDEF First Post-Retrieval Symposium, NASA CP-3134, 1991, pp. 1477ff.

[20] J.W. Haffner et al, "Natural Environmental Effects on SDI Spacecraft Surface Materials," Rockwell International, Report No. AFGL-TR-89-0084, Air Force Geophysical Laboratory, May 20, 1989.

[21] G.N. Raikar, J.C. Gregory, and C.L. Christl, "The Interaction of Atomic Oxygen with Copper: An XPS, AES, XRD , Optical Transmission, and Stylus Profilometry Study, LDEF Second Post-Retrieval Symposium, NASA CP-3194, 1993, pp. 1169ff.

[22] T.M. Donovan, J.M. Bennett, R.Z. Dalbey, D.K. Burge, and S. Gyetvay, "Space Environmental Effects on Coated Optics," LDEF First Post-Retrieval Symposium, NASA CP-3134, 1991, pp. 1361ff.

[23] J.W. Watts, T.W. Armstrong, and B.L. Colborn, "Revised Prediction of LDEF Exposure to Trapped Radiation," LDEF Second Post-Retrieval Symposium, NASA CP 3194, 1993, Part 1.

[24] F. Bonnemason, "Ruled & Holographic Diffraction Gratings Experiment (A0138-5), LDEF First Post-Retrieval Symposium, NASA CP-3194, 1991, pp. 1301.

13.0 ELECTRONIC SYSTEMS

13.1 INTRODUCTION

The LDEF flight experiment provides most of the information available on the effects of the space environment on electronic systems. Information for this section was exerpted from the NASA Contractor Report by Harry Dursch.[1]

13.2 LDEF FLIGHT EXPERIMENTS

LDEF carried a remarkable variety of electrical and electronic systems, resulting from the great diversity in experiment objectives and approaches to data collection. Many experiments carried electronic components or systems, generally for data and control purposes. NASA also made available a data collection and storage system, the Experiment Power and Data System (EPDS). Hence, most of the electronics carried on LDEF were used to support active experiments, rather than being flown as part of an experiment. An exception was the Boeing Electronics Experiment, which was an investigation of the effects of LEO on inexpensive, commercial quality components.

It should be noted that very few electronic components were directly exposed to the external environment. Most electronic systems were shielded by metal enclosures and/or thermal control materials, and experienced only moderate temperature excursions above or below the nominal 0° to 25°C range. The discrete components of the Boeing Electronics Experiment were mounted on circuit boards in such a way that they were protected from direct exposure to the external environment, and many were powered up periodically during data collection periods. Post-flight data were compared against pre-flight data. No failures or significant degradation were observed.

Most systems had power applied only during short periods for control or data collection periods, not during the entire mission. This, plus the shielding, may explain the absence of any observed radiation effects. Generally, ionizing radiation effects require power to be applied, to redistribute and trap charge prior to recombination.

13.2.1 Electronic System Anomalies

Most LDEF components were not "space rated," i.e., they had not been subjected to the rigorous testing and inspections normally required of spacecraft system components (e.g., MIL-STD-883, Class S). Some were off-the-shelf commercial quality parts, while most were MIL-STD-883, Class B or equivalent. Table 13-1 shows the electrical anomalies that occurred during the LDEF mission, and Table 13-2 provides the details of the known component failures (ref 1.).

Table 13-1. Electrical System Anomalies

Anomalies	Description	LDEF Experiment
Relays and other Electromechanical Devices	One tray initiate relay failed	A0038
	MTM[1] 4-track changeover relay failed	S0069
	One unused status indicator failed	EIS[2]
System Anomalies	Only 1 of 35 pairs of pyro cable cutters fired	A0038
	Premature shutoff	A0076
	Clam shells not closed on retrieval	A0187-1
	Gulton data system failed after retrieval	S0014
	Magnetic tape took mechanical set	MTM's
	Magnetic tape oxide lost adhesion in dry N_2	A0180
Component Anomalies	E-cell coulombmeters leaked (5 of 70 = 7%)	A0038
	E-cell coulombmeters leaked (6 of 152 = 4%)	A0054
	Transistor/resistor failed	A0076
	One fiber optic cable severed by micrometeoroid impact	M0004
	DAC: bit 25 latched high	S0069
	NiCd battery cells bulging (may have been overcharged)	S1001

(1) MTM = Magnetic Tape Module
(2) EIS = Experiment Initiate System

Table 13-2. Known Electrical Component Failures

Part	Part Number	Manufacturer	LDEF Experiment
Relay, Latching	FL11D	P&B	A0038
Capacitor, Tantalum	137D, 33uF	Sprague	A0187-1
Indicator, Miniature	BHGD21T	Minelco	EIS
Transistor	JAN2N2222A	Unknown	A0076
Microcoulombmeter	550	Pacific Electron	A0038
Microcoulombmeter	500-0002	Plessey	A0054
Relay	J422D-12WL	Teledyne	S0069 MTM

13.2.2 On-Orbit Data Storage Systems

LDEF was a passive satellite with no telemetry of data to Earth during the mission. However, several experiments required on-orbit collection of data. Seven Experiment Power and Data Systems (EPDS's) were supplied by NASA, and two other experiments used data storage systems of their own design and construction. All EPDS units were similar, consisting of a Data Processor and Control Assembly (DPCA), a tape recorder (the Magnetic Tape Module (MTM), and two lithium sulfur dioxide ($LiSO_2$) batteries, all of which were attached to a mounting plate designed to fit into the backside of the experiment tray. The EPDS components were not directly exposed to the exterior environment, being protected by their mounting plate and by external thermal shields. Although simple compared with today's data systems, the EPDS contained many elements common to most such systems, including various control and "handshake" lines, programmable data formats and timing, and a data storage system. EPDS electronic components were procured to MIL-SPEC-883, Class B standards, and were not rescreened prior to installation. Data analysis and post-flight functional testing showed that all EPDS functioned normally during and after the LDEF flight.

During post-flight inspections, it was noted that the magnetic tape on all but one MTM unit had taken a "set" where it was wrapped around the phenolic capstan. The exception was the single unit which had operated periodically throughout the flight (experiment S0014). The MTM's were backfilled with dry nitrogen prior to flight. During post-flight deintegration at Lockheed, the tapes were exposed to a controlled humidity, and the mechanical set gradually disappeared. Evidently, some level of humidity is necessary in the sealed units to avoid this problem under long-term, inactive storage. Interestingly, it has been reported that a different type of tape (a ruggedized cassette) used in experiment A0180 did not encounter this problem even though it too had been backfilled with dry nitrogen. The University of Toronto used a custom-designed and built data storage system also based on the magnetic tape cassette concept. This unit performed as designed. All magnetic tape cassette recorders worked well. They are simple, well proven, and reliable. It has been speculated that outgassing of some other material in that tape recorder housing prevented excessive drying of the tape.[2,3]

The remaining data storage system was based on semiconductor technology using an Electrically Alterable Read Only Memory (EAROM)-based storage system. During post-flight inspection, it was determined that on-orbit data did not exist. The resulting failure analysis showed that data had been stored on the EAROM at one time, but failed to identify the cause of data loss. However, this particular EAROM is thought to be radiation sensitive.

13.2.3 Experiment Initiate System

The Experiment Initiate System (EIS) was the sole "communications" link between the spacecraft and the individual experiments. Its proper operation was vital to the success of all active experiments, for it provided the initiate signal to those experiments, directing them to turn on their power and begin their operational programs. Consequently it was designed conservatively and thoroughly tested prior to installation. It was located in the spacecraft interior in a well protected location, and was not exposed to extremes of temperature or other environmental hazards. The experiment initiate relays and related components (connectors and diodes) were also supplied by NASA, and were well proven, space-rated items. Complete isolation was maintained between the EIS ground return for these relays and the experiment electrical systems. Thus, the experiments only saw sets of contacts which were closed at initiation and opened when the EIS was reset. The original EIS design included use of two parallel systems, each capable of turning on up to 40 experiments. For the actual flight, however, only 24 initiate circuits were required, serving 20 experiments (some experiments utilized more than one initiate relay).

A task conducted early in the deintegration phase was to inspect and document the state of the visual indicators on the EIS control box, which provided a record that the experiment initiate latching relays had been activated. These small electromagnetic devices rotate a ball to display either black or white sides through a window. One was used for each of the 24 active experiment initiate relays. The signal to set the indicator to white came through a separate set of contacts on the experiment initiate relay. These could only be reset using ground support equipment (GSE), so a white indication was a reliable record that the relay had been set. Shortly after removal of the EIS from LDEF, it was tested at KSC using original GSE. The initial reset functional test was completely successful: all indicators which had been set (white) were observed to reset (black). However, when the system was given its first set test, it was noted that one of the previously unused visual indicators failed to shit from black to white, although its associated relay circuit functioned correctly. On two subsequent reset/set cycles, this indicator shifted properly when exercised.

The faulty indicator and three other spares were removed and transported to Boeing Space & Defense Group (ref. 1) for analysis. Two of the three extra units had not been connected and therefore had not been exercised. All units were subjected to marginal voltage testing at the minimum specified operating pulse width of 40 milliseconds. The three "spare" units all functioned consistently at 5V to 6V. The faulty unit, however, exhibited highly variable behavior, operating twice at 9.4V to 10.3V, and a third time at 5.6V. This type of

intermittence is characteristic of contamination, and indeed the failure was found to be caused by a small particle which could jam the magnet. Particle contamination is an all-too-common problem with small electromechanical devices, including relays.

It should be noted that the failing unit operated normally during pre-flight testing of the EIS, and under normal voltages and with long input voltage on-times. It is often necessary to subject components to testing at the limits of the manufacturer's specifications (e.g., voltage, temperature, pulse widths and timing) to detect marginal parts. These indicators did not receive such testing prior to use.

13.2.4 Wire Harnesses

The LDEF wire harness was essential to the success of all active experiments, as it carried the experiment initiate signals. It was assembled in-place on the LDEF frame, using Teflon insulated wire and nylon cable ties. Much of the harness also was protected by shielded braid and an outer Teflon jacket. The majority of the harness was well shielded from direct exposure to the external environment. Extensive testing included in-place visual inspection, connector disconnect torques, continuity measurements, and 500 Vdc insulation resistance.

All tests were nominal. There were no reported instances of experimenter-provided harnessing exhibiting deterioration of electrical properties.[4]

13.2.5 Relays

Electrical/mechanical relays continue to be a design concern. Two of the most significant LDEF active system failures involved relay failures. The Interstellar Gas Experiment was one of the more complex experiments on LDEF, with seven cameras located on four trays. Each camera contained five copper-beryllium foil platens, which were to sequentially rotate out of their exposed position at predetermined intervals. This experiment was never initiated due to a failure of the experiment's master initiate relay. The Thermal Control Surfaces Experiment recorded on-orbit optical properties of various thermal control coatings using a four-track MTM (the other six MTM's were two track). The latching relay which switched track sets failed to operate when switching from track 3 to track 4. Consequently, portions of the early flight data on track 1 were overwritten and lost (ref. 4).

13.2.6 Electronic Support Hardware

Most of the electronics carried on LDEF were used to support active experiments, rather than being flown as part of an experiment. An exception was the Boeing Electronics Experiment, which was an investigation of the effects of LEO on inexpensive, commercial quality components. These included a number of plastic packaged integrated circuits and discrete components such as transistors, resistors, capacitors, and diodes. A total of over 400 components were mounted on a pair of circuit boards with half the components conformally coated with Hysol PC18. All hardware was mounted such that they were protected from direct exposure to the external environment, and many were powered up periodically during data collection periods. Post-flight data were compared against pre-flight data. No failures or significant degradation were observed.

Many low cost, nonspace-qualified components performed quite well, without any measurable degradation. Hence, the use of commercial or Class B parts in space applications can survive long-term exposure to LEO and their use may often be justified for low cost systems when failures would not result in safety concerns or other major mission costs (ref. 4).

13.2.7 Electrical Systems Lessons Learned

Most electrical systems on LDEF performed well. Actual failures were few, and these appear to be caused by traditional culprits: design oversights; testing limitations, component or assembly problems. Lessons learned from these failures are listed below (ref. 1).

- No anomalies occurred which indicate any new, fundamental limitations to extended mission lifetimes in LEO. Protection from the effects of atomic oxygen, micrometeoroids, and ultraviolet radiation must be provided, however.

- In considering the impact of unexpected mission extensions, designers should examine circuit behavior as batteries approach their discharge state. Some circuits may continue to function (perhaps with changing characteristics) at much lower voltages than their normal limits, particularly when interfaced with other systems operating at higher voltages.

- A key requirement (in addition to following good design practices) is a well planned component and system test plan. Testing of components at temperature, voltage and timing limits, and extensive testing of systems (including thermal-vacuum and noise tolerance testing) is essential. This must include thorough evaluation of the interfaces between systems, and special efforts to detect unanticipated noise or spurious signals which can affect system timing or operation.

- Extensive UV, and atomic oxygen effects were observed on many experiments and on the LDEF structure. Use of metallized Teflon and other films resulted in quantities of loose, conductive material which could cause problems. This area requires considerably more investigation, including long-term degradation studies and controls on allowable materials for long mission lifetimes.

- Electromechanical relays are a continuing problem area, well known in many production situations. Efforts have been made in some systems to eliminate them entirely, substituting solid state switches, or utilizing other design approaches (e.g., redundancy, error detection and provision for reset). There is no simple solution, but part of the answer is to use well-qualified vendors with a proven track record of supplying high-reliability parts. In addition, testing at the component and the system level is essential.

- In a stand alone such as LDEF, with no monitoring of system performance during the mission, attention needs to be given to backup systems. On-board sensing of some critical activities, with provision for detecting failures and recycling those functions, may prevent loss of data. This requires a very thorough design review (e.g., Failure Modes and Effects Analysis) to anticipate possible failures and look for ways to minimize their effects. Designers should seek to avoid single-point failures which can shut down major portions or entire operating systems.

- New developments in imaging and data storage technology would make it possible to document the external appearance of a spacecraft such as LDEF, rather than be forced to relay on initial and final appearance. Such monitoring might detect deterioration prior to major problems, or document the time history of changes in future long life missions.

- Many low cost, non-space-qualified components performed quite well on LDEF, but there were several failures. The question of whether to permit use of commercial or MIL-STD parts in space applications is complex and involves many considerations. However, it is evident that such components can survive in some space applications, and that their use may be justified for low-cost systems when failures would not result in safety concerns or loss of mission objectives. Key to use of such components is conservative design and testing.

- Long-term storage of materials such as magnetic tape in a sealed enclosure filled with a low humidity gas can result in changes in mechanical properties, including adhesion and flexibility. Optimum storage conditions, including upper and lower limits on humidity, and considering effects of other volatile materials in the same enclosure may have to be determined for such materials on an individual basis.

REFERENCES

1 H.W. Dursch, W.S. Spear, E.A. Miller, G.L. Bohnhoff-Hlavacek, and J. Edelman, "Analysis of Systems Hardware Flown on LDEF - Results of the Systems Special Investigation Group," NASA Contractor Report 189628, April 1992.

2 R.C. Tennyson, G.E. Mabson, W.D. Morison, and J. Kleiman, "Preliminary Results From the LDEF/UTIAS Composite Materials Experiment," LDEF First Post-Retrieval Conference, NASA CP-3134, 1992, pp. 1057-1072.

3 R.C. Tennyson and R. Matthews, "Outgassing and Dimensional Changes of Polymer Matrix Composites in Space," LDEF Second Post-Retrieval Conference, NASA CP-3194, 1993, pp. 877-888.

4 H. Dursch, G. Pippin, and L. Teichman, "Summary of Materials and Hardware Performance on LDEF,"LDEF Materials Results for Spacecraft Applications," NASA CP-3257, 1994, pp. 355-369.

14 APPLICATIONS

This chapter provides design tradeoffs case studies for the design of components for future spacecraft missions. The intent is to illustrate the issues involved during the materials selectivity and the component design process, as well as to provide examples of materials performance data.

14.1 CERES INSTRUMENT

14.1.1 Introduction

The Cloud and the Earth's Radiant Energy System (CERES) instrument is designed to measure the total energy reflected or emitted from Earth. Hence, its objective is to measure the Earth's greenhouse effects. The CERES instrument is scheduled to be launched on the Tropical Rainfall Measuring Mission (TRMM) satellite in August 1997. Information in this section is based on work performed by TRW under the NASA LaRC CERES Contract NAS1-19039.

14.1.2 Space Environment

The CERES instrument is required to survive a total ram mission fluence of 8.9×10^{22} atoms of AO/cm^2 during the 3.55 year TRMM orbit without significant degradation in performance. However, the CERES instrument will be exposed to less than the total ram mission fluence due to orientation of the spacecraft, co-rotation of the atmosphere, and other factors. Therefore, the adjusted worse case total AO fluence exposure predicted for the ram facing pedestal is 5.20×10^{22} atoms/cm^2 over the 3.5 year operating period on TRMM.

14.1.3 Thermal Control Applications: Radiators and MLI Blankets

The CERES instrument baseline thermal design control materials are based on the space environments specified for the Earth Observing System (EOS) platform and for TRMM platform. These materials are presented in Table 14-1.[1]

Table 14-1. CERES Baseline Thermal Design Control Materials

Application	Thermal Control Material
Radiators	2" wide perforated 5.0 mil Type A Teflon x vacuum deposited silver x vacuum deposited Inconel x 966 acrylic pressure sensitive adhesive tape
Multilayer Insulation (MLI) Blankets*	3.0 mil Type A Teflon x vacuum deposited aluminum outer layer
	10 - 0.3 mil Kapton x vacuum deposited aluminum filler layers
	2.0 mil Type A Teflon x vacuum deposited aluminum inside layer
	1" & 2" wide perforated 3.0 mil Teflon x vacuum deposited aluminum x 966 acrylic pressure sensitive adhesive tape (used for fastening MLI)
*Aluminized Teflon was previously chosen for the baseline MLI blanket material since Teflon performed satisfactorily in prior AO environment assessments. However, since an alternative blanket material is clearly required for the TRMM, the CERES baseline MLI blanket material has been changed recently to aluminized Kapton because it is more cost effective and easier to procure than aluminized Teflon. In addition, the aluminized Kapton MLI is sufficient to satisfy the thermal design requirements for CERES.	

Since the preliminary selection of the CERES instrument baseline design, published LDEF data point to higher erosion rates for certain CERES thermal design materials, such as FEP Teflon, than previously predicted. In addition, since the retrieval of the LDEF in 1991, new data have become available regarding the resistance of materials to degradation in such an environment. This section investigates materials that exhibit a high AO resistance for the specified environment. A summary of an atomic oxygen materials trade study is presented in Table 14-2 (ref. 1). Candidate materials investigated in this study are listed in decreasing order of recommendation. Key factors considered in this trade are discussed in the subsequent sections below.

Table 14-2. Atomic Oxygen Materials Trade Off Study for Thermal Control Applications

	CANDIDATE MATERIAL	HERITAGE	AVAILABILITY	TRW EXPERIENCE	BOL	EOL	COST	ADVANTAGES/DISADVANTAGES
					a/s	a/s		
RADIATORS	5 mil Silver Teflon Tape (SiOx)	At the time of this study, SiOx coated Silver Teflon tape had not been flight or ground tested in a reliable experiment.	Outside Vendor - Custom (Sheldahl)	CERES personnel have experience with application and handling of Silver Teflon Tape. TRW personnel are familiar with application and handling of other coated tapes such as ITO.	0.09/0.75*	~0.09/0.75	Material - medium to high; Labor - low	Excellent AO Resistance; TRW familiar with handling, repair, and processing. Minimal impact to current project planning.
	10 mil Silver Teflon Tape (Untreated)	TRW uses Silver Teflon Tape on many of their spacecraft and instruments including the CERES predecessor, ERBE.	Outside Vendor - Custom (Sheldahl)	CERES personnel have experience with application and handling of Silver Teflon Tape.	0.10/0.85*	~0.09/0.55	Material - low; Labor - low	Poor AO resistance; TRW familiar with handling, repair, and processing; No impact to current project planning. Cost effective.
	Second Surface Mirrors (Fused Silica)	TRW uses Fused Silica Second Surface Mirrors on many of their spacecraft and instruments such as VUE.	Outside Vendor	TRW personnel have experience with application and handling of Second Surface Mirrors.	0.066/0.75	~0.006/0.75	Material - high; Labor - high	Can be used on flat surfaces only. Silver Teflon tape or similar material must be used on curved surfaces. Requires silicone adhesive which generates contamination when exposed to AO.
	Z-93	Z-93 has been flown on LDEF. TRW has used Z-93 on many of their spacecraft such as DCSC-2 and TDRSS.	Outside Vendor (IITRI)	TRW personnel have experience with the application and handling of Z-93.	0.14/0.91#	0.15/0.92#	Material - high; Labor - high	Excellent AO resistance.
	MS-74 / YB-71 (Zinc Orthotitanate)	ZOT paints have been used on many of TRW's spacecraft such as DSP and Mil-Star. YB-71 has also flown on LDEF.	GFE/Outside Vendor (MSFC/IITRI)	TRW personnel have experience in the application and handling of ZOT paints other than MS-74.	0.13/0.90#	0.15/0.89#	Material - low (GFE) or high, Labor - high	Excellent AO resistance. Handling, cleaning, and repair difficult; Generates ground particulate contamination.
	S13G/LO	TRW uses S13G/LO on many of their spacecraft such as the GRO. This paint has also flown on LDEF.	Outside Vendor (IITRI)	TRW personnel are familiar with application and handling of paints such as S13G/LO.	0.18/0.90#	0.37/0.89#	Material - high, Labor - high	Yellows upon exposure to AO.
BLANKETS (OUTER LAYER)	3 mil Aluminized-Kapton MLI (SiOx)	Baselined for Space Station Solar Array Panels. Extensive AO ground simulation testing performed by NASA Lewis Research Center, Sheldahl Inc., and LMSC.	Outside Vendor - Custom (Sheldahl)	TRW personnel are familiar with manufacturing/procurement and handling of Aluminized-Kapton MLI. TRW personnel are familiar with coatings which are similar to SiOx such as ITO.	0.46/0.77*	~0.44/0.71	Material - low; Labor - low	Excellent AO resistance. TRW familiar with handling, repair, and processing.
	3 mil Aluminized-Teflon MLI (SiOx)	None	Outside Vendor - Custom (Sheldahl)	TRW personnel are familiar with manufacturing/procurement and handling of Aluminized-Teflon MLI. TRW personnel are familiar with coatings which are similar to SiOx such as ITO.	0.14/0.65*	~0.14/0.60	Material - medium to high, Labor - low	Excellent AO resistance. TRW familiar with handling, repair, and processing.
	S13G/LO	TRW uses S13G/LO on many of their spacecraft such as the GRO. This paint has also flown on LDEF.	Outside Vendor (IITRI)	TRW personnel are familiar with application and handling of paints such as S13G/LO.	0.18/0.90#	0.37/0.89#	Material - high, Labor - high	May be applied to blankets. Yellows upon exposure to AO.
	Beta Cloth	Beta cloth is used widely as a thermal blanket by the Shuttle. TRW has used Beta cloth on spacecraft such as GRO.	Outside Vendor - Custom (Sheldahl)	TRW personnel are familiar with manufacturing/procurement and handling of Beta Cloth MLI.	0.22/0.90	Not Available	Material - high, Labor -low	Significant source of on-orbit contamination when exposed to AO. Difficult to form into a blanket. Blanket must be pre-formed prior to use.
	Aluminized-Teflon MLI (Untreated)	Aluminized-Teflon MLI blankets have been flown on TRW spacecraft such as DCSC-2.	Outside Vendor - Custom	TRW personnel are familiar with manufacturing/procurement and handling of Aluminized-Teflon MLI.	0.14/0.6*	Completely erodes	Material - medium, Labor - low	Substantial erosion with AO exposure.
	Aluminized-Kapton MLI (Untreated)	TRW uses Aluminized-Kapton MLI on many of their spacecraft and instruments including the CERES predecessor, ERBE.	TRW Standard Stock	TRW personnel are familiar with manufacturing/procurement and handling of Aluminized-Kapton MLI.	0.46/0.77*	Completely erodes	Material - low; Labor - low	Substantial erosion with AO exposure.
	Chromic Acid Anodize/Aluminum	Used on [illegible] in flat applications.	Outside Vendor - Custom	TRW uses anodization processes over metals in many of their designs. Anodization is generally applied to rigid surfaces and not recommended for flexible applications. TRW does not generally use chromic acid anodization.	0.40/0.84#	0.47/0.84#	Material - high, Labor - medium	Excellent AO resistance. Good thermal properties; Incompatible with propellant by-products.
	MS-74 / YB-71 (Zinc Orthotitanate)	TRW is not familiar with the use of ZOT paints as overcoats in blanket applications.	GFE/Outside Vendor (MSFC/IITRI)	TRW's experience with ZOT paints is that it is an extremely brittle paint. TRW does not recommend using these paints as an overcoat in a blanket type application.	0.13/0.90#	0.15/0.89#	Material - high, Labor - high	Excellent AO resistance. Paint not well suited for blanket application.

Notes: * Reference 2
Reference 3

14.1.3.1 Silicon Oxide Coatings

14.1.3.1.1 SiO_x Coated Kapton

SiO_x coated Kapton was chosen as the baseline design material by the Lockheed Missiles and Space Company (LMSC) for use on the solar array panels of the Space Station Freedom (SSF), now the International Space Station Alpha. The SiO_x coating, produced by Sheldahl Inc. for LMSC, is a 1300 Å thick sputter deposited overcoating. The total AO mission fluence requirement for SSF is 5.0×10^{22} atoms/cm^2 at the ram facing CERES pedestal during the TRMM mission.

The SiO_x coating is an effective barrier against AO. AO plasma asher testing of the SiO_x coated Kapton performed at NASA Lewis Research Center indicated that the erosion rate of SiO_x coated Kapton is reduced to 1% the erosion rate of unprotected Kapton.[4] The amount of erosion of SiO_x coated Kapton which occurs upon exposure to AO is due to pinhole defects in the SiO_x coating which allow a small amount of AO to reach the Kapton. These results indicate that 88% of the Kapton blanket will remain after 15 years in LEO on SSF. Tests were also conducted on samples of SiO_x coated Kapton which had undergone a lamination process to determine if the scratches introduced during the handling of the SiO_x coated Kapton decrease the effectiveness of the SiO_x to protect the Kapton. However, the erosion rate of the SiO_x coated Kapton after handling is still very low - the erosion rate for the handled sample was measured to be 10% of the erosion rate for unprotected Kapton.

Tests were also conducted at NASA Lewis to determine the effect of Kapton surface roughness on erosion rate.[5] The roll side of Kapton is inherently rougher than the air side of Kapton. It was determined that the roll (rough) side of the Kapton had more pinhole defects and hence a higher erosion rate than the air (smooth) side of the Kapton. LMSC has chosen to have the roll side of the Kapton facing towards the environment because it is not as tacky as the smooth side. This is an important factor in the LMSC design because the solar array is folded during launch and unfolds during deployment. Since CERES does not have this unfolding deployment requirement, the air (smooth) side of the Kapton, which has inherently less defects, was selected by TRW.

In terms of handling, the SiO_x coating produced for LMSC is fragile and easily scratched. The SiO_x coating is clear, so once the materials are applied or bonded onto the radiator surface, there is no practical way to inspect for scratches. LMSC's approach is to accept a certain amount damage and hence erosion.[6] Since it has been demonstrated by tests performed at NASA Lewis

Research Center that the scratches introduced as a result of handling only increase the erosion rate slightly, LMSC is in the process of testing additional samples which have been cycled through the fabrication and assembly process in order to further quantify the increase in erosion rate. However, the advantage in using the SiO_x coated products is that the application, cleaning, and repair of the thermal materials is very similar or identical to the methods used for uncoated materials. LMSC is using the SiO_x coated Kapton on radii as small as 30 mil, which is consistent with the smallest on the CERES instrument, without having problems with the flexibility of the material of causing damage to the SiO_x layer.

14.1.3.1.2 SiO_x Coated Aluminized Teflon and Aluminized Kapton

Samples of 5.0 mil Type A Teflon/vacuum deposited silver/vacuum deposited Inconel/966 acrylic pressure sensitive adhesive tape (uncoated and SiO_x coated on Teflon side) and samples of 2.0 mil Type H Kapton/vacuum deposited aluminum (uncoated and SiO_x coated on Kapton side) are available from Sheldahl, Inc. A Sheldahl proprietary ion-beam assist process applies the SiO_x coating to the substrate in thin layers by allowing multiple passes of the depositing cathode. The total SiO_x coating thickness resulting from the multiple pass application process is 1000 Å. This is in contrast to a 1300 Å thick SiO_x coating produced using a single pass sputtering process resulting in.

The 1000 Å SiO_x coated is expected to exhibit superior handling and AO resistance qualities than the 1300 Å SiO_x coated materials. According to TRW Contamination Engineers, any particulate flakes which result from handling the 1000 Å SiO_x coated Kapton are not large due to the thinness of the SiO_x layer. With the ion-beam assisted SiO_x coated materials, it is expected that even less, if any flaking would result during handling of the material. Since the ion-beam assist deposition process involves the application of very thin multiple layers, any particulate flakes generated as a result of handling would be even smaller than the particulate flakes generated from handling of the 1300 Å material. It is recommended that a particle counter be mounted during plasma asher tests at NASA Lewis Research Center so that a reliable particle count can be obtained.

According to Sheldahl, the materials coated with the multiple pass ion-beam assist process exhibit excellent handling qualities. The SiO_x adheres so well to the substrate, that when a MIL-STD adhesion test is conducted, the adhesive is pulled off the tape and sticks to the SiO_x coating. The SiO_x coating produced by the ion-beam assist process also contains less pinhole type defects due to the multiple passes of the depositing cathode. Pinhole defects have been shown to decrease the AO resistance of the LMSC material.

The cost of the SiO_x coated materials is approximately two to three times the cost of uncoated materials. This additional cost includes testing of optical properties, thermal shock, adhesion, blocking, flexibility, outgassing, thermal cycling, solvent wipe, and humidity resistance. Sheldahl estimates a procurement time of eight to ten weeks. Sheldahl recommends that the SiO_x coated materials be handled with plastic gloves. Cloth or nylon gloves are not recommended since human oils may leach through these types of gloves. The SiO_x coated materials may be cleaned using alcohol and a soft cloth or "rimple" cloth. Repairs or patching is performed by applying an SiO_2 adhesive promoter over the area in need of repair.

An alternate coating is the use of a 1000 Å Teflon amorphous fluoro-polymer (Teflon A.F.) over the SiO_x coating. Application of the Teflon A.F. film over the SiO_x coating has the added benefit of filling pinholes in the SiO_x coating and reducing scratches during the handling of the SiO_x.

14.1.3.2 Unprotected Teflon/Kapton

Both unprotected Teflon and unprotected Kapton degrade severely when exposed to atomic oxygen. The option of using a 3 mil outer blanket layer of either unprotected Teflon or unprotected Kapton is undesirable because the material would be eroded in the TRMM environment. Increasing the thickness of the blanket outer layer to counteract erosion effects would make the material too stiff to work with. In terms of using unprotected Teflon or unprotected Kapton in a MLI blanket application, it is recommended that an alternate design be implemented.

An option considered for the CERES radiators was to increase the thickness of the unprotected Silver Teflon Tape to 10 mil. After the 3.5 year TRMM mission, approximately 2 mil Teflon would be remaining. From LDEF, it was observed that as long as approximately 2 mil of Teflon was remaining, the thermal performance of the system would not be severely degraded.[7,8]

TRW has used silver Teflon tape on many of its spacecraft and instruments including the CERES predecessor, ERBE. CERES manufacturing personnel are familiar with the application, handling, repair, and cleaning of silver Teflon tape. The use of silver Teflon tape for the radiators would be the least impact to the CERES program in terms of cost and schedule.

The major disadvantage of the silver Teflon tape is the erosion which occurs on-orbit. Although the major by products of the erosion process are gaseous and are not detrimental to the

performance of the CERES instrument, it has been theorized that the fluoride in FEP Teflon was a major contributor to the build-up of a contamination layer on LDEF (ref. 3).

14.1.3.3 Fused Silica Second Surface Mirrors

Fused silica second surface mirrors were used on the radiator surfaces of the VUE instrument. Fused silica is stable in LEO, however it has been determined that the silicone adhesive required to bond the mirrors to the radiator surfaces is incompatible with the AO environment. Silicones were a major contributor to the contamination layer on LDEF and have been demonstrated to promote degradation by AO (ref. 3). Hence, it was recommended that second surface mirrors not be used in the CERES thermal design.

14.1.3.4 White Silicate Paints

White silicate thermal control paints, such as Z-93, MS-74, and YB-71, perform extremely well in Low Earth Orbit. Although it has been demonstrated in ground simulation testing that these white paints discolor under severe AO environments, the phenomena has not been observed on actual flight samples.[9] MS-74 white silicate paint will be used on the TRMM spacecraft and is manufactured by GSFC. YB-71 and Z-93 which are manufactured by IITRI, have both been used by TRW in spacecraft thermal designs. The white silicate paints perform extremely well in an AO environment and are well suited for application on large, flat surfaces. TRW does not recommend the use of brittle paints such as MS-74, Z-93, or YB-71 as coatings on blankets. S13G/LO which is a more flexible formulation, has been used as a blanket coating on spacecraft such as the Gamma Ray Observatory (GRO). However, S13G/LO yellows upon exposure to AO as demonstrated on LDEF (ref. 3).

The main concern with the use of MS-74 or similar paints on the radiator surfaces for the CERES instrument is that it is extremely brittle and would generate particulate contamination during handling. Repairs are performed by sanding the surface and reapplying the paint. General cleaning is difficult. TRW spacecraft personnel design lucite or fiberglass shields to protect the painted surfaces during handling. This additional engineering effort would need to be performed for CERES if a white paint is chosen for the radiator surface. In addition, the labor associated with the application of white paint would have to be factored into the cost and schedule. The use of white paint on the CERES radiator surfaces is recommended only after all other feasible methods have been considered.

14.1.3.5 Beta Cloth

Beta cloth has been used for MLI blanket material on the Shuttle and many other spacecraft and is baselined for the Space Station. Although beta cloth lends the durability and AO resistance necessary for the TRMM environment, research recently performed from LDEF hardware indicate that beta cloth may be a significant source of on-orbit contamination (ref. 3).

In terms of instrument assembly, the major disadvantage of beta cloth is that the blankets would have to be performed prior to use. With Teflon or Kapton MLI, the material is cut to approximate size, and taped in place so that the contours of the MLI can be easily changed.

14.1.3.6 Chromic Acid Anodization

Chromic acid anodize coating was used on the clamps and experiment trays on the LDEF. Results from LDEF indicate that chromic acid anodized surfaces did not degrade upon exposure to AO. However, the chromic acid anodize finishing process is not well suited for a blanket application since the anodize process stiffens the aluminum making it too difficult to work with. The main limitation with the chromic acid anodization process is that it is incompatible with nitric acid which is a by-product of many propellants. Since the CERES instrument sees a large majority of the thruster contamination produced on TRMM, it is recommended that an alternate material be chosen.

14.1.4 Recommendations

The use of SiO_x coated aluminized Teflon tape and SiO_x coated Kapton MLI blankets for the TRMM instrument is highly recommended. Data generated from ground simulation testing indicates that 88% of the LMSC Kapton solar blanket will remain after 15 years of LEO on SSF. Although it has been demonstrated in ground simulation testing that SiO_x coated Kapton is prone to AO undercutting via inherent manufacturing pinhole defects or via scratches caused by handling, Monte Carlo modeling predicts that the mass loss of SiO_x overcoated Kapton upon exposure to actual space conditions is approximately 1/3 of the mass loss observed in plasma ashers.[10] In addition, SiO_x coatings applied to CERES thermal materials would be deposited with a different process which produces superior coatings than the SiO_x coating produced for LMSC.

Similar tests should be performed on SiO_x coated Teflon as were performed on the SiO_x coated Kapton. LMSC recommends that the amount of inherent manufacturing pinhole defects produced as a result of the SiO_x application process be closely scrutinized since FEP Teflon has a higher thermal expansion coefficient than Kapton. This difference in thermal expansion coefficients may lead to higher induced stresses in the SiO_x coating over Teflon than over Kapton.

14.2 TROPICAL RAINFALL MEASURING MISSION

14.2.1 Introduction

TRMM (Tropical Rainfall Measuring Mission) is a joint United States and Japan observatory program that will conduct systematic measurements of tropical rainfall required for weather and climate research. Launch date is scheduled for August 1997 using the Japanese H-11 rocket. NASA Goddard Space Flight Center is responsible for designing, building, and testing TRMM. Information for this section is based on the paper presented by S.A. Straka at the LDEF Third Post-Retrieval Symposium.[11]

14.2.2 Space Environment

The LEO environmental concerns for the TRMM mission are summarized in Table 14-3.

Table 14-3. Environmental Issues for the TRMM Mission

Environmental Issues	Comments
Maximum solar activity expected to occur	• April 2000 (Nominal phasing)
High atomic oxygen fluence predicted	• Design Requirement: 8.9×10^{22} atoms/cm^2 • Fluence is 10 times higher than LDEF ram direction • Fluence is almost double Space Station design AO fluence
Mechanism exists for SiO_x buildup	• Reaction between outgassed silicones and atomic oxygen can form a permanent contaminant layer • TRMM's major on-orbit contamination concern
Mechanism exists for glow to occur	• Mechanisms not well defined • Atomic oxygen and atomic nitrogen involved in reaction

Spacecraft material degradation expected	• Resulting from interaction with atomic oxygen or synergetic effects between atomic oxygen, solar UV, and temperature
	• Commonly used spacecraft outer layers will not survive mission
	• Material thicknesses required to survive mission based on LDEF and Shuttle erosion rates:
	  • Kapton > 105 mil
	  • Z306 > 12 mil
	  • Teflon > 13 mil
	  • Carbon Epoxy > 91 mil
	  • Unprotected Silver > 368 mil
	• All exterior surfaces need to be protected against atomic oxygen since spacecraft has no true "wake"

Ambient atmosphere approximately 26 times the density at 600 km	• Thrusters fire approximately every two days to maintain orbit near end of mission • High return flux to spacecraft • High potential for contamination build-up
Ambient Density "build up" around spacecraft	• Areas between solar array and spacecraft

14.2.3 Thermal Control Application

14.2.3.1 Multilayer Insulation Outer Layer Trade Off Study

OCLI Proprietary Coating Over VDA Backed White Tedlar. This TRMM primary MLI outer layer material is described in Table 14-4.:

Table 14-4. OCLI Proprietary Coating Over VDA Backed White Tedlar MLI for TRMM

Material Layers	Comment
OCLI proprietary coating	Developed by Optical Coating Laboratories, Inc. Coating consists of 11-13 layers of 3 oxides
White Tedlar (substrate)	1.5 mil polyvinylflouride film produced by DuPont Thermal properties: $\alpha = 0.301$, $\varepsilon = 0.890$
Vapor Deposited Aluminum (VDA)	Applied for conductivity Thickness 350Å
Scrim	Attached to back for added strength

Sheldahl SiO_x Over Kapton or Beta Cloth. This MLI material is for instruments and back-up spacecraft MLI materials.

14.2.3.2 Radiator Surfaces Trade Off Study

Materials selected for the radiator are summarized in Table 14-4.

Table 14-5. Radiator Surfaces Trade Off Study

Material	Status	Comments
MS 74 white silicate paint	Yes	UV and AO stable Low outgassing properties
OSRs	Yes	Used on instruments
OCLI over White Tedlar	Yes	Used on instruments
IITRI Z-93P white paint	Yes	Reformulation of the Z-93 paint flown on LDEF due to change in the potassium silicate binder
Vapor deposited aluminum	Yes	Used on a cooler
Silver Teflon	No	Erosion of Teflon is a synergetic effect between AO, UV, and temperature 13 mil of Teflon will be eroded on TRMM based on LDEF measured erosion rates Protective coatings do not adhere to the Teflon

14.3 SPACE STATION FREEDOM

14.3.1 Introduction

Long-life, manned space stations are one of the important space structures receiving attention today. Such stations must be constructed from long-life materials, structures, and components to minimize external maintenance by suited astronauts/cosmonauts, since extravehicular activities (EVA) are very restricted. For Space Station Freedom (SSF), now called the International Space Station Alpha, the goal was to provide 30-year life with as little maintenance and servicing as possible.

The following sections present the material trade studies (refs. 12 17) that were conducted for the Space Station Freedom (SSF), now called the International Space Station Alpha. The goals for the Space Station Freedom, intended for a 28.5° orbit inclination at an altitude between 180 to 240 nm, was to provide 30-year life with as little maintenance and servicing as possible. Although the International Space Station Alpha is being considered for a higher orbit inclination of 51.6° at 230 nm and for only a 10-year mission, the results of these material trade studies can provide utility for spacecraft designers considering similar space environmental interactions.

14.3.2 Space Environment

At an orbital inclination of ±28.5°, the environments that influenced the material selections for SSF are AO, UV, micrometeoroid and debris, vacuum, and the day-night cycle. Penetrating radiation was analyzed based on th expected dosage at the end of 30 years, and few materials approached the threshold dosage at which degradation begins. In contrast, for higher orbital inclinations of ±60°, which is now being considered for the International Space Station Alpha, penetrating radiation effects are a more important consideration.

14.3.3 Design Considerations

14.3.3.1 Thermal Control Applications

The requirement for long life in LEO at relatively low altitudes precludes many of the thermal control coatings that have been used on other programs. Organic coatings will erode in an AO environment unless they are on the wake side of the spacecraft. To minimize the number

of different finishes for hardware exposed to the environments, it is proposed to maximize the use of coatings that will provide the desired thermal properties and survive in all locations.

The material properties that control surface temperatures are absorptivity (α), emissivity (ε), and the ratio of these two properties. Optical property requirements for the Space Station include a low α/ε ratio coating for the radiators, and coatings with α/ε ratios near 1:1 to minimize the use of heaters where equipment must be maintained at relatively high temperatures. Hence, the higher the α/ε ratio, the higher the temperature of the part. One important restriction on the α/ε ratio is that an astronaut's glove should not contact surfaces hotter than 112.8°C for more than 30 seconds. Meeting this restriction is easily achieved as long as the α/ε ratio does not exceed a limit that is determined by the mass of the object, solar exposure of the surface, and other geometric considerations.

14.3.3.1.1 Anodized Aluminum Structure

Anodizing is recommended for all Space Station exposed aluminum hardware (e.g., truss structure, utility trays, HVI shields) except the radiators, which have extremely low α/ε requirements.[12,13] Anodized aluminum provides a corrosion-resistant coating on the ground, is resistant to AO in space, and reduces spectral reflection.

Aluminum anodizing using chromic or sulfuric acid can produce α/ε ratios between 0.2 and 2.0. In addition, adding inorganic dyes to sulfuric acid anodized aluminum can produce additional optical property options. Table 14-6 lists the optical properties of a number of chromic acid and sulfuric acid anodized aluminum alloys. The optical properties of chromic acid anodizing (CAA) can be varied over a wider range than sulfuric acid anodized (SAA) surfaces, but CAA requires greater process control to ensure repeatability to obtain the desired optical properties. Based on the processing studies conducted at McDonnell Douglas sulfuric acid anodizing was selected as the baseline for the 2219-T851 aluminum truss structure.

Table 14-6. Optical Properties of a Number of Anodized Aluminum Alloys

Alloy	Anodizing process			
	Chromic		Sulphuric	
	α	ε	α	ε
2219-T37 sheet	0.42	0.71	0.35	0.82
5052-H34 sheet	0.55	0.60	0.32	0.82
5657-H25 sheet	0.45	0.55	0.16	0.80
6061-T6 sheet	0.43	.0.50	0.40	0.84

Changes in thermal control coating properties are viewed as critical. Temperature changes associated with changes in absorptivity are not considered important for the truss tubes and utility trays. For the HVI shields and equipment covers, which are used for thermal control when no protection from HVI is required, changes in thermal control properties are important due to the maximum touch-temperature limits for the astronauts. An α/ε ratio of greater than 1:1 minimizes heat loss, reducing the need for heaters. Although there has been no final design decision, an α/ε ratio of less than 1:1 for the shields and covers allows for an increase in absorptivity due to UV radiation or contamination deposition without exceeding temperature limits.

Although anodic coatings offer many attractive features, there are a number of unfavorable characteristics that must be accommodated in a design. Because UV radiation normally causes the absorptivity of anodic coatings to increase with exposure while the emissivity remains constant, the α/ε increases. The coating should be designed to accommodate this increase without exceeding the allowable touch temperature limits. UV exposure of uncontaminated sulfuric acid anodized 2219-T851 samples resulted in no change in absorptance although a small increase occurred after AO exposure. This was in contrast to the nonstructural, low absorptance aluminum alloys that had been tested previously which showed substantial increases in absorptance when exposed to VUV (see Table 14-7) (ref. 13). In addition silicone contaminated sulfuric acid anodized 2219-T851 samples exposed to VUV exhibited no changes in optical properties after exposure. The results were so surprising that surface analyses were conducted which verified the presence of the silicone contaminant. The tests were repeated and the same results were obtained. The thickness of the contamination layer was slightly less than 4000Å and only one type of silicone oil was used as a model material. No fundamental understanding has been developed to explain why the absorptance did not increase. More details of the experiments conducted can be found in the reference by C.A. Jones et al.[14]

Table 14-7. Environmental Exposure of Clean and Silicone Contaminated 2219 and 7075 Aluminum

Alloy	Coating and Condition	Exposure	Results
2219-T851	SAA, Clean	Near UV	No change
		VUV	No change
		AO	$\Delta\alpha$ = -0.03
	SAA, Contaminated ≤ 4000Å	VUV	No change
7075-T7351	SAA, Clean	AO	No change
		VUV	$\Delta\alpha$ = +0.04
7075-T6 clad	Black SAA, clean	VUV	No change
	Black SAA, Cor taminated 375 Å - 4000Å	VUV and AO	No change

Absorptance/emittance ratio of approximately one can be provided by an anodizing process with inorganic black dyes known as the "Duranodic process." Trade studies and evaluations conducted leading to this selection are reported by the study of R.J. Le Vesque et al.[15] BOL tolerances were tighter than for standard SAA. Contamination deposition and UV exposures showed that the absorptance of this coating was not changed just as had been found for the standard SAA (see Table 14-5).

Commercial sulfuric acid anodizing processes including the Duranodic process were found to provide consistent, reproducible results, avoiding the need for additional specialized processing controls. Furthermore, for the alloys tested, no change in absorptance on VUV exposed, silicone contaminated samples was seen. These results were completely unexpected based on the literature data and the increases in absorptance seen on the CAA specimens on LDEF. These results are shown in Table 14-5.

Finally, anodic coatings can also begin to craze if thermally cycled, particularly when cycled to high temperatures. In one study, this crazing increased the absorptivity of several nominally 0.025 mm thick anodized coatings by about 0.02 to 0.03 and decreased emissivity by 0.04 to 0.07.[16] Other investigators using other alloys have reported no change in optical properties with thermal cycling.

14.3.3.1.2 Radiator Thermal Control Coatings

The original baseline for the large radiators was 5-mil thick embossed silver-Teflon. With the higher Teflon erosion rates experienced on LDEF, it would have been necessary to increase the Teflon thickness from 5 to 10 mils. This led to a trade study comparing 10 mil silver-Teflon with Z-93 inorganic paint and anodized 5657-H25 aluminum. Table 14-8 shows the number of panels required for various thermal control coatings for a continuously rotating radiator (ref. 12).

Table 14-8. Panels Required for a Continuously Rotating Radiator for Different Coatings

Coating	BOL α/ε	EOL α/ε	Total no. of station panels	Approx. weight change (kgs)
Z-93 (design baseline)	0.17/0.91	0.3/0.90	84	-540
Silver Teflon 10 mil (proposed) 5.5 mil - (original baseline)	0.09/0.92 0.08/0.83	0.2/0.81 0.2/0.65	88 104	0 +1220
Anodized 5657 Al (design values)	0.19/0.90	0.4/0.85	92	0

Because of the 1200 pound weight savings, and the excellent performance of Z-93 on LDEF, Z-93 was selected for the new baseline for the active thermal control radiators as well as for many smaller, passive radiators.

For weight economies, McDonnell Douglas designers selected 2219 Al for the passive radiators rather than 6061 aluminum, the latter being the substrate most commonly used for Z-93. Since 2219 Al has poorer corrosion resistance, an evaluation was made of whether Z-93 could be applied to anodized aluminum, a process which had not been seriously studied previously. The results were highly successful and the baseline was changed from applying Z-93 to bare 2219 Al to applying Z-93 to anodized 2219 aluminum. The application of Z-93 to anodized aluminum is now generally accepted.

The margins associated with thermal activities required a high confidence in the optical properties used. Measurements of the absorptance of Z-93 by various instruments led to the understanding that significantly different results are obtained depending on the instrument. A comparison of three instruments is shown in Table 14-9 (ref. 12).

Table 14-9. Comparison of Z-93 Absorptance Measurements with Three Different Instruments

Measurement Device	Absorptance Value
Gier-Dunkle MS-251	0.101
Spectrophotometer, Perkin-Elmer Lambda 9	0.134
Surface Optics Spectrophotometer and Infrared Reflectometer	0.169

The results using an infrared reflectometer that measures reflectance from 1.6 to 25.0 microns showed that there is a large drop in reflection between 2500 and 3000 nanometers and the reflection remains low above 3000 nanometers. Spectrophotometers used to measure solar absorptance have a cutoff at or below 2500 nm. The true thermal behavior of Z-93 is best approximated by the value 0.169 instead of 0.12, which was used in conjunction with tolerances in our thermal design analysis. The differences described above had not been reported previously in the open literature. Most other coatings tested did not exhibit such differences because their reflectance's did not change as dramatically as Z-93 in this region, in which there is still a significant portion of solar energy present.

14.3.3.1.3 Multilayer Insulation (MLI) Blankets

MLI blankets are efficient, lightweight insulation systems for use in a vacuum. They have not been designed and qualified with AO-resistant outer layers. The outer layers of these blankets frequently use materials such as Kapton and Mylar (DuPont trademarks), which are eroded by AO. In order to achieve long life for blankets directly exposed to the LEO environment, AO-resistant MLI outer layers must be developed.

Post flight analysis of LDEF has provided the technical community, in general, with an understanding of the effects of long space exposure on MLI. On LDEF, a 0.14 m^2 sample of a ram-facing MLI blanket provided an opportunity to study the effects of HVI. The 1.3 mm thick single aluminized Kapton outer layer had been eroded away by AO, releasing vapor-deposited aluminum on the back surface. The first layer of Dacron (DuPont trademark) isolator cloth was then exposed and also eroded away. The underlying double aluminized reflector layers and the remaining Dacron layers were intact except for eight small tears in the first reflector layer, caused by HVI. Reflector layers are commonly perforated with 3%-10% open area to aid venting during assent into space. The additional open area due to HVI damage was negligible in terms of the blanket performance.

The primary material issue with MLI appears to be the development of an AO-resistant outer layer. Materials under consideration for an AO-resistant outer layer are fiberglass or ceramic woven fabrics and aluminum foil laminated to Mylar or some other flexible, metalized material.

Fiberglass/Ceramic Woven Fabrics. While fiberglass and ceramics are both impervious to AO, the fiber-sizing materials normally used are not resistant to AO attack. At this time, the best sizing for AO resistance is Teflon, but the thin layer of Teflon sizing will erode from AO exposure. If the sizing is completely removed, the brittle fiberglass or ceramic fibers may break as the blanket is flexed, creating additional debris in the local space environment. The extent to which the sizing will erode is under investigation.

Aluminum Foil Laminates. Aluminum foil laminates are also under consideration. Specifically, the candidate material is a thin Mylar film sandwiched between two aluminum foil layers to form a foil laminate. Such a laminate would be very resistant to AO. Preliminary thermal vacuum tests indicate that there are design problems associates with using a thermally conductive material as an outer layer on an insulation blanket. Heat conduction at blanket overlaps and at areas where the MLI is compressed (for example, at seams and penetrations) may dominate the insulative properties.

Teflon Impregnated Beta Cloth. In addition to being AO resistant, the thermal designers require a light block (zero transmission of solar radiation) and optical properties similar to that of Beta cloth, i.e., high emittance and low absorptance. After conducting various screening tests, PTFE Teflon impregnated Beta cloth was selected with vapor deposited aluminum on the back side. The tight weave used in fabricating the Beta cloth helps protect the underlying Teflon from AO erosion. The Beta cloth is to be woven without the use of a silicon or other sizing material that darkens under UV exposure. The trade studies conducted are reported by C.A. Smith et al.[17]

REFERENCES

[1] C.W. Woo, "Atomic Oxygen Special Study Report," TRW CERES.93.310.001 Report, April 15, 1993.

[2] Sheldahl Thermal Control Material & Metalized Films part Number Listing and General Specifications Manual.

[3] A.S. Levine, editor, "LDEF 69 Months in Space", LDEF First Post-Retrieval Symposium, NASA CP-3134, June 2-8, 1991.

[4] B. A. Banks, S.K. Rutledge, L. Gebauer, and C. LaMoreaux, "SiO_x Coatings for Atomic Oxygen Protection of Polyimide Kapton in Low Earth Orbit," AIAA-92-2151-CP, AIAA Materials Specialist Conference, Dalla, TX, April 1992.

[5] S.K. Rutledge and R.M. Olle, "Space Station Freedom Solar Array Blanket Coverlay Atomic Oxygen Durability Testing Results," 38th International SAMPE Symposium & Exhibition, May 10-13, 1993.

[6] Private communication with Hiroshi Takeo of LMSC.

[7] D.R. Wilkes et al., "Initial Materials Evaluation of the Thermal Control Surfaces Experiment (S0069)," LDEF First Post-Retrieval Symposium, NASA CP-3134, 1991, pp. 899-917.

[8] K. Rousslang, E.R. Crutcher, and G. Pippin, "Results of Examination of Silver Teflon from LDEF," LDEF First Post-Retrieval Symposium, NASA CP 3134, 1991, pp. 847-859.

[9] J.A. Dever, S.K. Rutledge, et.al., "The Effects of Simulated Low Earth Orbit Environments on Spacecraft Thermal Control Coatings," 38th International SAMPE Symposium & Exhibition, May 10-13, 1993.

[10] B.A. Banks, B.M. Auer, S.K. Rutledge, and C.M. Hill, "Atomic Oxygen Interaction With Solar Array Blankets at Protective Coating Defect Sites," Fourth Annual Workshop on Space Operations Automation and Robotics (SOAR 90), June 1990.

[11] S.A. Straka, "Long Duration Exposure Facility Post-Flight Data as It Influences the Tropical Rainfall Measuring Mission," paper presented at the LDEF Third Post-Retrieval Symposium, November, 1993.

[12] H.W. Babel, K.E. Simpson, and C.A. Jones, "Material Considerations for Space Station Freedom", IAF-90-278, 1990.

[13] H.W. Babel, "LDEF's Contribution to the Selection of Thermal Control Coatings for the Space Station," presented at LDEF Third Post-Retrieval Symposium, November 1993.

[14] C.A. Jones, K.E. David, R.J. LeVesque, and H.W. Babel, "Environmental Effects on Passive Thermal Control Materials of the Space Station Freedom", Paper IAF-93-1.4.223, 44th IAF Conference, Graz, Austria, October 16-22, 1993.

[15] R.J. LeVesque, M.M. Ho, B.D. Vickers, and H.W. Babel, "Black Anodize as a Thermal Control Coating for Space Station Freedom," AIAA Paper 92-2160 and MDC Paper No 91H1111, Dallas, Texas, April 16-17 1992.

[16] D.Duffy, Final Report on Development off Durable/Long-Life Radiator Coatings. Acurex Technical Report FR-88-100/ESD for NASA Lyndon B. Johnson Space Center, Acurrex Corp. Environmental Systems Division, Mountain View, CA, April 1988.

[17] C.A. Smith, M.M. Hasegawa, and C.A. Jones, "Space Station WP-2 Application of LDEF MLI results," Presented at the LDEF Materials Results for Spacecraft Conference, Huntsville, Alabama, 27-28 October 1992.

REPORT DOCUMENTATION PAGE

Form Approved
OMB No. 0704-0188

1. AGENCY USE ONLY (*Leave blank*)	2. REPORT DATE	3. REPORT TYPE AND DATES COVERED
	August 1995	Contractor Report(April 1993 - March 1995)

4. TITLE AND SUBTITLE
Space Environmental Effects on Spacecraft: LEO Materials Selection Guide

5. FUNDING NUMBERS
C NAS1-19291
TA 12
WU 233-01-01-02

6. AUTHOR(S)
Edward M. Silverman

7. PERFORMING ORGANIZATION NAME(S) AND ADDRESS(ES)
TRW Space & Electronics Group
One Space Park
Redondo Beach, CA 90278

8. PERFORMING ORGANIZATION REPORT NUMBER

9. SPONSORING / MONITORING AGENCY NAME(S) AND ADDRESS(ES)
National Aeronautics and Space Administration
Langley Research Center
Hampton, VA 23681-0001

10. SPONSORING / MONITORING AGENCY REPORT NUMBER
NASA CR-4661, Part 2

11. SUPPLEMENTARY NOTES
Langley Technical Monitors: Joan G. Funk and Stephen S. Tompkins

12a. DISTRIBUTION / AVAILABILITY STATEMENT
Unclassified--Unlimited

Subject Category 18

12b. DISTRIBUTION CODE

13. ABSTRACT (*Maximum 200 words*)

This document provides performance properties on major spacecraft materials and subsystems that have been exposed to the low-Earth (LEO) space environment. Spacecraft materials include metals, polymers, composites, white and black paints, thermal-control blankets, adhesives, and lubricants. Spacecraft subsystems include optical components, solar cells, and electronics. Information has been compiled from LEO short-term spaceflight experiments (e.g., Space Shuttle) and from retrieved satellites of longer mission durations (e.g., Long Duration Exposure Facility). Major space environment effects include atomix oxygen, ultraviolet radiation, micrometeoroids and debris, contamination, and particle radiation

The main objective of this document is to provide a decision tool to designers for designing spacecraft and structures. This document identifies the space environments that will affect the performance of materials and components, e.g., thermal-optical property changes of paints due to UV exposures, AO-induced surface erosion of composites, dimensional changes due to thermal cycling, vacuum-induced moisture outgassing, and surface optical changes due to AO/UV exposures. Where appropriate, relationships between the space environment and the attendant material/system effects are identified.

14. SUBJECT TERMS	15. NUMBER OF PAGES
Space environmental effects; Atomic oxygen; Micrometeoroids and debris; Low-Earth orbit; Space Shuttle; Long Duration Exposure Facility (LDEF)	411
	16. PRICE CODE: A18

17. SECURITY CLASSIFICATION OF REPORT	18. SECURITY CLASSIFICATION OF THIS PAGE	19. SECURITY CLASSIFICATION OF ABSTRACT	20. LIMITATION OF ABSTRACT
Unclassified	Unclassified		